frontiers | Research Topics

New insights into fibrotic signaling in cancer

Edited by
Patrick Ming-Kuen Tang, Eric W-F Lam, Francis Jay Mussai, Dongmei Zhang and Chunjie Li

Published in
Frontiers in Oncology
Frontiers in Cell and Developmental Biology

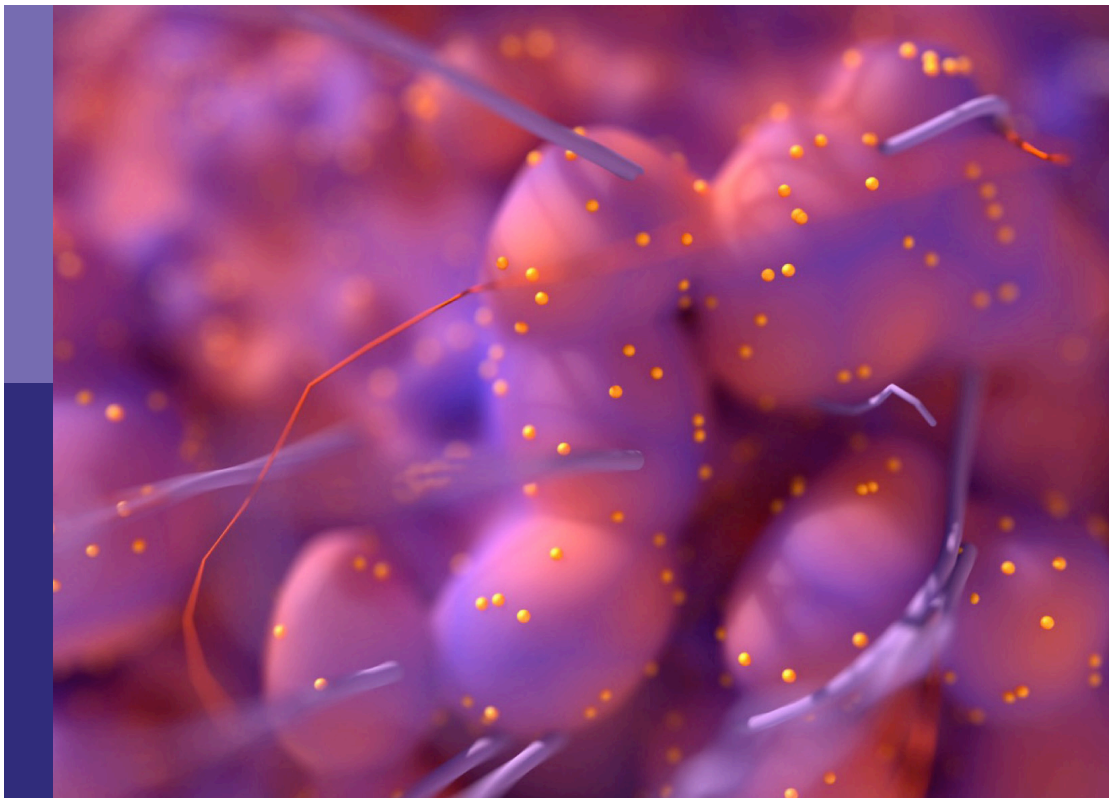

ISSN 1664-8714
ISBN 978-2-8325-4475-4
DOI 10.3389/978-2-8325-4475-4

About Frontiers

Frontiers is more than just an open access publisher of scholarly articles: it is a pioneering approach to the world of academia, radically improving the way scholarly research is managed. The grand vision of Frontiers is a world where all people have an equal opportunity to seek, share and generate knowledge. Frontiers provides immediate and permanent online open access to all its publications, but this alone is not enough to realize our grand goals.

Frontiers journal series

The Frontiers journal series is a multi-tier and interdisciplinary set of open-access, online journals, promising a paradigm shift from the current review, selection and dissemination processes in academic publishing. All Frontiers journals are driven by researchers for researchers; therefore, they constitute a service to the scholarly community. At the same time, the *Frontiers journal series* operates on a revolutionary invention, the tiered publishing system, initially addressing specific communities of scholars, and gradually climbing up to broader public understanding, thus serving the interests of the lay society, too.

Dedication to quality

Each Frontiers article is a landmark of the highest quality, thanks to genuinely collaborative interactions between authors and review editors, who include some of the world's best academicians. Research must be certified by peers before entering a stream of knowledge that may eventually reach the public - and shape society; therefore, Frontiers only applies the most rigorous and unbiased reviews. Frontiers revolutionizes research publishing by freely delivering the most outstanding research, evaluated with no bias from both the academic and social point of view. By applying the most advanced information technologies, Frontiers is catapulting scholarly publishing into a new generation.

What are Frontiers Research Topics?

Frontiers Research Topics are very popular trademarks of the *Frontiers journals series*: they are collections of at least ten articles, all centered on a particular subject. With their unique mix of varied contributions from Original Research to Review Articles, Frontiers Research Topics unify the most influential researchers, the latest key findings and historical advances in a hot research area.

Find out more on how to host your own Frontiers Research Topic or contribute to one as an author by contacting the Frontiers editorial office: frontiersin.org/about/contact

New insights into fibrotic signaling in cancer

Topic editors

Patrick Ming-Kuen Tang — The Chinese University of Hong Kong, China
Eric W-F Lam — Sun Yat-sen University Cancer Center (SYSUCC), China
Francis Jay Mussai — University of Birmingham, United Kingdom
Dongmei Zhang — Jinan University, China
Chunjie Li — Sichuan University, China

Citation

Tang, P. M.-K., Lam, E. W.-F., Mussai, F. J., Zhang, D., Li, C., eds. (2024). *New insights into fibrotic signaling in cancer*. Lausanne: Frontiers Media SA.
doi: 10.3389/978-2-8325-4475-4

Table of contents

frontiers | Frontiers in Oncology

TYPE Editorial
PUBLISHED 02 February 2024
DOI 10.3389/fonc.2024.1369457

OPEN ACCESS

EDITED AND REVIEWED BY
Tao Liu,
University of New South Wales, Australia

*CORRESPONDENCE
Patrick Ming-Kuen Tang
patrick.tang@cuhk.edu.hk

RECEIVED 12 January 2024
ACCEPTED 26 January 2024
PUBLISHED 02 February 2024

CITATION
Tang PM-K, Lam EW-F, Mussal F, Zhang D and Li C (2024) Editorial: New insights into fibrotic signaling in cancer.
Front. Oncol. 14:1369457.
doi: 10.3389/fonc.2024.1369457

Editorial: New insights into fibrotic signaling in cancer

Patrick Ming-Kuen Tang[1]*, Eric W-F. Lam[2], Francis Mussal[3], Dongmei Zhang[4] and Chunjie Li[5]

[1]Department of Anatomical and Cellular Pathology, State Key Laboratory of Translational Oncology, The Chinese University of Hong Kong, Hong Kong, Hong Kong SAR, China, [2]Sun Yat-sen University Cancer Center, State Key Laboratory of Oncology in South China, Collaborative Innovation Center for Cancer Medicine, Guangdong, China, [3]Paediatric Oncology, Birmingham Children's Hospital, University of Birmingham, Birmingham, United Kingdom, [4]College of Pharmacy, Jinan University, Guangzhou, China, [5]Department of Head and Neck Oncology, West China Hospital of Stomatology, Sichuan University, Chengdu, Sichuan, China

KEYWORDS

cancer, tumor microenvironment, fibrotic signaling, cancer therapy, macrophage-myofibroblast transition (MMT), macrophage to Neuron-like cell Transition (MNT)

Editorial on the Research Topic
New insights into fibrotic signaling in cancer

Cancer is still a top leading cause of death worldwide. Ineffective treatments, severe side effects, drug resistance, recurrence, and metastasis are major barriers to curing cancers with the conventional therapeutic methods. Immunotherapies show promise on blood cancers, but various response rates were observed on the treated patients with solid cancers, 30% of patients with non-small-cell lung cancer response to the T-cell based therapies including CAR-T and PD-1/L1 blockades in clinics.

Increasing evidence shows the importance of fibrotic signaling in solid cancers. For example, TGF-beta, a well-documented fibrotic cytokine, was first discovered as an anticancer regulator in cancer cells, but it has been found as a strong immunosuppressor for the host anticancer immunity (1, 2). Therefore, better understanding the potential roles of the fibrotic signaling in cancer cells as well as their microenvironment may eventually identify suitable strategies for improving the efficiency of cancer therapies in clinics.

This Research Topic serves as an interactive platform for sharing the latest insights of molecular mechanisms, translational potential, and clinical observations of the fibrotic singling in cancer. We have received manuscripts from research groups all over the world, and eventually accepted 6 original research and 4 review articles for publication. The articles widely covered findings from the clinical prognostic, molecular mechanisms, and therapeutic development based on the cancer cells as well as the tumor microenvironments.

Clinical discovery

The importance of fibrotic signaling in diseases beyond tissue fibrosis has been recognized. For examples, a well-documented phenomenon "Macrophage-Myofibroblast Transition" has been widely reported in kidney fibrosis (3), its implications in solid cancer has been started to be investigated nowadays (4). In this Research Topic, the clinical implications of fibrotic signaling in clinical solid cancers have been examined, where Chen

et al. observed that intratumorally fibrosis and pseudo-capsule fibrosis are positively correlated to the disease progression of renal cell. While Shan et al. observed 10 fibrotic signaling (e.g. TLR4, Hedgehog, TGF-β, etc) are closely related to the biological activities of hepatocellular carcinoma cells after reviewing 264 related studies. Qin et al. has developed a new prognostic nomogram combined with desmoplastic reaction for predicting the progression of synchronous peritoneal metastasis in colorectal cancer patients.

Molecular mechanism

Fibrotic signaling may contribute to pathogenesis that are beyond the end stage organ diseases. Myofibroblast formation is one of the critical steps for tissue scarring (5, 6) as well as tumor formation (4). Zhang et al. reported a pathogenic role of cancer-associated fibroblasts in the irradiation driven cancer progression. Cheng et al. further summarized the clinical implications of a myofibroblast-based targeting strategies for pancreatic cancer treatment. Besides, by transcriptome profiling of patient biopsies, Tulalamba et al. identified a Wnt signaling mediator FZD10 as potential biomarker for nasopharyngeal carcinoma recurrence and Chen et al. examined the clinical relevance of FGFR signaling in head and neck carcinoma. Sukphokkit et al. demonstrated a 3-dimensional culture system which can reformed the phenotype of cholangiocarcinoma cells compared to the conventional 2D system, may serve as an ideal platform for elucidating the underlying mechanisms as well as clinical potential of fibrotic signaling in cancer *in vitro*.

Therapeutic development

Indeed, a new study demonstrated that targeting of TGF-β/Smads signaling with a natural compound formula effectively overcome drug resistance of liver cancer cells via suppressing a multidrug resistant gene MDR1 (7). Here, Gao et al. reported Icaritin, an active component of the traditional Chinese herb Epimedium genus can inhibit cancer migration via targeting Akt/mTOR signaling of the cisplatin-resistant ovarian cancer cells *in vitro*. Ji et al. summarized the dynamics and therapeutic potentials of tumor-associated macrophages in solid cancer, such as a novel neuron type derived from "Macrophage to Neuron-like Cell Transition" in lung cancer (Figure 1) (8). Single-cell RNA-sequencing allows researchers to dissect the TME in a cell-type specific manner, therefore the contributions of fibrotic signaling in the cancer immunity which was hidden in the conventional bulk sequencing at population level can be unmasked (9).

In conclusion, this Research Topic gathered the latest findings about fibrotic signaling in solid cancer, highlighting their clinical relevance and translational potential beyond fibrosis. We hope the collected articles can inspire both pre-clinical and translational researchers, clinical strategy targeting fibrotic signaling may eventually be developed for cancer therapy.

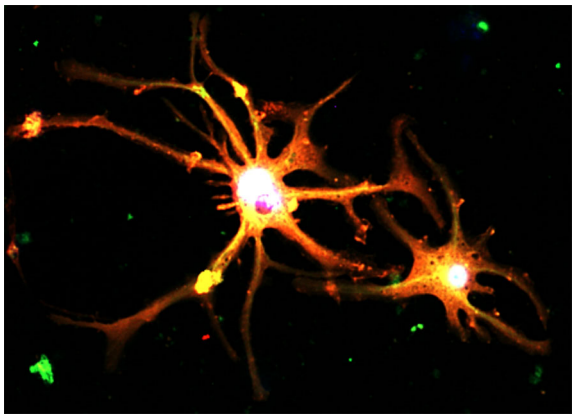

FIGURE 1
Cancer pain associated neurons formed by a TGF-β1-driven novel phenomenon "Macrophage to Neuron-like Cell Transition" in tumor microenvironment, expressing neuronal markers Synaptophysin (red) and Tubb3 (green) detecting by immunofluorescence *in vitro* (8).

Author contributions

PT: Conceptualization, Funding acquisition, Resources, Visualization, Writing – original draft, Writing – review & editing. EL: Validation, Writing – review & editing. FM: Writing – review & editing. DZ: Writing – review & editing. CL: Writing – review & editing.

Funding

The author(s) declare that financial support was received for the research, authorship, and/or publication of this article. This work was supported by the Research Grants Council of Hong Kong (14106518, 14111019, 14111720, 24102723); RGC Postdoctoral Fellowship Scheme (PDFS2122-4S06); Health and Medical Research Fund (10210726, 11220576); CU Medicine Passion for Perfection Scheme (PFP202210-004) and Faculty Innovation Award (4620528), CUHK Strategic Seed Funding for Collaborative Research Scheme (178896941), Direct Grant for Research (4054722), Postdoctoral Fellowship Scheme (NL/LT/PDFS2022/0360/22lt, WW/PDFS2023/0640/23en).

Conflict of interest

The authors declare that the research was conducted in the absence of any commercial or financial relationships that could be construed as a potential conflict of interest.

Publisher's note

References

1. Chan MK, Chung JY, Tang PC, Chan AS, Ho JY, Lin TP, et al. TGF-beta signaling networks in the tumor microenvironment. *Cancer Lett* (2022) 550:215925. doi: 10.1016/j.canlet.2022.215925

2. Chung JY, Chan MK, Li JS, Chan AS, Tang PC, Leung KT, et al. TGF-beta signaling: from tissue fibrosis to tumor microenvironment. *Int J Mol Sci* (2021) 22 (14):7575. doi: 10.3390/ijms22147575

3. Tang PC, Chan AS, Zhang CB, Garcia Cordoba CA, Zhang YY, To KF, et al. TGF-beta1 signaling: immune dynamics of chronic kidney diseases. *Front Med (Lausanne)* (2021) 8:628519. doi: 10.3389/fmed.2021.628519

4. Tang PC, Chung JY, Xue VW, Xiao J, Meng XM, Huang XR, et al. Smad3 promotes cancer-associated fibroblasts generation via macrophage-myofibroblast transition. *Adv Sci (Weinh)* (2022) 9:e2101235. doi: 10.1002/advs.202101235

5. Tang PM, Zhang YY, Xiao J, Tang PC, Chung JY, Li J, et al. Neural transcription factor Pou4f1 promotes renal fibrosis via macrophage-myofibroblast transition. *Proc Natl Acad Sci U.S.A.* (2020) 117:20741–52. doi: 10.1073/pnas.1917663117

6. Tang PM, Zhou S, Li CJ, Liao J, Xiao J, Wang QM, et al. The proto-oncogene tyrosine protein kinase Src is essential for macrophage-myofibroblast transition during renal scarring. *Kidney Int* (2018) 93:173–87. doi: 10.1016/j.kint.2017.07.026

7. Chung JY, Chan MK, Tang PC, Chan AS, Chung JS, Meng XM, et al. AANG: A natural compound formula for overcoming multidrug resistance via synergistic rebalancing the TGF-beta/Smad signalling in hepatocellular carcinoma. *J Cell Mol Med* (2021) 25:9805–13. doi: 10.1111/jcmm.16928

8. Tang PC, Chung JY, Liao J, Chan MK, Chan AS, Cheng G, et al. Single-cell RNA sequencing uncovers a neuron-like macrophage subset associated with cancer pain. *Sci Adv* (2022) 8:eabn5535. doi: 10.1126/sciadv.abn5535

9. Tang PC, Chan MK, Chung JY, Chan AS, Zhang D, Li C, et al. Hematopoietic transcription factor RUNX1 is essential for promoting macrophage-myofibroblast transition in non-small-cell lung carcinoma. *Adv Sci (Weinh)* (2023) 11(1):e2302203. doi: 10.1002/advs.202302203

frontiers in Cell and Developmental Biology

ORIGINAL RESEARCH
published: 14 February 2022
doi: 10.3389/fcell.2021.801715

Investigation of an FGFR-Signaling-Related Prognostic Model and Immune Landscape in Head and Neck Squamous Cell Carcinoma

Qi Chen [1,2,3†], Ling Chu [4†], Xinyu Li [2†], Hao Li [1], Ying Zhang [1], Qingtai Cao [5] and Quan Zhuang [1,6]*

[1]Transplantation Center, Third Xiangya Hospital, Central South University, Changsha, China, [2]Xiangya School of Medicine, Central South University, Changsha, China, [3]Xiangya School of Stomatology, Central South University, Changsha, China, [4]Department of Pathology, Third Xiangya Hospital, Central South University, Changsha, China, [5]Hunan Normal University School of Medicine, Changsha, China, [6]Research Center of National Health Ministry on Transplantation Medicine, Changsha, China

OPEN ACCESS

Edited by:
Patrick Ming-Kuen Tang, The Chinese University of Hong Kong, China

Reviewed by:
Ying Hu, Harbin Institute of Technology, China
Yiping Jin, University of California, Los Angeles, United States
Guoliang Wang, Huazhong University of Science and Technology, China

***Correspondence:**
Quan Zhuang
zhuangquansteven@163.com

[†]These authors have contributed equally to this work

Specialty section:
This article was submitted to Molecular and Cellular Oncology, a section of the journal Frontiers in Cell and Developmental Biology

Received: *25 October 2021*
Accepted: *29 December 2021*
Published: *14 February 2022*

Citation:
Chen Q, Chu L, Li X, Li H, Zhang Y, Cao Q and Zhuang Q (2022) Investigation of an FGFR-Signaling-Related Prognostic Model and Immune Landscape in Head and Neck Squamous Cell Carcinoma. Front. Cell Dev. Biol. 9:801715. doi: 10.3389/fcell.2021.801715

Background: There is accumulating evidence on the clinical importance of the fibroblast growth factor receptor (FGFR) signal, hypoxia, and glycolysis in the immune microenvironment of head and neck squamous cell carcinoma (HNSCC), yet reliable prognostic signatures based on the combination of the fibrosis signal, hypoxia, and glycolysis have not been systematically investigated. Herein, we are committed to establish a fibrosis–hypoxia–glycolysis–related prediction model for the prognosis and related immune infiltration of HNSCC.

Methods: Fibrotic signal status was estimated with microarray data of a discovery cohort from the TCGA database using the UMAP algorithm. Hypoxia, glycolysis, and immune-cell infiltration scores were imputed using the ssGSEA algorithm. Cox regression with the LASSO method was applied to define prognostic genes and develop a fibrosis–hypoxia–glycolysis–related gene signature. Immunohistochemistry (IHC) was conducted to identify the expression of specific genes in the prognostic model. Protein expression of several signature genes was evaluated in HPA. An independent cohort from the GEO database was used for external validation. Another scRNA-seq data set was used to clarify the related immune infiltration of HNSCC.

Results: Six genes, including AREG, THBS1, SEMA3C, ANO1, IGHG2, and EPHX3, were identified to construct a prognostic model for risk stratification, which was mostly validated in the independent cohort. Multivariate analysis revealed that risk score calculated by our prognostic model was identified as an independent adverse prognostic factor ($p < .001$). Activated B cells, immature B cells, activated $CD4^+$ T cells, activated $CD8^+$ T cells, effector memory $CD8^+$ T cells, MDSCs, and mast cells were identified as key immune cells between high- and low-risk groups. IHC results showed that the expression of SEMA3C, IGHG2 were slightly higher in HNSCC tissue than normal head and neck squamous cell tissue. THBS1, ANO1, and EPHX3 were verified by IHC in HPA. By using single-cell analysis, FGFR-related genes and highly expressed DEGs in low-survival patients were more active in monocytes than in other immune cells.

Conclusion: A fibrosis–hypoxia–glycolysis–related prediction model provides risk estimation for better prognoses to patients diagnosed with HNSCC.

Keywords: head and neck squamous cell carcinoma, fibroblast growth factor receptor, hypoxia, glycolysis, prognosis, immune-cell infiltration

INTRODUCTION

Head and neck squamous cell carcinoma (HNSCC) has a worldwide incidence of more than 600,000 cases per year (Ferlay et al., 2015), including a heterogeneous group of tumors that arise from the oral cavity, oropharynx, larynx, hypopharynx, nasopharynx, and sinonasal cavity (Kim et al., 2021). Due to its special anatomical location, patients with HNSCC often experience vital dysfunction, especially in the aspects of swallowing, feeding, breathing, and psychological health (Zhu et al., 2017). Despite significant progress in available therapies, the 5-year overall survival (OS) rate of HNSCC patients has not obviously improved in recent decades (Siegel et al., 2019). Therefore, there is an urgent need for a way to predict the progression of HNSCC (Shield et al., 2017).

The fibroblast growth factor receptor (FGFR) is a receptor tyrosine kinase (RTK) signaling pathway involved in the regulation of angiogenesis, invasion, and metastasis of tumors (Chae et al., 2017). It is considered to be a contributory factor in the development of fibrosis, causing the exacerbation of liver fibrosis (Seitz and Hellerbrand, 2021), systemic sclerosis (SS) (Chakraborty et al., 2020), idiopathic pulmonary fibrosis (IPF) (Wollin et al., 2015), and so on. A recent study also revealed the clinically activity of an FGFR inhibitor against HNSCC (Schuler et al., 2019). However, few investigations focus on the potential mechanisms about this profibrotic mediator in HNSCC.

Hypoxia, as a hallmark of tumor, is a potent microenvironmental factor facilitating proliferation and progression in a variety of cancers (Rankin and Giaccia, 2016). Previous research suggests that hypoxic HNSCC cells trigger glycolysis to obtain energy and balance metabolic and bioenergetic (Zhu et al., 2017). Furthermore, activated fibroblasts synthesized excessive collagen, leading to a microenvironment of hypoxia, which might deteriorate the progression of disease, whereas there were few records on the prognosis of HNSCC by combining a profibrotic signal with hypoxia and glycolysis. The immune landscape associated with the factors mentioned above also demands exploration.

Therefore, in this study, we establish an FGFR-signaling–hypoxia–glycolysis–related prediction model for the prognosis of HNSCC with a series of bioinformatics analyses. Immune cell infiltration associated with prognosis and profibrotic signaling is also revealed.

METHODS

Patient Cohort and Data Preparation

The discovery cohort of the study contained 483 HNSCC patients from the Cancer Genome Atlas (TCGA, available at https://portal.gdc.cancer.gov/) data set. To obtain a validation cohort, RNA-seq data and related clinicopathological data were downloaded from the Gene Expression Omnibus (GEO, available at https://www.ncbi.nlm.nih.gov/geo/) database (GSE41613), including 97 patients with HPV-negative oral squamous cell carcinoma (OSCC). The microarray data of GSE41613 was built upon the GPL570 Platform (Affymetrix Human Genome U133 Plus 2.0 Array). A single-cell RNA sequencing (scRNA-seq) data set (GSE139324) was also used for analyzing tumor immune infiltration in HNSCC patients, including tumor-infiltrating immune cells from 18 HNSCC patients and tissue resident immune cells from five healthy donor tonsils (Cillo et al., 2020).

The mRNA expression profiles from the TCGA database were normalized using fragments per kilobase of exon per million reads mapped (FPKM). Background correction and normalization has been performed for each series before downloading GSE41613 from the GEO database. Additionally, the harmony algorithm was used in the integration of the single-cell RNA-seq data set GSE139324 considering biological and technical differences (Korsunsky et al., 2019). The general idea and methodologies of our study are shown in a flowchart (**Figure 1**).

Distinction of Fibrotic Signal Status and FGFR-Related DEGs

An algorithm of uniform manifold approximation and projection (UMAP) was applied to deduce the fibrotic signal status of HNSCC patients. Based on the given hallmarks or signatures, UMAP, a nonlinear reductive dimension method, is able to assign a group of patients to diverse clusters. The gene set of the FGFR signal pathway was downloaded from the Molecular Signatures Database (MSigDB version 6.0), identifying the relative activation degree of fibrotic signal in patients. Based on the limma algorithm (Korsunsky et al., 2019) and functional enrichment analysis, two clusters including "fibrosis^{low}" and "fibrosis^{high}" were identified to estimate the fibrotic signal status. The limma algorithm was applied to identify DEGs between the two clusters based on the standards of false discovery rate (FDR) adjusted p-value <.0001 and $|\log2(\text{Fold change})| > 1$. To confirm biological functions and pathway enrichment of the fibrosis-related DEGs, we performed Gene Ontology (GO) functional analysis and Kyoto Encyclopedia of Genes and Genomes (KEGG) pathway enrichment analysis using the "Metascape" website (https://metascape.org/) (Zhou et al., 2019).

Distinction of Hypoxia–Glycolysis–Related DEGs

The ssGSEA algorithm was applied to explore the hypoxia and glycolysis degree in the HNSCC expression profile of the TCGA database. According to hypoxia and glycolysis scores calculated

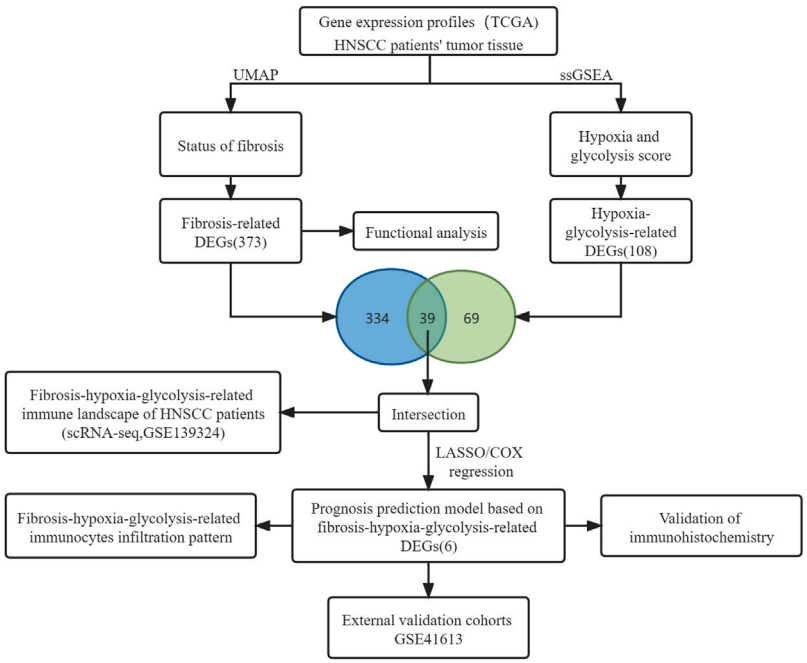

FIGURE 1 | Flowchart diagram of the study.

previously, two groups of patients were stratified. An optimal cutting point for classifying was determined by maximally selected rank statistics using the "survival" and "survminer" R package. Subsequently, "hypoxia^{high}," "hypoxia^{low}," "glycolysis^{high}," and "glycolysis^{low}" groups were identified, respectively. We further considered hypoxia and glycolysis together by combining them into a two-dimensional index; that is, patients were divided into three groups, i.e., hypoxia^{low}/glycolysis^{low}, hypoxia^{high}/glycolysis^{low}, and "mix" groups. Hypoxia–glycolysis–related DEGs were identified based on the standards of FDR adjusted p-value <.0001 and $|\log2(\text{Fold change})| > 1$ using the R package "limma".

Prognosis Prediction Model of HNSCC Based on Fibrosis–Hypoxia–Glycolysis–Related DEGs

Hypoxia–glycolysis–related DEGs and fibrosis–related DEGs were intersected to obtain the 39 shared fibrosis–hypoxia–glycolysis–related DEGs by Venn analysis. To obtain prognostic shared DEGs, univariate Cox regression analyses were further performed among all 39 DEGs mentioned above to screen those risk or protective shared DEGs with $p < .05$. Thereafter, we applied the least absolute shrinkage and selection operator (LASSO) (Friedman et al., 2010; Liu et al., 2013) to preserve valuable variables in 21 prognostic shared DEGs, implementing a high-dimensional prediction and avoiding overfitting. The LASSO Cox regression model was scientifically built up depending on threefold cross-validation and 1000 iterations, which decreased the underlying instability of the results. The optimal tuning parameter λ was identified *via* 1-SE (standard error) criterion. Eventually, the selected prognostic gene signatures were used to establish the prognosis prediction model of HNSCC based on fibrosis–hypoxia–glycolysis–related DEGs. The risk score computing formula is:

$$Risk\ score = \sum_{i=1}^{n} (coefficient_i \times \exp ression\ of\ signature\ gene_i).$$

Based on the risk scores, we computed the optimal cutting point to stratify HNSCC patients into high- and low-risk groups.

Identification of Immune Cell Infiltration Status

To predict the immune cell infiltration status, the ssGSEA algorithm was applied to identify the abundance of 28 immunocytes in each HNSCC patient, confirming the underlying correlation between immune infiltration status and prognostic model. The gene set from Charoentong et al. was obtained to calculate ssGSEA scores for immune cell populations. (Charoentong et al., 2017).

Evaluation of Immunohistochemical Staining

Formalin-fixed, paraffin-embedded tumor tissues were collected from eight patients with HNSCC diagnosed at the 3rd Xiangya Hospital from January 2020 to December 2020. This study was approved by the Ethics Committee of the 3rd Xiangya Hospital (No: 21158). The immunohistochemical process was performed as described previously (Guan et al., 2020). Our procedure used

TABLE 1 | Basic information of HNSCC patients in discovery cohort.

Characteristics	Whole cohort (483)	Low risk (327)	High risk (156)
Gender			
Male	355 (0.735)	246 (0.752)	109 (0.699)
Female	128 (0.265)	81 (0.248)	47 (0.301)
Age			
≥60 years	156 (0.323)	190 (0.581)	80 (0.513)
<60 years	213 (0.441)	137 (0.419)	76 (0.487)
original diagnosis			
Squamous cell carcinoma, NOS	409 (0.847)	272 (0.832)	137 (0.878)
Squamous cell carcinoma, keratinizing, NOS	52 (0.108)	33 (0.101)	19 (0.122)
Squamous cell carcinoma, large cell, nonkeratinizing, NOS	11 (0.023)	11 (0.034)	0 (0.000)
Basaloid squamous cell carcinoma	10 (0.021)	10 (0.031)	0 (0.000)
Squamous cell carcinoma, spindle cell	1 (0.002)	1 (0.003)	0 (0.000)
UMAP clustering			
Cluster1	309 (0.640)	173 (0.529)	136 (0.872)
Cluster2	174 (0.360)	154 (0.471)	20 (0.128)
Hypoxia status			
High	381 (0.789)	242 (0.740)	139 (0.891)
Low	102 (0.211)	85 (0.260)	17 (0.109)
Glycolysis status			
High	318 (0.658)	189 (0.578)	129 (0.827)
Low	165 (0.342)	138 (0.422)	27 (0.173)
Risk group			
High	156 (0.323)	0 (0.000)	156 (1.000)
Low	327 (0.677)	327 (1.000)	0 (0.000)

the following antibodies: Polyclonal rabbit anti-Semaphorin 3c (1:200 dilution; ab135842; Abcam Biochemicals, UK); monoclonal rabbit anti-human IgG2 (1:1000 dilution; ab134050; Abcam Biochemicals, UK). IHC results for IGHG2 and SEMA3C were evaluated by computerizing optical density (OD) measurements using ImageJ software, which depends on the degree and area of staining. Samples were scored by two trained pathologists according to the percentage contribution of high positive, positive, low positive, and negative. The immunoreactive score (IRS) was evaluated as follows: 4, high positive; 3, positive; 2, low positive; and 1 negative (Varghese et al., 2014).

The Human Protein Atlas (HPA, https://www.ptroteinatlas.org/) provides us the IHC staining data in HNSCC and normal tissue (Uhlen et al., 2010). The expression level of target protein was classified into high, medium, low, and not detected according to degree of staining (strong, moderate, weak, or negative) and the proportion of stained cells (>75%, 25%–75%, or <25%).

Single-Cell Analysis of Tumor Infiltrating Immune Cells From HNSCC Patients

After dimension reduction through principal component analysis (PCA), the *t*-distributed stochastic neighbor embedding (t-SNE) algorithm (Kobak and Berens, 2019), a technique that maps a set of high-dimensional points to two dimensions, was used to compute the degree of similarity between cells, which is visualized by the distances among the plotted points on the graph. It also potently governed how many of its nearest neighbors each point is attracted to. Here, each point represented a cell. The scores of individual cells for pathway activities were estimated by the R package "AUCell." According to gene expression rankings in each cell for a certain gene set, area under the curve (AUC) values were calculated to represent the proportion of top-ranking genes in the gene set for each cell (Corridoni et al., 2020).

Statistical Analysis

Using R version 4.0.2 (www.r-project.org/) and the appropriate packages, all statistical analysis was carried out. We implemented the UMAP algorithm using R package "umapr" for nonlinear dimension reduction and the ssGSEA algorithm using R package "GSVA" for the hypoxia and glycolysis score. The Lasso Cox regression model was conducted, and standard statistical tests were guaranteed by using the R package "glmnet." The FDR method was performed to adjust multiple tests. Risk factors were eventually identified through multivariate Cox regression analysis.

RESULTS

Fibrosis Signal and Fibrosis-Related DEGs in HNSCC

The expression profiles and clinical information of 483 HNSCC patients were contained in the discovery cohort downloaded from the TCGA database. The clinical information of patients is shown in **Table 1**. Seventy genes positively correlated with the FGFR signaling pathway were used to evaluate the status of fibrosis signal activation in patients. Based on the algorithm UMAP, we divided the patients into two clusters using the fibrosis-related expression matrix, enabling us to assign each patient to the

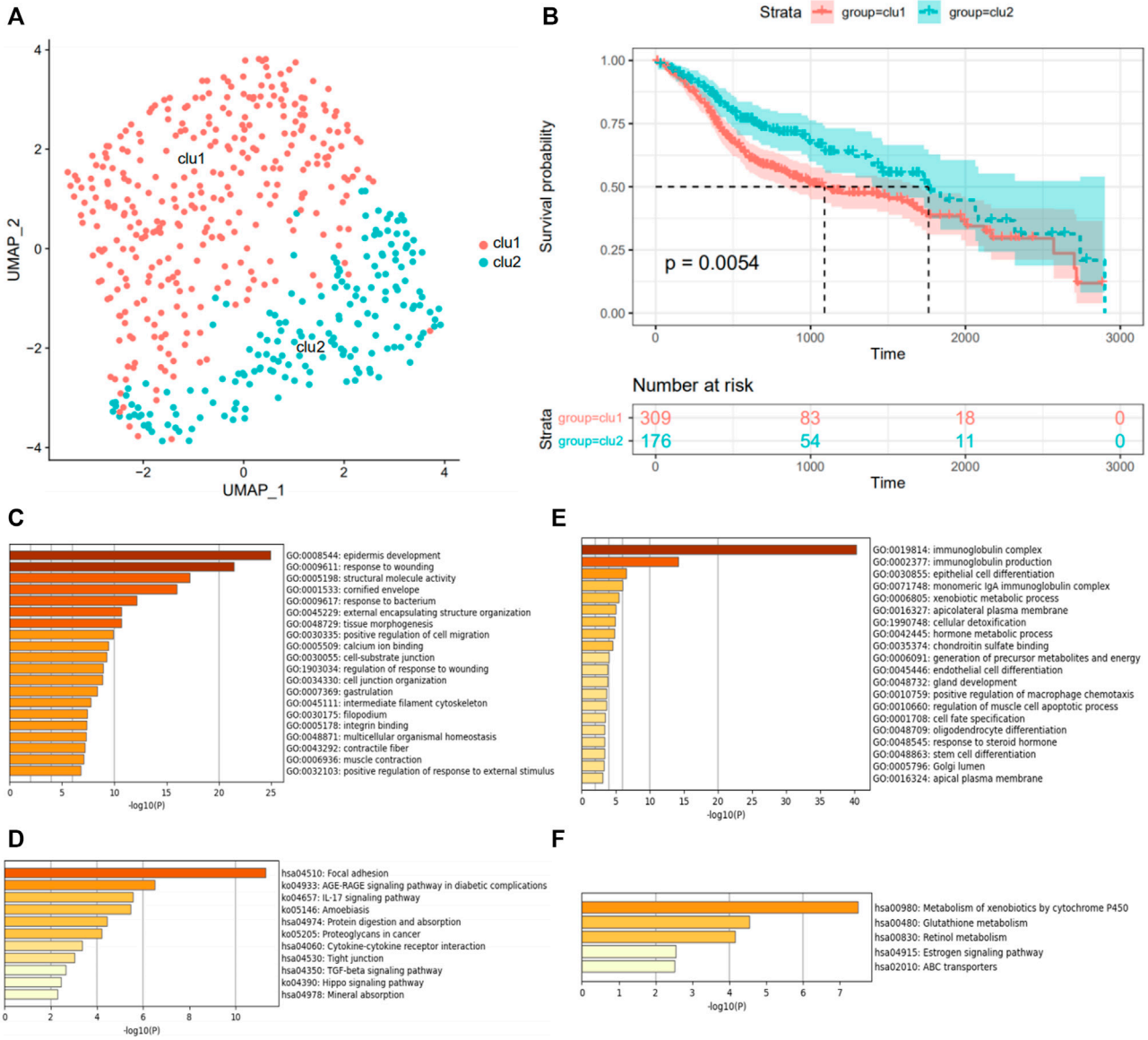

FIGURE 2 | Grouping of patients according to FGFR signaling pathway. **(A)** The UMAP algorithm classifies HNSCC patients into two clusters, indicated by different colors. **(B)** The survivorship analysis plot of OS in two clusters. GO function enrichment **(C,E)** and KEGG pathway enrichment analysis **(D,F)** of differentially expressed genes in the fibrosis$^{low\text{-}survival}$ group, colored by *p*-values. **(C,D)** Analysis of the high expression genes in the fibrosis$^{low\text{-}survival}$ group. **(E,F)** Analysis of the low expression genes in the fibrosis$^{low\text{-}survival}$ group.

nearest cluster (**Figure 2A**). A Kaplan–Meier plot demonstrates that significant differences in survival were witnessed between the two clusters (**Figure 2B**). There were 309 and 176 patients included in clusters 1 and 2, respectively. To obtain fibrosis-related DEGs, we compared the expression profiles between the clusters. A total of 187 fibrosis-related DEGs overexpressed in cluster 1, where patients had worse survival, which were enriched in "response to wounding" (**Figure 2C**), "TGF-beta signaling pathway" (**Figure 2D**). This implied the patients in cluster 1 were in a higher state of fibrosis activation. Enrichment analysis showed 186 DEGs overexpressed in cluster 2 were enriched in "immunoglobulin complex" (**Figure 2E**), "metabolism of xenobiotics cytochrome P450" (**Figure 2F**). These findings are consistent with the previous research that patients with good immune status have a better prognosis.

Hypoxia Status, Glycolysis Status, and Hypoxia–Glycolysis–Related DEGs in HNSCC

Meanwhile, using the "GSVA" package, the ssGSEA algorithm was implemented to quantify the hypoxia or glycolysis enrichment score of each HNSCC patient in hypoxia or glycolysis hallmark genes from the MSigDB. To identify the

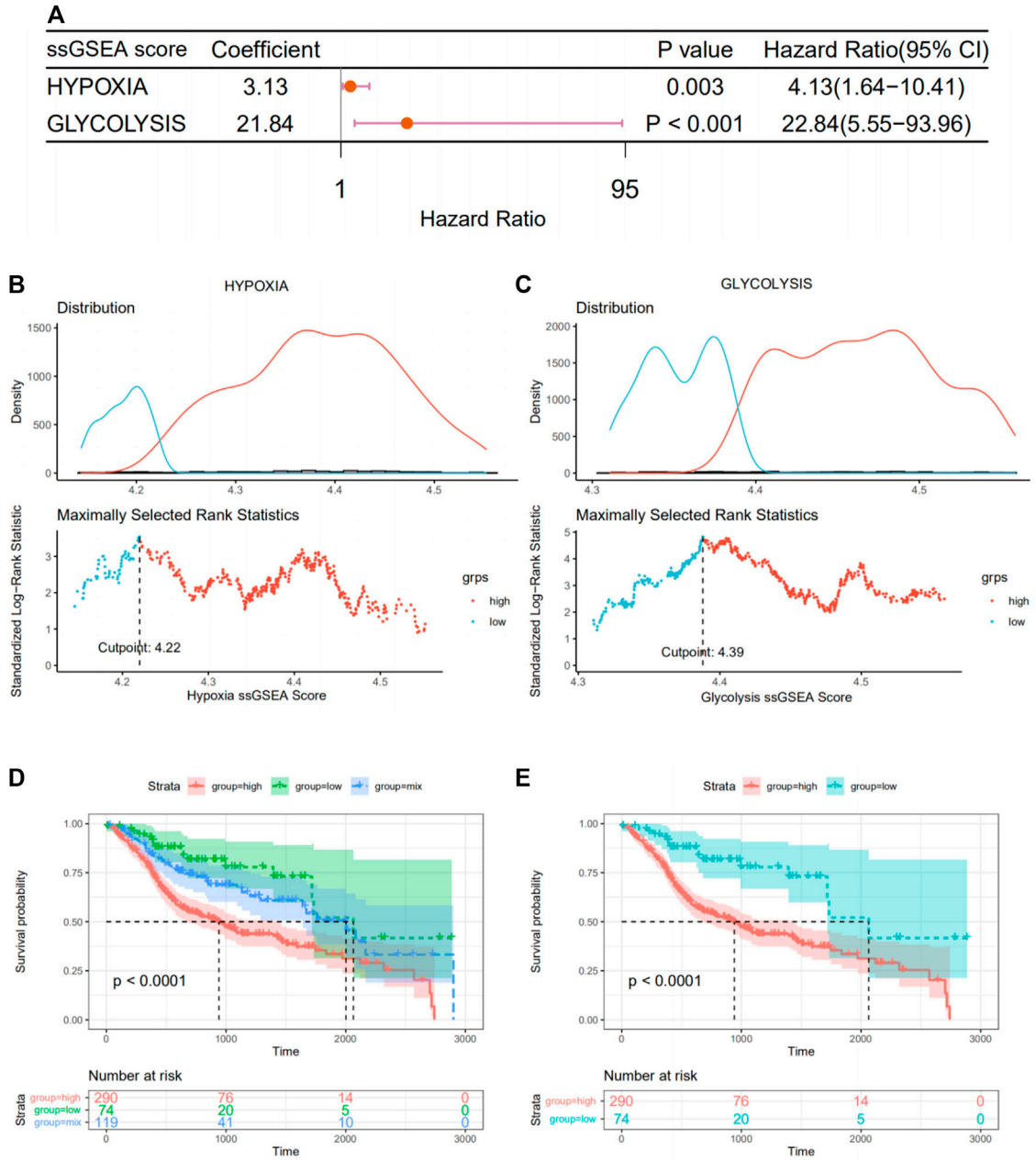

FIGURE 3 | Grouping of patients according to their hypoxia and glycolysis status. **(A)** Forest plot of hypoxia and glycolysis scores by univariate Cox regression. **(B,C)** A vertical dashed line was used to mark the cutoff point with the maximum standard log-rank statistic based on hypoxia and glycolysis scores. **(D)** Kaplan–Meier plot of OS among hypoxia^{high}/glycolysis^{high}, hypoxia^{low}/glycolysis^{low}, and mix groups. **(E)** Kaplan–Meier plot of OS between hypoxia^{high}/glycolysis^{high} and hypoxia^{low}/glycolysis^{low}.

effect of hypoxia and glycolysis on prognosis, univariate Cox regression analyses were further performed among patients' hypoxia and glycolysis scores. Hypoxia and glycolysis, as illustrated in the forest diagram in **Figure 3A**, were considered risk factors for prognosis in HNSCC patients. Based on maximally selected rank statistics, we divided patients into two groups according to hypoxia (**Figure 3B**) and glycolysis (**Figure 3C**) scores. We further synthesized the hypoxia and glycolysis status into a two-dimensional index, dividing patients into three groups, i.e., hypoxia^{high}/glycolysis^{high}, hypoxia^{low}/glycolysis^{low}, and "mix" groups. Significant differences in survival were observed among three groups (**Figure 3D**, log rank test, $p < .0001$). The survivorship analysis (Kaplan–Meier) showed a better survival in the hypoxia^{high}/glycolysis^{high} group than the hypoxia^{low}/glycolysis^{low} group as we expected (**Figure 3E**). Besides this, the mix group was at an intermediate level. A total of 108 hypoxia–glycolysis–related DEGs were obtained after

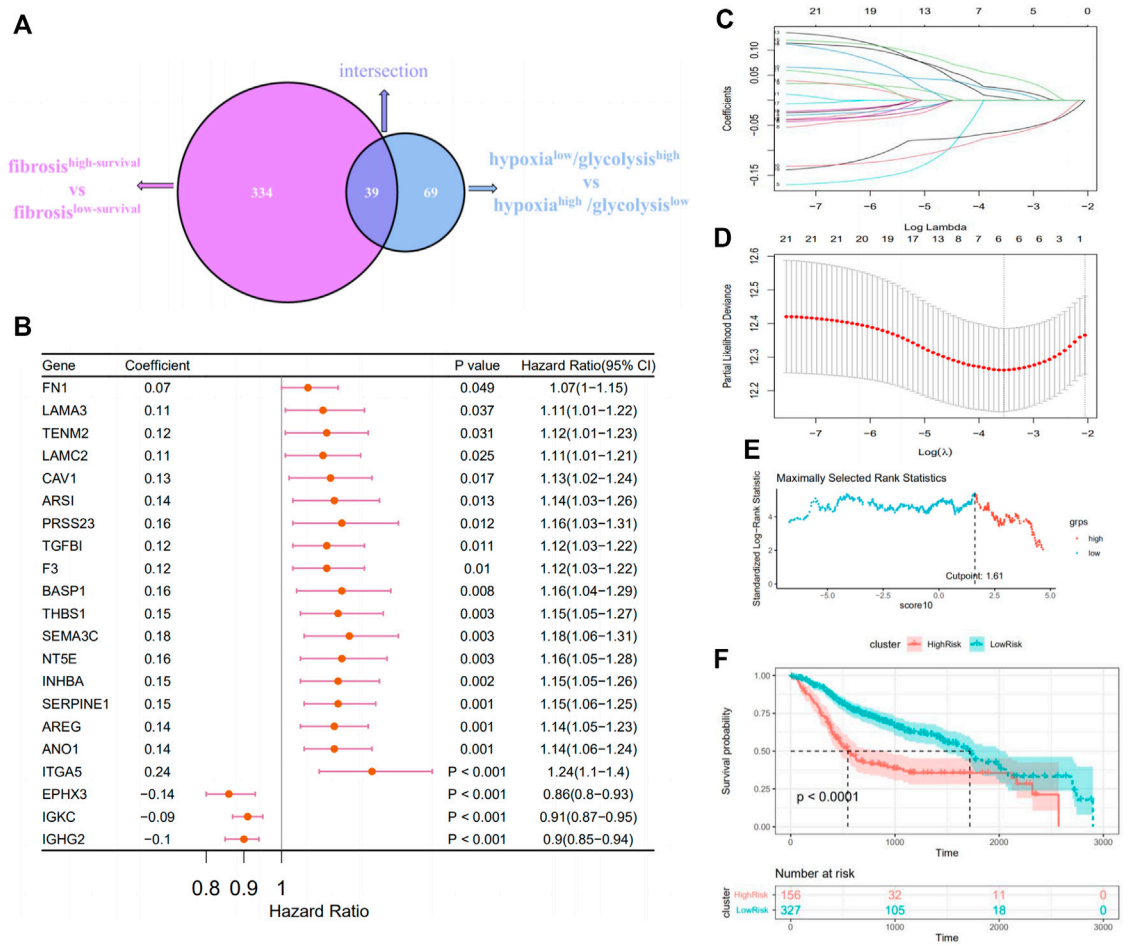

FIGURE 4 | Constructing a prognostic survival model in patients with HNSCC. **(A)** Venn diagrams show the fibrosis–hypoxia–glycolysis related DEGs (39). **(B)** Forest plot of the prognostic effects of 21 DEGs with $p < .05$ on a univariate Cox regression analysis. **(C)** LASSO coefficient profiles of 21 screened DEGs. **(D)** Threefold cross-validation for LASSO analysis was performed to calculate the minimum criteria. **(E)** A vertical dashed line was used to mark the cutoff point with the maximum standard log-rank statistic. **(F)** Kaplan–Meier plot established the survival differences between high- and low-risk groups.

comparing expression profiles between hypoxia^{high}/glycolysis^{high} and hypoxia^{low}/glycolysis^{low}.

Construction of the Fibrosis–Hypoxia–Glycolysis–Related Prognostic Model in the TCGA Data set

The above 334 fibrosis-related and 108 hypoxia–glycolysis–related DEGs screened from HNSCC were intersected to obtain the 39 shared genes (**Figure 4A**). To further filtrate the prognostic DEGs, univariate Cox regression analysis was conducted on 39 shared DEGs, and 21 DEGs with $p < .05$ were identified (**Figure 4B**). Among them, most of them (18 out of 21, 85.7%) were risk DEGs. Six critical variables were selected from the above 21 prognostic DEGs using the LASSO regression method, among which four were risk DEGs and two were protective (**Figures 4C,D**). For each HNSCC patient, a risk score was calculated based on the expression levels of the six characteristic DEGs and corresponding coefficients from the LASSO Cox regression: risk score = 0.0369 × expression of AREG+ 0.03432 × expression of THBS1+ 0.02182 × expression of SEMA3C+ 0.07125 × expression of ANO1+(-0.07718) × expression of IGHG2+ (-0.09177) × expression of EPHX3. Using the maximum selective rank method as the basis of demarcation, patients were divided into high- and low-risk groups according to their risk scores (**Figure 4E**). The low-risk group showed a significantly better effect on prognosis compared with the high-risk group (**Figure 4F**, log rank test, $p < .0001$).

Supplementary Information on Prognostic Model and its Relationship With Immunocyte Infiltration

We performed survival analysis on 483 HNSCC patients, which reorganized according to the location of the primary tumor in an attempt to verify the reliability of the prognostic model. In several regions with high incidence of HNSCC, such as tongue and

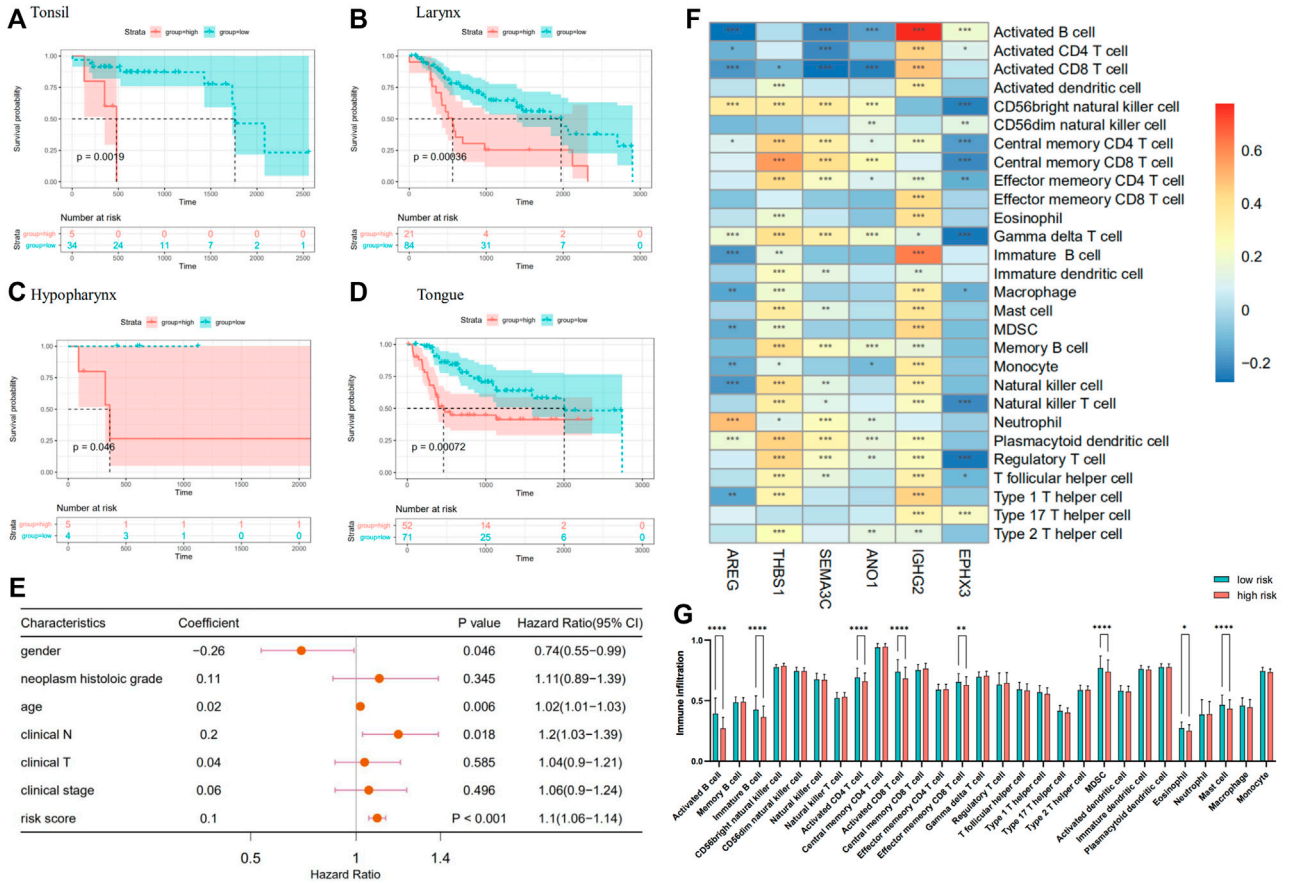

FIGURE 5 | (A–D) A Kaplan–Meier plot establishes the survival differences between high- and low-risk groups in HNSCC with different primary sites. **(E)** Forest plot of other clinical characteristic and risk scores on a univariate Cox regression analysis. **(F)** Heatmap plotted by the correlations between the expression of genes in prognostic model and immune infiltrate level in HNSCC. **(G)** Comparison of immunocyte infiltration between high- and low-risk groups.

TABLE 2 | Basic information of OSCC patients in validation cohort.

Characteristics	Whole cohort (97)
Gender	
Male	66 (0.680)
Female	31 (0.320)
Age	
≥60 years	47 (0.485)
<60 years	50 (0.515)
treatment	
uni-modality	43 (0.443)
multii-modality	53 (0.546)
unknown	1 (0.010)
tumor stage	
I/II	41 (0.423)
III/IV	56 (0.577)

larynx (**Figures 5B,D**), survival comparison revealed that the high-risk group was associated with a worse prognosis of the patients. The same went for tonsil, hypopharynx, and so on (**Figures 5A,C**). Univariate Cox regression analyses indicate that the risk score, similar to other clinical characteristics, such as age, could be deemed as an independent risk factor to assess the prognosis of patients with HNSCC (**Figure 5E**). Additionally, ssGSEA was used to estimate the immune cell infiltration in the patients. To explore the correlation between prognostic model and immune cell infiltration, correlation analysis was performed between six optimal prognostic signatures and the immunocyte infiltration score (**Figure 5F**). Furthermore, significantly decreased infiltration of eight specific immune cells was observed in the high- compared with the low-risk group, that is, activated B cells, immature B cells, activated $CD4^+$ T cells, activated $CD8^+$ T cells, effector memory $CD8^+$ T cells, MDSCs, and mast cells (**Figure 5G**).

External Independent Cohort Validation of the Fibrosis–Hypoxia–Glycolysis–Related Prognostic Model in the GEO Data set

The fibrosis–hypoxia–glycolysis–based prognosis model was further validated in an independent cohort "GSE41613." Searching for six genes from the prognosis model in the expression matrix of 97 OSCC patients, five of them were found. The clinical information of patients is shown in **Table 2**. Univariate Cox regression analyses confirmed that

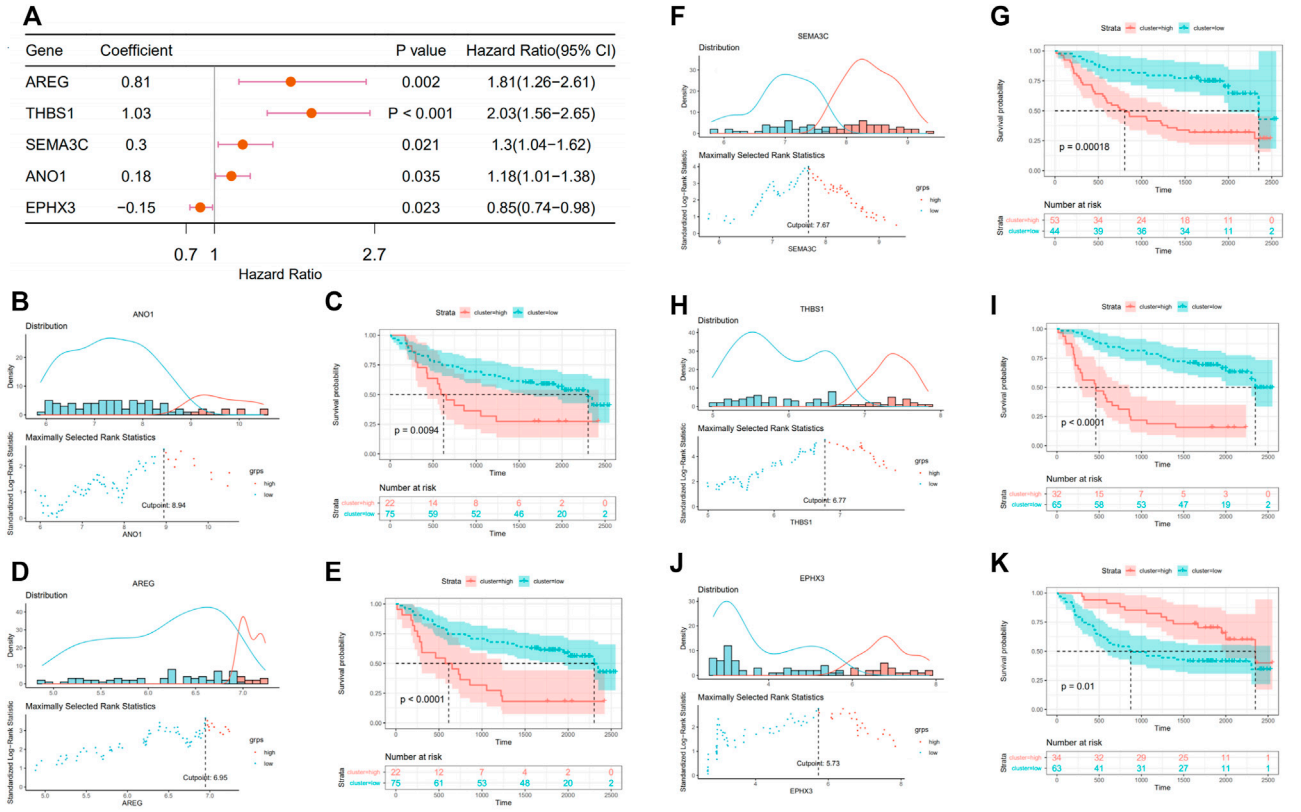

FIGURE 6 | Validation in external data set (GSE416130). **(A)** Forest plot of the prognostic effects of five genes in prognostic model on a univariate Cox regression analysis. **(B,D,F,H,J)** A vertical dashed line was used to mark the cutoff point with the maximum standard log-rank statistic based on the expression of each gene. **(C,E,G,I,K)** Kaplan–Meier plot established the survival differences between high (high expression of target gene) and low (low expression of target gene) groups.

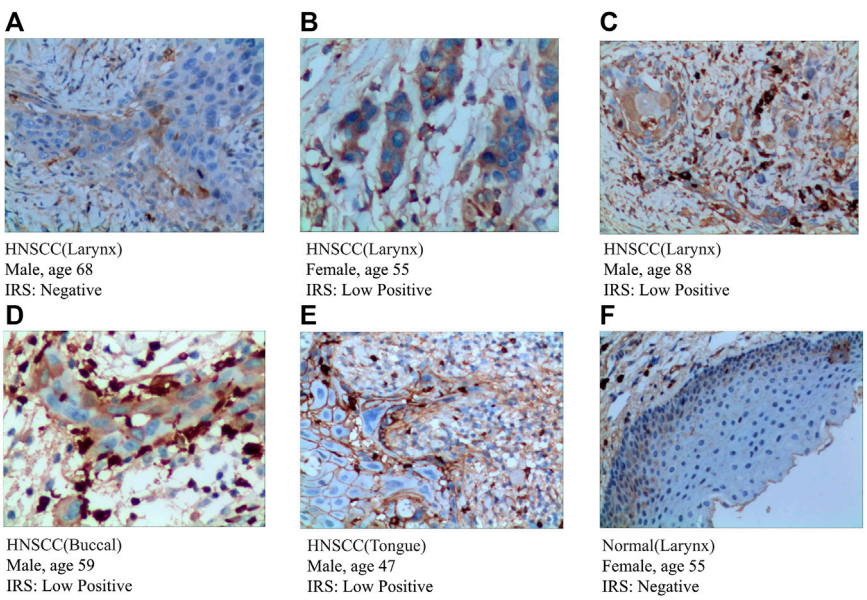

FIGURE 7 | IHC analysis of the protein expression of SEMA3C in HNSCC and normal tissues. **(A–E)** The expression of SEMA3C was detected by IHC in five patients with HNSCC (Magnification ×200). **(F)** The expression of SEMA3C was detected by IHC in normal head and neck squamous cell tissue (Magnification ×200).

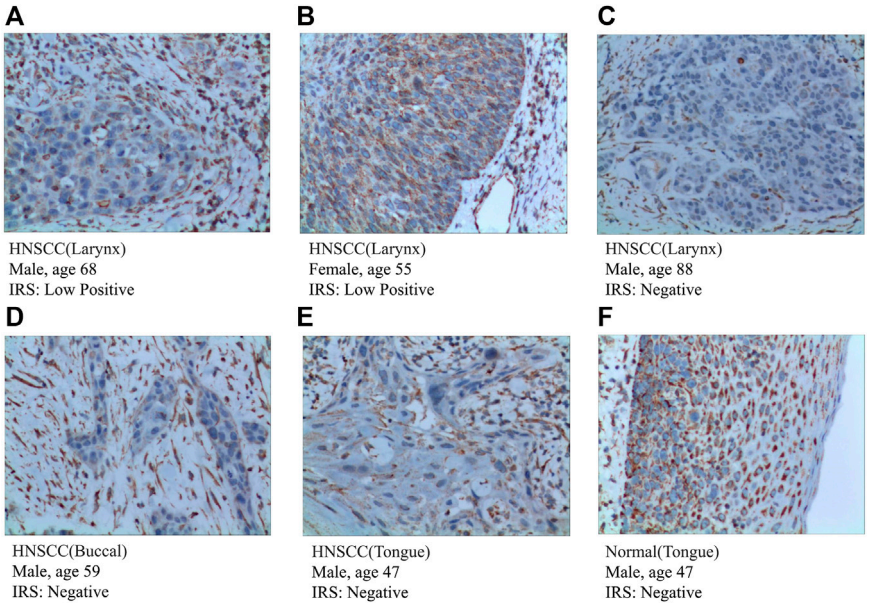

FIGURE 8 | IHC analysis of the protein expression of IGHG2 in HNSCC and normal tissues. **(A–E)** The expression of IGHG2 was detected by IHC in five patients with HNSCC (Magnification ×200). **(F)** The expression of IGHG2 was detected by IHC in normal head and neck squamous cell tissue (Magnification ×200).

AREG, THBS1, SEMA3C, and ANO1 were risk factors in the prognosis of patients. On the contrary, EPHX3 was a protective one, which is consistent with the model previously conducted (**Figure 6A**). Based on maximally selected rank statistics, patients were classified into two groups according to the level of each gene expression (**Figures 6B,D,F,H,J**), and survival analysis was performed (**Figures 6C,E,G,I,K**). Kaplan–Meier curves showing that patients with higher expression levels of four risk genes in the prognostic model had worse OS (**Figures 6C,E,G,I**), whereas the opposite was true for protective genes (**Figure 6K**).

IHC Analysis of Prognostic Signatures

To further validate the expression of prognosis-related molecules in HNSCC specimens and normal squamous epithelium of head and neck, we performed IHC staining analysis of paraffin section of HNSCC. IHC staining analysis suggested that the expression of SEMA3C and IGHG2 were slightly higher in HNSCC tissue quantified by the antibodies ab135842 (**Figures 7A–F**) and ab134050 (**Figures 8A–F**).

According to the protein expression data from the HPA, we compared the protein expression of six-gene signatures in HNSCC tissue and squamous epithelium normally located in the head and neck, such as oral squamous epithelium. We preliminarily inferred that the protein expression of these genes differed between HNSCC and normal tissues. The detailed results are presented in **Supplementary Figure S1**.

Fibrosis-Related Immune Landscape of HNSCC Patients Based on scRNA-Seq

To further understand the correlation between the fibrosis signal and immunity, we analyzed scRNA-seq data downloaded from the GEO data set "GSE139324." A total of 23 samples were used for analysis. Of these, 18 samples were tumor-infiltrating immune cells from HNSCC patients (HPV negative), and five were tissue-resident immune cells from healthy donor tonsils. After integrating data by the harmony algorithm and binning by the t-SNE algorithm, 20 cell clusters were successfully classified. Moreover, there was a significant difference in the number of each cell subset between HNSCC patients and healthy donors (HD) (**Figure 9A**). By the expression of several cell surface and intracellular markers, clusters 4 and 11 were defined as monocytes. Clusters 3, 9, 13, 14, and 20 expressed markers associated with B cells (e.g., CD79A), and the rest of the clusters expressed genes associated with T cells (e.g., CD3D) (**Figure 9B**). The cells with a high expression of FGF-receptor-signaling–related genes and highly expressed DEGs in low-survival patients were severally highlighted in **Figures 9C,D**, most of which were highly expressed in clusters 4 and 11. An obviously higher composition of monocytes is shown in patients compared with healthy controls (**Figure 9E**). Significant differences in the number of cells in clusters 4 and 11 were witnessed between HNSCC and HD (**Figures 9F,G**). The dot-plot heatmap implies that the genes mentioned are more enriched in monocytes than in other kinds of immune cells (**Figure 9H**).

DISCUSSION

Considering the poor therapeutic effect and prognosis of patients with HNSCC, it is necessary to construct an accurate prognostic staging system, which might bring personalized treatment and timely follow-up to them. In this study, a total of 483 HNSCC

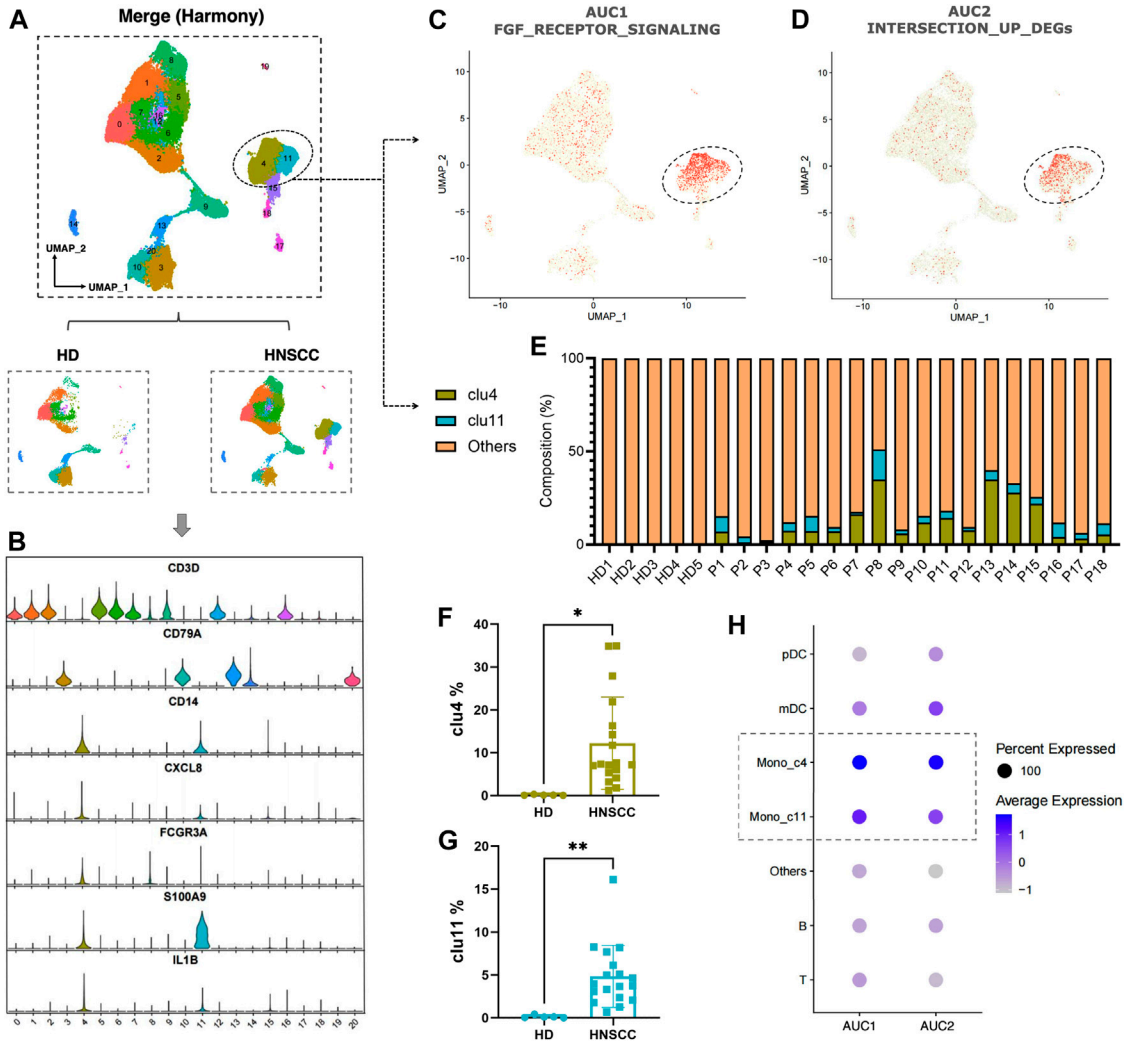

FIGURE 9 | (A) Twenty cell clusters were successfully classified by t-SNE algorithm. **(B)** Expression of several cell surface and intracellular markers in each cell subpopulation. **(C,D)** Individual cell AUC score overlay for FGF receptor signaling and highly expressed DEGs in low-survival patients (cells from n = 18 HNSCC, n = 5 HD). **(E)** Composition of clusters 4 and 11 in each sample. **(F)** Comparison of cluster 4 between HNSCC and HD. **(G)** Comparison of cluster 11 between HNSCC and HD. **(H)** Dot plot heatmap showing AUC1 and AUC2 enriched in monocyte (clusters 4 and 11).

patients from the TCGA data set were included in our discovery cohort to exploit the prognostic value of FGFR-signal, hypoxia, and glycolysis. The effect of immune status of the tumor microenvironment (TME) was also the focus of our research. We found that profibrotic signaling, hypoxia, and glycolysis were associated with the survival of patients with HNSCC. Furthermore, we constructed a new fibrosis–hypoxia–glycolysis–related prognostic classifier including a six-gene signature for HNSCC patients under the guarantee of an external independent validation cohort. IHC was used to determine the protein expression of these genes in HNSCC tissues. The single-cell analysis of monocyte infiltration also revealed marked differences between HNSCC patients and healthy controls. These findings represent a new insight into the prognosis and tumor immune microenvironment of patients with HNSCC.

Multiple studies suggest that the FGFR signal, hypoxia, and glycolysis play a critical role in the tumorigenesis and progression of HNSCC. On the one hand, it is reported that FGFR1 amplification is a frequent event (Göke et al., 2013) and might act as a candidate prognostic biomarker in primary and metastatic HNSCC (Koole et al., 2016). Rogaratinib, an inhibitor that effectively and selectively inhibits pan-FGFR, presents a broad antitumor activity in the FGFR-overexpressing preclinical HNSCC model, revealing the potentially important role of FGFR in disease development (Grünewald et al., 2019). In the mechanism of drug resistance in head and neck cancer stem cells, the FGFR signal also shows latent vitality (McDermott et al., 2018). In addition, the FGFR signal exerts high correlation with sustaining proliferative signaling, resisting cell death, inducing angiogenesis, and

activating invasion by cell migration (Ipenburg et al., 2016). However, FGFR signal–related prognostic study was still lacking in HNSCC. On the other hand, to support rapid and unlimited proliferation, solid cancer cells adopt unique energy metabolism properties, such as anaerobic glycolysis (Pavlova and Thompson, 2016) with the faster rate of ATP production and reducing the generation of reactive oxygen species (ROS) mainly produced by the electron transport chain (ETC) in the mitochondria during respiration (Yamamoto et al., 2017). This rule was also applied to HNSCC; glycolysis occurs in HNSCC cells along with a hypoxia microenvironment (Zhu et al., 2017). In the current analysis, hypoxia and glycolysis were presented as risk factors in HNSCC, which was consistent with previous studies. The FGFR signal, hypoxia, and glycolysis play a synergistic role in HNSCC prognosis. Thus, the fibrosis signal, hypoxia, and glycolysis accompanied with their interaction and its relationship with the development of HNSCC could provide improved special insight about the prognosis.

The results of single-cell analysis show that the infiltration of monocytes in the HNSCC group was higher than the HD group. Fibroblasts could communicate with the tumor cells by secreting cytokines in TME. It is reported that monocyte chemotactic protein (MCP)-1, a kind of cytokine associated with poor long-term survival of HNSCC patients (Ji et al., 2014), could be produced by fibroblasts infiltrating in TME to facilitate the recruitment of monocytes into the local inflammatory tissues and regulate their functions (Kondoh et al., 2019). This provides an explanation for the increased infiltration of monocytes in the tumor group and its close interconnection with the FGFR signal.

Significant roles of the predictive signature genes identified above are reported previously in diversified types of cancers. AREG, a ligand of epidermal growth factor receptor (EGFR), is abnormally expressed in multiple types of cancers, such as pancreatic cancer, implicated in mediating the motility, metastasis, and proliferation of tumor cells (Liu et al., 2021). It is proved that the AREG mRNA levels in cancer cells was significantly correlated with the metastatic phenotype of HNSCC tissues (Zhang et al., 2015). THBS1, known as encoding thrombospondin 1, plays a vital role in angiogenesis and tumor progression, overexpression of which was significantly associated with tumor differentiation (Yang et al., 2020). TGFB1 was reported to induce the expression of THBS1, resulting in stimulating migration of cancer cells and driving the expression of MMP3 (matrix metalloprotease 3) *via* integrin signaling, conducive to OSCC intrusion (Pal et al., 2016). Though the activation of the p-ERK pathway, SEMA3C promotes cervical cancer growth, which is related to poor prognosis (Liu et al., 2019a). ANO1 encodes a calcium-dependent chloride channel protein and commonly amplifies to facilitate several cancers' progression, including ovarian (Liu et al., 2019b), prostate (Liu et al., 2012), breast (Britschgi et al., 2013), and head and neck cancers (Filippou et al., 2021). After neoadjuvant chemoradiotherapy, the expression level of IGHG2 increased significantly in rectal cancer, indicating that IGHG2 was originally with a low expression in tumor cells and existed as a protective factor, which was consistent with our prognostic analysis. The protective gene EPHX3, known as epoxide hydrolase 3, whose hypermethylation is responsible for the development of OSCC (Morandi et al., 2017), contributes to predict the survival of HNSCC patients (Bai et al., 2019). However, six signature genes in this study were barely mentioned in the context of combination of the FGFR signal, hypoxia, and glycolysis. Thus, the abovementioned signature genes could provide therapeutic targets and directions for the elucidation of molecular mechanisms in HNSCC.

There were inevitable limitations in this study. The first limitation is that IGHG2 was not detected in the independent external cohort, so we could not validate the effect of it. More independent HNSCC cohorts should be used for the validation of the established prognostic model. Using expression profiles downloaded from publicly available databases, it is difficult for us to ensure that the validation samples including all primary tissue sites of tumors in TCGA. Thus, verification of findings above requires more well-designed, comprehensive, and thorough study.

CONCLUSION

In conclusion, the status of the FGFR signal, hypoxia, and glycolysis correlate with the prognosis of HNSCC patients. The prognostic model conducted above might provide potential application value for prognosis prediction and individualized treatment.

DATA AVAILABILITY STATEMENT

The data sets presented in this study can be found in online repositories. The names of the repository/repositories and accession number(s) can be found in the article/Supplementary Material.

ETHICS STATEMENT

The studies involving human participants were reviewed and approved by the Ethics Committee of the 3rd Xiangya Hospital (No: 21158). The patients/participants provided their written informed consent to participate in this study. Written informed consent was obtained from the individual(s) for the publication of any potentially identifiable images or data included in this article.

AUTHOR CONTRIBUTIONS

The study was conceived and designed by QZ. Statistical analyses were performed by QC and XL. Software package was prepared by LC, YZ, and QC. Manuscript was written by QC and LC. QC, LC, and XL. contributed equally to this study. All authors contributed to the article and approved the submitted version.

FUNDING

This study was supported by grants of the National Natural Science Foundation of China (81700658) and the Hunan Provincial Natural Science Foundation-Outstanding Youth Foundation (2020JJ3058).

SUPPLEMENTARY MATERIAL

The Supplementary Material for this article can be found online at: https://www.frontiersin.org/articles/10.3389/fcell.2021.801715/full#supplementary-material

REFERENCES

Bai, G., Song, J., Yuan, Y., Chen, Z., Tian, Y., Yin, X., et al. (2019). Systematic Analysis of Differentially Methylated Expressed Genes and Site-specific Methylation as Potential Prognostic Markers in Head and Neck Cancerfic Methylation as Potential Prognostic Markers in Head and Neck Cancer. *J. Cel Physiol* 234 (12), 22687–22702. doi:10.1002/jcp.28835

Britschgi, A., Bill, A., Brinkhaus, H., Rothwell, C., Clay, I., Duss, S., et al. (2013). Calcium-activated Chloride Channel ANO1 Promotes Breast Cancer Progression by Activating EGFR and CAMK Signaling. *Proc. Natl. Acad. Sci. USA* 110 (11), E1026–E1034. doi:10.1073/pnas.1217072110

Chae, Y. K., Ranganath, K., Hammerman, P. S., Vaklavas, C., Mohindra, N., Kalyan, A., et al. (2017). Inhibition of the Fibroblast Growth Factor Receptor (FGFR) Pathway: the Current Landscape and Barriers to Clinical Application. *Oncotarget* 8 (9), 16052–16074. doi:10.18632/oncotarget.14109

Chakraborty, D., Zhu, H., Jüngel, A., Summa, L., Li, Y.-N., Matei, A.-E., et al. (2020). Fibroblast Growth Factor Receptor 3 Activates a Network of Profibrotic Signaling Pathways to Promote Fibrosis in Systemic Sclerosis. *Sci. Transl. Med.* 12 (563), eaaz5506. doi:10.1126/scitranslmed.aaz5506

Charoentong, P., Finotello, F., Angelova, M., Mayer, C., Efremova, M., Rieder, D., et al. (2017). Pan-cancer Immunogenomic Analyses Reveal Genotype-Immunophenotype Relationships and Predictors of Response to Checkpoint Blockade. *Cel Rep.* 18 (1), 248–262. doi:10.1016/j.celrep.2016.12.019

Cillo, A. R., Kürten, C. H. L., Tabib, T., Qi, Z., Onkar, S., Wang, T., et al. (2020). Immune Landscape of Viral- and Carcinogen-Driven Head and Neck Cancer. *Immunity* 52 (1), 183–199. doi:10.1016/j.immuni.2019.11.014

Corridoni, D., Antanaviciute, A., Gupta, T., Fawkner-Corbett, D., Aulicino, A., Jagielowicz, M., et al. (2020). Single-cell Atlas of Colonic CD8+ T Cells in Ulcerative Colitis. *Nat. Med.* 26 (9), 1480–1490. doi:10.1038/s41591-020-1003-4

Ferlay, J., Soerjomataram, I., Dikshit, R., Eser, S., Mathers, C., Rebelo, M., et al. (2015). Cancer Incidence and Mortality Worldwide: Sources, Methods and Major Patterns in GLOBOCAN 2012. *Int. J. Cancer* 136 (5), E359–E386. doi:10.1002/ijc.29210

Filippou, A., Pehkonen, H., Karhemo, P.-R., Väänänen, J., Nieminen, A. I., Klefström, J., et al. (2021). ANO1 Expression Orchestrates p27Kip1/MCL1-Mediated Signaling in Head and Neck Squamous Cell Carcinoma. *Cancers* 13 (5), 1170. doi:10.3390/cancers13051170

Friedman, J., Hastie, T., and Tibshirani, R. (2010). Regularization Paths for Generalized Linear Models via Coordinate Descent. *J. Stat. Softw.* 33 (1), 1–22. doi:10.18637/jss.v033.i01

Göke, F., Bode, M., Franzen, A., Kirsten, R., Goltz, D., Göke, A., et al. (2013). Fibroblast Growth Factor Receptor 1 Amplification Is a Common Event in Squamous Cell Carcinoma of the Head and Neck. *Mod. Pathol.* 26 (10), 1298–1306. doi:10.1038/modpathol.2013.58

Grünewald, S., Politz, O., Bender, S., Héroult, M., Lustig, K., Thuss, U., et al. (2019). Rogaratinib: A Potent and Selective pan-FGFR Inhibitor with Broad Antitumor Activity in FGFR-overexpressing Preclinical Cancer Models. *Int. J. Cancer* 145 (5), 1346–1357. doi:10.1002/ijc.32224

Guan, K., Liu, X., Li, J., Ding, Y., Li, J., Cui, G., et al. (2020). Expression Status and Prognostic Value of M6A-Associated Genes in Gastric Cancer. *J. Cancer* 11 (10), 3027–3040. doi:10.7150/jca.40866

Ipenburg, N. A., Koole, K., Liem, K. S., van Kempen, P. M. W., Koole, R., van Diest, P. J., et al. (2016). Fibroblast Growth Factor Receptor Family Members as Prognostic Biomarkers in Head and Neck Squamous Cell Carcinoma: A Systematic Review. *Targ Oncol.* 11 (1), 17–27. doi:10.1007/s11523-015-0374-9

Ji, W.-T., Chen, H.-R., Lin, C.-H., Lee, J.-W., and Lee, C.-C. (2014). Monocyte Chemotactic Protein 1 (MCP-1) Modulates Pro-survival Signaling to Promote Progression of Head and Neck Squamous Cell Carcinoma. *PLoS One* 9 (2), e88952. doi:10.1371/journal.pone.0088952

Kim, H. A. J., Zeng, P. Y. F., Shaikh, M. H., Mundi, N., Ghasemi, F., Di Gravio, E., et al. (2021). All HPV-Negative Head and Neck Cancers Are Not the Same: Analysis of the TCGA Dataset Reveals that Anatomical Sites Have Distinct Mutation, Transcriptome, Hypoxia, and Tumor Microenvironment Profiles. *Oral Oncol.* 116, 105260. doi:10.1016/j.oraloncology.2021.105260

Kobak, D., and Berens, P. (2019). The Art of Using T-SNE for Single-Cell Transcriptomics. *Nat. Commun.* 10 (1), 5416. doi:10.1038/s41467-019-13056-x

Kondoh, N., Mizuno-Kamiya, M., Umemura, N., Takayama, E., Kawaki, H., Mitsudo, K., et al. (2019). Immunomodulatory Aspects in the Progression and Treatment of Oral Malignancy. *Jpn. Dental Sci. Rev.* 55 (1), 113–120. doi:10.1016/j.jdsr.2019.09.001

Koole, K., Brunen, D., van Kempen, P. M. W., Noorlag, R., de Bree, R., Lieftink, C., et al. (2016). FGFR1 Is a Potential Prognostic Biomarker and Therapeutic Target in Head and Neck Squamous Cell Carcinoma. *Clin. Cancer Res.* 22 (15), 3884–3893. doi:10.1158/1078-0432.Ccr-15-1874

Korsunsky, I., Millard, N., Fan, J., Slowikowski, K., Zhang, F., Wei, K., et al. (2019). Fast, Sensitive and Accurate Integration of Single-Cell Data with Harmony. *Nat. Methods* 16 (12), 1289–1296. doi:10.1038/s41592-019-0619-0

Liu, B., Fu, T., He, P., Du, C., and Xu, K. (2021). Construction of a Five-Gene Prognostic Model Based on Immune-Related Genes for the Prediction of Survival in Pancreatic Cancer. *Biosci. Rep.* 41 (7), BSR20204301. doi:10.1042/bsr20204301

Liu, R., Shuai, Y., Luo, J., and Zhang, Z. (2019a). SEMA3C Promotes Cervical Cancer Growth and Is Associated with Poor Prognosis. *Front. Oncol.* 9, 1035. doi:10.3389/fonc.2019.01035

Liu, W., Lu, M., Liu, B., Huang, Y., and Wang, K. (2012). Inhibition of Ca2+-Activated Cl− Channel ANO1/TMEM16A Expression Suppresses Tumor Growth and Invasiveness in Human Prostate Carcinoma. *Cancer Lett.* 326 (1), 41–51. doi:10.1016/j.canlet.2012.07.015

Liu, X.-Y., Liang, Y., Xu, Z.-B., Zhang, H., and Leung, K.-S. (2013). AdaptiveL1/2Shooting Regularization Method for Survival Analysis Using Gene Expression Data. *Scientific World J.* 2013, 1–5. doi:10.1155/2013/475702

Liu, Z., Zhang, S., Hou, F., Zhang, C., Gao, J., and Wang, K. (2019b). Inhibition of Ca2+-Activated Chloride Channel ANO1 Suppresses Ovarian Cancer through Inactivating PI3K/Akt Signaling. *Int. J. Cancer* 144 (9), 2215–2226. doi:10.1002/ijc.31887

McDermott, S. C., Rodriguez-Ramirez, C., McDermott, S. P., Wicha, M. S., and Nör, J. E. (2018). FGFR Signaling Regulates Resistance of Head and Neck Cancer Stem Cells to Cisplatin. *Oncotarget* 9 (38), 25148–25165. doi:10.18632/oncotarget.25358

Morandi, L., Gissi, D., Tarsitano, A., Asioli, S., Gabusi, A., Marchetti, C., et al. (2017). CpG Location and Methylation Level Are Crucial Factors for the Early Detection of Oral Squamous Cell Carcinoma in Brushing Samples Using Bisulfite Sequencing of a 13-gene Panel. *Clin. Epigenet* 9, 85. doi:10.1186/s13148-017-0386-7

Pal, S. K., Nguyen, C. T. K., Morita, K.-i., Miki, Y., Kayamori, K., Yamaguchi, A., et al. (2016). THBS1 Is Induced by TGFB1 in the Cancer Stroma and Promotes Invasion of Oral Squamous Cell Carcinoma. *J. Oral Pathol. Med.* 45 (10), 730–739. doi:10.1111/jop.12430

Pavlova, N. N., and Thompson, C. B. (2016). The Emerging Hallmarks of Cancer Metabolism. *Cel Metab.* 23 (1), 27–47. doi:10.1016/j.cmet.2015.12.006

Rankin, E. B., and Giaccia, A. J. (2016). Hypoxic Control of Metastasis. *Science* 352 (6282), 175–180. doi:10.1126/science.aaf4405

Schuler, M., Cho, B. C., Sayehli, C. M., Navarro, A., Soo, R. A., Richly, H., et al. (2019). Rogaratinib in Patients with Advanced Cancers Selected by FGFR mRNA Expression: a Phase 1 Dose-Escalation and Dose-Expansion Study. *Lancet Oncol.* 20 (10), 1454–1466. doi:10.1016/s1470-2045(19)30412-7

Seitz, T., and Hellerbrand, C. (2021). Role of Fibroblast Growth Factor Signalling in Hepatic Fibrosis. *Liver Int.* 41 (6), 1201–1215. doi:10.1111/liv.14863

Shield, K. D., Ferlay, J., Jemal, A., Sankaranarayanan, R., Chaturvedi, A. K., Bray, F., et al. (2017). The Global Incidence of Lip, Oral Cavity, and Pharyngeal Cancers by Subsite in 2012. *CA: A Cancer J. Clinicians* 67 (1), 51–64. doi:10.3322/caac.21384

Siegel, R. L., Miller, K. D., and Jemal, A. (2019). Cancer Statistics, 2019. *CA A. Cancer J. Clin.* 69 (1), 7–34. doi:10.3322/caac.21551

Uhlen, M., Oksvold, P., Fagerberg, L., Lundberg, E., Jonasson, K., Forsberg, M., et al. (2010). Towards a Knowledge-Based Human Protein Atlas. *Nat. Biotechnol.* 28 (12), 1248–1250. doi:10.1038/nbt1210-1248

Varghese, F., Bukhari, A. B., Malhotra, R., and De, A. (2014). IHC Profiler: an Open Source Plugin for the Quantitative Evaluation and Automated Scoring of Immunohistochemistry Images of Human Tissue Samples. *PLoS One* 9 (5), e96801. doi:10.1371/journal.pone.0096801

Wollin, L., Wex, E., Pautsch, A., Schnapp, G., Hostettler, K. E., Stowasser, S., et al. (2015). Mode of Action of Nintedanib in the Treatment of Idiopathic Pulmonary Fibrosis. *Eur. Respir. J.* 45 (5), 1434–1445. doi:10.1183/09031936.00174914

Yamamoto, M., Inohara, H., and Nakagawa, T. (2017). Targeting Metabolic Pathways for Head and Neck Cancers Therapeutics. *Cancer Metastasis Rev.* 36 (3), 503–514. doi:10.1007/s10555-017-9691-z

Yang, X., Chen, L., Mao, Y., Hu, Z., and He, M. (2020). Progressive and Prognostic Performance of an Extracellular Matrix-Receptor Interaction Signature in Gastric Cancer. *Dis. Markers* 2020, 1–23. doi:10.1155/2020/8816070

Zhang, J., Wang, Y., Chen, X., Zhou, Y., Jiang, F., Chen, J., et al. (2015). MiR-34a Suppresses Amphiregulin and Tumor Metastatic Potential of Head and Neck Squamous Cell Carcinoma (HNSCC). *Oncotarget* 6 (10), 7454–7469. doi:10.18632/oncotarget.3148

Zhou, Y., Zhou, B., Pache, L., Chang, M., Khodabakhshi, A. H., Tanaseichuk, O., et al. (2019). Metascape Provides a Biologist-Oriented Resource for the Analysis of Systems-Level Datasets. *Nat. Commun.* 10 (1), 1523. doi:10.1038/s41467-019-09234-6

Zhu, G., Peng, F., Gong, W., She, L., Wei, M., Tan, H., et al. (2017). Hypoxia Promotes Migration/invasion and Glycolysis in Head and Neck Squamous Cell Carcinoma via an HIF-1α-MTDH Loop. *Oncol. Rep.* 38 (5), 2893–2900. doi:10.3892/or.2017.5949

Conflict of Interest: The authors declare that the research was conducted in the absence of any commercial or financial relationships that could be construed as a potential conflict of interest.

Publisher's Note: All claims expressed in this article are solely those of the authors and do not necessarily represent those of their affiliated organizations, or those of the publisher, the editors and the reviewers. Any product that may be evaluated in this article, orclaim that may be made by its manufacturer, is not guaranteed or endorsed by the publisher.

frontiers in Oncology

ORIGINAL RESEARCH
published: 11 March 2022
doi: 10.3389/fonc.2022.826830

Development and Validation of a Novel Prognostic Nomogram Combined With Desmoplastic Reaction for Synchronous Colorectal Peritoneal Metastasis

Xiusen Qin[1,2†], Mingpeng Zhao[3†], Weihao Deng[4†], Yan Huang[4], Zhiqiang Cheng[4], Jacqueline Pui Wah Chung[3], Xufei Chen[5], Keli Yang[1,2], David Yiu Leung Chan[3*] and Hui Wang[1,2*]*

[1] Department of Colorectal Surgery, The Sixth Affiliated Hospital of Sun Yat-sen University, Guangzhou, China, [2] Guangdong Institute of Gastroenterology, Guangdong Provincial Key Laboratory of Colorectal and Pelvic Floor Diseases, Supported by the National Key Clinical Discipline, The Sixth Affiliated Hospital of Sun Yat-sen University, Guangzhou, China, [3] Assisted Reproductive Technology Unit, Department of Obstetrics and Gynaecology, Faculty of Medicine, Chinese University of Hong Kong, Hong Kong, Hong Kong SAR, China, [4] Department of Pathology, The Sixth Affiliated Hospital of Sun Yat-sen University, Guangzhou, China, [5] Department of Obstetrics and Gynaecology, Songshan Lake Central Hospital, Affiliated Dongguan Shilong People's Hospital of Southern Medical University, Dongguan, China

Purpose: The prognostic value of desmoplastic reaction (DR) has not been investigated in colorectal cancer (CRC) patients with synchronous peritoneal metastasis (SPM). The present study aimed to identify whether DR can predict overall survival (OS) and develop a novel prognostic nomogram.

Methods: CRC patients with SPM were enrolled from a single center between July 2007 and July 2019. DR patterns in primary tumors were classified as mature, intermediate, or immature according to the existence and absence of keloid-like collagen or myxoid stroma. Cox regression analysis was used to identify independent factors associated with OS and a nomogram was developed subsequently.

Results: One hundred ninety-eight and 99 patients were randomly allocated into the training and validation groups. The median OS in the training group was 36, 25, and 12 months in mature, intermediate, and immature DR categories, respectively. Age, T stage, extraperitoneal metastasis, differentiation, cytoreductive surgery (CRS), hyperthermic intraperitoneal chemotherapy (HIPEC), and DR categorization were independent variables for OS, based on which the nomogram was developed. The C-index of the nomogram in the training and validation groups was 0.773 (95% CI 0.734–0.812) and 0.767 (95% CI 0.708–0.826). The calibration plots showed satisfactory agreement

OPEN ACCESS

Edited by:
Eric W.-F. Lam, Sun Yat-sen University Cancer Center (SYSUCC), China

Reviewed by:
Dario Baratti, Fondazione IRCCS Istituto Nazionale Tumori, Italy
Yanwu Sun, Fujian Medical University Union Hospital, China

***Correspondence:**
Keli Yang
yangkl3@mail2.sysu.edu.cn
David Yiu Leung Chan
drdcyl16@cuhk.edu.hk
Hui Wang
wang89@mail.sysu.edu.cn

†These authors have contributed equally to this work

Specialty section:
This article was submitted to Molecular and Cellular Oncology, a section of the journal Frontiers in Oncology

Received: *01 December 2021*
Accepted: *15 February 2022*
Published: *11 March 2022*

Citation:
Qin X, Zhao M, Deng W, Huang Y, Cheng Z, Chung JPW, Chen X, Yang K, Chan DYL and Wang H (2022) Development and Validation of a Novel Prognostic Nomogram Combined With Desmoplastic Reaction for Synchronous Colorectal Peritoneal Metastasis. Front. Oncol. 12:826830. doi: 10.3389/fonc.2022.826830

between the actual outcome and nomogram-predicted OS probabilities in the training and validation cohorts.

Conclusions: DR classification in the primary tumor is a potential prognostic index for CRC patients with SPM. The novel prognostic nomogram combined with DR classification has good discrimination and accuracy in predicting the OS for CRC patients with SPM.

Keywords: colorectal cancer, synchronous peritoneal metastasis, prognosis, desmoplastic reaction, cancer-associated fibroblasts

INTRODUCTION

Peritoneal metastasis (PM) occurs in 5%–10% of newly diagnosed colorectal cancer (CRC) patients, which is defined as synchronous peritoneal metastasis (SPM) (1, 2). PM often has a poorer prognosis than liver or lung metastasis in CRC patients (3, 4). Patients with colorectal PM are classified into the M1c group in the eighth edition of the American Joint Committee on Cancer tumor–node–metastasis classification (5), representing a heterogeneous population of oncological prognosis.

With the increasing understanding of colorectal PM over the past decades, the treatment has changed from palliative chemotherapy to selective cytoreductive surgery (CRS) plus hyperthermic intraperitoneal chemotherapy (HIPEC) (6, 7). CRS can remove macroscopic tumors, and HIPEC can remove residual cancer cells and microscopic lesions, which significantly prolong the survival of patients (8, 9). However, studies reported considerable variations in the overall survival (OS) for CRC patients with PM due to unknown tumor heterogeneity and lack of unified treatments. Therefore, it is crucial to understand the mechanism of SPM further and predict patients' survival accurately for better clinical decision-making.

Recent studies on basic tumor biology have shown that the tumor microenvironment (TME) plays a vital role in remodeling metastatic capacity and determining tumor prognosis (10–12). Cancer-associated fibroblasts (CAFs) are the major cellular components of the TME and have recently been regarded as critical factors to modulate the TME (13, 14). Fibroblasts and myofibroblasts are representative CAFs in fibrotic tumor stroma and are associated with tumor progression (14, 15). Their histological entities at the front of the tumor are called desmoplastic reaction (DR), which was first described in advanced rectal cancer at St. Mark's Hospital in the UK (16). DR category is divided into three types, namely, mature, intermediate, and immature, and the prognosis deteriorates accordingly (17, 18). Studies have revealed that DR classification is associated with the prognosis of T2 CRC (19), stage II and stage III CRC (20–23), and resectable and unresectable stage IV CRC (24). In comparison, relatively few studies involved stage IV CRC. Ueno et al. found that DR classification was associated with the prognosis of resectable colorectal liver metastasis in 2014 (25). Furthermore, Ao et al. demonstrated that the DR patterns of liver and lymphatic metastases were morphologically consistent between primary and metastatic lesions in 2019 (26). In addition, Ubink et al. reported that molecular and histopathological classification of most primary tumors is consistent with corresponding metastasic tumors in colorectal cancer (27). Therefore, for CRC patients with SPM, the DR category of the primary tumor may be consistent with corresponding metastatic tumors.

However, the TME of colorectal SPM is poorly understood. DR is an embodiment of TME, whose role in SPM has not been revealed. Based on current advances, we postulate that the DR category in the primary tumor of CRC patients with SPM is associated with aggressive tumor behavior and may be a potential prognostic factor.

Therefore, this study aimed to evaluate the value of the DR category in predicting the overall survival of colorectal cancer patients with SPM who underwent CRS and to develop and validate an innovative prognostic nomogram using DR classification combined with traditional clinico-pathological parameters.

MATERIALS AND METHOD

Patients and Study Criteria

A total of 297 CRC patients with SPM were enrolled from the Sixth Affiliated Hospital of Sun Yat-sen University between July 2007 and July 2019. These patients were randomly divided into the training cohort (198 patients) and the validation cohort (99 patients) by the R software.

The inclusion criteria were patients who underwent CRS with histologically diagnosed SPM and patients with available clinicopathological data. The exclusion criteria were patients with other primary tumors.

A retrospective analysis of medical records, including surgical, pathological, and follow-up information, was conducted by the authors. Baseline clinicopathological data included sex, age at diagnosis, tumor location, tumor differentiation, tumor histology, lymph node metastasis, depth of invasion, CRS, and HIPEC. In addition, two pathologists (WD and YH) independently identified the DR classification of the primary tumor without knowing the patient's clinical outcomes.

Histology Categorization of DR

Hematoxylin and eosin (H&E)-stained glass slides of the primary tumor with a single longitudinal section and deepest part were obtained from the pathology department. DR was evaluated according to previous reports and histologically categorized into three categories (immature, intermediate, or mature) based on whether keloid-like collagen or myxoid stroma at the

extramural of the desmoplastic front existed (16). Keloid-like collagen is characterized by bundles of hypocellular collagen with bright eosinophilic hyalinization. Myxoid stroma is an amorphous material composed of an amphoteric or slightly basophilic extracellular matrix, usually intermixed with randomly oriented keloid-like collagen (16, 17).

More specifically, mature DR was defined as fibrotic stroma stratified into multiple layers by fine collagen fibers without keloid-like collagen or myxoid stroma. Keloid-like collagen intermingled in the mature stroma was regarded as intermediate DR. Fibrotic stroma with myxoid stroma was designated as immature DR (**Figure 1**).

Treatment Approaches

CRS involved removal of the primary tumor, removal of the invading organs, lymph node dissection, and/or peritonectomy, usually performed after evaluation by the multidisciplinary team (MDT). Residual lesions were evaluated by the completeness of cytoreduction score (CC score): CC0, no macroscopic peritoneal tumor remained following cytoreduction; CC1, presence of tumor nodules <2.5 mm; CC2, presence of residual disease measuring 2.5 to 2.5 cm; and CC3, presence of tumor nodules >2.5 cm, or a confluence of unresectable tumor nodules at any site within the abdomen or pelvis (28). HIPEC was performed with the closed abdomen technique. Briefly, four tubes (two for inflow of chemotherapeutic drugs and saline and two for outflow) were placed in the abdominal cavity at the end of the procedure. There were several drugs (including 5-FU, oxaliplatin, or loplatin) for HIPEC. The duration was usually at least 1 h and the fluid temperature in the abdominal cavity was kept at 42°C by a thermal perfusion device. All patients received at least two HIPEC treatments within 24 to 72 h postoperatively. Systematic chemotherapy and targeted therapy were carried out under the guidance of oncologists. Sixteen (5.4%) patients received preoperative chemotherapy and 182 (61.3%) patients received postoperative chemotherapy (adjuvant or palliative chemotherapy). For some patients, targeted therapy was added based on the results of the genetic tests. The chemotherapy regimens were mainly 5-fluorouracil-based chemotherapy, including FOLFOX, FOLFIRI, XELOX, etc. Targeted agents contained cetuximab or bevacizumab. At least three courses of continuous chemotherapy were performed for patients with chemotherapy.

Follow-Up and Outcome

The last date of follow-up was conducted until June 20, 2021. The primary endpoint was OS, defined as the date of initial treatment (chemotherapy or surgical intervention) to the date of death or last follow-up in censored patients. Follow-up information was obtained from the hospital's follow-up office.

Development of the Nomogram

In the training cohort, the Kaplan–Meier method was used to generate survival curves of different variables, and the log-rank test was conducted to identify variables with *P*-values less than 0.05. Cox univariate proportional hazard regression was further used to verify the above variables. These variables with $P < 0.05$ were included in Cox multivariate regression to identify independent prognostic factors. Based on the results of multivariate analysis, a nomogram was established using the R software.

Validation of the Nomogram

Firstly, the nomogram was subjected to 1,000 bootstrap resamples for internal validation with the training cohort and for external validation with the validation cohort. The coherence of the nomogram for predicting OS between predicted and actual outcomes was evaluated by C-index. The C-index is between 0.5 and 1, with 0.5 being completely random and 1 being perfectly predictive. Furthermore, calibration plots were constructed by comparing the predicted and actual survival of 1, 2, and 3 years. Finally, the relative operating characteristic (ROC) curve was used to further verify the prediction performance in both cohorts.

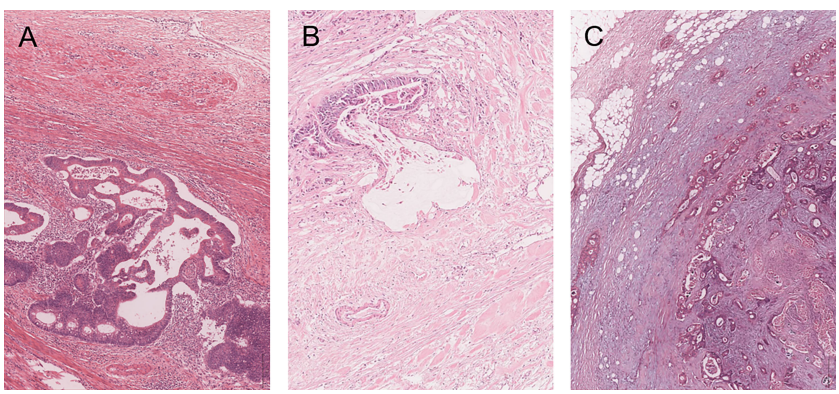

FIGURE 1 | Categorization of desmoplastic reaction (DR) in the primary tumor of colorectal cancer patients with SPM. Mature DR has neither keloid-like collagen nor myxoid stroma in the fibrotic stroma and elongated collagen fibers stratified into multiple layers by fine collagen fibers **(A)**. Intermediate DR has keloid-like collagen, which is characterized by bundles of hypocellular collagen with bright eosinophilic hyalinization **(B)**. Immature DR has an amphoteric or slightly basophilic extracellular matrix that forms myxoid stroma **(C)**.

Statistical Analysis

In this study, the continuous variable age was converted to a categorical variable. The chi-square test and Fisher's exact test were used to compare differences between categorical variables. The Kaplan–Meier curve and log-rank test were used to estimate differences in overall survival. Cox proportional hazard regression analysis was conducted to compute HR and 95% confidence intervals and to identify prognostic variables. R software (Version 4.0.3) and SPSS software (version 25.0 for Windows; Chicago, IL, USA) were used for statistical analysis. R packages of "rms," "survival," "foreign," and "survivalROC" were used to construct the prognostic nomogram, calculate the C-index, and plot calibration curves and ROC curves. Decision-curve analysis (DCA) was performed with the package of "ggDCA" to evaluate the clinical practicality of the prognostic nomogram by quantifying the net benefit. A two-sided P <0.05 was considered to be statistically significant.

RESULTS

Patients Characteristics and Overall Survival

There were no statistically significant differences in the baseline clinicopathological characteristics of the training and validation cohorts (**Table 1**). Among the 198 patients in the training cohort, 75.3% were younger than 65 years, with 122 (61.6%) men. Of the 99 patients in the validation cohort, 77.8% were younger than 65 years, with 57 (57.6%) men. The median follow-up duration (interquartile range, IQR) for all patients was 46 (29–64) months, and the median OS (IQR) for the whole cohort was 20 (10–63) months. In the training cohort, the median OS (IQR) was 22 (10–49) months and 130 patients died, and the 1-, 2-, and 3-year OS rates were 67.4%, 46.2%, and 33.7%, respectively. In the validation cohort, the median OS (IQR) was 18 (9–63) months and 68 patients died, and the 1-, 2-, and 3-year OS rates were 87.9%, 39.9%, and 30.5%, respectively.

TABLE 1 | Characteristics of the patients in the training and validation cohorts.

Variable	Training cohort (n = 198)	Validation cohort (n = 99)	P-value
Sex			0.502
Male	122 (61.6)	57 (57.6)	
Female	76 (38.4)	42 (42.4)	
Age (years)			0.631
≤65	149 (75.3)	77 (77.8)	
>65	49 (24.7)	22 (22.2)	
Tumor location			0.756
Right side	93 (47.0)	43 (43.4)	
Left side	75 (37.9)	38 (38.4)	
Rectum	30 (15.2)	18 (18.2)	
T stage			0.869
T1–3	88 (44.4)	45 (45.5)	
T4	110 (55.6)	54 (54.5)	
Lymph node metastasis			0.492
No	28 (14.1)	17 (17.2)	
Yes	170 (85.9)	82 (82.8)	
Extraperitoneal metastasis			0.930
No	133 (67.2)	67 (67.7)	
Yes	65 (32.8)	32 (32.3)	
Histology			0.210
Adenocarcinoma	134 (67.7)	74 (74.7)	
Mucinous adenocarcinoma and signet ring cell carcinoma	64 (32.3)	25 (25.3)	
Differentiation status			0.505
Poor and undifferentiated	84 (42.4)	38 (38.4)	
Moderate and well	114 (57.6)	61 (61.6)	
CRS			0.108
CC0–1	69 (34.8)	44 (44.4)	
CC2–3	129 (65.2)	55 (55.6)	
HIPEC			0.609
No	124 (62.6)	65 (65.7)	
Yes	74 (37.4)	34 (34.3)	
Desmoplastic reaction			0.498
Mature	72 (36.4)	37 (37.4)	
Intermediate	70 (35.4)	40 (40.4)	
Immature	56 (28.3)	22 (22.2)	

Prognostic Impact of DR Category

In the training cohort, the DR category was classified as mature, intermediate, or immature for 72, 70, and 56 primary tumors, respectively. The Kaplan–Meier curves showed OS in the three groups (**Figure 2**). Patients with immature stroma had a worse prognosis (median OS = 36 months in mature DR, 25 months in intermediate DR, and 12 months in immature DR; $P < 0.001$, log-rank test). Similar analyses were conducted in the validation cohort. DR category was classified as mature, intermediate, or immature for 37, 40, and 22 primary tumors, respectively, in the validation cohort. The median OS was 31, 15, and 11 months, respectively ($P = 0.002$, log-rank test).

Univariate and Multivariate Analyses in the Training Cohort

In the univariate analysis, eight variables (age > 65 years at diagnosis, T4 stage, extraperitoneal metastasis, histology of mucinous adenocarcinoma and signet ring cell carcinoma, poor differentiation, CRS, HIPEC, and DR category) were significantly associated with OS (**Table 2**). However, histology was not an independent prognostic factor when these factors above were incorporated into the multivariate analysis (**Table 2**).

Construction and Validation of the Nomogram

Based on the results of multivariate analysis, seven variables (age > 65 years at diagnosis, T4 stage, extraperitoneal metastasis, poor differentiation, CRS, HIPEC, and DR category) were used to construct the nomogram. This model can be used to predict the 1-, 2-, and 3-year postoperative survival probability of SPM patients treated with CRS (**Figure 3**).

Next, C-indices were calculated for the nomogram in predicting the 1-, 2-, and 3-year OS of patients. C-indices were 0.773 (95% CI 0.734–0.812) and 0.767 (95% CI 0.708–0.826) in the training and validation cohorts, respectively. These results indicated that the model has excellent predictive ability. Furthermore, calibration plots at 1, 2, or 3 years showed good

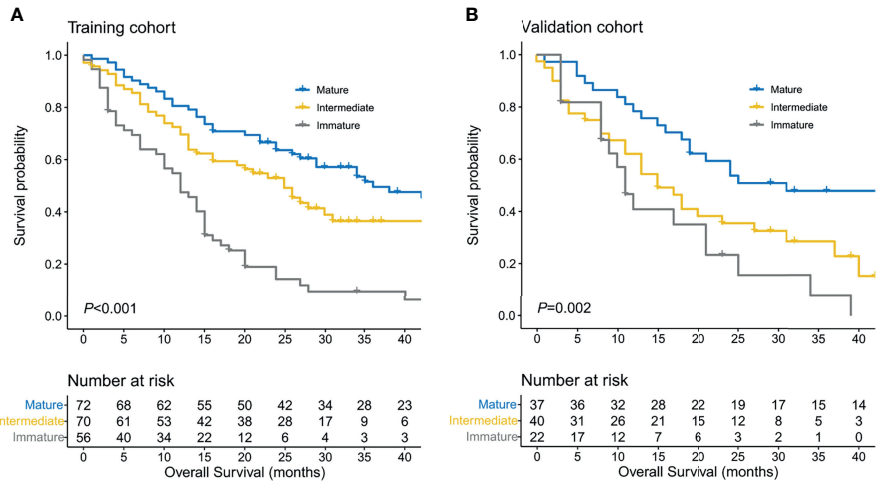

FIGURE 2 | Survival estimates of the training cohort **(A)** and validation cohort **(B)** using the Kaplan–Meier method based on desmoplastic reaction (DR) categorization in the primary tumor.

TABLE 2 | Univariate and multivariate analyses for overall survival (OS) by the Cox proportional hazards regression model in the training cohort.

Variable	Univariate analysis		Multivariate analysis	
	HR (95% CI)	*P*-value	HR (95% CI)	*P*-value
Sex		0.856		
Male	Reference			
Female	1.033 (0.725–1.473)			
Age (years)		0.003		
≤65	Reference		Reference	<0.001
>65	1.780 (1.217–2.603)		2.844 (1.894–4.270)	
Tumor location		0.221		
Right side	Reference			
Left side	0.719 (0.492–1.050)			
Rectum	0.807 (0.484–1.344)			
T stage		0.005		
T1–3	Reference		Reference	0.022
T4	1.664 (1.165–2.379)		1.549 (1.067–2.249)	
Lymph node metastasis		0.311		
No	Reference			
Yes	1.302 (0.781–2.172)			
Extraperitoneal metastasis		0.015		
No	Reference		Reference	0.002
Yes	1.559 (1.092–2.227)		1.855 (1.252–2.750)	
Histology		0.004		
Adenocarcinoma	Reference		Reference	0.122
Mucinous adenocarcinoma and signet ring cell carcinoma	1.678 (1.176–2.395)		1.612 (0.880–2.955)	
Differentiation status		0.002		
Poor and undifferentiated	Reference		Reference	0.001
Moderate and well	0.579 (0.409–0.818)		0.340 (0.180–0.643)	
CRS		<0.001		<0.001
CC0–1	Reference		Reference	
CC2–3	3.162 (2.096–4.769)		3.430 (2.234–5.267)	
HIPEC		0.022		0.015
No	Reference		Reference	
Yes	0.649 (0.448–0.840)		0.614 (0.414–0.910)	
Desmoplastic reaction		<0.001		
Mature	Reference		Reference	<0.001
Intermediate	1.380 (0.889–2.143)		1.671 (1.057–2.641)	
Immature	3.288 (2.140–5.052)		3.673 (2.317–5.822)	

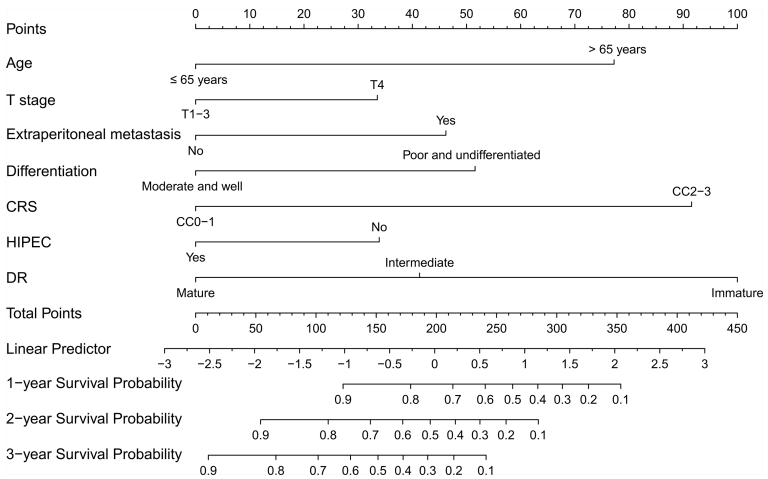

FIGURE 3 | Nomogram for predicting the overall survival of colorectal cancer patients with SPM. The C-index of the nomogram is 0.773 (95% CI 0.734–0.812).

consistency between predicted survival and actual survival, either in the training cohort or the validation cohort. Similar results were further verified by the ROC curve (**Figure 4**). Besides, DCA showed better net clinical benefit of the nomogram than the model without DR classification (**Figure S1**).

DISCUSSION

To our knowledge, the present study is the first to reveal that fibrotic characteristics in the front of the primary tumor, known as DR classification, played an important role in predicting the

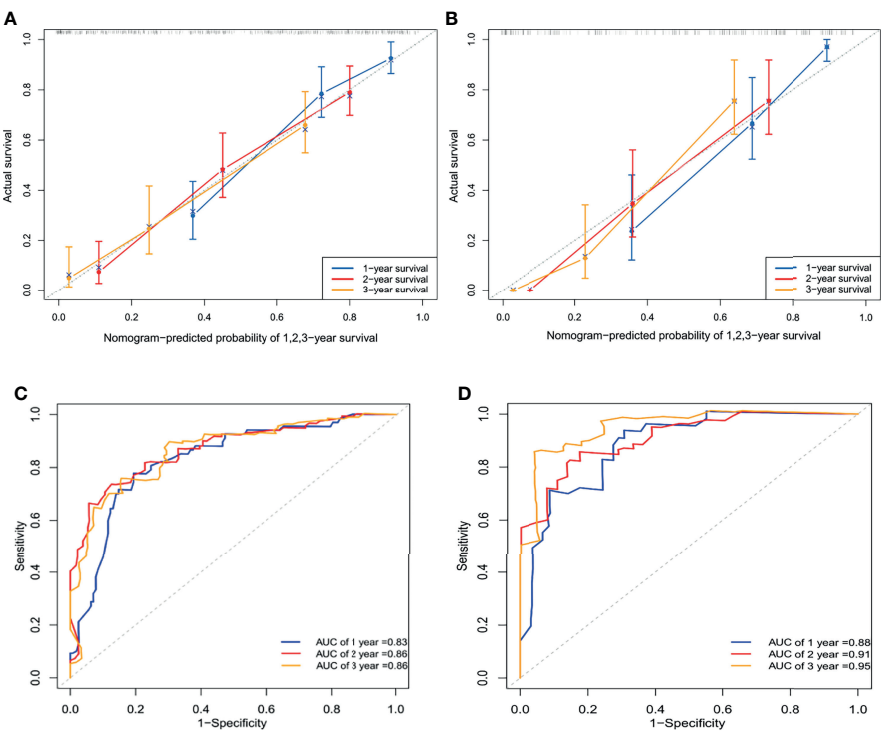

FIGURE 4 | Calibration curve to validate the nomogram for 1-, 2-, and 3-year overall survival with the training cohort and its C-index was 0.773 (95% CI 0.734–0.812) **(A)**. Calibration curve to validate the nomogram for 1-, 2-, and 3-year overall survival with the validation cohort and its C-index was 0.767 (95% CI 0.708–0.826) **(B)**. ROC curve of 1-, 2-, and 3-year survival prediction in the training cohort **(C)**. ROC curve of 1-, 2-, and 3-year survival prediction in the validation cohort **(D)**. AUC, the area under the curve.

OS of CRC patients with SPM. Firstly, the Kaplan–Meier method was used to analyze the prognosis of SPM patients with different DR classifications. Cox multivariate analysis revealed that DR classification could be an independent prognostic factor. Secondly we constructed and validated a prognostic nomogram to demonstrate that DR classification of the primary tumor can be a robust prognostic factor independent of traditional tumor factors in predicting overall survival.

In recent years, studies on tumor biology have shown that genes associated with poor prognosis are expressed in tumor stromal cells rather than cancer cells (29, 30). The potential for tumor growth and metastasis may depend on how tumor cells benefit by reshaping the stroma through different molecular mechanisms. Keloid-like collagen and myxoid stroma are distinct fibrotic stroma features formed by activated CAFs, although these features can also be seen in non-malignant diseases (31, 32), such as inflammatory responses to infection and benign tumors. However, the present study found that these features are mainly located in the front of the primary tumor of colorectal cancer. Our results suggested that these features were location-specific prognostic markers.

Although the mechanism of DR formation in different morphologies cannot be elucidated, it may be related to the following mechanisms. TGF-β family signaling is a possible mechanism. Keloid-like collagen bundles can be seen not only in intermediate DR but also in immature DR and are the main histological feature of scar and keloid. Compared with normal fibroblasts, fibroblasts in keloid upregulate the expression of several growth factors, including TGF-β (33). Elevated TGF-β levels have been reported to be associated with CRC recurrence (34), and non-mature DR types are associated with unfavorable survival outcomes (17). Moreover, epithelial–mesenchymal transition (EMT) is more common in malignant tumors, which is related to tumor invasion and progression (35). TGF-β can induce the activation of EMT (36). In addition, immature DR is characterized by excessive extracellular matrix deposition, including fibronectin, which affects pro-tumor functions and is associated with EMT activation (21). Therefore, it is speculated that the TGF-β signaling pathway activates EMT as a possible mechanism for non-mature DR formation.

Histological features of unfavorable DR classifications also include reduced immune cell infiltration (20, 21) and reduced microvascular formation (21). Ozdemir et al. observed that myofibroblast depletion in pancreatic cancer led to immunosuppression and increased tumor aggressiveness in transgenic mice using deleted αSMA+ myofibroblasts (37). Therefore, it can be speculated that CAFs are involved in tumor stroma remodeling and immunosuppression. On the other hand, mature DR is characterized by thin, multilayered, mature collagen and neatly arranged fibroblasts, which can encapsulate the tumor nests and inhibit metastasis. These results suggest that different CAF subgroups may be involved in forming different DR types, and future studies need to confirm this conjecture further.

DR classification as a prognostic factor has been validated not only in different stages of colorectal cancer but also in pancreatic ductal carcinoma (38), cervical squamous cell carcinoma (39), intrahepatic cholangiocarcinoma (40), and esophageal squamous cell carcinoma (41). In particular, a recent retrospective phase III clinical trial concluded that DR might be a valuable prognostic indicator to identify patients who will benefit from postoperative chemotherapy in stage II colorectal cancer (22). This result further confirms the prognostic value of DR. The prospective phase III clinical trial (JCOG1805) launched in 2020 in Japan is expected to further clarify the role of DR in stage II CRC patients at high risk of developing recurrence according to T stage and three selected pathological factors. In a word, we found that DR classifications could be used to predict postoperative OS of CRC patients with SPM, which is in accordance with expectation. Of course, further multicenter, prospective validation is needed.

This study has some strengths. Firstly, this is the first study to reveal that DR category is associated with OS of CRC patients with SPM. It may guide clinical decision-making and provide a new perspective for further understanding the mechanism of the occurrence and progression of colorectal PM. Secondly, the nomogram in this study may be superior to the peritoneal surface disease severity score (PSDSS) and the colorectal peritoneal metastases prognostic surgical score (COMPASS) in terms of prediction of OS for patients with colorectal peritoneal metastasis, which did not include the factor of tumor stroma (42, 43). Geert et al. performed an external validation of the PSDSS, showing a Harrell's C statistic of 0.62, and further developed the COMPASS with a Harrell's C statistic of 0.72, while the nomogram in the present study showed C-indices of 0.773 (95% CI 0.734-0.812) in the training group and 0.767 (95% CI 0.708–0.826) in the validation group. Thirdly, in terms of the clinical significance of the nomogram model, it may help select patients who could benefit from CRS and HIPEC preoperatively by endoscopic biopsy and provide a reference for clinical decision-making. For example, aggressive CRS may not be necessary for patients who are not expected to achieve complete CRS and with adverse DR classification. Modern palliative chemotherapy may be a better selection for these patients.

This study also has some limitations. First of all, this is a retrospective study, and the single-center data used in this study may have some bias. However, it is the largest cohort reported to determine the prognostic value of DR classification in CRC patients with SPM. Although we conducted a validation with data of random allocation, prospective, multicenter studies are needed for further validation. Secondly, some of the SPM patients enrolled in this study failed to achieve complete CRS. Limited by sample size, the effect of DR classification on relapse-free survival in CRC patients with SPM cannot be further clarified. Thirdly, due to no CRC cases with metachronous peritoneal metastasis being included in this study, we apologize for not presenting the prognostic value of desmoplastic reaction in patients with metachronous peritoneal metastasis. Future studies to validate the prognostic value of desmoplastic reaction in patients with metachronous peritoneal metastasis are expected. Finally, the current classification of DR relies on the artificial classification of pathologists. If collagen features can be extracted and quantified, the prognosis may be better predicted.

CONCLUSIONS

In conclusion, we developed and validated an innovative nomogram to predict the OS of CRC patients with SPM based on fibrotic stroma classification in the primary tumor. This model can provide a vital prognosis-predicting tool for these patients.

DATA AVAILABILITY STATEMENT

The raw data supporting the conclusions of this article will be made available by the authors, without undue reservation.

ETHICS STATEMENT

The studies involving human participants were reviewed and approved by the Institutional Review Board of The Sixth Affiliated Hospital of Sun Yat-sen University (No. 2020ZSLYEC–109). The ethics committee waived the requirement of written informed consent for participation.

AUTHOR CONTRIBUTIONS

XQ, KY, DC, and HW contributed to the conception and design of the study. XQ, MZ, WD, YH, ZC, JC, and XC contributed to data acquisition. XQ, MZ, and WD performed the statistical analysis. XQ wrote the first draft of the manuscript. MZ and WD wrote sections of the manuscript. All authors contributed to manuscript revision and read and approved the submitted version.

FUNDING

This study was supported by Sun Yat-sen University Clinical Research 5010 Programs (grant numbers 2017008 and 2019021).

SUPPLEMENTARY MATERIAL

The Supplementary Material for this article can be found online at: https://www.frontiersin.org/articles/10.3389/fonc.2022.826830/full#supplementary-material

Supplementary Figure 1 | Decision curve analyses (DCA) of nomogram prediction model and model without DR category for 1,2,3-year OS in the training cohort **(A-C)**, and the validation cohort **(D-F)**.

REFERENCES

1. Jayne DG, Fook S, Loi C, Seow-Choen F. Peritoneal Carcinomatosis From Colorectal Cancer. *Br J Surg* (2002) 89(12):1545–50. doi: 10.1046/j.1365-2168.2002.02274.x
2. Kobayashi H, Enomoto M, Higuchi T, Uetake H, Iida S, Ishikawa T, et al. Validation and Clinical Use of the Japanese Classification of Colorectal Carcinomatosis: Benefit of Surgical Cytoreduction Even Without Hyperthermic Intraperitoneal Chemotherapy. *Dig Surg* (2010) 27(6):473–80. doi: 10.1159/000320460
3. Franko J, Shi Q, Meyers JP, Maughan TS, Adams RA, Seymour MT, et al. Prognosis of Patients With Peritoneal Metastatic Colorectal Cancer Given Systemic Therapy: An Analysis of Individual Patient Data From Prospective Randomised Trials From the Analysis and Research in Cancers of the Digestive System (ARCAD) Database. *Lancet Oncol* (2016) 17(12):1709–19. doi: 10.1016/S1470-2045(16)30500-9
4. Veld JV, Wisselink DD, Amelung FJ, Consten ECJ, de Wilt JHW, de Hingh I, et al. Synchronous and Metachronous Peritoneal Metastases in Patients With Left-Sided Obstructive Colon Cancer. *Ann Surg Oncol* (2020) 27(8):2762–73. doi: 10.1245/s10434-020-08327-7
5. Tanaka T, Ozawa H, Nakagawa Y, Hirata A, Fujita S, Sugihara K. Verifying the M1c Category of CRC: Analysis of the Data From a Japanese Multi-Institutional Database. *Int J Colorectal Dis* (2020) 35(1):125–31. doi: 10.1007/s00384-019-03408-w
6. Weber T, Roitman M, Link KH. Current Status of Cytoreductive Surgery With Hyperthermic Intraperitoneal Chemotherapy in Patients With Peritoneal Carcinomatosis From Colorectal Cancer. *Clin Colorectal Cancer* (2012) 11(3):167–76. doi: 10.1016/j.clcc.2012.01.001
7. Verwaal VJ, Bruin S, Boot H, van Slooten G, van Tinteren H. 8-Year Follow-Up of Randomized Trial: Cytoreduction and Hyperthermic Intraperitoneal Chemotherapy Versus Systemic Chemotherapy in Patients With Peritoneal Carcinomatosis of Colorectal Cancer. *Ann Surg Oncol* (2008) 15(9):2426–32. doi: 10.1245/s10434-008-9966-2
8. Esquivel J. Cytoreductive Surgery and Hyperthermic Intraperitoneal Chemotherapy for Colorectal Cancer: Survival Outcomes and Patient Selection. *J Gastrointest Oncol* (2016) 7(1):72–8. doi: 10.3978/j.issn.2078-6891.2015.114
9. Hashiguchi Y, Muro K, Saito Y, Ito Y, Ajioka Y, Hamaguchi T, et al. Japanese Society for Cancer of the Colon and Rectum (JSCCR) Guidelines 2019 for the Treatment of Colorectal Cancer. *Int J Clin Oncol* (2020) 25(1):1–42. doi: 10.1007/s10147-019-01485-z
10. Sorolla MA, Hidalgo I, Sorolla A, Montal R, Pallise O, Salud A, et al. Microenvironmental Reactive Oxygen Species in Colorectal Cancer: Involved Processes and Therapeutic Opportunities. *Cancers (Basel)* (2021) 13(20). doi: 10.3390/cancers13205037
11. Quail DF, Joyce JA. Microenvironmental Regulation of Tumor Progression and Metastasis. *Nat Med* (2013) 19(11):1423–37. doi: 10.1038/nm.3394
12. Tang YQ, Chen TF, Zhang Y, Zhao XC, Zhang YZ, Wang GQ, et al. The Tumor Immune Microenvironment Transcriptomic Subtypes of Colorectal Cancer for Prognosis and Development of Precise Immunotherapy. *Gastroenterol Rep (Oxf)* (2020) 8(5):381–9. doi: 10.1093/gastro/goaa045
13. Cirri P, Chiarugi P. Cancer-Associated-Fibroblasts and Tumour Cells: A Diabolic Liaison Driving Cancer Progression. *Cancer Metastasis Rev* (2012) 31(1-2):195–208. doi: 10.1007/s10555-011-9340-x
14. Sahai E, Astsaturov I, Cukierman E, DeNardo DG, Egeblad M, Evans RM, et al. A Framework for Advancing Our Understanding of Cancer-Associated Fibroblasts. *Nat Rev Cancer* (2020) 20(3):174–86. doi: 10.1038/s41568-019-0238-1
15. Tsujino T, Seshimo I, Yamamoto H, Ngan CY, Ezumi K, Takemasa I, et al. Stromal Myofibroblasts Predict Disease Recurrence for Colorectal Cancer. *Clin Cancer Res* (2007) 13(7):2082–90. doi: 10.1158/1078-0432.CCR-06-2191
16. Ueno H, Jones A, Jass JR, Talbot IC. Clinicopathological Significance of the 'Keloid-Like' Collagen and Myxoid Stroma in Advanced Rectal Cancer. *Histopathology* (2002) 40(4):327–34. doi: 10.1046/j.1365-2559.2002.01376.x
17. Ueno H, Jones AM, Wilkinson KH, Jass JR, Talbot IC. Histological Categorisation of Fibrotic Cancer Stroma in Advanced Rectal Cancer. *Gut* (2004) 53(4):581–6. doi: 10.1136/gut.2003.028365
18. Ueno H, Kajiwara Y, Ajioka Y, Sugai T, Sekine S, Ishiguro M, et al. Histopathological Atlas of Desmoplastic Reaction Characterization in Colorectal Cancer. *Jpn J Clin Oncol* (2021) 51(6):1004–12. doi: 10.1093/jjco/hyab040
19. Kajiwara Y, Ueno H, Hashiguchi Y, Mochizuki H, Hase K. Risk Factors of Nodal Involvement in T2 Colorectal Cancer. *Dis Colon Rectum* (2010) 53 (10):1393–9. doi: 10.1007/DCR.0b013e3181ec5f66

20. Crispino P, De Toma G, Ciardi A, Bella A, Rivera M, Cavallaro G, et al. Role of Desmoplasia in Recurrence of Stage II Colorectal Cancer Within Five Years After Surgery and Therapeutic Implication. *Cancer Invest* (2008) 26(4):419–25. doi: 10.1080/07357900701788155
21. Ueno H, Shinto E, Shimazaki H, Kajiwara Y, Sueyama T, Yamamoto J, et al. Histologic Categorization of Desmoplastic Reaction: Its Relevance to the Colorectal Cancer Microenvironment and Prognosis. *Ann Surg Oncol* (2015) 22(5):1504–12. doi: 10.1245/s10434-014-4149-9
22. Ueno H, Ishiguro M, Nakatani E, Ishikawa T, Uetake H, Murotani K, et al. Prognostic Value of Desmoplastic Reaction Characterisation in Stage II Colon Cancer: Prospective Validation in a Phase 3 Study (SACURA Trial). *Br J Cancer* (2021) 124(6):1088–97. doi: 10.1038/s41416-020-01222-8
23. Ueno H, Kanemitsu Y, Sekine S, Ishiguro M, Ito E, Hashiguchi Y, et al. A Multicenter Study of the Prognostic Value of Desmoplastic Reaction Categorization in Stage II Colorectal Cancer. *Am J Surg Pathol* (2019) 43 (8):1015–22. doi: 10.1097/PAS.0000000000001272
24. Ueno H, Shinto E, Kajiwara Y, Fukazawa S, Shimazaki H, Yamamoto J, et al. Prognostic Impact of Histological Categorisation of Epithelial-Mesenchymal Transition in Colorectal Cancer. *Br J Cancer* (2014) 111(11):2082–90. doi: 10.1038/bjc.2014.509
25. Ueno H, Konishi T, Ishikawa Y, Shimazaki H, Ueno M, Aosasa S, et al. Histologic Categorization of Fibrotic Cancer Stroma in the Primary Tumor Is an Independent Prognostic Index in Resectable Colorectal Liver Metastasis. *Am J Surg Pathol* (2014) 38(10):1380–6. doi: 10.1097/PAS.0000000000000232
26. Ao T, Kajiwara Y, Yonemura K, Shinto E, Mochizuki S, Okamoto K, et al. Morphological Consistency of Desmoplastic Reactions Between the Primary Colorectal Cancer Lesion and Associated Metastatic Lesions. *Virchows Arch* (2020) 477(1):47–55. doi: 10.1007/s00428-019-02742-2
27. Ubink I, van Eden WJ, Snaebjornsson P, Kok NFM, van Kuik J, van Grevenstein WMU, et al. Histopathological and Molecular Classification of Colorectal Cancer and Corresponding Peritoneal Metastases. *Br J Surg* (2018) 105(2):e204–11. doi: 10.1002/bjs.10788
28. Jacquet P, Sugarbaker PH. Clinical Research Methodologies in Diagnosis and Staging of Patients With Peritoneal Carcinomatosis. *Cancer Treat Res* (1996) 82:359–74. doi: 10.1007/978-1-4613-1247-5_23
29. Isella C, Terrasi A, Bellomo SE, Petti C, Galatola G, Muratore A, et al. Stromal Contribution to the Colorectal Cancer Transcriptome. *Nat Genet* (2015) 47 (4):312–9. doi: 10.1038/ng.3224
30. Calon A, Lonardo E, Berenguer-Llergo A, Espinet E, Hernando-Momblona X, Iglesias M, et al. Stromal Gene Expression Defines Poor-Prognosis Subtypes in Colorectal Cancer. *Nat Genet* (2015) 47(4):320–9. doi: 10.1038/ng.3225
31. Saglam EA, Usubutun A, Kart C, Ayhan A, Kucukali T. Reactive Nodular Fibrous Pseudotumor Involving the Pelvic and Abdominal Cavity: A Case Report and Review of Literature. *Virchows Arch* (2005) 447(5):879–82. doi: 10.1007/s00428-005-0027-y
32. Allison DB, VandenBussche CJ, Rooper LM, Wakely PE, Rossi ED, Faquin WC, et al. Nodular Fasciitis of the Parotid Gland: A Challenging Diagnosis on FNA. *Cancer Cytopathol* (2018) 126(10):872–80. doi: 10.1002/cncy.22049
33. Bran GM, Goessler UR, Hormann K, Riedel F, Sadick H. Keloids: Current Concepts of Pathogenesis (Review). *Int J Mol Med* (2009) 24(3):283–93. doi: 10.3892/ijmm_00000231
34. Calon A, Espinet E, Palomo-Ponce S, Tauriello DV, Iglesias M, Cespedes MV, et al. Dependency of Colorectal Cancer on a TGF-Beta-Driven Program in Stromal Cells for Metastasis Initiation. *Cancer Cell* (2012) 22(5):571–84. doi: 10.1016/j.ccr.2012.08.013
35. Dongre A, Weinberg RA. New Insights Into the Mechanisms of Epithelial-Mesenchymal Transition and Implications for Cancer. *Nat Rev Mol Cell Biol* (2019) 20(2):69–84. doi: 10.1038/s41580-018-0080-4
36. Hao Y, Baker D, Ten Dijke P. TGF-Beta-Mediated Epithelial-Mesenchymal Transition and Cancer Metastasis. *Int J Mol Sci* (2019) 20(11). doi: 10.3390/ijms20112767
37. Ozdemir BC, Pentcheva-Hoang T, Carstens JL, Zheng X, Wu CC, Simpson TR, et al. Depletion of Carcinoma-Associated Fibroblasts and Fibrosis Induces Immunosuppression and Accelerates Pancreas Cancer With Reduced Survival. *Cancer Cell* (2014) 25(6):719–34. doi: 10.1016/j.ccr.2014.04.005
38. von Ahrens D, Bhagat TD, Nagrath D, Maitra A, Verma A. The Role of Stromal Cancer-Associated Fibroblasts in Pancreatic Cancer. *J Hematol Oncol* (2017) 10(1):76. doi: 10.1186/s13045-017-0448-5
39. Cao L, Sun PL, He Y, Yao M, Gao H. Desmoplastic Reaction and Tumor Budding in Cervical Squamous Cell Carcinoma Are Prognostic Factors for Distant Metastasis: A Retrospective Study. *Cancer Manag Res* (2020) 12:137–44. doi: 10.2147/CMAR.S231356
40. Kojima S, Hisaka T, Midorikawa R, Naito Y, Akiba J, Tanigawa M, et al. Prognostic Impact of Desmoplastic Reaction Evaluation for Intrahepatic Cholangiocarcinoma. *Anticancer Res* (2020) 40(8):4749–54. doi: 10.21873/anticanres.14476
41. Sakai A, Nakashima Y, Miyashita Y, Ao T, Kimura Y, Shinto E, et al. Histological Categorisation of the Desmoplastic Reaction Is a Predictor of Patient Prognosis in Oesophageal Squamous Cell Carcinoma. *Histopathology* (2021) 79(2):219–26. doi: 10.1111/his.14357
42. Pelz JO, Stojadinovic A, Nissan A, Hohenberger W, Esquivel J. Evaluation of a Peritoneal Surface Disease Severity Score in Patients With Colon Cancer With Peritoneal Carcinomatosis. *J Surg Oncol* (2009) 99(1):9–15. doi: 10.1002/jso.21169
43. Simkens GA, van Oudheusden TR, Nieboer D, Steyerberg EW, Rutten HJ, Luyer MD, et al. Development of a Prognostic Nomogram for Patients With Peritoneally Metastasized Colorectal Cancer Treated With Cytoreductive Surgery and HIPEC. *Ann Surg Oncol* (2016) 23(13):4214–21. doi: 10.1245/s10434-016-5211-6

Conflict of Interest: The authors declare that the research was conducted in the absence of any commercial or financial relationships that could be construed as a potential conflict of interest.

The handling editor declared a shared parent affiliation with several of the authors XQ, WD, YH, ZC, KY, HW at the time of review.

frontiers | Frontiers in Oncology

ORIGINAL RESEARCH
published: 01 April 2022
doi: 10.3389/fonc.2022.843489

Icaritin Inhibits Migration and Invasion of Human Ovarian Cancer Cells *via* the Akt/mTOR Signaling Pathway

Lvfen Gao[1], Yuan Ouyang[2], Ruobin Li[1], Xian Zhang[1], Xuesong Gao[1], Shaoqiang Lin[3] and Xiaoyu Wang[1]**

[1] Department of Obstetrics and Gynecology, The First Affiliated Hospital of Jinan University, Guangzhou, China, [2] Department of Obstetrics and Gynecology, Guangzhou Panyu Central Hospital, Guangzhou, China, [3] Integrated Traditional and Western Medicine Research Center, The First Affiliated Hospital of Guangdong Pharmaceutical University, Guangzhou, China

Ovarian cancer (OC) is the most lethal of all gynecologic malignancies with poor survival rates. Although surgical treatment and chemotherapy had advanced to improve survival, platinum-based chemoresistance remains a major hurdle in the clinical treatment of OC. The search for novel active ingredients for the treatment of drug-resistant OC is urgently needed. Here, we demonstrated that icaritin, the main active ingredient derived from the traditional Chinese herb *Epimedium* genus, significantly suppressed the proliferation, migration, and invasion of both drug-susceptible and cisplatin-resistant OC cells *in vitro*. Mechanistically, icaritin at 20 μM significantly inhibited the phosphorylation of Akt and mTOR, as well as decreased the expression of vimentin and increased the expression of E-cadherin. Our data indicate that icaritin, a prenylated flavonoid natural product, could serve as a potential inhibitor of cisplatin-resistant OC by inhibiting the Akt/mTOR signaling pathway.

Keywords: ovarian cancer, icaritin, drug-resistant, migration, invasion, Akt, mTOR

OPEN ACCESS

Edited by:
Dongmei Zhang,
Jinan University, China

Reviewed by:
Jun Shan Liu,
Southern Medical University, China
Xueping Lei,
Guangzhou Medical University, China

****Correspondence:***
Shaoqiang Lin
shaotsiang@163.com
Xiaoyu Wang
twxy163@163.com

Specialty section:
This article was submitted to Molecular and Cellular Oncology, a section of the journal Frontiers in Oncology

Received: *26 December 2021*
Accepted: *07 March 2022*
Published: *01 April 2022*

Citation:
Gao L, Ouyang Y, Li R, Zhang X, Gao X, Lin S and Wang X (2022) Icaritin Inhibits Migration and Invasion of Human Ovarian Cancer Cells via the Akt/mTOR Signaling Pathway. Front. Oncol. 12:843489. doi: 10.3389/fonc.2022.843489

INTRODUCTION

Ovarian cancer (OC) is the 5th leading cause of cancer deaths among women in the developed world (1). It remains a challenge to screen or detect OC at the early stages due to non-specific symptoms and lack of reliable biomarkers, resulting in OC being diagnosed at the advanced stage (2). Currently, surgery together with radiotherapy and chemotherapy remains the standard treatment for OC (3). Cisplatin is a front-line chemotherapeutic agent for OC (4). Cisplatin can block DNA transcription by direct covalent binding to nuclear DNA, thus exerting an anticancer activity (5, 6). Unfortunately, the 5-year survival rate is still hovering at about 30% because of cisplatin resistance, which is the major reason for chemotherapy failure. Therefore, to investigate novel target agents to effectively prevent or overcome cisplatin resistance is urgently needed.

Icaritin, a prenylated flavonoid natural product, is commonly recognized as one of the active compounds of the traditional Chinese herb *Epimedium* genus, which has been widely used as a tonic, an aphrodisiac, and an antirheumatic drug in China, Japan, and Korea for thousands of years

(7). It has been demonstrated that icaritin possesses a range of different biological and pharmacological functions in non-neoplastic diseases, such as preventing osteoporosis (8) and having cardioprotective (9), neuroprotective (10), and immunoregulatory effects (11). Lately, icaritin and its derivates have attracted great attention in terms of its antitumor effects against various solid tumors including lung cancer (12), prostate cancer (13), hepatocellular carcinoma (14), glioblastoma multiforme (15), and esophageal cancer (16). Moreover, it still exerts promising activity in female tumors, such as breast cancer (17), cervical cancer (18), and also OC in our previous work (19). Icaritin exerts antitumor effects mainly by inhibiting cell proliferation, inducing cell differentiation and apoptosis, suppressing cell migration and invasion, regulating the function of microRNAs, targeting stem cells, and reversing multidrug resistance (12, 13, 16, 20). Numerous signaling pathways are involved in the anticancer activities of icaritin, such as PTEN/Akt, Akt/mTOR, NF-κB, and MAPK/ERK pathways (12, 19, 21). In our previous work, we clarified that the anti-proliferative effects of icaritin on OC may be associated with the activation of p53 and the suppression of the Akt/mTOR pathway. However, the efficacies of icaritin against the migration and invasion of the OC cells and its underlying mechanism have not yet been illuminated.

Here, we sought to investigate the anticancer effect and the underlying mechanism of icaritin on the migration and invasion of human cisplatin-sensitive cells A2780s and the corresponding cisplatin-resistant cells A2780cp. Our results showed that icaritin significantly suppressed the epithelial–mesenchymal transformation (EMT) and migration of both A2780s and A2780cp cells *in vitro* through inhibition of the Akt/mTOR signaling pathway. Our study indicates that icaritin has the potential to inhibit the tumor metastases associated with cisplatin-resistant OC.

MATERIALS AND METHODS

Reagents

Icaritin was a gift from the Laboratory of the Department of Obstetrics and Gynecology, National University Hospital, Yong Loo Lin School (Singapore). RPMI-1640 medium, fetal bovine serum (FBS), and penicillin–streptomycin (PS) were purchased from Gibco (Life Technologies, NY, USA). Matrigel was from BioCoat (Corning, New York, NY, USA). The antibodies against GADPH, p-mTOR, $mTOR^{2448}$, $p\text{-}Akt^{473}$, and Akt were from Cell Signaling Technology (Danvers, MA, USA). Cisplatin, MTT (3-(4,5-dimethylthiazol-2-yl)-2,5-diphenyltetrazolium bromide), and other chemicals were obtained from Sigma (St Louis, MO, USA).

Cells and Cell Culture

The human cisplatin-sensitive OC cell line A2780s and human cisplatin-resistant OC cell line A2780cp were kindly provided by Dr. Benjamin K. Tsang (Ottawa Hospital Research Institute, Ottawa, ON, Canada) (22). These cells were cultured in RPMI-1640 and supplemented with 10% FBS (v/v) and 1% PS (v/v) in a humidified atmosphere of 5% CO_2 at 37°C. All cell lines were authenticated by STR Multi-amplification Kit and tested negative for mycoplasma using the Mycoplasma Detection Set (M&C Gene Technology, Beijing, China).

Cell Viability Assays

MTT assay was used to evaluate the cell viability. Cells (1×10^4/well) were seeded in 96-well plates and treated with icaritin at final concentrations of 10–50 μM for 24, 48, and 72 h. MTT (10 μl) solution was added to each well for 4 h after the preset time; then the supernatant was removed. Dimethyl sulfoxide (DMSO) (150 μl) was added to the well for 10 min. The absorbance was measured at 490 nm using a microplate reader (BioTek Synergy HT, Winooski, VT, USA). All experiments were performed three times to determine their reproducibility.

Wound-Healing Scratch Assay

A2780s and A2780cp cells (5×10^6/well) were seeded in 6-well plates in RPMI-1640 medium containing 10% FBS for 24 h, and the adherent monolayer cells of each plate were scratched at the same size and then treated with icaritin (20 μM) or cisplatin (1.6 μg/ml) for 0, 12, and 24 h. The size at the site of each scratch was recorded by a microscope at 0, 12, and 24 h. The data of the healing condition were calculated by software ImageJ.

Cell Migration and Invasion Analysis

A2780s and A2780cp cells were firstly cultured in serum-free media condition for 12 h, and the cells were then collected and counted after being exposed to icaritin (20 μM) or cis-platinum (1.6 μg/ml) for 12 h. Cells (1×10^4/well) were cultured in the upper chamber of transwell covered with (invasion) or without (migration) matrigel in the absence of FBS, while RPMI-1640 was added in the bottom well containing 20% FBS as a chemoattract factor. After being cultured for 12 h (for cell migration assay) or 24 h (for cell invasion assay), the migrated or invaded cells were fixed with 3% paraformaldehyde for 20 min and then stained by crystal violet for 10 min. The cells were then randomly photographed and counted.

Western Blotting

A2780s and A2780cp cells were treated with or without icaritin (10 or 20 μM) for 24 h. Afterward, the cell pellets were collected by centrifugation and rinsed with phosphate-buffered saline (PBS). Whole lysates were prepared with radioimmunoprecipitation assay (RIPA) buffer (1× PBS, 0.1% sodium dodecyl sulfate (SDS), 1% NP-40, and 0.5% sodium deoxycholate) supplemented with protease inhibitor cocktail, 10 mM of β-glycerophosphate, 1 mM of sodium orthovanadate, 10 mM of sodium fluoride, and 1 mM of phenylmethylsulfonyl fluoride; protein samples were subsequently obtained. Bicinchoninic Acid Assay Kit was used to examine the expression of total proteins, and equal amounts of protein were separated on 10% SDS–polyacrylamide gel electrophoresis (PAGE) gels at 125 V for 1.2 h. Transfer to nitrocellulose membranes was performed at 100 V for 1 h. Membranes were blocked using blocking buffer [(bovine serum albumin (BSA)] and then probed with primary antibodies. After incubation with horseradish peroxidase (HRP)-

conjugated secondary antibodies in blocking buffer, a chemiluminescence detection system (Thermo Fisher Scientific, Waltham, MA, USA) was used to detect visualized protein bands. GAPDH was used as an internal control. Densitometry was performed using ImageJ software.

Statistical Analysis

GraphPad Prism 5.0 software was used for statistical analyses (GraphPad Software, Inc., San Diego, CA, USA). All data are presented as the mean values with a standard error of the mean (SEM). Significant differences between the two groups were evaluated using the 2-tailed unpaired *t*-test, and significant differences between more than two groups were evaluated using 1-way ANOVA followed by Tukey's *post-hoc* test. $p < 0.05$ was considered significant.

RESULTS

Icaritin Inhibits the Proliferation of Human Ovarian Cancer A2780s and A2780cp Cells

To evaluate the effects of icaritin (**Figure 1A**) on the growth of OC cells, cells were treated with icaritin at different concentrations for 24, 48, and 72 h, and the cell viability was assessed by MTT assay. The results showed that icaritin inhibited both the proliferation of cisplatin-sensitive OC cells A2780s and the cisplatin-resistant OC cells A2780cp in a dose- and time-dependent manner (**Figures 1B, C**). The IC_{50} values of icaritin on A2780s cells were 23.41, 21.42, and 14.9 μM after drug treatment for 24, 48, and 72 h, respectively. And the IC_{50} values of icaritin on A2780cp cells were 28.59, 25, and 22.06 μM after drug treatment for 24, 48, and 72 h, respectively. These data suggest that icaritin inhibits the proliferation of both the cisplatin-sensitive and cisplatin-resistant OC cells.

Icaritin Suppresses the Wound Healing Ability of A2780s and A2780cp Cells

To determine whether icaritin affected the wound healing ability of both A2780s and A2780cp cells, we performed the scratch assay. Our results showed that icaritin (20 μM) inhibited the wound healing ability of both A2780s and A2780cp cells in a time-dependent manner (**Figures 2A, B**). The inhibitory rates of icaritin on the wound healing of A2780s were 51.9% and 26.6% at 12 and 24 h as compared to the CTL group, respectively. And the inhibitory rates of icaritin on the wound healing of A2780cp were 19.6% and 12.4% at 12 and 24 h as compared to the CTL group, respectively.

Icaritin Inhibits the Migration of A2780s and A2780cp Cells

We next investigated the effect of icaritin in the cell migration of human OC cells. Transwell assays showed that icaritin treatment significantly decreased the number of migrated A2780s and A2780cp cells in a dose-dependent manner, when compared to the control group (**Figures 3A, B**). The inhibitory rates of icaritin on the migration of A2780s were 51.20% and 70.13% at doses of 10 and 20 μM, respectively. And the inhibitory rates of icaritin on the migration of A2780cp were 33.63% and 81.95% at doses of 10 and 20 μM, respectively.

Icaritin Attenuates the Invasion of A2780s and A2780cp Cells

We utilized matrigel invasion chambers to evaluate the effect of icaritin on the *in vitro* invasion of A2780s and A2780cp cells. Transwell assays showed that icaritin treatment significantly decreased the number of invaded A2780s and A2780cp cells in a dose-dependent manner, when compared to the control group (**Figures 4A, B**). The inhibitory rates of icaritin on the invasion of A2780s were 22.15% and 63.83% at doses of 10 and 20 μM, respectively. And the inhibitory rates of icaritin on the invasion of A2780cp were 22.83% and 58.58% at doses of 10 and 20 μM, respectively.

Icaritin Inhibits the Akt/mTOR Signaling Pathway in A2780s and A2780cp Cells

We further evaluated the underlying mechanism of icaritin on inhibition of OC cell migration and invasion. Given that Akt and its important downstream executor mTOR played a critical role in controlling the ability of cell migration and invasion, we investigated whether icaritin can restrain the Akt/mTOR signaling pathway. We found that icaritin significantly suppressed the phosphorylation of Akt and mTOR, but it has a negligible effect on the expression of Akt and mTOR in both the A2780s and A2780cp cells (**Figures 5A, B**). EMT was critical for

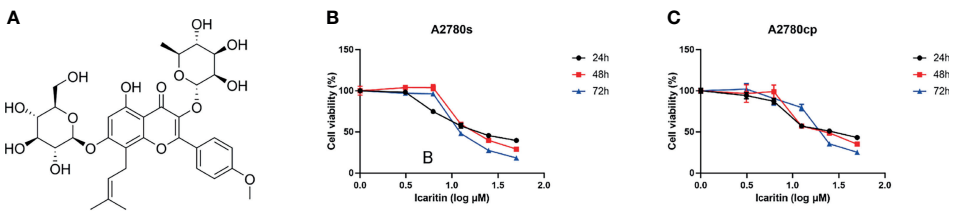

FIGURE 1 | Chemical structure of icaritin and its effects on cell viability in A2780s and A2780cp cells. **(A)** The chemical structure of icaritin. **(B)** A2780s cells were treated with different concentrations (0–50 μM) of icaritin for 24, 48, and 72 h. The cell viability was measured by MTT assay. The data are indicated as means ± SEM of three independent experiments. **(C)** A2780cp cells were treated with different concentrations (0–50 μM) of icaritin for 24, 48, and 72 h. The cell viability was measured by MTT assay. The data are represented as means ± SEM of three independent experiments.

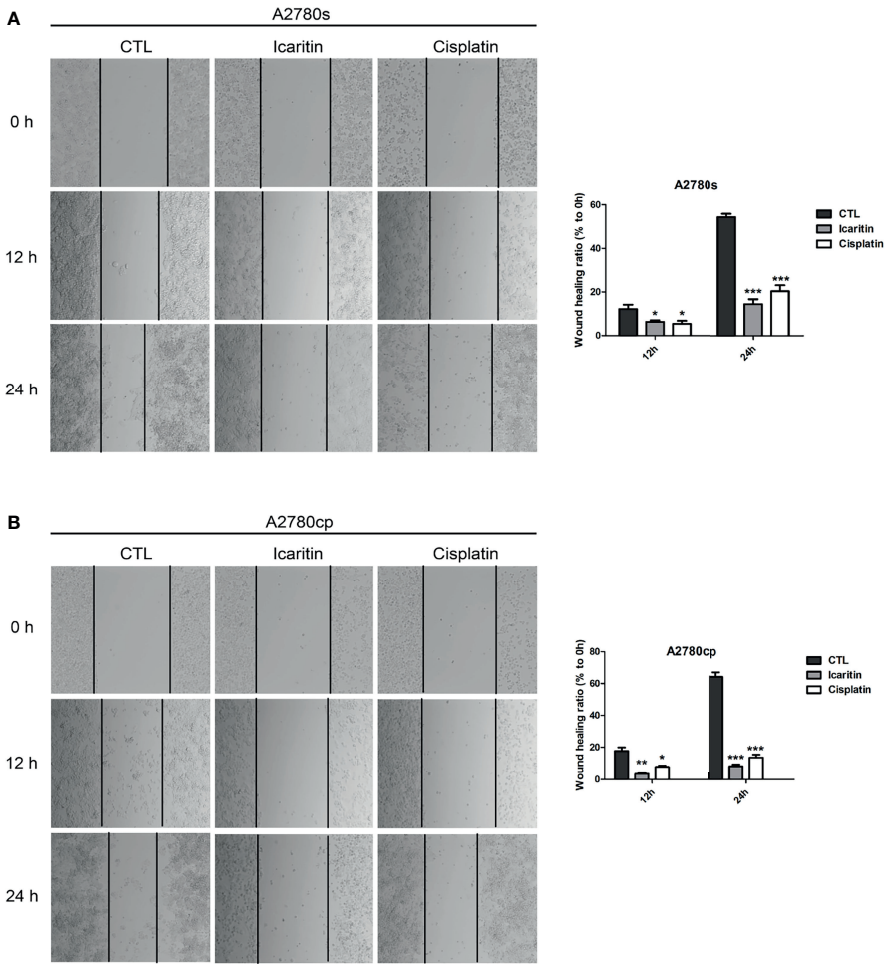

FIGURE 2 | The effects of icaritin or cisplatin on the horizontal motility of A2780s and A2780cp cells by wound-healing scratch assay. **(A)** A2780s were treated with icaritin (20 μM) or cisplatin (1.6 μg/ml) for 12 h or 24 h, respectively. Representative images and quantification of the migrated cells are shown. Data are represented as means ± SEM. ***$p < 0.001$ by 2-tailed Student's *t*-test. **(B)** A2780cp cells were treated with icaritin (20 μM) or cisplatin (1.6 μg/ml) for 12 h or 24 h, respectively. Representative images and quantification of the migrated cells are shown. Data are represented as means ± SEM. *$p < 0.05$, ***$p < 0.001$ compared to CTL group by 1-way ANOVA followed by Tukey's *post-hoc* test. **p < 0.01.

tumor cell migration, invasion, and tumor metastasis (23); our results showed that icaritin significantly decreased the expression of mesenchymal markers (including N-cadherin and vimentin) and increased expression of epithelial marker E-cadherin in both the A2780s and A2780cp cells (**Figures 5A, B**). Taken together, these data indicate that icaritin inhibited tumor cell motility by suppressing EMT.

DISCUSSION

Icaritin is the major bioactive component of *Epimedium*, which has been used as Chinese traditional medicine for thousands of years. Many studies demonstrated that numerous traditional Chinese medicine monomers have the effect of reversing tumor resistance (24–26). Extensive evidence showed that icaritin displayed anti-neoplastic activities in a variety of human malignancies both *in vitro* and *in vivo* (13, 27–29). For the first time, our previous study revealed that icaritin induced OC cell apoptosis through activating p53 and suppressing the Akt/mTOR signaling pathway (19). However, the effects of icaritin on migration and invasion of OC cells had not been thoroughly investigated. Therefore, we explored in the present study if icaritin had a significant repressive effect on migration and invasion of both cisplatin-sensitive and cisplatin-resistant OC cells by inhibiting the Akt/mTOR signaling pathway.

It is well established that the migratory and invasive capacity of tumor and stromal cells is linked with tumor metastasis. At present, it is widely believed that the fatal harm of a malignant tumor to the human body mainly lies in tumor metastasis. The migratory phenotype is the precondition for metastatic spreading. Thus, determining the effect of novel agents on migratory and invasive capabilities of tumor cells and clarifying the underlying mechanisms is highly relevant for

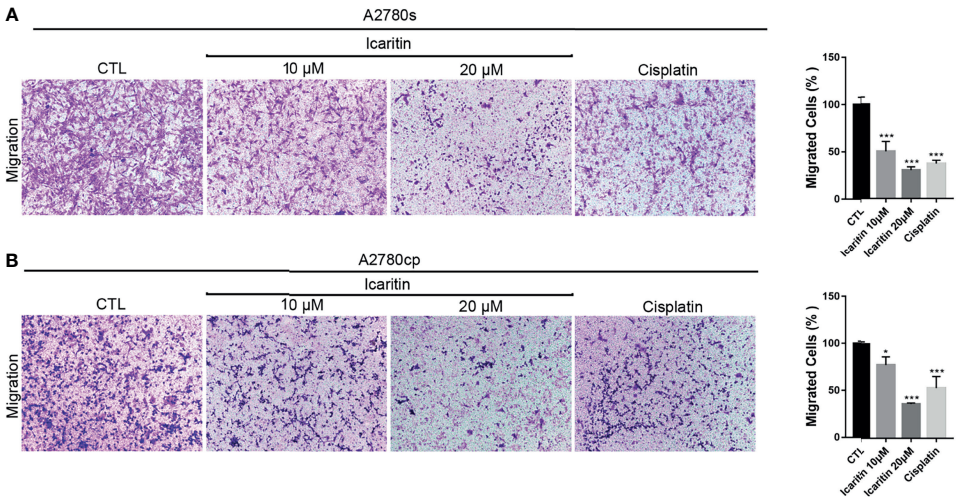

FIGURE 3 | Icaritin suppresses the migration of ovarian cancer (OC) cells. **(A)** A2780s were treated with icaritin (20 μM) or cisplatin (1.6 μg/ml) for 12 h. Representative images and quantification of the migrated cells are shown. Data are represented as means ± SEM. ***$p < 0.001$ by 2-tailed Student's *t*-test. **(B)** A2780cp cells were treated with icaritin (20 μM) or cisplatin (1.6 μg/ml) for 12 h. Representative images and quantification of the migrated cells are shown. Data are represented as means ± SEM. *$p < 0.05$, ***$p < 0.001$ compared to CTL group by 1-way ANOVA followed by Tukey's *post-hoc* test.

cancer diagnosis, prognosis, and treatment. It is of great significance to inhibit the motility of tumor cells and prevent the cells from breaking through the basal layer and leaving the primary lesion. A wide variety of assays can be used to assess the migratory or invasion potential and activity of cells *in vitro*, such as wound-healing assay, transwell migration assay, cell exclusion zone assay, transwell assay, 3D cell tracking, and spheroid confrontation assay. In our present experiments, the emphasis was placed on examining the inhibitory activity of icaritin on migratory and invasive motility of OC cells by using wound-healing assay and transwell migration/invasion assay. The results of our study demonstrated that icaritin inhibited the proliferation, migration, and invasion of both A2780s and A2780cp cells in a dose- and time-dependent manner, whose activities were comparable to those of cisplatin. However, for the cisplatin-resistant A2780cp cells, the anti-migration and anti-invasion effects of icaritin were better than those of cisplatin, and it was important to note that cisplatin-resistant OC had the

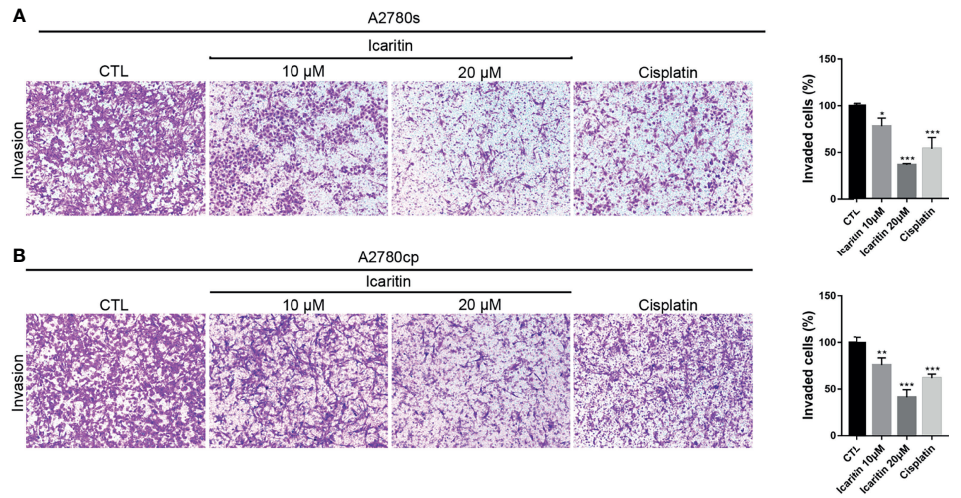

FIGURE 4 | Icaritin inhibits the invasion of ovarian cancer (OC) cells. **(A)** A2780s were treated with icaritin (20 μM) or cisplatin (1.6 μg/ml) for 24 h. Representative images and quantification of the invaded cells are shown. Data are represented as means ± SEM. ***$p < 0.001$ by 2-tailed Student's *t*-test. **(B)** A2780cp cells were treated with icaritin (20 μM) or cisplatin (1.6 μg/ml) for 24 h. Representative images and quantification of the invaded cells are shown. Data are represented as means ± SEM. *$p < 0.05$, **$p < 0.01$, ***$p < 0.001$ compared to CTL group by 1-way ANOVA followed by Tukey's *post-hoc* test.

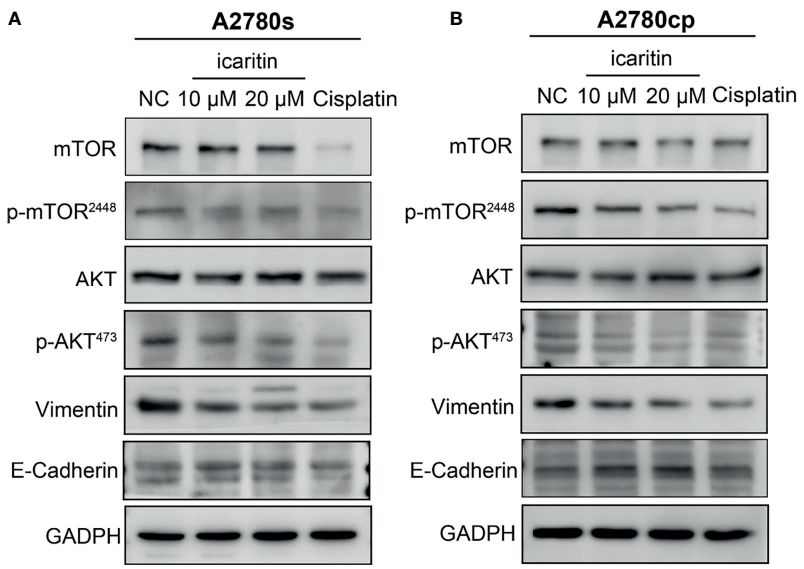

FIGURE 5 | Icaritin inhibits epithelial–mesenchymal transformation (EMT) of ovarian cancer (OC) cells *via* the Akt/mTOR signaling pathways. **(A)** Icaritin decreased the phosphorylation levels of Akt and mTOR, and the expression of vimentin, accompanied by increased expression of E-cadherin in A2780s cells. **(B)** Icaritin decreased the phosphorylation levels of Akt and mTOR, and the expression of vimentin, accompanied by increased expression of E-cadherin in A2780cp cells.

ability to metastasize. Taken together, icaritin is a promising antitumor agent for both cisplatin-sensitive and cisplatin-resistant OC.

Drug resistance is a complicated phenomenon, which has been recognized to severely limit therapeutic outcomes. OC is one of the lethal malignancies in women and cisplatin-based chemotherapy remains the main treatment of OC patients. However, its clinical success is often diminished by chemoresistance. The chemoresistance mechanisms are usually classified into two categories, intrinsic and acquired resistance, but the underlying mechanism of chemoresistance in OC is not completely understood (30). Aberrant activation of the PI3K/Akt/mTOR pathway had been found in various cancers and had been suggested to stimulate proliferation and drug resistance (31). It was reported that the PI3K/Akt/mTOR signaling pathway, EMT, and cancer stem cells played important roles in tumor progression, metastasis, and chemoresistance (32). Numerous studies demonstrated that inhibition of the PI3K/Akt/mTOR signaling pathway alleviated OC chemoresistance (33–35). Icaritin has been shown to have an anticancer effect against various drug-resistance cell types *via* different signaling pathways. For example, icaritin can effectively reverse the multidrug resistance of multiple myeloma cell line KM3/BTZ by decreasing the expression of HSP27 and increasing the expression of Par-4 (36). Icaritin possessed a potential effect on MG-63 doxorubicin-resistant (MG-63/DOX) cells by decreasing the mRNA and protein levels of multidrug resistance protein 1 (MDR1) and multidrug resistance-associated protein 1 (MRP1) and blocking the phosphorylation of STAT3 (20). Icaritin reversed multidrug resistance of HepG2/ADR human hepatoma cells *via* downregulation of MDR1 and P-glycoprotein expression (37). Here, we found that icaritin inhibited the migration and invasion of cisplatin-resistant OC cells. In addition, the Western blotting analysis revealed that icaritin suppressed the Akt/mTOR signaling pathway and process of EMT on both the cisplatin-sensitive and cisplatin-resistant OC cells. Taken together, this study proposes the anticancer mechanism of icaritin in OC.

In conclusion, icaritin could be a potential anti-metastatic agent in cisplatin-resistant OC, and the mechanism might be associated with the inhibition of the Akt/mTOR signaling pathway.

DATA AVAILABILITY STATEMENT

The raw data supporting the conclusions of this article will be made available by the authors, without undue reservation.

AUTHOR CONTRIBUTIONS

LG and YO are considered joint co-first authors for this study. LG, SL, and XW conceived and designed the experiments. YO and RL performed the experiments. XZ and XG analyzed statistical data. LG was a major contributor in writing the manuscript. All authors read and approved the final version of the manuscript.

FUNDING

This research was supported by the Medical Scientific Research Foundation of Guangdong Province (no. A2017203) and the Project of Traditional Chinese Medicine in Guangdong (no. 20162045).

REFERENCES

1. Siegel RL, Miller KD. Cancer Statistics, 2019. *CA Cancer J Clin* (2019) 69:7–34. doi: 10.3322/caac.21551
2. Chou JL, Su HY, Chen LY, Liao YP, Hartman-Frey C, Lai YH, et al. Promoter Hypermethylation of FBXO32, a Novel TGF-Beta/SMAD4 Target Gene and Tumor Suppressor, Is Associated With Poor Prognosis in Human Ovarian Cancer. *Lab Investigation J Tech Methods Pathol* (2010) 90:414–25. doi: 10.1038/labinvest.2009.138
3. Romero I, Bast RCJr.Minireview: Human Ovarian Cancer: Biology, Current Management, and Paths to Personalizing Therapy. *Endocrinology* (2012) 153:1593–602. doi: 10.1210/en.2011-2123
4. Boulikas T, Vougiouka M. Cisplatin and Platinum Drugs at the Molecular Level (Review). *Oncol Rep* (2003) 10:1663–82. doi: 10.3892/or.10.6.1663
5. Chu G. Cellular Responses to Cisplatin. The Roles of DNA-Binding Proteins and DNA Repair. *J Biol Chem* (1994) 269:787–90. doi: 10.1016/S0021-9258(17)42175-2
6. Kelland L. The Resurgence of Platinum-Based Cancer Chemotherapy, Nature Reviews. *Cancer* (2007) 7:573–84. doi: 10.1038/nrc2167
7. Ma H, He X, Yang Y, Li M, Hao D, Jia Z. The Genus Epimedium: An Ethnopharmacological and Phytochemical Review. *J Ethnopharmacol* (2011) 134:519–41. doi: 10.1016/j.jep.2011.01.001
8. Liu YQ, Yang QX, Cheng MC, Xiao HB. Synergistic Inhibitory Effect of Icariside II With Icaritin From Herba Epimedii on Pre-Osteoclastic RAW264.7 Cell Growth. *Phytomed: Int J Phytother Phytopharmacol* (2014) 21:1633–7. doi: 10.1016/j.phymed.2014.07.016
9. Zhu DY, Lou YJ. Inducible Effects of Icariin, Icaritin, and Desmethylicaritin on Directional Differentiation of Embryonic Stem Cells Into Cardiomyocytes *In Vitro*. *Acta Pharmacol Sin* (2005) 26:477–85. doi: 10.1111/j.1745-7254.2005.00076.x
10. Wang Z, Zhang X, Wang H, Qi L, Lou Y. Neuroprotective Effects of Icaritin Against Beta Amyloid-Induced Neurotoxicity in Primary Cultured Rat Neuronal Cells *via* Estrogen-Dependent Pathway. *Neuroscience* (2007) 145:911–22. doi: 10.1016/j.neuroscience.2006.12.059
11. Liao J, Liu Y, Wu H, Zhao M, Tan Y, Li D, et al. The Role of Icaritin in Regulating Foxp3/IL17a Balance in Systemic Lupus Erythematosus and Its Effects on the Treatment of MRL/lpr Mice. *Clin Immunol (Orlando Fla)* (2016) 162:74–83. doi: 10.1016/j.clim.2015.11.006
12. Lu X, Xue B, Zhang T, Zhou X, Zhang Y. Down-Regulation of microRNA-10a Mediates the Anti-Tumor Effect of Icaritin in A549 Cells *via* the PTEN/AKT and ERK Pathway. *Gen Physiol Biophysics* (2019) 38:525–33. doi: 10.4149/gpb_2019041
13. Hu J, Wu X, Yang C, Rashid K, Ma C, Hu M, et al. Anticancer Effect of Icaritin on Prostate Cancer via Regulating miR-381-3p and Its Target Gene UBE2C. *Cancer Med* (2019) 8:7833–45. doi: 10.1002/cam4.2630
14. Wang S, Wang Q, Wang H, Qin C, Cui X, Li L, et al. Induction of ROS and DNA Damage-Dependent Senescence by Icaritin Contributes to Its Antitumor Activity in Hepatocellular Carcinoma Cells. *Pharm Biol* (2019) 57:424–31. doi: 10.1080/13880209.2019.1628073
15. Liu Y, Shi L, Liu Y, Li P, Jiang G, Gao X, et al. Activation of PPARgamma Mediates Icaritin-Induced Cell Cycle Arrest and Apoptosis in Glioblastoma Multiforme. *Biomed Pharmacother Biomed Pharmacother* (2018) 100:358–66. doi: 10.1016/j.biopha.2018.02.006
16. Han S, Gou Y, Jin D, Ma J, Chen M, Dong X. Effects of Icaritin on the Physiological Activities of Esophageal Cancer Stem Cells. *Biochem Biophys Res Commun* (2018) 504:792–6. doi: 10.1016/j.bbrc.2018.08.060
17. Wang X, Zheng N, Dong J, Wang X, Liu L, Huang J. Estrogen Receptor-Alpha36 Is Involved in Icaritin Induced Growth Inhibition of Triple-Negative Breast Cancer Cells. *J Steroid Biochem Mol Biol* (2017) 171:318–27. doi: 10.1016/j.jsbmb.2017.05.009
18. Chen X, Song L, Hou Y, Li F. Reactive Oxygen Species Induced by Icaritin Promote DNA Strand Breaks and Apoptosis in Human Cervical Cancer Cells. *Oncol Rep* (2019) 41:765–78. doi: 10.3892/or.2018.6864
19. Gao L, Chen M, Ouyang Y, Li R, Zhang X, Gao X, et al. Icaritin Induces Ovarian Cancer Cell Apoptosis Through Activation of P53 and Inhibition of Akt/mTOR Pathway. *Life Sci* (2018) 202:188–94. doi: 10.1016/j.lfs.2018.03.059
20. Wang ZD, Wang RZ, Xia YZ, Kong LY, Yang L. Reversal of Multidrug Resistance by Icaritin in Doxorubicin-Resistant Human Osteosarcoma Cells. *Chin J Nat Med* (2018) 16:20–8. doi: 10.1016/S1875-5364(18)30026-8
21. Hwang E, Lin P, Ngo HTT, Gao W, Wang YS, Yu HS, et al. Icariin and Icaritin Recover UVB-Induced Photoaging by Stimulating Nrf2/ARE and Reducing AP-1 and NF-kappaB Signaling Pathways: A Comparative Study on UVB-Irradiated Human Keratinocytes. *Photochem Photobiol Sci: Off J Eur Photochem Assoc Eur Soc Photobiol* (2018) 17:1396–408. doi: 10.1039/C8PP00174J
22. Du M, Qiu Q, Gruslin A, Gordon J, He M, Chan CC, et al. SB225002 Promotes Mitotic Catastrophe in Chemo-Sensitive and -Resistant Ovarian Cancer Cells Independent of P53 Status *In Vitro*. *PloS One* (2013) 8:e54572. doi: 10.1371/journal.pone.0054572
23. Brabletz T, Kalluri R, Nieto MA, Weinberg RA. EMT in Cancer. *Nat Rev Cancer* (2018) 18:128–+. doi: 10.1038/nrc.2017.118
24. Sui H, Liu X, Jin BH, Pan SF, Zhou LH, Yu NA, et al. Zuo Jin Wan, a Traditional Chinese Herbal Formula, Reverses P-Gp-Mediated MDR *In Vitro* and *In Vivo*. *Evid Based Complement Alternat Med* (2013) 2013:957078. doi: 10.1155/2013/957078
25. Li XJ, Zhang HY. Western-Medicine-Validated Anti-Tumor Agents and Traditional Chinese Medicine. *Trends Mol Med* (2008) 14:1–2. doi: 10.1016/j.molmed.2007.11.002
26. Chai S, To KK, Lin G. Circumvention of Multi-Drug Resistance of Cancer Cells by Chinese Herbal Medicines. *Chin Med* (2010) 5:26. doi: 10.1186/1749-8546-5-26
27. Tong JS, Zhang QH, Huang X, Fu XQ, Qi ST, Wang YP, et al. Icaritin Causes Sustained ERK1/2 Activation and Induces Apoptosis in Human Endometrial Cancer Cells. *PloS One* (2011) 6:e16781. doi: 10.1371/journal.pone.0016781
28. Guo Y, Zhang X, Meng J, Wang ZY. An Anticancer Agent Icaritin Induces Sustained Activation of the Extracellular Signal-Regulated Kinase (ERK) Pathway and Inhibits Growth of Breast Cancer Cells. *Eur J Pharmacol* (2011) 658:114–22. doi: 10.1016/j.ejphar.2011.02.005
29. Li S, Priceman SJ, Xin H, Zhang W, Deng J, Liu Y, et al. Icaritin Inhibits JAK/STAT3 Signaling and Growth of Renal Cell Carcinoma. *PloS One* (2013) 8:e81657. doi: 10.1371/journal.pone.0081657
30. Liu X, Chan D, Ngan H. Gynecology & Obstetrics Mechanisms of Chemoresistance in Human Ovarian Cancer at a Glance. *Gynecol Obstetr* (2012) 2:e104. doi: 10.4172/2161-0932.1000e104
31. Ghayad SE, Cohen PA. Inhibitors of the PI3K/Akt/mTOR Pathway: New Hope for Breast Cancer Patients. *Recent Patents Anti-Cancer Drug Discov* (2010) 5:29–57. doi: 10.2174/157489210789702208
32. Deng J, Wang L, Chen H, Hao J, Ni J, Chang L, et al. Targeting Epithelial-Mesenchymal Transition and Cancer Stem Cells for Chemoresistant Ovarian Cancer. *Oncotarget* (2016) 7:55771–88. doi: 10.18632/oncotarget.9908
33. Deng J, Bai X, Feng X, Ni J, Beretov J, Graham P, et al. Inhibition of PI3K/Akt/mTOR Signaling Pathway Alleviates Ovarian Cancer Chemoresistance Through Reversing Epithelial-Mesenchymal Transition and Decreasing Cancer Stem Cell Marker Expression. *BMC Cancer* (2019) 19:618. doi: 10.1186/s12885-019-5824-9
34. Gasparri ML, Besharat ZM, Farooqi AA, Khalid S, Taghavi K, Besharat RA, et al. MiRNAs and Their Interplay With PI3K/AKT/mTOR Pathway in Ovarian Cancer Cells: A Potential Role in Platinum Resistance. *J Cancer Res Clin Oncol* (2018) 144:2313–8. doi: 10.1007/s00432-018-2737-y
35. Lengyel CG, Altuna SC, Habeeb BS, Trapani D, Khan SZ. The Potential of PI3K/AKT/mTOR Signaling as a Druggable Target for Endometrial and Ovarian Carcinomas. *Curr Drug Targets* (2019) 21(10):946–61. doi: 10.2174/1389450120666191120123612
36. Li ZY, Li ZJ, Chen X, Huang XR, Fang ZQ, Zhang JG, et al. [Icaritin Reverses Multidrug Resistance of Multiple Myeloma Cell Line KM3/BTZ]. *Zhongguo Shi Yan Xue Ye Xue Za Zhi* (2017) 25:1690–5. doi: 10.7534/j.issn.1009-2137.2017.06.020
37. Sun L, Chen W, Qu L, Wu J, Si J. Icaritin Reverses Multidrug Resistance of HepG2/ADR Human Hepatoma Cells *via* Downregulation of MDR1 and Pglycoprotein Expression. *Mol Med Rep* (2013) 8:1883–7. doi: 10.3892/mmr.2013.1742

Conflict of Interest: The authors declare that the research was conducted in the absence of any commercial or financial relationships that could be construed as a potential conflict of interest.

this article, or claim that may be made by its manufacturer, is not guaranteed or endorsed by the publisher.

frontiers | Frontiers in Oncology

TYPE Review
PUBLISHED 03 October 2022
DOI 10.3389/fonc.2022.969731

OPEN ACCESS

EDITED BY
Patrick Ming-Kuen Tang,
The Chinese University of Hong Kong,
Hong Kong SAR, China

REVIEWED BY
Chiu Tsun Philip Tang,
The Chinese University of Hong Kong,
Hong Kong SAR, China
Li-Juan Deng,
Jinan University, China

*CORRESPONDENCE
Zhen Chen
zchenzl@fudan.edu.cn

†These authors have contributed equally to this work and share first authorship

SPECIALTY SECTION
This article was submitted to Molecular and Cellular Oncology, a section of the journal Frontiers in Oncology

RECEIVED 15 June 2022
ACCEPTED 29 August 2022
PUBLISHED 03 October 2022

CITATION
Cheng C-s, Yang P-w, Sun Y, Song S-l and Chen Z (2022) Fibroblast activation protein-based theranostics in pancreatic cancer.
Front. Oncol. 12:969731.
doi: 10.3389/fonc.2022.969731

Fibroblast activation protein-based theranostics in pancreatic cancer

Chien-shan Cheng[1,2,3†], Pei-wen Yang[1,2†], Yun Sun[4], Shao-li Song[2,5] and Zhen Chen[1,2*]

[1]Department of Integrative Oncology, Shanghai Cancer Center, Fudan University, Shanghai, China, [2]Department of Oncology, Shanghai Medical College, Fudan University, Shanghai, China, [3]Department of Traditional Chinese Medicine, Shanghai Jiao Tong University School of Medicine Affiliated Ruijin Hospital, Shanghai, China, [4]Department of Research and Development, Shanghai Proton and Heavy Ion Center, Fudan University Cancer Hospital, Shanghai, China, [5]Nuclear Medicine Department, Shanghai Cancer Center, Fudan University, Shanghai, China

Fibroblast activation protein-α (FAP) is a type II transmembrane serine protease that has specific endopeptidase activity. Given its well-established selective expression in the activated stromal fibroblasts of epithelial cancers, although not in quiescent fibroblasts, FAP has received substantial research attention as a diagnostic marker and therapeutic target. Pancreatic cancer is characterized by an abundant fibrotic or desmoplastic stroma, leading to rapid progression, therapeutic resistance, and poor clinical outcomes. Numerous studies have revealed that the abundant expression of FAP in cancer cells, circulating tumor cells, stromal cells, and cancer-associated fibroblasts (CAFs) of pancreatic adenocarcinoma is implicated in diverse cancer-related signaling pathways, contributing to cancer progression, invasion, migration, metastasis, immunosuppression, and resistance to treatment. In this article, we aim to systematically review the recent advances in research on FAP in pancreatic adenocarcinoma, including its utility as a diagnostic marker, therapeutic potential, and correlation with prognosis. We also describe the functional role of FAP-overexpressing stromal cells, particulary CAFs, in tumor immuno- and metabolic microenvironments, and summarize the mechanisms underlying the contribution of FAP-overexpressing CAFs in pancreatic cancer progression and treatment resistance. Furthermore, we discuss whether targeting FAP-overexpressing CAFs could represent a potential therapeutic strategy and describe the development of FAP-targeted probes for diagnostic imaging. Finally, we assess the emerging basic and clinical studies regarding the bench-to-bedside translation of FAP in pancreatic cancer.

KEYWORDS

pancreatic adenocarcinoma, fibroblast activation protein-α, cancer-associated fibroblasts, FAPI imaging, cancer theranostics

1 Introduction

Pancreatic adenocarcinoma (PAAD) is a highly aggressive and lethal cancer requiring novel diagnostic and therapeutic approaches. Characterized by an abundant fibrotic and extensive desmoplastic stromal response, cancer-associated fibroblasts (CAFs) are the most abundant component of the PAAD stroma. CAFs accumulate in pancreatic tumor tissue, wherein they enhance collagen family protein and fibronectin expression in a paracrine manner, thereby maintaining and remodeling the extracellular matrix structure. They also generate multiple factors, including exosomes, growth factors, immune- and metabolism-associated metabolites in an autocrine manner to communicate with cancer cells. Moreover, they contribute to promoting the desmoplastic response and mediate the early invasion, high recurrence rate, and treatment resistance of PAAD (1). Owing to abundant extracellular matrix deposition, vasculature, and fibroblasts, the pancreatic cancer stroma acts as a firm haven protecting cancer cells from different interventions, thereby contributing to treatment resistance. Thus, rather than playing the roles of a mere tumorigenic onlooker, the desmolastic stroma functions as an active participant in pancreatic cancer progression, invasion, migration, metastasis, immunosuppression, and resistance to treatment. Therefore, CAFs have become an attractive therapeutic target in the stroma of pancreatic cancers (Figure 1).

Fibroblast activation protein-α (FAP), named after its activating role, is a type II transmembrane serine protease with specific endopeptidase activity that is upregulated in different cancer types. Given its well-established selective expression in the activated stromal fibroblasts of epithelial cancers, although not in quiescent fibroblasts, FAP has received considerable research attention as a diagnostic marker and therapeutic target. FAP was first identified in 1986 by Wolfgang Rettig based on its role in activating fibroblasts (2). Initial research conducted on FAP focused on its role as a cell surface antigen. Subsequent studies, however, revealed that FAP could be shed from the cell membrane, thereby undergoing conversion to a soluble derivative referred to as circulating antiplasmin-cleaving enzyme (APCE) (3). In normal tissues and plasma, FAP is typically expressed at low levels and appears to serve as a redundant or non-essential protease in developmental processes. However, FAP was subsequently established to be involved in diverse pathological processes, including wound healing; inflammation, such as arthritis, atherosclerosis, and fibrosis; and epithelial cancers. The abundant expression of FAP in cancer and stromal cells, and particularly in CAFs, has been implicated in different cancer-related signaling pathways, thereby contributing to cancer progression, invasion, migration, metastasis, immunosuppression, and resistance to treatment. Consequently, FAP^+ CAFs have emerged as important regulators and potential treatment targets.

The high levels of FAP expression in pancreatic cancer stroma have also been correlated with the poor prognosis of patients and desmoplasia (4, 5), and FAP has been identified as an independent predictor of pancreatic cancer survival (6, 7). The extensive fibrotic matrix of PAAD serves as a physical barrier that contributes to resistance to chemoradiotherapy or immunotherapy. Treatment paradigms targeting cancer cells are unable to overcome this obstacle, and consequently, considerable research effort has been devoted to characterizing the mechanisms underlying the treatment resistance of PAAD and identifying novel therapeutic strategies that can target the associated stroma and fibroblasts. In this review article, we summarize the promising theragnostic role of FAP in PAAD, with the aim of gaining further insights regarding the clinical implications.

Abbreviations: FAP, fibroblast activation protein-α; APCE, antiplasmin-cleaving enzyme; CAFs, cancer-associated fibroblasts; PAAD, pancreatic adenocarcinoma; CPTAC, national cancer institute clinical proteomic tumor analysis consortium; PDAC, pancreatic ductal adenocarcinoma; DPP, dipeptidyl peptidase; ECM, extracellular matrix; BIBH 1, humanized version unconjugated sibrotuzumab; CAR-T, chimeric antigen receptor T; CXCL12, chemokine (C-X-C motif) ligand 12; CXCR4, chemokine (C-X-C motif) receptor 4; MDSCs, myeloid-derived suppressor cells; CCR2, CCL2 receptor; TAM, tumor-associated macrophage; HO-1, heme oxygenase-1; VEGF, vascular endothelial growth factor; TNF, tumor necrosis factor; PSCs, pancreatic stellate cells; TGFβ1, transforming growth factor-β; CTLA-4, cytotoxic T-lymphocyte-associated protein 4; PD-1, programmed cell death protein 1; PD-L1, programmed cell death protein ligand 1; CAT-T cells, chimeric antigen receptor T cells; CAP, cleavable amphiphilic peptide; BMSCs, bone marrow stromal cells; lncRNAs, long non-coding RNAs.

2 Clinicopathological significance and prognostic value of FAP in PAAD

2.1 FAP expression and its clinical significance in PAAD

According to the National Cancer Institute Clinical Proteomic Tumor Analysis Consortium (CPTAC) dataset, FAP protein expression is significantly higher in primary PAAD tumor tissues than in normal tissues. Similarly, stromal FAP expression has been detected in approximately 98% of specimens in a sample of 48 patients with surgically resected PAAD (7). Consistently, the findings of a further immunohistochemical study involving 134 patients with PAAD revealed that FAP was expressed in both stromal fibroblasts (98/134, 73.1%) and cancer cells (102/134, 76.1%), with expression being significantly associated with patient age ($p < 0.001$), tumor size ($p < 0.001$), fibrotic foci ($p = 0.003$), and

perineural invasion (p = 0.009) (4), thereby highlighting the importance of FAP in the clinicopathological characterization of PAAD.

In humans and some mammals, plasma contains small amounts of FAP, at concentrations of approximately 100 ng/mL or 0.6 nmol/L (8). FAP is also detectable in peripheral blood, the levels of which have been used for disease characterizations. For example, FAP has been used as a molecular marker in the identification of subpopulations of circulating tumor cell (9). Moreover, the measurement of FAP-specific substrates in body fluids has also been reported (10). However, as to whether the levels of FAP enzyme activity can serve as an informative diagnostic tool and in the assessment of disease progression in the clinical setting has yet to be sufficiently ascertained. Although the potential utility of FAP immunohistochemistry and plasma FAP as a biomarker in renal tumors for the differential diagnosis at an early stage have previously been reported (11), there have to date been no comparable studies with respect to pancreatic cancer.

2.2 FAP as a prognostic marker in PAAD

The overexpression of FAP has also been implicated in the poor prognosis of PAAD patients (shown in Figure 2). Survival analyses have revealed that high FAP expression is associated with lower overall survival (12). A KPC mice model in which FAP had been deleted was characterized by delayed primary tumor onset and a more prolonged survival (13). Studies have also shown that higher CD8 expression and lower FAP expression in stromal cells can independently predict the prognosis in PAAD patients, and that blockade of FAP may improve the prognosis of patients with PAAD. It may increase CD8 cell levels (6). Furthermore, a comprehensive transcriptome analysis (14) identified two four-hub gene modules (including FAP) as specific predictive features for PAAD diagnosis and prognosis, thereby providing a new perspective with respect to clinical trials. Moreover, by applying weighted gene co-expression network analysis, Wang et al. (15) established that FAP is involved in a core module associated with PAAD type. Collectively, the findings of these studies highlight the potential utility of FAP expression patterns as a prognostic marker and an immune checkpoint target in PAAD.

3 The role of FAP in the PAAD tumor microenvironment

Previous diagnostic and therapeutic paradigms have tended to focus almost exclusively on tumor cells, and have failed to make any significant breakthroughs in PAAD therapy during the past decade. In this context, it has been established that FAP is expressed predominantly in stromal cells, whereas only very low levels of expression are detected in cancer cells in resected pancreatic ductal adenocarcinoma (PDAC) tissues (7). At the cellular level, pancreatic cancer cell lines have been shown to express FAP protein to a greater or lesser extent (4), and mRNA at different levels (Figure 3). Furthermore, the expression of FAP has been shown to alter the expression of stromal extracellular matrix proteins, including tenascin C, collagen I, fibronectin, and α-SMA, and also to enhance fibronectin fiber patterned

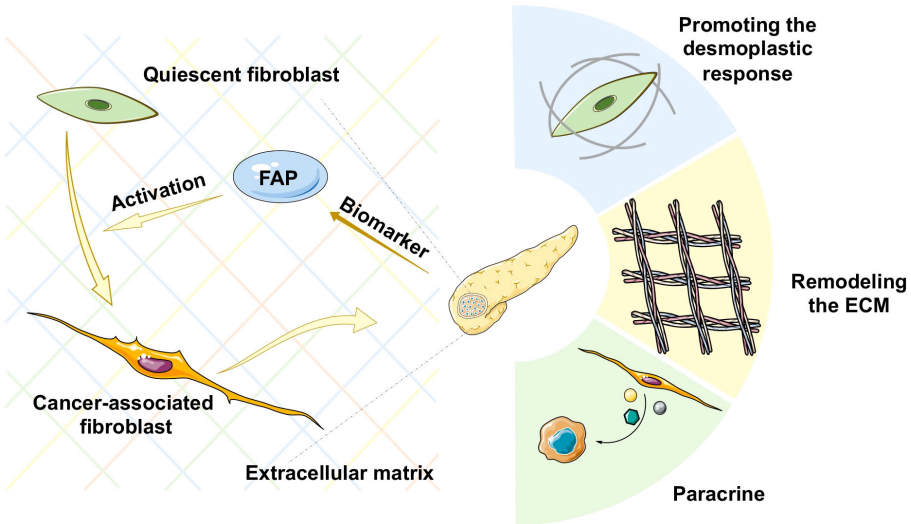

FIGURE 1
Schematic representation of various mechanisms of cancer-associated fibroblast (CAF) activation in pancreatic cancer. ECM, extracellular matrix.

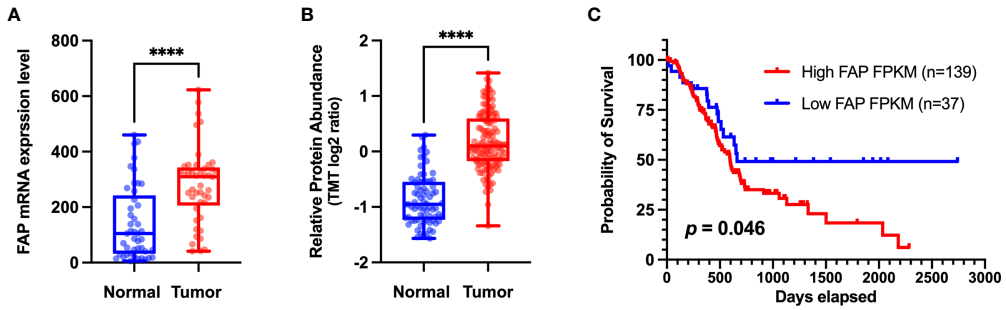

FIGURE 2
(A) Different levels of FAP mRNA expression in normal and tumor tissues. Transcriptome data of pancreatic adenocarcinoma (PAAD) and matched normal tissue were obtained from the Gene Expression Omnibus dataset (http://www.ncbi.nlm.nih.gov/geo) (GSE28735) for validation at the transcriptomic level. **(B)** Different levels of FAP protein expression in normal and tumor tissues. Proteome data were obtained from the CPTAC dataset (12) for validation at the protein level. **(C)** Overall survival analysis of two groups of patients with PAAD from The Cancer Genome Atlas (TCGA) database (https://portal.gdc.cancer.gov/). The Kaplan–Meier method was used to compare the survival of different FAP expression groups (the expression cutoff = 2.8), and the log-rank method was used for statistical analysis. GraphPad 9.0 software was used for data visualization. ****p < 0.0001.

orientation, thereby resulting in the rapid disease progression and increasing resistance to treatment (16). PAAD cells communicate with stromal cells, recruit fibroblasts, and activate these to yield cancer-associated fibroblasts. The finding of numerous studies have established the link between stromal-expressed FAP, particularly FAP$^+$ CAFs, and pancreatic cancer, thereby indicating the potential ultility of FAP as a target in PAAD treatment (Figure 4). Moreover, it has been found that FAP$^+$ stroma promotes cancer immune escape (17). In addition, findings relating to the enzymatic role, expressional patterns, and stroma modulation role of FAP in PAAD have provided insights for further examination of its pro-tumorigenic role and provided evidence to indicate that FAP could serve as both a novel marker in PAAD diagnosis and as therapeutic target (Figure 5).

3.1 The enzymatic role of FAP

FAP is a member of the dipeptidyl peptidase (DPP) 4 family of proteins that hydrolyzes a prolyl bond at sites two amino acids from the N-terminus of a protein. The cyclic character of proline residue makes targeting the specific catalytic ability of FAP attractive. However, the finding that mice in which FAP is not expressed show no an aberrant phenotype would tend to indicate that under physiological conditions, FAP is a redundant or non-essential protease (18).Moreover, in preclinical or clinical research, it has been demonstrated that inhibitors of FAP fail to have significant anti-cancer effect in preclinical or clinical research (19–21). These observations could be ascribed to one of several possible factors. Firstly, FAP could act indirectly on tumor cells, as has been indicated by the finding

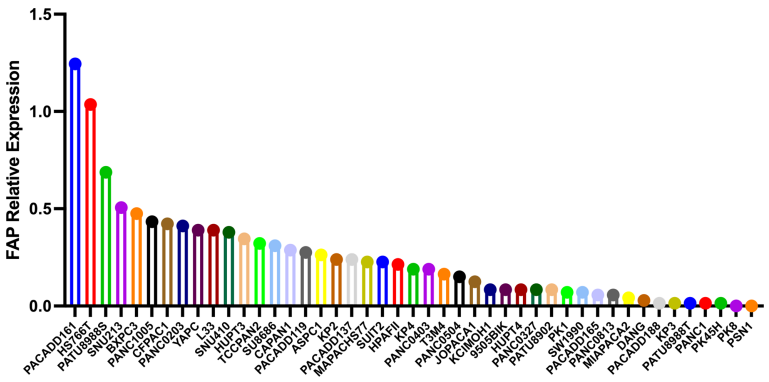

FIGURE 3
The different mRNA levels of FAP protein expression in pancreatic cancer cell lines using data obtained from the Motivations for the Cancer Cell Line Encyclopedia database (https://portals.broadinstitute.org/ccle).

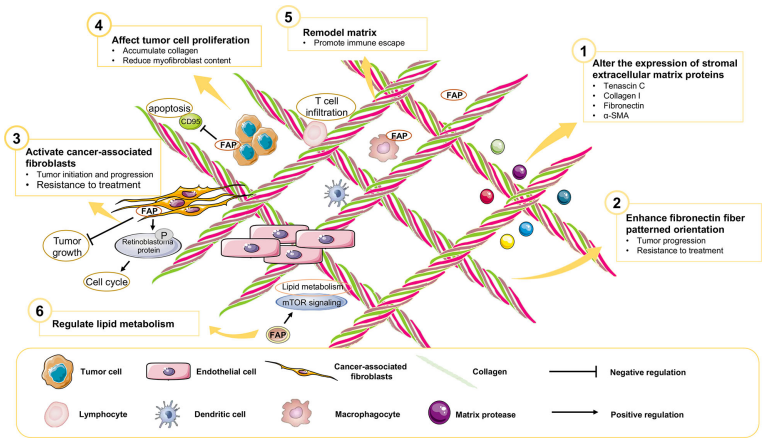

FIGURE 4
The role of FAP in the PAAD tumor microenvironment.

that the depletion of FAP indirectly inhibits tumor cell proliferation *via* an enhancement of collagen accumulation and the impediment of myofibroblast content (19). Mechanistically, it has been found that the regulation of FAP-1 enzymatic activity negatively regulates CD95 (Fas, APO-1)-mediated apoptosis in pancreatic cancer cells (22). Additionally, as a known collagen-degrading enzyme, FAP mediates matrix remodeling and in part regulates lipid metabolism *via* mTOR signaling (23). Secondly, the development of talabostat as an anti-cancer agent has focused mainly on its immune-mediated activity, and to date, there have been no studies that have specifically sought to evaluate the efficacy of talabostat in FAP-expressing tumors, or its use in combination with other targeted therapies. Collectively, these findings provide evidence to indicate a potential regulatory role of FAP under pathological conditions, and that this FAP-mediated regulation of lipid metabolism and remodeling of the extracellular matrix (ECM) could serve as a potential novel therapeutic target.

3.2 FAP$^+$ cells within the PAAD tumor microenvironment

Despite efforts designed to suppress the expression and enzymatic activity of FAP as anti-cancer treatments, studies, such as those involving the development of a murine anti-FAP mAb F19 and its humanized version unconjugated sibrotuzumab (BIBH 1) (24–26), have failed to demonstrate promising clinical

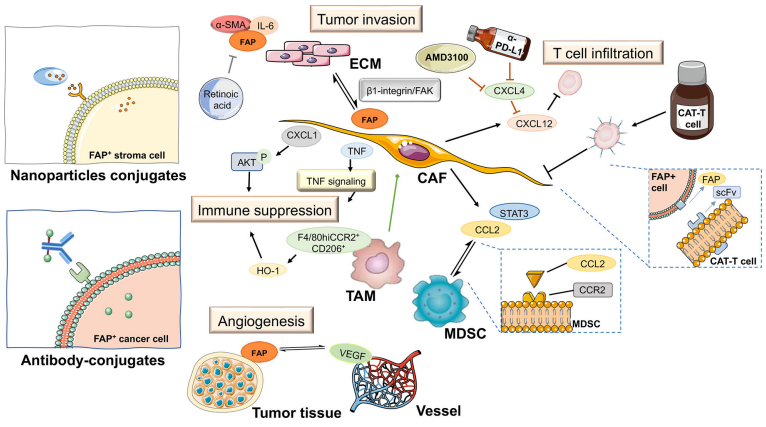

FIGURE 5
FAP-targeted therapies and their expected impact on pancreatic tumor tissue. ECM, extracellular matrix; TAM, tumor-associated macrophage; CAT-T cell, chimeric antigen receptor T cell; MDSC, myeloid-derived suppressor cell; CAF, cancer-associated fibroblast; scFv, fragments of single-chain antibody.

efficacy. On the basis of the studies conducted to date, there is no evidence to indicate that direct targeting of FAP would be either safe or effective. Consequently, given the overexpression of FAP in a wide variety of stromal cells during tumorigenesis, this would tend to identify the stroma as a target for anti-cancer drugs. Indeed, it has been found that depletion of FAP^+ cells has the effect of delaying subcutaneous tumor growth and contributes to the development of a more immunogenic environment, thereby indicating that FAP-expressing stromal cells could play important roles as immunomodulators (27).

Malignant cells drive the generation of desmoplastic and immunosuppressive tumor microenvironments, and emerging evidence indicates that FAP is aberrantly expressed in CAFs, chimeric antigen receptor T (CAR-T) cells, and a subset of M2 macrophages. Furthermore, FAP-expressing cells have also been associated with the degradation of extracellular matrix proteins and glycosaminoglycans, as well as a reduction in tumor vessel density, which jointly contributes to the continual remodeling of the tumor microenvironment during the progression of PAAD. Furthermore, the emerging development of nanoparticle conjugates and antibody-conjugates is offering a potentially wide range of therapeutic options from the perspective of targeting FAP in cancer.

3.2.1 FAP^+ CAFs associated with immunosuppressive tumor stroma

CAFs are the main component of the PAAD stroma, thereby indicating that targeting CAFs could represent a viable therapeutic strategy. CAFs play a pleiotropic role in PAAD initiation and progression, and in line with expectations, it has been demonstrated that depletion of CAFs can accelerate tumor progression (28, 29). In this context, attention has focused on targeting precise subpopulations of CAFs that are known to be oncogenic and pro-progression, particularly FAP-positive CAFs. These FAP-expressing CAFs have been proposed to accelerate proliferation, invasion, and therapeutic resistance in ovarian cancer cells (30), and have also been suggested to reprogram tumor inflammatory environments in human intrahepatic cholangiocarcinoma *via* FAP-STAT3-CCL2 signaling (31). However, in-depth research on PAAD cells is still lacking. By promoting retinoblastoma protein phosphorylation, FAP^+ CAFs have been suggested to alter the cell cycle of co-cultured PAAD cells (7). Furthermore, the depleting of FAP-expressing cells (including all FAP^+ CAFs), has been found to delay tumor growth in a subcutaneous model of PAAD (27).

It is well established that PAAD is highly resistant to immunotherapy, and it has been demonstrated that FAP-positive stromal cells (including almost all the CAFs) mediated local immunosuppression and immune escape, thereby compromising the efficacy of immunotherapy, and in particular, immune checkpoint blockade treatment (27, 32). Studies have indicated that the production of chemokine (C-X-C motif) ligand 12 (CXCL12) by FAP^+ CAFs within the cancer cell-rich region of a tumor impedes T cell infiltration leading to immunosuppression (32). To counteract this suppressive effect, a synergized treatment approach has been proposed, which entails inhibition of the CXCL12 receptor by the suppression of chemokine (C-X-C motif) receptor 4 (CXCR4) using α-PD-L1, a checkpoint antagonist. This was demonstrated to promote T-cell accumulation and contribute to tumor regression (32). Recently, a CXCR4 small-molecule inhibitor, AMD3100 (plerixafor), was assessed in a phase I clinical trial (NCT02179970) that aimed to evaluate its safety in PAAD patients. The findings of the comparative transcriptional analysis revealed an unusually rapid enhancement of intra-tumoral B and T cell responses within 7 days of treatment, thereby indicating the possible induction of an integrated anti-cancer immune response. Given these promising findings, further clinical trials are warranted that evaluate responses in a larger number of patients who have undergone repeated cycles of combination therapy with CXCR4 inhibitor and immune checkpoint antagonist, along with additional studies examining tolerability, pharmacokinetics, and pharmacodynamics to further assess the therapeutic activity.

However, the fact that several well-established biomarkers of CAFs are also typically expressed on the surface of other cell types, raises the likelihood that CAF-targeted therapy might have certain unwanted side effects. As an alternative strategy for the treatment of PAAD, researchers are examining the effects of blocking the interactions between CAFs and their neighboring cells. Determining the mechanisms underlying the accumulation of CAFs in cancer and developing methods that can be used to identify different CAF subsets in the tumor microenvironment will contribute to establishing therapeutic strategies that could convert the tumor-promoting microenvironment into a tumor-suppressing microenvironment. Considerable evidence has accumulated to indicate that FAP plays an important role in this alteration, and thus further research on the synergetic roles of FAP^+ CAFs in PAAD immunotherapy is warranted.

3.2.2 Crosstalk between FAP^+ CAFs and MDSCs and TAMs

The infiltration of immature myeloid cells, including the myeloid-derived suppressor cells (MDSCs) and macrophages, is one of the well-defined hallmarks of cancer (33). In this regard, Yang et al. (31) have demonstrated that FAP^+ CAFs can enhance the recruitment of MDSCs *via* STAT3-CCL2 signaling and thereby promote tumor progression in a murine liver tumor model. FAP^+ CAFs are characterized by a distinct inflammatory phenotype of STAT3 activation and pro-inflammatory cytokine CCL2 upregulation. As the primary source of CCL2, FAP^+ CAFs undergo crosstalk with circulating MDSCs expressing the CCL2 receptor (CCR2), thereby forming a CCL2–CCR2 axis that plays a role in mediating tumor promotion. In line with expectations, it has been observed that the tumor progression promoting and MDSC recruiting effects of FAP^+ CAFs are abolished in Ccr2-

deficient mice. However, current evidence indicates that the activity of tumoral FAP^+ stromal cells contributes to immune suppression, the function of FAP^+ CAFs in the recruitment of MDSCs in PAAD remains largely undetermined, and accordingly warrants further investigations.

Recently, a direct mechanism has been proposed for the generation of CAFs, which indicates that tumor-associated macrophage (TAMs) expressing CAF markers could be a potential source of CAFs (34, 35). The findings of research have indicated that these FAP-positive cells comprise two subpopulations, namely, a $CD45^-$ mesenchymal subset and a $CD45^+$ hematopoietic subset (36). In this regard, a previous study on immunogenic Lewis lung carcinoma cells identified FAP^+CD45^+ cells as a subset of $F4/80^{hi}CCR2^+CD206^+$ M2 macrophages and the main tumoral source of the immune inhibitory enzyme heme oxygenase-1 (HO-1). The depletion of FAP^+CD45^+ cells or administration of the HO-1 inhibitor Sn mesoporphyrin has been shown to promote the immune-dependent arrest of subcutaneous tumor growth (36). Moreover, $FAP^+/F4/80^+/HO\text{-}1^+$ stromal cells have been identified in a PAAD subcutaneous tumor model. Sn mesoporphyrin has been established to induce an immune response to a currently unidentified antigen(s) and inhibits tumor growth in a tumor-bearing mouse model of PAAD (37). In PAAD, TAMs in the tumor stroma also secretes FAP, shifting their phenotype to an immunosuppressive M2 macrophage type, suppressing the adaptive immune response, and promoting a positive feedback loop in PAAD progression (37).

3.2.3 T cells and tumor-infiltrating lymphocytes

PAAD is histologically characterized by a large stroma volume, and previous studies have consistently reported the suppression of intra-tumoral effector T-cells by the FAP-expressing stromal cells among different cancer types (27, 32, 38). In PAAD, FAP^+ CAF-abundant areas have been shown to be characterized by limited $CD8^+$ lymphocytes infiltration, thereby indicating the contribution to the spatial exclusion of intra-tumoral $CD8^+$ T cells (39), along with Tregs and neutrophil accumulation and cancer-associated pathways modulation (40). Given that heterogeneous and differential FAP^+ CAFs in PAAD tumors may be involved to varying degrees in stromal variation, immunosuppression, and differential responses to potential immunotherapy, further experimental studies are necessary to clarify the potential causal inference.

3.2.4 The extracellular matrix and tumor vascularity

In addition to cellular constituents, important components of the tumor microenvironment include the ECM, blood vessels, and cytokines (41). FAP activity has been found to direct stromal ECM organization *via* β1-integrin-dependent cell matrix interactions, in which suppression of FAP activity limits β1-integrin/FAK-mediated invasive capacity in PAAD cells (16). Moreover, the findings of a further study have indicated that retinoic acid, a vitamin A derivative, plays a role in transforming FAP-activated CAFs into static fibroblasts *via* the down-regulated expression of α-SMA, FAP, and IL-6 and the inhibition of the ECM production (42). These findings provide important insights regarding the selective targeting of the main source of ECM proteins and highlight the potential utility of FAP-mediated disruption of the ECM as a novel therapeutic approach for PAAD.

Levels of vascular endothelial growth factor (VEGF), a promotor of angiogenesis and biomarker of vessel density, are found to be raised in PDAC tissues and are linked to liver metastases and poor prognosis. It has previously been demonstrated that in the cancerous tissues of PAAD patients, the expression of FAP is positively correlated with VEGF (41). This significant positive correlation between FAP and VEGF indicates that the two factors conjunctly influence PAAD survival, and that contributing to the complexity of these interactions are pericytes, inflammatory cells, and fibroblastic cells, which together with PAAD cells, shape the tumor vasculature.

Cytokines and chemokines, including tumor necrosis factor (TNF), and CXCL1, secreted by FAP^+ CAFs contribute to the further suppression of adaptive immunity in PAAD (38, 43) and are currently attracting considerable attention among researchers. Moreover, with an increasing number of studies focusing on TNF, its roles in fibroblasts within the tumor microenvironment have gradually become more precisely elucidated, and it has accordingly been established that its functions are not confined to merely driving fibroblast activation. However, the tumor-promoting and immunosuppressive activity of FAP^+ fibroblasts have been demonstrated to suppress TNF signaling (27, 44, 45), thereby contributing to cancer–stroma–cancer interaction loop that promotes tumor progression (46). For example, the pancreatic stellate cells (PSCs), the FAP^+ resident cells of the pancreas, have been implicated in cancer-related fibrosis, induction of PAAD migration, and invasion *via* the activation of CXCL1-mediated AKT phosphorylation. Furthermore, the secretion of transforming growth factor-β1 (TGF-β1) PAAD cells has been observed to induce the expression of FAP in hitherto quiescent PSCs, thereby promoting a further releasing CXCL1, promoting tyrosine kinase receptors phosphorylation, and forming a positive feed-forward loop promoting PAAD progression (47). Collectively, the multifarious aspects of the tumor microenvironment provide a pool of secreted cytokines that stimulates or suppresses different components of this microenvironment, thereby contributing to the progression of PAAD.

4 Immunotherapeutic targeting of FAP$^+$ cells

As previously mentioned, the FAP$^+$ stroma and CAFs play pivotal roles in mediating the immunosuppressive characteristics of PAAD (32) and are responsible for the ineffective activity of known T-cell checkpoint antagonists. Cytotoxic T-lymphocyte-associated protein 4 (CTLA-4) and programmed cell death protein 1 (PD-1) or its ligand PD-L1 function as important checkpoint receptors on T cells, and accordingly present ideal targets for inhibition by antagonistic antibodies. However, given the ineffectual nature of immunotherapy and therapeutic approaches. In this regard, targeting tumoral FAP$^+$ stromal cells is seen as a novel alternative therapeutic option. Emerging evidence indicates that the malignant behavior of PAAD, such as resistance to treatment, immune escape, and metastasis, is associated with the complex interaction between stromal and tumor cells. However, the current therapeutic paradigm focuses on tumor-stroma interactions in PAAD rather than the expression of FAP protein. It is believed that gaining a better understanding of the role of this protein in the FAP-mediated interaction between stroma and tumor cells could contribute to optimizing the FAP-inhibition strategy.

4.1 The FAP$^+$ CAR-T

Chimeric antigen receptor T cells (CAT-T cells) are genetically engineered T cells that are becoming increasingly widely used as components in novel types of anti-cancer immunotherapy. T cells contain fragments of a single-chain antibody that can recognize predefined surface antigens, thus enabling T cells to effectively identify and target cancer cells, and thereby affording a considerable range of opportunities to modify and improve CAR T cell therapy. Traditionally, predefined surface antigens on cancer cells have been the primary targets in anti-cancer therapy. However, the findings of recent studies have identified a number of antigens, which, although expressed at very low levels on normal cells, are highly expressed on the surface of tumor stromal cells, thereby indicating their potential value as novel targets for CAR T cell therapy that can minimize on-target/off-tumor toxicity. This has thus stimulated an increasing interest in the development of CAR tools with FAP specificity for T cell modification.

Studies using mouse models have shown that FAP-CAR T cells can exhaust FAP-expressing stromal cells and inhibit tumor growth by producing immunostimulatory cytokines, promoting tumor cytolysis (48), and enhancing the anti-tumor response of endogenous CD8$^+$ T cells (49). Moreover, synchronously targeting both malignant cells and FAP$^+$ stroma has been established to produce a robust anti-tumor effect. However, the findings of a further study have indicated that the presence of highly reactive FAP-specific CAR-modified T cells can promote severe cachexia and dose-limiting bone toxicity without significantly affecting tumor suppression among different syngeneic tumor implantation models in mice. These observations tend to indicate that FAP-expressing stroma derived from different sources might contribute to contrasting outcomes. Hence, this emphasizes the necessity to take into consideration the location of FAP expression in stromal cells during PAAD initiation and progression and the requirement for a more precise biomarker of FAP+ CAFs. These results warrant further assessment for optimizing FAP-specific CAR in preclinical and clinical trials of human PAAD.

The findings of studies that have used murine pancreatic cancer models have tended to indicate that the adoptive transfer of FAP-CAR T can also inhibit tumor growth in an immune-independent manner (50–52). Furthermore, the adoptive transfer of FAP-targeted CAT-T cells has been demonstrated to reduce tumor vascularity, ECM proteins, and glycosaminoglycans (48, 53, 54). Moreover, FAP-specific CAR T transfer has been found to selectively recognizes and depletes the FAP$^+$ subsets of cancer stem cells, which play a vital role in maintaining the tumor stroma and eliminating FAP$^+$ CAFs. Consequently, the adoptive transfer of FAP-CAR T has provided insights that will contribute to the further development of FAP$^+$-specific stromal cell-targeted therapies for treating PAAD by targeting FAP$^+$ cells in the tumor microenvironment.

4.2 PD-1/PD-L1

Investigations that have focused on the depletion of FAP$^+$ cells in the PAAD tumor microenvironment have revealed an anti-tumor effect associated with α-CTLA-4 and α-PD-L1 treatment, thereby providing further evidence in support of the immune-suppressive role of FAP$^+$ stromal cells in the poor responsiveness to T-cell checkpoints antagonists. As previously mentioned, CXCL12 produced by FAP$^+$ CAFs may direct tumor immune evasion in a model of human PAAD and synergized treatment of CXCL12 receptor inhibition with α-PD-L1 (32), thereby remodeling the immunosuppressive microenvironment. In this context, Ji et al. (55) designed a cleavable amphiphilic peptide (CAP) marker to be specifically responsive to FAP stroma, in which, at the site of FAP$^+$ cell abundance, the CAP was cleaved, and nanoparticles rapidly disassembled and unloaded the drug into a solid tumor. In addition, an amphiphilic bifunctional PD-1/PD-L1 peptide antagonist has been developed to deliver doxorubicin and R848 after being cleaved by FAP, which in combination with PD-1 blockade therapy was observed to trigger a stronger immune response on activating immunogenic cell death and reprogramming tumor-associated macrophages (56). Furthermore, it is worth noting that stromal factors such as TGF-β and FAP, which are commonly characterized by altered expression in PAAD, were found to be associated with resistance to neoadjuvant

atezolizumab therapy (targeting PD-1, PD-L1) in operable urothelial carcinoma in the ABACUS trial (NCT02662309) (57). The findings of these studies thus indicate the utility of FAP as a clinical biomarker in T-cell checkpoint antagonist treatments, and consequently, have potential implications for comparable treatment in PAAD warrants further studies.

Currently, several clinical trials targeting FAP, especially RO6874281, are ongoing across cancers. An immunocytokine RO6874281 is composed of an interleukin-2 variant (IL-2v) targeting FAP and pembrolizumab (anti-PD-1), leading to the blockade of T cells migration. RO6874281 is applied to immunotherapy of several cancers, including renal cell carcinoma (NCT03063762), metastatic melanoma (NCT03875079), solid tumor, breast cancer, and cancer of head and neck (NCT02627274), and metastatic PAAD (NCT03193190). These trials are active or recruiting, without results yet, but their preclinical studies are promising. Therefore, it is valuable to keep a watchful eye on the results.

4.3 Novel nanoparticle conjugates and antibody-conjugates

As a protease, FAP has also been exploited in drug innovation studies, and several methods have been adopted that target FAP-expressing cells based on FAP enzyme activity. For example, nanomaterial-based drug delivery systems are a common platform used to deliver drugs to tumor sites. In this regard, the stroma can act as a barrier that impedes the passage of drugs targeting tumor sites. However, the aberrant expression of FAP provides a strategy for overcoming this impediment, namely, the development of smart nanomaterials that respond to FAP-positive CAFs. Nanomaterial-based drug delivery systems have shown considerable opportunity to optimize the drug specificity, biocompatibility, and pharmacokinetic features of these materials.

Sum et al. (58) have assessed a bispecific FAP-CD40 antibody that triggers a potent FAP-dependent stimulation of CD40, thereby enhancing tumor-specific T-cell priming and inducing tumor growth inhibition *in vivo*. By specifically inducing CD40 stimulation in the presence of FAP, this novel bispecific antibody was demonstrated to overcome the systemic toxicity associated with the CD40 agonist, thereby providing a promising approach for cancer immunotherapy. A further antibody-conjugate targeting FAP, FAP5-DM1, has also been shown to have an inhibitory effect on tumor progression, inducing complete regression in a PAAD xenograft model with good efficacy and tolerability (59). These studies have accordingly demonstrated the potential utility of combined targeting antibody conjugates as novel drug candidates for PAAD and stimulated further clinical translational studies toward clinical applications.

Although immune checkpoint blockade has shown promising results in the treatment of various cancers, the extensive fibrotic matrix and immunosuppressive effect of the PAAD tumor microenvironment have tended to hinder its wider application. In this respect, Yu et al. have proposed the use of novel thermo- and fibrotic matrix-sensitive liposomes encapsulating small-sized albumin nanoparticles loaded with an immune checkpoint inhibitor (BMS-202). Exposure to FAP and near-infrared laser radiation, with a mild elevation in localized temperature, induces the release of this agent at localized sites, thereby promoting the recovery of T lymphocyte activities within the immunosuppressive tumor microenvironment (60). By enhancing the accumulation of immune checkpoint inhibitors at the tumor site, these novel nanoparticles can promote the localized secretion of cytokines such as TNF-α and INF-γ, and potentiates the anti-tumor immune response in PAAD.

4.4 Safety concerns

Despite significant advances in research on FAP as an anti-cancer target candidate with broad clinical application prospects in conjunction with checkpoint blockade immunotherapy of solid tumors, the potentiality of lethal adverse effects should be taken into consideration when targeting FAP for immunotherapeutic purposes. The findings of previous studies have indicated that targeting FAP triggers the recognition of multipotent bone marrow stromal cells, whereas cachexic mouse and human pluripotent bone marrow mesenchymal stem cells (BMSCs) are recognized by FAP-reactive T cells (61). Fatal ototoxicity and cachexia observed following cell-based immunotherapy against FAP accordingly cautions against its use as a generic target. Furthermore, as FAP expression by pluripotent BMSCs may point to the cellular origin of tumor stromal fibroblasts and at least in part result from the universal recognition of FAP-reactive T cells on multipotent BMSCs, lethal bone marrow hypocellularity and necrosis, and cachexia have been observed subsequently to FAP-targeting immunotherapy (61). Additionally, long non-coding RNAs (lncRNAs), which are expressed in cell-type and disease-specific manners, have been demonstrated to contribute to the development and activation of CAFs (62, 63). In turn, these activated CAFs can promote tumor development by affecting the gene expression and secretory properties of cells, altering the tumor microenvironment, and enhancing malignant biological processes in cancer cells *via* lncRNAs. These observations provide evidence to indicate that FAP^+CAFs-specific lncRNAs could potentially be targeted for PAAD therapy without affecting the FAP expression of normal cells. In addition to these plausible obstacles, other challenges remain and should be carefully assessed to avert the potential risks of systemic toxicity when targeting FAP. Accordingly, prior to translational research evaluating the utility of FAP-related therapy, a comprehensive assessment of the safety and toxicity of these treatments using different animal models is of the utmost necessity.

5 Targeting FAP$^+$ CAF using diagnostic imaging and radioligand therapy probes

In preclinical and clinical trials, FAP-targeting molecular imaging radiotracers have shown promising results with respect to tumor diagnosis. At present, the clinical assessment of FAP-targeting radiotracers is primarily performed in small cohorts of patients in single-center studies. However, small sample populations and certain disparities among studies have led to difficulties in drawing definitive conclusions. Given the widely reported potential for oncological diagnosis, application of the [^{68}Ga]Ga-FAPI-04 probe, for example, has been reported in clinical trials (NCT04554719 and NCT04605939) with the uptake of [^{68}Ga]Ga-FAPI-04 in benign pancreatic lesions being demonstrated (64). Nevertheless, in low [^{18}F]F-FDG-avid tumors, such as in PAAD, [^{68}Ga]Ga-FAPI PET/CT shows high sensitivity in detecting primary pancreatic tumors, involved lymph nodes, and metastases, and is superior in terms of TNM staging (65), thereby indicating the potential utility of [^{68}Ga]Ga-FAPI-PET/CT as an effective imaging tool. Consequently, upon diagnosis, it is essential to undertake a comprehensive pathological assessment.

Furthermore, when applied in combination with magnetic resonance imaging (MRI), the [^{68}Ga]Ga-FAPI-04 PET/MR probe may enhance diagnostic sensitivity and prevent the misdiagnosis of certain pancreatic lesions. Although compared with the current gold standard contrast-enhanced CT, FAPI-PET/CT appears to be a superior imaging modality for pancreatic cancer (66), prospective trials with larger patient populations are needed to evaluate whether [^{68}Ga]Ga-FAPI PET/CT can elicit treatment modification in PAAD when compared with other imaging methodologies. Similarly, a preliminary study has reported the diagnostic potential of ^{18}F-FAPI-74 in FAP-expressing PAAD xenografts with higher tumoral uptake than [^{68}Ga]Ga-FAPI-04, thereby highlighting the advantageous properties of ^{18}F, notably the higher rate of detection and wide availability [https://jnm.snmjournals.org/content/62/supplement_1/1492/tab-article-info].

In pancreatic cancer, FAP-targeted radiotracers have been proposed as a diagnostic and therapeutic tool. For example, [^{64}Cu]FAPI-04 and [^{225}Ac]FAPI-04 have shown utility in theranostics for the treatment of FAP-expressing PAAD (67), whereas application of the albumin binder-conjugated FAPI radiotracers [^{177}Lu]TEFAPI-06 and [^{177}Lu]TEFAPI-07 has been found to promote substantial growth inhibition in patient-derived PAAD xenografts with negligible side effects (68). Other radiotracers, such as [177Lu]FAPI-46 and [225Ac]FAPI-4, have both demonstrated rapid renal clearance, relatively high intra-tumoral accumulation, and tumor-suppressive effects in PAAD xenografts, with a slight reduction in body weight (69). Furthermore, FAP-targeted radioligand therapy with ^{90}Y-FAPI-46 has also been assessed in three patients with advanced PAAD (70). The administration of low radiation doses to at-risk organs suggests the feasibility of repeat cycles of ^{90}Y-FAPI-46 with well-tolerated treatment and a low rate of attributable adverse events. However, although evidence of tumor response was observed following ^{90}Y-FAPI-46 treatment, further studies are warranted to determine efficacy and the toxicity profile in a larger cohort (71).

Given that the FAP is generally expressed at low levels on non-malignant cells, numerous studies have focused on targeting FAP$^+$ CAF to achieve precise imaging of solid tumors and assess potential treatments (72). Since the development of [^{89}Zr]Zr-B12 IgG as a selective imaging probe for FAP-expressing tumors, a series of compounds with the general structure of EB-FAPI-Bn have been synthesized based on FAP inhibitor (FAPI) variants (73), including 99mTc-labeled FAPI tracers for SPECT imaging and 188Re therapy (74). However, the rapid clearance of these molecules and their inadequate tumor retention have hindered them from further clinical translation into cancer therapeutics.

6 Conclusion

Examination of the complex and highly heterogeneous characteristics of tumors and the tumor microenvironment may lead to the development of novel treatments that can contribute to reducing suffering and enhance the overall prognosis of PAAD patients. Studies have shown that the desmoplastic response in PAAD is not only a "bystander" but also a source of dynamic cellular and non-cytokinetic factors that promote tumor progression, immunosuppression, and metastasis. To date, the findings of numerous studies have confirmed the potential value of FAP expression patterns as prognostic markers and immune checkpoint targets in PAAD. They have also unraveled the role of this enzyme in crosstalk with other cellular components of the tumor microenvironment, as well as non-cellular components, such as cytokines and chemokines, and have thereby provided insights on angiogenesis, matrix remodeling, and immunosuppression.

As an oncogenic subset of CAFs, FAP$^+$ CAFs mediate local immunosuppression and immune escape. FAP$^+$ CAFs have emerged as a therapeutic paradigm for new PAAD drug candidates with the development of novel nanoparticle conjugates and antibody-conjugates, which will contribute to overcoming matrix barriers to drug delivery, thereby facilitating the rapid accumulation of immune checkpoint inhibitors at tumor sites. Moreover, FAP-specific modification of CAR T cells can contribute to the depletion of FAP-expressing stromal cells and inhibit tumor growth by promoting the production of immunostimulatory cytokines, inducing tumor cell lysis, enhancing the anti-tumor response of endogenous CD8$^+$ T cells, and favoring the anti-tumor effects of α-CTLA-4 and α-PD-L1 therapy.

Nevertheless, deciphering the complex interactive processes between tumor and stroma cells in PAAD warrants considerable further study. Although investigations that focus on the target-

specific elimination of cancerous cells or pro-tumorigenesis components of the tumor microenvironment will undoubtedly contribute to identifying specific treatment options, future research should not be limited to singular components of PAAD. Studies on multiple compartments of the tumor microenvironment that evaluate combinations of drugs that target both tumors and stroma, as well as the inhibition of cancer-promoting signaling pathways and checkpoints, will aid in developing therapeutic targets and agents that are cytotoxic to cancerous cells and activate anti-tumor immune responses. In PAAD in particular, approaches designed to overcome the current therapeutic dilemma by suppressing desmoplastic responses, overcoming immunosuppression, and inhibiting tumor-promoting signaling pathways, may provide novel therapeutics that will comtribute to enhancing the overall treatment outcomes of PAAD patients.

Author contributions

ZC, C, S-lS, and YS contributed to the conception and design of the review. C-sC and P-wY wrote the first draft of the manuscript. YS and S-lS wrote sections of the manuscript. All authors contributed to the article and approved the submitted version.

Funding

This work was supported by the National Natural Science Foundation of China (81930115), Shanghai Science and Technology Commission (22YF1425800), and the Natural Science Foundation of Shanghai (21ZR1481800).

Conflict of interest

The authors declare that the research was conducted in the absence of any commercial or financial relationships that could be construed as a potential conflict of interest.

Publisher's note

References

1. Hosein AN, Brekken RA, Maitra A. Pancreatic cancer stroma: an update on therapeutic targeting strategies. *Nat Rev Gastroenterol Hepatol* (2020) 17(8):487–505. doi: 10.1038/s41575-020-0300-1

2. Rettig WJ, Chesa PG, Beresford HR, Feickert HJ, Jennings MT, Cohen J, et al. Differential expression of cell surface antigens and glial fibrillary acidic protein in human astrocytoma subsets. *Cancer Res* (1986) 46(12 Pt 1):6406–12.

3. Lee KN, Jackson KW, Christiansen VJ, Lee CS, Chun JG, McKee PA, et al. Antiplasmin-cleaving enzyme is a soluble form of fibroblast activation protein. *Blood* (2006) 107(4):1397–404. doi: 10.1182/blood-2005-08-3452

4. Shi M, Yu DH, Chen Y, Zhao CY, Zhang J, Liu QH, et al. Expression of fibroblast activation protein in human pancreatic adenocarcinoma and its clinicopathological significance. *World J Gastroenterol* (2012) 18(8):840–6. doi: 10.3748/wjg.v18.i8.840

5. Cohen SJ, Alpaugh RK, Palazzo I, Meropol NJ, Rogatko A, Xu Z, et al. Fibroblast activation protein and its relationship to clinical outcome in pancreatic adenocarcinoma. *Pancreas* (2008) 37(2):154–8. doi: 10.1097/MPA.0b013e31816618ce

6. MacNeil T, Vathiotis IA, Shafi S, Aung TN, Zugazagoitia J, Gruver AM, et al. Multiplex quantitative analysis of tumor-infiltrating lymphocytes, cancer-associated fibroblasts, and CD200 in pancreatic cancer. *Cancers (Basel)* (2021) 13 (21):5501. doi: 10.3390/cancers13215501

7. Kawase T, Yasui Y, Nishina S, Hara Y, Yanatori I, Tomiyama Y, et al. Fibroblast activation protein-α-expressing fibroblasts promote the progression of pancreatic ductal adenocarcinoma. *BMC Gastroenterol* (2015) 15:109. doi: 10.1186/s12876-015-0340-0

8. Busek P, Mateu R, Zubal M, Kotackova L, Sedo A. Targeting fibroblast activation protein in cancer - prospects and caveats. *Front Biosci (Landmark Ed)* (2018) 23(10):1933–68. doi: 10.2741/4682

9. Witek MA, Aufforth RD, Wang H, Kamande JW, Jackson JM, Pullagurla SR, et al. Discrete microfluidics for the isolation of circulating tumor cell subpopulations targeting fibroblast activation protein alpha and epithelial cell adhesion molecule. *NPJ Precis Oncol* (2017) 1:24. doi: 10.1038/s41698-017-0028-8

10. Keane FM, Yao TW, Seelk S, Gall MG, Chowdhury S, Poplawski SE, et al. Quantitation of fibroblast activation protein (FAP)-specific protease activity in mouse, baboon and human fluids and organs. *FEBS Open Bio* (2013) 4:43–54. doi: 10.1016/j.fob.2013.12.001

11. Solano-Iturri JD, Errarte P, Etxezarraga MC, Echevarria E, Angulo J, López JI, et al. Altered tissue and plasma levels of fibroblast activation protein-α (FAP) inxrenal tumours. *Cancers (Basel)* (2020) 12(11):3393. doi: 10.3390/cancers 12113393

12. Wei L, Jin Z, Yang S, Xu Y, Zhu Y, Ji Y. TCGA-assembler 2: software pipeline for retrieval and processing of TCGA/CPTAC data. *Bioinformatics* (2018) 34(9):1615–7. doi: 10.1093/bioinformatics/btx812

13. Lo A, Li CP, Buza EL, Blomberg R, Govindaraju P, Avery D, et al. Fibroblast activation protein augments progression and metastasis of pancreatic ductal adenocarcinoma. *JCI Insight* (2017) 2(19): e92232. doi: 10.1172/jci.insight.92232

14. Zhou YY, Chen LP, Zhang Y, Hu SK, Dong ZJ, Wu M, et al. Integrated transcriptomic analysis reveals hub genes involved in diagnosis and prognosis of pancreatic cancer. *Mol Med* (2019) 25(1):47. doi: 10.1186/s10020-019-0113-2

15. Wang W, Xing H, Huang C, Pan H, Li D. Identification of pancreatic cancer type related factors by weighted gene Co-expression network analysis. *Med Oncol* (2020) 37(4):33. doi: 10.1007/s12032-020-1339-0

16. Lee HO, Mullins SR, Franco-Barraza J, Valianou M, Cukierman E, Cheng JD. FAP-overexpressing fibroblasts produce an extracellular matrix that enhances invasive velocity and directionality of pancreatic cancer cells. *BMC Cancer* (2011) 11:245. doi: 10.1186/1471-2407-11-245

17. Roberts EW, Deonarine A, Jones JO, Denton AE, Feig C, Lyons SK, et al. Depletion of stromal cells expressing fibroblast activation protein-α from skeletal muscle and bone marrow results in cachexia and anemia. *J Exp Med* (2013) 210 (6):1137–51. doi: 10.1084/jem.20122344

18. Niedermeyer J, Kriz M, Hilberg F, Garin-Chesa P, Bamberger U, Lenter MC, et al. Targeted disruption of mouse fibroblast activation protein. *Mol Cell Biol* (2000) 20(3):1089–94. doi: 10.1128/MCB.20.3.1089-1094.2000

19. Santos AM, Jung J, Aziz N, Kissil JL, Puré E. Targeting fibroblast activation protein inhibits tumor stromagenesis and growth in mice. *J Clin Invest* (2009) 119 (12):3613–25. doi: 10.1172/JCI38988

20. Eager RM, Cunningham CC, Senzer N, Richards DA, Raju RN, Jones Bc . Phase II trial of talabostat and docetaxel in advanced non-small cell lung cancer. *Clin Oncol (R Coll Radiol)* (2009) 21(6):464–72. doi: 10.1016/j.clon.2009.04.007

21. Eager RM, Cunningham CC, Senzer NN, Stephenson Jr Anthony J SP, O'Day SJ, et al. Phase II assessment of talabostat and cisplatin in second-line stage IV melanoma. *BMC Cancer* (2009) 9:263. doi: 10.1186/1471-2407-9-263

22. Ungefroren H, Kruse ML, Trauzold A, Roeschmann S, Roeder C, Arlt A, et al. FAP-1 in pancreatic cancer cells: functional and mechanistic studies on its inhibitory role in CD95-mediated apoptosis. *J Cell Sci* (2001) 114(Pt 15):2735–46. doi: 10.1242/jcs.114.15.2735

23. Blomberg R, Beiting DP, Wabitsch M, Puré Ec , et al. Fibroblast activation protein restrains adipogenic differentiation and regulates matrix-mediated mTOR signaling. *Matrix Biol* (2019) 83:60–76. doi: 10.1016/j.matbio.2019.07.007

24. Hofheinz RD, al-Batran SE, Hartmann F, Hartung G, Jäger D, Renner C, et al. Stromal antigen targeting by a humanised monoclonal antibody: an early phase II trial of sibrotuzumab in patients with metastatic colorectal cancer. *Onkologie* (2003) 26(1):44–8. doi: 10.1159/000069863

25. Welt S, Divgi CR, Scott AM, Garin-Chesa P, Finn RD, Graham M, et al. Antibody targeting in metastatic colon cancer: a phase I study of monoclonal antibody F19 against a cell-surface protein of reactive tumor stromal fibroblasts. *J Clin Oncol* (1994) 12(6):1193–203. doi: 10.1200/JCO.1994.12.6.1193

26. Scott AM, Wiseman G, Welt S, Adjei A, Lee FT, Hopkins W, et al. A phase I dose-escalation study of sibrotuzumab in patients with advanced or metastatic fibroblast activation protein-positive cancer. *Clin Cancer Res* (2003) 9(5):1639–47.

27. Kraman M, Bambrough PJ, Arnold JN, Roberts EW, Magiera L, Jones JO, et al. Suppression of antitumor immunity by stromal cells expressing fibroblast activation protein-alpha. *Science* (2010) 330(6005):827–30. doi: 10.1126/science.1195300

28. Özdemir BC, Pentcheva-Hoang T, Carstens JL, Zheng X, Wu CC, Simpson TR, et al. Depletion of carcinoma-associated fibroblasts and fibrosis induces immunosuppression and accelerates pancreas cancer with reduced survival. *Cancer Cell* (2014) 25(6):719–34. doi: 10.1016/j.ccr.2014.04.005

29. Hingorani SR, Wang L, Multani AS, Combs C, Deramaudt TB, Hruban RH, et al. Trp53R172H and KrasG12D cooperate to promote chromosomal instability and widely metastatic pancreatic ductal adenocarcinoma in mice. *Cancer Cell* (2005) 7(5):469–83. doi: 10.1016/j.ccr.2005.04.023

30. Hussain A, Voisin V, Poon S, Karamboulas C, Bui NHB, Meens J, et al. Distinct fibroblast functional states drive clinical outcomes in ovarian cancer and are regulated by TCF21. *J Exp Med* (2020) 217(8):e20191094. doi: 10.1084/jem.20191094

31. Yang X, Lin Y, Shi Y, Li B, Liu W, Yin W, et al. FAP promotes immunosuppression by cancer-associated fibroblasts in the tumor microenvironment *via* STAT3-CCL2 signaling. *Cancer Res* (2016) 76(14):4124–35. doi: 10.1158/0008-5472.CAN-15-2973

32. Feig C, Jones JO, Kraman M, Wells RJ, Deonarine A, Chan DS, et al. Targeting CXCL12 from FAP-expressing carcinoma-associated fibroblasts synergizes with anti-PD-L1 immunotherapy in pancreatic cancer. *Proc Natl Acad Sci U.S.A.* (2013) 110(50):20212–7. doi: 10.1073/pnas.1320318110

33. Gabrilovich DI, Ostrand-Rosenberg S, Bronte V. Coordinated regulation of myeloid cells by tumours. *Nat Rev Immunol* (2012) 12(4):253–68. doi: 10.1038/nri3175

34. Muliaditan T, Caron J, Okesola M, Opzoomer JW, Kosti P, Georgouli M, et al. Macrophages are exploited from an innate wound healing response to facilitate cancer metastasis. *Nat Commun* (2018) 9(1):2951. doi: 10.1038/s41467-018-05346-7

35. Tang PC, Chung JY, Xue VW, Xiao J, Meng XM, Huang XR, et al. Smad3 promotes cancer-associated fibroblasts generation *via* macrophage-myofibroblast transition. *Adv Sci (Weinh)* (2022) 9(1):e2101235. doi: 10.1002/advs.202101235

36. Arnold JN, Magiera L, Kraman M, Fearon DT, et al. Tumoral immune suppression by macrophages expressing fibroblast activation protein-α and heme oxygenase-1. *Cancer Immunol Res* (2014) 2(2):121–6. doi: 10.1158/2326-6066.CIR-13-0150

37. Mu W, Wang Z, Zöller M. Ping-Pong-Tumor and host in pancreatic cancer progression. *Front Oncol* (2019) 9:1359. doi: 10.3389/fonc.2019.01359

38. Kalluri R. The biology and function of fibroblasts in cancer. *Nat Rev Cancer* (2016) 16(9):582–98. doi: 10.1038/nrc.2016.73

39. Ogawa Y, Masugi Y, Abe T, Yamazaki K, Ueno A, Fujii-Nishimura Y, et al. Three distinct stroma types in human pancreatic cancer identified by image analysis of fibroblast subpopulations and collagen. *Clin Cancer Res* (2021) 27 (1):107–19. doi: 10.1158/1078-0432.CCR-20-2298

40. McAndrews KM, Chen Y, Darpolor JK, Zheng X, Yang S, Carstens JL, et al. Identification of functional heterogeneity of carcinoma-associated fibroblasts with distinct IL6-mediated therapy resistance in pancreatic cancer. *Cancer Discovery* (2022) 12(6):1580–97. doi: 10.1158/2159-8290.CD-20-1484

41. Patsouras D, Papaxoinis K, Kostakis A, Safioleas MC, Lazaris AC, Nicolopoulou-Stamati P, et al. Fibroblast activation protein and its prognostic significance in correlation with vascular endothelial growth factor in pancreatic adenocarcinoma. *Mol Med Rep* (2015) 11(6):4585–90. doi: 10.3892/mmr.2015.3259

42. Guan J, Zhang H, Wen Z, Gu Y, Cheng Y, Sun Y, et al. Retinoic acid inhibits pancreatic cancer cell migration and EMT through the downregulation of IL-6 in cancer associated fibroblast cells. *Cancer Lett* (2014) 345(1):132–9. doi: 10.1016/j.canlet.2013.12.006

43. Whittle MC, Hingorani SR. Fibroblasts in pancreatic ductal adenocarcinoma: Biological mechanisms and therapeutic targets. *Gastroenterology* (2019) 156(7):2085–96. doi: 10.1053/j.gastro.2018.12.044

44. Chaudhry SI, Hooper S, Nye E, Williamson P, Harrington K, Sahai E. Autocrine IL-1β-TRAF6 signalling promotes squamous cell carcinoma invasion through paracrine TNFα signalling to carcinoma-associated fibroblasts. *Oncogene* (2013) 32(6):747–58. doi: 10.1038/onc.2012.91

45. Lau TS, Chan LK, Wong EC, Hui CW, Sneddon K, Cheung TH, et al. A loop of cancer-stroma-cancer interaction promotes peritoneal metastasis of ovarian cancer *via* TNFα-TGFα-EGFR. *Oncogene* (2017) 36(25):3576–87. doi: 10.1038/onc.2016.509

46. Sahai E, Astsaturov I, Cukierman E, DeNardo DG, Egeblad M, Evans RM, et al. A framework for advancing our understanding of cancer-associated fibroblasts. *Nat Rev Cancer* (2020) 20(3):174–86. doi: 10.1038/s41568-019-0238-1

47. Wen Z, Liu Q, Wu J, Xu B, Wang J, Liang Lc , et al. Fibroblast activation protein α-positive pancreatic stellate cells promote the migration and invasion of pancreatic cancer by CXCL1-mediated akt phosphorylation. *Ann Transl Med* (2019) 7(20):532. doi: 10.21037/atm.2019.09.164

48. Kakarla S, Chow KK, Mata M, Shaffer DR, Song XT, Wu MF, et al. Antitumor effects of chimeric receptor engineered human T cells directed to tumor stroma. *Mol Ther* (2013) 21(8):1611–20. doi: 10.1038/mt.2013.110

49. Wang LC, Lo A, Scholler J, Sun J, Majumdar RS, Kapoor V, et al. Targeting fibroblast activation protein in tumor stroma with chimeric antigen receptor T cells can inhibit tumor growth and augment host immunity without severe toxicity. *Cancer Immunol Res* (2014) 2(2):154–66. doi: 10.1158/2326-6066.CIR-13-0027

50. Roybal KT, Williams JZ, Morsut L, Rupp LJ, Kolinko I, Choe JH, et al. Engineering T cells with customized therapeutic response programs using synthetic notch receptors. *Cell* (2016) 167(2):419–432.e16. doi: 10.1016/j.cell.2016.09.011

51. Bansal R, Reshef R. Revving the CAR - combination strategies to enhance CAR T cell effectiveness. *Blood Rev* (2021) 45:100695. doi: 10.1016/j.blre.2020.100695

52. D'Aloia MM, Zizzari IG, Sacchetti B, Pierelli L, Alimandi M. CAR-T cells: the long and winding road to solid tumors. *Cell Death Dis* (2018) 9(3):282. doi: 10.1038/s41419-018-0278-6

53. Lo A, Scholler J, Monslow J, Avery D, Newick K, et al. Tumor-promoting desmoplasia is disrupted by depleting FAP-expressing stromal cells. *Cancer Res* (2015) 75(14):2800–10. doi: 10.1158/0008-5472.CAN-14-3041

54. Schuberth PC, Hagedorn C, Jensen SM, Gulati P, van den Broek M, Mischo A, et al. Treatment of malignant pleural mesothelioma by fibroblast activation protein-specific re-directed T cells. *J Transl Med* (2013) 11:187. doi: 10.1186/1479-5876-11-187

55. Ji T, Zhao Y, Ding Y, Wang J, Zhao R, Lang J, et al. Transformable peptide nanocarriers for expeditious drug release and effective cancer therapy *via* cancer-associated fibroblast activation. *Angew Chem Int Ed Engl* (2016) 55(3):1050–5. doi: 10.1002/anie.201506262

56. Sun M, Yao S, Fan L, Fang Z, Miao W, Hu Z, et al. Fibroblast activation protein-α responsive peptide assembling prodrug nanoparticles for remodeling the immunosuppressive microenvironment and boosting cancer immunotherapy. *Small* (2022) 18(9):e2106296. doi: 10.1002/smll.202106296

57. Powles T, Kockx M, Rodriguez-Vida A, Duran I, Crabb SJ, Van Der Heijden MS, et al. Clinical efficacy and biomarker analysis of neoadjuvant atezolizumab in operable urothelial carcinoma in the ABACUS trial. *Nat Med* (2019) 25(11):1706–14. doi: 10.1038/s41591-019-0628-7

58. Sum E, Rapp M, Fröbel P, Le Clech M, Dürr H, Giusti AM, et al. Fibroblast activation protein α-targeted CD40 agonism abrogates systemic toxicity and enables administration of high doses to induce effective antitumor immunity. *Clin Cancer Res* (2021) 27(14):4036–53. doi: 10.1158/1078-0432.CCR-20-4001

59. Ostermann E, Garin-Chesa P, Heider KH, Kalat M, Lamche H, Puri C, et al. Effective immunoconjugate therapy in cancer models targeting a serine protease of tumor fibroblasts. *Clin Cancer Res* (2008) 14(14):4584–92. doi: 10.1158/1078-0432.CCR-07-5211

60. Yu Q, Tang X, Zhao W, Qiu Y, He J, Wan D, et al. Mild hyperthermia promotes immune checkpoint blockade-based immunotherapy against metastatic pancreatic cancer using size-adjustable nanoparticles. *Acta Biomater* (2021) 133:244–56. doi: 10.1016/j.actbio.2021.05.002

61. Tran E, Chinnasamy D, Yu Z, Morgan RA, Lee CC, Restifo NP, et al. Immune targeting of fibroblast activation protein triggers recognition of

multipotent bone marrow stromal cells and cachexia. *J Exp Med* (2013) 210 (6):1125–35. doi: 10.1084/jem.20130110

62. Tang PM, Tang PC, Chung JY, Lan HY. TGF-β1 signaling in kidney disease: From smads to long non-coding RNAs. *Noncoding RNA Res* (2017) 2(1):68–73. doi: 10.1016/j.ncrna.2017.04.001

63. Fang Z, Xu J, Zhang B, Wang W, Liu J, Liang C, et al. The promising role of noncoding RNAs in cancer-associated fibroblasts: an overview of current status and future perspectives. *J Hematol Oncol* (2020) 13(1):154. doi: 10.1186/s13045-020-00988-x

64. Zhang X, Song W, Qin C, Liu F, Lan X, et al. Non-malignant findings of focal (68)Ga-FAPI-04 uptake in pancreas. *Eur J Nucl Med Mol Imaging* (2021) 48 (8):2635–41. doi: 10.1007/s00259-021-05194-6

65. Dendl K, Finck R, Giesel FL, Kratochwil C, Lindner T, Mier W, et al. FAP imaging in rare cancer entities-first clinical experience in a broad spectrum of malignancies. *Eur J Nucl Med Mol Imaging* (2022) 49(2):721–31. doi: 10.1007/s00259-021-05488-9

66. Liermann J, Syed M, Ben-Josef E, Schubert K, Schlampp I, Sprengel SD, et al. Impact of FAPI-PET/CT on target volume definition in radiation therapy of locally recurrent pancreatic cancer. *Cancers (Basel)* (2021) 13(4):796. doi: 10.3390/cancers13040796

67. Watabe T, Liu Y, Kaneda-Nakashima K, Shirakami Y, Lindner T, Ooe K, et al. Theranostics targeting fibroblast activation protein in the tumor stroma: (64) Cu- and (225)Ac-labeled FAPI-04 in pancreatic cancer xenograft mouse models. *J Nucl Med* (2020) 61(4):563–9. doi: 10.2967/jnumed.119.233122

68. Xu M , Zhang P, Ding J, Chen J, Huo LLiu Z. Albumin binder-conjugated fibroblast activation protein inhibitor radiopharmaceuticals for cancer therapy. *J Nucl Med* (2022) 63(6):952–8. doi: 10.2967/jnumed.121.262533

69. Liu Y, Watabe T, Kaneda-Nakashima K, Shirakami Y, Naka S, Ooe K. Fibroblast activation protein targeted therapy using [(177)Lu]FAPI-46 compared with [(225)Ac]FAPI-46 in a pancreatic cancer model. *Eur J Nucl Med Mol Imaging* (2022) 49(3):871–80. doi: 10.1007/s00259-021-05554-2

70. Ferdinandus J, Costa PF, Kessler L, Weber M, Hirmas N, Kostbade K, et al. Initial clinical experience with (90)Y-FAPI-46 radioligand therapy for advanced-stage solid tumors: A case series of 9 patients. *J Nucl Med* (2022) 63(5):727–34. doi: 10.2967/jnumed.121.262468

71. Gilardi L, Airò Farulla LS, Demirci E, Clerici I, Omodeo Salè E, Ceci F. Imaging cancer-associated fibroblasts (CAFs) with FAPi PET. *Biomedicines* (2022) 10(3):523. doi: 10.3390/biomedicines10030523

72. Roy J, Hettiarachchi SU, Kaake M, Mukkamala R, Low PS. Design and validation of fibroblast activation protein alpha targeted imaging and therapeutic agents. *Theranostics* (2020) 10(13):5778–89. doi: 10.7150/thno.41409

73. Wen X, Xu P, Shi M, Liu J, Zeng X, Zhang Y, et al. Evans Blue-modified radiolabeled fibroblast activation protein inhibitor as long-acting cancer therapeutics. *Theranostics* (2022) 12(1):422–33. doi: 10.7150/thno.68182

74. Lindner T, Altmann A, Krämer S, Kleist C, Loktev A, Kratochwil C, et al. Design and development of (99m)Tc-labeled FAPI tracers for SPECT imaging and (188)Re therapy. *J Nucl Med* (2020) 61(10):1507–13. doi: 10.2967/jnumed.119.239731

frontiers | Frontiers in Oncology

TYPE Original Research
PUBLISHED 19 October 2022
DOI 10.3389/fonc.2022.965660

OPEN ACCESS

EDITED BY
Dongmei Zhang,
Jinan University, China

REVIEWED BY
Melissa Fishel,
Purdue University Indianapolis, United States
Pengfei Dong,
Icahn School of Medicine at Mount Sinai, United States
Cheng Zhou,
Southern Medical University, China

*CORRESPONDENCE
Yi Yao
yaoyi2018@whu.edu.cn
Zhongliang Zheng
yivanrobin@sina.com
Qibin Song
qibinsong@whu.edu.cn

†These authors have contributed equally to this work and share first authorship

SPECIALTY SECTION
This article was submitted to Molecular and Cellular Oncology, a section of the journal Frontiers in Oncology

RECEIVED 10 June 2022
ACCEPTED 15 September 2022
PUBLISHED 19 October 2022

CITATION
Zhang Z, Dong Y, Wu B, Li Y, Liu Z, Liu Z, Gao Y, Gao L, Song Q, Zheng Z and Yao Y (2022) Irradiation enhances the malignancy-promoting behaviors of cancer-associated fibroblasts. *Front. Oncol.* 12:965660. doi: 10.3389/fonc.2022.965660

Irradiation enhances the malignancy-promoting behaviors of cancer-associated fibroblasts

Ziyue Zhang[1,2†], Yi Dong[1,2†], Bin Wu[1,3†], Yingge Li[1,2], Zehui Liu[4], Zheming Liu[1,2], Yanjun Gao[1,2], Likun Gao[5], Qibin Song[1,2*], Zhongliang Zheng[4*] and Yi Yao[1,2*]

[1]Cancer Center, Renmin Hospital of Wuhan University, Wuhan, China, [2]Hubei Provincial Research Center for Precision Medicine of Cancer, Wuhan, China, [3]Department of Oncology, Huang-gang Central Hospital, Huanggang, China, [4]College of Life Sciences, Wuhan University, Wuhan, China, [5]Department of Pathology, Renmin Hospital of Wuhan University, Wuhan, China

Background: Cancer-associated fibroblasts (CAFs) are the important component of the tumor microenvironment (TME). Previous studies have found that some pro-malignant CAFs participate in the resistance to radiotherapy as well as the initiation and progression of tumor recurrence. However, the exact mechanism of how radiation affects CAFs remains unclear. This study aimed to explore the effect and possible mechanism of radiation-activated CAFs, and its influence on lung cancer.

Methods: CAFs were isolated from surgical specimens *in situ* and irradiated with 8Gy x-rays. The changes in cell morphology and subcellular structure were observed. CAFs marker proteins such as FAP and α-SMA were detected by Western Blotting. Cell counting kit-8 (CCK8) assay, flow cytometry, wound healing assay, and transwell chamber assay was used to detect the activation of cell viability and migration ability. A nude mouse xenograft model was established to observe the tumorigenicity of irradiated CAFs *in vivo*. The genomic changes of CAFs after radiation activation were analyzed by transcriptome sequencing technology, and the possible mechanisms were analyzed.

Results: The CAFs showed a disorderly growth pattern after X-ray irradiation. Subcellular observations suggested that metabolism-related organelles exhibited more activity. The expression level of CAFs-related signature molecules was also increased. The CAFs irradiated by 8Gy had good proliferative activity. In the (indirect) co-culture system, CAFs showed radiation protection and migration induction to lung cancer cell lines, and this influence was more obvious in radiation-activated CAFs. The radiation protection was decreased after exosome inhibitors were applied. Vivo study also showed that radiation-activated CAFs have stronger tumorigenesis. Transcriptome analysis showed that genes were enriched in several pro-cancer signaling pathways in radiation-activated CAFs.

Conclusions: Our study confirmed that CAFs could be activated by ionizing radiation. Irradiation-activated CAFs could promote cancer cell proliferation, migration, radiotherapy tolerance, and tumorigenesis. These results suggested that irradiation-activated CAFs might participate in the recurrence of lung cancer after radiotherapy, and the inhibition of CAFs activation may be an important way to improve clinical radiotherapy efficacy.

KEYWORDS

cancer-associated fibroblasts, irradiation, lung cancer, activation, malignant, biological behavior

Introduction

In the past decades, advances in radiotherapy have improved overall survival for malignant tumors. However, primary resistance and acquired tolerance to radiotherapy remain significant challenges in clinical practice (1). Previous studies have found that bidirectional communication between cells and their microenvironment is critical for the malignant biological behavior of tumors (2–4).

As an important cellular component in the tumor stroma, cancer-associated fibroblasts (CAFs) can promote the malignant biological behavior of cancer cells. α-smooth muscle actin (α-SMA) (5), fibroblast specific protein-1 (FSP-1) (6), fibroblast activation protein (FAP) (7), and platelet-derived growth factor receptor-β (PDGFR-β) (8) are considered as traditional CAFs biomarkers. CAFs influence the chemotaxis of endothelial progenitor cells and monocytes (9) and promote survival (10), invasion and metastasis (11), and tumor angiogenesis (12) of cancer cells. Also, it has been suggested that CAFs can induce acquired drug resistance (13) and radiation resistance (14). In short, CAFs confer a mesenchymal-like phenotype and enhance metastasis of both premalignant and malignant epithelial cells, whereas normal fibroblasts promote an epithelial-like phenotype and suppress metastasis (15). CAFs have a diverse origin, which also leads to their heterogeneity; yet, they are mainly differentiated from normal fibroblast (NF) located close to cancer cells. When specific stimulation occurs, some NF can be activated into CAFs with different forms and functions, triggering various "pro-malignant" effects (16).

Previous studies on improving the efficacy of radiotherapy have mainly focused on cancer cells alone while ignoring the complex biological interactions between them and the tumor microenvironment (TME) (17). Numerous studies have suggested that radiation breaks the DNA strands of tumor cells and increases the secretion of transforming growth factor-β (TGF-β) and hypoxia-inducible factor 1-α (HIF-1α), thus suppressing the immune system and inducing radio-resistance (18).

Over the years, the variation and role of tumor stroma have attracted increasing attention during radiotherapy (19). Previous studies have found that some pro-malignant CAFs participate in the resistance to radiotherapy as well as the initiation and progression of tumor recurrence. In addition, a multivariate analysis showed that α-SMA/epithelial area ratio was an independent prognostic value associated with poor recurrence-free survival, suggesting that neoadjuvant treatment impacts on CAFs (20). Moreover, some CAFs activation following radiation led to altered growth factor secretion and release of numerous modulators of the ECM and cytokines, including TGF-β, which is a complex and pleiotropic cytokine that directly affects tumor cells and CAFs, driving HIF-1 signaling, reducing the activation of T-cells and dendritic cells (DCs), remolding the tumor microenvironment, and resulting in the progression of cancer (17).

The aim of this study was to explore the effect of radiation on the activation of CAFs *in vitro* and *in vivo* experiments and to further explore the influence of radiation-activated CAFs on the development of lung cancer and its possible mechanism.

Materials and methods

Materials and reagents

The antibodies used in this study were anti-GAPDH (60004-1-Ig, Proteintech, China), anti-α-SMA (14395-1-AP, Proteintech, China), anti-FAP (A11572, Abclonal, China), anti-VIM (60330-1-Ig, Proteintech, China), and anti-KI67 (27309-1-AP, Proteintech, China). Flow cytometry Kit (Multi Sciences, China), CCK8 reagent (Dojindo, Japan), MTT Reagent (Sigma, Germany), BCA1-1KT kit (Sigma, Germany), RIPA lysate (Beyotime, China), and inhibitor of exosome GW4869 (MCE, Shanghai) were purchased from Baitengruida Biotechnology. Optical microscope (Nikon, Japan), HT7800 Transmission Electron microscope (Hitachi, Japan), microplate reader (Bio-RAD, USA), and flow cytometry (BIO-RAD, USA) were provided by

the central lab of Renmin Hospital of Wuhan University. The Elekta Infinity™ linear accelerator (Elekta, Sweden) was provided by Renmin Hospital of Wuhan University. Four-week-old female BALB/c nude mice were purchased from Weitonglihua Experimental Animal Technology.

Primary CAFs isolation and cell culture

Primary CAFs were isolated and extracted from the lung cancer tissue of an adult male NSCLC patient who underwent surgical resection (the study was approved by the Ethics Committee of the Renmin Hospital of Wuhan University). The peritumoral tissue was taken from an area 1.0 cm away from the edge of lung cancer tissue, cleaned with 1% penicillin/streptomycin in PBS at 4°C, and cut into 1.0 mm^3. The tissue was then put into the dish with 1 ml of fetal bovine serum, cultured in a CO_2 incubator for 1 h, and then mixed by inverting the dish overnight. An appropriate amount of DMEM containing 10% fetal bovine serum was added to each dish after 24 h for upright culture, and the medium was changed every 3 days. When spindle cells migrated away from the edges of the tissue clumps and were fused to about 85%, the subculture was carried out. CAFs were used for further experiments after 5-8 passages.

CAFs were grown in Dulbecco's Modified Eagle Medium (DMEM, HyClone, USA); MRC-5 cells were cultured in Eagle's Minimal Essential Medium (EMEM, HyClone, USA); lung cancer cells A549 and H1299 were cultured in Roswell Park Memorial Institute 1640 Medium (RPMI-1640, HyClone, USA). All mediums were supplemented with 10% fetal bovine serum (FBS) and 1% penicillin/streptomycin. If not specified, all cells were maintained in a humidified atmosphere containing 5% CO_2/95% air at 37°C. A549, H1299, and MRC5 cells were kind gifts from Wuhan University School of Life Sciences laboratory.

Cell radiation and conditioned medium

Confluent CAF cultures were irradiated using a clinical 6MV X-ray beam produced by the Elekta Infinity™ linac. The source-to-surface distance was 100 cm with a dose rate of 300 MU/min. Except for where otherwise indicated, CAF received 8Gy, while A549 was 6Gy as reported previously (19). Conditioned medium (CM) was obtained as described below.

After conventional culture, the human lung adenocarcinoma cell line (A549) was divided into the irradiated group and the unirradiated group. Then these two groups were divided into three subgroups, respectively, by adding the supernatant of ordinary DMEM (blank), non-irradiated CAFs supernatant (CAF_0-CM), and CAFs supernatant that underwent 8Gy X-ray irradiation (CAF8-CM) at a ratio of 7:5 (volume ratio). After 2 h of culture, the irradiated group was given a single dose of 6Gy X-ray at room temperature, and the pseudo-irradiated group was placed in the irradiation chamber for 1 min. The cells from both groups were cultured. The human NSCLC cell line H1299 and human embryonic lung fibroblast cell line MRC-5 were routinely cultured for the following experiments.

The primary cultured CAFs with or without irradiation were pretreated with GW4869 (10 μmol/L) for 48 h, and their supernatants were prepared at 4°C for later use. Each group was cultured in normal DMEM (blank), supernatant of GW4869 treated CAF_0 (G+CAF_0-CM), and supernatant of GW4869 treated CAF_8 (G+CAF_8-CM) with a ratio of 7:5 (volume ratio), respectively. After 2 h in the incubator, the irradiation group A549 was given X-ray irradiation at room temperature with a single dose of 6Gy, and the cells of the two groups continued to be cultured. The processes are detailed in Figure 1F.

Morphology and subcellular structure observation of CAFs

After reaching a confluency of 60%, cells were treated with 8 Gy irradiation and then cultured for 8 h. The morphology and subcellular structure of CAFs were observed by an optical microscope. As for the transmission electron microscope, the collected cell sediment was fixed using 4% glutaraldehyde after centrifugation. This was further processed into ultra-thin slices of 60 nm in thickness, followed by observation for target subcellular structures like mitochondria, endoplasmic reticulum, etc.

Western blotting

Protein lysates were obtained according to the previously described procedures (21). BCA1-1KT kit was used for the protein quantification assay. An appropriate amount of protein was mixed with 5× loading buffer and loaded on the 10% SDS-PAGE. After membranes were blocked with 5% non-fat milk, they were incubated with primary antibodies at 4°C overnight and appropriate horseradish peroxidase (HRP)-conjugated secondary antibodies at room temperature for 1.5 h. Protein bands were visualized using the enhanced chemiluminescence system. All experiments were performed three times. Protein levels were normalized as a ratio to GAPDH. The primary antibodies were: FAP (1:1000, Abclonal), Vimentin (1:50000, proteintech), and α-SMA (1:5000, proteintech).

Cell apoptosis assay

Flow cytometry was used to analyze the apoptosis of A549 cells. The cells were seeded into a 6-well plate (1×10^6/well) overnight. The medium was changed with a conditional medium

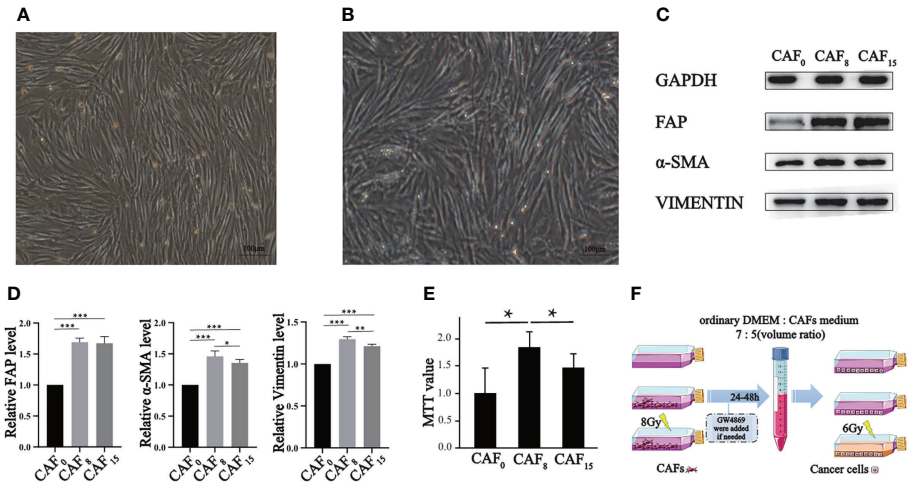

FIGURE 1
Effect of irradiation on the morphology, molecular markers, and proliferation of CAFs. **(A, B)** Morphology of CAFs without irradiation **(A)** and CAFs that received 8Gy irradiation **(B)** were compared under a light microscope (100×), and both groups of cells were spindle-shaped, but the irradiated cells were slightly disorganized; **(C)** Representative western blotting for FAP, α-SMA, and vimentin in CAFs that received 0Gy, 8Gy, and 15Gy irradiation; **(D)** The relative expression differences of the biomarkers after normalization of the GAPDH were analyzed by quantitatively comparing the density differences of the immunoblot bands; **(E)** MTT experiment was used to analyze the proliferation activity of CAFs under 0Gy, 8Gy, and 15Gy irradiation. T-test, *$P < 0.05$; **(F)** The sketch map of supernatants preparations of CAFs. (T-test, data are presented as the mean ± S.D. *P < 0.05, **P < 0.01, ***P < 0.001).

2 h before irradiation. After 24-hour incubation, cells in each group with different treatments were washed with PBS 3 times; the supernatant was discarded, digested with trypsin without EDTA, and then gently mixed with 500 μL binding buffer, 5μL Annexin V-FITC, and 5 μL PI. The cells were incubated at 4°C for 20 min under dark conditions and detected by flow cytometry.

Cell viability assay

The viability of A549 cells was analyzed using CCK-8 kits. The cells were digested by trypsin and then suspended. Approximately 3.5×10^4 cells per well were placed in 96-well plates and cultured for 24, 48, and 72 h, respectively. After each time point, a 10 μL of CCK-8 was added to each well at 37°C for 2 h. The absorbance at 450nm was determined using a microplate reader. Three wells were taken from each group to calculate the average value and draw the proliferation curve.

The viability of CAFs was analyzed using a MTT assay. The cells were seeded in 96-well plates (5×10^3 cells/well) after irradiation and cultured for 24 h. Then, 20 μl MTT reagent was added to each well for 4 h. After removal of the medium, 150 μl of DMSO was added to each well and properly mixed for another 10 min. The absorbance at 570 nm was determined using a microplate reader. A blank well (medium, MTT, DMSO) was included for comparison. All experiments were performed three times.

Wound healing assay

A549 cells were placed into 6-well plates (2.5×10^6 cells/well). The two groups (irradiated and irradiated groups) were divided into three subgroups, respectively (see above). The irradiated group was given a single dose of 6Gy X-ray. After the cell reached 90% confluence, a line was drawn using a marker on the bottom of the dish, and then a sterile 1,000-μl pipet tip was used to scratch five separate wounds through the cells, moving perpendicular to the line. The cells were gently rinsed twice with PBS to remove floating cells and incubated in a fresh culture medium containing 1% FBS. Images of the scratches were taken by using an inverted microscope at ×10 magnification at 0, 12, 24, 36, and 48 h of incubation. Image J software (Version 1.53n) was used to calculate the percentage of migration area and draw the time-healing area curve. The percentage of migration area was quantitatively analyzed using cells migration area when measuring divided by the wound area at 0 h.

Transwell migration assay

Transwell migration assay was performed using 24-well culture plates. Briefly, 500 μl of CAFs/MRC5 suspension (2×10^4) was added to each well (lower chamber) overnight. The experimental group was given single X-ray irradiation of 8Gy, after which they were cultured for an additional 2 h. A549 or H1299 cells (5×10^4/200μL) were seeded in the upper chamber and

allowed to migrate the lower chamber. The cells were removed after co-culture for 24 h. A549 or H1299 cells passing through the polycarbonate membrane were observed and counted under the microscope after cleaning, fixed with 4% paraformaldehyde, and stained with crystal violet dye.

Construction of xenografted mouse model

All animal studies (including the mice euthanasia procedure) were done in compliance with the regulations and guidelines of Renmin Hospital of Wuhan University institutional animal care and conducted according to the AAALAC and the IACUC guidelines. All the animals were housed in an environment with a temperature of 22 ± 1 °C, relative humidity of 50 ± 1%, and a light/dark cycle of 12/12 h.

Eighteen 4-week-old female BALB/c nude mice were divided into three groups. A549 cells (2×10^6 cells), A549 and CAFs mixed cells (A549: CAF_0, 1:1, a total of 4×10^6 cells), and A549 and 8Gy irradiated CAFs mixed cells (A549: CAF_8, 1:1, a total of 4×10^6 cells) were subcutaneously inoculated under the right axilla of animals. The living status, body weight, and tumorigenesis of mice were observed and recorded daily. At the end of the animal experiments (about 25 days), the subcutaneous tumor tissue was completely removed. The long diameter (D) and short diameter (d) of the tumor size were measured. The tumor volume was calculated by $V= d^2 \times D/2$, and the tumor volumetric time growth curve was plotted.

Immunohistochemistry

The dissected subcutaneous tumor tissues were fixed using 4% paraformaldehyde. The expression of nuclear proliferation antigen ki67 and α-SMA in tumor tissues of each group was analyzed by immunohistochemistry. The experimental steps followed the previous standard protocols (22). In short, the tumor tissues of each group were fixed, embedded, sectioned, stained, and mounted, and then observed under a common light microscope. The collected pictures were calculated and analyzed by Image J software (Version 1.53n). The mean density was calculated and analyzed using the integrated density of the pre-processed images divided by the total area.

RNA extraction and transcriptome sequencing

Primary cultured CAFs and 8Gy irradiated CAFs (CAF_8) were used for RNA sequencing. Cells were treated as described above (see the materials and methods section). Then, cells were incubated for 24 h after irradiation and then collected. Total RNA was isolated using Trizol (Invitrogen, USA) according to the manufacturer's instructions. By analyzing the RNA-seq raw data obtained from the HiSeq platform, we compared the differential expressed genes, and the enrichment analysis, including GO, and KEGG was further conducted. The differentially expressed genes that underwent GO and KEGG enrichment analyses with a q value < 0.05 were screened. The enrichment results were visualized by R software. Heat maps of differential oncogenic genes were visualized using "heatmap" R package.

Statistical analysis

Data was statistically analyzed and plotted by GraphPad Prism (Version 8.0.1) and SPSS (Version 20.0). A two-tailed unpaired Student's t-test was used for inter-group comparison. All data was represented as mean ± SD. Differences were considered statistically significant if P-value < 0.05.

Results

Activation of CAFs proliferation by ionizing radiation and its potential mechanism

Under a light microscope, CAFs showed a long spindle shape with dense growth and a slightly disordered and non-directional arrangement (Figure 1A). The contact and density inhibition were lost when reaching a certain density. Under 8Gy X-ray irradiation, the shape, size, and growth mode of CAFs did not significantly change (Figure 1B), thus suggesting that irradiation does not cause morphological changes to the cells.

Next, we detected intrinsic changes in cells at the protein level. Western blot showed that CAFs biomarkers were up-regulated with relatively low-dose irradiation (Figure 1C). FAP, vimentin and α-SMA were significantly increased after single irradiation of 8Gy and 15Gy compared with 0Gy. The expression level of α-SMA and vimentin under the 8Gy condition were slightly higher than under the 0Gy condition but not under the 15Gy condition (Figure 1D). The increased expression of the above cytoskeleton-associated proteins indicates that irradiated CAFs have an enhanced motor migration capacity, promoting an aggressive phenotype in metastasis.

To further explore the alteration of CAFs in other functional phenotypes after irradiation, we verified the proliferation alteration of CAFs by MTT assay. According to the MTT results, irradiation boosted the proliferative capacity of CAFs. The proliferation rate of CAFs irradiated with 8Gy and 15Gy was double that of 0Gy, and 1.5 times that of 0Gy, respectively (P < 0.001). CAFs exposed to 8Gy exhibited the highest proliferation capacity (Figure 1E). The above changes suggest that CAFs can exhibit malignant behavior after treated with 8Gy, which also

imply that the CAFs organelles related to heredity, metabolism, and synthesis from the observation have been modified. The electron microscopic results further confirmed these changes.

There was no significant change in subcellular morphology after ionizing radiation; yet, double nucleoli, double nuclei, and lobulated nuclei were found in CAFs (Figures 2A, E, F). The rough endoplasmic reticulum increased and expanded in the cytoplasm (Figures 2D, H). As shown in Figures 2B, G, the microtubules increased in bundles. Mitochondria fission and Golgi apparatus also showed an increased status (Figures 2C, G, H).

Several investigations have reported that low-dose ionizing radiation could enhance cell proliferation *via* transient ERK1/2 and p38 activation in normal human lung fibroblasts (23). The phenotype of irradiated CAFs did reveal its activation, and the transcriptome data also provided an insight into the potential mechanism of activation of CAFs when exposed to 8Gy. Ionizing radiation activated multiple proliferation-related and cancer-promoting signaling pathways in CAFs.

Differentially expressed analysis showed that large amounts of oncogenic genes were up-regulated (fold-change>2, FDR<0.05) (Figure 3A). Genes associated with cell proliferation like MITF, ABL2, and XIAP, and oncogenes like PDGFB and ERG were highly expressed in CAF_8. The enrichment of Gene Ontology (GO) further showed that differentially expressed oncogenes were mainly enriched in cell proliferation, regulation of cell proliferation, positive regulation of the biological process, and positive regulation of cellular process (Figure 3B). The Kyoto Encyclopedia of Genes and Genomes (KEGG) analysis showed that differentially expressed oncogenes were enriched in pathways in cancer, Ras signaling pathway, PI3K-Akt signaling pathway, MAPK signaling pathway, and TGF-β and other signaling pathways (Figure 3C). To sum up, this data confirms that an irradiation dose of 8Gy can promote malignant transformation.

CAFs promote the deterioration of lung cancer cells after ionizing irradiation

Clinical practice has revealed the presence of tumor recurrence in patients treated with low radiation doses and that the TME has an important role in this process (14). This study further explored whether activated CAFs are involved in this process. The wound healing assay demonstrated that CAFs enhance the proliferation of A549 cells after ionizing irradiation. The wound healed faster in the non-irradiated A549 cells of the CAF_0-CM and CAF_8-CM subgroups compared to the DMEM subgroup ($P < 0.05$) (Figures 4A, B). After 72 h, the wounds of the CAF_0-CM and CAF_8-CM subgroups were nearly completely healed. In the irradiation group, the wound healing of all subgroups slowed down; it was almost stationary in the DMEM subgroup, while it was faster in the CAF_8-CM subgroup than that of the CAF_0-CM subgroup ($P < 0.05$). Thus, we concluded that CAFs could promote the migration of A549 or radiation-damaged A549, and this ability could be enhanced by irradiated-activated CAFs.

To further investigate the effect of CAFs on lung cancer cells (A549), we conducted the CCK8 assay to detect their effect on

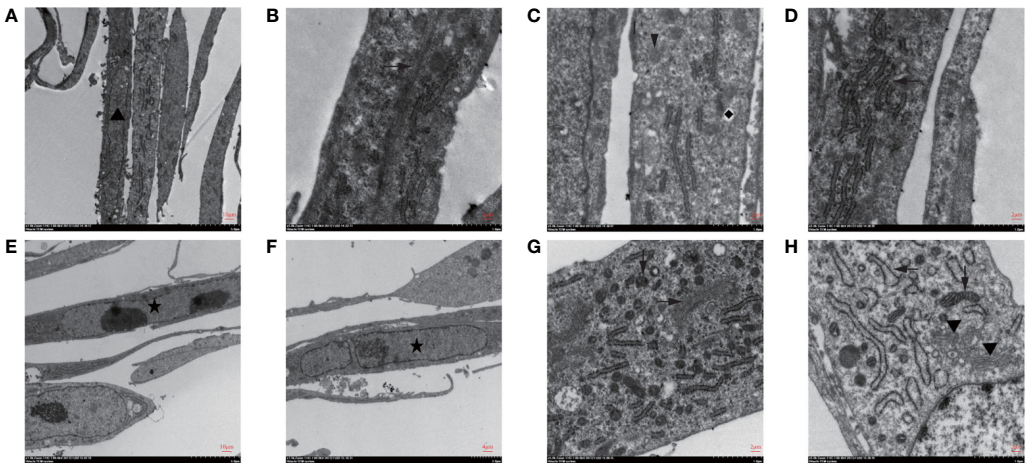

FIGURE 2
Subcellular structure of CAFs changed after irradiation was seen under transmission electron microscopy. **(A–D)** The observation of the subcellular structure of CAFs before irradiation showed that the nuclei were oval with obvious nucleoli (▲). Rough endoplasmic reticulum (←), mitochondria (↓), vesicles (◆), microtubules (→), and microfilaments can be seen in the cytoplasm; **(E–H)** The observation of the subcellular structure of CAFs after 8Gy irradiation revealed double nucleoli and double nuclei (★) and lobulated nuclei in the nucleus. The rough endoplasmic reticulum increased and expanded, and mitochondria were divided and increased, while Golgi apparatus (▼) increased in the cytoplasm.

the proliferation of A549. As shown in Figure 4C, the proliferation capacity of A549 cells irradiated by 6Gy X-ray (solid black line) was significantly lower than 0Gy (solid gray line). However, the number of A549 cells in the CAF_0-CM subgroup (gray dotted line) and CAF_8-CM subgroup (gray dash line) was significantly higher than in the DMEM group (solid gray line) after 72 h in the unirradiation group (0Gy). From the proliferation rate, the slope within 72 h of the CAF_0-CM subgroup (gray dotted line) and CAF_8-CM subgroup (gray dash line) was similar but significantly higher than the control ($P < 0.05$). Under 6Gy irradiation, the CAF_0-CM subgroup (black dotted line) and the CAF_8-CM subgroup (black dash line) showed a similar proliferation trend to the A549 cells of the DMEM irradiation group. The proliferation rate of the CAF_8-CM subgroup was the fastest within 48 h, while the slope of the CAF_0-CM subgroup (black dotted line) decreased rapidly after 48 h and showed the inhibition of proliferation. All these analyses revealed that irradiated CAFs have a stronger promotion effect on A549 cell proliferation.

Apart from the adenocarcinoma, another non-small cell lung cancer cell line, H1299, was also applied for validation. CAFs had a stronger inductive effect on the migration ability of lung cancer cells H1299 by transwell cell co-culture experiment. H1299 cells immersed in irradiated CAFs (CAF_8) culture medium had a higher number and density of transmembrane cell clones ($P < 0.05$) compared with un-irradiated CAFs (CAF_0) (Figures 4D, E). The

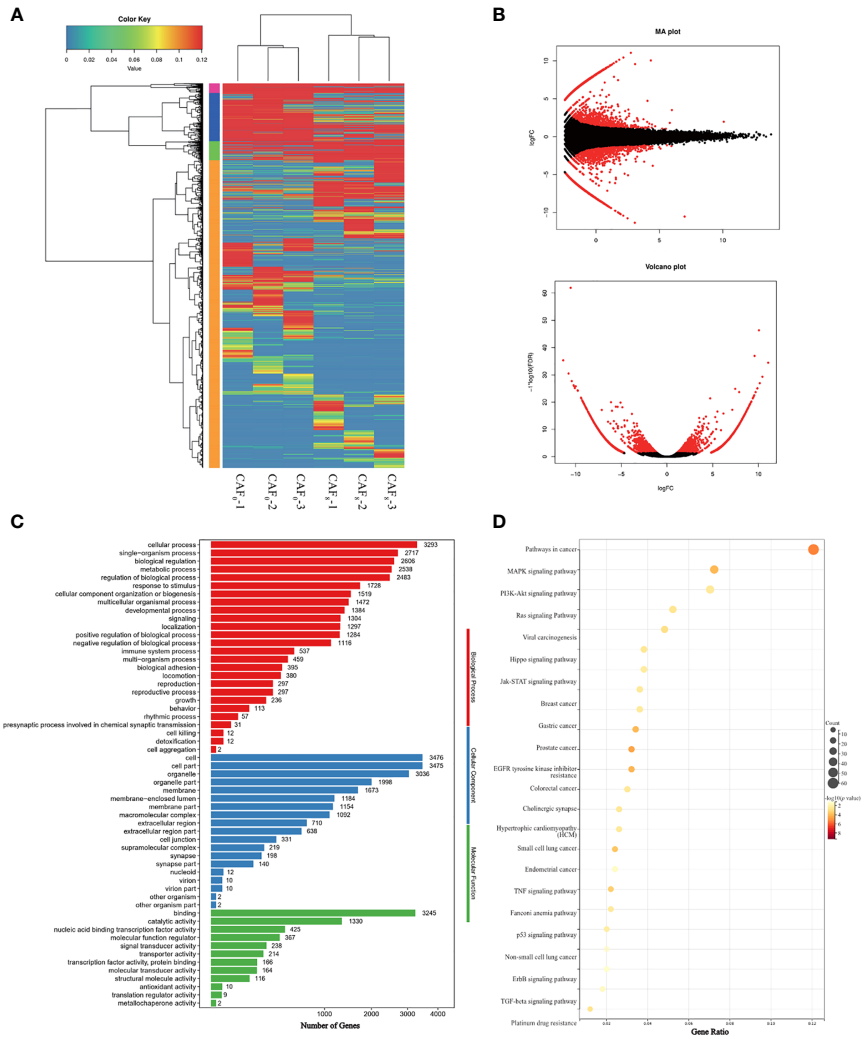

FIGURE 3
Identification and functional characterization of CAFs under 0Gy and 8Gy irradiation. **(A)** The cluster analysis of 0Gy compared to 8Gy irradiated CAFs (3 samples for each group) and the heat map showed that the irradiated CAFs differed more significantly at the gene level; **(B)** Volcano plot of differential genes after 0Gy vs. 8Gy irradiation of CAFs; **(C)** Gene Ontology (GO) analysis of differentially expressed genes; **(D)** Kyoto Encyclopedia of Genes and Genomes (KEGG) analysis of differentially expressed genes.

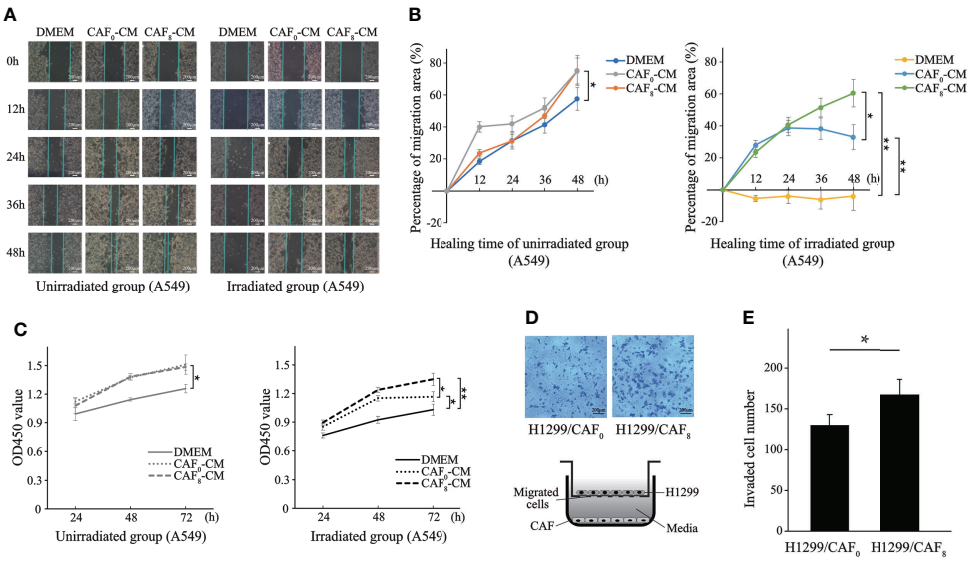

FIGURE 4
CAFs' conditioned medium (CM) promoted proliferation and migration of lung cancer cells after ionizing irradiation. **(A)** Representative images of wound healing assay for the A549 cells in irradiated group and unirradiated group treated with DMEM, CAF_0-CM, and CAF_8-CM; **(B)** Quantification of the change in healing area (%) over time in different subgroups; **(C)** Differences in the proliferation of A549 after irradiation with or without 6Gy in different conditioned medium were analyzed by the CCK8 assay; **(D)** Transwell assay analyzed the migration of H1299 cells co-cultured with CAF_0 and CAF_8; **(E)** The histogram showed the number of transmembrane H1299 cells in two groups. (T-test, data are presented as the mean ± S.D. *$P < 0.05$, **$P < 0.01$).

number of transmembrane cell clones in the H1299/CAF_8 subgroup was about 20% more than that in H1299/CAF_0 subgroup.

Flow cytometry results showed that irradiated CAFs had a stronger inhibitory effect on apoptosis of A549 cells (Figure 5). In the unirradiated A549 cell group, the apoptosis rate of the CAF_0-CM and CAF_8-CM subgroups was about 50% and 80% lower than the DMEM control ($P < 0.05$). In the irradiation group, the apoptosis rate of the CAF_0-CM subgroup and CAF_8-CM subgroup showed the same inhibitory trend ($P < 0.05$).

The enrichment analyses of transcriptome sequencing data showed that DEGs were related to transcriptional factors, membrane-enclosed lumen, as well as pancarcinoma-related pathways and drug resistance (Figure 3). Based on the complex mechanism involved in the activation of CAFs and its effect on cancer cells, we proposed that the exosome from CAFs

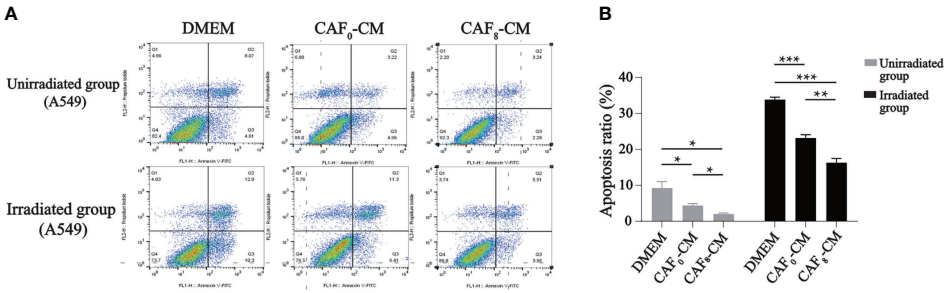

FIGURE 5
Flow cytometry analyzed the apoptosis of A549 cells received irradiation or not and treated with DMEM, CAF_0-CM, CAF_8-CM. **(A)** CAFs exhibited an inhibitory effect on A549 cells apoptosis, which showed more obvious in radiation-activated CAFs. In the unirradiated group, the CAF_8-CM subgroup displayed more normal cells with less viable apoptotic cells. And when A549 received 6Gy irradiation, the number of the viable apoptotic cells in DMEM subgroup was twice as many as that in the CAF_8-CM subgroup, which indicated the protective value of CAFs for irradiated A549; **(B)** A quantitative statistical analysis of the apoptotic cells in the different groups was carried out, and the bar graphs visualized the differences in apoptosis. (T-test, data are presented as the mean ± S.D. *P < 0.05, **P < 0.01, ***P < 0.001).

might participate in the modulation by paracrine mechanisms. CAF exosomes contain various components such as proteins, DNA, and RNA that could activate many signaling pathways and facilitate intercellular communication (21). GW4869 is a kind of exosome inhibitor that can decrease CAF exosome secretion by ~70% *in vitro* (24). Also, local injection in the late scar formation period with GW4869 reduced α-SMA$^+$ fibroblasts and extracellular matrix production, including collagen I and collagen II (25). The results of exosome inhibition experiments demonstrated that exosome was an important mediator for accelerating the proliferation and migration of A549 cells induced by irradiated CAFs. There was no difference in apoptosis rate ($P > 0.05$) between non-irradiated A549 cells in the G+CAF_0-CM subgroup and G +CAF_8-CM subgroup compared with G+DMEM (Figures 6A, B). In irradiated A549 cells, the apoptosis rate was lower in the G +CAF_0-CM subgroup ($P < 0.001$) and G+CAF_8-CM subgroup ($P < 0.01$) compared with the control.

In the transwell culture system, compared with CAFs, fewer A549 cells could penetrate the polycarbonate membrane regardless of whether the MRC5 cells in the lower chamber underwent ionizing radiation or not, and there was no significant difference in the number of transmembrane cells between the $MRC5_0$ subgroup and $MRC5_8$ subgroup ($P > 0.05$). The number was about 6 times that of the $MRC5_0$ subgroup when under the induction of non-irradiated CAFs (CAF_0) in the lower chamber ($P < 0.001$). However, ionized CAFs (CAF_8) induced more A549 cells to migrate downwards, and the number of transmembrane cells was about 1.5 times that of the CAF_0 group ($P < 0.001$). This result was similar to the migration and the induction of H1299 cells. Nevertheless, when GW4869 was added into the lower chamber, the number of A549 cells induced to transmembrane was significantly lower than that in the non-GW4869 treated subgroup (CAF_0 or CAF_8) ($P < 0.001$) regardless if CAFs in the lower chamber were irradiated or not (CAF_0+G or CAF_8+G) (Figures 6C, D).

Radiated CAFs promote the deterioration of A549 xenograft

Mice were subcutaneously inoculated with CAFs (CAF_0, CAF_8) and A549 cells with a ratio of 1:1 to establish a subcutaneously implanted tumor model; the control group was inoculated with A549 cells only. All mice successfully developed tumors and gradually gained weight. The rates of weight gain were similar among groups from the slope of the curve (Figure 7A). According to the tumor volume growth curve (Figure 7B), the volume of implanted tumors in the A549+CAF_0 group increased faster than in the A549 group ($P < 0.05$), while the A549+CAF_8 group was the fastest one ($P < 0.05$). After 13 days of inoculation, the volume of

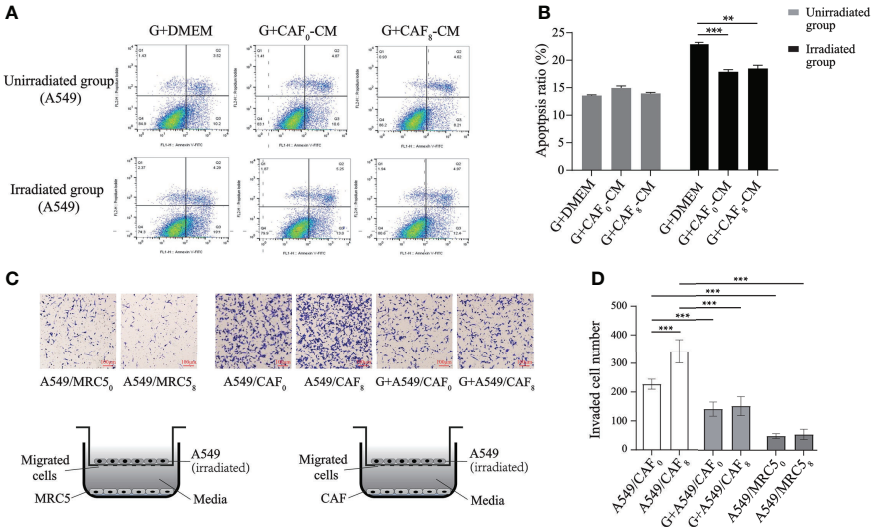

FIGURE 6
Exosome inhibitor GW4869 (G) inhibited the proliferation and migration of A549 cells induced by irradiated CAFs. **(A)** Flow cytometry analyzed the apoptosis of A549 cells received irradiation or not and treated with G+DMEM, G+CAF_0-CM, and G+CAF_8-CM. GW4869 (exosome releasing inhibitor) can inhibit "apoptosis protection" effect of CAFs on A549 cells in unirradiated group almost completely, but partially in irradiated group; **(B)** The histogram of apoptosis ratio (%) of the A549 cells in different subgroups of A; **(C)** Designation of transwell assay and the results of transmembrane A549 cells when co-cultured with $MRC5_0$, $MRC5_8$, CAF_0 ± GW4869, CAF_8 ± GW4869. Radiation-activated CAFs promoted migration of lung cancer cell, which can be inhibited by GW4869. All A549 cells received 6Gy irradiation before seeding on the upper chamber and co-cultured with CAFs or MRC5; **(D)** Statistics histogram of the numbers of invaded cells of different subgroups in **(C)**. (T-test, data are presented as the mean ± S.D. **P < 0.01, ***P < 0.001).

implanted tumors in the A549+CAF_8 group was larger than that in the A549+CAF_0 and A549 groups ($P < 0.05$). This difference gradually increased in tumor volume among all groups. On the 22nd day of inoculation, the implanted tumor size of several animals reached 15 mm in length (Figure 7C). Consequently, all the animals were anesthetized and sacrificed, and *ex vivo* analysis was performed. The tumor of the A549+CAF_8 group was heavier than the A549+CAF_0 and A549 group ($P < 0.05$, $P < 0.001$ respectively) (Figure 7D). These data indicated that irradiated-CAFs have a stronger promotion effect on the tumor initiation and progression.

Hematoxylin and eosin (H&E) and immunohistochemical staining suggested that CAFs after ionizing irradiation had higher proliferation ability in A549 transplanted tumors. H&E staining results showed no significant difference in tumor histomorphology among the three groups, which were all distributed in sheet or nest shapes. All tumor cells had obvious atypia, with large and dark nuclei, coarse nuclear chromatin, and mitotic images (Figures 8A–C). In comparison to the A549 group, the staining of α -SMA seemed more in the A549+CAF0 and A549+CAF8 groups, but the difference was not significant (Figures 8D–F, J). The immunohistochemical results of ki67 also showed that irradiated CAFs promoted the growth of A549 cell tumor and its chromogenic area in the A549+CAF_8 group was significantly higher than in A549 control ($P < 0.01$) and A549 +CAF_0 group ($P < 0.05$) (Figures 8G–I, K).

Discussion

Radiotherapy (RT) is an important treatment for malignant tumors, and more than 70% of tumor patients receive radiotherapy at different stages of the disease course. However, the emergence of tumor radiotherapy resistance and secondary malignant tumors are matters of utmost importance (26). RT can lead to high load mutations in the tumor genome, and the tumor genome mainly manifests in the form of small fragment deletion, which may be an important mechanism explaining poor prognosis in recent studies (27).

In the RT process, radiation kills tumor cells and affects the TME, forming a special radiation tumor microenvironment (RTME). Moreover, the interaction between tumor cells and TME is also considered a potential factor in inducing RT tolerance (28, 29). Radiation induces a series of interrelated processes in TME, including inflammatory response, local hypoxia, immune regulation, microcirculation reconstruction, interstitial tumor remodeling, and fibrosis (17). Numerous studies have shown that CAFs, a key player in TME, can promote the occurrence, development, metastasis, and formation of treatment tolerance in malignant tumors (10, 11). In the present study, we used A549 and H1299 cell lines as models to validate the effect of irradiated CAFs on tumor cells. Although higher doses of radiation could cause CAFs growth inhibition (30), CAFs irradiated by 8Gy X-rays still had the highest activity (Figures 1C–E). Therefore, our subsequent experiments were all based on this radiation dose.

Our results showed that the irradiation of 8Gy X-ray could promote the accelerated replication of nuclei, resulting in double nucleoli, double nuclei, and lobulated nuclei. Moreover, it could increase and expand the rough endoplasmic reticulum and Golgi apparatus in the cytoplasm, indicating that the synthesis ability of proteins, lipids, and sugars was improved. It also increased mitochondrial division, suggesting the enhancement of cellular energy metabolism. The up-regulated expression of α-SMA, FAP, vimentin, and the result of the MTT assay showed that irradiation could enhance the proliferation ability of CAFs. Transcriptome analysis showed a characteristic gene expression profile of radiated CAFs. The oncogenic genes significantly increased after irradiation, and these differentially expressed genes were mainly enriched in several common signaling pathways for promoting cancer progression, including the Ras signaling pathway, PI3K-Akt signaling pathway, and MAPK signaling pathway. CAFs irradiated at a higher dose may show similar genetic changes; however, these cells are prone to growth inhibition due to the activation of p53 signaling and the cell cycle arrest signaling pathway (30).

We further explored the effect of radiation-activated CAFs on lung cancer cells. To simulate the pathophysiological changes of tumors after RT, irradiated A549 cells were used to prepare cancer cell models. Firstly, we found that A549 cells were sensitive to ionizing irradiation, and 6Gy irradiation partially inhibited their growth, while the treatment with a conditioned medium of radiation-activated CAFs could reverse the apoptosis of irradiated A549 cells and promote their growth (Figure 4C), thus reflecting the "apoptosis protection" effect of radiation-activated CAFs on cancer cells. These results were further verified in wound healing. Transwell assay demonstrated that radiation-activated CAFs could induce the migration of H1299 cells. Also, these results could help explaining some clinical phenomena, such as local fibrous hyperplasia and distant metastasis induced by RT, where a higher interstitial ratio (TSR) was associated with a worse prognosis. CAFs have a strong radiation tolerance. Although the dose of RT used in clinical practice causes continuous DNA damage, CAFs only undergo senescence and are not eliminated in the tumor. The latter can continue to promote tumor growth and participate in the induction of tumor radiation resistance through the secretion of certain cytokines and growth factors, cooperating with the modified RTME by ionizing radiation (31). The conditioned medium of 8Gy-activated CAFs promoted the migration of A549 cells in the A549-irradiated and non-irradiated groups. The difference among DMEM, CAF_0-CM and CAF_8-CM culture groups was greater when A549 received 6-Gy irradiation (Figure 4B), and we wonder if there were some special factors that participate in the repair of damaged cancer cells but had no effect on undamaged cells, which could be triggered by DNA

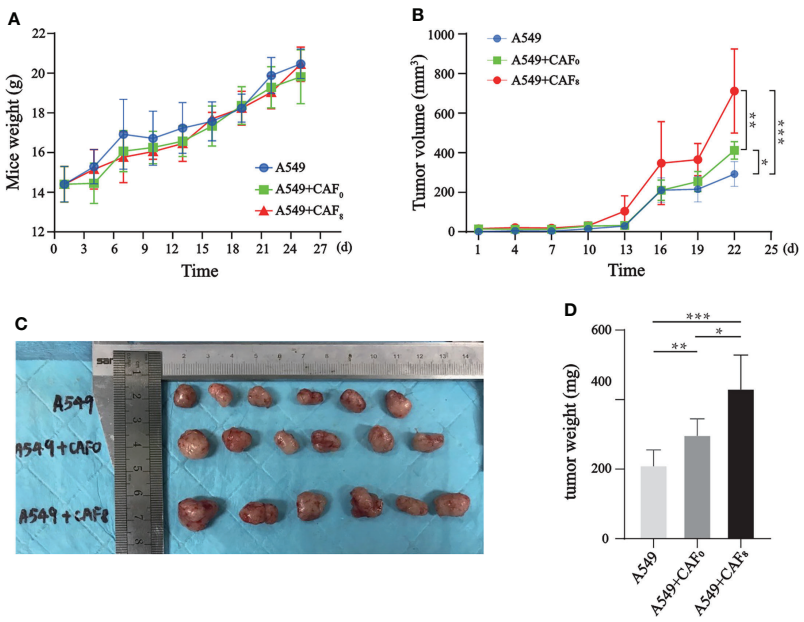

FIGURE 7
CAFs promoted the tumor volume and weight of the A549 cells tumor model after ionizing irradiation. **(A)** The line graph of mice weight showed that differences of body weight changes for each mouse in different groups was no significant; **(B)** The line graph of tumor volume indicated that CAF_8 had the greatest promotion on the tumorigenicity of A549 cells; **(C)** An overview of implanted tumors in three subgroups revealed that the tumor volume of the A549+CAF8 group was the biggest, and the A549 group was the smallest; **(D)** The tumor volume was measured for each group of mice and the t-test was applied for statistical analysis. The histogram displayed that CAF8 had the strongest promotion on the tumorigenicity of A549 cells. (T-test, data are presented as the mean ± S.D. *P < 0.05, **P < 0.01, ***P < 0.001).

breakage or by proteins that related to radiation-induced apoptosis-associated pathway. Nonetheless, the above assumption needs to be further confirmed by subsequent experiments. Moreover, after irradiation of A549, all cells in the irradiated group showed decreased ability to migrate compared to non-irradiated cells, suggesting that activated CAFs could at least partially reverse the damage caused by radiation to cancer cells. However, in the proliferation CCK8 assay, we could also find the difference between DMEM and CAF0-CM in the irradiated group, which indicated that even not activated by irradiation, CAFs exhibited partially pro-malignant behavior, resulting the protection of cancer cells throughout tumorigenesis.

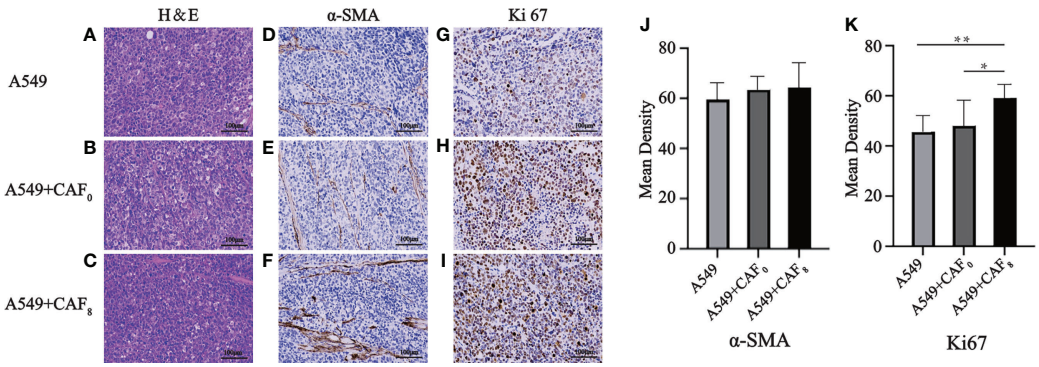

FIGURE 8
Hematoxylin and eosin (H&E) and immunohistochemical staining of the exfoliated tumor tissues were used to detect histopathological features and expression of α-SMA and Ki67 in A549, A549+CAF_0, and A549+CAF_8 subgroups. **(A–C)** Representative images of H&E staining for three subgroups; **(D–F)** Immunohistochemical staining of α-SMA of three subgroups; **(G–I)**. Immunohistochemical staining of Ki67 of three subgroups; **(J, K)** The histogram of the mean density of α-SMA positive staining area **(J)** and Ki67 positive staining area **(K)** in the samples from all groups. (T-test, data are presented as the mean ± S.D. *P < 0.05, **P < 0.01).

Some previous studies have reported that the release of exosomes is the main way for CAFs to exert the ability to "promote malignancy" (32–34). GW4869 is a cellular permeable, non-competitive N-Smase (neutral sphinomatidylase) inhibitor that inhibits exosome release by blocking neuramide-mediated cellular multivesicular germination (35). In the present study, we obtained similar results by using GW4869. It has also been reported that the exosomes from CAFs can activate the TGF-β signaling pathway in cancer cells and promote the stem-cell nature of colorectal cancer (CRC) cells, thereby increasing radiation resistance and promoting the normal growth of CRC cells in colorectal cancer (36). This was also verified in our transcriptome, which detected upregulation of TGF-β signaling pathways in radiation-activated CAFs (Figure 3). Finally, we demonstrated the *in vivo* pro-malignancy effect of radiation-activated CAFs by constructing a rodent model of subcutaneous implantation of tumors. This is similar to previous reports suggesting that CAFs can accelerate the growth rate of implanted cancer cells in animals (13). Our results not only confirmed this conclusion but also found that radiation-activated CAFs have a stronger tumorigenic effect *in vivo* than primary CAFs with regard to tumor size and growth rate.

The previous studies suggested that CAFs have a vital role in the occurrence and development of malignant tumors and the formation of tolerance to RT and chemotherapy; however, few reported on the effects of RT on CAFs (14). Therefore, we proposed that radiation not only kills cancer cells but also transforms CAFs in tumor tissues, named "radiation activation", thus facilitating cancer cells to survive, migrate, and develop tolerance to RT and chemotherapy. Indeed, TME has undergone great changes compared with ordinary conditions *via* irradiation, which will be beneficial or mediate the qualitative changes of tumor resistance to treatment. Therefore, targeting CAFs or preventing CAFs activation will be beneficial for improving the therapeutic effect of radiotherapy and reducing the occurrence of local tissue fibrosis.

To sum up, the present study confirmed that CAFs could be activated by a certain dose of ionizing radiation and that activated CAFs showed stronger "pro-malignant" biological behavior. Our results also suggested that inhibiting CAFs activation would have a significant effect on improving clinical RT efficacy. With the continuous elucidation of the complicated mechanism as well as the continuous research of CAFs inhibitors or CAFs activation blockers, the CAFs-inhibiting treatment may become a necessary supplement for tumor precision radiotherapy in the future.

Data availability statement

The original contributions presented in the study are included in the Supplementary Material, further inquiries can be directed to the corresponding author (YY).

Ethics statement

The studies involving human participants were reviewed and approved by Medical Ethics Committee of Renmin Hospital of Wuhan University. The patients/participants provided their written informed consent to participate in this study. The animal study was reviewed and approved by Medical Ethics Committee for Animal Experiments, Renmin Hospital of Wuhan University.

Author contributions

YY, ZLZ and QS contributed to the conception of the study; ZYZ, YD, BW, YL contributed significantly to carry out experiments and analysis; ZHL and ZML performed the data analyses and wrote the manuscript; YG and LG helped perform the analysis with constructive discussions. All authors contributed to the article and approved the submitted version.

Funding

This work was supported by Key Youth Training Foundation of Renmin Hospital of Wuhan University (No. 2013-18); Beijing Medical and Health Foundation (No. YWJKJJHKYJJ-BXS5-22006); Chen Xiao-ping Foundation for the Development of Science and Technology of Hubei Province (CXPJJH122006-1005).

Acknowledgments

We thank Wuhan Frasergen Bioinformatics Co. Ltd for technical support with sequencing and data analysis.

Conflict of interest

The authors declare that the research was conducted in the absence of any commercial or financial relationships that could be construed as a potential conflict of interest.

Publisher's note

Supplementary material

The Supplementary Material for this article can be found online at: https://www.frontiersin.org/articles/10.3389/fonc.2022.965660/full#supplementary-material

References

1. Hoffman D, Dragojević I, Hoisak J, Hoopes D, Manger R. Lung stereotactic body radiation therapy (SBRT) dose gradient and PTV volume: a retrospective multi-center analysis. *Radiat Oncol* (2019) 14:162. doi: 10.1186/s13014-019-1334-9

2. Sato A, Rahman NIA, Shimizu A, Ogita H. Cell-to-cell contact-mediated regulation of tumor behavior in the tumor microenvironment. *Cancer Sci* (2021) 112(10):4005–12. doi: 10.1111/cas.15114

3. Mao X, Xu J, Wang W, Liang C, Hua J, Liu J, et al. Crosstalk between cancer-associated fibroblasts and immune cells in the tumor microenvironment: new findings and future perspectives. *Mol Cancer* (2021) 20:131. doi: 10.1186/s12943-021-01428-1

4. Kalluri R. The biology and function of fibroblasts in cancer. *Nat Rev Cancer* (2016) 16(9):582–98. doi: 10.1038/nrc.2016.73

5. Nomura S. Identification, friend or foe: Vimentin and alpha-smooth muscle actin in cancer-associated fibroblasts. *Ann Surg Oncol* (2019) 26:4191–92. doi: 10.1245/s10434-019-07894-8

6. Borriello L, Nakata R, Sheard MA, Fernandez GE, Sposto R, Malvar J, et al. Cancer-associated fibroblasts share characteristics and protumorigenic activity with mesenchymal stromal cells. *Cancer Res* (2017) 77(18):5142–57. doi: 10.1158/0008-5472

7. Fitzgerald AA, Weiner LM. The role of fibroblast activation protein in health and malignancy. *Cancer Metastasis Rev* (2020) 39:783–803. doi: 10.1007/s10555-020-09909-3

8. Primac I, Maquoi E, Blacher S, Heljasvaara R, Van Deun J, Smeland HY, et al. Stromal integrin alpha11 regulates PDGFR-beta signaling and promotes breast cancer progression. *J Clin Invest* (2019) 129(11):4609–28. doi: 10.1172/JCI125890

9. Kaps L, Schuppan D. Targeting cancer associated fibroblasts in liver fibrosis and liver cancer using nanocarriers. *Cells* (2020) 9(9):2027. doi: 10.3390/cells9092027

10. Alexander J, Cukierman E. Cancer associated fibroblast: Mediators of tumorigenesis. *Matrix Biol* (2020) 91-92:19–34. doi: 10.1016/j.matbio.2020.05.004

11. Fiori ME, Di Franco S, Villanova L, Bianca P, Stassi G, De Maria R. Cancer-associated fibroblasts as abettors of tumor progression at the crossroads of EMT and therapy resistance. *Mol Cancer* (2019) 18:70. doi: 10.1186/s12943-019-0994-2

12. Heichler C, Scheibe K, Schmied A, Geppert CI, Schmid B, Wirtz S, et al. STAT3 activation through IL-6/IL-11 in cancer-associated fibroblasts promotes colorectal tumour development and correlates with poor prognosis. *Gut* (2020) 69 (7):1269–82. doi: 10.1136/gutjnl-2019-31920

13. Su S, Chen J, Yao H, Liu J, Yu S, Lao L, et al. CD10(+)GPR77(+) cancer-associated fibroblasts promote cancer formation and chemoresistance by sustaining cancer stemness. *Cell* (2018) 172(4):841–56. doi: 10.1016/j.cell.2018.01.009

14. Tommelein J, De Vlieghere E, Verset L, Melsens E, Leenders J, Descamps B, et al. Radiotherapy-activated cancer-associated fibroblasts promote tumor progression through paracrine IGF1R activation. *Cancer Res* (2018) 78(3):659–70. doi: 10.1158/0008-5472

15. Dumont N, Liu B, Defilippis RA, Chang H, Rabban JT, Karnezis AN, et al. Breast fibroblasts modulate early dissemination, tumorigenesis, and metastasis through alteration of extracellular matrix characteristics. *Neoplasia* (2013) 15 (3):249–62. doi: 10.1593/neo.121950

16. Sahai E, Astsaturov I, Cukierman E, DeNardo DG, Egeblad M, Evans RM, et al. A framework for advancing our understanding of cancer-associated fibroblasts. *Nat Rev Cancer* (2020) 20(3):174–86. doi: 10.1038/s41568-019-0238-1

17. Barker HE, Paget JT, Khan AA, Harrington KJ. The tumour microenvironment after radiotherapy: mechanisms of resistance and recurrence. *Nat Rev Cancer* (2015) 15:409–25. doi: 10.1038/nrc3958

18. Xia WY, Feng W, Zhang CC, Shen YJ, Zhang Q, Yu W, et al. Radiotherapy for non-small cell lung cancer in the immunotherapy era: the opportunity and challenge-a narrative review. *Transl Lung Cancer Res* (2020) 9(5):2120–36. doi: 10.21037/tlcr-20-827

19. Menon H, Ramapriyan R, Cushman TR, Verma V, Kim HH, Schoenhals JE, et al. Role of radiation therapy in modulation of the tumor stroma and microenvironment. *Front Immunol* (2019) 10:193. doi: 10.3389/fimmu.2019.00193

20. Verset L, Tommelein J, Moles Lopez X, Decaestecker C, Boterberg T, De Vlieghere E, et al. Impact of neoadjuvant therapy on cancer-associated fibroblasts in rectal cancer. *Radiother Oncol* (2015) 116(3):449–54. doi: 10.1016/j.radonc.2015.05.007

21. Shi L, Zhu W, Huang Y, Zhuo L, Wang S, Chen S, et al. Cancer-associated fibroblast-derived exosomal microRNA-20a suppresses the PTEN/PI3K-AKT pathway to promote the progression and chemoresistance of non-small cell lung cancer. *Clin Transl Med* (2022) 12:e989. doi: 10.1002/ctm2.989

22. Cheng Y, Mo F, Li Q, Han X, Shi H, Chen S, et al. Targeting CXCR2 inhibits the progression of lung cancer and promotes therapeutic effect of cisplatin. *Mol Cancer* (2021) 20:62. doi: 10.1186/s12943-021-01355-1

23. Kim CS, Kim JM, Nam SY, Yang KH, Jeong M, Kim HS, et al. Low-dose of ionizing radiation enhances cell proliferation *via* transient ERK1/2 and p38 activation in normal human lung fibroblasts. *J Radiat Res* (2007) 48(5):407–15. doi: 10.1269/jrr.07032

24. Richards KE, Zeleniak AE, Fishel ML, Wu J, Littlepage LE, Hill R. Cancer-associated fibroblast exosomes regulate survival and proliferation of pancreatic cancer cells. *Oncogene* (2017) 36(13):1770–78. doi: 10.1038/onc.2016.353

25. Chen J, Zhou R, Liang Y, Fu X, Wang D, Wang C. Blockade of lncRNA-ASLNCS5088-enriched exosome generation in M2 macrophages by GW4869 dampens the effect of M2 macrophages on orchestrating fibroblast activation. *FASEB J* (2019) 33(11):12200–12. doi: 10.1096/fj.201901610

26. Lee SY, Jeong EK, Ju MK, Jeon HM, Kim MY, Kim CH, et al. Induction of metastasis, cancer stem cell phenotype, and oncogenic metabolism in cancer cells by ionizing radiation. *Mol Cancer* (2017) 16:10. doi: 10.1186/s12943-016-0577-4

27. Kocakavuk E, Anderson KJ, Varn FS, Johnson KC, Amin SB, Sulman EP, et al. Radiotherapy is associated with a deletion signature that contributes to poor outcomes in patients with cancer. *Nat Genet* (2021) 53(7):1088–96. doi: 10.1038/s41588-021-00874-3

28. Ashrafizadeh M, Farhood B, Eleojo Musa A, Taeb S, Najafi M. The interactions and communications in tumor resistance to radiotherapy: Therapy perspectives. *Int Immunopharmacol* (2020) 87:106807. doi: 10.1016/j.intimp.2020.106807

29. McLaughlin M, Patin EC, Pedersen M, Wilkins A, Dillon MT, Melcher AA, et al. Inflammatory microenvironment remodelling by tumour cells after radiotherapy. *Nat Rev Cancer* (2020) 20(4):203–17. doi: 10.1038/s41568-020-0246-1

30. Wang Z, Tang Y, Tan Y, Wei Q, Yu W. Cancer-associated fibroblasts in radiotherapy: challenges and new opportunities. *Cell Commun Signal* (2019) 17:47. doi: 10.1186/s12964-019-0362-2

31. Donlon NE, Power R, Hayes C, Reynolds JV, Lysaght J. Radiotherapy, immunotherapy, and the tumour microenvironment: Turning an immunosuppressive milieu into a therapeutic opportunity. *Cancer Lett* (2021) 502:84–96. doi: 10.1016/j.canlet.2020.12.045

32. Luga V, Wrana JL. Tumor-stroma interaction: Revealing fibroblast-secreted exosomes as potent regulators of wnt-planar cell polarity signaling in cancer metastasis. *Cancer Res* (2013) 73(23):6843–7. doi: 10.1158/0008-5472.CAN-13-1791

33. Miki Y, Yashiro M, Okuno T, Kitayama K, Masuda G, Hirakawa K, et al. CD9-positive exosomes from cancer-associated fibroblasts stimulate the migration ability of scirrhous-type gastric cancer cells. *Br J Cancer* (2018) 118:867–77. doi: 10.1038/bjc.2017.487

34. Xu K, Zhang C, Du T, Gabriel ANA, Wang X, Li X, et al. Progress of exosomes in the diagnosis and treatment of lung cancer. *BioMed Pharmacother* (2021) 134:111111. doi: 10.1016/j.biopha.2020.111111

35. Dinkins MB, Dasgupta S, Wang G, Zhu G, Bieberich E. Exosome reduction *in vivo* is associated with lower amyloid plaque load in the 5XFAD mouse model of alzheimer's disease. *Neurobiol Aging* (2014) 35(8):1792–800. doi: 10.1016/j.neurobiolaging.2014.02.012

36. Liu L, Zhang Z, Zhou L, Hu L, Yin C, Qing D, et al. Cancer associated fibroblasts-derived exosomes contribute to radioresistance through promoting colorectal cancer stem cells phenotype. *Exp Cell Res* (2020) 391(2):111956. doi: 10.1016/j.yexcr.2020.111956

frontiers | Frontiers in Oncology

TYPE Original Research
PUBLISHED 12 January 2023
DOI 10.3389/fonc.2022.999158

OPEN ACCESS

EDITED BY
Eric W-F Lam,
State Key Laboratory of Oncology in South China, Sun Yat-sen University Cancer Center (SYSUCC), China

REVIEWED BY
Malinee Thanee,
Khon Kaen University, Thailand
Tomoaki Koga,
Kumamoto University, Japan

*CORRESPONDENCE
Tavan Janvilisri
tavan.jan@mahidol.ac.th

SPECIALTY SECTION
This article was submitted to Molecular and Cellular Oncology, a section of the journal Frontiers in Oncology

RECEIVED 20 July 2022
ACCEPTED 02 December 2022
PUBLISHED 12 January 2023

CITATION
Sukphokkit S, Kiatwuthinon P, Kumkate S and Janvilisri T (2023) Distinct cholangiocarcinoma cell migration in 2D monolayer and 3D spheroid culture based on galectin-3 expression and localization. *Front. Oncol.* 12:999158. doi: 10.3389/fonc.2022.999158

Distinct cholangiocarcinoma cell migration in 2D monolayer and 3D spheroid culture based on galectin-3 expression and localization

Siriwat Sukphokkit[1], Pichamon Kiatwuthinon[2], Supeecha Kumkate[3] and Tavan Janvilisri[1]*

[1]Department of Biochemistry, Faculty of Science, Mahidol University, Bangkok, Thailand, [2]Department of Biochemistry, Faculty of Science, Kasetsart University, Bangkok, Thailand, [3]Department of Biology, Faculty of Science, Mahidol University, Bangkok, Thailand

Introduction: Cholangiocarcinoma (CCA) is difficult to cure due to its ineffective treatment and advanced stage diagnosis. Thoroughly mechanistic understandings of CCA pathogenesis crucially help improving the treatment success rates. Using three-dimensional (3D) cell culture platform offers several advantages over a traditional two-dimensional (2D) culture as it resembles more closely to *in vivo* tumor.

Methods: Here, we aimed to establish the 3D CCA spheroids with lowly (KKU-100) and highly (KKU-213A) metastatic potentials to investigate the CCA migratory process and its EMT-associated galectin-3 in the 3D setting.

Results and discussion: Firstly, the growth of lowly metastatic KKU-100 cells was slower than highly metastatic KKU-213A cells in both 2D and 3D systems. Hollow formation was observed exclusively inside the KKU-213A spheroids, not in KKU-100. Additionally, the migration activity of KKU-213A cells was higher than that of KKU-100 cells in both 2D and 3D systems. Besides, altered expression of galectin-3 were observed across all CCA culture conditions with substantial relocalization from inside the 2D cells to the border of spheroids in the 3D system. Notably, the CCA migration was inversely proportional to the galectin-3 expression in the 3D culture, but not in the 2D setting. This suggests the contribution of culture platforms to the alternation of the CCA cell migration process.

Conclusions: Thus, our data revealed that 3D culture of CCA cells was phenotypically distinct from 2D culture and pointed to the superiority of using the 3D culture model for examining the CCA cellular mechanisms, providing knowledges that are better correlated with CCA phenotypes *in vivo*.

KEYWORDS

3D culture, spheroid, cholangiocarcinoma, galectin-3, cell migration

1 Introduction

Cholangiocarcinoma (CCA) is an epithelial malignancy of the biliary ducts. The global incidence of CCA is on the rising trend with the highest rate in Southeast Asia, especially in the northeastern part of Thailand (33.4 and 12.3 cases per 100,000 people in men and women, respectively) (1, 2). Studies of CCA patients in the regions with high parasitic prevalence revealed a strong association between chronic liver fluke and CCA carcinogenesis (1, 3, 4). CCA has also been implicated with biliary duct disorders, hepatitis B and C infection, and primary sclerosing cholangitis (5, 6). Asymptomatic and non-specific symptoms often make an early diagnosis of CCA difficult, causing patients to be diagnosed at an advanced stage (7). Surgical resection is usually represented as the standard therapy while radiation and chemotherapy are deemed less effective. However, the success rate of CCA treatment remains poor as the surgical treatment by liver resection and transplantation only yield ~25-40% 5-year survival rate (8). As a result, a profound understanding in CCA molecular pathways is crucially required to improve the treatment efficiency and to identify novel potent molecular target for future CCA therapy.

In order to thoroughly gain knowledge on CCA pathogenesis and carcinogenesis, *in vitro* studies using CCA cell lines have been implemented as tools to discern the cellular and molecular alteration of the disease without the involvement of patient participants or animal studies (9–11). Despite easy manipulation, the traditional *in vitro* 2D culture system lacks several biological cues that are established *in vivo*, posing major pitfalls in correlating the *in vitro* with *in vivo* results (12). Alternatively, an *in vitro* three-dimensional (3D) culture has therefore been developed to overcome these problems and bridges the gap between the 2D culture and the animal model. The 3D culture system has been established to be more resembling to *in vivo* tumor properties, including histomorphology, functions, and microenvironments in terms of cellular heterogeneity, nutrients and oxygen gradients, cell-cell interaction, matrix deposition, and gene expression (13–15). Currently, there are several methods to establish tumor spheroids including forced-floating method (16), hanging drop method (17), agitation-based approach (18), matrix- and scaffold-based culture (19, 20), and microfluid cell culture platforms (21, 22). Among these methods, the matrix-based cell culture recapitulates cellular organization and functions due to the presence of various types of cell-extracellular matrix (ECM) interactions (23). As a result, the ECM proteins are important for cell growth and differentiation as well as maintenance of cellular homoeostasis including the epithelial-mesenchymal transition (EMT). EMT is the central process which changes non-motile epithelial phenotypic cells into motile or invasive mesenchymal phenotypic cells (24). Its crucial role is evident toward cancer cell properties, especially its migration and metastatic potentials. Furthermore, EMT in hepatocellular and CCA has been found to involve with TGF-β signaling which leads to the inflammatory and fibrotic processes and pathogenesis (25).

Galectin-3, one key EMT proteins, is a β-galactoside-binding protein that is involved in many cellular functions of non-cancerous and cancerous tissues such as cell proliferation and survival, differentiation, inflammation, and cell migration and metastasis through the interaction between cells and ECM (26). Its structure consists of a carbohydrate recognition domain (CRD) and an N-terminal domain (ND), containing highly conserved proline and glycine-rich for 12 amino acid lengths. The ND can multimerize into dimers or pentamers when the ligand is present in CRD, transducing various extracellular and intracellular signals, causing diverse cellular activities (27, 28). Its expression is found in various organs, including the small intestine, kidney, colon, and lung tissue (29). Furthermore, galectin-3 is localized in diverse subcellular compartments, mainly in cytoplasm, cell surface membrane, and nucleus (30), responsible for the regulation of cell differentiation, apoptosis, and proliferation, respectively (29, 30). Remarkably, a previous study reported that galectin-3 could shuttle between nucleus and cytoplasm to mediate its functions (30). An aberrant expression of galectin-3 in distinct localization, specifically in cancers, has been associated with unique functions (9, 31, 32). In prostate cancer, galectin-3 is mainly localized at the cytoplasmic compartment of cancer specimens and its low expression is also related to poor progression of patients (31). Additional findings illustrated that cytoplasmic galectin-3 was associated with tumor progression (31, 33). Also, the loss of galectin-3 expression was associated with higher T-stage and the reduction of survival rate in renal carcinoma (32). A previous study on CCA showed that galectin-3 expression in intrahepatic CCA was lower than that in the normal bile duct (9). Moreover, gene suppression of galectin-3 in CCA cell lines also induces cell motility and cell invasion (9). In addition to cell mobility and invasion, galectin-3 displayed an association with chronic inflammation, enhancing the fibrotic pathogenesis in many types of tissues and cancers (34, 35). A recent study on intrahepatic CCA patients with COVID-19 infection displayed that the expression of galectin-3 was directly correlated with the level of MMP-9, another key indicator for the inflammation and the promotion of lung fibrosis (35). To date, there has been no report on other cell culture models, for example, 3D cultures and organoids, to confirm the role of galectin -3.

In this study, we established the 3D culture of CCA cells including lowly-metastatic KKU-100 and highly metastatic KKU-213A, formally known as KKU-M213, cells using the Matrigel-based culture to provide the cells with ECM environments (10). The cancer characteristics in terms of cell proliferation, cell migration, cell organization and protein expression between the 2D culture and 3D culture were evaluated. The level of proteins involved in cancer metastasis, including EMT and galectin-3, were compared among CCA cells and 2D- and 3D-based culture

systems. Furthermore, the role of galectin-3 in cell migration of both culture systems was examined using gene silencing and rescue assays. Our results highlighted the distinct patterns of galectin-3 expression in both cells in 2D and 3D settings, resulting in different migration activities.

2 Materials and methods

2.1 Reagents

Ham's F12 nutrient mix, Roswell Park Memorial Institute (RPMI) 1640, fetal bovine serum (FBS), penicillin/streptomycin, and Lab-Tek II 8-well chamber slide were purchased from Thermo Fisher Scientific (Waltham, MA, USA). Corning® Matrigel® Growth Factor Reduced (GFR) basement membrane matrix and cell recovery solution were acquired from Corning (Corning, NY, USA). Ribonuclease A and phenylmethylsulphonyl fluoride (PMSF) protease inhibitor were purchased from Sigma Chemicals (St. Louis, MO, USA). Bradford solution was purchased from Bio-Rad (Hercules, CA, USA). Hoechst 33342, TRITC-conjugated phalloidin, primary antibodies against galectin-3, ZEB-1, N-cadherin, E-cadherin, β-catenin, vimentin, horseradish peroxidase (HRP)-conjugated secondary antibodies against anti-rabbit and anti-mouse antibodies, Alexa Fluor® 647-conjugated secondary antibody against anti-rabbit antibodies and SignalFire™ ECL Reagent were purchased from Cell Signaling Technologies (Denver, MA, USA). The primary antibody against β-actin was purchased from Sigma-Aldrich. Triton X-100 was obtained from Bio-Rad. Recombinant human galectin-3 (rGal-3) was purchased from Merck (Dorset, UK).

2.2 Cell lines and culture conditions

Human poorly differentiated KKU-100 and mixed papillary and non-papillary KKU-213A CCA cell lines, derived from Thai CCA patients, respectively, were employed to represent lowly and highly invasive CCA models in this study (10, 11). Both cell lines were purchased from the Japanese Collection of Research Bioresources Cell Bank and maintained in Ham's F12 nutrient mix supplemented with 10% FBS, 100 U/ml penicillin and 100 µg/ml streptomycin. Human intrahepatic CCA RBE cell line, kindly gifted from Prof. David Bates (University of Nottingham, UK), was maintained in RPMI 1640 supplemented with 10% FBS, 100 U/ml penicillin and 100 µg/ml streptomycin. All cell lines were cultured at 37°C in a 5% CO_2 incubator.

2.3 Tumor spheroid formation

To produce tumor spheroids of CCA cell lines, 35 µl of GFR Matrigel at a concentration of 5,000 µg/ml was filled into a 96-well plate and incubated at 37°C for 2 h. Then, 5 x 10^3 CCA cells were seeded into Matrigel-coated wells and were further incubated for 15 min to allow cell attachment. Ham's F12 nutrient mix supplemented with 10% FBS, 2% of 5 mg/ml Matrigel, 100 U/ml penicillin and 100 µg/ml streptomycin were added at a total volume of 120 µl each well. The 3D spheroids were formed and incubated 37°C in a 5% CO_2 incubator and the culture medium were changed every two days.

2.4 Cell proliferation assay

For monolayer culture, ~5 x 10^3 cells were seeded in a 96-well plate and incubated for 24 h at 37°C in 5% CO_2 incubator. The cells were collected by trypsinization. The number of cells was counted by a dye exclusion method using 0.4% trypan blue. For 3D culture proliferation assay, the diameters of tumor spheroids were observed under a phase-contrast inverted microscope (Nikon model eclipse TS100, Minato, Tokyo, Japan) with 40x magnification for 5 fields per well and were measured using an ImageJ program (NIH image, National Institutes of Health, Bethesda, MD, USA). The cellular morphology was observed under a phase-contrast microscope using 100x magnification.

2.5 Migration assay for monolayer cells

Wound healing assay was performed by creating a scratch on the monolayer cells as our previous study (36). Migration activity of the cells was recorded at different timepoints. First, ~1 x 10^5 CCA cells were seeded in a 24-well plate and incubated for 24 h. Then, culture medium was discarded, and the cells were washed with phosphate buffer saline (PBS). Scratches were created, and scattered cells were removed. Cells were then supplemented with Ham's F12 nutrient mix containing 0.1% FBS, 100 U/ml penicillin and 100 µg/ml streptomycin. Wound images were captured under a phase-contrast microscope at 0 and 12 h to reduce the contribution of cell proliferation to fill the gap. The migration areas were determined using ImageJ analysis software version 1.8.0. The relative migration was calculated as the ratio between the difference in migration wound area at time 12 h relative to 0 h and migration wound area at time 0 h.

2.6 Migration assay for 3D CCA spheroids

The 3D migration assay for CCA spheroids was modified from a previously published protocol (37). Briefly, the 96-well plate was coated with 50 µl of 125 µg/ml GFR Matrigel and incubated at 37°C for 2 h. Twenty thousand (2 x 10^4) CCA cells were then seeded on Matrigel-pre-coated wells and grew for 4 days. They were then collected and pipetted into Matrigel-coated

wells. After that, the CCA spheroids were supplemented with 180 µl of Ham's F12 nutrient mix, 0.1% FBS, 100 U/ml penicillin, and 100 µg/ml streptomycin. Spheroid images were taken at 0 and 12 h to prevent the effect of cell proliferation under a phase-contrast microscope. Next, cell migration areas were determined using ImageJ analysis software. The relative cell migration was subsequently calculated as the difference in the migrating area between time at 12h and 0 h.

2.7 Gene expression by qPCR

Total RNA was extracted from CCA cells in 2D and 3D culture systems using TRIzol reagent (Invitrogen, MA, USA). Then, 1 µg of the extracted RNA was used as a template to synthesize first strand cDNA using iScript^{TM} cDNA synthesis kit (Biorad, CA, USA). Then, the relative gene expression of galectin-3 was evaluated using quantitative real-time polymerase chain reaction using specific galectin-3 primers and iTaq Universal SYBR Green Supermix (Bio-Rad, CA, USA). All reactions were performed in triplicate using the CFX Connect Real-Time system (Bio-Rad, CA, USA) with the following thermocycling conditions: initial denaturation at 95°C for 5 min, extension at 95°C for 30 s, 60°C for 30 s, 70°C for 60 s (40 cycles), and final extension at 70°C for 1 min. Actin gene expression was used as an internal housekeeping gene control to normalize gene expression between samples. The relative fold change was calculated using the $2^{-\Delta\Delta Cq}$ method. The gene primer sequences of galectin-3 F: 5' GCCAACGAGCGGAAAATGG 3′, R: 5′ CAGGCCATCCTTGAGGGTTT 3′ and actin F: 5′ GCACAGACCTCGCCTT 3′, R: 5′ CTTGCACATGCCGAG 3′ were used.

2.8 Protein extraction and western blotting

Total proteins were retrieved using RIPA lysis buffer and a PMSF protein inhibitor. One hundred microliters of lysis cocktail were pipetted onto monolayer cells, which were harvested using a cell scraper. The supernatant was transferred into a microcentrifuge tube and was centrifuged at 4°C 15,000 x *g* for 10 min. The supernatant as protein lysate was collected for further analysis. For tumor spheroids, spheroids were collected using cell recovery solution and transferred into a 1.5 ml-microcentrifuge tube. The tumor spheroids were washed three times with cell recovery solution to eliminate ECM. The cell pellet was then filled with 50 µl of protein lysis cocktail and sonicated for 10 min on ice. The protein concentrations were determined using the Bradford assay. Then, 20 µg of protein sample was subjected to 10% SDS-PAGE at 100 V. The separated proteins were transferred to a nitrocellulose membrane using semi-dry electroblotting (Trans-Blot Turbo^{TM} Transfer System, Bio-Rad laboratories, Hercules, CA, USA). The membrane was washed 3 times with tris buffer saline containing 0.1% tween and then incubated with 5% skim milk for 1 h to block non-specific binding. Primary antibodies for ZEB1 (1:1,000), E-cadherin (1:1,000), N-cadherin (1:1,000), β-catenin (1:500), vimentin (1:500), galectin-3 (1:500) and β-actin (1:10,000) were probed on the membranes at 4°C overnight. The membranes were then washed 3 times and incubated with HRP-conjugated secondary antibodies (1:500) for 1.5 h. The immunoreactivity of protein bands was determined using an enhanced chemiluminescent (ECL) substrate. Protein intensities were evaluated using ImageJ analysis software.

2.9 Immunofluorescence

For monolayer culture, cells were seeded into an 8-well Lab-Tek II chamber slide (Sigma-Aldrich, St. Louis, MO, USA) and incubated for 48 h. Then, cells were fixed using 4% paraformaldehyde for 15 min and washed with PBS for 5 min three times. The slide was blocked with 5% BSA for 30 min and then washed with PBS. Galectin-3 antibody (1:500) was added to the cells with incubation at 4°C overnight. The supernatant was discarded, and the cells were washed PBS for 5 min three times. Then, Alexa 647-conjugated secondary antibody was added to the cells with 1 h incubation in the dark. Hoechst 33342 (5 µg/µl) was added to the cells for 10 min in the dark. Cells were then washed with PBS for 5 min thrice and observed using a confocal laser scanning microscope (Olympus model FV10i-DOC, Shinjuku, Tokyo, Japan). For 3D culture, tumor spheroids were formed using a 3D Matrigel overlay culture for 6 days. Tumor spheroids were then retrieved with ice-cold PBS and centrifugation at 3,500 x *g* for 5 min. A tissue clearing protocol was adopted to improve image quality (38). Briefly, tumor spheroids were incubated with 25% formamide and 10% PEG for 10 min, followed by 50% formamide and 20% PEG for 1 h. Subsequently, the spheroids were washed extensively with PBS for 3 times and fixed with 4% paraformaldehyde for 1 h at room temperature. Tributyl phosphate solution was then added to the samples for 30 min at room temperature, followed by washing step with PBS 3 times. For cellular organization, the CCA spheroids were counterstained with TRITC-phalloidin and Hoechst33342 for actin filament and nucleus, respectively. For the localization of galactin-3, the CCA spheroids were incubated with galectin-3 antibody (1:500) overnight at 4°C and were washed with PBS 3 times. Alexa 647-conjugated secondary antibody was then added with 1 h incubation in the dark. Next, the stained CCA spheroids were wash with PBS. After that, Hoechst 33342 and TRITC-phalloidin were counterstained for 10 min in the dark. The CCA spheroids were then washed 3 times with PBS and transferred into an 8-well chamber slide before being observed using a confocal laser scanning microscope.

2.10 shRNA silencing of galectin-3

The galectin-3 shRNA plasmid (sc-155994-SH) containing a pool of three to five lentiviral vector plasmids each encoding galectin-3-specific 19-25 nucleotides (plus hairpin) shRNAs, and scramble shRNA plasmid-A (sc-108060) were purchased from Santa Cruz Biotechnology (Dallas, TX, USA). The knockdown experiment was slightly modified from our previous study (39). Briefly, galectin-3 shRNA or scramble plasmids were mixed with shRNA transfection reagent (sc-108061) and shRNA transfection media (sc-108062). Then, the plasmid mixture was transferred into the cells with 6 h incubation. Cells were then cultured in Ham's F-12 nutrient mix supplemented with 20% FBS, 100 U/ml penicillin and 100 µg/ml streptomycin. After 48 h, transfected cells were selected using 1 µg/ml of puromycin in normal culture media. Non-transfected cells were removed, and transfected cells were maintained for verification using qPCR and Western blotting.

2.11 Galection-3 rescue experiment in galectin-3-knockdowned CCA cells

To investigate the effect of galectin-3 in CCA cell mobility in 2D culture, galectin-3-knockdowned CCA cells were pre-plated in 24-well plate and wound scratches were generated, followed by an incubation with 1.0 or 5.0 µg/mL rGal-3 containing medium (Ham's F12 nutrient mix containing 0.1% FBS and 100U/ml penicillin/100 µg/ml streptomycin) for 6 or 12 h prior to experiment. For the 3D culture experiment, galectin-3-knockdowned CCA spheroids were pre-grown on Matrigel-coated wells for 4 days as previously described. Then, the galectin-3-knockdowned CCA spheroids were transferred to newly Matrigel-coated wells and incubated with 1.0 or 5.0 µg/mL rGal-3 containing medium (Ham's F12 nutrient mix or RPMI 1640 containing 0.1% FBS and 100U/ml penicillin/100 µg/ml streptomycin) for 6 or 12 h prior to experiment. The culture medium containing 1% PBS was used as a control for the rescue experiments.

2.12 Galection-3 expression in CCA patients and survival analysis

To evaluate the correlation between galectin-3 expression and survival in CCA patients, publicly available web-based tools for analyzing RNA sequencing data (GEPIA), the Cancer Genome Atlas (TCGA) and the Genotype-Tissue Expression (GTEx) databases were used (40). The RNA sequencing data from 36 tumor specimens were divided into two groups according to their expression levels and overall survival and disease-free survival rates were created.

2.13 Statistical analysis

All experiments were performed at least in three biological replicates. All data were evaluated using two-tailed unpaired student's T-test and presented as the mean ± standard error of the mean. The GraphPad Prism version 6.0 software was used for statistical analysis. Significant value cutoffs were set at $p < 0.05$.

3 Results

3.1 Characterization of CCA cells in 2D and 3D culture systems

To determine the growth rate of both CCA cell lines in 2D and 3D culture systems, the numbers of cells and the diameters of CCA tumor spheroids were determined, respectively. For 2D monolayers, the numbers of both KKU-100 and KKU-213A cells gradually increased from 0 to 48 h. Then, a drastic growth of KKU-213A cells was observed from 72 h onwards, whereas the growth pattern of KKU-100 cells was much slower. The doubling time of KKU-100 and KKU-213A cells was 168 h and 54.6 h, respectively, confirming that highly metastatic KKU-213A exhibited a higher growth rate than lowly metastatic KKU-100 (Figure 1A). In 3D culture, the formation of both CCA spheroids were clearly observed at 48 h and the growth of both CCA spheroids was evaluated using the spheroid diameters (Figure 1B). During the first 4 days, KKU-100 and KKU-213A spheroids appeared comparable in sizes (Figure 1B). Then, the size of KKU213A spheroids significantly increased, exceeding that of KKU-100 spheroids. The largest sizes of KKU-100 and KKU- 213A spheroids were observed at the diameters of 76.4 and 99.2 µm on days 8 and 10, respectively. Interestingly, the size of KKU-213A spheroids reduced after day 10 of cultivation, while the size of KKU-100 spheroids was comparable after day 5 of cultivation (Figure 1B). Furthermore, the morphological structure of the growing CCA spheroids demonstrated a round colony outline of both CCA spheroids (Figure 1C). Additionally, the internal cellular organization of both CCA spheroids was examined using a confocal microscope. Z-stack images showed that both CCA spheroids possessed mass-forming properties with distorted cell rearrangement, oppositely observed in 2D CCA monolayers (Figure 1D). Notably, the highly metastatic KKU-213A developed luminal space inside its spheroids whereas lowly metastatic KKU-100 possessed a relatively uniformed spheroids, indicating a distinctively internal cellular organization in 3D culture.

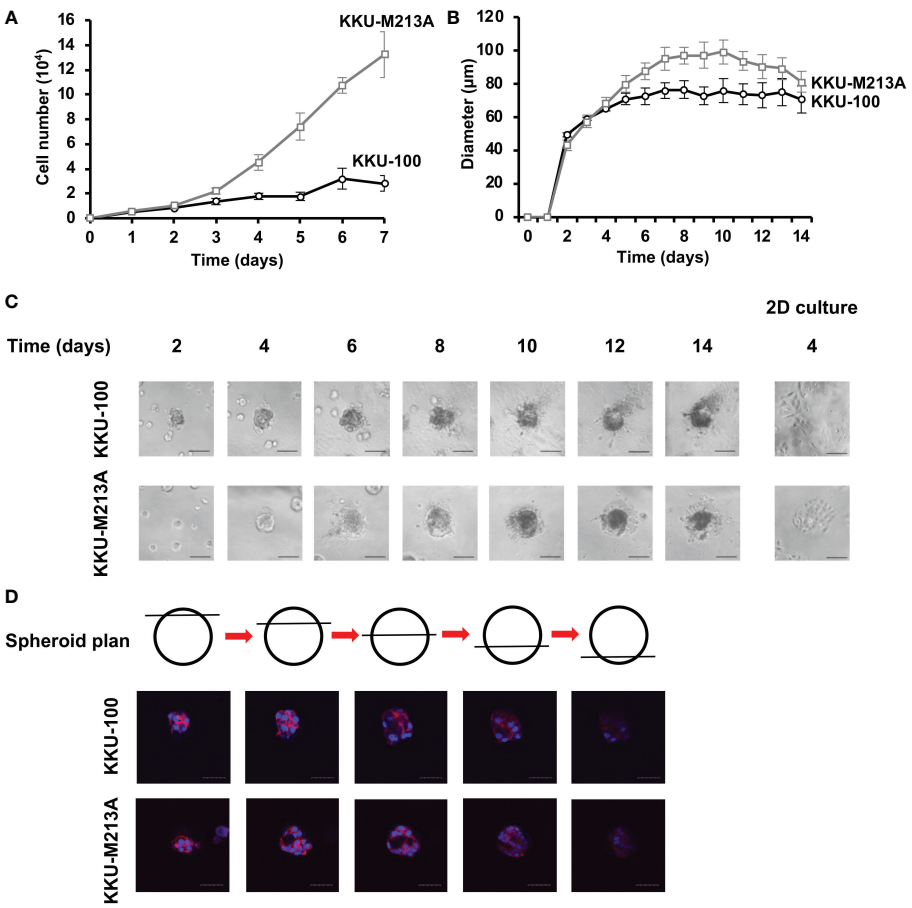

FIGURE 1
The growth rate of CCA cells in 2D and 3D cultures. **(A)** The growth rate of CCA cells in 2D culture as determined by cell counting. The cell numbers were counted every 24 h. Black circle and grey square represent KKU-100 and KKU-213A cells, respectively. **(B)** The growth rate of CCA cells in 3D culture as determined by diameter measurement. The diameter was measured every 24 h. Black circle and grey square represent KKU-100 and KKU-213A cells, respectively. The data represent means and ± standard error. **(C)** The tumor spheroid morphologies of KKU-100 and KKU-213A cells in 3D Matrigel-overlayed culture. The images were taken every 2 days using a phase-contrast microscope. The scale bars represent 100 μm. **(D)** Cellular organization of CCA spheroids. KKU-100 and KKU-213A cells were grown in 3D culture for 6 days. The CCA spheroids were permeabilized, blocked and subsequently stained with Hoechst 33342 for nucleus and TRITC-phalloidin for F-actin. Their structures were observed under a confocal microscope and Z-stack images were obtained. Red represents F-actin and blue represents nuclei. The scale bars represent 100 μm.

3.2 Migration ability of CCA cells in 2D and 3D culture systems

The migration activity of CCA cells was observed using the wound healing assay for 2D culture and 3D migration assay for 3D culture. For the 2D wound healing assay, KKU-100 cells exhibited significantly lower migration, compared with KKU-213A cells (Figures 2A, B). Interestingly, KKU-100 barely migrated toward the scratch wound area, indicating the incompetence in cell mobility of KKU-100. Also, the 3D migration assay showed that KKU-100 spheroids substantially possessed lower migratory ability, compared to KKU- 213A spheroids which exhibited approximately ~5.1-fold migrative activity (Figures 2C, D). Although the migrative activities between 2D and 3D culture systems were not readily comparable, these findings demonstrated that KKU-213A cells exhibited higher migrative potential compared with KKU-100 cells in both 2D and 3D cultures.

3.3 Differential EMT protein expression in 2D and 3D CCA cultures

To further understand the role of EMT in 2D and 3D CCA migration, EMT markers including β-catenin, together with epithelial (E-cadherin), and mesenchymal markers (N-cadherin, vimentin, ZEB1) were investigated at a protein level in both CCA monolayers and spheroids (Figures 3A, B).

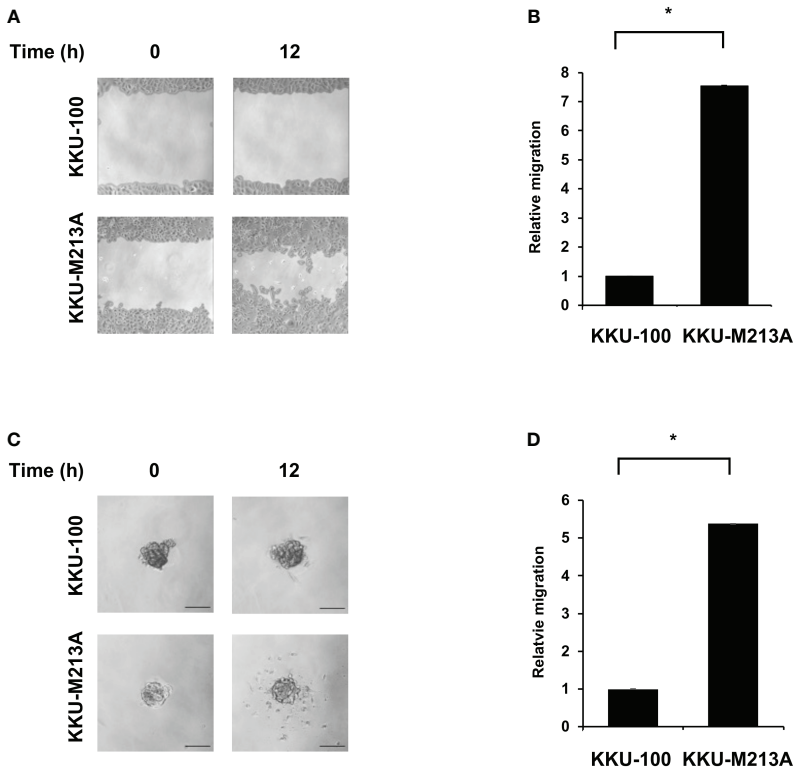

FIGURE 2
Migration activity of CCA cells in 2D and 3D cultures. KKU-100 and KKU-213A cells were grown as monolayers and spheroids for 4 days. **(A)** Wounds were created on CCA monolayer cells and size of the wound was photographed at 0 and 12 h following the wound scratch. **(B)** The relative migration is shown as the average value of migration index compared to KKU-100. **(C)** Representative images of 3D culture migration at 0 h and 12 h. The scale bars represent 100 μm. **(D)** The relative migration is represented by bar graph of the percentage migration area of KKU-213A in 3D culture compared with KKU-100. Data were presented as mean ± standard error, which were derived from three independent experiments, *$p < 0.05$.

For 2D monolayers, lowly metastatic KKU-100 and highly metastatic KKU-213A cells displayed no expression of vimentin. Moreover, the 2D KKU-100 cells demonstrated decreased expression of ZEB1, N-cadherin, and E-cadherin compared to the KKU-213A cells. Intriguingly, galectin-3, a multi-functional protein which has various ligands and locations, was expressed at a higher level in KKU-100 cells in relative to KKU-213A monolayers. In addition, the 3D KKU-100 spheroids exhibited reduced expression of ZEB1, N-cadherin, and E-cadherin while overexpressed galectin-3, compared to the 3D KKU-213A spheroids (Figures 3A, B). These results unveiled that galectin-3 was differentially expressed across culture conditions and CCA cell lines, causing it to be a good EMT candidate to examining the effect of EMT proteins on CCA migration. Subsequently, the intracellular localization of galectin-3 was examined to draw a correlation between cellular localization and migratory activities using immunofluorescence technique (Figure 4). In 2D culture, galectin-3 expressed throughout the nucleus and cytoplasmic compartment of the cells with a higher fluorescence intensity in KKU-100 than KKU-213A cells. In contrast, in 3D culture, galectin-3 was distinctively located on the outer layer of both KKU-100 and KKU-213A spheroids. Furthermore, KKU-100 spheroids had higher galectin-3 expression than KKU-213A spheroids, which is in accordance with Western blot analysis (Figure 3). Altogether, our data point to the different patterns of expression and localization of galectin-3 in 2D and 3D settings of highly and lowly metastatic CCA cells which potentially correlate with migratory activities in CCA.

3.4 Differential expression of galectin-3 revealed distinct migration activities in 2D and 3D CCA cells

Galectin-3 gene knockdown and recombinant galectin-3 (rGal-3) rescue assays were employed to investigate the correlation between galectin-3 and migration ability in CCA cells. KKU-213A was chosen as a CCA model due to the most distinguishable galectin-3 expression and migration ability. Gal-3-

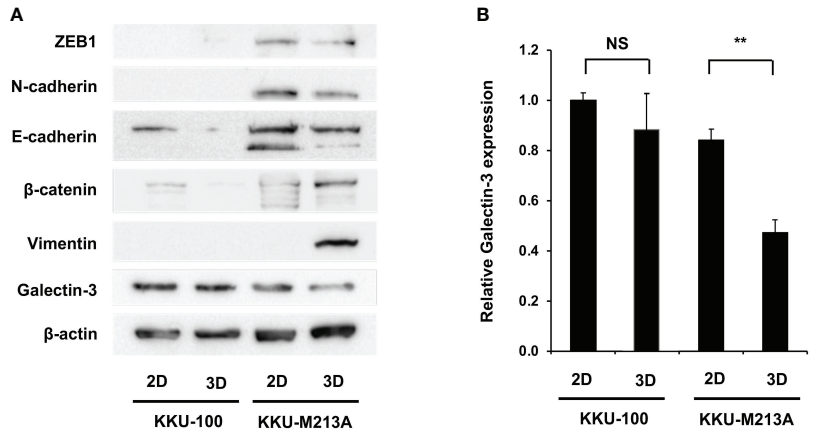

FIGURE 3
Migration-related expression in CCA cells in 2D and 3D culture systems. **(A)** CCA cells were grown as monolayers and spheroids for 6 days. Cells were harvested and lysed. Protein expression was determined by Western blotting. Migration-related proteins were compared between the two culture systems in each cell line. β-actin was used as an internal control. **(B)** Expressions of galectin-3 was quantified as relative intensity to β-actin. The data represent means and ± standard error. $^{**}p < 0.01$, NS represents not significant.

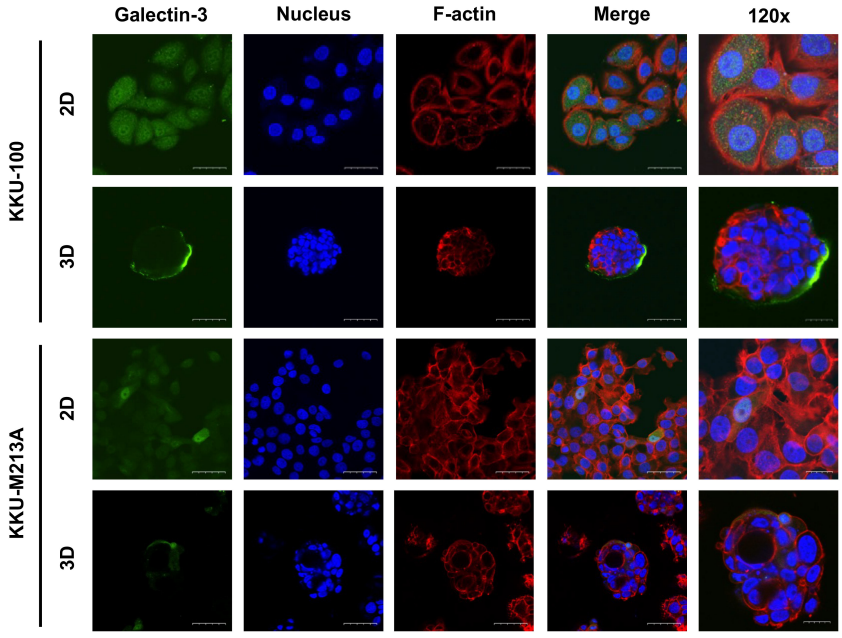

FIGURE 4
Localization of galectin-3 in 2D and 3D CCA cells. CCA cells were cultured as monolayer and spheroids for 10 days before harvesting for the immunofluorescence. CCA cells were fixed, permeabilized and blocked before staining with galectin-3 antibody (green). TRITC-phalloidin and Hoechst 33342 were used as counterstains for F-actin (red) and nuclei (blue), respectively. The tumor spheroid images were taken under a confocal microscope using 60x and 120x magnifications. The scale bars in 2D and 3D systems indicate 25 μm and 10 μm, respectively.

shRNA plasmids were transfected into the KKU-213A cells and showed a diminution in galectin-3 in both transcriptional and translational levels (Figures 5A–C). Additionally, the morphological study revealed no change in cellular structure in a comparison to its control cells in both 2D and 3D cultures (Figure 5D). We then performed the wound-healing assay for monolayer cells and the 3D migration assay for tumor spheroids, comparing between galectin-3-knockdown and control KKU-213A cells. The galectin-3-knockdown KKU-213A monolayers exhibited significantly lower cell migration compared to the control KKU-213A cells and their migration was resumed after adding the rGal-3 (Figures 5E, F). In contrast to 2D wound healing, the tumor spheroids of galectin-3-depleted KKU-213A cells revealed ~1.5-fold higher cell migration ability compared to KKU-213A spheroid control ($p < 0.01$) (Figures 5E, G). Furthermore, the rescue experiments displayed a strong adverse correlation between galectin-3 and migration ability in the 3D KKU-213A spheroids. To further confirm the role of galectin-3 on CCA cell migration, we additionally performed a stable knockdown of galectin-3 in RBE cells using shRNA transfection and evaluated cell migration in both 2D and 3D settings. The results coincided well with the findings observed for KKU-213A, suggesting the implication of galectin-3-associated pathways in 2D and 3D cultures of CCA cells (Supplementary Figure 1).

3.5 Clinical association between the expression of galectin-3 and overall survival in CCA TCGA database

As previously demonstrated, the expression and localization of galectin-3 in 3D CCA spheroids were explicitly deviated from that in 2D CCA monolayers and it was negatively correlated with the CCA migration ability. According to the high metastatic phenotype, poor prognosis and low overall survival were witnessed in a variety of cancers (26, 32). We then used

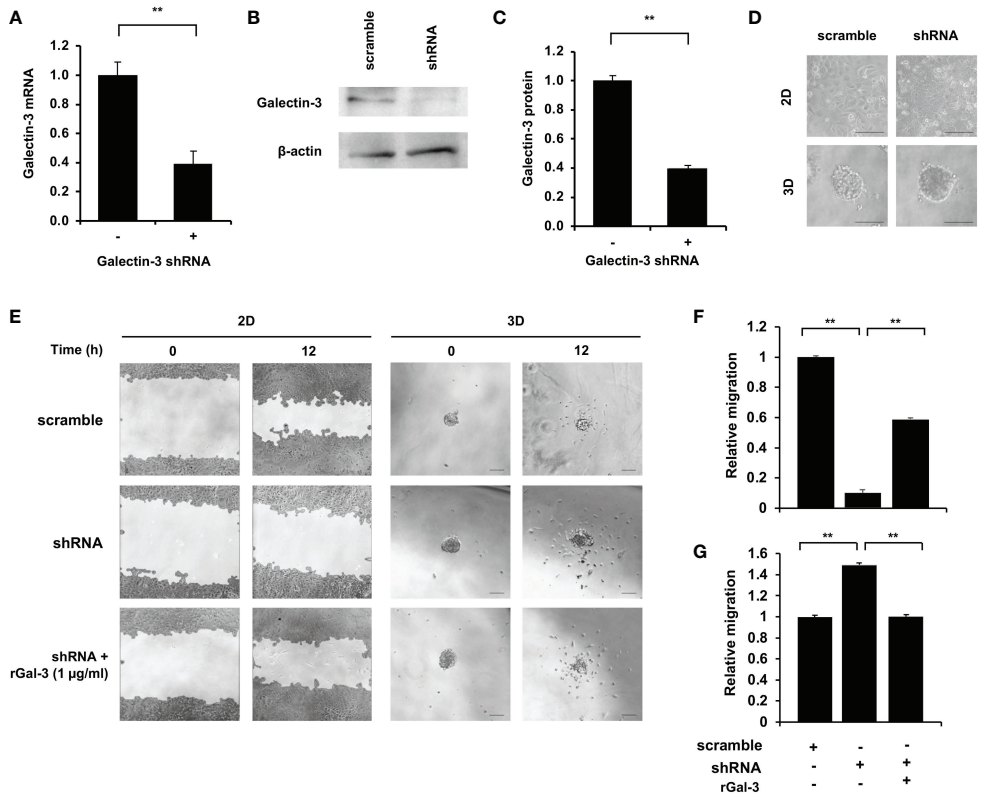

FIGURE 5
Effect of galectin-3 on 2D and 3D KKU-213A cell migration. **(A)** The relative galectin-3 mRNA level of KKU-213A knockdown cells compared to the control. **(B)** Representative galectin-3 immunoblots of KKU-213A cells subjected to *gal-3* and scrambled shRNA. β-actin was used as the loading control. **(C)** The relative galectin-3 protein expression of KKU-213A knockdown cells compared to the control. **(D)** The morphology of galectin-3 knockdown cells in 2D and 3D cultures. The 2D culture images were taken before cells reached confluence and 3D culture images were taken on day 6. **(E)** Control and galectin-3 knockdown KKU-213A cells were grown as monolayer or tumor spheroids for 4 days. rGal-3 was treated during the migration assay. The migration area of KKU-213A monolayer and tumor spheroids were collected at 0 h and 12 h. The scale bars represent 100 μm. **(F, G)** Bars represent the relative migration of galectin-3 knockdown cells with and without the treatment of rGal-3 in **(F)** 2D and **(G)** 3D conditions compared to the control cells. The data represent means and ± standard error. $^{**}p < 0.01$.

Kaplan-Meier analysis to validate the correlation of galectin-3 and survival in CCA patients using clinical TCGA database (n =18). The results showed that CCA patients with low galectin-3 expression, albeit not statistically significant, seemed to exhibit poor prognosis (Figure 6). The propensity of these data coincided with our experimental results. Collectively, we propose that the 3D CCA culture, which potentially recapitulate an CCA *in vivo* condition, provided knowledge on the probable negative association between galectin-3 and cell migration, leading to clinically lower survival outcome.

4 Discussion

CCA is a cancer arising from the epithelial cells of biliary trees. The incidence of CCA in Thailand is extremely high, especially in the Northeast part of Thailand (2, 3). Treatment failure for CCA is common due to patient presentation at late stages, thereby often causing metastasis (1). Hence, further understanding in the cellular and molecular pathways of CCA is urgently required to enhance the treatment efficiency. The use of a conventional 2D *in vitro* system in CCA research could greatly fulfil the fundamental knowledge on cellular mechanisms of CCA (9, 36, 41, 42). Nevertheless, the 2D cell monolayer culture lack a number of vital biological signals and intracellular interactions such as cell-cell and cell-extracellular matrix interactions, normally observed *in vivo* (23). Recently, an *in vitro* 3D culture in which the cells are surrounded by ECM proteins, could potentially recapitulate *in vivo*-like environment and render *in vivo* characteristics, bridging and overcoming the experimental gap (23). Although, there are a few studies on CCA 3D culture, none have attempted to compare the characteristics of CCA migration in 2D and 3D culture. Hence, we established the 3D CCA culture model using Matrigel as a scaffold and evaluated the migration ability of lowly and highly metastatic CCA cells in 2D and 3D settings with a reference to the expression of galectin-3.

3D culture produces cell aggregates or tumor spheroids *in vitro*, which are more physiologically relevant to tumor tissues than the traditional 2D culture. While the cells in 2D culture are uniformly enriched with both oxygen and nutrient, tumor spheroids receive differential amounts of oxygen and nutrients, of which cells inside the core are exposed to less amount than the cells at the border, resulting in the necrotic core (43–45). At an early stage, the size of CCA tumor spheroids increased rapidly. Smaller spheroids thoroughly allow diffusion of oxygen and nutrients sufficient for their growth. When the size of tumor spheroids increases, cells tend to disassociate from spheroids, which could be resulted from the insufficient amount of oxygen and nutrients. This phenomenon can also be observed in other types of cancer. For example, the proliferation rate of endometrial cancer cells, including Ishikawa, RL-95-2, KLE, and EN-10780 reduced when grown in 3D reconstituted basement membranes (46). The growth rate of colorectal cancer cells, including CACO-2, DLD-1, HT-29, 3w480, LOVO, and COLO-206F, decreased when cultured on the laminin-rich-extracellular matrix compared to the 2D culture (47). The structures of tumor spheroids can differ even if they are from the same type of cancer. Here, we report mass-forming spheroids with disorganized structures in both KKU-100 and KKU-213A cells. Confocal images revealed the lumen formation in KKU-213A spheroids, not in KKU-100 spheroids. The luminal structure was also observed in other types of cancer such as breast and colorectal cancer spheroids (48, 49). The hollow formation was contributed to the TRAIL-mediated autophagy or caspase-induced apoptosis as a result of hypoxia and nutrient deprivation condition, typically observed in the 3D culture (48, 50, 51). Additionally, in the colorectal cancer, there was a strong relationship between hollow-forming spheroids and tumor metastasis and poor prognosis (49). Cancer stem cells in primary colorectal tumors could moreover be identified using the 3D culture method (51). Furthermore, the fluorescent signals from the confocal microscope were dimmed at the lower z-stack

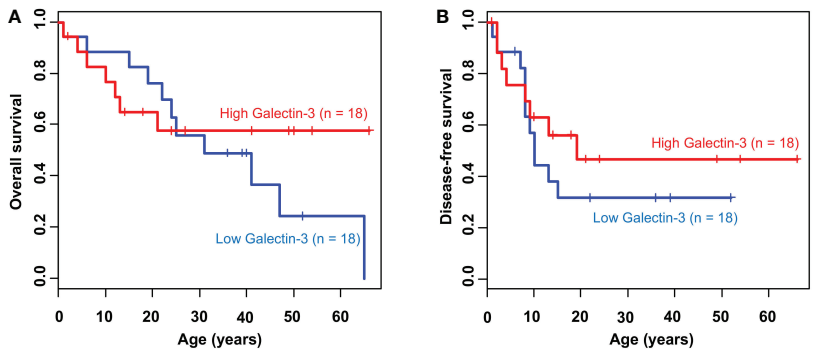

FIGURE 6
Kaplan-Meier survival curve of CCA patients according to galectin-3 expression. The cumulative **(A)** overall survival (P = 0.54) and **(B)** disease-free survival (P = 0.41) plot stratified by the level of galectin-3 expression.

due to the limitation of laser at z-depth around 20–30 μm. This phenomenon has been noted in tumor spheroids produced from 25 breast cancer cell lines, which were categorized into 4 groups based on their organization and cell-cell interaction. These structure formations depend on the properties of each cell line, such as metastatic properties (52).

Our data showed that the KKU-213A compared to KKU-100 cells exhibited higher migration activity in both 2D and 3D settings. Our scratch wound healing results in 2D culture were comparable to the previous data using the Transwell migration assay (53). Additionally, KKU-213A cells exhibited both collective and individual cell migration while KKU-100 cells showed only collective migration. In 3D culture, the migration activity of CCA tumor spheroids was measured on Matrigel-coated wells to preserve adhesion molecules resembling the tumor microenvironment. Both CCA spheroids migrated individually rather than collectively migrated and some cells represented a mesenchymal phenotype, elongated cell shape, which is the malignant feature of cancer (54).

The migration of tumor cells is regulated by various pathways. The central pathway of migration is EMT, which is the process that allows non-motile epithelial cells to become motile mesenchymal cells. EMT is contributed by many proteins and transcription factors. To migrate, E-cadherin expression, which is an epithelial marker, has been reported to be reduced to suppress epithelial phenotypes (55). Then, β-catenin, which normally binds to the cytosolic part of E-cadherin is released and moves into the nucleus to turn on the target genes such as Snail1 and MMP-7 (56). The β-catenin accumulation in the nuclei is often found with the loss of E-cadherin expression (57). These data are correlated with our results showing that reduced E-cadherin and induced β-catenin expression in 3D CCA culture, reflecting the malignant form of CCA cells. Among the mesenchymal markers investigated, we found the reduction of ZEB1 and N-cadherin expression, which function as an EMT inducer and a mesenchymal marker, respectively. As galectin-3 interacts with and regulates other proteins, which contribute to EMT during tumor cell migration and invasion. We therefore further investigated the expression and localization of galectin-3 in KKU-100 and KKU-213A in both 2D and 3D culture. Our results revealed that galectin-3 expression was lower in highly metastatic KKU-213A compared with lowly metastatic KKU-100 cells and was significantly reduced in KKU-213A spheroids, but not in KKU-100. These results agreed with a previous study that reported the association of decreased expression of galectin-3 with the metastatic potential of liver fluke-associated cholangiocarcinoma (9). Although the vast majority of research focused on galectin-3 expression, a few studies have attempted to investigate its localization. In 2D culture, galectin-3 was uniformly distributed in KKU-100 cells at the higher level compared to KKU-213A cells. So, the evenly distributed galectin-3 in 2D CCA monolayers might confer additional functions on the 2D CCA cells, interfering with the migratory activity of CCA cells (26). In contrast, galectin-3 in 3D culture was strongly expressed at the border of KKU-100 spheroids, but to a much lesser extent in KKU-213A spheroids. Typically, the formation of 3D spheroids promotes the expression of the cell adhesion molecules on the cell surface membrane and, hence, increased cell-cell interaction which could recruit the accumulation of galectin-3 near the edge of spheroids (58). Noticeably, the intensely high membrane-associated galectin-3 in 3D epithelial KKU-100 spheroids might be attributed to the demand of the cells on interacting with Matrigel and galactoside-conjugated glycans on their adjacent cells, enhancing the cell attachment and reducing the cell migration activity (58). Besides, galectin-3 might interact with ECM and form a tumor capsule, a fibrotic capsule that harasses migratory cells. This tumor capsule has been shown as a mechanical barrier against local invasion (59).

The verification of the association between galectin-3 and CCA cell migration was performed in KKU-213A cells, due to its most distinguishable galectin-3 expression and migratory activity. The galectin-3 gene knockdown showed contradictory observations between 2D and 3D cell migration which was already discussed in the abovementioned paragraph together with galectin-3 localization and intensity. In addition, other cancer studies also reported contrast cell mobility between 2D and 3D cultures (33, 60, 61). Notably, it has been demonstrated that the suppression of galectin-3 *via* siRNA in 2D highly metastatic KKU-213B cells, formally recognized as KKU-M214, led to the promotion of cell migration (9). These could potentially be due to the cell line-specific behaviors which exclusively displayed distinct phenotypes including differentially gene expression profiles (10). Furthermore, although Kaplan-Meier analyses denoted non-significant correlation between galectin-3 overall and disease-free survival rates, which was similar to the work reported previously, however, lower galectin-3 expression has been significantly associated with lymphatic metastasis (9). Also a recent study hinted to the therapeutic potential of galectin-3 for treating intrahepatic CCA patients (35). Hence, our data revealed the differential expression level of galectin-3 in a relation to culture systems. Also, the diminished galectin-3 in the 3D spheroid culture system was inversely correlated with CCA cell migration. This 3D cell migration behavior potentially pointed to the closer resemblance of that in CCA *in vivo* conditions.

5 Conclusions

In summary, we established and characterized the 3D lowly- and highly-metastatic CCA spheroids. The 3D CCA spheroids demonstrated distinct patterns of growth and migration, compared to the 2D CCA monolayers. We further revealed differential expression and localization of galectin-3 and other EMT proteins in different culture settings. Galectin-3 uniquely accumulated at the outer surface of the 3D CCA spheroids, potentially facilitating the

cell attachment and cellular binding characteristics. The expression of galectin-3 produced by the 3D CCA spheroids displayed a negative correlation with cell migration, which coincided well with previous observations in the clinical data. Altogether, the disparity in the culture systems described here illustrates the advantage of employing a 3D culture, which more resembles to *in vivo* conditions in investigating the CCA pathogenesis and carcinogenesis. It could potentially be developed as a CCA drug screening platform that offers a stronger correlation and more accurate interpretation to *in vivo* conditions.

Data availability statement

The original contributions presented in the study are included in the article/Supplementary Material. Further inquiries can be directed to the corresponding author.

Author contributions

SS and TJ designed and conceived the study. Material preparation, data collection and analyses were performed by SS, PK, SK. Analyses of the data were performed by SS, PK and TJ. The first draft of the manuscript was written by SS and PK and all authors commented on previous versions of the manuscript. All authors contributed to the article and approved the submitted version.

Funding

This research project is supported by Mahidol University (Basic Research Fund: fiscal year 2021).

Acknowledgments

We thank the Central Instrument Facility at Faculty of Science, Mahidol University and a scholarship from the Development and Promotion of Science and Technology Talents Project (SS). We also thank Thapakorn Sripramong, Pongphol Prattapong and Thanyapit Thita for their technical assistance.

Conflict of interest

The authors declare that the research was conducted in the absence of any commercial or financial relationships that could be construed as a potential conflict of interest.

Publisher's note

Supplementary material

The Supplementary Material for this article can be found online at: https://www.frontiersin.org/articles/10.3389/fonc.2022.999158/full#supplementary-material

References

1. Brindley PJ, Bachini M, Ilyas SI, Khan SA, Loukas A, Sirica AE, et al. Cholangiocarcinoma. *Nat Rev Dis Primers* (2021) 7(1):65. doi: 10.1038/s41572-021-00300-2

2. Sripa B, Pairojkul C. Cholangiocarcinoma: lessons from Thailand. *Curr Opin Gastroenterol* (2008) 24(3). doi: 10.1097/MOG.0b013e3282fbf9b3

3. Crellen T, Sithithaworn P, Pitaksakulrat O, Khuntikeo N, Medley GF, Hollingsworth TD, et al. Towards evidence-based control of opisthorchis viverrini. *Trends Parasitol* (2021) 37(5):370–80. doi: 10.1016/j.pt.2020.12.007

4. Sripa B, Tangkawattana S, Brindley PJ. Chapter five - update on pathogenesis of opisthorchiasis and cholangiocarcinoma. In: Sripa B, Brindley PJ, editors. *Advances in parasitology*. Cambridge, MA: Academic Press (2018). p. 97–113.

5. Rizvi S, Gores GJ. Pathogenesis, diagnosis, and management of cholangiocarcinoma. *Gastroenterology* (2013) 145(6):1215–29. doi: 10.1053/j.gastro.2013.10.013

6. Cigliano A, Chen X, Calvisi DF. Current challenges to underpinning the genetic basis for cholangiocarcinoma. *Expert Rev Gastroenterol Hepatol* (2021) 15 (5):511–26. doi: 10.1080/17474124.2021.1915128

7. Banales JM, Marin JJG, Lamarca A, Rodrigues PM, Khan SA, Roberts LR, et al. Cholangiocarcinoma 2020: the next horizon in mechanisms and management. *Nat Rev Gastroenterol Hepatol* (2020) 17(9):557–88. doi: 10.1038/s41575-020-0310-z

8. Mazzaferro V, Gorgen A, Roayaie S, Droz dit Busset M, Sapisochin G. Liver resection and transplantation for intrahepatic cholangiocarcinoma. *J Hepatol* (2020) 72(2):364–77. doi: 10.1016/j.jhep.2019.11.020

9. Junking M, Wongkham C, Sripa B, Sawanyawisuth K, Araki N, Wongkham S., et al. Decreased expression of galectin-3 is associated with metastatic potential of liver fluke-associated cholangiocarcinoma. *Eur J Cancer* (2008) 44(4):619–26. doi: 10.1016/j.ejca.2008.01.014

10. Sripa B, Seubwai W, Vaeteewoottacharn K, Sawanyawisuth K, Silsirivanit A, Kaewkong W, et al. Functional and genetic characterization of three cell lines derived from a single tumor of an opisthorchis viverrini-associated cholangiocarcinoma patient. *Hum Cell* (2020) 33(3):695–708. doi: 10.1007/s13577-020-00334-w

11. Sripa B, Leungwattanawanit S, Nitta T, Wongkham C, Bhudhisawasdi V, Puapairoj A, et al. Establishment and characterization of an opisthorchiasis-

associated cholangiocarcinoma cell line (KKU-100). *World J Gastroenterol* (2005) 11(22):3392–7. doi: 10.3748/wjg.v11.i22.3392

12. Lv D, Hu Z, Lu L, Lu H, Xu X. Three–dimensional cell culture: A powerful tool in tumor research and drug discovery (Review). *Oncol Lett* (2017) 14(6):6999–7010. doi: 10.3892/ol.2017.7134

13. Wang H, Brown PC, Chow ECY, Ewart L, Ferguson SS, Fitzpatrick S, et al. 3D cell culture models: Drug pharmacokinetics, safety assessment, and regulatory consideration. *Clin Transl Sci* (2021) 14(5):1659-80. doi: 10.1111/cts.13066

14. Barbosa MAG, Xavier CPR, Pereira RF, Petrikaitė V, Vasconcelos MH. 3D cell culture models as recapitulators of the tumor microenvironment for the screening of anti-cancer drugs. *Cancers* (2022) 14(1):190. doi: 10.3390/cancers14010190

15. Habanjar O, Diab-Assaf M, Caldefie-Chezet F, Delort L. 3D cell culture systems: Tumor application, advantages, and disadvantages. *Int. J. Mol. Sci* (2021) 22(22):12200. doi: 10.3390/ijms222212200

16. Amaral RLF, Miranda M, Marcato PD, Swiech K. *Comparative analysis of 3D bladder tumor spheroids obtained by forced floating and hanging drop methods for drug screening* (2017) 8:605. doi: 10.3389/fphys.2017.00605

17. Eder T, Eder IE. 3D hanging drop culture to establish prostate cancer organoids. In: Koledova Z, editor. *3D cell culture: Methods and protocols*. New York, NY: Springer New York (2017). p. 167–75.

18. Santo VE, Estrada MF, Rebelo SP, Abreu S, Silva I, Pinto C, et al. Adaptable stirred-tank culture strategies for large scale production of multicellular spheroid-based tumor cell models. *J Biotechnol* (2016) 221:118–29. doi: 10.1016/j.jbiotec.2016.01.031

19. Ngaokrajang U, Janvilisri T, Sae-Ueng U, Prungsak A, Kiatwuthinon P.. Integrin α5 mediates intrinsic cisplatin resistance in three-dimensional nasopharyngeal carcinoma spheroids via the inhibition of phosphorylated ERK /caspase-3 induced apoptosis. *Exp Cell Res* (2021) 406(2):112765. doi: 10.1016/j.yexcr.2021.112765

20. Unnikrishnan K, Thomas LV, Ram Kumar RM. *Advancement of scaffold-based 3D cellular models in cancer tissue engineering: An update* (2021) 11. doi: 10.3389/fonc.2021.733652

21. Mehling M, Tay S. Microfluidic cell culture. *Curr Opin Biotechnol* (2014) 25:95–102. doi: 10.1016/j.copbio.2013.10.005

22. Polidoro MA, Ferrari E, Marzorati S, Lleo A, Rasponi M. *Experimental liver models: From cell culture techniques to microfluidic organs-on-chip* (2021) 41 (8):1744–61. doi: 10.1111/liv.14942

23. Jensen C, Teng Y. *Is it time to start transitioning from 2D to 3D cell culture?*, Vol. 7. (2020). doi: 10.3389/fmolb.2020.00033

24. Chaffer CL, San Juan BP, Lim E, Weinberg RA. EMT, cell plasticity and metastasis. *Cancer Metastasis Rev* (2016) 35(4):645–54. doi: 10.1007/s10555-016-9648-7

25. Reichl P, Haider C, Grubinger M, Mikulits W. TGF-β in epithelial to mesenchymal transition and metastasis of liver carcinoma. *Curr Pharm Design* (2012) 18(27):4135–47. doi: 10.2174/138161212802430477

26. Hara A, Niwa M, Noguchi K, Kanayama T, Niwa A, Matsuo M, et al. Galectin-3 as a next-generation biomarker for detecting early stage of various diseases. *Biomolecules* (2020) 10(3):389. doi: 10.3390/biom10030389

27. Nangia-Makker P, Hogan V, Raz A. Galectin-3 and cancer stemness. *Glycobiology* (2018) 28(4):172–81. doi: 10.1093/glycob/cwy001

28. Song L, Tang J-w, Owusu L, Sun M-Z, Wu J, Zhang J. Galectin-3 in cancer. *Clinica Chimica Acta* (2014) 431:185–91. doi: 10.1016/j.cca.2014.01.019

29. Sciacchitano S, Lavra L, Morgante A, Ulivieri A, Magi F, De Francesco GP, et al. *Galectin-3: One molecule for an alphabet of diseases, from a to z* (2018) 19 (2):379. doi: 10.3390/ijms19020379

30. Funasaka T, Raz A, Nangia-Makker P. Nuclear transport of galectin-3 and its therapeutic implications. *Semin Cancer Biol* (2014) 27:30–8. doi: 10.1016/j.semcancer.2014.03.004

31. van den Brûle FA, Waltregny D, Liu F-T, Castronovo V. Alteration of the cytoplasmic/nuclear expression pattern of galectin-3 correlates with prostate carcinoma progression. *Int J Cancer Res* (2000). 89(4)361–7. doi: 10.1002/1097-0215(20000720)89:4<361::AID-IJC8>3.0.CO;2-U

32. Merseburger AS, Kramer MW, Hennenlotter J, Serth J, Kruck S, Gracia A, et al. Loss of galectin-3 expression correlates with clear cell renal carcinoma progression and reduced survival. *World J Urol* (2008) 26(6):637. doi: 10.1007/s00345-008-0294-8

33. Califice S, Castronovo V, Bracke M, van den Brûle F., et al. Dual activities of galectin-3 in human prostate cancer: tumor suppression of nuclear galectin-3 vs tumor promotion of cytoplasmic galectin-3. *Oncogene* (2004) 23(45):7527–36. doi: 10.1038/sj.onc.1207997

34. Slack RJ, Mills R, Mackinnon AC. The therapeutic potential of galectin-3 inhibition in fibrotic disease. *Int J Biochem Cell Biol* (2021) 130:105881. doi: 10.1016/j.biocel.2020.105881

35. Li H, Li J, Xiao W, Zhang Y, Lv Y, Yu X, et al. The therapeutic potential of galectin-3 in the treatment of intrahepatic cholangiocarcinoma patients and those compromised with COVID-19. *Mol Biol* (2021) 8. doi: 10.3389/fmolb.2021.666054

36. Pearngam P, Kumkate S, Okada S, Janvilisri T. Andrographolide inhibits cholangiocarcinoma cell migration by down-regulation of claudin-1 via the p-38 signaling pathway. *Pharmacology* (2019) 10. doi: 10.3389/fphar.2019.00827

37. Vinci M, Box C, Zimmermann M, Eccles SA. Tumor spheroid-based migration assays for evaluation of therapeutic agents. *Methods Mol Biol* (2013) 986:253–66. doi: 10.1007/978-1-62703-311-4_16

38. Boutin ME, Hoffman-Kim D. Application and assessment of optical clearing methods for imaging of tissue-engineered neural stem cell spheres. *Tissue Eng Part C Methods* (2015) 21(3):292–302. doi: 10.1089/ten.tec.2014.0296

39. Aimjongjun S, Reamtong O, Janvilisri T. Lectin affinity chromatography and quantitative proteomic analysis reveal that galectin-3 is associated with metastasis in nasopharyngeal carcinoma. *Sci Rep* (2020) 10(1):16462. doi: 10.1038/s41598-020-73498-y

40. Tang Z, Li C, Kang B, Gao G, Li C, Zhang Z. GEPIA: a web server for cancer and normal gene expression profiling and interactive analyses. *Nucleic Acids Res* (2017) 45(W1):W98–w102. doi: 10.1093/nar/gkx247

41. Vaeteewoottacharn K, Kariya R, Pothipan P, Fujikawa S, Pairojkul C, Waraasawapati S, et al. Attenuation of CD47-SIRPα signal in cholangiocarcinoma potentiates tumor-associated macrophage-mediated phagocytosis and suppresses intrahepatic metastasis. *Trans Oncol* (2019) 12(2):217–25. doi: 10.1016/j.tranon.2018.10.007

42. Liang T, Shen L, Ji Y, Jia L, Dou Y, Guo L. NOV/CCN3 promotes cell migration and invasion in intrahepatic cholangiocarcinoma via miR-92a-3p. *Genes* (2021) 12(11). doi: 10.3390/genes12111659

43. Tung Y-C, Hsiao AY, Allen SG, Torisawa YS, Ho M, Takayama S. High-throughput 3D spheroid culture and drug testing using a 384 hanging drop array. *Analyst* (2011) 136(3):473–8. doi: 10.1039/C0AN00609B

44. Huang H, Ding Y, Sun XS, Nguyen TA. Peptide hydrogelation and cell encapsulation for 3D culture of MCF-7 breast cancer cells. *PloS One* (2013) 8(3): e59482. doi: 10.1371/journal.pone.0059482

45. Mehta G, Hsiao AY, Ingram M, Luker GD, Takayama S. Opportunities and challenges for use of tumor spheroids as models to test drug delivery and efficacy. *J Controlled Release* (2012) 164(2):192–204. doi: 10.1016/j.jconrel.2012.04.045

46. Chitcholtan K, Sykes PH, Evans JJ. The resistance of intracellular mediators to doxorubicin and cisplatin are distinct in 3D and 2D endometrial cancer. *J Trans Med* (2012) 10(1):38. doi: 10.1186/1479-5876-10-38

47. Luca AC, Mersch S, Deenen R, Schmidt S, Messner I, Schäfer K-L. Impact of the 3D microenvironment on phenotype, gene expression, and EGFR inhibition of colorectal cancer cell lines. *PloS One* (2013) 8(3):e59689. doi: 10.1371/journal.pone.0059689

48. do Amaral JB, Rezende-Teixeira P, Freitas VM, Machado-Santelli GM. MCF-7 cells as a three-dimensional model for the study of human breast cancer. *Tissue Eng Part C Methods* (2011) 17(11):1097–107. doi: 10.1089/ten.tec.2011.0260

49. Tamura K, Yokoyama S, Ieda J, Takifuji K, Hotta T, Matsuda K, et al. Hollow spheroids beyond the invasive margin indicate the malignant potential of colorectal cancer. *BMJ Open* (2011) 1(1):e000179. doi: 10.1136/bmjopen-2011-000179

50. Mills KR, Reginato M, Debnath J, Queenan B, Brugge JS. Tumor necrosis factor-related apoptosis-inducing ligand (TRAIL) is required for induction of autophagy during lumen formation *in vitro*. *Proc Natl Acad Sci USA* (2004) 101 (10):3438–43. doi: 10.1073/pnas.0400443101

51. Ashley N, Yeung TM, Bodmer WF. Stem cell differentiation and lumen formation in colorectal cancer cell lines and primary tumors. *Cancer Res* (2013) 73 (18):5798–809. doi: 10.1158/0008-5472.CAN-13-0454

52. Kenny PA, Lee GY, Myers CA, Neve RM, Semeiks JR, Spellman PT, et al. *The morphologies of breast cancer cell lines in three-dimensional assays correlate with their profiles of gene expression* (2007) 1(1)84–96. doi: 10.1016/j.molonc.2007.02.004

53. Treekitkarnmongkol W, Suthiphongchai T. High expression of ErbB2 contributes to cholangiocarcinoma cell invasion and proliferation through AKT/p70S6K. *World J Gastroenterol* (2010) 16(32):4047–54. doi: 10.3748/wjg.v16.i32.4047

54. Wang X, Enomoto A, Asai N, Kato T, Takahashi M. Collective invasion of cancer: Perspectives from pathology and development. *J Pathol* (2016) 66(4):183–92. doi: 10.1111/pin.12391

55. Eger A, Stockinger A, Schaffhauser B, Beug H, Foisner R. Epithelial mesenchymal transition by c-fos estrogen receptor activation involves nuclear translocation of β-

catenin and upregulation of β-Catenin/Lymphoid enhancer binding factor-1 transcriptional activity. *J Cell Biol* (2000) 148(1):173–87. doi: 10.1083/jcb.148.1.173

56. Stockinger A, Eger A, Wolf J, Beug H, Foisner R. E-cadherin regulates cell growth by modulating proliferation-dependent β-catenin transcriptional activity. *J Cell Biol* (2001) 154(6):1185–96. doi: 10.1083/jcb.200104036

57. Kim K, Lu Z, Hay ED. Direct evidence for a role of β-catenin/LEF-1 signaling pathway in induction of EMT. *Cell Biol Int* (2002) 26(5):463–76. doi: 10.1006/cbir.2002.0901

58. Yu LG. Circulating galectin-3 in the bloodstream: An emerging promoter of cancer metastasis. *World J Gastrointest Oncol* (2010) 2(4):177–80. doi: 10.4251/wjgo.v2.i4.177

59. Lunevicius R, Nakanishi H, Ito S, Kozaki K-I, Kato T, Tatematsu M, et al. Clinicopathological significance of fibrotic capsule formation around liver metastasis from colorectal cancer. *J Cancer Res Clin Oncol* (2001) 127(3):193–9. doi: 10.1007/s004320000199

60. Ingeson-Carlsson C, Martinez-Monleon A, Nilsson M. Differential effects of MAPK pathway inhibitors on migration and invasiveness of BRAFV600E mutant thyroid cancer cells in 2D and 3D culture. *Exp Cell Res* (2015) 338(2):127–35. doi: 10.1016/j.yexcr.2015.08.003

61. Baskaran JP, Weldy A, Guarin J, Munoz G, Shpilker PH, Kotlik M, et al. Cell shape, and not 2D migration, predicts extracellular matrix-driven 3D cell invasion in breast cancer. *APL Bioengineerig* (2020) 4(2):026105. doi: 10.1063/1.5143779

frontiers | Frontiers in Oncology

TYPE Original Research
PUBLISHED 20 January 2023
DOI 10.3389/fonc.2022.1084713

OPEN ACCESS

EDITED BY
Patrick Ming-Kuen Tang,
The Chinese University of Hong Kong,
Hong Kong SAR, China

REVIEWED BY
Hong Lok Lung,
Hong Kong Baptist University, Hong Kong SAR, China
Jeff Chung,
The Chinese University of Hong Kong,
Hong Kong SAR, China

*CORRESPONDENCE
Tavan Janvilisri
tavan.jan@mahidol.ac.th

SPECIALTY SECTION
This article was submitted to Molecular and Cellular Oncology, a section of the journal Frontiers in Oncology

RECEIVED 30 October 2022
ACCEPTED 28 December 2022
PUBLISHED 20 January 2023

CITATION
Tulalamba W, Ngernsombat C, Larbcharoensub N and Janvilisri T (2023) Transcriptomic profiling revealed FZD10 as a novel biomarker for nasopharyngeal carcinoma recurrence.
Front. Oncol. 12:1084713.
doi: 10.3389/fonc.2022.1084713

Transcriptomic profiling revealed FZD10 as a novel biomarker for nasopharyngeal carcinoma recurrence

Warut Tulalamba[1,2], Chawalit Ngernsombat[3], Noppadol Larbcharoensub[4] and Tavan Janvilisri[5]*

[1]Siriraj Center of Research Excellence in Advanced Gene and Cell Therapy (Si-CORE-AGCT) and Thalassemia Center, Faculty of Medicine Siriraj Hospital, Mahidol University, Bangkok, Thailand, [2]Faculty of Science, Mahidol University, Bangkok, Thailand, [3]Division of Biochemistry, Department of Preclinical Science, Faculty of Medicine, Thammasat University, Pathumthani, Thailand, [4]Department of Pathology, Faculty of Medicine Ramathibodi Hospital, Mahidol University, Bangkok, Thailand, [5]Department of Biochemistry, Faculty of Science, Mahidol University, Bangkok, Thailand

Background: Nasopharyngeal carcinoma (NPC) is a type of cancers that develops in the nasopharynx, the very upper part of the throat behind the nose. NPC is typically diagnosed in later stages of the disease and has a high rate of recurrence due to the location of the tumor growth site. In this study, we compared the gene expression profiles of NPC tissues from patients with and without recurrence to identify potential molecular biomarkers of NPC recurrence.

Methods: Microarrays were used to analyze the expression of genes in 15 NPC tissues taken at the time of diagnosis and at the site of recurrence following therapeutic treatment. Pathway enrichment analysis was used to examine the biological interactions between the major differentially expressed genes. The target identified was then validated using immunohistochemistry on 86 NPC tissue samples.

Results: Our data showed that the Wnt signaling pathway was enhanced in NPC tissues with recurrence. FZD10, a component of the Wnt signaling pathway, was significantly expressed in NPC tissues, and was significantly associated with NPC recurrence.

Conclusion: Our study provides new insights into the pathogenesis of NPC and identifies FZD10 as a potential molecular biomarker for NPC recurrence. FZD10 may be a promising candidate for NPC recurrence and a potential therapeutic target.

KEYWORDS

nasopharyngeal carcinoma, transcriptome, microarray, biomarkers, recurrence, Wnt signaling

1 Introduction

Nasopharyngeal carcinoma (NPC) is a type of head and neck cancer that is uncommon in most parts of the world, but is more prevalent in some regions, such as East and Southeast Asia (1–3). The physical examination of the patient is frequently used to identify cervical lymphadenopathy, which serves as the basis for the diagnosis of NPC. It is common practice to conduct radiographic imaging, including magnetic resonance imaging of the primary and nodal areas and computer tomography to check for bone degradation at the base of the skull, which may be visible at first glance (4). However, due to the vague symptoms and the painless, quiet tumor growth at the primary site, NPC is typically detected at a late stage. Additionally, advanced NPC has a higher risk for metastasis than other head and neck squamous cell carcinomas (5). Although radiotherapy is the recommended course of action for NPC, follow-up research has shown that patients with advanced NPC have poor response rates, locoregional recurrences, and distant metastases (6–8). In order to improve patient outcomes for advanced NPC, concurrent chemotherapy and radiotherapy have been implemented; however, responses from patients with recurrent or metastatic NPC have not been very successful (9, 10). Because NPC has such a poor prognosis, it is critical that we understand the molecular mechanisms behind its pathogenesis and progression, identify appropriate biomarkers for early detection, and search for potential treatment targets (11, 12). Unfortunately, relatively little is known about the pathophysiology of NPC, especially the molecular causes of recurrent NPC.

Gene expression profiling has gained a lot of attention in the fields of biomedicine, especially cancer biology, to retrieve molecular biomarkers. Many public databases, such as ArrayExpress and the Gene Expression Omnibus (GEO), have quickly accumulated transcriptomic data. According to reports, between 76% and 96% of diagnostic platforms based on genetic signatures correctly identify a variety of primary and metastatic cancers (13, 14). Recent articles on transcriptome investigations of NPC in various experimental and clinical settings are available (15, 16). However, efficient biomarkers for NPC recurrence are still unknown. Research on the signalling pathways involved in NPC development is still in its early stages compared to other types of cancer. Therefore, it is very intriguing to study their role in the pathogenesis and growth of NPC in the future.

Here, we conducted a transcriptome analysis to assess the expression profiles of NPC histological tissue sections. The differentially expressed genes in the NPC tissues from patients at the time of diagnosis and the point of recurrence, after receiving therapeutic treatments, were identified using microarray technology. Validation of the target protein was performed using immunohistochemistry. Our findings provide new insights to the pathophysiology of NPC, which may lead to identification of biomarkers for NPC recurrence and potential therapeutics.

2 Materials and methods

2.1 Nasopharyngeal carcinoma tissues

The tissues that were histopathologically confirmed to be NPC were collected from Ramathibodi Hospital. Table 1 shows the patient characteristics including age, gender, WHO type, and stage. To evaluate the NPC stages, examiners used physical examination, CT, and MRI according to the TNM categorization system of the AJCC staging system. According to the WHO classification, histological grades were assigned. All patients were treated with concurrent chemotherapy and radiation. The patients received radiation to the primary tumor five times per week at a dose of 18 to 20 Gy, for a total of about 70 Gy. During weeks 1, 4, 7, 10, 13, and 16 of radiotherapy, three rounds of chemotherapy (cisplatin 100 mg/m^2) were administered concurrently.

The patients underwent chemotherapy consisting of cisplatin (80 mg/m^2) on day 1 and 5-fluorouracil (1000 mg/m^2/day) on days 1 to 5 every 4 weeks for three cycles after the concurrent chemoradiotherapy was finished. All patients were followed up every three to six months for at least 5 years. Tissue samples were fixed in formalin overnight at room temperature. Samples were first dehydrated in a series of ethanol (70%, 90%, and 100%, respectively) and then xylene before being heated to 60°C and embedded in paraffin block. The formalin-fixed paraffin-embedded (FFPE) tissue blocks were stored at room temperature. The use of human materials was approved by the research ethics committee of Faculty of Medicine Ramathibodi Hospital, Mahidol University, which waived the need for consents from the donors.

TABLE 1 Clinicopathological characteristics of nasopharyngeal carcinoma patients for transcriptomic study.

Relapse	Case no.	Age	Gender	WHO type	TNM stage	
Without NPC relapse	1	60	Female	2a	T1N1M0	2B
	2	47	Female	2b	T4N1M0	4A
	3	53	Female	2b	T2N3M0	4B
	4	30	Female	2b	T2N3M0	4B
	5	51	Male	2a	T3N2M0	3
With 1 NPC relapse	6	46	Female	2a	T4N0M0	4A
	7	44	Male	2a	T3N2M0	3
With 2 NPC relapse	8	43	Female	2a	T2N2M0	3
	9	45	Male	2a	T3N2M0	3

2.2 PALM laser-capture microdissection and pressure catapulting

The FFPE tissues were cut into 8 µm tissue sections and placed on the coated microscope slides as samples for LMPC. This was done using a conventional microtome. After deparaffinization in xylene, tissue sections were rehydrated in a series of decreasing ethanol concentrations (100%, 90%, and 70%, respectively). Tissue slides were dried in a sequence of ethanol before being kept in xylene until laser-capture microdissection, after which they were stained with 0.1% cresyl violet in 50% ethanol for histological markers. Each slide was put onto the PALM® laser-capture microdissection system stage (PALM MicroBeam with PALM RoboMover module and RoboSoftware; Carl Zeiss MicroImaging GmbH, Germany) for light microscopy observation of cresyl violet-stained cells. The laser cut around the NPC cells while being focused through a 40X objective lens, and some cells were then launched into the lid of a 0.6 ml microcentrifuge tube. Per sample and tube, 1 to 2 × 10^6 NPC cells were dissected and collected. The tubes holding the catapulted cells were then briefly centrifuged to move the cells from the lid to the bottom of the tube for RNA extraction.

2.3 RNA preparation

Total RNA from micro-dissected-FFPE samples were extracted using RNeasy FFPE kit (Qiagen, Valencia, CA, USA) according to the manufacturer's instruction. The extracted RNA was then subjected to a 10-minute RNase-free DNase I treatment at 65°C. Using visible and UV/visible spectrophotometers, a ratio of 260/280 nm absorbance was measured to estimate the amount and purity of the total RNA (Thermo Scientific, Wilmington, DE, USA). A total of 25 ng of total RNA was utilized as a template for TransPlex® Complete Whole Transcriptome Amplification Kit, or WTA (Sigma, St. Louis, MO, USA). In the first phase, sample RNA was reverse transcribed with substantially non-self-complementary primers without 3' bias. The resulting Omniplex® cDNA library was then amplified by PCR using the universal primer to create WTA products. This library is made up of random, overlapping fragments flanked by universal end sequences. WTA products were re-amplified using REPLI-g FFPE kit (Qiagen, Valencia, CA, USA) according to the company's recommendation. The resultant amplified products were purified using a PCR purification kit after amplification (Qiagen, Valencia, CA, USA). Using visible and UV/visible spectrophotometers, the concentration and purity of purified cDNA were determined (Thermo Scientific, Wilmington, DE, USA).

2.4 Gene expression profiling

Each patient's amplified cDNA was utilized as a template to stain DNA using Cy3. In brief, 3 µg of DNA were sonicated before being combined with 5 µg of random hexamers (Roche, Madison, WI, USA), 200 µM of dATP/dGTP/dTTP, 100 g of dCTP, 60 g of Cy3-dCTP (GE Healthcare, Little Chalfont, UK), and 10 units of Klenow Fragment (exo-) (Fermentas, Madison, WI, USA) and incubated at 37°C for an overnight period. Cy3-labeled DNA was purified with PCR purification Kit (Qiagen, Valencia, CA, USA). By measuring optical density with visible and UV/visible spectrophotometers (Thermo Scientific Wilmington, DE, USA), the quantity of pure Cy3-labeled cDNA was determined, and frequency of incorporation was estimated. For the gene expression profiling, the Human Whole Genome OneArray™ Version 5 was used (Phalanx Biotech Group, Inc., Hsinchu, Taiwan). Each microarray underwent a pre-hybridization phase in 5X SSPE, 0.1% SDS, and 1% BSA for an hour at 42°C before being spun dry. The microarray was blocked using sheared salmon sperm DNA to lessen non-specific binding (Agilent Technologies, Santa Clara, CA, USA). Three micrograms of Cy3-labeled DNA derived from each NPC sample was hybridized to the microarray. Following 18-h hybridization at 42°C with humidity, non-specific binding was washed away by a series of SSC buffer. The microarray slides were dried by centrifugation. The arrays were then scanned using the Agilent G2565CA Microarray Scanner System with Scan Control Software 8.5 (Agilent Technologies, Santa Clara, CA, USA). The images of microarray slide were exported as a TIFF format.

2.5 Data analysis

The Cy3-fluorescent intensities were extracted from the generated images by the Genepix Pro software 6.3 (Molecular Devices, Sunnyvale, CA, USA). The Cy3 signal intensity of each spot was corrected by subtracting background signal intensities in the immediate surroundings. The poor spots were flagged manually and eliminated from the analysis. Following the $\log_2$ transformation, the normalization was achieved using median with absolute deviation and RANK with RANKIT on SPSS, respectively. The data have been deposited in GEO database (accession number GSE62328). To identify the differentially expressed genes, the MultiExperiment Viewer (MeV) version 4.6 in TM4 software suite (Dana-Farber Cancer Institute, Boston, MA, USA) was used. The level of significance for t-tests statistic was set at $P < 0.01$. The significant gene lists were selected according to their *P* values and fold difference, both up- and down-regulation. The hierarchical clustering was performed on the set of significant genes to cluster similar groups of samples or genes together. Up-regulated and down-regulated genes then were included in gene set enrichment analysis. Web-based functional annotation tools, WebGastalt (17) was used to analyse clusters of related hits such as enrich signalling pathways (KEGG pathway) as well as gene ontology (GO) term of biological process. Gene set enrichment analysis generated multiple clusters of high significance showed a common trend as to function. The global interaction networks of the protein encoded by differentially expressed genes were predicted using STRING database (18).

2.6 qRT-PCR

The expression of selected genes including *CTNNB1*, *FZD10*, and *Wnt8b* was validated through qRT-PCR. The cDNA from FFPE samples were used to perform realtime qRT-PCR using qPCRBIO SyGreen Mix (PCR Biosystems, London, United Kingdom) following the kit's instruction. The primer sequences are CTNNB1-forward; 5'-AGC TTC CAG ACA CGC TAT CAT-3'; CTNNB1-reverse; 5'-CGG

TAC AAC GAG CTG TTT CTA C-3'; Fzd10- forward; 5'-GCT CAT GGT GCG TAT CGG G-3'; Fzd10- reverse; 5'-GAG GCG TTC GTA AAA GTA GCA-3'; Wnt8b- forward; 5'-CAC CTG TGT CCT CCA ACT CA-3', and Wnt8b- reverse; 5'-CTT CAA TAC CAC TCT GGG CA-3'.

2.7 Immunohistochemistry

Tissue microarrays containing 86 human NPC and 6 normal nasopharyngeal epithelial tissues were constructed using paraffin blocks from Ramathibodi Hospital as described previously (19). Briefly, 5 µm TMA sections were blocked with bovine serum albumin and incubated with rabbit anti-FZD10 antibody (1:200 dilution; catalog number ab83044, Abcam, USA) at 4°C overnight in a humidified chamber. The IgG1 was used for negative control. The TMA sections were targeted to stain with SignalStain® Boost IHC Detection Reagent (Cell Signaling Technology, Danvers, MA 01923, USA) for 30 min at room temperature, and visualized with 3-amino-9- ethylcarbazole peroxidase substrate containing H_2O_2 for 20 min. Immunohistochemical staining was evaluated independently by 2 pathologists. The FZD10 labeling was divided into five grades: 0 (no FZD10 labeling), 1 (>0-25% cells labeling), 2 (26-50% cells labeling), 3 (51-75% cells labeling), and 4 (76-100% cells labeling). The staining intensity for FZD10 were categorized as 0 for negative, 1 for weakly positive, 2 for moderately positive, and 3 for strongly positive. The staining positivity was calculated by the formula: labeling score × intensity score. A score less than 4 was considered low FZD10 expression while score 4-12 indicated high expression. The correlation between expression of FZD10 protein and NPC clinical features was evaluated by Pearson Chi-Square test. All *P*-values were calculated based on two-sided statistical analysis, and a probability level < 0.05 was considered statistically significant.

3 Results

3.1 Differentially expressed genes involved in NPC recurrence

Using a non-parametric approach, the mRNA profiles of NPC tissues at the time of diagnosis from patients with and without relapse were compared. Table 1 displays the clinicopathological features of our NPC cohort. A total of 1,180 genes showed substantially different expression between NPC with and without disease recurrence following treatment, with a *P*-value of less than 0.05. Figure 1A shows a hierarchical clustering (HCL) tree of significant genes. According to HCL, genes with similar expression patterns were clearly clustered together and connected by a network of branches that showed which genes were up- and down-regulated. Top 50 significant up- and down-regulated genes are summarized in Table S1. To further shed light on the biological activities of differentially expressed genes in NPC, we carried out a gene ontology analysis to group these genes into clusters based on their biological functions,

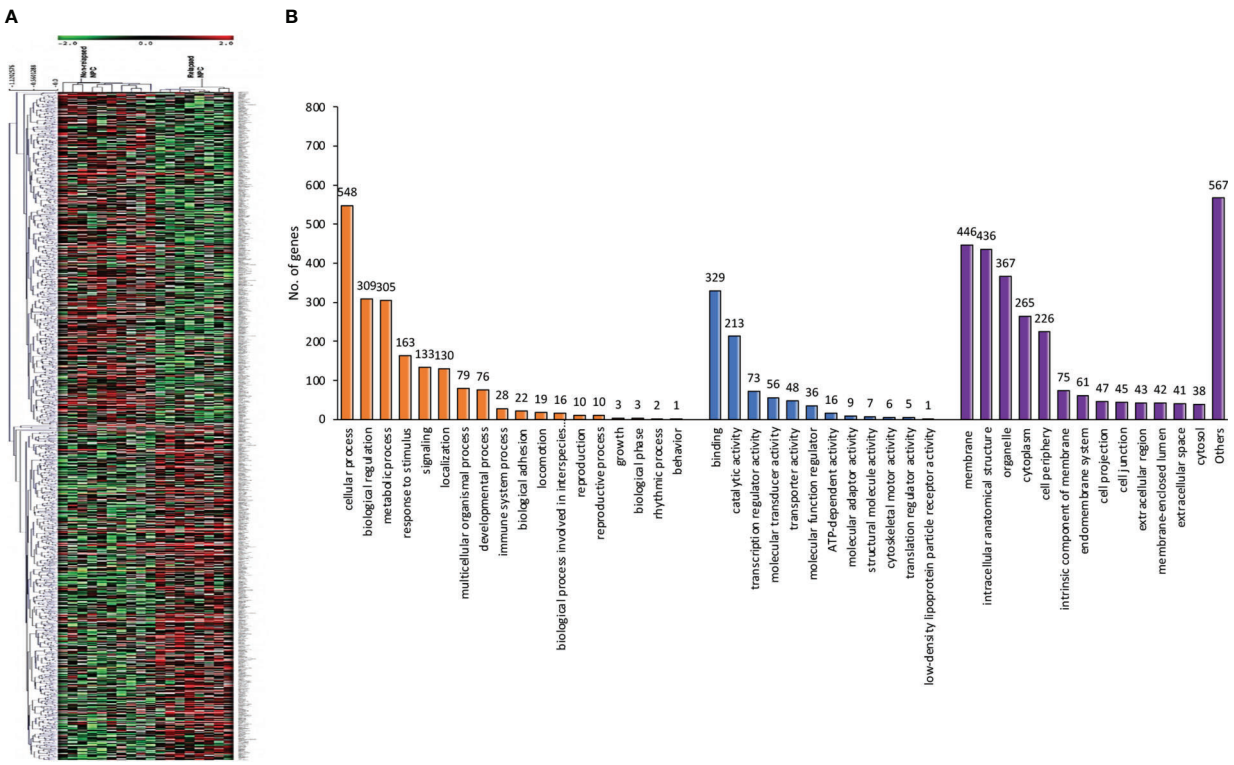

FIGURE 1
Differentially expressed genes involved in NPC recurrence. **(A)** Hierarchical clustering of significant genes involved in NPC recurrence. Each row represents each significant gene, and each column corresponds to a specific sample. The status of each gene is indicated by the intensity as indicated by the scale bar with $\log_2$ scale. **(B)** Gene ontology classification of differentially expressed genes. A bar represents each gene ontology category. The height of the bar represents the number of genes observed in each category. The number of genes per category is indicated upon the bars text.

cellular components, and molecular functions (Figure 1B). Our findings showed that more than 50% of the genes were involved in biological activities such as biological regulation, metabolism, and cell signaling, while less than 5% of the genes were involved in growth. Fourteen categories of cellular compartments were identified. Most of the differentially expressed genes were primarily found in the membrane and intracellular compartments. Protein binding, catalytic activity, and transcriptional regulator activity were among the top ranks in molecular function.

3.2 Identification of key signaling pathway of recurrent NPC

KEGG pathway enrichment analysis was carried out to gain an understanding of the functional roles of differentially expressed genes. Figure 2A shows 20 enriched KEGG pathways that were retrieved at a significant level of $P < 0.01$. The osteoclast differentiation pathway, RIG-I-like receptor signaling pathway, antiviral innate immunity pathway, and several carcinogenic pathways were among the notable KEGG pathways that we discovered. The carcinogenic pathways, Hedgehog and Wnt, are well known, and have been shown to be implicated in malignancies like NPC in the past. To confirm the importance of the projected molecular pathways from gene enrichment studies in NPC, we built protein-protein networks using STRING from the genes of the top 20 pathways in the KEGG pathway database (Figure 2B). In this work, the Wnt signaling pathway was highlighted. In the relapse cases, it was discovered that several Wnt-related genes were dysregulated (Table 2).

We verified the accuracy of our transcriptomic findings using quantitative RT-PCR. With the use of the $2^{-\Delta\Delta Ct}$ method and ACTB as an endogenous reference, the expression of Wnt-related genes was quantified in the cDNA from FFPE samples of non-relapse and relapse NPC patients. β-catenin, FZD10, and WNT8B proteins were selected for validation. The Spearman's rho test showed that the correlation between the microarray and qPCR results was 0.837 (Supplementary Figure S1).

3.3 FZD10 as a biomarker for NPC recurrence

To further investigate the role of FZD10 in NPC recurrence, we initially conducted qPCR on NPC tissue samples from patients with and without relapse at the time of diagnosis (Table 1). Our results showed that the relative expression of the *FZD10* gene was higher in NPC tissues with recurrence compared to those without relapse (Figure 3A). We then performed immunohistochemistry on a cohort of 86 NPC and 6 normal nasopharyngeal tissue samples to assess the level of FZD10 protein expression (Table 3). The staining patterns for FZD10 protein were mostly found in the cytoplasm of both normal and NPC tissues, as shown in Figure 3B. We also evaluated the relationship between FZD10

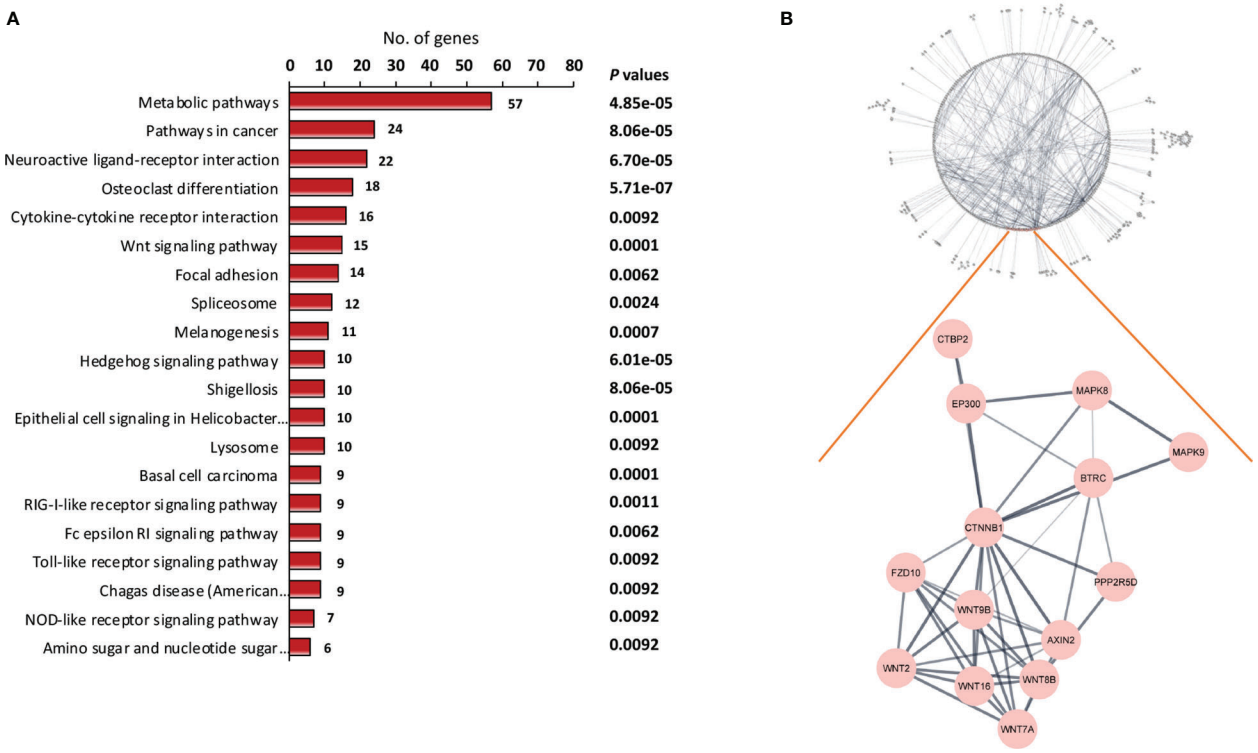

FIGURE 2
Identification of key signaling pathway of recurrent NPC. **(A)** Pathway enrichment analysis of differentially expressed genes. The differentially expressed genes between relapse and non-relapse NPC were identified using t test with *P* values less than 0.01 and were used as input into pathway enrichment analysis. Based on KEGG database, multiple clusters of highly significant pathways in NPC were identified. **(B)** Protein-protein interaction networks were discovered *via* network analysis. Among the dysregulated mechanisms in NPC recurrence is the Wnt signaling pathway. Several Wnt pathway members have been found to be differentially expressed in recurrent NPC.

TABLE 2 List of differentially expressed genes between relapsed and non-relapsed NPC following Wnt signaling pathway enrichment analysis.

Wnt signaling pathway		KEGG ID: 04310	$P = 0.0001$
Index	Symbol	Gene Name	EntrezGene
1	*AXIN2*	axin 2	8313
2	*BTRC*	beta-transducin repeat containing E3 ubiquitin protein ligase	8945
3	*CTBP2*	C-terminal binding protein 2	1488
4	*CTNNB1*	catenin (cadherin-associated protein), beta 1, 88kDa	1499
5	*EP300*	E1A binding protein p300	2033
6	*FZD10*	frizzled family receptor 10	11211
7	*MAPK8*	mitogen-activated protein kinase 8	5599
8	*MAPK9*	mitogen-activated protein kinase 9	5601
9	*PPP2R5D*	protein phosphatase 2, regulatory subunit B', delta	5528
10	*PRKX*	protein kinase, X-linked	5613
11	*WNT16*	wingless-type MMTV integration site family, member 16	51384
12	*WNT2*	wingless-type MMTV integration site family member 2	7472
13	*WNT7A*	wingless-type MMTV integration site family, member 7A	7476
14	*WNT8B*	wingless-type MMTV integration site family, member 8B	7479
15	*WNT9B*	wingless-type MMTV integration site family, member 9B	7484

expression and clinicopathological features in NPC patients. Our findings revealed that elevated FZD10 expression was observed in 57/86 (66.3%) of NPC patients and was significantly associated with recurrence status ($P = 0.044$) (Figure 3C). However, FZD10 expression was not significantly associated with age, gender, WHO classification, AJCC staging, T stage, lymph node metastasis, or systemic metastasis ($P > 0.05$).

Based on our cohort, there was no statistically significant association between NPC patient survival and FZD10 expression. The data from the human protein atlas (https://www.proteinatlas.org/) of head and neck cancer were then used to analyze patient survival with varied Fzd10 expression levels. The 499 patients with head and neck cancer were divided into two groups: those with low Fzd10 expression (n = 343) and those with high Fzd10 expression (n = 156). The Kaplan-Meier survival analysis revealed that those with low Fzd10 mRNA expression outlived those with high expression ($P = 0.046$) (Supplementary Figure S2).

4 Discussion

Most NPC patients present in later stages and have a poor prognosis due to metastasis and the recurrence of the disease. However, to date, there is no report on the molecular biomarkers for NPC recurrence as the recurrence often occurs months or years after the primary diagnosis and treatment and obtaining tissue samples from patients at this point is difficult. Moreover, tissue samples from patients with recurrent disease are limited in quantity or quality because of previous treatment. A lack of knowledge of molecular pathophysiology and adequate biomarkers contributes to a poor response to existing therapy. In this study, the NPC biopsies from patients were taken at the time of diagnosis and after relapses following therapy to better understand the pathophysiology of NPC recurrence. The expression patterns of NPCs that had relapsed and those that had not were examined to identify the key players in NPC development and therapeutic response. A total of 1,180 genes were significantly identified. Among the significantly enriched pathways, the osteoclast differentiation pathway is predominant. The MAPK and NF-B gene families, which are present in other important pathways including the focal adhesion pathway and the Fc epsilon RI signaling pathway, are among many relevant genes enriched in this study (20, 21). The signaling pathway of the RIG-I-like receptors, which are important in antiviral innate immunity (22), was also discovered. MAVS (mitochondrial antiviral signaling protein), one of the key components of this signaling, is dysregulated in relapsed NPC. In response to viral infection, MAVS, a membrane-bound protein, transmits signals from RIG-I to downstream signaling molecules *via* the transcription factors NF-B, IRF3, and IRF7 to create inflammatory cytokines such as IFN-beta (23). There is no direct data of MAVS dysregulation in NPC yet. Evidence suggests that EBV infection is linked to recurrent NPC, and plasma EBV DNA is essential for the early identification of local or distant failure (24, 25). Increased MAVS expression in relapsed NPC may indicate the presence of EBV infection, which is causally connected to the etiology and recurrence of NPC. The radiation treatment of NPC can cause microvasculature damage by affecting the tumor microenvironment (26, 27). Hyperactivation of the hedgehog (HH) pathway was also upregulated in relapsed NPC. The basal cell carcinoma related pathway is also enriched, which is closely associated with hedgehog signaling. The HH pathway is dysregulated in head and neck cancer, including NPC. Aberrant of GLI1 has been reported in NPC tissues and cell lines (28). Interestingly, HH signaling has been associated to NPC metastasis, as suggested by the effect of *MTA1* (metastasis-associated gene 1) on the aggressive phenotypes of NPC cells (29).

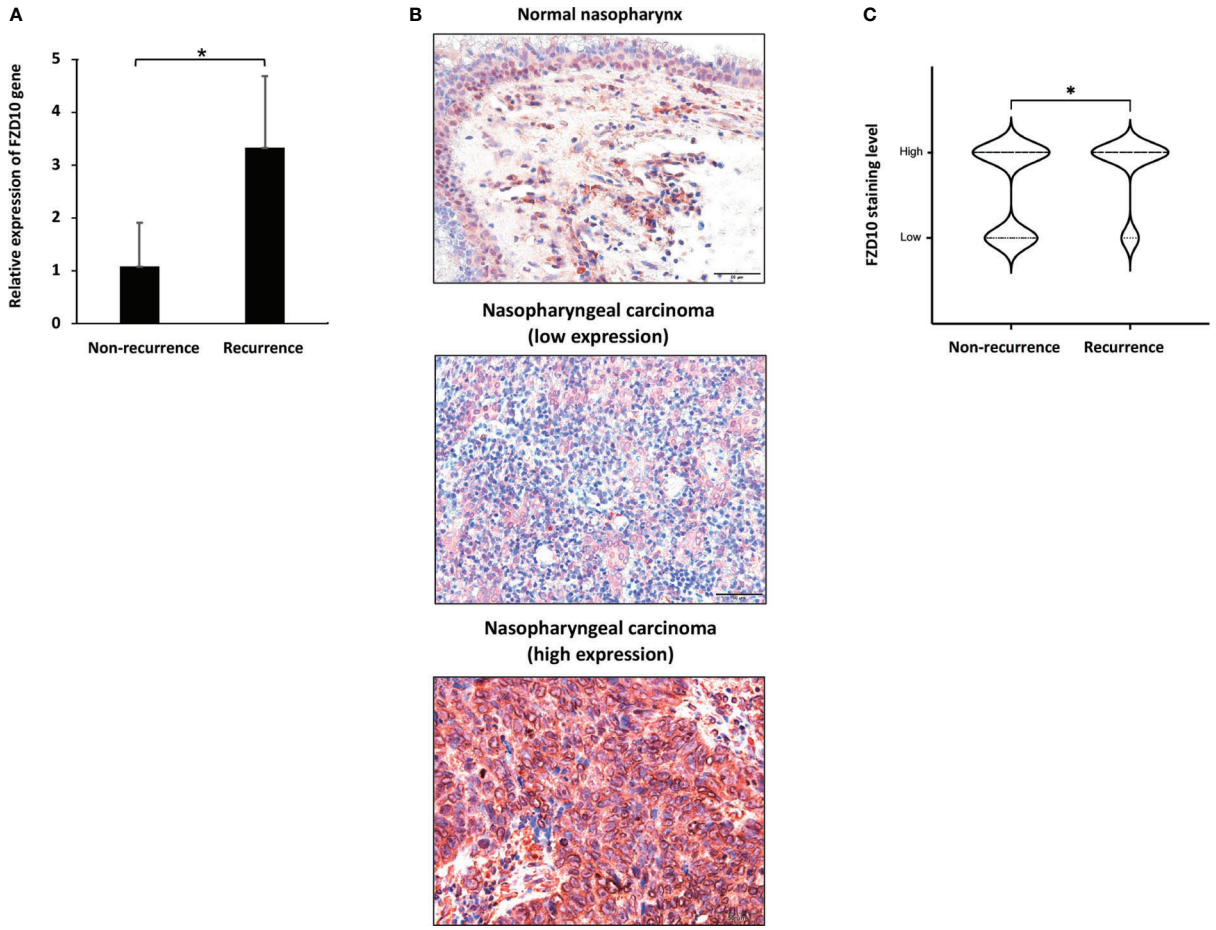

FIGURE 3
FZD10 as a biomarker for NPC recurrence. **(A)** The relative *FZD10* mRNA level of non-recurrent NPC compared to recurrent NPC. **(B)** FZD10 protein expression in normal nasopharynx and NPC tissues. Shown are representative photomicrographs at magnification X200 of normal nasopharynx and cancerous nasopharyngeal tissues that were subjected to immunostaining of FZD10. **(C)** The correlation of recurrent status of NPC patients and the FZD10 expression level. The NPC tissues was stratified into non-recurrent (N=59) and recurrent (N=27). Recurrent NPC represented higher FZD10 expression than non-recurrent NPC with *P* value of 0.044. *$P < 0.05$

Moreover, the stem cell-like characteristics of NPC are maintained by EBV infection through the HH signaling pathway (30). Overall, our data suggest that a few factors contribute to the recurrence of NPCs, and further research is necessary to confirm their contributions.

The Wnt signaling pathway plays an important role in cancer development. Dysregulation of this pathway can cause unwanted cell growth and movement, which can lead to tumor development, including NPC (2, 31). Additionally, it has been suggested that the Wnt signaling pathway contributes to fibrosis by interacting with other signals, such as TGF- β, and inducing fibroblast activation and fibrogenesis (32). Our transcriptomic analyses resulted in the considerable identification of the Wnt signaling pathway using pathway enrichment analysis. Several Wnt signaling pathway members have previously been identified as being up-regulated in several types of cancers, including NPC (19, 33 – 35). Remarkably, the relapse cases of NPC exhibited the different expression of Wnt signaling compared to the point of diagnosis, including various *WNT* isoforms, *FZD10*, *CTNNB1*, and *AXIN2* expression. Moreover, up-regulation of WNT5A has recently been reported in primary NPC tissue samples and cell lines associated with EBV infection (36), which promotes aggressiveness and stem characteristics in NPC (37). Our previous tissue microarray analysis illustrated that WNT8B is associated with NPC patients' survival, which could be used as a prognostic biomarker for NPC patients (19). As the NPC development comprises multi-step carcinogenesis, the differential expression of Wnt components in our studies may affect the mechanisms of NPC pathogenesis.

Frizzled (FZD) is a protein that is crucial for many aspects of cell development, including cell polarity, cell proliferation, and the development of both embryonic and adult cells. It is also a potential target for the treatment of cancer (38). Several Frizzled isoforms have been identified as possible targets for treating human cancer. FZD10 is among the genes that are aberrantly expressed in the Wnt signaling pathway. Previous studies have shown that FZD10 is involved in the progression of several types of cancer, including colorectal cancer, gastric cancer, and synovial sarcomas (39 – 41). Additionally, a therapeutic targeting FZD10 (OTSA101) is currently in clinical trials (42). However, the role of FZD10 in NPC has not been thoroughly studied, making it a potential target for further research. The immunohistochemical analyses suggested that high FZD10 expression was significantly associated with recurrent NPC. Based on our validating cohort, there was no correlation between

10.3389/fonc.2022.1084713

TABLE 3 Clinicopathological characteristics of nasopharyngeal carcinoma patients in this study.

Characteristics		No. of patients	
Age			
	mean	50.3	years
	median	51.0	years
	range	16-77	years
Gender			%
	Male	62	72.1
	Female	24	27.9
WHO classification			%
	Type 1	2	2.3
	Type 2	51	59.3
	Type 3	33	38.4
AJCC staging			%
	Stage I-II	11	12.8
	Stage III-IV	73	84.9
	N/A	2	2.3
T stage			%
	T1-T2	31	36.0
	T3-T4	54	62.8
	N/A	1	1.2
Regional lymph node metastasis			%
	No	21	24.4
	Yes (N1-N3)	65	75.6
systemic metastasis			%
	No	74	86.0
	Yes (M1)	11	12.8
	N/A	1	1.2
recurrence			%
	No	59	68.6
	Yes	27	31.4
FZD10 expression			%
	Low	29	33.7
	High	57	66.3
	Total	86	100.0

N/A, Not available.

other clinicopathological parameters including survival with FZD10. This is possibly due to the small cohort. As NPC is a distinct subtype of head and neck cancer, we evaluated the mRNA expression of FZD10 in head and neck cancer based on the Human Protein Atlas datasets and found that it is associated with the poor prognosis. It is noteworthy that although there is several mRNA profiling on NPC tissues, the patient characteristics including survival are not readily available in the public databases. In addition, a study reported that FZD10 expression negatively exhibited correlation with overall survival of NPC patients in a Chinese cohort (43). Moreover, FZD10 was upregulated and cross talked with TGF-β1, which activate the HH signaling pathway in myofibroblast differentiation and pulmonary fibrosis (44). To date, there has been no report on the role of FZD10 in the recurrent cancers. Other Frizzled isoforms have

been associated with recurrence in some cancers. For example, FZD2 was upregulated in the hepatocellular carcinoma and was significantly associated metastasis and cancer recurrence (45). FZD3 expression was correlated with recurrent or metastatic CRC (46). Triple-negative breast cancer was found to highly express FZD5 mRNA, which correlated with shorter overall survival, recurrence-free survival, distal metastasis-free survival, and post-progression survival (47). Therefore, one of the key signaling pathways involved in the development of NPC was the Wnt signaling pathway. FZD10 may be an important cancer recurrent biomarker and a potentially effective target for cancer therapy.

In summary, our transcriptomic findings identified several signaling pathways involved in NPC recurrence. One of these mechanisms, Wnt signaling, appears to be a disrupted during recurrence and its participation may help is better understand how NPC recurrence is regulated. FZD10, a Wnt signaling receptor, is involved in NPC recurrence, and could serve as an independent predictive biomarker for cancer recurrence. Further research into prospective FZD10-targeted therapies is necessary, as it may improve the survival outcomes of these patients.

Data availability statement

The data presented in the study are deposited in the Gene Expression Omnibus repository, accession number GSE62328 (https://www.ncbi.nlm.nih.gov/geo/query/acc.cgi?acc=GSE62328/).

Ethics statement

The studies involving human participants were reviewed and approved by the research ethics committee of Faculty of Medicine Ramathibodi Hospital, Mahidol University. Written informed consent for participation was not required for this study in accordance with the national legislation and the institutional requirements.

Author contributions

Conceptualization: TJ. Methodology: WT, CN and TJ. Validation: CN. Investigation: WT and CN. Resources: NL and TJ. Writing—original draft preparation: WT and CN. Writing—review and editing: CN and TJ. Supervision: TJ. Project administration: TJ. Funding acquisition: TJ. All authors contributed to the article and approved the submitted version.

Funding

This research project is supported by Mahidol University (Fundamental Fund: Fiscal Year 2023 by National Science Research and Innovation Fund (NSRF)).

Acknowledgments

The authors acknowledge Krittika Khotthong (MD) and Pongphol Prattapong for the data analysis.

Conflict of interest

The authors declare that the research was conducted in the absence of any commercial or financial relationships that could be construed as a potential conflict of interest.

Publisher's note

Supplementary material

The Supplementary Material for this article can be found online at: https://www.frontiersin.org/articles/10.3389/fonc.2022.1084713/full#supplementary-material

References

1. Chang ET, Ye W, Zeng YX, Adami HO. The evolving epidemiology of nasopharyngeal carcinoma. *Cancer Epidemiol Biomarkers Prev* (2021) 30(6):1035–47. doi: 10.1158/1055-9965.EPI-20-1702

2. Richardo T, Prattapong P, Ngernsombat C, Wisetyaningsih N, Iizasa H, Yoshiyama H, et al. Epstein-barr virus mediated signaling in nasopharyngeal carcinoma carcinogenesis. *Cancers (Basel).* (2020) 12(9):2441. doi: 10.3390/cancers12092441

3. Chen YP, Chan ATC, Le QT, Blanchard P, Sun Y, Ma J. Nasopharyngeal carcinoma. *Lancet* (2019) 394(10192):64–80. doi: 10.1016/S0140-6736(19)30956-0

4. Su ZY, Siak PY, Leong CO, Cheah SC. Nasopharyngeal carcinoma and its microenvironment: Past, current, and future perspectives. *Front Oncol* (2022) 12:840467. doi: 10.3389/fonc.2022.840467

5. Jiromaru R, Nakagawa T, Yasumatsu R. Advanced nasopharyngeal carcinoma: Current and emerging treatment options. *Cancer Manag Res* (2022) 14:2681–9. doi: 10.2147/CMAR.S341472

6. Lee AWM, Ng WT, Chan JYW, Corry J, Mäkitie A, Mendenhall WM, et al. Management of locally recurrent nasopharyngeal carcinoma. *Cancer Treat Rev* (2019) 79:101890. doi: 10.1016/j.ctrv.2019.101890

7. Xu T, Tang J, Gu M, Liu L, Wei W, Yang H. Recurrent nasopharyngeal carcinoma: A clinical dilemma and challenge. *Curr Oncol* (2013) 20(5):e406–19. doi: 10.3747/co.20.1456

8. Lee AW, Fee WE Jr, Ng WT, Chan LK. Nasopharyngeal carcinoma: Salvage of local recurrence. *Oral Oncol* (2012) 48(9):768–74. doi: 10.1016/j.oraloncology.2012.02.017

9. Wong KCW, Hui EP, Lo KW, Lam WKJ, Johnson D, Li L, et al. Nasopharyngeal carcinoma: An evolving paradigm. *Nat Rev Clin Oncol* (2021) 18(11):679–95. doi: 10.1038/ s41571-021-00524-x

10. Liu Z, Chen Y, Su Y, Hu X, Peng X. Nasopharyngeal carcinoma: Clinical achievements and considerations among treatment options. *Front Oncol* (2021) 11:635737. doi: 10.3389/fonc.2021.635737

11. Tulalamba W, Larbcharoensub N, Sirachainan E, Tantiwetrueangdet A, Janvilisri T. Transcriptome meta-analysis reveals dysregulated pathways in nasopharyngeal carcinoma. *Tumour Biol* (2015) 36(8):5931–42. doi: 10.1007/s13277-015-3268-7

12. Tulalamba W, Janvilisri T. Nasopharyngeal carcinoma signaling pathway: An update on molecular biomarkers. *Int J Cell Biol* (2012) 2012:594681. doi: 10.1155/2012/ 594681

13. Bloom G, Yang IV, Boulware D, Kwong KY, Coppola D, Eschrich S, et al. Multi-platform, multi-site, microarray-based human tumor classification. *Am J Pathol* (2004) 164(1):9–16. doi: 10.1016/S0002-9440(10)63090-8

14. Tothill RW, Kowalczyk A, Rischin D, Bousioutas A, Haviv I, van Laar RK, et al. An expression-based site of origin diagnostic method designed for clinical application to cancer of unknown origin. *Cancer Res* (2005) 65(10):4031–40. doi: 10.1158/0008-5472.CAN-04-3617

15. Janvilisri T. Omics-based identification of biomarkers for nasopharyngeal carcinoma. *Dis Markers.* (2015) 2015:762128. doi: 10.1155/2015/762128

16. Zhang SQ, Pan SM, Liang SX, Han YS, Chen HB, Li JC. Research status and prospects of biomarkers for nasopharyngeal carcinoma in the era of high–throughput omics. *Int J Oncol* (2021) 58(4):9. doi: 10.3892/ijo.2021.5188

17. Zhang B, Kirov S, Snoddy J. WebGestalt: An integrated system for exploring gene sets in various biological contexts. *Nucleic Acids Res* (2005) 33(Web Server issue):W741–8. doi: 10.1093/nar/gki475

18. Jensen LJ, Kuhn M, Stark M, Chaffron S, Creevey C, Muller J, et al. STRING 8–a global view on proteins and their functional interactions in 630 organisms. *Nucleic Acids Res* (2009) 37(Database issue):D412–6. doi: 10.1093/nar/gkn760

19. Ngernsombat C, Prattapong P, Larbcharoensub N, Khotthong K, Janvilisri T. WNT8B as an independent prognostic marker for nasopharyngeal carcinoma. *Curr Oncol* (2021) 28(4):2529–39. doi: 10.3390/curroncol28040230

20. Guan X. Cancer metastases: challenges and opportunities. *Acta Pharm Sin B* (2015) 5(5):402–18. doi: 10.1016/j.apsb.2015.07.005

21. Karin M. Nuclear factor-kappaB in cancer development and progression. *Nature* (2006) 441(7092):431–6. doi: 10.1038/nature04870

22. Schlee M, Hartmann G. The chase for the RIG-i ligand–recent advances. *Mol Ther* (2010) 18(7):1254–62. doi: 10.1038/mt.2010.90

23. Akira S, Uematsu S, Takeuchi O. Pathogen recognition and innate immunity. *Cell* (2006) 124(4):783–801. doi: 10.1016/j.cell.2006.02.015

24. An X, Wang FH, Ding PR, Deng L, Jiang WQ, Zhang L, et al. Plasma epstein-barr virus DNA level strongly predicts survival in metastatic/recurrent nasopharyngeal carcinoma treated with palliative chemotherapy. *Cancer* (2011) 117(16):3750–7. doi: 10.1002/cncr.25932

25. Chan JY, Wong ST. The role of plasma epstein-barr virus DNA in the management of recurrent nasopharyngeal carcinoma. *Laryngoscope* (2014) 124(1):126– 30. doi: 10.1002/lary.24193

26. Chen TC, Chen CH, Wang CP, Lin PH, Yang TL, Lou PJ, et al. The immunologic advantage of recurrent nasopharyngeal carcinoma from the viewpoint of galectin-9/Tim-3-related changes in the tumour microenvironment. *Sci Rep* (2017) 7(1):10349. doi: 10.1038/s41598-017-10386-y

27. Straub JM, New J, Hamilton CD, Lominska C, Shnayder Y, Thomas SM. Radiation-induced fibrosis: Mechanisms and implications for therapy. *J Cancer Res Clin Oncol* (2015) 141(11):1985–94. doi: 10.1007/s00432-015-1974-6

28. Yue Y, Zhong W, Pei G, Xiao B, Zhang G, Jiang F, et al. Aberrant activation of hedgehog pathway in nasopharyngeal carcinoma. *Clin Exp Med* (2013) 13(4):315–22. doi: 10.1007/s10238-012-0198-1

29. Song Q, Li Y, Zheng X, Fang Y, Chao Y, Yao K, et al. MTA1 contributes to actin cytoskeleton reorganization and metastasis of nasopharyngeal carcinoma by modulating rho GTPases and hedgehog signaling. *Int J Biochem Cell Biol* (2013) 45(7):1439–46. doi: 10.1016/j.biocel.2013.04.017

30. Port RJ, Pinheiro-Maia S, Hu C, Arrand JR, Wei W, Young LS, et al. Epstein-barr virus induction of the hedgehog signalling pathway imposes a stem cell phenotype on human epithelial cells. *J Pathol* (2013) 231(3):367–77. doi: 10.1002/path.4245

31. Zhan T, Rindtorff N, Boutros M. Wnt signaling in cancer. *Oncogene* (2017) 36 (11):1461–73. doi: 10.1038/onc.2016.304

32. Akhmetshina A, Palumbo K, Dees C, Bergmann C, Venalis P, Zerr P, et al. Activation of canonical wnt signalling is required for TGF-beta-mediated fibrosis. *Nat Commun* (2012) 3:735. doi: 10.1038/ncomms1734

33. Sriuranpong V, Mutirangura A, Gillespie JW, Patel V, Amornphimoltham P, Molinolo AA, et al. Global gene expression profile of nasopharyngeal carcinoma by laser capture microdissection and complementary DNA microarrays. *Clin Cancer Res* (2004) 10(15):4944–58. doi: 10.1158/1078-0432.CCR-03-0757

34. Zeng ZY, Zhou YH, Zhang WL, Xiong W, Fan SQ, Li XL, et al. Gene expression profiling of nasopharyngeal carcinoma reveals the abnormally regulated wnt signaling pathway. *Hum Pathol* (2007) 38(1):120–33. doi: 10.1016/j.humpath.2006.06.023

35. Morrison JA, Gulley ML, Pathmanathan R, Raab-Traub N. Differential signaling pathways are activated in the epstein-barr virus-associated malignancies nasopharyngeal carcinoma and hodgkin lymphoma. *Cancer Res* (2004) 64(15):5251–60. doi: 10.1158/0008-5472.CAN-04-0538

36. Yap LF, Ahmad M, Zabidi MM, Chu TL, Chai SJ, Lee HM, et al. Oncogenic effects of WNT5A in epstein-barr virus–associated nasopharyngeal carcinoma. *Int J Oncol* (2014) 44(5):1774–80. doi: 10.3892/ijo.2014.2342

37. Qin L, Yin YT, Zheng FJ, Peng LX, Yang CF, Bao YN, et al. WNT5A promotes stemness characteristics in nasopharyngeal carcinoma cells leading to metastasis and tumorigenesis. *Oncotarget* (2015) 6(12):10239–52. doi: 10.18632/oncotarget.3518

38. Sompel K, Elango A, Smith AJ, Tennis MA. Cancer chemoprevention through frizzled receptors and EMT. *Discovery Oncol* (2021) 12(1):32. doi: 10.1007/s12672-021-00429-2

39. Scavo MP, Rizzi F, Depalo N, Armentano R, Coletta S, Serino G, et al. Exosome released FZD10 increases ki-67 expression *via* phospho-ERK1/2 in colorectal and gastric cancer. *Front Oncol* (2021) 11:730093. doi: 10.3389/fonc.2021.730093

40. Scavo MP, Fucci L, Caldarola L, Mangia A, Azzariti A, Simone G, et al. Frizzled-10 and cancer progression: Is it a new prognostic marker? *Oncotarget* (2018) 9(1):824–30. doi: 10.18632/oncotarget.23159

41. Fukukawa C, Nagayama S, Tsunoda T, Toguchida J, Nakamura Y, Katagiri T. Activation of the non-canonical dvl-Rac1-JNK pathway by frizzled homologue 10 in human synovial sarcoma. *Oncogene* (2009) 28(8):1110–20. doi: 10.1038/onc.2008.467

42. Sudo H, Tsuji AB, Sugyo A, Harada Y, Nagayama S, Katagiri T, et al. FZD10-targeted a-radioimmunotherapy with 225 ac-labeled OTSA101 achieves complete remission in a synovial sarcoma model. *Cancer Sci* (2022) 113(2):721–32. doi: 10.1111/cas.15235

43. Chen J, Zhang F, Ren X, Wang Y, Huang W, Zhang J, et al. Targeting fatty acid synthase sensitizes human nasopharyngeal carcinoma cells to radiation *via* downregulating frizzled class receptor 10. *Cancer Biol Med* (2020) 17(3):740–52. doi: 10.20892/j.issn.2095-3941.2020.0219

44. Chen X, Shi C, Cao H, Chen L, Hou J, Xiang Z, et al. The hedgehog and wnt/beta-catenin system machinery mediate myofibroblast differentiation of LR-MSCs in pulmonary fibrogenesis. *Cell Death Dis* (2018) 9(6):639. doi: 10.1038/s41419-018-0692-9

45. Ou H, Chen Z, Xiang L, Fang Y, Xu Y, Liu Q, et al. Frizzled 2-induced epithelial-mesenchymal transition correlates with vasculogenic mimicry, stemness, and hippo signaling in hepatocellular carcinoma. *Cancer Sci* (2019) 110(4):1169–82. doi: 10.1111/cas.13949

46. Wong SC, He CW, Chan CM, Chan AK, Wong HT, Cheung MT, et al. Clinical significance of frizzled homolog 3 protein in colorectal cancer patients. *PloS One* (2013) 8 (11):e79481. doi: 10.1371/journal.pone.0079481

47. Sun Y, Wang Z, Na L, Dong D, Wang W, Zhao C. FZD5 contributes to TNBC proliferation, DNA damage repair and stemness. *Cell Death Dis* (2020) 11(12):1060. doi: 10.1038/s41419-020-03282-3

frontiers | Frontiers in Cell and Developmental Biology

TYPE Review
PUBLISHED 21 February 2023
DOI 10.3389/fcell.2023.1056964

OPEN ACCESS

EDITED BY
Jianping Chen,
Shenzhen Traditional Chinese Medicine Hospital, China

REVIEWED BY
Ila Pant,
Icahn School of Medicine at Mount Sinai, United States
Libang Yang,
University of Minnesota Twin Cities, United States

*CORRESPONDENCE
Sydney Chi-Wai Tang,
scwtang@hku.hk

SPECIALTY SECTION
This article was submitted to Cancer Cell Biology, a section of the journal Frontiers in Cell and Developmental Biology

RECEIVED 29 September 2022
ACCEPTED 17 January 2023
PUBLISHED 21 February 2023

CITATION
Chen J-Y, Yiu W-H, Tang PM-K and Tang SC-W (2023), New insights into fibrotic signaling in renal cell carcinoma. *Front. Cell Dev. Biol.* 11:1056964. doi: 10.3389/fcell.2023.1056964

New insights into fibrotic signaling in renal cell carcinoma

Jiao-Yi Chen[1], Wai-Han Yiu[1], Patrick Ming-Kuen Tang[2] and Sydney Chi-Wai Tang[1]*

[1]Division of Nephrology, Department of Medicine, The University of Hong Kong, Hong Kong, Hong Kong SAR, China, [2]Department of Anatomical and Cellular Pathology, State Key Laboratory of Translational Oncology, The Chinese University of Hong Kong, Hong Kong, China

Fibrotic signaling plays a pivotal role in the development and progression of solid cancers including renal cell carcinoma (RCC). Intratumoral fibrosis (ITF) and pseudo-capsule (PC) fibrosis are significantly correlated to the disease progression of renal cell carcinoma. Targeting classic fibrotic signaling processes such as TGF-β signaling and epithelial-to-mesenchymal transition (EMT) shows promising antitumor effects both preclinically and clinically. Therefore, a better understanding of the pathogenic mechanisms of fibrotic signaling in renal cell carcinoma at molecular resolution can facilitate the development of precision therapies against solid cancers. In this review, we systematically summarized the latest updates on fibrotic signaling, from clinical correlation and molecular mechanisms to its therapeutic strategies for renal cell carcinoma. Importantly, we examined the reported fibrotic signaling on the human renal cell carcinoma dataset at the transcriptome level with single-cell resolution to assess its translational potential in the clinic.

KEYWORDS

renal fibrosis, renal cell carcinoma, cancer-associated fibroblast, mTOR, TGF-β

1 Introduction

Renal cell carcinoma accounts for approximately 3% of all adult malignant diseases and over 90% of kidney cancer (Ferlay et al., 2015). In 2020, the new cases of kidney cancer have reached 431,288 worldwide, with 179,368 related deaths reported accordingly (Siegel et al., 2021). Although the 5-year survival is 60% overall for kidney cancer, it drops to 10% in patients with metastasis (Sengupta et al., 2005; Bianchi et al., 2012; Howlader et al., 2019). Currently, over 10 histological and molecular subtypes of RCC have been identified (Lopez-Beltran et al., 2006; Moch et al., 2016), of which clear cell renal cell carcinoma (ccRCC) is the most common RCC subtype (75% in all RCCs) (Creighton et al., 2013), followed by papillary RCC (pRCC, about 15% in all RCCs) (Linehan et al., 2016) and chromophobe RCC (chRCC, about 5% in total RCCs) (Davis et al., 2014). The discovery of von Hippel–Lindau (VHL) and other epigenetic regulatory gene mutations further advanced the knowledge of RCC development (Creighton et al., 2013; Alaghehbandan et al., 2019; Lin et al., 2021). However, how immune escape and distant metastasis initiate in RCC remains obscure.

Cancer-associated fibrosis was found to play a critical role in tumorigenesis, immune evasion, metastasis, and drug resistance in various solid tumors (Coffman et al., 2016; Kalluri, 2016; Piersma et al., 2020). Epidemiological findings strongly indicate a prognostic relevance between tissue fibrosis and epithelial cancers, such as hepatic, gastroesophageal, lung, and renal cancers (Neglia et al., 1995; Leek et al., 1996; Maisonneuve et al., 2013; Joung et al., 2018; Ballester et al., 2019). Moreover, fibrosis in the tumor immune microenvironment (TME), characterized by ITF (Chandler et al., 2019; Liu et al., 2019),

activation of cancer-associated fibroblasts (CAFs) (Kalluri, 2016), and extracellular matrix (ECM) deposition (Chandler et al., 2019), supports tumor growth by producing growth factors, stimulating angiogenesis (Ziani et al., 2018; Inoue et al., 2019). Fibrotic signaling can also mediate immunosuppression by facilitating Treg cell and myeloid-derived suppressor cell (MDSC) differentiation and recruitment (Costa et al., 2018; Givel et al., 2018; Lin et al., 2022), metabolic reprogramming (Hamanaka and Mutlu, 2021), and long non-coding RNA (lncRNA) regulation (Shi et al., 2021). Therefore, fibrotic signaling has become a promising therapeutic target for cancer.

In this review, we summarized the pathogenic roles and underlying mechanisms of various RCC-associated fibrosis in the development and progression of RCC. In addition, we validated the reported findings in RCC patients datasets by using gene set enrichment analysis (GSEA) and single-cell RNA sequencing (scRNA-seq) data mining. Furthermore, the translational potentials of new therapeutic strategies targeting fibrotic signaling in RCC were also discussed.

2 Prognostic relevance between fibrosis and RCC

Fibrosis is a common feature frequently observed in RCC (Cheville et al., 2003), characterized by ITF, CAFs, ECM deposition, peritumoral PC fibrosis, and EMT. CAFs play an essential and versatile role in all stages of RCC. They are a group of robustly proliferative and metabolically activated fibroblasts (Guido et al., 2012; Kalluri, 2016), characterized by high expression of α-smooth muscle actin (α-SMA), fibroblast activation protein (FAP), S100A4, and platelet-derived growth factor receptors α and β (PDGFα and PDGFβ) (Kalluri, 2016). CAFs can be derived from multiple sources including resident fibroblasts (Kojima et al., 2010), mesenchymal stem cells (MSCs) (Barcellos-de-Souza et al., 2016), and epithelial and endothelial cells (Petersen et al., 2003; Yeon et al., 2018). Mechanistically, CAFs continuously interplay with tumor cells by producing pro-tumor cytokines, activating immunosuppressive leukocytes, and promoting ECM deposition, thus offering a tumor-favorable microenvironment (Kalluri, 2016). A recent cohort study revealed that the CAFs are significantly correlated with shorter disease-free survival (DFS), poorer overall survival (OS), and lymph node metastasis among ccRCC patients (Ambrosetti et al., 2022). Xu et al. further specified CD248 + CAFs as the pivotal CAF phenotype that was remarkably related to poor prognosis and immunosuppressive TME during RCC progression (Xu et al., 2021).

CAFs can directly form fibrotic tumor stroma *via* cross-linked collagen matrix deposition. Such ITF is associated with decreased lymphocyte infiltration, poorer patient survival, and various carcinomas, including breast cancer (Solinas et al., 2017; Li et al., 2019), lung cancer (Ballester et al., 2019), colorectal cancer (Nazemalhosseini-Mojarad et al., 2019), pancreatic cancer (Sinn et al., 2014), and advanced rectal cancer (Ueno et al., 2004). A retrospective cohort study involving 204 RCC patients found that over 80% of ccRCC cases had intratumoral fibrosis (Joung et al., 2018). Although ITF itself does not have a significant association with ccRCC prognosis, it is correlated with other prognostic factors such as Fuhrman nuclear grade, intratumoral necrosis, and lymphovascular invasion (Joung et al., 2018).

CAFs are also the major source of tumor-associated ECM (Bond et al., 2021). A recent proteomics study revealed that the composition of ECM in ccRCC varies significantly from their respective counterparts in the neighboring healthy cortex. RCC-associated ECM is more abundant, denser, and stiffer, with increased deposition of fibronectin (*FN1*), collagen 1 (*COL1A1* and *COL1A2*), and collagen 6 (*COL6A1*, *COL6A2*, and *COL6A3*) (Bond et al., 2021). Also, some of these overexpressed fibrotic ECM proteins, including fibronectin 1 and collagen 1, are correlated with a poorer prognosis among ccRCC and pRCC patients (Steffens et al., 2012; Majo et al., 2020).

Interestingly, in contrast to the previous findings, several studies show that tumor-related fibrosis might limit tumor growth and metastasis at the early stages of cancer (Bruno et al., 2013; Alkasalias et al., 2014). In terms of RCC, such protective fibrosis is referred to as the fibrotic PC (Xi et al., 2018). PC is a common pathologic feature that exists in almost all the early-stage RCCs and is composed of fibrous tissue, compressed normal renal tissue, and scaffolding of vascular tissues in the RCC surrounding area (Huang et al., 1992; Tsili et al., 2012; Minervini et al., 2014; Cheng et al., 2015; Cho et al., 2017). The frequency of PC appearance varies from 33% to 72% in RCC. As the only barrier interposing between RCC and the surrounding normal renal parenchyma, the intact PC indicates a limited tumor-to-immune cell and tumor-to-matrix interaction in the TME and lower aggressiveness of RCCs. Several clinical observations revealed that the tumor invasion of the PC suggested a poor prognosis with a higher risk of local recurrence and metastasis (Yamashita et al., 1996; Cho et al., 2009; Xi et al., 2018). Qin et al. (2020) mentioned that fibrosis in PCs might strengthen the vital barriers to prevent tumor penetration. By quantifying collagen distribution in PCs among RCC patients, they further noticed that fibrosis in PCs is an independent marker of PC integrity. Lower PC fibrosis is significantly associated with shorter progression-free survival.

3 Transcriptome profile uncovered enriched fibrotic signaling in RCC

With the emerging RNA sequencing technologies, from bulk RNA sequencing (bulk RNA-seq) to scRNA-seq, transcriptome profiling of RCC has been greatly utilized in biomarker discovery, cancer heterogeneity characterization, and studies regarding distant metastasis and therapy resistance. More importantly, understanding the role of fibrosis in RCC development enlightens further therapeutic target identification by data mining the transcriptomic database of RCC patients. Here, we performed gene set enrichment analysis, as previously described (Chen et al., 2022), of a public human RCC scRNA-seq dataset (Young et al., 2018) and summarized the activated fibrotic signaling pathways identified in different subtypes and stages of human RCC.

Early in 2010, López-Lago et al. (2010) used RNA sequencing to provide evidence for the association of increased metastatic activity with the acquisition of a myofibroblast-like feature in both RCC cell lines and human metastatic RCC biopsies. Later, activation of the pro-fibrotic

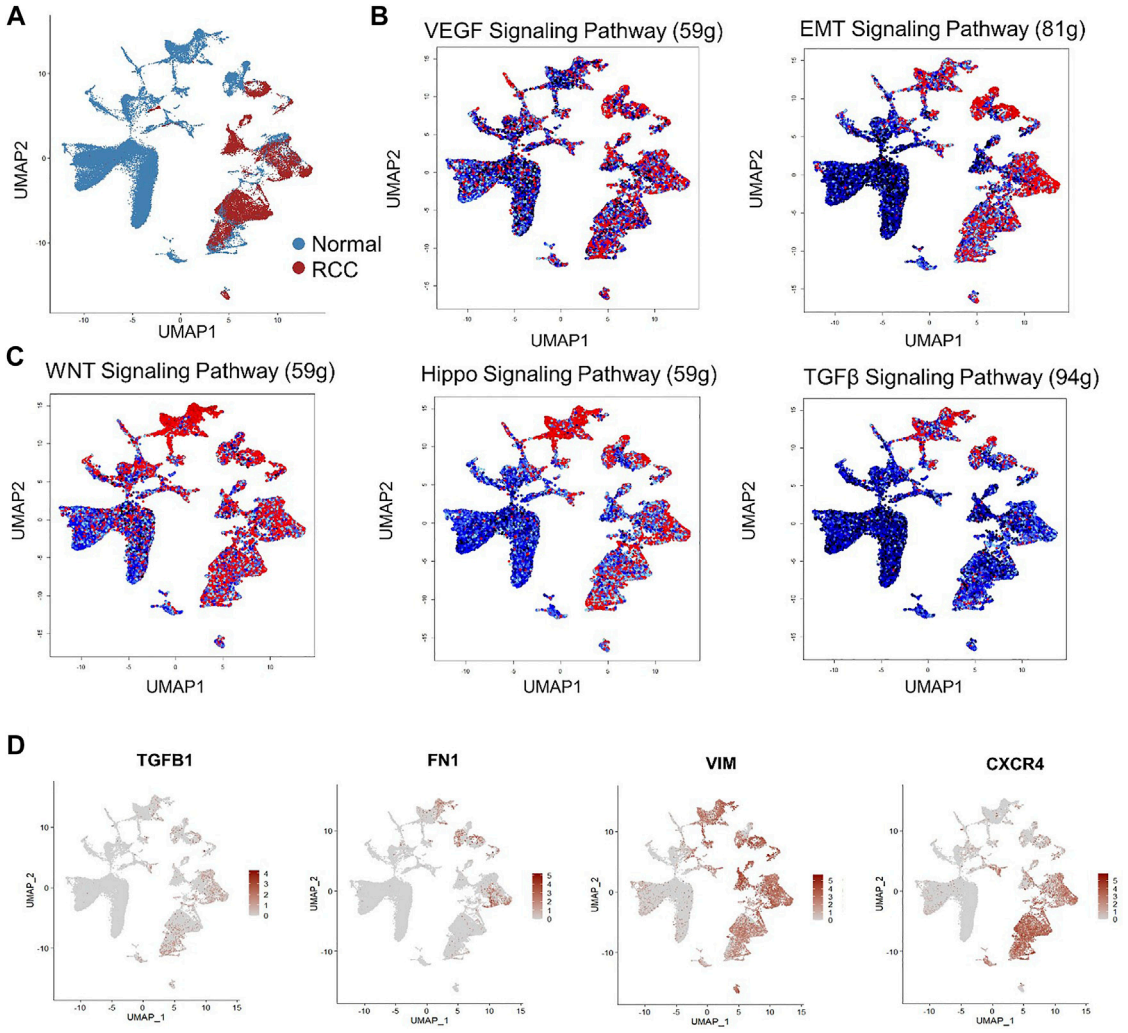

FIGURE 1
Single-cell RNA sequencing (scRNA-seq) reveals activated fibrotic signaling pathways in human renal cell carcinoma. **(A)** Non-linear dimensionality reduction on Uniform Manifold Approximation and Projection (UMAP) visualization of renal cells from RCC patients and the healthy control group. Each point depicts a single cell, colored according to group designation. Colored UMAP plots of highlighted cells with activated gene set expression in **(B)** VEGF and EMT signaling and **(C)** WNT, Hippo, and TGF-β signaling pathways in renal cells based on AUC scores. Each point represents a single cell. Cells with indicated signaling activation are colored in shades of red and those without signaling activation are colored in black–blue. **(D)** UMAP plots of gene expression gradients identified. Each point depicts a single cell, colored according to normalized expression levels. The average expression scale is shown on the right side of each UMAP plot.

TGF-β signaling pathway was further identified in the transcriptome profile of MiTF/TFE translocation RCC (Malouf et al., 2014). Another two bulk RNA-seq datasets, comparing mRNA expression between human ccRCC and normal kidney tissue, also revealed pro-fibrosis signatures *ACTA2* (α-SMA), *COL1A1*, *COL23A1*, *VEGFA*, and *TGFB1* as the top differentially expressed genes (DEGs) upregulated in ccRCC (Xiong et al., 2014; Eikrem et al., 2016). Elevated TGF-β signaling was also identified in the transcriptomic profile of 176 ccRCC patients, correlated with poor disease survival and tumor metastasis (Zhao et al., 2006; Sjölund et al., 2011). Sven Wach et al. (2019) reported over 5,000 DEGs with the criteria $|\log_2$ fold change$| \geq 1$ in collecting duct carcinoma (CDC), in comparison with the normal kidney tissue. Enrichment analysis targeting those DEGs further identified the pro-fibrosis collagen signaling pathway as the top-ranked enriched pathway activated in the CDC group. *KRT17* (keratin 17), a wounded stratified epithelium-induced filament protein, was identified as the top DEG with the highest fold change of expression in CDC [Wach et al. (2019)]. More recently, *KRT17* high-expressing basal-like cells were defined in fibrotic hypersensitivity pneumonitis patients with higher expression levels of *COL1A1*, *FN1*, and *COL6A2* and upregulated activities in ECM organization by scRNA-seq analysis (Wang et al., 2022b). Findings of the scRNA-seq profile, in combination with the CDC bulk RNA profile, suggest a potential pathogenic role of KRT17-mediated fibrosis during RCC development.

Nevertheless, the aforementioned studies mainly focused on biomarker identification and RCC heterogenetic phenotype characterization without an in-depth study of fibrotic signaling participation in RCC at single-cell resolution. To address this question, we performed GSEA of a published human RCC scRNA-seq dataset (Young et al., 2018)

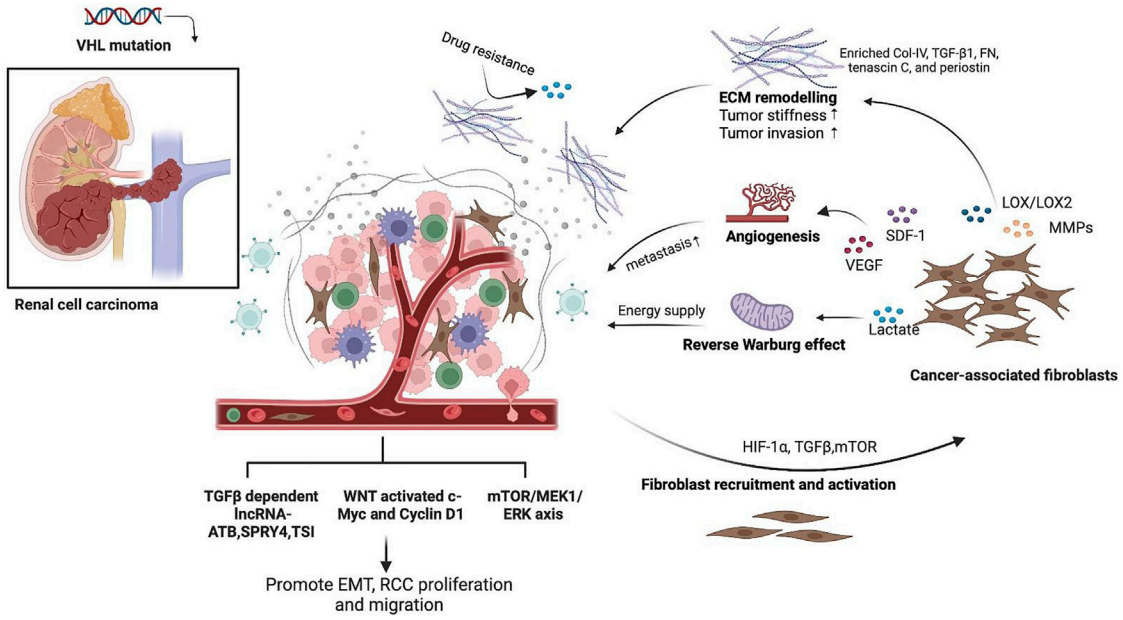

FIGURE 2
Schematic representation of the role of fibrotic signaling in renal cell carcinoma (RCC). CAFs are the major source of fibrotic stroma in the RCC TME, which could be activated due to HIF-1α accumulation and TGF-β and mTOR signaling regulation from cancer cells. Activated CAFs secreted MMPs and LOX to promote ECM remodeling with enriched collagen IV, TGF-β1, fibronectin, tenascin C, and periostin, thus promoting tumor stiffness, drug resistance, and tumor invasion. CAFs in RCC also produce SDF-1 and VEGF to promote tumor angiogenesis and favor RCC metastasis. CAFs fed cancer cells with increased lactate as a direct energy supply *via* aerobic glycolysis, which is known as the "reverse Warburg effect." RCC also expressed pro-fibrotic signaling pathways, including TGF-β and its downstream lncRNA, WNT, and mTOR signaling pathways, to mediate the EMT process, tumor cell proliferation, and migration. This figure was created in BioRender.com.

downloaded from the European Genome-phenome Archive (EGA) under study IDs EGAS00001002171, EGAS00001002486, EGAS00001002325, and EGAS00001002553. Subsequently, raw UMI counts of the scRNA-seq dataset were imported into R (version 4.1.2) using the Seurat package (version 4.0.5) for quality control. Next, sequencing data from normal control and RCC patients were normalized, scaled, and mapped *via* non-linear dimensionality reduction on the Uniform Manifold Approximation and Projection (UMAP) plot by using the Normalized, ScaleData, and FindVariableFeatures functions, respectively, in the Seurat package to map the comprehensive cell landscape as shown in Figure 1A. Next, fibrosis-related gene set enrichment was tested using GSEABase (version 1.56.0) and GSVA R packages (version 1.42.0) within a panel of annotated gene databases (Gene Ontology, Reactome, and Kyoto Encyclopedia of Genes and Genomes). The enrichment of gene sets at the single-cell level was visualized using the AUCell (version 1.16.0) R Bioconductor package. The transcriptomes of RCC cells were significantly enriched in pro-fibrotic EMT and VEGF signaling (Figure 1B). Fibrotic signaling pathways including WNT and Hippo signaling pathways were also significantly upregulated in RCC (Figure 1C). Although TGF-β signaling is less enriched in RCC cells, *TGFB1* expression, together with three other key fibrosis regulators, *FN1*, *VIM*, and *CXCR4*, was also elevated under the RCC condition (Figure 1D). Taken together, the above findings provided solid evidence of the activation and participation of fibrotic signaling during RCC progression.

4 Mechanism of the interplay between fibrosis and RCC

4.1 CAF-centered crosstalk between fibrotic stroma and RCC

CAFs have long been recognized as a substantial element in the TME that support tumor growth and invasion through diverse mechanisms, including ECM remodeling, cytokine production, immune regulation, and metabolic alteration. In this study, we reviewed and summarized the role of CAF-centered interaction and other critical fibrotic signaling pathways in RCC oncogenesis and metastasis (Figure 2). In RCC, activation of CAFs results from von Hippel–Lindau gene malfunction-induced HIF-1α accumulation (Razorenova et al., 2011; Shen and Kaelin, 2013; Yang et al., 2020). During tumor progression, CAFs continuously produce matrix-crosslinking enzymes, such as LOX family oxidases and matrix metalloproteinases (MMPs), to promote ECM remodeling. This leads to the reorganization of collagen and fibronectin fibers and consequently increases tumor stiffness and contributes to RCC invasion and metastasis (Gilkes et al., 2014). Higher expression levels of LOX family genes, for instance, LOX and LOXL2, indicate poor survival in ccRCC patients (Hase et al., 2014; Lin et al., 2020). Mechanistically, LOX and LOXL2 promote collagen stiffness increment, integrin α5β1 stabilization, and fiber formation while suppressing the protease and proteasome system in ccRCC (Hase et al., 2014). Furthermore, MMPs, including MMP-9 and MMP-2 produced by CAFs, also contribute to tumor invasion and metastasis

and have been recognized as potential prognostic biomarkers in ccRCC (Awakura et al., 2006; Chen et al., 2017). In addition, microRNA mir-124-mediated suppression of MMP-9 can attenuate RCC invasiveness *in vitro* (Wang et al., 2018). Regulated by TGF-β1, MMP-13 is more related to bone metastasis of RCC than to primary RCC and healthy kidneys (Kominsky et al., 2008). Moreover, CAFs are also the major producers of the stromal cell-derived factor (SDF-1) (Orimo et al., 2005; Wang et al., 2021). In RCC, CAF-secreted SDF-1 interacts with the chemokine receptor 4 (CXCR4) on renal cancer cells and consequently promotes tumor angiogenesis and organ metabolism (Pan et al., 2006).

CAFs are also capable of transducing the non-muscular myosin II- and PDGFRα-mediated contractility and traction forces to fibronectin *via* integrin α5β1, thus aligning the fibronectin-rich ECM to favor tumor migration (Erdogan et al., 2017; Gopal et al., 2017). Previous scRNA-seq transcriptomic analysis revealed CAF-specific feature expression and identified CAFs as the major sources of ECM in human ccRCC (Young et al., 2018; Bond et al., 2021; Liu et al., 2021). In contrast to the healthy cortex, CAF-contributed ECM production in ccRCC was characterized by high enrichment of collagen VI, fibronectin, tenascin C, TGF-β1, and periostin (Bond et al., 2021). Fibronectin and collagen were the most abundant components in CAF-produced ECM. CAF-induced fibronectin promotes the proliferation and inhibits the apoptosis of precancerous bronchial epithelial and carcinoma cells through the activation of PI3K/AKT signaling in the lung (Han et al., 2006; Han and Roman, 2006). As for RCC patients, higher fibronectin 1 expression showed an increased disease-related mortality rate (Steffens et al., 2012) and a more advanced clinical stage (Dong et al., 2021). Competing endogenous RNA networks further proved the direct correlations between FN1 and C3, FN1 and pro-fibrotic signaling pathways, including WNT, HIF, PI3K/AKT, MAPK, and TGF-β pathways, in ccRCC (Dong et al., 2021). The TGF-β1/Src axis is a well-studied pro-fibrotic signaling pathway that promotes renal fibrosis and tumor progression by promoting macrophage-to-myofibroblast transition (MMT) (Meng et al., 2016; Tang et al., 2018). An *in vitro* study on human RCC cells showed that silencing fibronectin *in vitro* attenuated cell proliferation and migration by suppressing TGF-β1/Src signaling (Ou et al., 2019). Collagen I, another essential CAF-produced ECM component, also facilitates EMT by upregulating MMP-2 and transcription factors ZEB2 and SNAIL in multiple RCC cell lines (Majo et al., 2020), which consequently enhances the proliferation, adhesion, and migration of RCC.

CAFs also influence tumor behavior by reprograming cancer cell metabolism (Martinez-Outschoorn et al., 2014). Aerobic glycolysis, also known as the Warburg effect (Warburg, 1925), has long been recognized as the hallmark metabolic pathway in various solid tumors, including RCC (Singer et al., 2011). During cancer development, anabolic cancer cells rapidly interact with the neighboring CAFs through metabolite exchange and oxidative stress induction and thus consequently promote aerobic glycolysis in CAFs. Such a "dual chamber" process is proposed as a CAF-dependent "reverse Warburg effect" (Pavlides et al., 2009; Benny et al., 2020). To be specific, aerobic glycolysis occurring within CAFs under Warburg metabolism results in lactate generation and deposition in RCC TME. Increased lactate not only acts as a major metabolic fuel for cancer cells directly (Guo et al., 2019), but also contributes to RCC progression and metastasis through indirect mechanisms. Accelerated lactate leads to acidification in TME, which consequently suppresses T-cell cytotoxicity against RCC (Sun et al., 2022). In addition, lactate also accelerates angiogenesis (Trabold et al., 2003), promotes EMT (Miranda-Gonçalves et al., 2020), and weakens cancer sensitivity to programmed cell death (Daneshmandi et al., 2019), thereby enhancing tumor aggressiveness.

CAFs in RCC expressed common fibrotic signaling pathways, including TGF-β, mTOR, MAPK, and WNT/β-catenin signaling pathways, which are similar to those found in most solid tumors (Wu et al., 2021a). Meanwhile, it is increasingly recognized that CAFs and their fibrotic signaling exhibit phenotypic and functional heterogeneity in different tissues/organs and origins. For example, CAFs in lung cancer express distinctively high levels of elastin and collagen (Hao et al., 2019a). Diverse CAF subpopulations with a distinguished transcriptome profile have been recognized in breast cancer (Bartoschek et al., 2018; Costa et al., 2018). Knowledge of CAF heterogeneity will help develop a precision cancer treatment. However, our understanding of RCC-specific CAFs is still very limited. A recent study combining scRNA-seq and cell line sequencing profile has identified the transcriptome signatures of RCC-specific CAFs, including COL1A1, COL1A2, COL5A1, COL16A1, elastin microfibril interfacer 1 (EMILIN1), lysyl oxidase-like 1 (LOXL1), and lumican (LUM) (Liu et al., 2020). Functional enrichment analysis indicates that RCC-specific CAF signatures are significantly associated with extracellular matrix function, collagen synthesis, cell surface interaction, and cell adhesion. Further studies are required to validate the phenotype and functional heterogeneity of CAFs among RCC patients.

4.2 TGF-β-centered regulation of fibrosis in RCC progression

TGF-β is the master regulator of renal fibrosis and immune escape in renal cancer (Meng et al., 2015; Chung et al., 2021). Early in 1998, Wunderlich et al. (1998) observed that the latent TGF-β1 was commonly and significantly elevated among RCC patients and even higher among those with pyelonephritis, indicating the oncogenetic role of TGF-β in RCC. With the emerging in-depth studies targeting the pathological role of TGF-β in cancer development, researchers have revealed the dual roles of TGF-β and its downstream cascades during cancer development (Massagué, 2008; Kubiczkova et al., 2012; Chan et al., 2022; Tang et al., 2022). Under normal conditions or at precancerous stages, TGF-β mainly exhibits antitumor activities by maintaining tissue homeostasis and inducing cell cycle arrest to regulate epithelial cell differentiation and apoptosis (Song, 2007; Xu et al., 2018). Nevertheless, cancer cells can always find ways to bypass TGF-β-mediated inhibition, in turn taking advantage of TGF-β signaling or directly producing TGF-β to benefit themselves (Biswas et al., 2014; Yang et al., 2016a; Tang et al., 2017; Rasti et al., 2021). In TME, TGF-β is the key mediator of EMT during tumor progression (Hao et al., 2019b; Xue et al., 2020; Chung et al., 2021). Stimulation with recombinant TGF-β1 significantly promotes EMT in renal carcinoma cells *in vitro* (Boström et al., 2012; Tretbar et al., 2019). Inhibition of TGF-β-induced EMT resulted in suppressed metastasis capacity of RCC (Boström et al., 2013; Wang et al., 2020). TGF-β also promotes EMT by regulating long non-coding RNA (lncRNA) expression in RCC TME. TGF-β1-dependent activation of lncRNA-ATB enhances EMT and tumor

cell invasion in hepatocellular carcinoma (Yuan et al., 2014). In RCC, lncRNA-ATB was found to be positively correlated with metastasis and poorer prognosis (Xiong et al., 2016; Qi et al., 2017). Mechanistically, lncRNA-ATB downregulates the tumor suppressor p53 through the regulation of the DNA methyltransferase enzyme DNMT1 and thus strengthens the proliferation and migration of RCC cells (Song et al., 2019). Meanwhile, silencing lncRNA-ATB represses EMT in RCC by suppressing the expression of mesenchymal signatures such as N-cadherin and vimentin (Xiong et al., 2016). Another TGF-β1-induced lncRNA SPRY4-IT1 also demonstrates similar pro-EMT functions both in human RCC and RCC cells *in vitro* (Zhang et al., 2014).

4.3 ITF shapes the immune landscape of RCC

Immune cells in TME are considered critical and versatile players in tumor development. Fibrotic tumoral stroma is a significant source of immunosuppressive activity in the TME (Yamauchi et al., 2018; Baker et al., 2021). By producing CXCL12, activated CAFs directly inhibit cytotoxic T-cell recruitment and upregulate immunosuppressive Treg cell infiltration *via* binding to the CXCR4 receptor on cytotoxic T cells and Treg cells in pancreatic cancer (Feig et al., 2013). Yang et al. (2016b) found that FAP + CAFs are the major producers of CCL2 through the uPAR-induced FAP/STAT3/CCL2 axis in the murine liver cancer model. CAF-derived CCL2 in turn induces the recruitment of MDSCs by interacting with CCR2 on circulating MDSCs, thus favoring tumor evasion from immune surveillance. Other molecules produced by CAFs such as MMPs, latent TGF-β, IL-10, and VEGFA were also found to reshape the immune system toward a pro-tumoral pattern (Baker et al., 2021). In addition, CAFs contribute to ECM remodeling by producing MMPs, fibronectin, and collagen, thus increasing ECM stiffness around tumors (Acerbi et al., 2015; Altorki et al., 2019). Consequently, the thickened ECM prevents T-cell infiltration and antitumor drug delivery to cancer cells. Till now, there are still very limited evidence regarding the fibrotic stroma and its interaction with immune activity in TME of kidney cancer. A recent cohort study of 45 ccRCC patients uncovered a significant association between intratumoral fibrosis and cytotoxic T-lymphocyte-associated protein 4 (CTLA4) expression (Han et al., 2022), indicating the potential regulatory role of fibrosis in the tumor immune microenvironment of RCC. However, the underlying mechanism of fibrosis interaction with TME of RCC needs further investigation.

4.4 The role of other fibrosis signaling in RCC tumorigenesis

Except for TGF-β/Smad signaling, other pro-fibrotic pathways such as WNT, mTOR, and NOTCH signaling pathways also contribute to tumorigenesis in renal cancer (Table 1). The WNT/β-catenin pathway is one of the most well-studied signaling pathways in renal fibrosis and is activated in human fibrotic chronic kidney disease and the unilateral ureteral obstruction (UUO) mouse model (Tan et al., 2014; Huffstater et al., 2020). In response to injury, renal cells from the tubular epithelium or interstitium ubiquitously produce WNT ligands, such as WNT1, WNT7A, and WNT10A (He et al., 2011; Kuma et al., 2014; Huffstater et al., 2020). The activation of WNT signaling upregulates β-catenin-mediated downstream gene expression, including fibronectin, Snail 1, MMP-7, PAI-1, FSP1, and HGF, which consequently leads to fibroblast activation, EMT, and renal fibrosis (Edeling et al., 2016; Zhou et al., 2017). In RCC, the activation of WNT signaling through WNT ligand secretion, WNT receptor overexpression, and function loss of WNT antagonists has been reported to promote tumorigenesis and metastasis (Xu et al., 2016). Ligands of the WNT canonical pathway, such as WNT1 and WNT10A, are associated with tumor progression, poor prognosis, and tumor invasiveness in ccRCC patients (Kruck et al., 2013; Piotrowska et al., 2020) by oncogene activation, such as c-Myc and cyclin D1 (Furge et al., 2007; Karim et al., 2016). On the contrary, some ligands of the WNT non-canonical pathway, including WNT5A and WNT7A, demonstrate a potential tumor-suppressive role in renal cancer (Tamimi et al., 2008; Kondratov et al., 2012). In addition, the functional loss of WNT antagonists is another vital trigger of WNT signaling activation in RCC. Early in 2006, Urakami et al. (2006) reported that RCC patients significantly demonstrated high methylation levels of WNT antagonists, including sFRP-1, sFRP-2, sFRP-4, sFRP-5, WIF-1, and Dkk-3, compared to healthy controls. Specifically, the methylation level of sFRP-1 serves as an independent biomarker for RCC prognosis. Later, the same team also identified that WIF-1, a WNT antagonist belonging to the secreted frizzled-related protein (sFRP) class, functions as a tumor suppressor in RCC cells. Overexpression of WIF-1 enhances RCC cell apoptosis and inhibits tumor growth *in vivo* (Kawakami et al., 2009). A similar antitumor potential has also been identified in IGFBP-4, DKK-1, and DKK-3 (Ueno et al., 2011; Xu et al., 2017; Chen et al., 2018).

Activation of the mTOR signaling cascade also plays a pro-fibrotic role during chronic kidney injury. In diabetic nephropathy, induced glomerular mesangial hypertrophy and matrix expansion were mediated by TGF-β1 and its downstream AKT/PRAS40/mTOR axis in glomerular mesangial cells (Dey et al., 2012; Maity et al., 2020). Further studies confirmed that the activation of either mTOR1 or mTOR2 promotes fibroblast activation and myofibroblast proliferation (Jiang et al., 2013; Li et al., 2015). Moreover, the activation of mTOR2 facilitates macrophage polarization toward the pro-fibrotic M2 phenotype through the Rictor/mTORC2/AKT axis in the UUO mouse model (Ren et al., 2017). Both activated myofibroblasts and M2 macrophages are the main contributors to collagen production and ECM deposition during renal fibrosis. Intriguingly, downstream cascades of mTOR signaling also contribute to RCC oncogenesis and metastasis. The activation of mTOR is correlated with poor prognosis and aggressive tumorigenesis in RCC (Pantuck et al., 2007; Damayanti et al., 2018). Wu et al. (2021b) further uncovered that the activation of the mTOR pathway initiated RCC development from renal proximal tubular cells. Mechanistically, activated mTOR signaling upregulates MEK1 expression and promotes ERK activation, which induces pro-proliferation cyclins and Myc expression. Meanwhile, activated mTOR also suppresses the anti-proliferation p53/p16 axis *via* MKK6/p38 MAPK signaling. As a result, the TSC1 or VHL mutation-induced pathologic mTOR activation and its downstream cascades lead to renal cyst formation

TABLE 1 Fibrotic signaling in RCC.

Key molecule	Associated pathway	Mechanism	Biological function
CAF-mediated fibrotic signaling in RCC			
LOX/LOX2	ECM remodeling	Promotes collagen stiffness increment and integrin stabilization and fiber formation and suppresses the protease and proteasome system	RCC invasion and metastasis
MMP-2/9	AKT/NF-κB/MMP-9 and collagen I/MMP-2	Degrades ECM proteins; proteolytic breakdown of tissue barriers to invasion; and promotes circulating tumor cell extravasation	RCC invasion and metastasis
MMP-13	TGF-β1/MMP-13	Promotes osteoblastic matrix degradation and osteoclastic activation	Bone metastasis
SDF-1	SDF-1/CXCR4 interaction	Promotes angiogenesis and organ metabolism	RCC proliferation and invasion
Collagen I	Upregulating MMP-2, ZEB2, and SNAIL	Facilitates EMT	Enhances RCC proliferation, adhesion, and migration
Fibronectin	Fibronectin/TGF-β1/Src/cyclin D1 and vimentin	Interacts with integrin α5 and integrin β1; promotes RCC cell migration; and promotes cyclin D1 and vimentin expression, TGF-β1 production, and Src and Smad phosphorylation	Enhances RCC cell growth and migration
Lactate	Aerobic glycolysis	Energy supply to the tumor; TME acidification; suppresses T-cell anticancer activities; and accelerates angiogenesis	Enhances RCC aggressiveness
TGF-β-centered fibrotic signaling in RCC			
lncRNA ATB	TGF-β1/ATB/DNMT1/p53	Regulates DNMT1 to suppress p53 and promotes the expression of N-cadherin and vimentin	Enhances RCC cell proliferation and migration
lncRNA SPRY4-IT1	ND	ND	Promotes RCC cell proliferation, migration, and invasion
Other fibrotic signaling in RCC			
WNT1 WNT10A	WNT canonical pathway	Activating oncogenes c-Myc and cyclin D1	Promotes ccRCC progression and invasiveness
WNT5A	WNT non-canonical pathway	Directly regulated by PAX2	Potentially related to blastemal predominant Wilms tumorigenesis
WNT7A		WNT7A hypermethylation due to genetic/epigenetic alterations and promotes ccRCC oncogenesis	ccRCC tumor suppressor
WIF-1	WNT antagonist	Loss function of WIF in ccRCC triggers WNT signaling activation and inhibits RCC apoptosis and proliferation	Enhances RCC cell apoptosis and inhibits tumor growth
mTOR	mTOR/MEK1/ERK and mTOR/MMK6/p38 MAPK	Induces pro-proliferation gene (cyclins and Myc) expression and suppresses the anti-proliferation p53/p16 axis	Promotes RCC tumorigenesis, proliferation, and metastasis
Notch2	Notch2/Jagged1 interaction	Notch2/Jagged1 interaction modifies histone and gene amplification of oncogenesis-related genes.	Promotes ECC proliferation and metastasis

and RCC carcinogenesis [Wu et al. (2021b)]. Other mTOR-regulated molecules, such as autophagy-related light chain (LC3), fatty acids, EMT-associated eIF4E-binding protein 1 (4E-BP1), and ribosomal S6 kinase (S6K), were also found to contribute to RCC development and invasion (Dey et al., 2019; Qu et al., 2020; Tao et al., 2020).

The pro-fibrotic Notch signaling pathway also contributes to tumorigenesis. The interaction of Notch2 with its receptor Jagged1 not only promotes renal fibrosis and metabolism by regulating TFAM and PGC1-α expression (Han et al., 2017; Huang et al., 2018) but is also associated with RCC proliferation and metastasis through histone modification and gene amplification of cell fate determination features, *KLF4* and *SOX9*, renal development-related features, *PAX2* and *SALL1*, the stem cell maintenance-associated features, *PROM1* and *ALDH1A*, and chromatin modification-related feature, *MYST3* (Fendler et al., 2020).

Efforts have also been made to identify how RCC-specific fibrotic signaling differs from that of other types of cancer. Yang et al. (2021) identified 11 cytokines that are significantly associated with fibrosis in ccRCC, including brevican, prolactin, presenilin 1, and GRO. The team further found that ccRCC expressed a distinctly higher level of prolactin

TABLE 2 Anticancer therapies targeting fibrosis in RCC.

Drug	Target	Mechanism	Type	Current status
Target mTOR signaling				
Everolimus	mTORC1	Selective inhibition of mTORC1	Small-molecule inhibitor	FDA approved
Temsirolimus	mTORC1	Selective inhibition of mTORC1	Small-molecule inhibitor	FDA approved
AZD2014	mTORC1/ mTORC2	Dual inhibition of mTORC1 and mTORC2	Small-molecule ATP competitive inhibitor	Phase II trial completed
NVP-BEZ235 combined with sorafenib	PI3K/mTOR	Dual inhibition of PI3K/Akt/mTOR	Small-molecule ATP competitive inhibitor	Preclinical study conducted on RCC cell lines
PP242 and PP30	mTORC2	Selective inhibition of mTORC2	Small-molecule ATP competitive inhibitor	Preclinical study conducted on RCC cell lines (UMRC6, 786-0, and UOK121)
WYE-125132	mTORC1/ mTORC2	Dual inhibition of mTORC1 and mTORC2	Small-molecule ATP competitive inhibitor	Preclinical study conducted on the mouse RCC model
Target TGF-β signaling				
Fresolimumab	TGF-β	Human TGF-β1/β2/β3 neutralizer	Human monoclonal antibody	Phase I trial completed
LY3022859	TGF-β2	Human TGF-β2 neutralizer	Human monoclonal antibody	Phase I trial completed
Valproic acid	Smad4	Smad4 suppressor		Preclinical study conducted on RCC cell lines (786-0 and Caki-1)
Pirfenidone	TGF-β	TGF-β inhibitor	Broad-based anti-fibrotic drug	Preclinical study conducted on the mouse RCC model

and prolactin receptors, compared to other malignant tumors like lung, liver, and breast cancers. Such ligand–receptor interactions are also correlated with the prognosis of ccRCC patients.

5 Therapeutic implications targeting fibrosis signaling

Due to the highly fibrotic feature of the RCC intratumoral environment, therapies targeting fibrosis signaling are exploited to suppress the progression of RCC (Table 2). In 2009, the mTORC1 inhibitors everolimus and temsirolimus had already been approved by the U.S. Food and Drug Administration (FDA) as single agents in the second-line setting and in the first-line in RCC patients' treatment at advanced stages (Hudes et al., 2007; Motzer et al., 2008). Interestingly, another mTORC1/2 dual inhibitor AZD-2014 was also able to downregulate HIF-1α/2α and cyclin D expression and further inhibit RCC cell proliferation preclinically (Zheng et al., 2015). However, the phase II randomized control study among 49 patients with VEGF-refractory metastatic ccRCC showed that AZD-2014 was less toxic but also less effective than everolimus in improving patients' overall survival and preventing tumor progression (Powles et al., 2016). Roulin et al. (2011) revealed that combined treatment with sorafenib and NVP-BEZ235, a novel dual PI3K/mTOR inhibitor, demonstrated enhanced antitumor efficacy in RCC cell lines, 786-0 and Caki-1, compared to either of the single treatments. Other mTOR inhibitors, such as mTORC2 inhibitors, PP242 and PP30 (Feldman et al., 2009; Li et al., 2021), and the mTORC1/2 dual inhibitor, WYE-125132 (Yu et al., 2010), all demonstrated ideal antitumor capacity in RCC preclinically. The aforementioned findings provide new insights into the development of mTOR-targeted novel antitumor therapeutic strategies for RCC.

The classic pro-fibrosis TGF-β signaling pathway is another promising therapeutic target of RCC. Early in 2014, a phase I clinical study used the human TGF-β1/β2/β3 neutralizer GC1008 (fresolimumab) to treat patients with advanced malignant melanoma and RCC (Morris et al., 2014). However, only seven out of the total 29 patients achieved a partial response. Later, in 2017, another phase I study among advanced cancer patients using the TGF-β receptor 2 monoclonal antibody LY3022859 failed to determine the maximum tolerated dose due to adverse side effects (Tolcher et al., 2017). The difficulties in the clinical application of anti-TGF-β antibodies among cancer patients might be related to the dual functions of the diverse TGF-β-dependent downstream cascades (Meng et al., 2012a). Smad3, one of the key downstream transcription factors of TGF-β signaling, plays a major pathogenic role during renal fibrosis and inflammation. However, the activation of TGF-β-dependent Smad2 and Smad7 pathways demonstrates anti-fibrosis and renal protective effects (Meng et al., 2012b). Nevertheless, efforts have been continuously made to improve the therapeutic effects of TGF-β-targeted treatments. Strauss et al. (2018) led another phase I study using a novel bifunctional fusion protein M7824 against PD-L1 and TGF-β among patients with an advanced solid tumor, and this novel targeted agent demonstrated encouraging antitumor effects with a good safety profile (Strauss et al., 2018). Previously, Lian et al. (2018) used a Smad7 inducer asiatic acid (AA) in combination with a Smad3 inhibitor naringenin (NG) to restore the balance of Smad3 and Smad7 signaling pathways in invasive melanoma and lung cancer mouse models and achieved significant anticancer effects by enhancing natural killer (NK) cell-mediated cytotoxicity through attenuating Smad3-induced suppression on two

transcription factors essential for NK development and functions, namely, ID2 and IRF2. In addition, the same group discovered SIS3, a small-molecule inhibitor of Smad3, which effectively delays tumor development by suppressing TGF-β-mediated angiogenesis and immune escape in lung cancer (Tang et al., 2017; Lian et al., 2022). Although there is still very limited clinical evidence, preclinical studies have already revealed the promising anti-RCC potential of TGF-β signal-targeted therapies. A study using valproic acid, a Smad4 suppressor, significantly decreased cancer cell viability by inducing cell apoptosis and inhibiting EMT marker (E-cadherin and vimentin) expression in RCC cell lines (Mao et al., 2017). More recently, the anti-fibrotic drug pirfenidone (PFD), which has been approved by the FDA for the treatment of renal fibrosis, has been shown to be capable of suppressing RCC progression *in vivo* (Wang et al., 2022a). Mechanistically, PFD significantly downregulates TGF-β production in the RCC mouse model, thus mitigating TGF-β-mediated EMT and immunosuppressive MDSC infiltration into the TME.

6 Conclusion

Fibrosis has long been recognized as a major contributor to cancer progression and invasion. In this review, we systematically summarized the clinical association between renal fibrosis and poorer RCC outcomes and how a fibrotic microenvironment interacts with RCC in the form of ITF, CAFs, and PC fibrosis. In addition, we further conducted transcriptomic analysis on an up-to-date scRNA-seq profile of human RCC to confirm the participation of diverse fibrotic signaling in RCC development at single-cell resolution. The crosstalk between common pro-fibrotic pathways, including TGF-β, WNT, mTOR, and NOTCH signaling pathways, and RCC has also been discussed. In conclusion, the discovery of the mechanisms through which fibrotic signaling promotes tumorigenesis and aggressiveness in RCC provides inspiration for the development of anti-fibrotic therapies, such as mTOR inhibitors or anti-TGF-β antibodies, as novel therapeutic strategies for renal cancer.

Author contributions

J-YC conceived and designed the study, analyzed the scRNA-seq dataset, and coordinated this work. JY-C and W-HY collected and reviewed the literature and composed the draft. PT contributed to the draft and revision. J-YC and ST organized the manuscript. All authors contributed to data interpretation and manuscript editing.

Funding

This project was supported by the Research Grants Council of Hong Kong (General Research Fund 14111720, 17117923), Dr. Rita T. Liu SBS of L&T Charitable Foundation Ltd., and Bingei Family of Indo Café, Mr. Winston Leung, Mr. K.K. Chan, Ms. Siu Suet Lau, and Dr. Y.Y. Cheung and an endowment fund established at the University of Hong Kong for the Yu Professorship in Nephrology awarded to ST.

Conflict of interest

The authors declare that the research was conducted in the absence of any commercial or financial relationships that could be construed as a potential conflict of interest.

Publisher's note

References

Acerbi, I., Cassereau, L., Dean, I., Shi, Q., Au, A., Park, C., et al. (2015). Human breast cancer invasion and aggression correlates with ECM stiffening and immune cell infiltration. *Integr. Biol. (Camb)* 7, 1120–1134. doi:10.1039/c5ib00040h

Alaghehbandan, R., Perez Montiel, D., Luis, A. S., and Hes, O. (2019). Molecular genetics of renal cell tumors: A practical diagnostic approach. *Cancers (Basel)* 12, 85. doi:10.3390/cancers12010085

Alkasalias, T., Flaberg, E., Kashuba, V., Alexeyenko, A., Pavlova, T., Savchenko, A., et al. (2014). Inhibition of tumor cell proliferation and motility by fibroblasts is both contact and soluble factor dependent. *Proc. Natl. Acad. Sci.* 111, 17188–17193. doi:10.1073/pnas.1419554111

Altorki, N. K., Markowitz, G. J., Gao, D., Port, J. L., Saxena, A., Stiles, B., et al. (2019). The lung microenvironment: An important regulator of tumour growth and metastasis. *Nat. Rev. Cancer* 19, 9–31. doi:10.1038/s41568-018-0081-9

Ambrosetti, D., Coutts, M., Paoli, C., Durand, M., Borchiellini, D., Montemagno, C., et al. (2022). Cancer-associated fibroblasts in renal cell carcinoma: Implication in prognosis and resistance to anti-angiogenic therapy. *BJU Int.* 129, 80–92. doi:10.1111/bju.15506

Awakura, Y., Ito, N., Nakamura, E., Takahashi, T., Kotani, H., Mikami, Y., et al. (2006). Matrix metalloproteinase-9 polymorphisms and renal cell carcinoma in a Japanese population. *Cancer Lett.* 241, 59–63. doi:10.1016/j.canlet.2005.10.005

Baker, A. T., Abuwarwar, M. H., Poly, L., Wilkins, S., and Fletcher, A. L. (2021). Cancer-associated fibroblasts and T cells: From mechanisms to outcomes. *J. Immunol.* 206, 310–320. doi:10.4049/jimmunol.2001203

Ballester, B., Milara, J., and Cortijo, J. (2019). Idiopathic pulmonary fibrosis and lung cancer: Mechanisms and molecular targets. *Int. J. Mol. Sci.* 20, 593. doi:10.3390/ijms20030593

Barcellos-De-Souza, P., Comito, G., Pons-Segura, C., Taddei, M. L., Gori, V., Becherucci, V., et al. (2016). Mesenchymal stem cells are recruited and activated into carcinoma-associated fibroblasts by prostate cancer microenvironment-derived TGF-β1. *Stem Cells* 34, 2536–2547. doi:10.1002/stem.2412

Bartoschek, M., Oskolkov, N., Bocci, M., Lövrot, J., Larsson, C., Sommarin, M., et al. (2018). Spatially and functionally distinct subclasses of breast cancer-associated fibroblasts revealed by single cell RNA sequencing. *Nat. Commun.* 9, 5150. doi:10.1038/s41467-018-07582-3

Benny, S., Mishra, R., Manojkumar, M. K., and Aneesh, T. (2020). From Warburg effect to Reverse Warburg effect; the new horizons of anti-cancer therapy. *Med. Hypotheses* 144, 110216. doi:10.1016/j.mehy.2020.110216

Bianchi, M., Sun, M., Jeldres, C., Shariat, S. F., Trinh, Q. D., Briganti, A., et al. (2012). Distribution of metastatic sites in renal cell carcinoma: A population-based analysis. *Ann. Oncol.* 23, 973–980. doi:10.1093/annonc/mdr362

Biswas, T., Gu, X., Yang, J., Ellies, L. G., and Sun, L. Z. (2014). Attenuation of TGF-β signaling supports tumor progression of a mesenchymal-like mammary tumor cell line in a syngeneic murine model. *Cancer Lett.* 346, 129–138. doi:10.1016/j.canlet.2013.12.018

Bond, K. H., Chiba, T., Wynne, K. P. H., Vary, C. P. H., Sims-Lucas, S., Coburn, J. M., et al. (2021). The extracellular matrix environment of clear cell renal cell carcinoma

determines cancer associated fibroblast growth. *Cancers (Basel)* 13, 5873. doi:10.3390/cancers13235873

Boström, A.-K., Möller, C., Nilsson, E., Elfving, P., Axelson, H., and Johansson, M. E. (2012). Sarcomatoid conversion of clear cell renal cell carcinoma in relation to epithelial-to-mesenchymal transition. *Hum. Pathol.* 43, 708–719. doi:10.1016/j.humpath.2011.06.019

Boström, A. K., Lindgren, D., Johansson, M. E., and Axelson, H. (2013). Effects of TGF-β signaling in clear cell renal cell carcinoma cells. *Biochem. Biophys. Res. Commun.* 435, 126–133. doi:10.1016/j.bbrc.2013.04.054

Bruno, S., Collino, F., Deregibus, M. C., Grange, C., Tetta, C., and Camussi, G. (2013). Microvesicles derived from human bone marrow mesenchymal stem cells inhibit tumor growth. *Stem cells Dev.* 22, 758–771. doi:10.1089/scd.2012.0304

Chan, M. K., Chung, J. Y., Tang, P. C., Chan, A. S., Ho, J. Y., Lin, T. P., et al. (2022). TGF-β signaling networks in the tumor microenvironment. *Cancer Lett.* 550, 215925. doi:10.1016/j.canlet.2022.215925

Chandler, C., Liu, T., Buckanovich, R., and Coffman, L. G. (2019). The double edge sword of fibrosis in cancer. *Transl. Res.* 209, 55–67. doi:10.1016/j.trsl.2019.02.006

Chen, J., Huang, X. R., Yang, F., Yiu, W. H., Yu, X., Tang, S. C. W., et al. (2022). Single-cell RNA sequencing identified novel Nr4a1(+) Ear2(+) anti-inflammatory macrophage phenotype under myeloid-TLR4 dependent regulation in anti-glomerular basement membrane (GBM) crescentic glomerulonephritis (cGN). *Adv. Sci. (Weinh)* 9, e2200668. doi:10.1002/advs.202200668

Chen, S., Liu, W., Wang, K., Fan, Y., Chen, J., Ma, J., et al. (2017). Tetrandrine inhibits migration and invasion of human renal cell carcinoma by regulating Akt/NF-κB/MMP-9 signaling. *PLoS One* 12, e0173725. doi:10.1371/journal.pone.0173725

Chen, Z. Y., Du, Y., Wang, L., Liu, X. H., Guo, J., and Weng, X. D. (2018). MiR-543 promotes cell proliferation and metastasis of renal cell carcinoma by targeting Dickkopf 1 through the Wnt/β-catenin signaling pathway. *J. Cancer* 9, 3660–3668. doi:10.7150/jca.27124

Cheng, X., He, J., Gan, W., Fan, X., Yang, J., Zhu, B., et al. (2015). Pseudocapsule of renal cell carcinoma associated with Xp11.2 translocation/TFE3 gene fusion: A clue for tumor enucleation? *Int. J. Clin. Exp. Pathol.* 8, 5403–5410.

Cheville, J. C., Lohse, C. M., Zincke, H., Weaver, A. L., and Blute, M. L. (2003). Comparisons of outcome and prognostic features among histologic subtypes of renal cell carcinoma. *Am. J. Surg. Pathology* 27, 612–624. doi:10.1097/00000478-200305000-00005

Cho, H. J., Kim, S. J., Ha, U. S., Hong, S. H., Kim, J. C., Choi, Y. J., et al. (2009). Prognostic value of capsular invasion for localized clear-cell renal cell carcinoma. *Eur. Urol.* 56, 1006–1012. doi:10.1016/j.eururo.2008.11.031

Cho, S., Lee, J. H., Jeon, S. H., Park, J., Lee, S. H., Kim, C. H., et al. (2017). A prospective, multicenter analysis of pseudocapsule characteristics: Do all stages of renal cell carcinoma have complete pseudocapsules? *Urol. Oncol.* 35, 370–378. doi:10.1016/j.urolonc.2017.01.003

Chung, J. Y., Chan, M. K., Li, J. S., Chan, A. S., Tang, P. C., Leung, K. T., et al. (2021). TGF-B signaling: From tissue fibrosis to tumor microenvironment. *Int. J. Mol. Sci.* 22, 7575. doi:10.3390/ijms22147575

Coffman, L. G., Choi, Y. J., Mclean, K., Allen, B. L., Di Magliano, M. P., and Buckanovich, R. J. (2016). Human carcinoma-associated mesenchymal stem cells promote ovarian cancer chemotherapy resistance via a BMP4/HH signaling loop. *Oncotarget* 7, 6916–6932. doi:10.18632/oncotarget.6870

Costa, A., Kieffer, Y., Scholer-Dahirel, A., Pelon, F., Bourachot, B., Cardon, M., et al. (2018). Fibroblast heterogeneity and immunosuppressive environment in human breast cancer. *Cancer Cell* 33, 463–479. doi:10.1016/j.ccell.2018.01.011

Creighton, C. J., Morgan, M., Gunaratne, P. H., Wheeler, D. A., Gibbs, R. A., Gordon Robertson, A., et al. (2013). Comprehensive molecular characterization of clear cell renal cell carcinoma. *Nature* 499, 43–49. doi:10.1038/nature12222

Damayanti, N. P., Budka, J. A., Khella, H. W. Z., Ferris, M. W., Ku, S. Y., Kauffman, E., et al. (2018). Therapeutic targeting of TFE3/IRS-1/PI3K/mTOR Axis in translocation renal cell carcinoma. *Clin. Cancer Res.* 24, 5977–5989. doi:10.1158/1078-0432.CCR-18-0269

Daneshmandi, S., Wegiel, B., and Seth, P. (2019). Blockade of lactate dehydrogenase-A (LDH-A) improves efficacy of anti-programmed cell death-1 (PD-1) therapy in melanoma. *Cancers (Basel)* 11, 450. doi:10.3390/cancers11040450

Davis, C. F., Ricketts, C. J., Wang, M., Yang, L., Cherniack, A. D., Shen, H., et al. (2014). The somatic genomic landscape of chromophobe renal cell carcinoma. *Cancer Cell* 26, 319–330. doi:10.1016/j.ccr.2014.07.014

Dey, N., Ghosh-Choudhury, N., Kasinath, B. S., and Choudhury, G. G. (2012). TGFβ-stimulated microRNA-21 utilizes PTEN to orchestrate AKT/mTORC1 signaling for mesangial cell hypertrophy and matrix expansion. *PLoS One* 7, e42316. doi:10.1371/journal.pone.0042316

Dey, P., Son, J. Y., Kundu, A., Kim, K. S., Lee, Y., Yoon, K., et al. (2019). Knockdown of pyruvate kinase M2 inhibits cell proliferation, metabolism, and migration in renal cell carcinoma. *Int. J. Mol. Sci.* 20, 5622. doi:10.3390/ijms20225622

Dong, Y., Ma, W. M., Yang, W., Hao, L., Zhang, S. Q., Fang, K., et al. (2021). Identification of C3 and FN1 as potential biomarkers associated with progression and prognosis for clear cell renal cell carcinoma. *BMC Cancer* 21, 1135. doi:10.1186/s12885-021-08818-0

Edeling, M., Ragi, G., Huang, S., Pavenstädt, H., and Susztak, K. (2016). Developmental signalling pathways in renal fibrosis: The roles of notch, wnt and hedgehog. *Nat. Rev. Nephrol.* 12, 426–439. doi:10.1038/nrneph.2016.54

Eikrem, O. S., Strauss, P., Beisland, C., Scherer, A., Landolt, L., Flatberg, A., et al. (2016). Development and confirmation of potential gene classifiers of human clear cell renal cell carcinoma using next-generation RNA sequencing. *Scand. J. Urol.* 50, 452–462. doi:10.1080/21681805.2016.1238007

Erdogan, B., Ao, M., White, L. M., Means, A. L., Brewer, B. M., Yang, L., et al. (2017). Cancer-associated fibroblasts promote directional cancer cell migration by aligning fibronectin. *J. Cell Biol.* 216, 3799–3816. doi:10.1083/jcb.201704053

Feig, C., Jones, J. O., Kraman, M., Wells, R. J., Deonarine, A., Chan, D. S., et al. (2013). Targeting CXCL12 from FAP-expressing carcinoma-associated fibroblasts synergizes with anti-PD-L1 immunotherapy in pancreatic cancer. *Proc. Natl. Acad. Sci. U. S. A.* 110, 20212–20217. doi:10.1073/pnas.1320318110

Feldman, M. E., Apsel, B., Uotila, A., Loewith, R., Knight, Z. A., Ruggero, D., et al. (2009). Active-site inhibitors of mTOR target rapamycin-resistant outputs of mTORC1 and mTORC2. *PLoS Biol.* 7, e38. doi:10.1371/journal.pbio.1000038

Fendler, A., Bauer, D., Busch, J., Jung, K., Wulf-Goldenberg, A., Kunz, S., et al. (2020). Inhibiting WNT and NOTCH in renal cancer stem cells and the implications for human patients. *Nat. Commun.* 11, 929. doi:10.1038/s41467-020-14700-7

Ferlay, J., Soerjomataram, I., Dikshit, R., Eser, S., Mathers, C., Rebelo, M., et al. (2015). Cancer incidence and mortality worldwide: Sources, methods and major patterns in GLOBOCAN 2012. *Int. J. Cancer* 136, E359–E386. doi:10.1002/ijc.29210

Furge, K. A., Chen, J., Koeman, J., Swiatek, P., Dykema, K., Lucin, K., et al. (2007). Detection of DNA copy number changes and oncogenic signaling abnormalities from gene expression data reveals MYC activation in high-grade papillary renal cell carcinoma. *Cancer Res.* 67, 3171–3176. doi:10.1158/0008-5472.CAN-06-4571

Gilkes, D. M., Semenza, G. L., and Wirtz, D. (2014). Hypoxia and the extracellular matrix: Drivers of tumour metastasis. *Nat. Rev. Cancer* 14, 430–439. doi:10.1038/nrc3726

Givel, A.-M., Kieffer, Y., Scholer-Dahirel, A., Sirven, P., Cardon, M., Pelon, F., et al. (2018). miR200-regulated CXCL12β promotes fibroblast heterogeneity and immunosuppression in ovarian cancers. *Nat. Commun.* 9, 1056. doi:10.1038/s41467-018-03348-z

Gopal, S., Veracini, L., Grall, D., Butori, C., Schaub, S., Audebert, S., et al. (2017). Fibronectin-guided migration of carcinoma collectives. *Nat. Commun.* 8, 14105. doi:10.1038/ncomms14105

Guido, C., Whitaker-Menezes, D., Capparelli, C., Balliet, R., Lin, Z., Pestell, R. G., et al. (2012). Metabolic reprogramming of cancer-associated fibroblasts by TGF-β drives tumor growth: Connecting TGF-β signaling with "Warburg-like" cancer metabolism and L-lactate production. *Cell Cycle* 11, 3019–3035. doi:10.4161/cc.21384

Guo, C., Huang, T., Wang, Q.-H., Li, H., Khanal, A., Kang, E.-H., et al. (2019). Monocarboxylate transporter 1 and monocarboxylate transporter 4 in cancer-endothelial co-culturing microenvironments promote proliferation, migration, and invasion of renal cancer cells. *Cancer Cell Int.* 19, 170. doi:10.1186/s12935-019-0889-8

Hamanaka, R. B., and Mutlu, G. M. (2021). The role of metabolic reprogramming and de novo amino acid synthesis in collagen protein production by myofibroblasts: Implications for organ fibrosis and cancer. *Amino Acids* 53, 1851–1862. doi:10.1007/s00726-021-02996-8

Han, S. H., Wu, M. Y., Nam, B. Y., Park, J. T., Yoo, T. H., Kang, S. W., et al. (2017). PGC-1α protects from notch-induced kidney fibrosis development. *J. Am. Soc. Nephrol.* 28, 3312–3322. doi:10.1681/ASN.2017020130

Han, S., Khuri, F. R., and Roman, J. (2006). Fibronectin stimulates non-small cell lung carcinoma cell growth through activation of Akt/mammalian target of rapamycin/S6 kinase and inactivation of LKB1/AMP-activated protein kinase signal pathways. *Cancer Res.* 66, 315–323. doi:10.1158/0008-5472.CAN-05-2367

Han, S. W., and Roman, J. (2006). Fibronectin induces cell proliferation and inhibits apoptosis in human bronchial epithelial cells: Pro-oncogenic effects mediated by PI3-kinase and NF-kappa B. *Oncogene* 25, 4341–4349. doi:10.1038/sj.onc.1209460

Han, S., Yang, W., Qin, C., Du, Y., Ding, M., Yin, H., et al. (2022). Intratumoral fibrosis and patterns of immune infiltration in clear cell renal cell carcinoma. *BMC Cancer* 22, 661. doi:10.1186/s12885-022-09765-0

Hao, J., Zeltz, C., Pintilie, M., Li, Q., Sakashita, S., Wang, T., et al. (2019a). Characterization of distinct populations of carcinoma-associated fibroblasts from non-small cell lung carcinoma reveals a role for ST8SIA2 in cancer cell invasion. *Neoplasia* 21, 482–493. doi:10.1016/j.neo.2019.03.009

Hao, Y., Baker, D., and Ten Dijke, P. (2019b). TGF-β-Mediated epithelial-mesenchymal transition and cancer metastasis. *Int. J. Mol. Sci.* 20, 2767. doi:10.3390/ijms20112767

Hase, H., Jingushi, K., Ueda, Y., Kitae, K., Egawa, H., Ohshio, I., et al. (2014). LOXL2 status correlates with tumor stage and regulates integrin levels to promote tumor progression in ccRCC. *Mol. Cancer Res.* 12, 1807–1817. doi:10.1158/1541-7786.MCR-14-0233

He, W., Kang, Y. S., Dai, C., and Liu, Y. (2011). Blockade of Wnt/β-catenin signaling by paricalcitol ameliorates proteinuria and kidney injury. *J. Am. Soc. Nephrol.* 22, 90–103. doi:10.1681/ASN.2009121236

Howlader, N., Noone, A., Krapcho, M. E., Miller, D., Brest, A., Yu, M., et al. (2019).SEER cancer statistics review, 1. National Cancer Institute, 1975–2016.

Huang, S., Park, J., Qiu, C., Chung, K. W., Li, S. Y., Sirin, Y., et al. (2018). Jagged1/Notch2 controls kidney fibrosis via Tfam-mediated metabolic reprogramming. *PLoS Biol.* 16, e2005233. doi:10.1371/journal.pbio.2005233

Huang, S. Q., Zou, S. S., and Huang, Q. L. (1992). MR appearance of the pseudocapsule of renal cell carcinoma and its pathologic basis. *Urol. Radiol.* 13, 158–161.

Hudes, G., Carducci, M., Tomczak, P., Dutcher, J., Figlin, R., Kapoor, A., et al. (2007). Temsirolimus, interferon alfa, or both for advanced renal-cell carcinoma. *N. Engl. J. Med.* 356, 2271–2281. doi:10.1056/NEJMoa066838

Huffstater, T., Merryman, W. D., and Gewin, L. S. (2020). Wnt/β-Catenin in acute kidney injury and progression to chronic kidney disease. *Semin. Nephrol.* 40, 126–137. doi:10.1016/j.semnephrol.2020.01.004

Inoue, K. I., Kishimoto, S., Akimoto, K., Sakuma, M., Toyoda, S., Inoue, T., et al. (2019). Cancer-associated fibroblasts show heterogeneous gene expression and induce vascular endothelial growth factor A (VEGFA) in response to environmental stimuli. *Ann. Gastroenterol. Surg.* 3, 416–425. doi:10.1002/ags3.12249

Jiang, L., Xu, L., Mao, J., Li, J., Fang, L., Zhou, Y., et al. (2013). Rheb/mTORC1 signaling promotes kidney fibroblast activation and fibrosis. *J. Am. Soc. Nephrol.* 24, 1114–1126. doi:10.1681/ASN.2012050476

Joung, J. W., Oh, H. K., Lee, S. J., Kim, Y. A., and Jung, H. J. (2018). Significance of intratumoral fibrosis in clear cell renal cell carcinoma. *J. Pathol. Transl. Med.* 52, 323–330. doi:10.4132/jptm.2018.07.21

Kalluri, R. (2016). The biology and function of fibroblasts in cancer. *Nat. Rev. Cancer* 16, 582–598. doi:10.1038/nrc.2016.73

Karim, S., Al-Maghrabi, J. A., Farsi, H. M., Al-Sayyad, A. J., Schulten, H. J., Buhmeida, A., et al. (2016). Cyclin D1 as a therapeutic target of renal cell carcinoma-a combined transcriptomics, tissue microarray and molecular docking study from the Kingdom of Saudi Arabia. *BMC Cancer* 16, 741. doi:10.1186/s12885-016-2775-2

Kawakami, K., Hirata, H., Yamamura, S., Kikuno, N., Saini, S., Majid, S., et al. (2009). Functional significance of Wnt inhibitory factor-1 gene in kidney cancer. *Cancer Res.* 69, 8603–8610. doi:10.1158/0008-5472.CAN-09-2534

Kojima, Y., Acar, A., Eaton, E. N., Mellody, K. T., Scheel, C., Ben-Porath, I., et al. (2010). Autocrine TGF-beta and stromal cell-derived factor-1 (SDF-1) signaling drives the evolution of tumor-promoting mammary stromal myofibroblasts. *Proc. Natl. Acad. Sci. U. S. A.* 107, 20009–20014. doi:10.1073/pnas.1013805107

Kominsky, S. L., Doucet, M., Thorpe, M., and Weber, K. L. (2008). MMP-13 is over-expressed in renal cell carcinoma bone metastasis and is induced by TGF-beta1. *Clin. Exp. Metastasis* 25, 865–870. doi:10.1007/s10585-008-9202-2

Kondratov, A. G., Kvasha, S. M., Stoliar, L. A., Romanenko, A. M., Zgonnyk, Y. M., Gordiyuk, V. V., et al. (2012). Alterations of the WNT7A gene in clear cell renal cell carcinomas. *PLoS One* 7, e47012. doi:10.1371/journal.pone.0047012

Kruck, S., Eyrich, C., Scharpf, M., Sievert, K. D., Fend, F., Stenzl, A., et al. (2013). Impact of an altered Wnt1/β-catenin expression on clinicopathology and prognosis in clear cell renal cell carcinoma. *Int. J. Mol. Sci.* 14, 10944–10957. doi:10.3390/ijms140610944

Kubiczkova, L., Sedlarikova, L., Hajek, R., and Sevcikova, S. (2012). TGF-β - an excellent servant but a bad master. *J. Transl. Med.* 10, 183. doi:10.1186/1479-5876-10-183

Kuma, A., Yamada, S., Wang, K. Y., Kitamura, N., Yamaguchi, T., Iwai, Y., et al. (2014). Role of WNT10A-expressing kidney fibroblasts in acute interstitial nephritis. *PLoS One* 9, e103240. doi:10.1371/journal.pone.0103240

Leek, R. D., Lewis, C. E., Whitehouse, R., Greenall, M., Clarke, J., and Harris, A. L. (1996). Association of macrophage infiltration with angiogenesis and prognosis in invasive breast carcinoma. *Cancer Res.* 56, 4625–4629.

Li, B., Zhang, X., Ren, Q., Gao, L., and Tian, J. (2021). NVP-BEZ235 inhibits renal cell carcinoma by targeting TAK1 and PI3K/Akt/mTOR pathways. *Front. Pharmacol.* 12, 781623. doi:10.3389/fphar.2021.781623

Li, J., Ren, J., Liu, X., Jiang, L., He, W., Yuan, W., et al. (2015). Rictor/mTORC2 signaling mediates TGFβ1-induced fibroblast activation and kidney fibrosis. *Kidney Int.* 88, 515–527. doi:10.1038/ki.2015.119

Li, Y., Wei, Y., Tang, W., Luo, J., Wang, M., Lin, H., et al. (2019). Association between the degree of fibrosis in fibrotic focus and the unfavorable clinicopathological prognostic features of breast cancer. *PeerJ* 7, e8067. doi:10.7717/peerj.8067

Lian, G. Y., Wan, Y., Mak, T. S., Wang, Q. M., Zhang, J., Chen, J., et al. (2022). Self-carried nanodrug (SCND-SIS3): A targeted therapy for lung cancer with superior biocompatibility and immune boosting effects. *Biomaterials* 288, 121730. doi:10.1016/j.biomaterials.2022.121730

Lian, G. Y., Wang, Q. M., Tang, P. M., Zhou, S., Huang, X. R., and Lan, H. Y. (2018). Combination of asiatic acid and Naringenin modulates NK cell anti-cancer immunity by rebalancing smad3/smad7 signaling. *Mol. Ther.* 26, 2255–2266. doi:10.1016/j.ymthe.2018.06.016

Lin, P. H., Huang, C. Y., Yu, K. J., Kan, H. C., Liu, C. Y., Chuang, C. K., et al. (2021). Genomic characterization of clear cell renal cell carcinoma using targeted gene sequencing. *Oncol. Lett.* 21, 169. doi:10.3892/ol.2021.12430

Lin, S., Zheng, L., Lu, Y., Xia, Q., Zhou, P., and Liu, Z. (2020). Comprehensive analysis on the expression levels and prognostic values of LOX family genes in kidney renal clear cell carcinoma. *Cancer Med.* 9, 8624–8638. doi:10.1002/cam4.3472

Lin, Y., Cai, Q., Chen, Y., Shi, T., Liu, W., Mao, L., et al. (2022). CAFs shape myeloid-derived suppressor cells to promote stemness of intrahepatic cholangiocarcinoma through 5-lipoxygenase. *Hepatology* 75, 28–42. doi:10.1002/hep.32099

Linehan, W. M., Spellman, P. T., Ricketts, C. J., Creighton, C. J., Fei, S. S., Davis, C., et al. (2016). Comprehensive molecular characterization of papillary renal-cell carcinoma. *N. Engl. J. Med.* 374, 135–145. doi:10.1056/NEJMoa1505917

Liu, B., Chen, X., Zhan, Y., Wu, B., and Pan, S. (2020). Identification of a gene signature for renal cell carcinoma-associated fibroblasts mediating cancer progression and affecting prognosis. *Front. Cell Dev. Biol.* 8, 604627. doi:10.3389/fcell.2020.604627

Liu, B., Chen, X., Zhan, Y., Wu, B., and Pan, S. (2021). Identification of a gene signature for renal cell carcinoma–associated fibroblasts mediating cancer progression and affecting prognosis. *Front. Cell Dev. Biol.* 8, 604627. doi:10.3389/fcell.2020.604627

Liu, T., Zhou, L., Li, D., Andl, T., and Zhang, Y. (2019). Cancer-associated fibroblasts build and secure the tumor microenvironment. *Front. Cell Dev. Biol.* 7, 60. doi:10.3389/fcell.2019.00060

Lopez-Beltran, A., Scarpelli, M., Montironi, R., and Kirkali, Z. (2006). 2004 WHO classification of the renal tumors of the adults. *Eur. Urol.* 49, 798–805. doi:10.1016/j.eururo.2005.11.035

López-Lago, M. A., Thodima, V. J., Guttapalli, A., Chan, T., Heguy, A., Molina, A. M., et al. (2010). Genomic deregulation during metastasis of renal cell carcinoma implements a myofibroblast-like program of gene expression. *Cancer Res.* 70, 9682–9692. doi:10.1158/0008-5472.CAN-10-2279

Maisonneuve, P., Marshall, B. C., Knapp, E. A., and Lowenfels, A. B. (2013). Cancer risk in cystic fibrosis: A 20-year nationwide study from the United States. *J. Natl. Cancer Inst.* 105, 122–129. doi:10.1093/jnci/djs481

Maity, S., Das, F., Kasinath, B. S., Ghosh-Choudhury, N., and Ghosh Choudhury, G. (2020). TGFβ acts through PDGFRβ to activate mTORC1 via the Akt/PRAS40 axis and causes glomerular mesangial cell hypertrophy and matrix protein expression. *J. Biol. Chem.* 295, 14262–14278. doi:10.1074/jbc.RA120.014994

Majo, S., Courtois, S., Souleyreau, W., Bikfalvi, A., and Auguste, P. (2020). Impact of extracellular matrix components to renal cell carcinoma behavior. *Front. Oncol.* 10, 625. doi:10.3389/fonc.2020.00625

Malouf, G. G., Su, X., Yao, H., Gao, J., Xiong, L., He, Q., et al. (2014). Next-generation sequencing of translocation renal cell carcinoma reveals novel RNA splicing partners and frequent mutations of chromatin-remodeling genes. *Clin. Cancer Res.* 20, 4129–4140. doi:10.1158/1078-0432.CCR-13-3036

Mao, S., Lu, G., Lan, X., Yuan, C., Jiang, W., Chen, Y., et al. (2017). Valproic acid inhibits epithelial-mesenchymal transition in renal cell carcinoma by decreasing SMAD4 expression. *Mol. Med. Rep.* 16, 6190–6199. doi:10.3892/mmr.2017.7394

Martinez-Outschoorn, U. E., Lisanti, M. P., and Sotgia, F. (2014). Catabolic cancer-associated fibroblasts transfer energy and biomass to anabolic cancer cells, fueling tumor growth. *Semin. Cancer Biol.* 25, 47–60. doi:10.1016/j.semcancer.2014.01.005

Massagué, J. (2008). TGFbeta in cancer. *Cell* 134, 215–230. doi:10.1016/j.cell.2008.07.001

Meng, X.-M., Nikolic-Paterson, D. J., and Lan, H. Y. (2016). TGF-B: The master regulator of fibrosis. *Nat. Rev. Nephrol.* 12, 325–338. doi:10.1038/nrneph.2016.48

Meng, X. M., Huang, X. R., Xiao, J., Chen, H. Y., Zhong, X., Chung, A. C., et al. (2012a). Diverse roles of TGF-β receptor II in renal fibrosis and inflammation *in vivo* and *in vitro*. *J. Pathol.* 227, 175–188. doi:10.1002/path.3976

Meng, X. M., Huang, X. R., Xiao, J., Chung, A. C., Qin, W., Chen, H. Y., et al. (2012b). Disruption of Smad4 impairs TGF-β/Smad3 and Smad7 transcriptional regulation during renal inflammation and fibrosis *in vivo* and *in vitro*. *Kidney Int.* 81, 266–279. doi:10.1038/ki.2011.327

Meng, X. M., Tang, P. M., Li, J., and Lan, H. Y. (2015). TGF-β/Smad signaling in renal fibrosis. *Front. Physiol.* 6, 82. doi:10.3389/fphys.2015.00082

Minervini, A., Rosaria Raspollini, M., Tuccio, A., Di Cristofano, C., Siena, G., Salvi, M., et al. (2014). Pathological characteristics and prognostic effect of peritumoral capsule penetration in renal cell carcinoma after tumor enucleation. *Urol. Oncol.* 32, 50.e15–e22. doi:10.1016/j.urolonc.2013.07.018

Miranda-Gonçalves, V., Lameirinhas, A., Macedo-Silva, C., Lobo, J., Dias, P, C., Ferreira, V., et al. (2020). Lactate increases renal cell carcinoma aggressiveness through sirtuin 1-dependent epithelial mesenchymal transition Axis regulation. *Cells* 9, 1053. doi:10.3390/cells9041053

Moch, H., Cubilla, A. L., Humphrey, P. A., Reuter, V. E., and Ulbright, T. M. (2016). The 2016 WHO classification of tumours of the urinary system and male genital organs-Part A: Renal, penile, and testicular tumours. *Eur. Urol.* 70, 93–105. doi:10.1016/j.eururo.2016.02.029

Morris, J. C., Tan, A. R., Olencki, T. E., Shapiro, G. I., Dezube, B. J., Reiss, M., et al. (2014). Phase I study of GC1008 (fresolimumab): A human anti-transforming growth factor-beta (TGFβ) monoclonal antibody in patients with advanced malignant melanoma or renal cell carcinoma. *PLoS One* 9, e90353. doi:10.1371/journal.pone.0090353

Motzer, R. J., Escudier, B., Oudard, S., Hutson, T. E., Porta, C., Bracarda, S., et al. (2008). Efficacy of everolimus in advanced renal cell carcinoma: A double-blind, randomised, placebo-controlled phase III trial. *Lancet* 372, 449–456. doi:10.1016/S0140-6736(08)61039-9

Nazemalhosseini-Mojarad, E., Mohammadpour, S., Torshizi Esafahani, A., Gharib, E., Larki, P., Moradi, A., et al. (2019). Intratumoral infiltrating lymphocytes correlate with improved survival in colorectal cancer patients: Independent of oncogenetic features. *J. Cell Physiol.* 234, 4768–4777. doi:10.1002/jcp.27273

Neglia, J. P., Fitzsimmons, S. C., Maisonneuve, P., Schöni, M. H., Schöni-Affolter, F., Corey, M., et al. (1995). The risk of cancer among patients with cystic fibrosis. Cystic Fibrosis and Cancer Study Group. *N. Engl. J. Med.* 332, 494–499. doi:10.1056/NEJM199502233320803

Orimo, A., Gupta, P. B., Sgroi, D. C., Arenzana-Seisdedos, F., Delaunay, T., Naeem, R., et al. (2005). Stromal fibroblasts present in invasive human breast carcinomas promote tumor growth and angiogenesis through elevated SDF-1/CXCL12 secretion. *Cell* 121, 335–348. doi:10.1016/j.cell.2005.02.034

Ou, Y. C., Li, J. R., Wang, J. D., Chang, C. Y., Wu, C. C., Chen, W. Y., et al. (2019). Fibronectin promotes cell growth and migration in human renal cell carcinoma cells. *Int. J. Mol. Sci.* 20, 2792. doi:10.3390/ijms20112792

Pan, J., Mestas, J., Burdick, M. D., Phillips, R. J., Thomas, G. V., Reckamp, K., et al. (2006). Stromal derived factor-1 (SDF-1/CXCL12) and CXCR4 in renal cell carcinoma metastasis. *Mol. Cancer* 5, 56. doi:10.1186/1476-4598-5-56

Pantuck, A. J., Seligson, D. B., Klatte, T., Yu, H., Leppert, J. T., Moore, L., et al. (2007). Prognostic relevance of the mTOR pathway in renal cell carcinoma: Implications for molecular patient selection for targeted therapy. *Cancer* 109, 2257–2267. doi:10.1002/cncr.22677

Pavlides, S., Whitaker-Menezes, D., Castello-Cros, R., Flomenberg, N., Witkiewicz, A. K., Frank, P. G., et al. (2009). The reverse Warburg effect: Aerobic glycolysis in cancer associated fibroblasts and the tumor stroma. *Cell Cycle* 8, 3984–4001. doi:10.4161/cc.8.23.10238

Petersen, O. W., Nielsen, H. L., Gudjonsson, T., Villadsen, R., Rank, F., Niebuhr, E., et al. (2003). Epithelial to mesenchymal transition in human breast cancer can provide a nonmalignant stroma. *Am. J. Pathol.* 162, 391–402. doi:10.1016/S0002-9440(10)63834-5

Piersma, B., Hayward, M. K., and Weaver, V. M. (2020). Fibrosis and cancer: A strained relationship. *Biochim. Biophys. Acta Rev. Cancer* 1873, 188356. doi:10.1016/j.bbcan.2020.188356

Piotrowska, Ż., Niezgoda, M., Młynarczyk, G., Acewicz, M., and Kasacka, I. (2020). Comparative assessment of the WNT/β-Catenin pathway, CacyBP/SIP, and the immunoproteasome subunit LMP7 in various histological types of renal cell carcinoma. *Front. Oncol.* 10, 566637. doi:10.3389/fonc.2020.566637

Powles, T., Wheater, M., Din, O., Geldart, T., Boleti, E., Stockdale, A., et al. (2016). A randomised phase 2 study of AZD2014 versus everolimus in patients with VEGF-refractory metastatic clear cell renal cancer. *Eur. Urol.* 69, 450–456. doi:10.1016/j.eururo.2015.08.035

Qi, J. J., Liu, Y. X., and Lin, L. (2017). High expression of long non-coding RNA ATB is associated with poor prognosis in patients with renal cell carcinoma. *Eur. Rev. Med. Pharmacol. Sci.* 21, 2835–2839.

Qin, C., Yin, H., Liu, H., Liu, F., Du, Y., and Xu, T. (2020). The significance of fibrosis quantification as a marker in assessing pseudo-capsule status and clear cell renal cell carcinoma prognosis. *Diagn. (Basel)* 10, 895. doi:10.3390/diagnostics10110895

Qu, Y. Y., Zhao, R., Zhang, H. L., Zhou, Q., Xu, F. J., Zhang, X., et al. (2020). Inactivation of the AMPK-GATA3-ECHS1 pathway induces fatty acid synthesis that promotes clear cell renal cell carcinoma growth. *Cancer Res.* 80, 319–333. doi:10.1158/0008-5472.CAN-19-1023

Rasti, A., Madjd, Z., Saeednejad Zanjani, L., Babashah, S., Abolhasani, M., Asgari, M., et al. (2021). SMAD4 expression in renal cell carcinomas correlates with a stem-cell phenotype and poor clinical outcomes. *Front. Oncol.* 11, 581172. doi:10.3389/fonc.2021.581172

Razorenova, O. V., Finger, E. C., Colavitti, R., Chernikova, S. B., Boiko, A. D., Chan, C. K. F., et al. (2011). VHL loss in renal cell carcinoma leads to up-regulation of CUB domain-containing protein 1 to stimulate PKCδ-driven migration. *Proc. Natl. Acad. Sci.* 108, 1931–1936. doi:10.1073/pnas.1011777108

Ren, J., Li, J., Feng, Y., Shu, B., Gui, Y., Wei, W., et al. (2017). Rictor/mammalian target of rapamycin complex 2 promotes macrophage activation and kidney fibrosis. *J. Pathol.* 242, 488–499. doi:10.1002/path.4921

Roulin, D., Waselle, L., Dormond-Meuwly, A., Dufour, M., Demartines, N., and Dormond, O. (2011). Targeting renal cell carcinoma with NVP-BEZ235, a dual PI3K/mTOR inhibitor, in combination with sorafenib. *Mol. Cancer* 10, 90. doi:10.1186/1476-4598-10-90

Sengupta, S., Lohse, C. M., Leibovich, B. C., Frank, I., Thompson, R. H., Webster, W. S., et al. (2005). Histologic coagulative tumor necrosis as a prognostic indicator of renal cell carcinoma aggressiveness. *Cancer* 104, 511–520. doi:10.1002/cncr.21206

Shen, C., and Kaelin, W. G., Jr. (2013). The VHL/HIF axis in clear cell renal carcinoma. *Semin. Cancer Biol.* 23, 18–25. doi:10.1016/j.semcancer.2012.06.001

Shi, T., Morishita, A., Kobara, H., and Masaki, T. (2021). The role of long non-coding RNA and microRNA networks in hepatocellular carcinoma and its tumor microenvironment. *Int. J. Mol. Sci.* 22, 10630. doi:10.3390/ijms221910630

Siegel, R. L., Miller, K. D., Fuchs, H. E., and Jemal, A. (2021). Cancer Statistics, 2021. *CA Cancer J. Clin.* 71 (1), 7–33. doi:10.3322/caac.21654

Singer, K., Kastenberger, M., Gottfried, E., Hammerschmied, C. G., Büttner, M., Aigner, M., et al. (2011). Warburg phenotype in renal cell carcinoma: High expression of glucose-transporter 1 (GLUT-1) correlates with low CD8(+) T-cell infiltration in the tumor. *Int. J. Cancer* 128, 2085–2095. doi:10.1002/ijc.25543

Sinn, M., Denkert, C., Striefler, J. K., Pelzer, U., Stieler, J. M., Bahra, M., et al. (2014). α-Smooth muscle actin expression and desmoplastic stromal reaction in pancreatic cancer: Results from the CONKO-001 study. *Br. J. Cancer* 111, 1917–1923. doi:10.1038/bjc.2014.495

Sjölund, J., Boström, A. K., Lindgren, D., Manna, S., Moustakas, A., Ljungberg, B., et al. (2011). The notch and TGF-β signaling pathways contribute to the aggressiveness of clear cell renal cell carcinoma. *PLoS One* 6, e23057. doi:10.1371/journal.pone.0023057

Solinas, C., Carbognin, L., De Silva, P., Criscitiello, C., and Lambertini, M. (2017). Tumor-infiltrating lymphocytes in breast cancer according to tumor subtype: Current state of the art. *Breast* 35, 142–150. doi:10.1016/j.breast.2017.07.005

Song, C., Xiong, Y., Liao, W., Meng, L., and Yang, S. (2019). Long noncoding RNA ATB participates in the development of renal cell carcinoma by downregulating p53 via binding to DNMT1. *J. Cell Physiol.* 234, 12910–12917. doi:10.1002/jcp.27957

Song, J. (2007). EMT or apoptosis: A decision for TGF-beta. *Cell Res.* 17, 289–290. doi:10.1038/cr.2007.25

Steffens, S., Schrader, A. J., Vetter, G., Eggers, H., Blasig, H., Becker, J., et al. (2012). Fibronectin 1 protein expression in clear cell renal cell carcinoma. *Oncol. Lett.* 3, 787–790. doi:10.3892/ol.2012.566

Strauss, J., Heery, C. R., Schlom, J., Madan, R. A., Cao, L., Kang, Z., et al. (2018). Phase I trial of M7824 (MSB0011359C), a bifunctional fusion protein targeting PD-L1 and TGFβ, in advanced solid tumors. *Clin. Cancer Res.* 24, 1287–1295. doi:10.1158/1078-0432.CCR-17-2653

Sun, Z., Tao, W., Guo, X., Jing, C., Zhang, M., Wang, Z., et al. (2022). Construction of a lactate-related prognostic signature for predicting prognosis, tumor microenvironment, and immune response in kidney renal clear cell carcinoma. *Front. Immunol.* 13, 818984. doi:10.3389/fimmu.2022.818984

Tamimi, Y., Ekuere, U., Laughton, N., and Grundy, P. (2008). WNT5A is regulated by PAX2 and may be involved in blastemal predominant Wilms tumorigenesis. *Neoplasia* 10, 1470–1480. doi:10.1593/neo.08442

Tan, R. J., Zhou, D., Zhou, L., and Liu, Y. (2014). Wnt/β-catenin signaling and kidney fibrosis. *Kidney Int. Suppl.* 4 (4), 84–90. doi:10.1038/kisup.2014.16

Tang, P. C., Chung, J. Y., Liao, J., Chan, M. K., Chan, A. S., Cheng, G., et al. (2022). Single-cell RNA sequencing uncovers a neuron-like macrophage subset associated with cancer pain. *Sci. Adv.* 8, eabn5535. eabn5535. doi:10.1126/sciadv.abn5535

Tang, P. M.-K., Zhou, S., Meng, X.-M., Wang, Q.-M., Li, C.-J., Lian, G.-Y., et al. (2017). Smad3 promotes cancer progression by inhibiting E4BP4-mediated NK cell development. *Nat. Commun.* 8, 14677. doi:10.1038/ncomms14677

Tang, P. M., Zhou, S., Li, C. J., Liao, J., Xiao, J., Wang, Q. M., et al. (2018). The proto-oncogene tyrosine protein kinase Src is essential for macrophage-myofibroblast transition during renal scarring. *Kidney Int.* 93, 173–187. doi:10.1016/j.kint.2017.07.026

Tao, R., Niu, W. B., Dou, P. H., Ni, S. B., Yu, Y. P., Cai, L. C., et al. (2020). Nucleobindin-2 enhances the epithelial-mesenchymal transition in renal cell carcinoma. *Oncol. Lett.* 19, 3653–3664. doi:10.3892/ol.2020.11526

Tolcher, A. W., Berlin, J. D., Cosaert, J., Kauh, J., Chan, E., Piha-Paul, S. A., et al. (2017). A phase 1 study of anti-TGFβ receptor type-II monoclonal antibody LY3022859 in patients with advanced solid tumors. *Cancer Chemother. Pharmacol.* 79, 673–680. doi:10.1007/s00280-017-3245-5

Trabold, O., Wagner, S., Wicke, C., Scheuenstuhl, H., Hussain, M. Z., Rosen, N., et al. (2003). Lactate and oxygen constitute a fundamental regulatory mechanism in wound healing. *Wound Repair Regen.* 11, 504–509. doi:10.1046/j.1524-475x.2003.11621.x

Tretbar, S., Krausbeck, P., Müller, A., Friedrich, M., Vaxevanis, C., Bukur, J., et al. (2019). TGF-β inducible epithelial-to-mesenchymal transition in renal cell carcinoma. *Oncotarget* 10, 1507–1524. doi:10.18632/oncotarget.26682

Tsili, A. C., Argyropoulou, M. I., Gousia, A., Kalef-Ezra, J., Sofikitis, N., Malamou-Mitsi, V., et al. (2012). Renal cell carcinoma: Value of multiphase MDCT with multiplanar reformations in the detection of pseudocapsule. *AJR Am. J. Roentgenol.* 199, 379–386. doi:10.2214/AJR.11.7747

Ueno, H., Jones, A. M., Wilkinson, K. H., Jass, J. R., and Talbot, I. C. (2004). Histological categorisation of fibrotic cancer stroma in advanced rectal cancer. *Gut* 53, 581–586. doi:10.1136/gut.2003.028365

Ueno, K., Hirata, H., Majid, S., Tabatabai, Z. L., Hinoda, Y., and Dahiya, R. (2011). IGFBP-4 activates the Wnt/beta-catenin signaling pathway and induces M-CAM

expression in human renal cell carcinoma. *Int. J. Cancer* 129, 2360–2369. doi:10.1002/ijc.25899

Urakami, S., Shiina, H., Enokida, H., Hirata, H., Kawamoto, K., Kawakami, T., et al. (2006). Wnt antagonist family genes as biomarkers for diagnosis, staging, and prognosis of renal cell carcinoma using tumor and serum DNA. *Clin. Cancer Res.* 12, 6989–6997. doi:10.1158/1078-0432.CCR-06-1194

Wach, S., Taubert, H., Weigelt, K., Hase, N., Köhn, M., Misiak, D., et al. (2019). RNA sequencing of collecting duct renal cell carcinoma suggests an interaction between miRNA and target genes and a predominance of deregulated solute carrier genes. *Cancers (Basel)* 12, 64. doi:10.3390/cancers12010064

Wang, G., Zhou, X., Guo, Z., Huang, N., Li, J., Lv, Y., et al. (2022a). The Anti-fibrosis drug Pirfenidone modifies the immunosuppressive tumor microenvironment and prevents the progression of renal cell carcinoma by inhibiting tumor autocrine TGF-β. *Cancer Biol. Ther.* 23, 150–162. doi:10.1080/15384047.2022.2035629

Wang, J., Zhang, L., Luo, L., He, P., Xiong, A., Jiang, M., et al. (2022b). Characterizing cellular heterogeneity in fibrotic hypersensitivity pneumonitis by single-cell transcriptional analysis. *Cell Death Discov.* 8, 38. doi:10.1038/s41420-022-00831-x

Wang, P., Chen, W., Ma, T., Lin, Z., Liu, C., Liu, Y., et al. (2020). lncRNA lnc-TSI inhibits metastasis of clear cell renal cell carcinoma by suppressing TGF-β-induced epithelial-mesenchymal transition. *Mol. Ther. Nucleic Acids* 22, 1–16. doi:10.1016/j.omtn.2020.08.003

Wang, P., Zhang, L. D., Sun, M. C., Gu, W. D., and Geng, H. Z. (2018). Over-expression of mir-124 inhibits MMP-9 expression and decreases invasion of renal cell carcinoma cells. *Eur. Rev. Med. Pharmacol. Sci.* 22, 6308–6314. doi:10.26355/eurrev_201810_16041

Wang, Y., Lan, W., Xu, M., Song, J., Mao, J., Li, C., et al. (2021). Cancer-associated fibroblast-derived SDF-1 induces epithelial-mesenchymal transition of lung adenocarcinoma via CXCR4/β-catenin/PPARδ signalling. *Cell Death Dis.* 12, 214. doi:10.1038/s41419-021-03509-x

Warburg, O. H. (1925). The metabolism of carcinoma cells. *J. Cancer Res.* 9, 148–163. doi:10.1158/jcr.1925.148

Wu, F., Yang, J., Liu, J., Wang, Y., Mu, J., Zeng, Q., et al. (2021a). Signaling pathways in cancer-associated fibroblasts and targeted therapy for cancer. *Signal Transduct. Target Ther.* 6, 218. doi:10.1038/s41392-021-00641-0

Wu, H., He, D., Biswas, S., Shafiquzzaman, M., Zhou, X., Charron, J., et al. (2021b). mTOR activation initiates renal cell carcinoma development by coordinating ERK and p38MAPK. *Cancer Res.* 81, 3174–3186. doi:10.1158/0008-5472.CAN-20-3979

Wunderlich, H., Steiner, T., Kosmehl, H., Junker, U., Reinhold, D., Reichelt, O., et al. (1998). Increased transforming growth factor beta1 plasma level in patients with renal cell carcinoma: A tumor-specific marker? *Urol. Int.* 60, 205–207. doi:10.1159/000030255

Xi, W., Wang, J., Liu, L., Xiong, Y., Qu, Y., Lin, Z., et al. (2018). Evaluation of tumor pseudocapsule status and its prognostic significance in renal cell carcinoma. *J. Urol.* 199, 915–920. doi:10.1016/j.juro.2017.10.043

Xiong, J., Liu, Y., Jiang, L., Zeng, Y., and Tang, W. (2016). High expression of long non-coding RNA lncRNA-ATB is correlated with metastases and promotes cell migration and invasion in renal cell carcinoma. *Jpn. J. Clin. Oncol.* 46, 378–384. doi:10.1093/jjco/hyv214

Xiong, Z., Yu, H., Ding, Y., Feng, C., Wei, H., Tao, S., et al. (2014). RNA sequencing reveals upregulation of RUNX1-runx1t1 gene signatures in clear cell renal cell carcinoma. *BioMed Res. Int.* 2014, 450621. doi:10.1155/2014/450621

Xu, C., Zhang, K., Yang, F., Zhou, X., Liu, S., Li, Y., et al. (2021). CD248+ cancer-associated fibroblasts: A novel prognostic and therapeutic target for renal cell carcinoma. *Front. Oncol.* 11, 773063. doi:10.3389/fonc.2021.773063

Xu, J., Sadahira, T., Kinoshita, R., Li, S. A., Huang, P., Wada, K., et al. (2017). Exogenous DKK-3/REIC inhibits Wnt/β-catenin signaling and cell proliferation in human kidney cancer KPK1. *Oncol. Lett.* 14, 5638–5642. doi:10.3892/ol.2017.6833

Xu, Q., Krause, M., Samoylenko, A., and Vainio, S. (2016). Wnt signaling in renal cell carcinoma. *Cancers (Basel)* 8, 57. doi:10.3390/cancers8060057

Xu, X., Zheng, L., Yuan, Q., Zhen, G., Crane, J. L., Zhou, X., et al. (2018). Transforming growth factor-β in stem cells and tissue homeostasis. *Bone Res.* 6, 2. doi:10.1038/s41413-017-0005-4

Xue, V. W., Chung, J. Y., Córdoba, C. a. G., Cheung, A. H., Kang, W., Lam, E. W., et al. (2020). Transforming growth factor-β: A multifunctional regulator of cancer immunity. *Cancers (Basel)* 12, 3099. doi:10.3390/cancers12113099

Yamashita, Y., Honda, S., Nishiharu, T., Urata, J., and Takahashi, M. (1996). Detection of pseudocapsule of renal cell carcinoma with MR imaging and CT. *AJR Am. J. Roentgenol.* 166, 1151–1155. doi:10.2214/ajr.166.5.8615260

Yamauchi, M., Barker, T. H., Gibbons, D. L., and Kurie, J. M. (2018). The fibrotic tumor stroma. *J. Clin. Invest.* 128, 16–25. doi:10.1172/JCI93554

Yang, D., He, Y., Wu, B., Deng, Y., Li, M., Yang, Q., et al. (2020). Drinking water and sanitation conditions are associated with the risk of malaria among children under five years old in sub-saharan africa: A logistic regression model analysis of national survey data. *J. Adv. Res.* 21, 1–13. doi:10.1016/j.jare.2019.09.001

Yang, J., Lu, Y., Lin, Y. Y., Zheng, Z. Y., Fang, J. H., He, S., et al. (2016a). Vascular mimicry formation is promoted by paracrine TGF-β and SDF1 of cancer-associated fibroblasts and inhibited by miR-101 in hepatocellular carcinoma. *Cancer Lett.* 383, 18–27. doi:10.1016/j.canlet.2016.09.012

Yang, W., Qin, C., Han, J., Han, S., Bai, W., Du, Y., et al. (2021). What mediates fibrosis in the tumor microenvironment of clear renal cell carcinoma. *Front. Genet.* 12, 725252. doi:10.3389/fgene.2021.725252

Yang, X., Lin, Y., Shi, Y., Li, B., Liu, W., Yin, W., et al. (2016b). FAP promotes immunosuppression by cancer-associated fibroblasts in the tumor microenvironment via STAT3-CCL2 signaling. *Cancer Res.* 76, 4124–4135. doi:10.1158/0008-5472.CAN-15-2973

Yeon, J. H., Jeong, H. E., Seo, H., Cho, S., Kim, K., Na, D., et al. (2018). Cancer-derived exosomes trigger endothelial to mesenchymal transition followed by the induction of cancer-associated fibroblasts. *Acta Biomater.* 76, 146–153. doi:10.1016/j.actbio.2018.07.001

Young, M. D., Mitchell, T. J., Vieira Braga, F. A., Tran, M. G. B., Stewart, B. J., Ferdinand, J. R., et al. (2018). Single-cell transcriptomes from human kidneys reveal the cellular identity of renal tumors. *Science* 361, 594–599. doi:10.1126/science.aat1699

Yu, K., Shi, C., Toral-Barza, L., Lucas, J., Shor, B., Kim, J. E., et al. (2010). Beyond rapalog therapy: Preclinical pharmacology and antitumor activity of WYE-125132, an ATP-competitive and specific inhibitor of mTORC1 and mTORC2. *Cancer Res.* 70, 621–631. doi:10.1158/0008-5472.CAN-09-2340

Yuan, J.-H., Yang, F., Wang, F., Ma, J.-Z., Guo, Y.-J., Tao, Q.-F., et al. (2014). A long noncoding RNA activated by TGF-β promotes the invasion-metastasis cascade in hepatocellular carcinoma. *Cancer Cell* 25, 666–681. doi:10.1016/j.ccr.2014.03.010

Zhang, H. M., Yang, F. Q., Yan, Y., Che, J. P., and Zheng, J. H. (2014). High expression of long non-coding RNA SPRY4-IT1 predicts poor prognosis of clear cell renal cell carcinoma. *Int. J. Clin. Exp. Pathol.* 7, 5801–5809.

Zhao, H., Ljungberg, B., Grankvist, K., Rasmuson, T., Tibshirani, R., and Brooks, J. D. (2006). Gene expression profiling predicts survival in conventional renal cell carcinoma. *PLoS Med.* 3, e13. doi:10.1371/journal.pmed.0030013

Zheng, B., Mao, J. H., Qian, L., Zhu, H., Gu, D. H., Pan, X. D., et al. (2015). Pre-clinical evaluation of AZD-2014, a novel mTORC1/2 dual inhibitor, against renal cell carcinoma. *Cancer Lett.* 357, 468–475. doi:10.1016/j.canlet.2014.11.012

Zhou, D., Fu, H., Zhang, L., Zhang, K., Min, Y., Xiao, L., et al. (2017). Tubule-derived wnts are required for fibroblast activation and kidney fibrosis. *J. Am. Soc. Nephrol.* 28, 2322–2336. doi:10.1681/ASN.2016080902

Ziani, L., Chouaib, S., and Thiery, J. (2018). Alteration of the antitumor immune response by cancer-associated fibroblasts. *Front. Immunol.* 9, 414. doi:10.3389/fimmu.2018.00414

frontiers | Frontiers in Cell and Developmental Biology

TYPE Mini Review
PUBLISHED 26 October 2023
DOI 10.3389/fcell.2023.1261749

OPEN ACCESS

EDITED BY
Yu Zhao,
Capital Medical University, China

REVIEWED BY
Yanruide Li,
University of California, Los Angeles, United States

*CORRESPONDENCE
Patrick Ming-Kuen Tang,
patrick.tang@cuhk.edu.hk

†These authors have contributed equally to this work

RECEIVED 19 July 2023
ACCEPTED 12 October 2023
PUBLISHED 26 October 2023

CITATION
Ji ZZ, Chan MK-K, Chan AS-W, Leung K-T, Jiang X, To K-F, Wu Y and Tang PM-K (2023), Tumour-associated macrophages: versatile players in the tumour microenvironment.
Front. Cell Dev. Biol. 11:1261749.
doi: 10.3389/fcell.2023.1261749

Tumour-associated macrophages: versatile players in the tumour microenvironment

Zoey Zeyuan Ji[1†], Max Kam-Kwan Chan[1†], Alex Siu-Wing Chan[2], Kam-Tong Leung[3], Xiaohua Jiang[4], Ka-Fai To[1], Yi Wu[5] and Patrick Ming-Kuen Tang[1*]

[1]Department of Anatomical and Cellular Pathology, State Key Laboratory of Translational Oncology, The Chinese University of Hong Kong, Shatin, Hong Kong SAR, China, [2]Department of Applied Social Sciences, The Hong Kong Polytechnic University, Kowloon, Hong Kong SAR, China, [3]Department of Paediatrics, The Chinese University of Hong Kong, Shatin, Hong Kong SAR, China, [4]Key Laboratory for Regenerative Medicine of the Ministry of Education of China, School of Biomedical Sciences, Faculty of Medicine, The Chinese University of Hong Kong, Shatin, Hong Kong SAR, China, [5]MOE Key Laboratory of Environment and Genes Related to Diseases, School of Basic Medical Sciences, Xi'an Jiaotong University, Xi'an, China

Tumour-Associated Macrophages (TAMs) are one of the pivotal components of the tumour microenvironment. Their roles in the cancer immunity are complicated, both pro-tumour and anti-cancer activities are reported, including not only angiogenesis, extracellular matrix remodeling, immunosuppression, drug resistance but also phagocytosis and tumour regression. Interestingly, TAMs are highly dynamic and versatile in solid tumours. They show anti-cancer or pro-tumour activities, and interplay between the tumour microenvironment and cancer stem cells and under specific conditions. In addition to the classic M1/M2 phenotypes, a number of novel dedifferentiation phenomena of TAMs are discovered due to the advanced single-cell technology, e.g., macrophage-myofibroblast transition (MMT) and macrophage-neuron transition (MNT). More importantly, emerging information demonstrated the potential of TAMs on cancer immunotherapy, suggesting by the therapeutic efficiency of the checkpoint inhibitors and chimeric antigen receptor engineered cells based on macrophages. Here, we summarized the latest discoveries of TAMs from basic and translational research and discussed their clinical relevance and therapeutic potential for solid cancers.

KEYWORDS

tumour-associated macrophages, tumour microenvironment, immunotherapy, macrophage plasticity, macrophage-myofibroblast transition, macrophage-neuron transition

Introduction

Tumour microenvironment (TME) is crucial for cancer initiation, progression, and drug resistance. TME is formed by various fundamental constituents including stromal cells and immune cells (Cassetta et al., 2019; Li et al., 2023; Wang et al., 2023). Cancer development can be facilitated by tissue inflammation (Nost et al., 2021; Rajamaki et al., 2021). Despite the diverse inflammatory components in various cancer types (Cheng et al., 2021), increasing evidence demonstrated the importance of macrophages in the progression of solid cancers (Christofides et al., 2022). Macrophage is the key inflammatory effector cells, better understanding its roles may uncover effective therapeutic strategy for cancer (Coussens et al., 2013).

Interestingly, macrophages are versatile in tissues under inflammation including cancer (Maier et al., 2020; Vayrynen et al., 2021; Xue et al., 2021; Nalio Ramos et al., 2022). Their phenotypes and functions are broadly categorized into pro-inflammatory M1 and anti-inflammatory M2 (Cho et al., 2022; Zhou et al., 2022). M1 macrophages eliminate cancer cells by phagocytosis, antibody-dependent cytotoxicity, vascular damage, and tumour necrosis. M2 macrophages promote tumour growth and progression via enhancing cancer cell survival, angiogenesis and immune suppression (Zhao et al., 2020; Chen et al., 2021; Ren et al., 2022). Beyond M1/M2 polarization, new transition mechanisms for TAMs have been recently identified by single-cell bioinformatic studies including MMT (Tang et al., 2022a) and MNT (Tang et al., 2022b), their roles in cancer remain unclear.

Clinical studies highlight the crucial roles of macrophages in cancer therapy response and resistance, including chemotherapy, radiotherapy, and PDL1-based immunotherapy (Furuse et al., 2020; Liu et al., 2020). Moreover, clinical trials of macrophage-targeted therapies have been started such as the engineered mononuclear phagocytes (Brempelis et al., 2020) and chimeric antigen receptor macrophages (CAR-M) (Klichinsky et al., 2020; Wang et al., 2022), these therapeutic approaches stem from bench-top discoveries like recruitment and differentiation (Hannan et al., 2023), functional reprogramming (Willingham et al., 2012), and integration (Dang et al., 2021), highlighting the importance of basic research and preclinical study for the development of effective cancer treatment.

In this review, we systematically summarized the functional roles and underlying mechanisms of macrophages in TME for cancer formation and progression, their translational potential, and related studies on patients for overcoming the barriers of conventional cancer treatments as well as the latest immunotherapy resistance in the clinic. Finally, we also discussed the prospects and further directions of TAMs in the clinical development for cancer treatment.

Physiological roles of macrophages

Macrophages release cytokines and chemokines for recruiting immune cells for wound healing and blood vessel formation (Hernandez et al., 2022), including vascular endothelial growth factor (VEGF) (Lu et al., 2020) and transforming growth factor-beta (TGF-β) (Chung et al., 2018). Macrophages maintain tissue integrity (Mosser et al., 2021), clearing apoptotic cells (Dooling et al.,

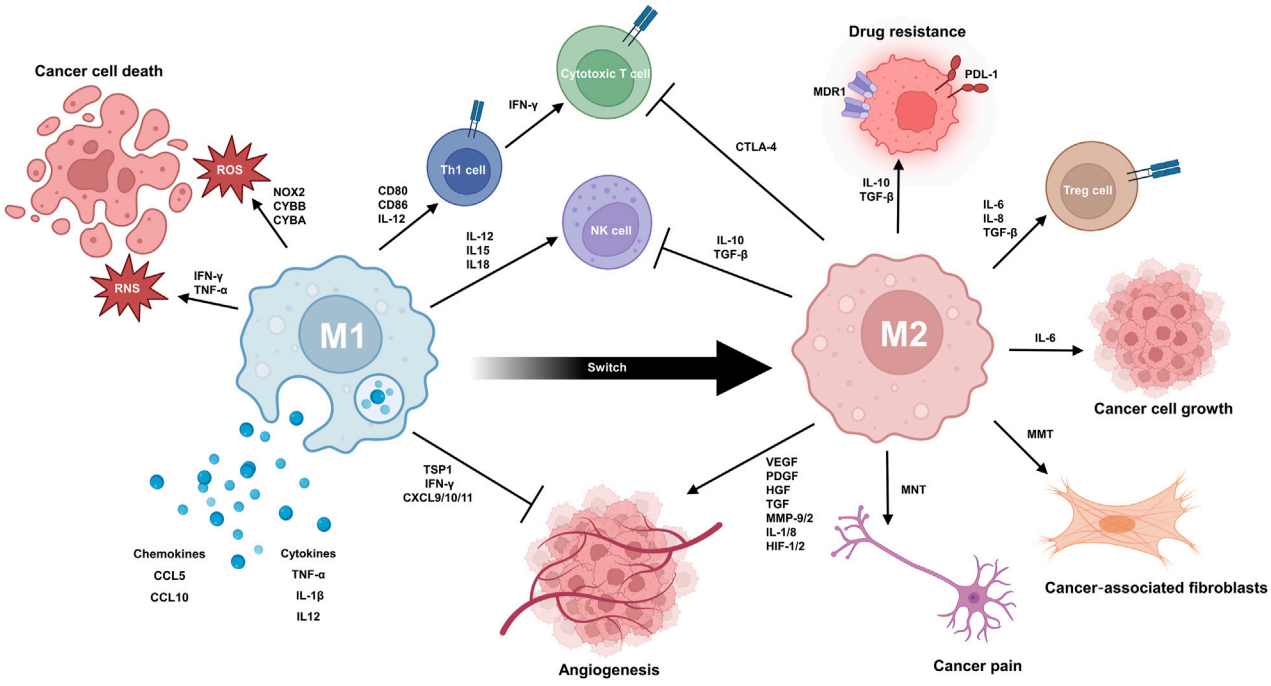

FIGURE 1
TAMs play a complex dual role in the progression of cancer. M1 TAMs contribute to the anticancer response via multiple mechanisms. They can produce reactive oxygen species (ROS) and reactive nitrogen species (RNS) to cause oxidative damage and kill cancer cells. The secretion of pro-inflammatory cytokines and chemokines (e.g., TNF-α, IL1B, IL12A/B, CCL5, and CXCL10) can mobilize other anticancer immune cells, like T cells and NK cells, into the TME. Anti-angiogenesis is promoted by secretion of thrombospondin-1 and angiostatic chemokines like CXCL9, CXCL10, and CXCL11. TAMs also express MHC class I and II molecules for antigen presentation to further priming and activation of T cells. The interaction between CD80/CD86 on TAMs and CD28 on T cells provides a second signal for T cell activation. M2 TAMs promote immunosuppression, angiogenesis, and tumour growth/metastasis while contributing to drug resistance. Immunosuppression involves secretion of TGF-β and IL-10, expression of PD-L1, and CCL22-induced Treg activation. In angiogenesis, TAMs secrete factors like VEGF, FGFs, PDGF, HGF, MMPs, and IL-8/1. During tumour growth and metastasis, M2 TAMs enhance proliferation, migration, and invasion. Factors like EGF, PDGF, VEGF, CCL-10, and MMPs play key roles. TAM can also undergo transformation to MNT and MMT, resulting in the generation of cancer pain and cancer-associated fibroblast. In drug resistance, TAM-derived TGF-β, IL-6/8, and PDGF stimulate survival pathways and enhance DNA repair in cancer cells. It is noteworthy that macrophages can switch from M1 phenotype to M2 phenotype during tissue repair.

2023), debris (Kim et al., 2020), and pathogens (Nau et al., 2002) via cell-mediated phagocytosis, where the targets are recognized by pattern recognition receptors (PRRs) dependent mechanisms (Li and Wu, 2021) i.e., Toll-like receptors (TLRs) (Irizarry-Caro et al., 2020) and NOD-like receptors (NLRs) (Fekete et al., 2018; Frising et al., 2022).

Furthermore, macrophages are involved in innate and adaptive immune responses by recognizing pathogen-associated molecular patterns (PAMPs) (Greene et al., 2022) and damage-associated molecular patterns (DAMPs) (Serbulea et al., 2018; Neu et al., 2022) through PRRs. Activated macrophages produce pro-inflammatory cytokines, i.e., tumour necrosis factor-alpha (TNF-α) (Lee et al., 2021; Lechner et al., 2022; Tanito et al., 2023) and interleukin-12 (IL-12) (Luo et al., 2022; Pfirschke et al., 2022), to promote inflammation and activate other immune cells. Macrophages also process and present antigens to T cells via major histocompatibility complex (MHC) molecules aiding adaptive immune response (Mascarau et al., 2023; van Elsas et al., 2023). Interestingly, tissue-specific macrophages display unique functions. For example, alveolar macrophages in lung, express high levels of surfactant protein A (SP-A) (Bain and MacDonald, 2022; Garcia-Fojeda et al., 2022; Yau et al., 2023) and surfactant protein D (SP-D) receptors (Guo et al., 2019; Hsieh et al., 2023) for clearing inhaled particles and pathogens. Liver-resident macrophages, Kupffer cells, express various scavenger receptors (Taban et al., 2022), complement receptors (Wen et al., 2021), and Fc receptors (Pfefferle et al., 2023), filtering blood-borne pathogens (Zhao et al., 2022a), toxins (Kermanizadeh et al., 2019), and debris (Liu and Sun, 2023).

Macrophages are classified into M1 and M2 phenotypes (Guilliams and Svedberg, 2021; De Vlaminck et al., 2022). M1 macrophages express high level of pro-inflammatory cytokines like Interleukin-1β (IL-1β), Interleukin-6 (IL-6), IL-12, Interleukin-23 (IL-23), and TNF-α (Hou et al., 2018; Akhtari et al., 2021; Beyranvand Nejad et al., 2021; Gunassekaran et al., 2021) polarized by Th1 cytokines including GM-CSF, TNF-α, and interferon-gamma (IFN-γ) (Wu et al., 2022a; Zhao et al., 2022b; Cho et al., 2022; Zhang et al., 2023), whereas, M2 macrophages actively produce anti-inflammatory cytokines Interleukin-10 (IL-10) and TGF-β (Nagata et al., 2019; Yang et al., 2023a) and polarized by Th2 cytokines like Interleukin-4 (IL-4) and Interleukin-13 (IL-13) (Celik et al., 2020; Lundahl et al., 2022). For metabolism, M1 macrophages rely on glycolysis (Yu et al., 2020; Mouton et al., 2023), while M2 macrophages depend on oxidative phosphorylation (Xu et al., 2021a; Zhou et al., 2022). During tissue repair, macrophages switch from an M1-like to an M2-like phenotype (Kim et al., 2019a; Alhamdi et al., 2019; Kohno et al., 2021). Interestingly, M1/M2 homeostasis is disrupted by inhibition of aspartate-aminotransferase (Wu et al., 2020a) and N-glycosylation (Wu et al., 2020a; Hu et al., 2023), altering immune responses and tissue damage. Moreover, various polarization and activation markers coexist in tissues, and factors like the macrophage-inducible C-type lectin (MINCLE) (Maier et al., 2020; Xue et al., 2021) or TLRs (Vidyarthi et al., 2018; Zhou et al., 2022) impact their balance. TAMs play multifaceted roles in cancer progression that are both beneficial and detrimental, highlighting the dual nature of their involvement (Figure 1).

Anticancer effects of TAMs

Reactive species production

M1 TAMs produce reactive oxygen species (ROS), mediated by NADPH oxidase (Fang et al., 2022; Tlili et al., 2023), causing cancer cell death. Activation by IFN-γ and TNF-α prompts TAMs to generate reactive nitrogen species (RNS) via nitric oxide synthase (iNOS) (Zhang et al., 2021a; Wei et al., 2022). Collectively, these ROS and RNS induce oxidative damage on cancer cells, leading to direct cancer cell-killing effect (Liang et al., 2019; Huang et al., 2022; Qi et al., 2022; Kidwell et al., 2023).

Pro-inflammatory cytokine and chemokine

TAMs secrete pro-inflammatory cytokines for mobilizing anticancer cells (e.g., T cells and natural killer cells) into TME, including TNF-α (Jiang et al., 2019; Kaplanov et al., 2019; Tu et al., 2021a), IL1B (interleukin-1 beta) (Revu et al., 2018), IL12A and IL12B (subunits of IL-12) (Yen et al., 2022). TAMs also produce chemokines, e.g., C-C Motif Chemokine Ligand 5 (CCL5) and C-X-C motif chemokine ligand 10 (CXCL10) to recruit and activate other immune cells to TME, driven by pro-inflammatory transcription factor NF-κB (nuclear factor kappa-light-chain-enhancer of activated B cells) (Taki et al., 2018). Furthermore, M1 macrophages produce IL-12, prompting $CD4^+$ T cells towards Th1 phenotype (Zhao et al., 2022b), these Th1 cells will produce IFN-γ to activate cytotoxic $CD8^+$ T cells in TME (Greaney et al., 2020; Liu et al., 2022). M1 macrophages also stimulate NK cell activation by IL-12, IL-15 and IL-18 (Mattiola et al., 2015).

Anti-angiogenesis

M1 macrophages secrete angiostatic factor thrombospondin-1(TSP1) (Yang et al., 2019; Kumar et al., 2020) for inhibiting angiogenesis by interacting with an endothelial cell receptor CD36 in various cancers, including hepatocellular carcinoma (Aburima et al., 2021). Moreover, M1 macrophages produce additional angiostatic chemokines to block vessel formation via CXCR3 (C-X-C Motif Chemokine Receptor 3) dependent mechanism, including CXCL9, 10, 11 (C-X-C Motif Chemokine Ligand 9, 10, 11) (Romagnani et al., 2004; Sahraei et al., 2019).

Antigen presentation

M1 macrophages express MHC class I and II molecules (Haloul et al., 2019; Ahmed and Ismail, 2020) to present cancer antigens, involving several genes, including MHC class I (Yao et al., 2020; Desterke et al., 2021; Piatakova et al., 2021) and II (He et al., 2021; Tang et al., 2022c; Scavuzzi et al., 2022). The interaction of MHC molecules with T cell receptors amplifies anti-tumour host immune response (Guerriero, 2019; Kawasaki et al., 2022). Interaction between CD80 and CD86 on the M1 macrophage and CD28 on

the T cell also provides crucial second signal for T cell activation (Trzupek et al., 2020).

Pro-tumour effects of TAM

Immunosuppression

TAMs contribute to immunosuppression in TME, including lung adenocarcinoma (LUAD) and bladder cancer (BLCA). They inhibit the anticancer activities of NK cells primarily through producing TGF-β (Nunez et al., 2018) and IL-10 (Xu et al., 2022). TGF-β hampers NK cell cytotoxicity by downregulating NKG2D receptor expression (Lazarova and Steinle, 2019). IL-10 inhibits the production of the anticancer cytokine IFN-γ in NK cells (Wang et al., 2021a). TAMs in these diverse cancer types express programmed death-ligand 1 (PD-L1) (Sumitomo et al., 2019; Shinchi et al., 2022; Xia et al., 2022; Elomaa et al., 2023), which interacts with the PD-1 receptor on T cells (Pereira et al., 2023; Puig-Saus et al., 2023) and NK cells (Zhou et al., 2023a; van der Sluis et al., 2023), leading to their exhaustion and promoting tumour immune evasion. TAM-derived CCL22 (C-C Motif Chemokine Ligand 22) contributes to the recruitment and activation of regulatory T cells (Tregs) (Rapp et al., 2019; Chen et al., 2022a), inducing immunosuppression in TME (Kraaij et al., 2010; Erlandsson et al., 2019). TAMs also enhance immunosuppressive function of Tregs, promote the transition of conventional $CD4^+$ T cells into Tregs (Morhardt et al., 2019; Saraiva et al., 2020; Maldonado et al., 2022), and activate myeloid-derived suppressor cells (MDSCs) via IL-10 (Yu et al., 2018; Yogev et al., 2022) and TGF-β (Becker et al., 2018; Astarita et al., 2023). Furthermore, TAMs express immune checkpoint molecule cytotoxic T-lymphocyte-associated protein 4 (CTLA-4) (Guan et al., 2021), interacting with CD80/CD86 of Tregs to amplify their immunosuppressive effects (Zappasodi et al., 2021; Kennedy et al., 2022).

Angiogenesis

TAMs play pivotal role in augmenting angiogenesis within the TME, integral to cancer progression (Cheng et al., 2021). Essential for tumor growth and metastasis (Liu et al., 2023a; Natale and Bocci, 2023), angiogenesis provides TME with necessary nutrients and oxygen, aiding in the growth of cancer cells (Schaaf et al., 2018; Lugano et al., 2020; Schito and Rey, 2020). TAMs secret factors for promoting angiogenesis, including VEGF (Schaaf et al., 2018), fibroblast growth factors (FGF1 and FGF2) (Schaaf et al., 2018; Im et al., 2020), platelet-derived growth factor (PDGF) (Ntokou et al., 2021), hepatocyte growth factor (HGF) (Choi et al., 2019; Dong et al., 2019), matrix metalloproteinases (MMP-9, MMP-2) (Diwanji and Bergmann, 2020; Tian et al., 2022), and cytokines like IL-8 and IL-1 (Liu et al., 2023b; Yang et al., 2023b). VEGF is crucial for tumoural angiogenesis (Lai et al., 2019; Hwang et al., 2020). Moreover, TAMs are concentrated in the hypoxic zones of tumours (Bai et al., 2022), where they upregulate the expression of numerous angiogenic genes including Hypoxia-inducible factors (HIF)-1 and −2 (Jeong et al., 2019; Cowman et al., 2020) for enhancing the production of angiogenic factors like VEGF in TME (Roda et al., 2012).

Cancer growth and metastasis

M2 TAMs promote primary tumour development and metastasis (Yao et al., 2018; Li et al., 2019a; Tu et al., 2021b). They increase tumour proliferation in breast cancer (Chen et al., 2022b; Zhou et al., 2023b), endometrial cancer (Xiao et al., 2020; Gu et al., 2021), and renal cell carcinoma (Xie et al., 2021; Ishii et al., 2022). Furthermore, M2 TAMs secrete Epidermal Growth Factor (EGF) (Zeng et al., 2019; Wu et al., 2020b), which binds to EGFR on cancer cells, for activating their growth signaling including MAPK/ERK (Liang et al., 2022) and PI3K/Akt pathways (Zhang et al., 2021b), promoting cell motility and invasion (Haque et al., 2019; Zeng et al., 2019; Onal et al., 2021). Growth Factor PDGF (Turrell et al., 2023) secreted from TAMs also contributes to tumour cell proliferation. Tumour metastasis is defining characteristic of advanced cancer stage, TAM-derived EGF accelerates metastasis by activating the EGFR-ERK signaling and inhibiting the expression of lncRNA LIMT (Zeng et al., 2019) in the epithelial ovarian cancer.

At the pre-metastasis stage, TAMs secrete VEGF, CCL-10 and MMPs, which remodel distant tissues to create pre-metastatic niche (Kim et al., 2019b; Winkler et al., 2020). TAMs release inflammatory factors TNF-α, IL-6, and IL-11 (Kaplanov et al., 2019; Yu et al., 2019; Beyranvand Nejad et al., 2021) to enhance cancer cell survival and proliferation by activating NF-κB and STAT3 pathways (Dorrington and Fraser, 2019; Balic et al., 2020). TGF-β from TAMs activates TGF receptors on cancer cells, initiating SMAD signaling for their growth (Chung et al., 2023; Lv et al., 2023). Importantly, TAM-derived TGF-β induces epithelial-to-mesenchymal transition (EMT) of cancer cells (Cai et al., 2019; Tiwari et al., 2021), allowing them to migrate into surrounding tissue and vasculature (Dongre and Weinberg, 2019; Wang et al., 2021b). Additionally, TAMs-secreted MMPs, such as MMP2 and MMP9 (Wang and Khalil, 2018; Liu et al., 2019; Muniz-Bongers et al., 2021), degrade the ECM in TME (Marigo et al., 2020), enabling metastasis into the bloodstream or lymphatic system (Winkler et al., 2020). TAMs produce chemokines like CCL18 and CCL22 (She et al., 2018; Kimura et al., 2019; Zhou et al., 2019; Chen et al., 2022a) to promote tumour cell migration. TAMs also release proteases like cathepsins (CTSB, CTSD) (Loeuillard et al., 2020; Shi et al., 2022) to stimulate tumour cells to produce tissue inhibitors of metalloproteinases, enhancing ECM degradation and metastasis (Bissinger et al., 2021).

TAMs transformation also contributes to cancer progression. Besides M1/M2 polarization, single-cell RNA-sequencing revealed new TAM phenomena. Macrophage to MNT, a process where TAMs transform into neuron-like cells contributing to the formation of cancer pain (Tang et al., 2022b). MMT, where TAMs trans-differentiate into myofibroblasts for increasing abundance of pro-tumour cancer-associated fibroblasts (CAFs) in TME, enhancing the progression of non-small-cell lung carcinoma (NSCLC) (Tang et al., 2022a).

Drug resistance

TAMs are associated with resistance of cancer therapy (Mantovani et al., 2022). TAM-derived TGF-β upregulates the expression of multidrug resistance protein 1 (MDR1) in cancer

TABLE 1 Selected clinical trials of drugs targeting TAMs.

Compound	Clinical phase	Tumour type	Status	NCT identifier	Year
CSF1R inhibitors					
PLX3397	Phase1	Drug Interaction Potential	Completed	NCT03291288	2017
	Phase3	Tenosynovial Giant Cell Tumour	Active_Not_Recruiting	NCT04488822	2020
	Phase4	Tenosynovial Giant Cell Tumour	Active_Not_Recruiting	NCT04526704	2020
	Phase2	Tenosynovial Giant Cell Tumour	Recruiting	NCT04703322	2021
HMPL-012	Phase2	Advanced Solid Tumours	Completed	NCT04169672	2019
	Phase2	Thyroid Cancer	Unknown	NCT04524884	2020
	Phase2	Neuroendocrine Tumours	Active_Not_Recruiting	NCT04579679	2020
	Phase2	Advanced Colorectal Cancer	Not_Yet_Recruiting	NCT04734249	2021
	Phase2	Advanced Colorectal Cancer	Recruiting	NCT04764006	2021
	Phase2	Advanced Non-Small Cell Lung Cancer	Recruiting	NCT04922658	2021
	Phase1 and 2	Advanced Colorectal Cancer	Recruiting	NCT04929652	2021
	Phase1	Small Cell Lung Carcinoma	Recruiting	NCT04996771	2021
	Phase2	Carcinoma, Non-Small-Cell Lung	Recruiting	NCT05003037	2021
	Phase2	Refractory Metastatic Digestive System Carcinoma and Peritoneal Cancer	Recruiting	NCT05030246	2021
	Na	Biliary Tract Cancer	Recruiting	NCT05056116	2021
	Phase1	Neuroendocrine Tumours and Non-hematologic Malignancy	Recruiting	NCT05077384	2021
	Phase1 and 2	Solid Tumour	Active_Not_Recruiting	NCT05093322	2021
	Phase2	Neuroendocrine Neoplasm	Recruiting	NCT05165407	2021
	Phase2	Hepatocellular Carcinoma	Recruiting	NCT05171439	2021
	Phase2	Breast Cancer and Breast Cancer Female	Recruiting	NCT05186545	2022
	Phase1 and 2	Pancreatic Cancer	Recruiting	NCT05218889	2022
	Phase2	Gastric Adenocarcinoma	Not_Yet_Recruiting	NCT05235906	2022
	Phase2	Pancreatic Neoplasms	Not_Yet_Recruiting	NCT05481463	2022
	Phase2	Pancreatic Neoplasms	Not_Yet_Recruiting	NCT05481476	2022
	Phase2	Advanced Solid Tumours	Not_Yet_Recruiting	NCT05527821	2022
	Phase2	Small Cell Lung Cancer	Not_Yet_Recruiting	NCT05595889	2022
	Phase2	Pancreatic Carcinoma	Recruiting	NCT05627427	2022
	Phase2	Extensive-stage Small-cell Lung Cancer	Not_Yet_Recruiting	NCT05668767	2022
	Phase1 and 2	Metastatic Triple-negative Breast Cancer	Not_Yet_Recruiting	NCT05746728	2023
	Phase1 and 2	Unresectable Locally Advanced	Not_Yet_Recruiting	NCT05832892	2023
	Phase1 and 2	Small Cell Lung Cancer	Not_Yet_Recruiting	NCT05882630	2023
	Phase2	Pancreatic Cancer	Recruiting	NCT05908747	2023
DCC-3014	Phase1	Advanced Sarcoma cancer	Active_Not_Recruiting	NCT04242238	2020
	Phase3	Giant Cell Tumour	Active_Not_Recruiting	NCT05059262	2021
	Phase1 and 2	Advanced Malignant Neoplasm	Recruiting	NCT03069469	2017
CS2164	Phase1	Small Cell Lung Cancer	Recruiting	NCT03216343	2017
	Phase1 and 2	Ovarian Cancer	Completed	NCT03166891	2017

(Continued on following page)

TABLE 1 (*Continued*) Selected clinical trials of drugs targeting TAMs.

Compound	Clinical phase	Tumour type	Status	NCT identifier	Year
	Phase2	Ovarian Cancer	Completed	NCT03901118	2019
	Phase3	Small Cell Lung Cancer	Recruiting	NCT04830813	2021
	Phase3	Ovarian Cancer and Relapsed or Refractory and Chiauranib and Paclitaxel	Recruiting	NCT04921527	2021
	Phase1 and 2	Small-cell Lung Cancer and Advanced Solid Malignant Tumour	Recruiting	NCT05271292	2022
Q702	Phase1	Solid Tumour and Advanced Cancer and Metastatic Cancer	Recruiting	NCT04648254	2020
	Phase1 and 2	Esophageal Cancer, Gastric Cancer, Hepatocellular Cancer and Cervical Cancer	Recruiting	NCT05438420	2022
TPX-0022	Phase1 and 2	Advanced Solid Tumour	Active_Not_Recruiting	NCT03993873	2019
X-82	Phase1	Solid Tumour	Terminated	NCT03511222	2018
	Phase1 and 2	Thymic Carcinoma, Non-small Cell Lung Cancer and Small-Cell Lung Cancer	Active_Not_Recruiting	NCT03583086	2018
	Phase1	Advanced Malignant Solid Tumours	Active_Not_Recruiting	NCT03792958	2019
	Phase2	Extensive-stage Small Cell Lung Cancer	Active_Not_Recruiting	NCT04373369	2020
Chemokine inhibitors					
BMS-813160	Phase1 and 2	Colorectal Cancer and Pancreatic Cancer	Active_Not_Recruiting	NCT03184870	2017
	Phase1 and 2	Pancreatic Ductal Adenocarcinoma	Active_Not_Recruiting	NCT03496662	2018
	Phase1 and 2	Locally Advanced Pancreatic Ductal Adenocarcinoma	Recruiting	NCT03767582	2018
	Phase2	Non-small Cell Lung Cancer and Hepatocellular Carcinoma	Recruiting	NCT04123379	2019
Maraviroc	Phase1	Metastatic Colorectal Cancer and MSS	Completed	NCT03274804	2017
	Phase1	Colorectal Cancer Metastatic and Pancreatic Cancer Metastatic	Unknown	NCT04721301	2021
	Phase1 and 2	HIV and Hematologic Malignancies	Recruiting	NCT05470491	2022
Anti-CD47/SIRPα antibodies					
Hu5F9-G4	Phase1	Hematological Malignancies	Active_Not_Recruiting	NCT03248479	2017
	Phase1	Ovarian Cancer	Completed	NCT03558139	2018
	Phase1	Acute Myeloid Leukemia	Terminated	NCT03922477	2019
	Phase1 and 2	Mycosis Fungoides and	Recruiting	NCT04541017	2020
	Phase1	Follicular Lymphoma	Recruiting	NCT04599634	2020
	Phase1	High Risk Neuroblastoma, Recurrent Neuroblastoma and Resectable Osteosarcoma	Suspended	NCT04751383	2021
	Phase2	Myeloid Malignancies	Active_Not_Recruiting	NCT04778410	2021
	Phase2	Solid Tumour	Recruiting	NCT04827576	2021
	Phase2	Triple-Negative Breast Cancer	Recruiting	NCT04958785	2021
	Phase1	Brain Cancer	Recruiting	NCT05169944	2021
	Phase2	Metastatic Colorectal Cancer	Recruiting	NCT05330429	2022
	Phase1	Advanced Malignant Solid Neoplasm	Not_Yet_Recruiting	NCT05807126	2023
BI 754091	Phase1	Neoplasms and Carcinoma, Non-Small-Cell Lung	Completed	NCT03156114	2017
	Phase1	Neoplasms and Neoplasm Metastasis and Carcinoma, Non-Small-Cell Lung	Terminated	NCT03166631	2017
	Early_Phase1	Neoplasms	Active_Not_Recruiting	NCT03433898	2018
	Phase1	Non-squamous, Non-Small-Cell Lung Cancer and Neoplasms	Active_Not_Recruiting	NCT03468426	2018

(Continued on following page)

TABLE 1 (*Continued*) Selected clinical trials of drugs targeting TAMs.

Compound	Clinical phase	Tumour type	Status	NCT identifier	Year
	Phase2	Neoplasm Metastasis	Active_Not_Recruiting	NCT03697304	2018
	Phase1	Carcinoma, Non-Small-Cell Lung and Head and Neck Neoplasms	Terminated	NCT03780725	2018
	Phase1	Neoplasms	Recruiting	NCT03964233	2019
	Phase1	Neoplasms	Completed	NCT03972150	2019
	Phase1	Solid Tumour, Adult	Recruiting	NCT03990233	2019
	Phase1 and 2	Colorectal Cancer	Recruiting	NCT04046445	2019
	Phase1	Neoplasm	Completed	NCT04138823	2019
	Phase1	Neoplasms	Active_Not_Recruiting	NCT04147234	2019
	Phase2	Anal Canal Squamous Cell Carcinoma	Withdrawn	NCT04499352	2020
	Phase1	Solid Tumours	Completed	NCT04653142	2020
	Phase2	Squamous Cell Carcinoma	Recruiting	NCT04719988	2021
	Phase1	Colorectal Neoplasms, Carcinoma and Non-Small-Cell Lung	Recruiting	NCT04752215	2021
	Phase1	Neoplasms	Recruiting	NCT04958239	2021
	Phase1	Head and Neck Squamous Cell Carcinoma	Recruiting	NCT05249426	2022
	Phase1	Solid Tumours	Recruiting	NCT05471856	2022
ALX148	Phase1	Metastatic Cancer and Solid Tumour and Advanced Cancer and NonHodgkin Lymphoma	Active	NCT03013218	2017
	Phase2 and 3	Gastric Cancer	Recruiting	NCT05002127	2021
	Phase1 and 2	HER2-expressing Cancers	Recruiting	NCT05027139	2021
	Phase2	Microsatellite Stable Metastatic Colorectal Cancer	Recruiting	NCT05167409	2021
	Phase2	Ovarian Cancer	Recruiting	NCT05467670	2022
	Phase2	Oropharynx Cancer	Not_Yet_Recruiting	NCT05787639	2023
	Phase1	HER2-positive Breast Cancer and Metastatic Cancer	Recruiting	NCT05868226	2023
AO-176	Phase1 and 2	Solid Tumour	Active_Not_Recruiting	NCT03834948	2019
IBI188	Phase1	Advanced Malignancies	Completed	NCT03763149	2018
SRF231	Phase1	Advanced Solid Cancers and Hematologic Cancers	Completed	NCT03512340	2018
Agonist anti-CD40 antibodies					
SEA-CD40	Phase2	Melanoma and Carcinoma, Non-Small- Cell Lung	Active_Not_Recruiting	NCT04993677	2021
APX005M	Phase1 and 2	Solid Cancers	Completed	NCT03123783	2017
	Phase2	Esophageal Cancer, Gastric Cancer and Hepatocellular Cancer	Active_Not_Recruiting	NCT03165994	2017
	Phase1	Glioblastoma Multiforme, Nos and Ependymoma, NOS and Medulloblastoma	Active_Not_Recruiting	NCT03389802	2018
	Phase1	Advanced Melanoma, Non-small Cell Lung Cancer and Renal Cell Carcinoma	Active_Not_Recruiting	NCT03502330	2018
	Phase1	Metastatic Melanoma	Terminated	NCT03597282	2018
	Phase2	Soft Tissue Sarcoma	Recruiting	NCT03719430	2018
	Phase2	Locally Advanced Rectal Adenocarcinoma	Active_Not_Recruiting	NCT04130854	2019
	Phase2	Ovarian Cancer	Not_Yet_Recruiting	NCT05201001	2022
	Phase1 and 2	Pancreatic Cancer	Recruiting	NCT05419479	2022

(Continued on following page)

TABLE 1 (*Continued*) Selected clinical trials of drugs targeting TAMs.

Compound	Clinical phase	Tumour type	Status	NCT identifier	Year
CDX-1140	Phase1	Solid Tumours	Completed	NCT03329950	2017
	Phase1 and 2	Non-Small Cell Lung Cancer	Recruiting	NCT04491084	2020
	Phase1	Malignant Epithelial Neoplasms	Recruiting	NCT04520711	2020
	Phase2	Pancreatic Cancer	Recruiting	NCT04536077	2020
	Phase1	Breast Cancer and Melanoma	Recruiting	NCT04616248	2020
	Phase1	Metastatic Triple Negative Breast Cancer	Recruiting	NCT05029999	2021
	Phase2	Solid Tumours	Not_Yet_Recruiting	NCT05231122	2022
	Phase1	Malignant Epithelial Neoplasms	Enrolling_By_Invitation	NCT05349890	2022
NG-350A	Phase1	Metastatic Cancer and Epithelial Tumour	Completed	NCT03852511	2019
	Phase1	Epithelial Tumour and Metastatic Cancer	Recruiting	NCT05165433	2021
TLR agonists					
Imiquimod	Phase1	Carcinoma, Non-Small-Cell Lung Cancer	Unknown	NCT03057340	2017
	Early_Phase1	Cervical Intraepithelial Neoplasia	Active_Not_Recruiting	NCT03196180	2017
	NA	Cervical Intraepithelial Neoplasia 3	Unknown	NCT03206138	2017
	Phase2	High Grade Intraepithelial Neoplasiaand Cervix Cancer	Completed	NCT03233412	2017
	Phase2	Basal Cell Carcinoma, Basal Cell Carcinoma of Skin and Invasive Carcinoma	Recruiting	NCT03534947	2018
	Phase1 and 2	Primary/Relapsed Acute Lymphoblastic Leukemia (ALL) of Childhood, Adolescents and Young Adults	Unknown	NCT03559413	2018
	Phase1	Solid Tumours	Recruiting	NCT03872947	2019
	Phase1	Malignant Glioma	Recruiting	NCT03893903	2019
	Phase1	Metastatic Breast Cancer	Terminated	NCT03982004	2019
	Phase1	Melanoma	Unknown	NCT04072900	2019
	Early_Phase1	Basal Cell Carcinoma	Completed	NCT04279535	2020
	Phase1	Glioblastoma	Active_Not_Recruiting	NCT04642937	2020
	Early_Phase1	Oral Cancer	Recruiting	NCT04883645	2021
	Phase1	Bladder Cancer and Bladder	Recruiting	NCT05055050	2021
	Phase3	Basal Cell Carcinoma	Not_Yet_Recruiting	NCT05212246	2022
	Phase1	Bladder Cance	Recruiting	NCT05375903	2022
Resiquimod	Phase1	Tumours	Completed	NCT00821652	2009
	Phase1 and 2	Advanced Malignancies	Completed	NCT00948961	2009
	Phase2	Melanoma	Completed	NCT00960752	2009
	Phase2	Bladder Cancer	Terminated	NCT01094496	2010
	Phase2	Glioma and Glioblastoma	Active_Not_Recruiting	NCT01204684	2010
	Early_Phase1	Recurrent Melanoma	Completed	NCT01748747	2012
	Phase1 and 2	Melanoma	Unknown	NCT02126579	2014
	Phase4	Postoperative Pain	Completed	NCT03570541	2018
	Phase1 and 2	Advanced Solid Tumour	Recruiting	NCT04799054	2021
	Phase1 and 2	Non-muscle-invasive Bladder Cancer	Recruiting	NCT05710848	2023

(Continued on following page)

TABLE 1 (*Continued*) Selected clinical trials of drugs targeting TAMs.

Compound	Clinical phase	Tumour type	Status	NCT identifier	Year
CpG ODN	Phase2	Lymphoma, Mantle-Cell	Completed	NCT00490529	2007
	Early_Phase1	Breast Cancer	Completed	NCT00640861	2008
	Phase2	Breast Cancer	Terminated	NCT00824733	2009
	Phase1	Melanoma	Completed	NCT01149343	2010
	Phase2	Malignant Melanoma	Recruiting	NCT04126876	2019
	Phase1	Pancreatic Cancer and Metastatic Pancreatic Cancer	Recruiting	NCT04612530	2020
	Phase1	Lung Cancer and Hepatocellular Carcinoma and Solid Tumour	Recruiting	NCT04952272	2021
Poly(I:C)	Phase1	Prostate Cancer	Completed	NCT03412786	2018
	Phase1	Leiomyosarcoma	Active_Not_Recruiting	NCT04420975	2020
	Early_Phase1	Advanced Hepatocellular Carcinoma	Terminated	NCT04777708	2021
CMP-001	Phase1 and 2	Advanced Cancer	Terminated	NCT02554812	2015
	Phase1	Non-Small Cell Lung Cancer	Completed	NCT03438318	2018
	Phase1	Colorectal Neoplasms Malignant and Liver Metastases	Completed	NCT03507699	2018
	Phase2	Melanoma and Lymph Node Cancer	Active_Not_Recruiting	NCT03618641	2018
	Phase1 and 2	Lymphoma	Recruiting	NCT03983668	2019
	Phase1 and 2	Locally Advanced Malignant Solid Neoplasm	Terminated	NCT04387071	2020
	Phase2	Melanoma	Recruiting	NCT04401995	2020
	Phase2	Squamous Cell Carcinoma of Head and Neck	Active_Not_Recruiting	NCT04633278	2020
	Phase2	Triple Negative Breast Cancer	Recruiting	NCT04807192	2021
	Phase2	Merkel Cell Carcinoma, Triple Negative Breast Cancer and Non-Small Cell Lung Cancer	Recruiting	NCT04916002	2021
	Phase3	Solid Tumours	Recruiting	NCT05059522	2021
	Phase2	Multiple Primary Cancers	Not_Yet_Recruiting	NCT05164510	2021
	Phase2	Metastatic Prostate Adenocarcinoma	Not_Yet_Recruiting	NCT05445609	2022
TREM2 inhibitor					
PY314	Phase1	Advanced Solid Tumour	Recruiting	NCT04691375	2020
Clever 1 inhibitor					
FP-1305	Phase1 and 2	Cancer	Recruiting	NCT03733990	2018
	Phase1	Non-small Cell Lung Cancer	Not_Yet_Recruiting	NCT05171062	2021
	Phase1 and 2	Acute Myeloid Leukemia	Recruiting	NCT05428969	2022
Complement inhibitor					
IPH5401	Phase1	Advanced Solid Tumours	Terminated	NCT03665129	2018
Macrophage cell therapy					
CT-0508	Phase1	Solid Tumours		NCT04660929	2020
TEMFERON	Phase1 and 2	Glioblastoma Multiforme	Recruiting	NCT03866109	2019
	Phase1 and 2	Multiple Myeloma	Terminated	NCT03875495	2019

cells (Badmann et al., 2020), leading to drug resistance. TAMs secrete IL-6 and IL-8 (Ahmed et al., 2021; Radharani et al., 2022), associated with resistance to therapies including EGFR tyrosine kinase inhibitors. TAMs-secreted PDGF enhances DNA repair in cancer cells against radiation therapy (Sakama et al., 2021).

Interplay between TME and cancer stem cells

The dynamic relationship between the TME and cancer stem cells (CSCs) is central to understanding the roles of TAMs. CSCs, distinguished by their pronounced expression of stemness markers like SOX2, NANOG, and OCT4 (Zhou et al., 2021), actively drive self-renewal, differentiation, and are influenced by signals from TME (Yang et al., 2020). Key pathways such as TGF-β, Wnt, and Hedgehog (Li et al., 2019b; Zhu et al., 2019; Wu et al., 2022b) mold the genetic landscape of CSCs. The crosstalk between CSCs and TME involves factors including IL-6 (Orange et al., 2023), IL-8 (Sun et al., 2018), IL-1β (Eyre et al., 2019), MMPs (Jin and Jin, 2020), VEGF (Lopez de Andres et al., 2020), and TGF-β1 (Yuan et al., 2022), which are encapsulated within extracellular vehicles (EVs) (Su et al., 2021; Cao et al., 2022). Given the immunomodulatory role of CSCs, further studies are essential to understand the clinical implications.

Importantly, interaction between TAMs and CSCs fosters an immunosuppressive TME (Wu et al., 2023). CSCs promote macrophage recruitment and polarization by ILs, ECM, TGF-β, and periostin (Ning et al., 2018; Kesh et al., 2020; Taniguchi et al., 2020; Li et al., 2022a; Lin et al., 2022). Moreover, TAMs increase CD47 expression in pancreatic, liver and lung cancer stem cells (Cioffi et al., 2015; Liu et al., 2017; Ruiz-Blazquez et al., 2021). When linked to SIRPα on macrophages, CD47 expression protects CSCs against immune cell-mediated phagocytosis (Li et al., 2018). TAM-secreted factors also upregulate immunological checkpoints like PD-L1 (Muraoka et al., 2019; Pu and Ji, 2022). The intricate interplay between CSCs and TAMs creates immunosuppressive TME, enhancing the survival of CSC and hindering tumour eradication post-immunotherapy.

Macrophage-targeted antitumour therapy

TAMs are essential for cancer immunotherapy (Lin et al., 2019). Macrophage-targeted treatments often deplete macrophages, modify their phenotypes, or enhance antigen presentation activity of TAM (Cassetta and Pollard, 2018). Combined with chemotherapy, radiation, or immunotherapy, these techniques may increase host antitumor immunity. They have been studied in animal models and clinical studies with immunological checkpoints and other immunotherapies (Table 1).

Depletion of macrophages

TAM recruitment by CCL2 and CCR2 is critical to tumour invasion and metastasis (Xu et al., 2021b). CCL2-CCR2 signaling controls the supply of circulating inflammatory monocytes (Argyle and Kitamura, 2018) and inhibiting CCR2 keeps monocytes in bone marrow, reducing TAMs at cancer sites (Flores-Toro et al., 2020). Blocking CCL2-CCR2 axis also hinders TAM recruitment, decreasing tumour incidence and enhancing $CD8^+$ T cells anti-tumour activity (Teng et al., 2017; Tu et al., 2020). Another target is CSF-1, which promotes monocyte and macrophage differentiation, proliferation, and function (Stanley and Chitu, 2014). Mouse models with CSF-1R inhibition had smaller tumors and better survival (Tan et al., 2021). Small molecule inhibitors of CSF1-R have also been shown to deplete some TAMs, enhancing tumour sensitivity to chemotherapy (O'Brien et al., 2021).

Alteration of macrophage phenotypes

TAMs change into a tumour-suppressing phenotype (Liu et al., 2021) which is a promising clinical strategy for cancer treatment. Inducing M1 macrophage phenotype through the use of selective class IIa HDAC inhibitors (Li et al., 2021a) enhances T cell responses to chemotherapy and immune checkpoint blockades (McCaw et al., 2019). The CD47/SIRP-α pathway is crucial for tumour immune escape, and blocking it enhances macrophages immune killing against tumours (Wang et al., 2020; Jia et al., 2021). Cancer immunotherapy research has also focused on anti-PD-1/PD-L1 treatment (Tomlins et al., 2023). TAMs, particularly M2 TAMs, express PD-L1 on their surface and contribute to immunosuppression by promoting T-cell apoptosis (Li et al., 2022b; Shinchi et al., 2022). In vitro-transcribed mRNA could stimulate effector molecule synthesis or cell reprogramming. mRNA in an injectable nanocarrier genetically reprogrammed TAMs into antitumour effectors. Nanoparticles formulated with mRNAs encoding the transcription factor interferon regulatory factor 5 (IRF5) and its activating kinase, inhibitor of NF-B kinase subunit-β (IKKβ), reversed the immunosuppressive TME and reprogrammed TAMs, regressing tumours in mouse cancer models (Zhang et al., 2019; Petty et al., 2021). The LILRB family, specifically LILRB2, is integral to the immune evasion strategies of cancer cells (Chen et al., 2018). LILRB2, an MHC-binding protein rich in TAMs, interacts with MHC class I molecules, which cancer cells often downregulate to dodge T cell recognition (Liu et al., 2023c). Blocking LILRB2 enhances macrophage pro-inflammatory and phagocytic activity. Its effect on macrophage activation and phagocytosis is unknown (Chen et al., 2018). MK-4830, an antibody against LILRB2, showed promising results in early trials with advanced-stage tumours (Siu et al., 2022). Responses correlated with the expression of pro-inflammatory cytokines and enhanced cytotoxic T cell-mediated anti-tumour immune response (Sharma et al., 2021). These approaches have been tested with other clinical used immunotherapies like immune checkpoints for their clinical potential with animal models and clinical trials.

Antigen presentation enhancement

Scavenger receptors on TAMs are becoming therapeutic targets for their role in promoting TME pro-inflammatory shifts. Scavenger receptor CD163 is associated to tumour progression in several

TABLE 2 Innovative strategies targeting TAMs in tumour microenvironment.

Cell type	Tumour type	Function
FRβ.CAR-T	Ovarian, Pancreatic, Colon, Melanoma	Recognize and eliminate TAMs, delay tumour progression and prolong life
F4.CAR-T	Orthotopic Lung Tumours	Deplete TAMs, inhibit tumour growth, enhance MHC upregulation via IFNγ, and boost CD8 T cell expansion and tumour cell immune editing
iNKT	Melanoma, Multiple myeloma, Ovarian	Use iNKT TCR/CD1d and CAR recognition to deplete TAMs
γδT		Raise MDSCs, induce antitumour responses with zoledronic acid, target monocytes, and kill macrophages
MCAR-MAIT		Kill OVCAR3-FG tumour cells, have dual CAR/TCR targeting mechanisms, sustain antitumour capacity in presence of macrophages, and target TAMs

malignancies but the mechanism is unclear (Xie et al., 2022). However, CD163+ macrophage depletion causes tumor regression and re-establish anti-PD1 treatment response (Etzerodt et al., 2019). Macrophage mannose receptor 1 (MRC1), also known as CD206, affects tumour immunity (Rahabi et al., 2020). Its activation induces immunosuppressive macrophages. Intriguingly, MRC1-binding peptide RP-182 converts TAMs into anti-tumour M1-like effector cells (Jaynes et al., 2020). The collagenous macrophage receptor (MARCO) is abundantly present on TAMs. Targeting MARCO potentially reprogrammes TAMs from tumour-supportive to pro-inflammatory effectors (Sa et al., 2020; La Fleur et al., 2021). Another scavenger receptor Clever 1 also suppresses macrophages and T helper 1 lymphocytes (Virtakoivu et al., 2021). Blocking it switches TAMs from immunosuppressive to pro-inflammatory (Viitala et al., 2019). Triggering receptor expressed on myeloid cells 2 (TREM2), upregulated on TAMs in human and mouse tumours, is a potential target (Katzenelenbogen et al., 2020; Molgora et al., 2020). Blocking TREM2+ macrophages limit tumour growth and augment anti-PD1 therapy (Binnewies et al., 2021). PSGL1, highly expressed in TAMs, represents a valuable target for TAMs re-education (Johnston et al., 2019). Using anti-PSGL1 monoclonal antibody potentially triggers a pro-inflammatory response in tumour tissues, exhibiting notable antitumour activity (DeRogatis et al., 2022; Lin et al., 2023).

Innovative strategies for TAM modulation

Recent strategies explore TAM modulation. One approach involves the engineering of T cells with chimeric antigen receptors (CAR) (Maalej et al., 2023) specifically tailored to recognize and eliminate TAMs. Research shows CAR T cells targeting macrophages are effective against various solid organ tumours, including ovarian and pancreatic cancer (Sanchez-Paulete et al., 2022). Eliminating M2-like FRβ+ TAMs in the murine models of ovarian cancer, colon cancer and melanoma TME through FR-specific CAR-T cells delay tumour progression and prolong life (Rodriguez-Garcia et al., 2021). These CAR-engineered T cells show potential in redirecting immune responses against the tumour. Another method focuses on harnessing invariant natural killer T (iNKT) cells (Li et al., 2021b). These cells possess innate and adaptive immune properties, CAR-iNKT cells use iNKT TCR/CD1d and CAR recognition to deplete TAMs and tumours (Simonetta et al., 2021). Recent studies harness iNKT cells to modulate TAMs, boosting antitumour responses. Other innate T cells, including MAIT, and γδT cells, have potential clinical applications as they target and eliminate TAMs (Li et al., 2022c). In synthesis, these innovative strategies signify a shift in tumour immunotherapy (Table 2).

Prospects of macrophages in cancer

TAMs are an important immune cell type that shapes TME properties. Targeting TAMs effectively blocks the progression of various cancer types. Moreover, popularity of single-cell RNA-sequencing analysis enhances the mechanistic study and preclinical research of TAMs in TME (Tang et al., 2020; Tang et al., 2021a; Chung et al., 2023). Dissecting the heterogeneity and regulatory mechanism of macrophages in cancer at single-cell resolution leads to the discovery of novel macrophage-specific therapeutics targets from the TME, for example, MMT and MNT (Xue et al., 2021; Tang et al., 2022a; Tang et al., 2022b). They are emphasizing the adaptive plasticity of macrophages. MMTs, derived from M2 TAMs with protumour activities, lead to the formation of CAFs. These CAFs are key in driving cancer progression (Chen and Song, 2019; Li et al., 2020). The roles of MMT-derived CAFs in functions, including adaptive immunity suppression, drug resistance, metastasis, and promoting cancer cell stemness warrant investigation. Conversely, MNTs highlight the transformation of TAMs into neuron-like entities, influencing *de novo* neurogenesis in the TME (Tang et al., 2022b) and contributing to cancer-associated pain (Shepherd et al., 2018). This transition, while prevalent in NSCLC, is also seen in other tumours, emphasizing its importance in cancer pain and tumour innervation (Tang et al., 2022b). Given the impact of cancer pain on quality of life, especially in patients with advanced stages of the disease (Wang et al., 2021c), understanding MNT is vital for pain management strategies. Notably, these transitions were found to be mediated by a Smad3-centric gene network in TAMs, highlighting the potential of macrophage-targeted Smad3 interventions as a promising therapeutic approach in cancer immunotherapy (Tang et al., 2017; Feng et al., 2018; Tang et al., 2021b; Tang et al., 2022b). These new findings lead to the development of effective therapeutic approaches to enhance the efficiency of conventional anticancer treatments as well as the latest immunotherapies which are not primary or secondary resistant in patients with solid cancers (Kim et al., 2019b; Kim et al., 2020; Tang et al., 2020; Chung et al., 2021;

Xue et al., 2021). Besides, macrophages are considered as a primary target of anti-inflammatory therapy for cancer prevention, their therapeutic potential is explored by new trials worldwide (Tang et al., 2019; Lee et al., 2021; Tang et al., 2022d). Despite the challenges, a better understanding of the immunodynamics of TAM shows a substantial potential for improving the therapeutic efficiency and clinical outcomes of cancer patients in the future.

Author contributions

ZZJ: Writing–original draft, Writing–review and editing, Visualization. MK-KC: Writing–original draft, Writing–review and editing, Visualization. AS-WC: Data curation. K-TL: Writing–review and editing. XJ: Writing–review and editing. K-FT: Writing–review and editing. YW: Writing–review and editing. PM-KT: Writing–original draft, Writing–review & editing Conceptualization, Funding acquisition, Investigation, Resources, Supervision. Validation: All authors have read and agreed to the published version.

Funding

The authors declare financial support was received for the research, authorship, and/or publication of this article. This study was supported by the Research Grants Council of Hong Kong (14106518, 14111019, 14111720, and 24102723); RGC Postdoctoral Fellowship Scheme (PDFS2122-4S06); Hong Kong Government Health and Medical Research Fund (10210726); CU Medicine Passion for Perfection Scheme (PFP202210-004) and Faculty Innovation Award (4620528), CUHK Strategic Seed Funding for Collaborative Research Scheme (178896941), Direct Grant for Research (4054722), Postdoctoral Fellowship Scheme (NL/LT/PDFS 2022/0360/22lt and WW/PDFS 2023/0640/23en).

Conflict of interest

The authors declare that the research was conducted in the absence of any commercial or financial relationships that could be construed as a potential conflict of interest.

Publisher's note

References

Aburima, A., Berger, M., Spurgeon, B. E. J., Webb, B. A., Wraith, K. S., Febbraio, M., et al. (2021). Thrombospondin-1 promotes hemostasis through modulation of cAMP signaling in blood platelets. *Blood* 137 (5), 678–689. doi:10.1182/blood.2020005382

Ahmed, I., and Ismail, N. (2020). M1 and M2 macrophages polarization via mTORC1 influences innate immunity and outcome of ehrlichia infection. *J. Cell. Immunol.* 2 (3), 108–115. doi:10.33696/immunology.2.029

Ahmed, S., Mohamed, H. T., El-Husseiny, N., El Mahdy, M. M., Safwat, G., Diab, A. A., et al. (2021). IL-8 secreted by tumor associated macrophages contribute to lapatinib resistance in HER2-positive locally advanced breast cancer via activation of Src/STAT3/ERK1/2-mediated EGFR signaling. *Biochim. Biophys. Acta Mol. Cell. Res.* 1868 (6), 118995. doi:10.1016/j.bbamcr.2021.118995

Akhtari, M., Zargar, S. J., Vojdanian, M., Jamshidi, A., and Mahmoudi, M. (2021). Monocyte-derived and M1 macrophages from ankylosing spondylitis patients released higher TNF-α and expressed more IL1B in response to BzATP than macrophages from healthy subjects. *Sci. Rep.* 11 (1), 17842. doi:10.1038/s41598-021-96262-2

Alhamdi, J. R., Peng, T., Al-Naggar, I. M., Hawley, K. L., Spiller, K. L., and Kuhn, L. T. (2019). Controlled M1-to-M2 transition of aged macrophages by calcium phosphate coatings. *Biomaterials* 196, 90–99. doi:10.1016/j.biomaterials.2018.07.012

Argyle, D., and Kitamura, T. (2018). Targeting macrophage-recruiting chemokines as a novel therapeutic strategy to prevent the progression of solid tumors. *Front. Immunol.* 9, 2629. doi:10.3389/fimmu.2018.02629

Astarita, J. L., Dominguez, C. X., Tan, C., Guillen, J., Pauli, M. L., Labastida, R., et al. (2023). Treg specialization and functions beyond immune suppression. *Clin. Exp. Immunol.* 211 (2), 176–183. doi:10.1093/cei/uxac123

Badmann, S., Heublein, S., Mayr, D., Reischer, A., Liao, Y., Kolben, T., et al. (2020). M2 macrophages infiltrating epithelial ovarian cancer express MDR1: a feature that may account for the poor prognosis. *Cells* 9 (5), 1224. doi:10.3390/cells9051224

Bai, R., Li, Y., Jian, L., Yang, Y., Zhao, L., and Wei, M. (2022). The hypoxia-driven crosstalk between tumor and tumor-associated macrophages: mechanisms and clinical treatment strategies. *Mol. Cancer* 21 (1), 177. doi:10.1186/s12943-022-01645-2

Bain, C. C., and MacDonald, A. S. (2022). The impact of the lung environment on macrophage development, activation and function: diversity in the face of adversity. *Mucosal Immunol.* 15 (2), 223–234. doi:10.1038/s41385-021-00480-w

Balic, J. J., Albargy, H., Luu, K., Kirby, F. J., Jayasekara, W. S. N., Mansell, F., et al. (2020). STAT3 serine phosphorylation is required for TLR4 metabolic reprogramming and IL-1β expression. *Nat. Commun.* 11 (1), 3816. doi:10.1038/s41467-020-17669-5

Becker, W., Nagarkatti, M., and Nagarkatti, P. S. (2018). miR-466a targeting of TGF-β2 contributes to FoxP3+ regulatory T cell differentiation in a murine model of allogeneic transplantation. *Front. Immunol.* 9, 688. doi:10.3389/fimmu.2018.00688

Beyranvand Nejad, E., Labrie, C., van Elsas, M. J., Kleinovink, J. W., Mittrücker, H. W., Franken, K. L. M. C., et al. (2021). IL-6 signaling in macrophages is required for immunotherapy-driven regression of tumors. *J. Immunother. Cancer* 9 (4), e002460. doi:10.1136/jitc-2021-002460

Binnewies, M., Pollack, J. L., Rudolph, J., Dash, S., Abushawish, M., Lee, T., et al. (2021). Targeting TREM2 on tumor-associated macrophages enhances immunotherapy. *Cell. Rep.* 37 (3), 109844. doi:10.1016/j.celrep.2021.109844

Bissinger, S., Hage, C., Wagner, V., Maser, I. P., Brand, V., Schmittnaegel, M., et al. (2021). Macrophage depletion induces edema through release of matrix-degrading proteases and proteoglycan deposition. *Sci. Transl. Med.* 13 (598), eabd4550. doi:10.1126/scitranslmed.abd4550

Brempelis, K. J., Cowan, C. M., Kreuser, S. A., Labadie, K. P., Prieskorn, B. M., Lieberman, N. A. P., et al. (2020). Genetically engineered macrophages persist in solid tumors and locally deliver therapeutic proteins to activate immune responses. *J. Immunother. Cancer* 8 (2), e001356. doi:10.1136/jitc-2020-001356

Cai, J., Xia, L., Li, J., Ni, S., Song, H., and Wu, X. (2019). Tumor-associated macrophages derived TGF-β–induced epithelial to mesenchymal transition in colorectal cancer cells through smad2,3-4/snail signaling pathway. *Cancer Res. Treat.* 51 (1), 252–266. doi:10.4143/crt.2017.613

Cao, M., Isaac, R., Yan, W., Ruan, X., Jiang, L., Wan, Y., et al. (2022). Cancer-cell-secreted extracellular vesicles suppress insulin secretion through miR-122 to impair systemic glucose homeostasis and contribute to tumour growth. *Nat. Cell. Biol.* 24 (6), 954–967. doi:10.1038/s41556-022-00919-7

Cassetta, L., and Pollard, J. W. (2018). Targeting macrophages: therapeutic approaches in cancer. *Nat. Rev. Drug Discov.* 17 (12), 887–904. doi:10.1038/nrd.2018.169

Cassetta, L., Fragkogianni, S., Sims, A. H., Swierczak, A., Forrester, L. M., Zhang, H., et al. (2019). Human tumor-associated macrophage and monocyte transcriptional landscapes reveal cancer-specific reprogramming, biomarkers, and therapeutic targets. *Cancer Cell.* 35 (4), 588–602. doi:10.1016/j.ccell.2019.02.009

Celik, M. O., Labuz, D., Keye, J., Glauben, R., and Machelska, H. (2020). IL-4 induces M2 macrophages to produce sustained analgesia via opioids. *JCI Insight* 5 (4), e133093. doi:10.1172/jci.insight.133093

Chen, X., and Song, E. (2019). Turning foes to friends: targeting cancer-associated fibroblasts. *Nat. Rev. Drug Discov.* 18 (2), 99–115. doi:10.1038/s41573-018-0004-1

Chen, H. M., van der Touw, W., Wang, Y. S., Kang, K., Mai, S., Zhang, J., et al. (2018). Blocking immunoinhibitory receptor LILRB2 reprograms tumor-associated myeloid cells and promotes antitumor immunity. *J. Clin. Invest.* 128 (12), 5647–5662. doi:10.1172/JCI97570

Chen, J., Zhang, K., Zhi, Y., Wu, Y., Chen, B., Bai, J., et al. (2021). Tumor-derived exosomal miR-19b-3p facilitates M2 macrophage polarization and exosomal LINC00273 secretion to promote lung adenocarcinoma metastasis via Hippo pathway. *Clin. Transl. Med.* 11 (9), e478. doi:10.1002/ctm2.478

Chen, J., Zhao, D., Zhang, L., Zhang, J., Xiao, Y., Wu, Q., et al. (2022a). Tumor-associated macrophage (TAM)-derived CCL22 induces FAK addiction in esophageal squamous cell carcinoma (ESCC). *Cell. Mol. Immunol.* 19 (9), 1054–1066. doi:10.1038/s41423-022-00903-z

Chen, Z., Wu, J., Wang, L., Zhao, H., and He, J. (2022b). Tumor-associated macrophages of the M1/M2 phenotype are involved in the regulation of malignant biological behavior of breast cancer cells through the EMT pathway. *Med. Oncol.* 39 (5), 83. doi:10.1007/s12032-022-01670-7

Cheng, S., Li, Z., Gao, R., Xing, B., Gao, Y., Yang, Y., et al. (2021). A pan-cancer single-cell transcriptional atlas of tumor infiltrating myeloid cells. *Cell.* 184 (3), 792–809 e23. doi:10.1016/j.cell.2021.01.010

Cho, H., Kwon, H. Y., Sharma, A., Lee, S. H., Liu, X., Miyamoto, N., et al. (2022). Visualizing inflammation with an M1 macrophage selective probe via GLUT1 as the gating target. *Nat. Commun.* 13 (1), 5974. doi:10.1038/s41467-022-33526-z

Choi, W., Lee, J., Lee, J., Lee, S. H., and Kim, S. (2019). Hepatocyte growth factor regulates macrophage transition to the M2 phenotype and promotes murine skeletal muscle regeneration. *Front. Physiol.* 10, 914. doi:10.3389/fphys.2019.00914

Christofides, A., Strauss, L., Yeo, A., Cao, C., Charest, A., and Boussiotis, V. A. (2022). The complex role of tumor-infiltrating macrophages. *Nat. Immunol.* 23 (8), 1148–1156. doi:10.1038/s41590-022-01267-2

Chung, S., Overstreet, J. M., Li, Y., Wang, Y., Niu, A., Wang, S., et al. (2018). TGF-beta promotes fibrosis after severe acute kidney injury by enhancing renal macrophage infiltration. *JCI Insight* 3 (21), e123563. doi:10.1172/jci.insight.123563

Chung, J. Y., Chan, M. K. K., Tang, P. C. T., Chan, A. S. W., Meng, X. M., Chung, J. S. Y., et al. (2021). AANG: a natural compound formula for overcoming multidrug resistance via synergistic rebalancing the TGF-β/Smad signalling in hepatocellular carcinoma. *J. Cell. Mol. Med.* 25 (20), 9805–9813. doi:10.1111/jcmm.16928

Chung, J. Y., Tang, P. C. T., Chan, M. K. K., Xue, V. W., Huang, X. R., Ng, C., et al. (2023). Smad3 is essential for polarization of tumor-associated neutrophils in non-small cell lung carcinoma. *Nat. Commun.* 14 (1), 1794. doi:10.1038/s41467-023-37515-8

Cioffi, M., Trabulo, S., Hidalgo, M., Costello, E., Greenhalf, W., Erkan, M., et al. (2015). Inhibition of CD47 effectively targets pancreatic cancer stem cells via dual mechanisms. *Clin. Cancer Res.* 21 (10), 2325–2337. doi:10.1158/1078-0432.CCR-14-1399

Coussens, L. M., Zitvogel, L., and Palucka, A. K. (2013). Neutralizing tumour-promoting chronic inflammation: a magic bullet? *Science* 339 (6117), 286–291. doi:10.1126/science.1232227

Cowman, S. J., Fuja, D. G., Liu, X. D., Tidwell, R. S. S., Kandula, N., Sirohi, D., et al. (2020). Macrophage HIF-1α is an independent prognostic indicator in kidney cancer. *Clin. Cancer Res.* 26 (18), 4970–4982. doi:10.1158/1078-0432.CCR-19-3890

Dang, M. T., Gonzalez, M. V., Gaonkar, K. S., Rathi, K. S., Young, P., Arif, S., et al. (2021). Macrophages in SHH subgroup medulloblastoma display dynamic heterogeneity that varies with treatment modality. *Cell. Rep.* 34 (13), 108917. doi:10.1016/j.celrep.2021.108917

De Vlaminck, K., Van Hove, H., Kancheva, D., Scheyltjens, I., Pombo Antunes, A. R., Bastos, J., et al. (2022). Differential plasticity and fate of brain-resident and recruited macrophages during the onset and resolution of neuroinflammation. *Immunity* 55 (11), 2085–2102 e9. doi:10.1016/j.immuni.2022.09.005

DeRogatis, J. M., Viramontes, K. M., Neubert, E. N., Henriquez, M. L., Guerrero-Juarez, C. F., and Tinoco, R. (2022). Targeting the PSGL-1 immune checkpoint promotes immunity to PD-1-resistant melanoma. *Cancer Immunol. Res.* 10 (5), 612–625. doi:10.1158/2326-6066.CIR-21-0690

Desterke, C., Turhan, A. G., Bennaceur-Griscelli, A., and Griscelli, F. (2021). HLA-dependent heterogeneity and macrophage immunoproteasome activation during lung COVID-19 disease. *J. Transl. Med.* 19 (1), 290. doi:10.1186/s12967-021-02965-5

Diwanji, N., and Bergmann, A. (2020). Basement membrane damage by ROS- and JNK-mediated Mmp2 activation drives macrophage recruitment to overgrown tissue. *Nat. Commun.* 11 (1), 3631. doi:10.1038/s41467-020-17399-8

Dong, N., Shi, X., Wang, S., Gao, Y., Kuang, Z., Xie, Q., et al. (2019). M2 macrophages mediate sorafenib resistance by secreting HGF in a feed-forward manner in hepatocellular carcinoma. *Br. J. Cancer* 121 (1), 22–33. doi:10.1038/s41416-019-0482-x

Dongre, A., and Weinberg, R. A. (2019). New insights into the mechanisms of epithelial-mesenchymal transition and implications for cancer. *Nat. Rev. Mol. Cell. Biol.* 20 (2), 69–84. doi:10.1038/s41580-018-0080-4

Dooling, L. J., Andrechak, J. C., Hayes, B. H., Kadu, S., Zhang, W., Pan, R., et al. (2023). Cooperative phagocytosis of solid tumours by macrophages triggers durable anti-tumour responses. *Nat. Biomed. Eng.* 7, 1081–1096. doi:10.1038/s41551-023-01031-3

Dorrington, M. G., and Fraser, I. D. C. (2019). NF-κB signaling in macrophages: dynamics, crosstalk, and signal integration. *Front. Immunol.* 10, 705. doi:10.3389/fimmu.2019.00705

Elomaa, H., Ahtiainen, M., Väyrynen, S. A., Ogino, S., Nowak, J. A., Lau, M. C., et al. (2023). Spatially resolved multimarker evaluation of CD274 (PD-L1)/PDCD1 (PD-1) immune checkpoint expression and macrophage polarisation in colorectal cancer. *Br. J. Cancer* 128 (11), 2104–2115. doi:10.1038/s41416-023-02238-6

Erlandsson, A., Carlsson, J., Lundholm, M., Fält, A., Andersson, S. O., Andrén, O., et al. (2019). M2 macrophages and regulatory T cells in lethal prostate cancer. *Prostate* 79 (4), 363–369. doi:10.1002/pros.23742

Etzerodt, A., Tsalkitzi, K., Maniecki, M., Damsky, W., Delfini, M., Baudoin, E., et al. (2019). Specific targeting of CD163+ TAMs mobilizes inflammatory monocytes and promotes T cell-mediated tumor regression. *J. Exp. Med.* 216 (10), 2394–2411. doi:10.1084/jem.20182124

Eyre, R., Alférez, D. G., Santiago-Gómez, A., Spence, K., McConnell, J. C., Hart, C., et al. (2019). Microenvironmental IL1β promotes breast cancer metastatic colonisation in the bone via activation of Wnt signalling. *Nat. Commun.* 10 (1), 5016. doi:10.1038/s41467-019-12807-0

Fang, T., Huang, Y. K., Wei, J., Monterrosa Mena, J. E., Lakey, P. S. J., Kleinman, M. T., et al. (2022). Superoxide release by macrophages through NADPH oxidase activation dominating chemistry by isoprene secondary organic aerosols and quinones to cause oxidative damage on membranes. *Environ. Sci. Technol.* 56 (23), 17029–17038. doi:10.1021/acs.est.2c03987

Fekete, T., Bencze, D., Szabo, A., Csoma, E., Biro, T., Bacsi, A., et al. (2018). Regulatory NLRs control the RLR-mediated type I interferon and inflammatory responses in human dendritic cells. *Front. Immunol.* 9, 2314. doi:10.3389/fimmu.2018.02314

Feng, M., Tang, P. M. K., Huang, X. R., Sun, S. F., You, Y. K., Xiao, J., et al. (2018). TGF-Beta mediates renal fibrosis via the smad3-erbb4-IR long noncoding RNA Axis. *Mol. Ther.* 26 (1), 148–161. doi:10.1016/j.ymthe.2017.09.024

Flores-Toro, J. A., Luo, D., Gopinath, A., Sarkisian, M. R., Campbell, J. J., Charo, I. F., et al. (2020). CCR2 inhibition reduces tumor myeloid cells and unmasks a checkpoint inhibitor effect to slow progression of resistant murine gliomas. *Proc. Natl. Acad. Sci. U. S. A.* 117 (2), 1129–1138. doi:10.1073/pnas.1910856117

Frising, U. C., Ribo, S., Doglio, M. G., Malissen, B., van Loo, G., and Wullaert, A. (2022). Nlrp3 inflammasome activation in macrophages suffices for inducing autoinflammation in mice. *EMBO Rep.* 23 (7), e54339. doi:10.15252/embr.202154339

Furuse, M., Kuwabara, H., Ikeda, N., Hattori, Y., Ichikawa, T., Kagawa, N., et al. (2020). PD-L1 and PD-L2 expression in the tumor microenvironment including peritumoral tissue in primary central nervous system lymphoma. *BMC Cancer* 20 (1), 277. doi:10.1186/s12885-020-06755-y

Garcia-Fojeda, B., Minutti, C. M., Montero-Fernández, C., Stamme, C., and Casals, C. (2022). Signaling pathways that mediate alveolar macrophage activation by surfactant protein A and IL-4. *Front. Immunol.* 13, 860262. doi:10.3389/fimmu.2022.860262

Greaney, S. K., Algazi, A. P., Tsai, K. K., Takamura, K. T., Chen, L., Twitty, C. G., et al. (2020). Intratumoral plasmid IL12 electroporation therapy in patients with advanced melanoma induces systemic and intratumoral T-cell responses. *Cancer Immunol. Res.* 8 (2), 246–254. doi:10.1158/2326-6066.CIR-19-0359

Greene, C. J., Nguyen, J. A., Cheung, S. M., Arnold, C. R., Balce, D. R., Wang, Y. T., et al. (2022). Macrophages disseminate pathogen associated molecular patterns through the direct extracellular release of the soluble content of their phagolysosomes. *Nat. Commun.* 13 (1), 3072. doi:10.1038/s41467-022-30654-4

Gu, X., Shi, Y., Dong, M., Jiang, L., Yang, J., and Liu, Z. (2021). Exosomal transfer of tumor-associated macrophage-derived hsa_circ_0001610 reduces radiosensitivity in endometrial cancer. *Cell. Death Dis.* 12 (9), 818. doi:10.1038/s41419-021-04087-8

Guan, X., Wang, Y., Sun, Y., Zhang, C., Ma, S., Zhang, D., et al. (2021). CTLA4-Mediated immunosuppression in glioblastoma is associated with the infiltration of macrophages in the tumor microenvironment. *J. Inflamm. Res.* 14, 7315–7329. doi:10.2147/JIR.S341981

Guerriero, J. L. (2019). Macrophages: their untold story in T cell activation and function. *Int. Rev. Cell. Mol. Biol.* 342, 73–93. doi:10.1016/bs.ircmb.2018.07.001

Guilliams, M., and Svedberg, F. R. (2021). Does tissue imprinting restrict macrophage plasticity? *Nat. Immunol.* 22 (2), 118–127. doi:10.1038/s41590-020-00849-2

Gunassekaran, G. R., Poongkavithai Vadevoo, S. M., Baek, M. C., and Lee, B. (2021). M1 macrophage exosomes engineered to foster M1 polarization and target the IL-4 receptor inhibit tumor growth by reprogramming tumor-associated macrophages into M1-like macrophages. *Biomaterials* 278, 121137. doi:10.1016/j.biomaterials.2021.121137

Guo, C. J., Atochina-Vasserman, E. N., Abramova, E., Smith, L. C., Beers, M. F., and Gow, A. J. (2019). Surfactant protein-D modulation of pulmonary macrophage phenotype is controlled by S-nitrosylation. *Am. J. Physiol. Lung Cell. Mol. Physiol.* 317 (5), L539–L549. doi:10.1152/ajplung.00506.2018

Haloul, M., Oliveira, E. R. A., Kader, M., Wells, J. Z., Tominello, T. R., El Andaloussi, A., et al. (2019). mTORC1-mediated polarization of M1 macrophages and their accumulation in the liver correlate with immunopathology in fatal ehrlichiosis. *Sci. Rep.* 9 (1), 14050. doi:10.1038/s41598-019-50320-y

Hannan, C. J., Lewis, D., O'Leary, C., Waqar, M., Brough, D., Couper, K. N., et al. (2023). Increased circulating chemokines and macrophage recruitment in growing vestibular schwannomas. *Neurosurgery* 92 (3), 581–589. doi:10.1227/neu.0000000000002252

Haque, A., Moriyama, M., Kubota, K., Ishiguro, N., Sakamoto, M., Chinju, A., et al. (2019). CD206+ tumor-associated macrophages promote proliferation and invasion in oral squamous cell carcinoma via EGF production. *Sci. Rep.* 9 (1), 14611. doi:10.1038/s41598-019-51149-1

He, L., Jhong, J. H., Chen, Q., Huang, K. Y., Strittmatter, K., Kreuzer, J., et al. (2021). Global characterization of macrophage polarization mechanisms and identification of M2-type polarization inhibitors. *Cell. Rep.* 37 (5), 109955. doi:10.1016/j.celrep.2021.109955

Hernandez, G. E., Ma, F., Martinez, G., Firozabadi, N. B., Salvador, J., Juang, L. J., et al. (2022). Aortic intimal resident macrophages are essential for maintenance of the non-thrombogenic intravascular state. *Nat. Cardiovasc Res.* 1 (1), 67–84. doi:10.1038/s44161-021-00006-4

Hou, Y., Zhu, L., Tian, H., Sun, H. X., Wang, R., Zhang, L., et al. (2018). IL-23-induced macrophage polarization and its pathological roles in mice with imiquimod-induced psoriasis. *Protein Cell.* 9 (12), 1027–1038. doi:10.1007/s13238-018-0505-z

Hsieh, M. H., Chen, P. C., Hsu, H. Y., Liu, J. C., Ho, Y. S., Lin, Y. J., et al. (2023). Surfactant protein D inhibits lipid-laden foamy macrophages and lung inflammation in chronic obstructive pulmonary disease. *Cell. Mol. Immunol.* 20 (1), 38–50. doi:10.1038/s41423-022-00946-2

Hu, M., Zhang, R., Yang, J., Zhao, C., Liu, W., Huang, Y., et al. (2023). The role of N-glycosylation modification in the pathogenesis of liver cancer. *Cell. Death Dis.* 14 (3), 222. doi:10.1038/s41419-023-05733-z

Huang, C., Hu, F., Song, D., Sun, X., Liu, A., Wu, Q., et al. (2022). EZH2-triggered methylation of SMAD3 promotes its activation and tumor metastasis. *J. Clin. Invest.* 132 (5), e152394. doi:10.1172/JCI152394

Hwang, I., Kim, J. W., Ylaya, K., Chung, E. J., Kitano, H., Perry, C., et al. (2020). Tumor-associated macrophage, angiogenesis and lymphangiogenesis markers predict prognosis of non-small cell lung cancer patients. *J. Transl. Med.* 18 (1), 443. doi:10.1186/s12967-020-02618-z

Im, J. H., Buzzelli, J. N., Jones, K., Franchini, F., Gordon-Weeks, A., Markelc, B., et al. (2020). FGF2 alters macrophage polarization, tumour immunity and growth and can be targeted during radiotherapy. *Nat. Commun.* 11 (1), 4064. doi:10.1038/s41467-020-17914-x

Irizarry-Caro, R. A., McDaniel, M. M., Overcast, G. R., Jain, V. G., Troutman, T. D., and Pasare, C. (2020). TLR signaling adapter BCAP regulates inflammatory to reparatory macrophage transition by promoting histone lactylation. *Proc. Natl. Acad. Sci. U. S. A.* 117 (48), 30628–30638. doi:10.1073/pnas.2009778117

Ishii, T., Mimura, I., Nagaoka, K., Naito, A., Sugasawa, T., Kuroda, R., et al. (2022). Effect of M2-like macrophages of the injured-kidney cortex on kidney cancer progression. *Cell. Death Discov.* 8 (1), 480. doi:10.1038/s41420-022-01255-3

Jaynes, J. M., Sable, R., Ronzetti, M., Bautista, W., Knotts, Z., Abisoye-Ogunniyan, A., et al. (2020). Mannose receptor (CD206) activation in tumor-associated macrophages enhances adaptive and innate antitumor immune responses. *Sci. Transl. Med.* 12 (530), eaax6337. doi:10.1126/scitranslmed.aax6337

Jeong, H., Kim, S., Hong, B. J., Lee, C. J., Kim, Y. E., Bok, S., et al. (2019). Tumor-associated macrophages enhance tumor hypoxia and aerobic glycolysis. *Cancer Res.* 79 (4), 795–806. doi:10.1158/0008-5472.CAN-18-2545

Jia, X., Yan, B., Tian, X., Liu, Q., Jin, J., Shi, J., et al. (2021). CD47/SIRPα pathway mediates cancer immune escape and immunotherapy. *Int. J. Biol. Sci.* 17 (13), 3281–3287. doi:10.7150/ijbs.60782

Jiang, P., Gao, W., Ma, T., Wang, R., Piao, Y., Dong, X., et al. (2019). CD137 promotes bone metastasis of breast cancer by enhancing the migration and osteoclast differentiation of monocytes/macrophages. *Theranostics* 9 (10), 2950–2966. doi:10.7150/thno.29617

Jin, M. Z., and Jin, W. L. (2020). The updated landscape of tumor microenvironment and drug repurposing. *Signal Transduct. Target Ther.* 5 (1), 166. doi:10.1038/s41392-020-00280-x

Johnston, R. J., Su, L. J., Pinckney, J., Critton, D., Boyer, E., Krishnakumar, A., et al. (2019). VISTA is an acidic pH-selective ligand for PSGL-1. *Nature* 574 (7779), 565–570. doi:10.1038/s41586-019-1674-5

Kaplanov, I., Carmi, Y., Kornetsky, R., Shemesh, A., Shurin, G. V., Shurin, M. R., et al. (2019). Blocking IL-1β reverses the immunosuppression in mouse breast cancer and synergizes with anti-PD-1 for tumor abrogation. *Proc. Natl. Acad. Sci. U. S. A.* 116 (4), 1361–1369. doi:10.1073/pnas.1812266115

Katzenelenbogen, Y., Sheban, F., Yalin, A., Yofe, I., Svetlichnyy, D., Jaitin, D. A., et al. (2020). Coupled scRNA-seq and intracellular protein activity reveal an immunosuppressive role of TREM2 in cancer. *Cell.* 182 (4), 872–885. doi:10.1016/j.cell.2020.06.032

Kawasaki, T., Ikegawa, M., Yunoki, K., Otani, H., Ori, D., Ishii, K. J., et al. (2022). Alveolar macrophages instruct CD8(+) T cell expansion by antigen cross-presentation in lung. *Cell. Rep.* 41 (11), 111828. doi:10.1016/j.celrep.2022.111828

Kennedy, A., Waters, E., Rowshanravan, B., Hinze, C., Williams, C., Janman, D., et al. (2022). Differences in CD80 and CD86 transendocytosis reveal CD86 as a key target for CTLA-4 immune regulation. *Nat. Immunol.* 23 (9), 1365–1378. doi:10.1038/s41590-022-01289-w

Kermanizadeh, A., Brown, D. M., Moritz, W., and Stone, V. (2019). The importance of inter-individual Kupffer cell variability in the governance of hepatic toxicity in a 3D primary human liver microtissue model. *Sci. Rep.* 9 (1), 7295. doi:10.1038/s41598-019-43870-8

Kesh, K., Gupta, V. K., Durden, B., Garrido, V., Mateo-Victoriano, B., Lavania, S. P., et al. (2020). Therapy resistance, cancer stem cells and ECM in cancer: the matrix reloaded. *Cancers (Basel)* 12 (10), 3067. doi:10.3390/cancers12103067

Kidwell, C. U., Casalini, J. R., Pradeep, S., Scherer, S. D., Greiner, D., Bayik, D., et al. (2023). Transferred mitochondria accumulate reactive oxygen species, promoting proliferation. *Elife* 12, e85494. doi:10.7554/eLife.85494

Kim, H., Wang, S. Y., Kwak, G., Yang, Y., Kwon, I. C., and Kim, S. H. (2019a). Exosome-guided phenotypic switch of M1 to M2 macrophages for cutaneous wound healing. *Adv. Sci. (Weinh)* 6 (20), 1900513. doi:10.1002/advs.201900513

Kim, H., Chung, H., Kim, J., Choi, D. H., Shin, Y., Kang, Y. G., et al. (2019b). Macrophages-Triggered sequential remodeling of endothelium-interstitial matrix to form pre-metastatic niche in microfluidic tumor microenvironment. *Adv. Sci. (Weinh)* 6 (11), 1900195. doi:10.1002/advs.201900195

Kim, S. H., Saeidi, S., Zhong, X., Gwak, S. Y., Muna, I. A., Park, S. A., et al. (2020). Breast cancer cell debris diminishes therapeutic efficacy through heme oxygenase-1-mediated inactivation of M1-like tumor-associated macrophages. *Neoplasia* 22 (11), 606–616. doi:10.1016/j.neo.2020.08.006

Kimura, S., Nanbu, U., Noguchi, H., Harada, Y., Kumamoto, K., Sasaguri, Y., et al. (2019). Macrophage CCL22 expression in the tumor microenvironment and implications for survival in patients with squamous cell carcinoma of the tongue. *J. Oral Pathol. Med.* 48 (8), 677–685. doi:10.1111/jop.12885

Klichinsky, M., Ruella, M., Shestova, O., Lu, X. M., Best, A., Zeeman, M., et al. (2020). Human chimeric antigen receptor macrophages for cancer immunotherapy. *Nat. Biotechnol.* 38 (8), 947–953. doi:10.1038/s41587-020-0462-y

Kohno, K., Koya-Miyata, S., Harashima, A., Tsukuda, T., Katakami, M., Ariyasu, T., et al. (2021). Inflammatory M1-like macrophages polarized by NK-4 undergo enhanced phenotypic switching to an anti-inflammatory M2-like phenotype upon co-culture with apoptotic cells. *J. Inflamm. (Lond)* 18 (1), 2. doi:10.1186/s12950-020-00267-z

Kraaij, M. D., Savage, N. D. L., van der Kooij, S. W., Koekkoek, K., Wang, J., van den Berg, J. M., et al. (2010). Induction of regulatory T cells by macrophages is dependent on production of reactive oxygen species. *Proc. Natl. Acad. Sci. U. S. A.* 107 (41), 17686–17691. doi:10.1073/pnas.1012016107

Kumar, R., Mickael, C., Kassa, B., Sanders, L., Hernandez-Saavedra, D., Koyanagi, D. E., et al. (2020). Interstitial macrophage-derived thrombospondin-1 contributes to hypoxia-induced pulmonary hypertension. *Cardiovasc Res.* 116 (12), 2021–2030. doi:10.1093/cvr/cvz304

La Fleur, L., Botling, J., He, F., Pelicano, C., Zhou, C., He, C., et al. (2021). Targeting MARCO and IL37R on immunosuppressive macrophages in lung cancer blocks regulatory T cells and supports cytotoxic lymphocyte function. *Cancer Res.* 81 (4), 956–967. doi:10.1158/0008-5472.CAN-20-1885

Lai, Y. S., Wahyuningtyas, R., Aui, S. P., and Chang, K. T. (2019). Autocrine VEGF signalling on M2 macrophages regulates PD-L1 expression for immunomodulation of T cells. *J. Cell. Mol. Med.* 23 (2), 1257–1267. doi:10.1111/jcmm.14027

Lazarova, M., and Steinle, A. (2019). Impairment of nkg2d-mediated tumor immunity by TGF-β. *Front. Immunol.* 10, 2689. doi:10.3389/fimmu.2019.02689

Lechner, A., Henkel, F. D. R., Hartung, F., Bohnacker, S., Alessandrini, F., Gubernatorova, E. O., et al. (2022). Macrophages acquire a TNF-dependent inflammatory memory in allergic asthma. *J. Allergy Clin. Immunol.* 149 (6), 2078–2090. doi:10.1016/j.jaci.2021.11.026

Lee, J., Son, W., Hong, J., Song, Y., Yang, C. S., and Kim, Y. H. (2021). Down-regulation of TNF-α via macrophage-targeted RNAi system for the treatment of acute inflammatory sepsis. *J. Control Release* 336, 344–353. doi:10.1016/j.jconrel.2021.06.022

Li, D., and Wu, M. (2021). Pattern recognition receptors in health and diseases. *Signal Transduct. Target Ther.* 6 (1), 291. doi:10.1038/s41392-021-00687-0

Li, F., Lv, B., Liu, Y., Hua, T., Han, J., Sun, C., et al. (2018). Blocking the CD47-SIRPα axis by delivery of anti-CD47 antibody induces antitumor effects in glioma and glioma stem cells. *Oncoimmunology* 7 (2), e1391973. doi:10.1080/2162402X.2017.1391973

Li, W., Zhang, X., Wu, F., Zhou, Y., Bao, Z., Li, H., et al. (2019a). Gastric cancer-derived mesenchymal stromal cells trigger M2 macrophage polarization that promotes metastasis and EMT in gastric cancer. *Cell. Death Dis.* 10 (12), 918. doi:10.1038/s41419-019-2131-y

Li, K., Yang, L., Li, J., Guan, C., Zhang, S., Lao, X., et al. (2019b). TGFβ induces stemness through non-canonical AKT-FOXO3a axis in oral squamous cell carcinoma. *EBioMedicine* 48, 70–80. doi:10.1016/j.ebiom.2019.09.027

Li, C., Xue, V. W., Wang, Q. M., Lian, G. Y., Huang, X. R., Lee, T. L., et al. (2020). The mincle/syk/NF-κB signaling circuit is essential for maintaining the protumoral activities of tumor-associated macrophages. *Cancer Immunol. Res.* 8 (8), 1004–1017. doi:10.1158/2326-6066.CIR-19-0782

Li, X., Su, X., Liu, R., Pan, Y., Fang, J., Cao, L., et al. (2021a). HDAC inhibition potentiates anti-tumor activity of macrophages and enhances anti-PD-L1-mediated tumor suppression. *Oncogene* 40 (10), 1836–1850. doi:10.1038/s41388-020-01636-x

Li, Y. R., Zhou, Y., Kim, Y. J., Zhu, Y., Ma, F., Yu, J., et al. (2021b). Development of allogeneic HSC-engineered iNKT cells for off-the-shelf cancer immunotherapy. *Cell. Rep. Med.* 2 (11), 100449. doi:10.1016/j.xcrm.2021.100449

Li, H., Yang, P., Wang, J., Zhang, J., Ma, Q., Jiang, Y., et al. (2022a). HLF regulates ferroptosis, development and chemoresistance of triple-negative breast cancer by activating tumor cell-macrophage crosstalk. *J. Hematol. Oncol.* 15 (1), 2. doi:10.1186/s13045-021-01223-x

Li, M., He, L., Zhu, J., Zhang, P., and Liang, S. (2022b). Targeting tumor-associated macrophages for cancer treatment. *Cell. Biosci.* 12 (1), 85. doi:10.1186/s13578-022-00823-5

Li, Y. R., Brown, J., Yu, Y., Lee, D., Zhou, K., Dunn, Z. S., et al. (2022c). Targeting immunosuppressive tumor-associated macrophages using innate T cells for enhanced antitumor reactivity. *Cancers (Basel)* 14 (11), 2749. doi:10.3390/cancers14112749

Li, Y. R., Dunn, Z. S., Yu, Y., Li, M., Wang, P., and Yang, L. (2023). Advancing cell-based cancer immunotherapy through stem cell engineering. *Cell. Stem Cell.* 30 (5), 592–610. doi:10.1016/j.stem.2023.02.009

Liang, S., Ma, H. Y., Zhong, Z., Dhar, D., Liu, X., Xu, J., et al. (2019). NADPH oxidase 1 in liver macrophages promotes inflammation and tumor development in mice. *Gastroenterology* 156 (4), 1156–1172. doi:10.1053/j.gastro.2018.11.019

Liang, N., Bing, Z., Wang, Y., Liu, X., Guo, C., Cao, L., et al. (2022). Clinical implications of EGFR-associated MAPK/ERK pathway in multiple primary lung cancer. *Clin. Transl. Med.* 12 (5), e847. doi:10.1002/ctm2.847

Lin, Y., Xu, J., and Lan, H. (2019). Tumor-associated macrophages in tumor metastasis: biological roles and clinical therapeutic applications. *J. Hematol. Oncol.* 12 (1), 76. doi:10.1186/s13045-019-0760-3

Lin, S. C., Liao, Y. C., Chen, P. M., Yang, Y. Y., Wang, Y. H., Tung, S. L., et al. (2022). Periostin promotes ovarian cancer metastasis by enhancing M2 macrophages and cancer-associated fibroblasts via integrin-mediated NF-κB and TGF-β2 signaling. *J. Biomed. Sci.* 29 (1), 109. doi:10.1186/s12929-022-00888-x

Lin, Y., Huang, S., Qi, Y., Xie, L., Jiang, J., Li, H., et al. (2023). PSGL-1 is a novel tumor microenvironment prognostic biomarker with cervical high-grade squamous lesions and more. *Front. Oncol.* 13, 1052201. doi:10.3389/fonc.2023.1052201

Liu, W., and Sun, Y. (2023). Epigenetics in glaucoma: a link between histone methylation and neurodegeneration. *J. Clin. Invest.* 133 (8), e173784. doi:10.1172/JCI173784

Liu, L., Zhang, L., Yang, L., Li, H., Li, R., Yu, J., et al. (2017). Anti-CD47 antibody as a targeted therapeutic agent for human lung cancer and cancer stem cells. *Front. Immunol.* 8, 404. doi:10.3389/fimmu.2017.00404

Liu, L., Ye, Y., and Zhu, X. (2019). MMP-9 secreted by tumor associated macrophages promoted gastric cancer metastasis through a PI3K/AKT/Snail pathway. *Biomed. Pharmacother.* 117, 109096. doi:10.1016/j.biopha.2019.109096

Liu, Y., Zugazagoitia, J., Ahmed, F. S., Henick, B. S., Gettinger, S. N., Herbst, R. S., et al. (2020). Immune cell PD-L1 colocalizes with macrophages and is associated with outcome in PD-1 pathway blockade therapy. *Clin. Cancer Res.* 26 (4), 970–977. doi:10.1158/1078-0432.CCR-19-1040

Liu, J., Geng, X., Hou, J., and Wu, G. (2021). New insights into M1/M2 macrophages: key modulators in cancer progression. *Cancer Cell. Int.* 21 (1), 389. doi:10.1186/s12935-021-02089-2

Liu, J. Q., Zhang, C., Zhang, X., Yan, J., Zeng, C., Talebian, F., et al. (2022). Intratumoral delivery of IL-12 and IL-27 mRNA using lipid nanoparticles for cancer immunotherapy. *J. Control Release* 345, 306–313. doi:10.1016/j.jconrel.2022.03.021

Liu, Z. L., Chen, H. H., Zheng, L. L., Sun, L. P., and Shi, L. (2023a). Angiogenic signaling pathways and anti-angiogenic therapy for cancer. *Signal Transduct. Target Ther.* 8 (1), 198. doi:10.1038/s41392-023-01460-1

Liu, H., Zhao, Q., Tan, L., Wu, X., Huang, R., Zuo, Y., et al. (2023b). Neutralizing IL-8 potentiates immune checkpoint blockade efficacy for glioma. *Cancer Cell.* 41 (4), 693–710 e8. doi:10.1016/j.ccell.2023.03.004

Liu, Y., Wang, Y., Yang, Y., Weng, L., Wu, Q., Zhang, J., et al. (2023c). Emerging phagocytosis checkpoints in cancer immunotherapy. *Signal Transduct. Target Ther.* 8 (1), 104. doi:10.1038/s41392-023-01365-z

Loeuillard, E., Yang, J., Buckarma, E., Wang, J., Liu, Y., Conboy, C., et al. (2020). Targeting tumor-associated macrophages and granulocytic myeloid-derived suppressor cells augments PD-1 blockade in cholangiocarcinoma. *J. Clin. Invest.* 130 (10), 5380–5396. doi:10.1172/JCI137110

Lopez de Andres, J., Griñán-Lisón, C., Jiménez, G., and Marchal, J. A. (2020). Cancer stem cell secretome in the tumor microenvironment: a key point for an effective personalized cancer treatment. *J. Hematol. Oncol.* 13 (1), 136. doi:10.1186/s13045-020-00966-3

Lu, C. Y., Santosa, K. B., Jablonka-Shariff, A., Vannucci, B., Fuchs, A., Turnbull, I., et al. (2020). Macrophage-derived vascular endothelial growth factor-A is integral to neuromuscular junction reinnervation after nerve injury. *J. Neurosci.* 40 (50), 9602–9616. doi:10.1523/JNEUROSCI.1736-20.2020

Lugano, R., Ramachandran, M., and Dimberg, A. (2020). Tumor angiogenesis: causes, consequences, challenges and opportunities. *Cell. Mol. Life Sci.* 77 (9), 1745–1770. doi:10.1007/s00018-019-03351-7

Lundahl, M. L. E., Mitermite, M., Ryan, D. G., Case, S., Williams, N. C., Yang, M., et al. (2022). Macrophage innate training induced by IL-4 and IL-13 activation enhances OXPHOS driven anti-mycobacterial responses. *Elife* 11, e74690. doi:10.7554/eLife.74690

Luo, W. J., Yu, S. L., Chang, C. C., Chien, M. H., Chang, Y. L., Liao, K. M., et al. (2022). HLJ1 amplifies endotoxin-induced sepsis severity by promoting IL-12 heterodimerization in macrophages. *Elife* 11, e76094. doi:10.7554/eLife.76094

Lv, W., Guo, H., Wang, J., Ma, R., Niu, L., and Shang, Y. (2023). PDLIM2 can inactivate the TGF-beta/Smad pathway to inhibit the malignant behavior of ovarian cancer cells. *Cell. Biochem. Funct.* 41, 542–552. doi:10.1002/cbf.3801

Maalej, K. M., Merhi, M., Inchakalody, V. P., Mestiri, S., Alam, M., Maccalli, C., et al. (2023). CAR-cell therapy in the era of solid tumor treatment: current challenges and emerging therapeutic advances. *Mol. Cancer* 22 (1), 20. doi:10.1186/s12943-023-01723-z

Maier, B., Leader, A. M., Chen, S. T., Tung, N., Chang, C., LeBerichel, J., et al. (2020). A conserved dendritic-cell regulatory program limits antitumour immunity. *Nature* 580 (7802), 257–262. doi:10.1038/s41586-020-2134-y

Maldonado, L. A. G., Nascimento, C. R., Rodrigues Fernandes, N. A., Silva, A. L. P., D'Silva, N. J., and Rossa, C., Jr (2022). Influence of tumor cell-derived TGF-β on macrophage phenotype and macrophage-mediated tumor cell invasion. *Int. J. Biochem. Cell. Biol.* 153, 106330. doi:10.1016/j.biocel.2022.106330

Mantovani, A., Allavena, P., Marchesi, F., and Garlanda, C. (2022). Macrophages as tools and targets in cancer therapy. *Nat. Rev. Drug Discov.* 21 (11), 799–820. doi:10.1038/s41573-022-00520-5

Marigo, I., Trovato, R., Hofer, F., Ingangi, V., Desantis, G., Leone, K., et al. (2020). Disabled homolog 2 controls prometastatic activity of tumor-associated macrophages. *Cancer Discov.* 10 (11), 1758–1773. doi:10.1158/2159-8290.CD-20-0036

Mascarau, R., Woottum, M., Fromont, L., Gence, R., Cantaloube-Ferrieu, V., Vahlas, Z., et al. (2023). Productive HIV-1 infection of tissue macrophages by fusion with infected CD4+ T cells. *J. Cell. Biol.* 222 (5), e202205103. doi:10.1083/jcb.202205103

Mattiola, I., Pesant, M., Tentorio, P. F., Molgora, M., Marcenaro, E., Lugli, E., et al. (2015). Priming of human resting NK cells by autologous M1 macrophages via the engagement of IL-1β, IFN-β, and IL-15 pathways. *J. Immunol.* 195 (6), 2818–2828. doi:10.4049/jimmunol.1500325

McCaw, T. R., Li, M., Starenki, D., Liu, M., Cooper, S. J., Arend, R. C., et al. (2019). Histone deacetylase inhibition promotes intratumoral CD8+ T-cell responses, sensitizing murine breast tumors to anti-PD1. *Cancer Immunol. Immunother.* 68 (12), 2081–2094. doi:10.1007/s00262-019-02430-9

Molgora, M., Esaulova, E., Vermi, W., Hou, J., Chen, Y., Luo, J., et al. (2020). TREM2 modulation remodels the tumor myeloid landscape enhancing anti-PD-1 immunotherapy. *Cell.* 182 (4), 886–900. doi:10.1016/j.cell.2020.07.013

Morhardt, T. L., Hayashi, A., Ochi, T., Quirós, M., Kitamoto, S., Nagao-Kitamoto, H., et al. (2019). IL-10 produced by macrophages regulates epithelial integrity in the small intestine. *Sci. Rep.* 9 (1), 1223. doi:10.1038/s41598-018-38125-x

Mosser, D. M., Hamidzadeh, K., and Goncalves, R. (2021). Macrophages and the maintenance of homeostasis. *Cell. Mol. Immunol.* 18 (3), 579–587. doi:10.1038/s41423-020-00541-3

Mouton, A. J., Aitken, N. M., Moak, S. P., do Carmo, J. M., da Silva, A. A., Omoto, A. C. M., et al. (2023). Temporal changes in glucose metabolism reflect polarization in resident and monocyte-derived macrophages after myocardial infarction. *Front. Cardiovasc Med.* 10, 1136252. doi:10.3389/fcvm.2023.1136252

Muniz-Bongers, L. R., McClain, C. B., Saxena, M., Bongers, G., Merad, M., and Bhardwaj, N. (2021). MMP2 and TLRs modulate immune responses in the tumor microenvironment. *JCI Insight* 6 (12), e144913. doi:10.1172/jci.insight.144913

Muraoka, D., Seo, N., Hayashi, T., Tahara, Y., Fujii, K., Tawara, I., et al. (2019). Antigen delivery targeted to tumor-associated macrophages overcomes tumor immune resistance. *J. Clin. Invest.* 129 (3), 1278–1294. doi:10.1172/JCI97642

Nagata, E., Masuda, H., Nakayama, T., Netsu, S., Yuzawa, H., Fujii, N., et al. (2019). Insufficient production of IL-10 from M2 macrophages impairs *in vitro* endothelial progenitor cell differentiation in patients with Moyamoya disease. *Sci. Rep.* 9 (1), 16752. doi:10.1038/s41598-019-53114-4

Nalio Ramos, R., Missolo-Koussou, Y., Gerber-Ferder, Y., Bromley, C. P., Bugatti, M., Núñez, N. G., et al. (2022). Tissue-resident FOLR2(+) macrophages associate with CD8(+) T cell infiltration in human breast cancer. *Cell.* 185 (7), 1189–1207 e25. doi:10.1016/j.cell.2022.02.021

Natale, G., and Bocci, G. (2023). Discovery and development of tumor angiogenesis assays. *Methods Mol. Biol.* 2572, 1–37. doi:10.1007/978-1-0716-2703-7_1

Nau, G. J., Richmond, J. F. L., Schlesinger, A., Jennings, E. G., Lander, E. S., and Young, R. A. (2002). Human macrophage activation programs induced by bacterial pathogens. *Proc. Natl. Acad. Sci. U. S. A.* 99 (3), 1503–1508. doi:10.1073/pnas.022649799

Neu, C., Thiele, Y., Horr, F., Beckers, C., Frank, N., Marx, G., et al. (2022). DAMPs released from proinflammatory macrophages induce inflammation in cardiomyocytes via activation of TLR4 and TNFR. *Int. J. Mol. Sci.* 23 (24), 15522. doi:10.3390/ijms232415522

Ning, Y., Cui, Y., Li, X., Cao, X., Chen, A., Xu, C., et al. (2018). Co-culture of ovarian cancer stem-like cells with macrophages induced SKOV3 cells stemness via IL-8/STAT3 signaling. *Biomed. Pharmacother.* 103, 262–271. doi:10.1016/j.biopha.2018.04.022

Nost, T. H., Alcala, K., Urbarova, I., Byrne, K. S., Guida, F., Sandanger, T. M., et al. (2021). Systemic inflammation markers and cancer incidence in the UK Biobank. *Eur. J. Epidemiol.* 36 (8), 841–848. doi:10.1007/s10654-021-00752-6

Ntokou, A., Dave, J. M., Kauffman, A. C., Sauler, M., Ryu, C., Hwa, J., et al. (2021). Macrophage-derived PDGF-B induces muscularization in murine and human pulmonary hypertension. *JCI Insight* 6 (6), e139067. doi:10.1172/jci.insight.139067

Nunez, S. Y., Ziblat, A., Secchiari, F., Torres, N. I., Sierra, J. M., Raffo Iraolagoitia, X. L., et al. (2018). Human M2 macrophages limit NK cell effector functions through secretion of TGF-beta and engagement of CD85j. *J. Immunol.* 200 (3), 1008–1015. doi:10.4049/jimmunol.1700737

O'Brien, S. A., Orf, J., Skrzypczynska, K. M., Tan, H., Kim, J., DeVoss, J., et al. (2021). Activity of tumor-associated macrophage depletion by CSF1R blockade is highly dependent on the tumor model and timing of treatment. *Cancer Immunol. Immunother.* 70 (8), 2401–2410. doi:10.1007/s00262-021-02861-3

Onal, S., Turker-Burhan, M., Bati-Ayaz, G., Yanik, H., and Pesen-Okvur, D. (2021). Breast cancer cells and macrophages in a paracrine-juxtacrine loop. *Biomaterials* 267, 120412. doi:10.1016/j.biomaterials.2020.120412

Orange, S. T., Leslie, J., Ross, M., Mann, D. A., and Wackerhage, H. (2023). The exercise IL-6 enigma in cancer. *Trends Endocrinol. Metab.* 34, 749–763. doi:10.1016/j.tem.2023.08.001

Pereira, J. A., Lanzar, Z., Clark, J. T., Hart, A. P., Douglas, B. B., Shallberg, L., et al. (2023). PD-1 and CTLA-4 exert additive control of effector regulatory T cells at homeostasis. *Front. Immunol.* 14, 997376. doi:10.3389/fimmu.2023.997376

Petty, A. J., Owen, D. H., Yang, Y., and Huang, X. (2021). Targeting tumor-associated macrophages in cancer immunotherapy. *Cancers (Basel)* 13 (21), 5318. doi:10.3390/cancers13215318

Pfefferle, M., Dubach, I. L., Buzzi, R. M., Dürst, E., Schulthess-Lutz, N., Baselgia, L., et al. (2023). Antibody-induced erythrophagocyte reprogramming of Kupffer cells prevents anti-CD40 cancer immunotherapy-associated liver toxicity. *J. Immunother. Cancer* 11 (1), e005718. doi:10.1136/jitc-2022-005718

Pfirschke, C., Zilionis, R., Engblom, C., Messemaker, M., Zou, A. E., Rickelt, S., et al. (2022). Macrophage-targeted therapy unlocks antitumoral cross-talk between ifnγ-secreting lymphocytes and IL12-producing dendritic cells. *Cancer Immunol. Res.* 10 (1), 40–55. doi:10.1158/2326-6066.CIR-21-0326

Piatakova, A., Polakova, I., Smahelova, J., Johari, S. D., Nunvar, J., and Smahel, M. (2021). Distinct responsiveness of tumor-associated macrophages to immunotherapy of tumors with different mechanisms of major histocompatibility complex class I downregulation. *Cancers (Basel)* 13 (12), 3057. doi:10.3390/cancers13123057

Pu, Y., and Ji, Q. (2022). Tumor-associated macrophages regulate PD-1/PD-L1 immunosuppression. *Front. Immunol.* 13, 874589. doi:10.3389/fimmu.2022.874589

Puig-Saus, C., Sennino, B., Peng, S., Wang, C. L., Pan, Z., Yuen, B., et al. (2023). Neoantigen-targeted CD8(+) T cell responses with PD-1 blockade therapy. *Nature* 615 (7953), 697–704. doi:10.1038/s41586-023-05787-1

Qi, Y. T., Jiang, H., Wu, W. T., Zhang, F. L., Tian, S. Y., Fan, W. T., et al. (2022). Homeostasis inside single activated phagolysosomes: quantitative and selective measurements of submillisecond dynamics of reactive oxygen and nitrogen species production with a nanoelectrochemical sensor. *J. Am. Chem. Soc.* 144 (22), 9723–9733. doi:10.1021/jacs.2c01857

Radharani, N. N. V., Yadav, A. S., Nimma, R., Kumar, T. V. S., Bulbule, A., Chanukuppa, V., et al. (2022). Tumor-associated macrophage derived IL-6 enriches cancer stem cell population and promotes breast tumor progression via Stat-3 pathway. *Cancer Cell. Int.* 22 (1), 122. doi:10.1186/s12935-022-02527-9

Rahabi, M., Jacquemin, G., Prat, M., Meunier, E., AlaEddine, M., Bertrand, B., et al. (2020). Divergent roles for macrophage C-type lectin receptors, dectin-1 and mannose receptors, in the intestinal inflammatory response. *Cell. Rep.* 30 (13), 4386–4398. doi:10.1016/j.celrep.2020.03.018

Rajamaki, K., Taira, A., Katainen, R., Välimäki, N., Kuosmanen, A., Plaketti, R. M., et al. (2021). Genetic and epigenetic characteristics of inflammatory bowel disease-associated colorectal cancer. *Gastroenterology* 161 (2), 592–607. doi:10.1053/j.gastro.2021.04.042

Rapp, M., Wintergerst, M. W. M., Kunz, W. G., Vetter, V. K., Knott, M. M. L., Lisowski, D., et al. (2019). CCL22 controls immunity by promoting regulatory T cell communication with dendritic cells in lymph nodes. *J. Exp. Med.* 216 (5), 1170–1181. doi:10.1084/jem.20170277

Ren, L., Yi, J., Yang, Y., Li, W., Zheng, X., Liu, J., et al. (2022). Systematic pan-cancer analysis identifies APOC1 as an immunological biomarker which regulates macrophage polarization and promotes tumor metastasis. *Pharmacol. Res.* 183, 106376. doi:10.1016/j.phrs.2022.106376

Revu, S., Wu, J., Henkel, M., Rittenhouse, N., Menk, A., Delgoffe, G. M., et al. (2018). IL-23 and IL-1β drive human Th17 cell differentiation and metabolic reprogramming in absence of CD28 costimulation. *Cell. Rep.* 22 (10), 2642–2653. doi:10.1016/j.celrep.2018.02.044

Roda, J. M., Wang, Y., Sumner, L. A., Phillips, G. S., Marsh, C. B., and Eubank, T. D. (2012). Stabilization of HIF-2α induces sVEGFR-1 production from tumor-associated macrophages and decreases tumor growth in a murine melanoma model. *J. Immunol.* 189 (6), 3168–3177. doi:10.4049/jimmunol.1103817

Rodriguez-Garcia, A., Lynn, R. C., Poussin, M., Eiva, M. A., Shaw, L. C., O'Connor, R. S., et al. (2021). CAR-T cell-mediated depletion of immunosuppressive tumor-associated macrophages promotes endogenous antitumor immunity and augments adoptive immunotherapy. *Nat. Commun.* 12 (1), 877. doi:10.1038/s41467-021-20893-2

Romagnani, P., Lasagni, L., Annunziato, F., Serio, M., and Romagnani, S. (2004). CXC chemokines: the regulatory link between inflammation and angiogenesis. *Trends Immunol.* 25 (4), 201–209. doi:10.1016/j.it.2004.02.006

Ruiz-Blazquez, P., Pistorio, V., Fernández-Fernández, M., and Moles, A. (2021). The multifaceted role of cathepsins in liver disease. *J. Hepatol.* 75 (5), 1192–1202. doi:10.1016/j.jhep.2021.06.031

Sa, J. K., Chang, N., Lee, H. W., Cho, H. J., Ceccarelli, M., Cerulo, L., et al. (2020). Transcriptional regulatory networks of tumor-associated macrophages that drive malignancy in mesenchymal glioblastoma. *Genome Biol.* 21 (1), 216. doi:10.1186/s13059-020-02140-x

Sahraei, M., Chaube, B., Liu, Y., Sun, J., Kaplan, A., Price, N. L., et al. (2019). Suppressing miR-21 activity in tumor-associated macrophages promotes an antitumor immune response. *J. Clin. Invest.* 129 (12), 5518–5536. doi:10.1172/JCI127125

Sakama, S., Kurusu, K., Morita, M., Oizumi, T., Masugata, S., Oka, S., et al. (2021). An enriched environment alters DNA repair and inflammatory responses after radiation exposure. *Front. Immunol.* 12, 760322. doi:10.3389/fimmu.2021.760322

Sanchez-Paulete, A. R., Mateus-Tique, J., Mollaoglu, G., Nielsen, S. R., Marks, A., Lakshmi, A., et al. (2022). Targeting macrophages with CAR T cells delays solid tumor progression and enhances antitumor immunity. *Cancer Immunol. Res.* 10 (11), 1354–1369. doi:10.1158/2326-6066.CIR-21-1075

Saraiva, M., Vieira, P., and O'Garra, A. (2020). Biology and therapeutic potential of interleukin-10. *J. Exp. Med.* 217 (1), e20190418. doi:10.1084/jem.20190418

Scavuzzi, B. M., van Drongelen, V., and Holoshitz, J. (2022). HLA-G and the MHC cusp theory. *Front. Immunol.* 13, 814967. doi:10.3389/fimmu.2022.814967

Schaaf, M. B., Garg, A. D., and Agostinis, P. (2018). Defining the role of the tumor vasculature in antitumor immunity and immunotherapy. *Cell. Death Dis.* 9 (2), 115. doi:10.1038/s41419-017-0061-0

Schito, L., and Rey, S. (2020). Hypoxia: turning vessels into vassals of cancer immunotolerance. *Cancer Lett.* 487, 74–84. doi:10.1016/j.canlet.2020.05.015

Serbulea, V., Upchurch, C. M., Ahern, K. W., Bories, G., Voigt, P., DeWeese, D. E., et al. (2018). Macrophages sensing oxidized DAMPs reprogram their metabolism to support redox homeostasis and inflammation through a TLR2-Syk-ceramide dependent mechanism. *Mol. Metab.* 7, 23–34. doi:10.1016/j.molmet.2017.11.002

Sharma, N., Atolagbe, O. T., Ge, Z., and Allison, J. P. (2021). LILRB4 suppresses immunity in solid tumors and is a potential target for immunotherapy. *J. Exp. Med.* 218 (7), e20201811. doi:10.1084/jem.20201811

She, L., Qin, Y., Wang, J., Liu, C., Zhu, G., Li, G., et al. (2018). Tumor-associated macrophages derived CCL18 promotes metastasis in squamous cell carcinoma of the head and neck. *Cancer Cell. Int.* 18, 120. doi:10.1186/s12935-018-0620-1

Shepherd, A. J., Mickle, A. D., Golden, J. P., Mack, M. R., Halabi, C. M., de Kloet, A. D., et al. (2018). Macrophage angiotensin II type 2 receptor triggers neuropathic pain. *Proc. Natl. Acad. Sci. U. S. A.* 115 (34), E8057–E8066. doi:10.1073/pnas.1721815115

Shi, Q., Shen, Q., Liu, Y., Shi, Y., Huang, W., Wang, X., et al. (2022). Increased glucose metabolism in TAMs fuels O-GlcNAcylation of lysosomal Cathepsin B to promote cancer metastasis and chemoresistance. *Cancer Cell.* 40 (10), 1207–1222 e10. doi:10.1016/j.ccell.2022.08.012

Shinchi, Y., Ishizuka, S., Komohara, Y., Matsubara, E., Mito, R., Pan, C., et al. (2022). The expression of PD-1 ligand 1 on macrophages and its clinical impacts and mechanisms in lung adenocarcinoma. *Cancer Immunol. Immunother.* 71 (11), 2645–2661. doi:10.1007/s00262-022-03187-4

Simonetta, F., Lohmeyer, J. K., Hirai, T., Maas-Bauer, K., Alvarez, M., Wenokur, A. S., et al. (2021). Allogeneic CAR invariant natural killer T cells exert potent antitumor effects through host CD8 T-cell cross-priming. *Clin. Cancer Res.* 27 (21), 6054–6064. doi:10.1158/1078-0432.CCR-21-1329

Siu, L. L., Wang, D., Hilton, J., Geva, R., Rasco, D., Perets, R., et al. (2022). Correction: first-in-Class anti-immunoglobulin-like transcript 4 myeloid-specific antibody MK-

4830 abrogates a PD-1 resistance mechanism in patients with advanced solid tumors. *Clin. Cancer Res.* 28 (8), 1734. doi:10.1158/1078-0432.CCR-22-0564

Stanley, E. R., and Chitu, V. (2014). CSF-1 receptor signaling in myeloid cells. *Cold Spring Harb. Perspect. Biol.* 6 (6), a021857. doi:10.1101/cshperspect.a021857

Su, C., Zhang, J., Yarden, Y., and Fu, L. (2021). The key roles of cancer stem cell-derived extracellular vesicles. *Signal Transduct. Target Ther.* 6 (1), 109. doi:10.1038/s41392-021-00499-2

Sumitomo, R., Hirai, T., Fujita, M., Murakami, H., Otake, Y., and Huang, C. L. (2019). PD-L1 expression on tumor-infiltrating immune cells is highly associated with M2 TAM and aggressive malignant potential in patients with resected non-small cell lung cancer. *Lung Cancer* 136, 136–144. doi:10.1016/j.lungcan.2019.08.023

Sun, L., Wang, Q., Chen, B., Zhao, Y., Shen, B., Wang, H., et al. (2018). Gastric cancer mesenchymal stem cells derived IL-8 induces PD-L1 expression in gastric cancer cells via STAT3/mTOR-c-Myc signal axis. *Cell. Death Dis.* 9 (9), 928. doi:10.1038/s41419-018-0988-9

Taban, Q., Mumtaz, P. T., Masoodi, K. Z., Haq, E., and Ahmad, S. M. (2022). Scavenger receptors in host defense: from functional aspects to mode of action. *Cell. Commun. Signal* 20 (1), 2. doi:10.1186/s12964-021-00812-0

Taki, M., Abiko, K., Baba, T., Hamanishi, J., Yamaguchi, K., Murakami, R., et al. (2018). Snail promotes ovarian cancer progression by recruiting myeloid-derived suppressor cells via CXCR2 ligand upregulation. *Nat. Commun.* 9 (1), 1685. doi:10.1038/s41467-018-03966-7

Tan, I. L., Arifa, R. D. N., Rallapalli, H., Kana, V., Lao, Z., Sanghrajka, R. M., et al. (2021). CSF1R inhibition depletes tumor-associated macrophages and attenuates tumor progression in a mouse sonic Hedgehog-Medulloblastoma model. *Oncogene* 40 (2), 396–407. doi:10.1038/s41388-020-01536-0

Tang, P. M., Zhou, S., Meng, X. M., Wang, Q. M., Li, C. J., Lian, G. Y., et al. (2017). Smad3 promotes cancer progression by inhibiting E4BP4-mediated NK cell development. *Nat. Commun.* 8, 14677. doi:10.1038/ncomms14677

Tang, P. M., Nikolic-Paterson, D. J., and Lan, H. Y. (2019). Macrophages: versatile players in renal inflammation and fibrosis. *Nat. Rev. Nephrol.* 15 (3), 144–158. doi:10.1038/s41581-019-0110-2

Tang, P. M., Zhang, Y. Y., Xiao, J., Tang, P., Chung, J. Y. F., Li, J., et al. (2020). Neural transcription factor Pou4f1 promotes renal fibrosis via macrophage-myofibroblast transition. *Proc. Natl. Acad. Sci. U. S. A.* 117 (34), 20741–20752. doi:10.1073/pnas.1917663117

Tang, P. M., Zhang, Y. Y., Hung, J. S. C., Chung, J. Y. F., Huang, X. R., To, K. F., et al. (2021a). DPP4/CD32b/NF-κB circuit: a novel druggable target for inhibiting CRP-driven diabetic nephropathy. *Mol. Ther.* 29 (1), 365–375. doi:10.1016/j.ymthe.2020.08.017

Tang, P. C., Chung, J. Y. F., Xue, V. W. W., Xiao, J., Meng, X. M., Huang, X. R., et al. (2021b). Smad3 promotes cancer-associated fibroblasts generation via macrophage-myofibroblast transition. *Adv. Sci. (Weinh)* 9, e2101235. doi:10.1002/advs.202101235

Tang, P. C., Chung, J. Y. F., Xue, V. W. W., Xiao, J., Meng, X. M., Huang, X. R., et al. (2022a). Smad3 promotes cancer-associated fibroblasts generation via macrophage-myofibroblast transition. *Adv. Sci. (Weinh)* 9 (1), e2101235. doi:10.1002/advs.202101235

Tang, P. C., Chung, J. Y. F., Liao, J., Chan, M. K. K., Chan, A. S. W., Cheng, G., et al. (2022b). Single-cell RNA sequencing uncovers a neuron-like macrophage subset associated with cancer pain. *Sci. Adv.* 8 (40), eabn5535. doi:10.1126/sciadv.abn5535

Tang, X. X., Shimada, H., and Ikegaki, N. (2022c). Macrophage-mediated anti-tumor immunity against high-risk neuroblastoma. *Genes Immun.* 23 (3-4), 129–140. doi:10.1038/s41435-022-00172-w

Tang, P. C., Zhang, Y. Y., Li, J. S. F., Chan, M., Chen, J., Tang, Y., et al. (2022d). LncRNA-dependent mechanisms of transforming growth factor-β: from tissue fibrosis to cancer progression. *Noncoding RNA* 8 (3), 36. doi:10.3390/ncrna8030036

Taniguchi, S., Elhance, A., Van Duzer, A., Kumar, S., Leitenberger, J. J., and Oshimori, N. (2020). Tumor-initiating cells establish an IL-33-TGF-β niche signaling loop to promote cancer progression. *Science* 369 (6501), eaay1813. doi:10.1126/science.aay1813

Tanito, K., Nii, T., Yokoyama, Y., Oishi, H., Shibata, M., Hijii, S., et al. (2023). Engineered macrophages acting as a trigger to induce inflammation only in tumor tissues. *J. Control Release* 361, 885–895. doi:10.1016/j.jconrel.2023.04.010

Teng, K. Y., Han, J., Zhang, X., Hsu, S. H., He, S., Wani, N. A., et al. (2017). Blocking the CCL2-CCR2 Axis using CCL2-neutralizing antibody is an effective therapy for hepatocellular cancer in a mouse model. *Mol. Cancer Ther.* 16 (2), 312–322. doi:10.1158/1535-7163.MCT-16-0124

Tian, K., Du, G., Wang, X., Wu, X., Li, L., Liu, W., et al. (2022). MMP-9 secreted by M2-type macrophages promotes Wilms' tumour metastasis through the PI3K/AKT pathway. *Mol. Biol. Rep.* 49 (5), 3469–3480. doi:10.1007/s11033-022-07184-9

Tiwari, J. K., Negi, S., Kashyap, M., Nizamuddin, S., Singh, A., and Khattri, A. (2021). Pan-cancer analysis shows enrichment of macrophages, overexpression of checkpoint molecules, inhibitory cytokines, and immune exhaustion signatures in EMT-high tumors. *Front. Oncol.* 11, 793881. doi:10.3389/fonc.2021.793881

Tlili, A., Pintard, C., Hurtado-Nedelec, M., Liu, D., Marzaioli, V., Thieblemont, N., et al. (2023). ROCK2 interacts with p22phox to phosphorylate p47phox and to control NADPH oxidase activation in human monocytes. *Proc. Natl. Acad. Sci. U. S. A.* 120 (3), e2209184120. doi:10.1073/pnas.2209184120

Tomlins, S. A., Khazanov, N. A., Bulen, B. J., Hovelson, D. H., Shreve, M. J., Lamb, L. E., et al. (2023). Development and validation of an integrative pan-solid tumor predictor of PD-1/PD-L1 blockade benefit. *Commun. Med. (Lond)* 3 (1), 14. doi:10.1038/s43856-023-00243-7

Trzupek, D., Dunstan, M., Cutler, A. J., Lee, M., Godfrey, L., Jarvis, L., et al. (2020). Discovery of CD80 and CD86 as recent activation markers on regulatory T cells by protein-RNA single-cell analysis. *Genome Med.* 12 (1), 55. doi:10.1186/s13073-020-00756-z

Tu, M. M., Abdel-Hafiz, H. A., Jones, R. T., Jean, A., Hoff, K. J., Duex, J. E., et al. (2020). Inhibition of the CCL2 receptor, CCR2, enhances tumor response to immune checkpoint therapy. *Commun. Biol.* 3 (1), 720. doi:10.1038/s42003-020-01441-y

Tu, M., Klein, L., Espinet, E., Georgomanolis, T., Wegwitz, F., Li, X., et al. (2021a). TNF-α-producing macrophages determine subtype identity and prognosis via AP1 enhancer reprogramming in pancreatic cancer. *Nat. Cancer* 2 (11), 1185–1203. doi:10.1038/s43018-021-00258-w

Tu, D., Dou, J., Wang, M., Zhuang, H., and Zhang, X. (2021b). M2 macrophages contribute to cell proliferation and migration of breast cancer. *Cell. Biol. Int.* 45 (4), 831–838. doi:10.1002/cbin.11528

Turrell, F. K., Orha, R., Guppy, N. J., Gillespie, A., Guelbert, M., Starling, C., et al. (2023). Age-associated microenvironmental changes highlight the role of PDGF-C in ER(+) breast cancer metastatic relapse. *Nat. Cancer* 4 (4), 468–484. doi:10.1038/s43018-023-00525-y

van der Sluis, T. C., Beyrend, G., van der Gracht, E. T. I., Abdelaal, T., Jochems, S. P., Belderbos, R. A., et al. (2023). OX40 agonism enhances PD-L1 checkpoint blockade by shifting the cytotoxic T cell differentiation spectrum. *Cell. Rep. Med.* 4 (3), 100939. doi:10.1016/j.xcrm.2023.100939

van Elsas, M. J., Labrie, C., Etzerodt, A., Charoentong, P., van Stigt Thans, J. J. C., Van Hall, T., et al. (2023). Invasive margin tissue-resident macrophages of high CD163 expression impede responses to T cell-based immunotherapy. *J. Immunother. Cancer* 11 (3), e006433. doi:10.1136/jitc-2022-006433

Vayrynen, J. P., Haruki, K., Lau, M. C., Väyrynen, S. A., Zhong, R., Dias Costa, A., et al. (2021). The prognostic role of macrophage polarization in the colorectal cancer microenvironment. *Cancer Immunol. Res.* 9 (1), 8–19. doi:10.1158/2326-6066.CIR-20-0527

Vidyarthi, A., Khan, N., Agnihotri, T., Negi, S., Das, D. K., Aqdas, M., et al. (2018). TLR-3 stimulation skews M2 macrophages to M1 through IFN-αβ signaling and restricts tumor progression. *Front. Immunol.* 9, 1650. doi:10.3389/fimmu.2018.01650

Viitala, M., Virtakoivu, R., Tadayon, S., Rannikko, J., Jalkanen, S., and Hollmén, M. (2019). Immunotherapeutic blockade of macrophage clever-1 reactivates the CD8+ T-cell response against immunosuppressive tumors. *Clin. Cancer Res.* 25 (11), 3289–3303. doi:10.1158/1078-0432.CCR-18-3016

Virtakoivu, R., Rannikko, J. H., Viitala, M., Vaura, F., Takeda, A., Lönnberg, T., et al. (2021). Systemic blockade of clever-1 elicits lymphocyte activation alongside checkpoint molecule downregulation in patients with solid tumors: results from a phase I/II clinical trial. *Clin. Cancer Res.* 27 (15), 4205–4220. doi:10.1158/1078-0432.CCR-20-4862

Wang, X., and Khalil, R. A. (2018). Matrix metalloproteinases, vascular remodeling, and vascular disease. *Adv. Pharmacol.* 81, 241–330. doi:10.1016/bs.apha.2017.08.002

Wang, H., Sun, Y., Zhou, X., Chen, C., Jiao, L., Li, W., et al. (2020). CD47/SIRPα blocking peptide identification and synergistic effect with irradiation for cancer immunotherapy. *J. Immunother. Cancer* 8 (2), e000905. doi:10.1136/jitc-2020-000905

Wang, Z., Guan, D., Huo, J., Biswas, S. K., Huang, Y., Yang, Y., et al. (2021a). IL-10 enhances human natural killer cell effector functions via metabolic reprogramming regulated by mTORC1 signaling. *Front. Immunol.* 12, 619195. doi:10.3389/fimmu.2021.619195

Wang, G., Xu, D., Zhang, Z., Li, X., Shi, J., Sun, J., et al. (2021b). The pan-cancer landscape of crosstalk between epithelial-mesenchymal transition and immune evasion relevant to prognosis and immunotherapy response. *NPJ Precis. Oncol.* 5 (1), 56. doi:10.1038/s41698-021-00200-4

Wang, K., Donnelly, C. R., Jiang, C., Liao, Y., Luo, X., Tao, X., et al. (2021c). STING suppresses bone cancer pain via immune and neuronal modulation. *Nat. Commun.* 12 (1), 4558. doi:10.1038/s41467-021-24867-2

Wang, S., Yang, Y., Ma, P., Zha, Y., Zhang, J., Lei, A., et al. (2022). CAR-macrophage: an extensive immune enhancer to fight cancer. *EBioMedicine* 76, 103873. doi:10.1016/j.ebiom.2022.103873

Wang, C., Barnoud, C., Cenerenti, M., Sun, M., Caffa, I., Kizil, B., et al. (2023). Dendritic cells direct circadian anti-tumour immune responses. *Nature* 614 (7946), 136–143. doi:10.1038/s41586-022-05605-0

Wei, Z., Oh, J., Flavell, R. A., and Crawford, J. M. (2022). LACC1 bridges NOS2 and polyamine metabolism in inflammatory macrophages. *Nature* 609 (7926), 348–353. doi:10.1038/s41586-022-05111-3

Wen, Y., Lambrecht, J., Ju, C., and Tacke, F. (2021). Hepatic macrophages in liver homeostasis and diseases-diversity, plasticity and therapeutic opportunities. *Cell. Mol. Immunol.* 18 (1), 45–56. doi:10.1038/s41423-020-00558-8

Willingham, S. B., Volkmer, J. P., Gentles, A. J., Sahoo, D., Dalerba, P., Mitra, S. S., et al. (2012). The CD47-signal regulatory protein alpha (SIRPa) interaction is a therapeutic target for human solid tumors. *Proc. Natl. Acad. Sci. U. S. A.* 109 (17), 6662–6667. doi:10.1073/pnas.1121623109

Winkler, J., Abisoye-Ogunniyan, A., Metcalf, K. J., and Werb, Z. (2020). Concepts of extracellular matrix remodelling in tumour progression and metastasis. *Nat. Commun.* 11 (1), 5120. doi:10.1038/s41467-020-18794-x

Wu, H., Zhong, Z., Wang, A., Yuan, C., Ning, K., Hu, H., et al. (2020a). LncRNA FTX represses the progression of non-alcoholic fatty liver disease to hepatocellular carcinoma via regulating the M1/M2 polarization of Kupffer cells. *Cancer Cell. Int.* 20, 266. doi:10.1186/s12935-020-01354-0

Wu, J., Yang, H., Cheng, J., Zhang, L., Ke, Y., Zhu, Y., et al. (2020b). Knockdown of milk-fat globule EGF factor-8 suppresses glioma progression in GL261 glioma cells by repressing microglial M2 polarization. *J. Cell. Physiol.* 235 (11), 8679–8690. doi:10.1002/jcp.29712

Wu, X., Wang, Z., Shi, J., Yu, X., Li, C., Liu, J., et al. (2022a). Macrophage polarization toward M1 phenotype through NF-κB signaling in patients with Behçet's disease. *Arthritis Res. Ther.* 24 (1), 249. doi:10.1186/s13075-022-02938-z

Wu, M., Zhang, X., Zhang, W., Chiou, Y. S., Qian, W., Liu, X., et al. (2022b). Cancer stem cell regulated phenotypic plasticity protects metastasized cancer cells from ferroptosis. *Nat. Commun.* 13 (1), 1371. doi:10.1038/s41467-022-29018-9

Wu, B., Shi, X., Jiang, M., and Liu, H. (2023). Cross-talk between cancer stem cells and immune cells: potential therapeutic targets in the tumor immune microenvironment. *Mol. Cancer* 22 (1), 38. doi:10.1186/s12943-023-01748-4

Xia, Q., Jia, J., Hu, C., Lu, J., Li, J., Xu, H., et al. (2022). Tumor-associated macrophages promote PD-L1 expression in tumor cells by regulating PKM2 nuclear translocation in pancreatic ductal adenocarcinoma. *Oncogene* 41 (6), 865–877. doi:10.1038/s41388-021-02133-5

Xiao, L., He, Y., Peng, F., Yang, J., and Yuan, C. (2020). Endometrial cancer cells promote M2-like macrophage polarization by delivering exosomal miRNA-21 under hypoxia condition. *J. Immunol. Res.* 2020, 9731049. doi:10.1155/2020/9731049

Xie, Y., Chen, Z., Zhong, Q., Zheng, Z., Chen, Y., Shangguan, W., et al. (2021). M2 macrophages secrete CXCL13 to promote renal cell carcinoma migration, invasion, and EMT. *Cancer Cell. Int.* 21 (1), 677. doi:10.1186/s12935-021-02381-1

Xie, T., Fu, D. J., Li, Z. M., Lv, D. J., Song, X. L., Yu, Y. Z., et al. (2022). CircSMARCC1 facilitates tumor progression by disrupting the crosstalk between prostate cancer cells and tumor-associated macrophages via miR-1322/CCL20/CCR6 signaling. *Mol. Cancer* 21 (1), 173. doi:10.1186/s12943-022-01630-9

Xu, M., Wang, X., Li, Y., Geng, X., Jia, X., Zhang, L., et al. (2021a). Arachidonic acid metabolism controls macrophage alternative activation through regulating oxidative phosphorylation in PPARγ dependent manner. *Front. Immunol.* 12, 618501. doi:10.3389/fimmu.2021.618501

Xu, M., Wang, Y., Xia, R., Wei, Y., and Wei, X. (2021b). Role of the CCL2-CCR2 signalling axis in cancer: mechanisms and therapeutic targeting. *Cell. Prolif.* 54 (10), e13115. doi:10.1111/cpr.13115

Xu, Y., Zeng, H., Jin, K., Liu, Z., Zhu, Y., Xu, L., et al. (2022). Immunosuppressive tumor-associated macrophages expressing interlukin-10 conferred poor prognosis and therapeutic vulnerability in patients with muscle-invasive bladder cancer. *J. Immunother. Cancer* 10 (3), e003416. doi:10.1136/jitc-2021-003416

Xue, V. W., Chung, J. Y. F., Tang, P. C. T., Chan, A. S. W., To, T. H. W., Chung, J. S. Y., et al. (2021). USMB-shMincle: a virus-free gene therapy for blocking M1/M2 polarization of tumor-associated macrophages. *Mol. Ther. Oncolytics* 23, 26–37. doi:10.1016/j.omto.2021.08.010

Yang, H. D., Kim, H. S., Kim, S. Y., Na, M. J., Yang, G., Eun, J. W., et al. (2019). HDAC6 suppresses let-7i-5p to elicit TSP1/CD47-mediated anti-tumorigenesis and phagocytosis of hepatocellular carcinoma. *Hepatology* 70 (4), 1262–1279. doi:10.1002/hep.30657

Yang, L., Shi, P., Zhao, G., Xu, J., Peng, W., Zhang, J., et al. (2020). Targeting cancer stem cell pathways for cancer therapy. *Signal Transduct. Target Ther.* 5 (1), 8. doi:10.1038/s41392-020-0110-5

Yang, K., Xie, Y., Xue, L., Li, F., Luo, C., Liang, W., et al. (2023a). M2 tumor-associated macrophage mediates the maintenance of stemness to promote cisplatin resistance by secreting TGF-β1 in esophageal squamous cell carcinoma. *J. Transl. Med.* 21 (1), 26. doi:10.1186/s12967-022-03863-0

Yang, Q., Dai, H., Cheng, Y., Wang, B., Xu, J., Zhang, Y., et al. (2023b). Oral feeding of nanoplastics affects brain function of mice by inducing macrophage IL-1 signal in the intestine. *Cell. Rep.* 42 (4), 112346. doi:10.1016/j.celrep.2023.112346

Yao, R. R., Li, J. H., Zhang, R., Chen, R. X., and Wang, Y. H. (2018). M2-polarized tumor-associated macrophages facilitated migration and epithelial-mesenchymal transition of HCC cells via the TLR4/STAT3 signaling pathway. *World J. Surg. Oncol.* 16 (1), 9. doi:10.1186/s12957-018-1312-y

Yao, Y., Zhang, T., Ru, X., Qian, J., Tong, Z., Li, X., et al. (2020). Constitutively expressed MHC class Ib molecules regulate macrophage M2b polarization and sepsis severity in irradiated mice. *J. Leukoc. Biol.* 107 (3), 445–453. doi:10.1002/JLB.1AB1219-125RR

Yau, E., Yang, L., Chen, Y., Umstead, T. M., Atkins, H., Katz, Z. E., et al. (2023). Surfactant protein A alters endosomal trafficking of influenza A virus in macrophages. *Front. Immunol.* 14, 919800. doi:10.3389/fimmu.2023.919800

Yen, J. H., Huang, W. C., Lin, S. C., Huang, Y. W., Chio, W. T., Tsay, G. J., et al. (2022). Metabolic remodeling in tumor-associated macrophages contributing to antitumor activity of cryptotanshinone by regulating TRAF6-ASK1 axis. *Mol. Ther. Oncolytics* 26, 158–174. doi:10.1016/j.omto.2022.06.008

Yogev, N., Bedke, T., Kobayashi, Y., Brockmann, L., Lukas, D., Regen, T., et al. (2022). CD4(+) T-cell-derived IL-10 promotes CNS inflammation in mice by sustaining effector T cell survival. *Cell. Rep.* 38 (13), 110565. doi:10.1016/j.celrep.2022.110565

Yu, L., Yang, F., Zhang, F., Guo, D., Li, L., Wang, X., et al. (2018). CD69 enhances immunosuppressive function of regulatory T-cells and attenuates colitis by prompting IL-10 production. *Cell. Death Dis.* 9 (9), 905. doi:10.1038/s41419-018-0927-9

Yu, Y., Ke, L., Xia, W. X., Xiang, Y., Lv, X., and Bu, J. (2019). Elevated levels of TNF-α and decreased levels of CD68-positive macrophages in primary tumor tissues are unfavorable for the survival of patients with nasopharyngeal carcinoma. *Technol. Cancer Res. Treat.* 18, 1533033819874807. doi:10.1177/1533033819874807

Yu, Q., Wang, Y., Dong, L., He, Y., Liu, R., Yang, Q., et al. (2020). Regulations of glycolytic activities on macrophages functions in tumor and infectious inflammation. *Front. Cell. Infect. Microbiol.* 10, 287. doi:10.3389/fcimb.2020.00287

Yuan, S., Stewart, K. S., Yang, Y., Abdusselamoglu, M. D., Parigi, S. M., Feinberg, T. Y., et al. (2022). Ras drives malignancy through stem cell crosstalk with the microenvironment. *Nature* 612 (7940), 555–563. doi:10.1038/s41586-022-05475-6

Zappasodi, R., Serganova, I., Cohen, I. J., Maeda, M., Shindo, M., Senbabaoglu, Y., et al. (2021). CTLA-4 blockade drives loss of T(reg) stability in glycolysis-low tumours. *Nature* 591 (7851), 652–658. doi:10.1038/s41586-021-03326-4

Zeng, X. Y., Xie, H., Yuan, J., Jiang, X. Y., Yong, J. H., Zeng, D., et al. (2019). M2-like tumor-associated macrophages-secreted EGF promotes epithelial ovarian cancer metastasis via activating EGFR-ERK signaling and suppressing lncRNA LIMT expression. *Cancer Biol. Ther.* 20 (7), 956–966. doi:10.1080/15384047.2018.1564567

Zhang, F., Parayath, N. N., Ene, C. I., Stephan, S. B., Koehne, A. L., Coon, M. E., et al. (2019). Genetic programming of macrophages to perform anti-tumor functions using targeted mRNA nanocarriers. *Nat. Commun.* 10 (1), 3974. doi:10.1038/s41467-019-11911-5

Zhang, F., Mears, J. R., Shakib, L., Beynor, J. I., Shanaj, S., Korsunsky, I., et al. (2021a). IFN-γ and TNF-α drive a CXCL10+ CCL2+ macrophage phenotype expanded in severe COVID-19 lungs and inflammatory diseases with tissue inflammation. *Genome Med.* 13 (1), 64. doi:10.1186/s13073-021-00881-3

Zhang, B., Zhang, Y., Jiang, X., Su, H., Wang, Q., Wudu, M., et al. (2021b). JMJD8 promotes malignant progression of lung cancer by maintaining EGFR stability and EGFR/PI3K/AKT pathway activation. *J. Cancer* 12 (4), 976–987. doi:10.7150/jca.50234

Zhang, S., Rautela, J., Bediaga, N. G., Kolesnik, T. B., You, Y., Nie, J., et al. (2023). CIS controls the functional polarization of GM-CSF-derived macrophages. *Cell. Mol. Immunol.* 20 (1), 65–79. doi:10.1038/s41423-022-00957-z

Zhao, S., Mi, Y., Guan, B., Zheng, B., Wei, P., Gu, Y., et al. (2020). Tumor-derived exosomal miR-934 induces macrophage M2 polarization to promote liver metastasis of colorectal cancer. *J. Hematol. Oncol.* 13 (1), 156. doi:10.1186/s13045-020-00991-2

Zhao, D., Yang, F., Wang, Y., Li, S., Li, Y., Hou, F., et al. (2022a). ALK1 signaling is required for the homeostasis of Kupffer cells and prevention of bacterial infection. *J. Clin. Invest.* 132 (3), e150489. doi:10.1172/JCI150489

Zhao, X., Di, Q., Liu, H., Quan, J., Ling, J., Zhao, Z., et al. (2022b). MEF2C promotes M1 macrophage polarization and Th1 responses. *Cell. Mol. Immunol.* 19 (4), 540–553. doi:10.1038/s41423-022-00841-w

Zhou, Z., Peng, Y., Wu, X., Meng, S., Yu, W., Zhao, J., et al. (2019). CCL18 secreted from M2 macrophages promotes migration and invasion via the PI3K/Akt pathway in gallbladder cancer. *Cell. Oncol. (Dordr)* 42 (1), 81–92. doi:10.1007/s13402-018-0410-8

Zhou, H. M., Zhang, J. G., Zhang, X., and Li, Q. (2021). Targeting cancer stem cells for reversing therapy resistance: mechanism, signaling, and prospective agents. *Signal Transduct. Target Ther.* 6 (1), 62. doi:10.1038/s41392-020-00430-1

Zhou, Y., Takano, T., Li, X., Wang, Y., Wang, R., Zhu, Z., et al. (2022). β-elemene regulates M1-M2 macrophage balance through the ERK/JNK/P38 MAPK signaling pathway. *Commun. Biol.* 5 (1), 519. doi:10.1038/s42003-022-03369-x

Zhou, Y., Cheng, L., Liu, L., and Li, X. (2023a). NK cells are never alone: crosstalk and communication in tumour microenvironments. *Mol. Cancer* 22 (1), 34. doi:10.1186/s12943-023-01737-7

Zhou, H., Gan, M., Jin, X., Dai, M., Wang, Y., Lei, Y., et al. (2023b). [Corrigendum] miR-382 inhibits breast cancer progression and metastasis by affecting the M2 polarization of tumor-associated macrophages by targeting PGC-1α. *Int. J. Oncol.* 62 (1), 1. doi:10.3892/ijo.2022.5449

Zhu, R., Gires, O., Zhu, L., Liu, J., Li, J., Yang, H., et al. (2019). TSPAN8 promotes cancer cell stemness via activation of sonic Hedgehog signaling. *Nat. Commun.* 10 (1), 2863. doi:10.1038/s41467-019-10739-3

frontiers | Frontiers in Oncology

TYPE Review
PUBLISHED 22 November 2023
DOI 10.3389/fonc.2023.1196298

OPEN ACCESS

EDITED BY
Chunjie Li,
Sichuan University, China

REVIEWED BY
Debanjali Dasgupta,
Mayo Clinic, United States
Jiaoyi Chen,
University Health Network (UHN), Canada

*CORRESPONDENCE
Jianjun Liu
Jianjun_liu2020@163.com
Xiongwen Lv
xiongwen_lv2019@163.com

RECEIVED 29 March 2023
ACCEPTED 06 November 2023
PUBLISHED 22 November 2023

CITATION
Shan L, Wang F, Xue W, Zhai D, Liu J and Lv X (2023) New insights into fibrotic signaling in hepatocellular carcinoma. *Front. Oncol.* 13:1196298. doi: 10.3389/fonc.2023.1196298

New insights into fibrotic signaling in hepatocellular carcinoma

Liang Shan[1,2,3,4], Fengling Wang[1], Weiju Xue[1], Dandan Zhai[1], Jianjun Liu[1*] and Xiongwen Lv[2,3,4*]

[1]Department of Pharmacy, The Second People's Hospital of Hefei, Hefei Hospital Affiliated to Anhui Medical University, Hefei, Anhui, China, [2]Anhui Province Key Laboratory of Major Autoimmune Diseases, Anhui Medical University, Hefei, China, [3]Inflammation and Immune Mediated Diseases Laboratory of Anhui Province, Hefei, China, [4]The Key Laboratory of Major Autoimmune Diseases, Hefei, Anhui, China

Hepatocellular carcinoma (HCC) mostly occurs in the background of liver fibrosis, and activated hepatic stellate cells (HSCs) exist in HCC tissues and adjacent tissues. HSC activation is involved throughout the development of HCC precancerous lesions, which has gradually attracted the attention of related researchers. In addition, HCC can promote the activation of HSCs, which in turn accelerates the occurrence and development of HCC by promoting tumor angiogenesis. In this review, we reviewed 264 studies from PubMed and ScienceDirect to summarize and analyze current significant fibrotic signaling in HCC. As a result, we found 10 fibrotic signaling pathways that are closely related to the activation, proliferation, invasion, migration, and promotion of apoptosis of HCC cells. In addition, we found that crosstalk between various fibrotic signaling pathways of HCC, hypoxia-induced energy metabolic reprogramming of HCC cells, matrix stiffness and stemness of HCC cells, and ferroptosis of HCC cells and HSCs are the latest research hotspots. Furthermore, related drugs that have been found to target these 10 fibrotic signaling pathways of HCC are listed. Our study provides a new reference for developing anti-HCC drugs.

KEYWORDS

fibrotic signaling, hepatocellular carcinoma, hepatic fibrosis, hepatic stellate cell, hepatocellular carcinoma cell

1 Introduction

1.1 Hepatocellular carcinoma

HCC is the fifth most common cancer worldwide and the third leading cause of cancer death (1). Recent epidemiological data indicate that death rates from HCC are increasing in the United States and Europe, and, together with incidence, are expected to double in the next 10–20 years (2). HCC can be primary or secondary. Primary HCC includes HCC and intrahepatic

cholangiocarcinoma (ICC), mixed HCC, and bile duct cell carcinoma. HCC and ICC are the two main types of primary HCC (3). HCC is the most common primary liver cancer and the fourth leading cause of cancer-related death globally, accounting for more than 90% of all primary HCC cases. Chronic hepatitis B or C virus infection is the main cause of HCC, while other causes include alcoholism, autoimmune liver disease, and nonalcoholic steatohepatitis (4). Constant inflammation damages deoxyribonucleic acid (DNA) in regenerating liver cells, which leads to genetic changes that increase the chance of cancer development (5) (Figure 1). Chronic hepatitis infection or long-term liver injury often leaves the liver in a state of chronic inflammation (6, 7). Moderate inflammation can fight pathogens and repair tissue damage in liver, however, persistent liver inflammation can disrupt the microenvironment and tip the balance in favor of liver carcinogenesis (8, 9). Over the past decade, new researches have demonstrated that the immune microenvironment plays critical roles in HCC progression, and therapies targeting tumor microenvironment (TME) have been reported to effectively inhibit HCC growth in both animal models and clinical trials (6–9).

1.2 Hepatic fibrosis

Numerous inflammatory factors continue to stimulate hepatic stellate cells, leading to their activation, which is the main cause of hepatic fibrosis (10). Approximately 80% of HCC cases occur in the context of chronic inflammation and cirrhosis caused by viral hepatitis. The hepatic inflammation and fibrosis environment play an important role in the development of HCC, and the treatment and prognosis of HCC are also complicated by the tumor stage and the degree of liver dysfunction (11). Various injury factors, including viral infection, alcohol, obesity, and insulin resistance, act on the liver, which can cause liver inflammation, immune response, hypoxia, oxidative stress, hepatocyte necrosis, and apoptosis (12). Injury and inflammation cause the regeneration of hepatocytes and the activation of HSCs, which are the main sources of liver scars. After activation, HSCs undergo a series of phenotypic and biological behavior changes, including fibroplasia promotion, migration, and release of many cytokines that promote proliferation, angiogenesis, and anti-

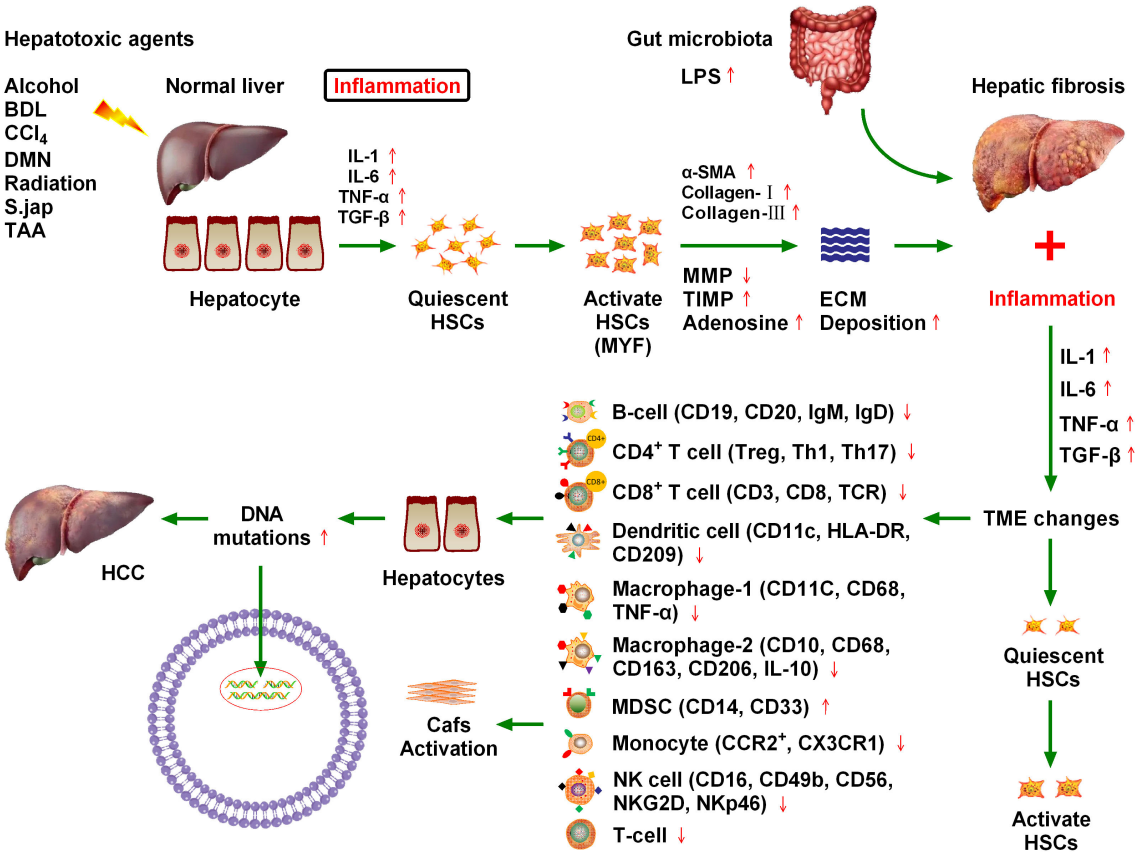

FIGURE 1
Chronic cytokine stimulation of liver cells leads to genetic mutations that induce hepatocellular carcinoma (HCC), and ultimately hepatic fibrosis. Various injury factors, including viral infection, alcohol, obesity, and insulin resistance, act on the liver, causing liver inflammation, an immune response, hypoxia, oxidative stress, hepatocyte necrosis, and apoptosis. Injury and inflammation cause regeneration of hepatocytes and activation of hepatic stellate cells (HSCs), which are the main sources of liver scarring. After activation, a series of phenotypic and biological behavior changes occur in HSCs, including the promotion of fibroplasia and migration and the release of many cytokines, which promote proliferation and angiogenesis, and prevent apoptosis. Inflammatory cells, such as macrophages, natural killer cell lymphoma and leukemia, T lymphocytes, and B lymphocytes, may be involved in liver injury and fibrosis. Chronic inflammation and regeneration processes lead to dysregulation of hepatocyte growth, genomic instability, DNA damage, dysplasia, and malignant transformation, which ultimately lead to HCC. The immune microenvironment composed of different immune cells plays a key role in HCC progression.

apoptosis (13). Inflammatory cells such as macrophages, natural killer (NK) cells, T lymphocytes, and B lymphocytes may be involved in liver injury and fibrosis. Chronic inflammation and regeneration processes lead to the loss of hepatocyte growth, regulatory genomic instability, DNA damage, dysplasia, and malignant transformation, ultimately leading to the development of HCC (13) (Figure 1).

1.3 Liver inflammation and the fibrosis microenvironment promote HCC progression

A close relationship exists between chronic liver inflammation, hepatic fibrosis, and HCC. Most chronic liver diseases are characterized by diffuse chronic inflammation, necrosis, and fibrosis. Chronic inflammation and fibrosis is a dynamic process of accumulation of lymphocytes, macrophages, and matrix cells that undergo secretory and paracrine interactions (11). Inflammatory cells belonging to innate immunity (e.g., NK cells and macrophages) and adaptive immunity (e.g., T lymphocytes and B lymphocytes) are involved in hepatic injury and fibrosis. By contrast, injured hepatocytes, Kupffer cells, and HSCs are involved in inflammation induction. Matrix cells can regulate the differentiation and function of antigen-presenting cells. The pattern of cytokine and chemokine secretion in the matrix determines T lymphocyte migration and polarization (14). Tumors may occur when chronic inflammation and injury healing processes become dysregulated. Malignant transformed hepatocytes may replace proliferative nodules, which are atypically altered during regeneration. In addition, hypoxia and inflammation are major factors that stimulate the proliferation of blood vessels and promote tumor growth (Figure 1). Inflammatory signals such as toll-like receptor 4 (TLR4) and nuclear factor kappa B (NFκB) promote tumor cell proliferation and migration by producing numerous cytokines and altering matrix, chemotactic growth, and lymphovascular hyperplasia factors (15). Because of the close relationship between hepatic fibrosis and HCC, it is crucial to explore the influence of fibrosis signaling on the occurrence, development, recurrence, and metastasis of HCC to improve the standard of HCC prevention and treatment (16).

2 Fibrotic signaling in HCC

The HCC TME comprises matrix cells, including Kupffer cells, HSCs, cancer-associated fibroblasts (CAFs), liver sinusoids endothelial cells (LSECs), tumor-associated macrophages (TAMs), and lymphocytes. The HCC–HSC dialog plays an important role in the development of HCC (17). HSCs play a central role in the occurrence and development of ICC, especially in the cytokine dialog between ICC and matrix cells. Metastatic cancer cells enter the sinusoidal spaces of the liver, where most are captured and killed by Kupffer and NK cells (18). Escaped cancer cells form micrometastases and induce a microenvironment conducive to metastasis. These cells are activated following liver damage, after which, they differentiate into myofibroblast (MYF)-like cells and produce a large amount of cytokines, chemokines, growth factors, and extracellular matrix (ECM). In addition to producing and secreting collagen and other scar tissue, HSCs have other important functions, including participating in liver regeneration, immune regulation, immune tolerance, and liver tumorigenesis. Various cytokines mediate the development of HCC through multiple fibrosis signaling pathways (19). Therefore, here we review recent advances in the field of hepatic fibrosis and HCC and consider several molecular signaling pathways that contribute to HCC in the hepatic fibrosis microenvironment (20) (Figures 2, 3, Table 1).

2.1 TLR4-MyD88-NFκB signaling pathways

Activation of the TLR4-myeloid differentiation primary response gene 88 (MyD88)-NFκB signaling pathway, an important pathway associated with the inflammatory response and hepatitis/hepatitis fibrosis, can lead to the release of downstream inflammatory factors and induce the production of interleukin (IL)-1, IL-6, and tumor necrosis factor (TNF)-α. TLR4 has been shown to pass through the Toll/IL-1 receptor domain (TIR domain) and use the TIR domain adaptor proteins MyD88, IL-1 receptor-associated kinase, and TNF receptor-s-sociated factor 6, to induce downstream NFκB activation to produce inflammatory factors (87). Extracellular inflammatory signals are presented to MyD88 via the TLR4-mediated signaling pathway, which activates NFκB, inducing its nuclear translocation and subsequent signal transduction (88) (Figure 2).

2.1.1 TLR4-MyD88-NFκB signaling and hepatic fibrosis

Hepatic fibrosis is the result of long-term chronic liver injury and repeated scar repair, which is mainly characterized by excessive deposition of ECM. HSCs are the main source of scar tissue in hepatic fibrosis. HSCs possess a complete TLR4 signaling pathway, which mediates important biological characteristics, including inflammation phenotype tolerance to apoptosis in fibrosis. Indeed, the degree of fibrosis in mice with *TLR4* mutation has been shown to be significantly reduced in the three hepatic fibrosis models of bile duct ligation (BDL), carbon tetrachloride (CCl_4), and thioacetamide (TAA), indicating that the TLR4 signaling pathway is involved in the occurrence of hepatic fibrosis (89, 90). Moreover, lipopolysaccharide (LPS) has been shown to cause swelling of hepatocytes, disappearance of the hepatic cord structure, and infiltration of numerous inflammatory cells. LPS has also been shown to upregulate the messenger ribonucleic acid (mRNA) and protein expression levels of TLR4, MyD88, IκBα, and NFκB, and increase the secretion of cytokines, including IL-1β, IL-4, IL-6, and TNF-α levels. Guo et al. (21) found that pretreatment with polysaccharide of Atractylodes macrocephala Koidz (PAMK) relieved LPS-induced histopathological damage in mice, and could activate TLR4-MyD88-NFκB signaling, reduce the levels of IL-1β, IL-6, and TNF-α, increase IL-4 levels, and inhibit the levels of glutathione peroxidase and malondialdehyde. These results indicate that PAMK could reduce inflammatory damage and

10.3389/fonc.2023.1196298

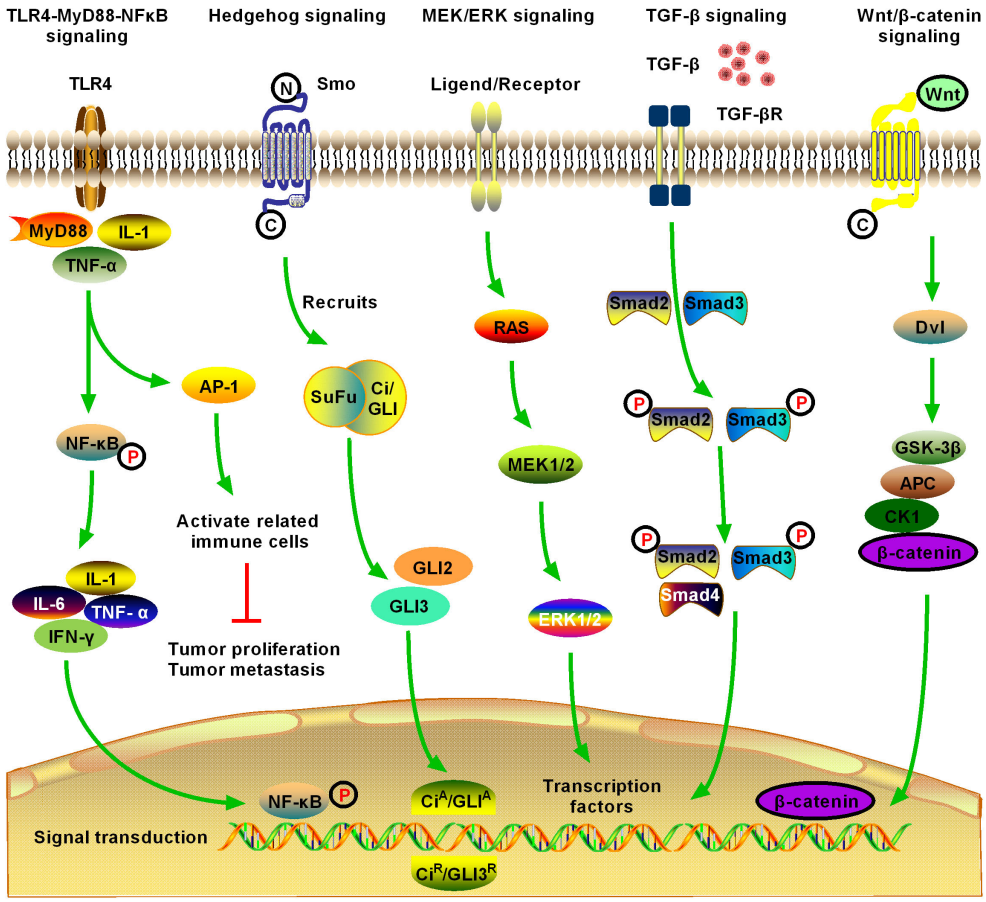

FIGURE 2
Schematic of five significant fibrotic signaling pathways in HCC, including toll-like receptor 4 (TLR4)-myeloid differentiation primary response gene 88 (MyD88)-nuclear factor kappa B (NFκB) signaling, Hedgehog (Hg) signaling, MAPK/extracellular signal-regulated kinase (MEK)/extracellular regulated protein kinase (ERK) signaling, transforming growth factor-β (TGF-β) signaling, and Wnt/β-catenin signaling (1). TLR4-MyD88-NFκB signaling is one of the most important inflammatory and fibrotic pathways discovered in recent years, the activation of which releases downstream inflammatory cytokines, inducing the production of interleukin (IL)-1, IL-6, and tumor necrosis factor (TNF)-α. Activation of NFκB downstream of the pathway is induced, and the signal enters the nucleus to induce activation, proliferation, invasion, and migration of HCC cells, and inhibit their apoptosis (2). Hg signaling is activated in different tumors and may contribute to the development of multiple tumor types by promoting the process of tumor initiation and metastasis. Novel Hg signaling inhibitors have entered the clinical research stage for the treatment of HCC; however, the development of Hg signaling targeted inhibitors still has broad prospects (3). MEK/ERK signaling is the most active research area in cell signal transduction recently. MEK/ERK signaling transfers a variety of extracellular signals to the nucleus through phosphorylation and activates various transcription factors, regulating cell proliferation, growth inhibition, differentiation, and apoptosis. MEK/ERK signaling is an important fibrosis signal in HCC (4). TGF-β1 is an important cytokine in the development of HCC, and it is also the strongest known fibrogenic factor. TGF-β1 signaling regulates the growth and proliferation of HCC cells. Currently, TGF-β1 is highly expressed in patients with HCC, where it is significantly correlated with the degree of tumor differentiation. The expression level of TGF-β1 increased with the decrease in tumor cell differentiation, suggesting that TGF-β1 can be used as an indicator for the early diagnosis of HCC. TGF-β signaling is an important fibrosis signaling of HCC (5). After activation of Wnt/β-catenin signaling, β-catenin accumulates continuously in the cytoplasm, which promotes part of β-catenin to enter the nucleus, activate and bind to the T cell factor/lymphoid enhancer transcription factor family, initiate the transcription of multiple downstream target genes, and promote the development of HCC. Activation of Wnt/β-catenin signaling promotes the activation and proliferation of HSCs and HCC cells and is an important fibrotic signaling pathway in HCC.

oxidative stress in mice and play a protective role in the early stages of LPS invasion of the liver. However, overexpression of the TLR4/MyD88/NFκB axis and its downstream pro-inflammatory mediators, such as TNF-α, IL-6, and interferon (IFN)-γ, were observed in mice with CCl_4-induced cirrhosis. Inhibiting the TLR4/MyD88/NFκB signaling pathway has protective effects on liver injury induced by various inflammatory cytokines (22). Activation of the TLR4-myD88-NFκB signaling pathway, an important pathway associated with hepatic fibrosis and HCC, can lead to the release of downstream inflammatory factors and induce the production of IL-1, IL-6, and TNF-α. These results suggest that inhibition of the TLR4-MyD88-NFκB-mediated inflammatory response can down-regulate the expression of TLR4 mRNA and protein, thereby improving hepatic fibrosis (91) (Table 1).

2.1.2 TLR4-MyD88-NFκB signaling pathway and HCC

At present, there are at least two views on the mechanism by which the TLR4-mediated signaling pathway induces HCC formation. The TLR4-MyD88-dependent signaling pathway can

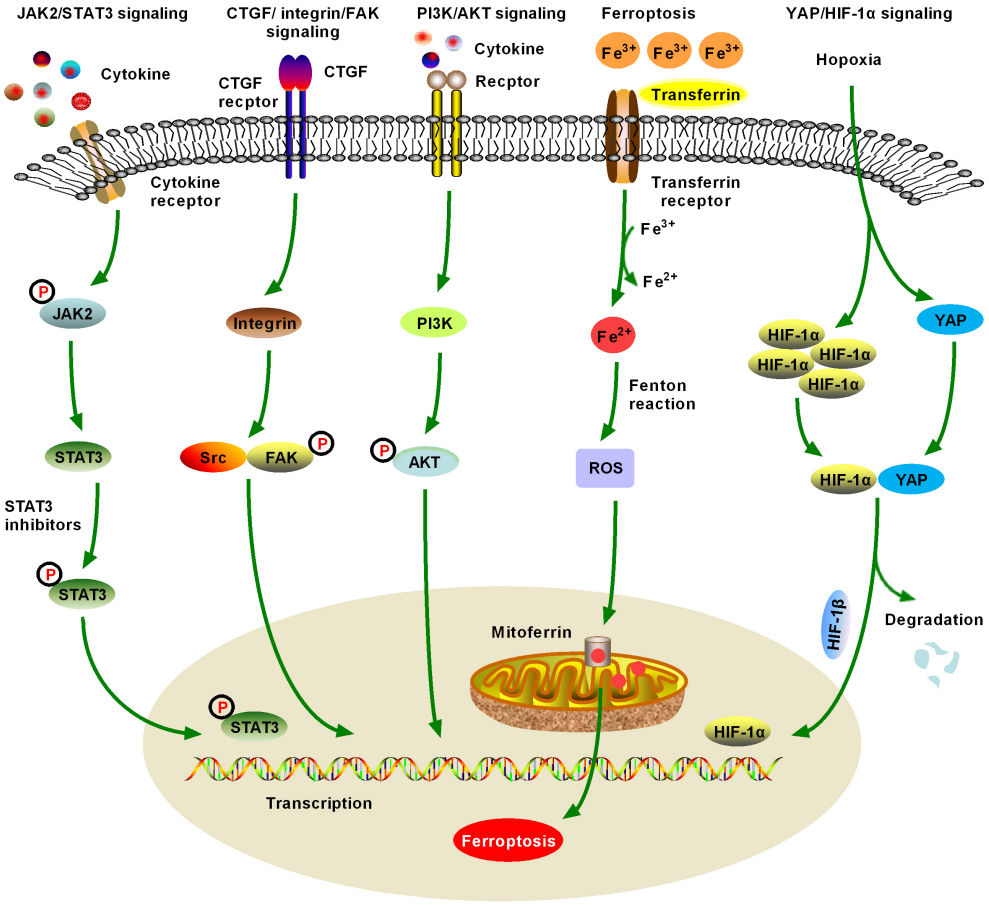

FIGURE 3
Schematic figure of another five significant fibrotic signaling pathways in HCC, including Janus kinase2 (JAK2)/signal transducer and activator of transcription 3 (STAT3), connective tissue growth factor (CTGF)/integrin/focal adhesion kinase (FAK), and Yes-associated protein (YAP)/hypoxia-inducible factor-1α (HIF-1α) signaling (6). JAK2/STAT3 signaling can be activated by various cytokines and growth factors, resulting in dysregulation of downstream target genes, which promote the formation and metastasis of malignant tumors by controlling cell proliferation, angiogenesis, immune surveillance, tumor invasion, and metastasis. JAK/STAT3 signaling is one of the important fibrotic signaling pathways in HCC (7). Increased expression and distribution of integrins have been observed in almost all human cancers, and multiple integrin-related genes are upregulated in HCC. Currently, crosstalk between CTGF/integrin/FAK and other signaling factors, such as TGF-β, has been extensively studied (8). Numerous studies have confirmed that the activation of phosphatidylinositol 3-kinase (PI3K)/AKT signaling promotes the proliferation, migration, and glycolysis of HCC cells, and is a widely studied fibrosis signal in the context of HCC. An increasing number of PI3K/AKT signaling-targeted inhibitors have been identified for preclinical or clinical trials (9). Ferroptosis was first proposed in 2012 and has quickly become a hot research topic. Various natural products improve hepatic fibrosis by inducing ferroptosis of HSCs and myofibroblasts and prevent HCC by inducing ferroptosis in HCC cells. However, as these studies are still in the initial stage and many research results are controversial, further studies are necessary (10). Hypoxia-induced YAP/HIF-1α signaling activation facilitates tumor cell growth, survival, and metastasis, and hypoxia is a central marker of HCC and its microenvironment. YAP/HIF-1α signaling is a widely studied fibrotic signaling in HCC. HIF-1α inhibitors may be developed as HCC therapeutic drugs in the future.

activate transcription factors such as *NFκB* and *activatorprotein-1* (*AP-1*), before activating related immune cells to play the role of immunosuppression and promote the development of tumor disease (92). It has been reported that intraperitoneal injection of diethylnitrosamine (DEN) to induce HCC in animals activates the TLR4-mediated MyD88 signaling pathway, resulting in the activation of Kupffer cells, the production of IL-6 and other pro-inflammatory mediators, and the induction of carcinogenic effects of the TLR4-MyD88-dependent pathway (93). Therefore, the activation of the TLR4-MyD88 signal is considered to be one of the important causes of HCC. In-depth studies on HCC have shown that the downstream multifunctional NFκB signaling pathway regulated by TLR4 plays a key role in the induction of tumor formation by inflammatory mediators. TLR4-MyD88-NFκB signaling plays a positive regulatory role in the inflammatory progression of HCC, suggesting that the TLR4-MyD88-NFκB signaling pathway may be a new target for the prevention or treatment of HCC (94). The regeneration of hepatocytes caused by inflammatory damage induced by the activation of TLR4-MyD88-NFκB signaling pathway mostly originates from the activation of HSCs, which lead to various biological changes, including promoting the proliferation and migration of fibrous tissue and secreting several cytokines with antiapoptotic effects and the ability to promote proliferation. Chronic inflammation leads to

TABLE 1 Major drugs targeting the 10 signaling pathways.

Targeting signaling	Agonist/Antagonist	Drugs	Characteristics	References
TLR4-MyD88-NFκB	(1) Antagonist	① Polysaccharide of Atractylodes	① Most are in clinical studies	(21)
		② Ginkgolide-A	② Most are natural products	(22)
Hedgehog	(1) Hg antagonist	① IPI-926 ② Vismodegib	① Treatment of some cancers	(23)
	(2) Smo antagonist	① Erismodegib (NVPLDE225)	① Lack specificity	
		② BMS-833923 (XL139) ③ IPI-926	② Susceptible to drug resistance	
	(3) Gli antagonist	① As_2O_3 ② Imiquimod ③ RU-SKI 43	① Inhibited Hg target gene Sufu expression	(24)
		④ GANT-61 ⑤ GANT-58 ⑥ FN1-8	② Good drug resistance	
MEK/ERK	(1) Antagonist	① NVP-AAL881 ② Sorafenib	① Effective against HCC	
		③ PD098059 ④ UO126 ⑤ Tanshinol	② Effective against advanced liver cancer	(25, 26)
TGF-β	Antagonist	① Physalin D ② Oxymatrine	① Numerous research works at present	
		③ Galunisertib ④ Fresolimumab	② Research hotspot	(27)
		⑤ 1D11 ⑥ EMD527040 ⑦ Cilengitide	③ Many research institutions are	(28)
		⑧ NIS793	researching	(29)
Wnt/β-catenin	Inhibitor	① ICG-001 ② PRI-724		(30, 31)
		③ OMP-54F28 (Ipafricept) ④ XAV939	① Most are in clinical studies	(32)
		⑤ OMP-54F28 ⑥ sFZD7 ⑦ DKN-01	② Broad prospects	(33)
		⑧ PKF115-548 ⑨ PKF222-815 ⑩ MG132	③ Many research institutions are	(34)
JAK2/STAT3	Inhibitor	① AG490 ② NSC74859 ③ Sorafenib	researching	(35, 36)
		④ SP600125 ⑤ Danshensu ⑥ Genistein		(37)
		⑦ Mg isoglycyrrhizinate ⑧ Mangiferin	④ More varieties ⑤ Lack specificity	(38)
		⑨ Cantharidin ⑩ Etomidate	① Research hotspot	(39, 40)
		⑪ AZD1480 ⑫ Cucurbitacin I ⑬ FLLL32	② Most are in clinical studies	(41, 42)
		⑭ S3I-201 ⑮ Toosendanin ⑯ Y705	③ Broad prospects	(43, 44)
		⑰ BP-1-102 ⑱ AZD1480	④ Includes many natural products	(45, 46)
CTGF/integrin/FAK	Integrin Antagonist	① CWHM-12 ② abciximab ③ Eptifibatide	⑤ Numerous varieties	(47)
		④ Tirofiban ⑤ EMD 525797 ⑥ CNTO-95		(48)
		⑦ EMD121974 ⑧ GLPG0187 ⑨ CWHM12		(49)
		⑩ MK-0429 ⑪ IDL-2965 ⑫ STX-100	① Excellent potential	(50)
		⑬ GSK3008348 ⑭ PLN-1474 ⑮ PLN-74809	② Poor targeting	(51)
		⑯ BG00011 ⑰ Natalizumab ⑱ IDL-2965	③ Many products have high toxicity	(52)
		⑲ PLN-1474 ⑳ Abciximab ㉑ Natalizumab	④ Many varieties used in research	(53)
		㉒ Vedolizumab ㉓ Lifitegrast	⑤ Broad prospects	
PI3K/AKT	(1) Inhibitor	① Curcumin ② MK2206 ③ LY294002	⑥ Includes many natural products	
		④ Kinsenoside ⑤ Maltitol	⑦ Most in thepreclinical research stage	(54, 55)
		⑥ Cytisine derivatives ⑦ Salvianolic acid A	① Currentresearch hotspot	(56, 57)
		⑧ Aloperine ⑨ BYL-719 ⑩ GDC-0941	② Poor targeting	(58, 59)
		⑪ Apatinib ⑫ Astragalin ⑬ Jolkinolide B	③ Combination medication required	(60, 61)
		⑭ Oxaliplatin ⑮ Bicyclol ⑯ Arenobufagin	④ Includes many natural products	(62, 63)
		⑰ Peurarin ⑱ Aloin ⑲ BEZ235 ⑳ Betulinic acid ㉑ Isoviolanthin ㉒ Ginsenoside Rk3	⑤ Drugs alreadyon the market	
		㉓ GSK690693	⑥ Many clinical studies underway	
	(2) Agonist	① Doxazosin ② Quercetin	⑦ Various types	
Ferroptosis	(1) Inducer	① Erastin ② Sorafenib ③ RSL3 ④ Sulfasalazine		(64, 65)
		⑤ RSL3 ⑥ RSL5 ⑦ DPI compounds	① Controversial ② Needs further research	(66, 67)
		⑧ FIN56 ⑨ CIL56 ⑩ Statins	① Recently discovered and reported	(68)
		⑪ FINO2 ⑫ 1,2-dioxolane ⑬ Artesunate	② Currentresearch hotspot	(69)
		⑭ Berberine ⑮ Ellagic Acid ⑯ Mg isoglycyrrhizinate ⑰ Chrysophanol ⑱ Wild bitter gourd extract ⑲ Altretamine ⑳ ML-162	③ Requires further research	
		㉑ Dihydroartemisinin ㉒ Artemether	④ Numerous types	(70)
			⑤ Includes many natural products	(71)

(Continued)

10.3389/fonc.2023.1196298

TABLE 1 Continued

Targeting signaling	Agonist/Antagonist	Drugs	Characteristics	References
YAP/HIF-1α	(2) Inhibitor	㉓ Sulfoximine Buthionine ㉔ Lanperisone ㉕ Acetaminophen ㉖ Cisplatin ㉗ Aferin A ① Deferoxamine Mesylate ② Liproxstatin-1 ③ Ferrostatin-1 ④ Vitamin E ⑤ 2-mercaptoethanol ⑥ Cycloheximide ⑦ Rosiglitazone ⑧ Pioglitazone	⑥ Controversial ⑦ Mechanism research is imperfect	(72) (73, 74) (75) (76) (68) (67) (72)
	(1) Inhibitor	① Curcumin ② PX-478 ③ Metformin ④ Nicotinamide mononucleotide ⑤ Oroxylin A ⑥ LW6 ⑦ Bruceine D ⑧ 32-134D	① Controversial ② Mechanism research is imperfect ③ Requires further research ④ Discovered late ① Currentresearch hotspot ② Discovered late ③ Requires further research ④ Mediates various liver diseases ⑤ Little variety	(72) (77, 78) (79, 80) (81, 82) (83, 84) (85, 86)

abnormal cell growth, gene expression disorders, and DNA damage in liver tissues, which further results in malignant tissue development and ultimately induces HCC.

2.2 Hedgehog signaling pathway

The discovery of the Hedgehog (Hg) signaling pathway stems from studies of embryonic development in Drosophila melanogaster. In humans, the pathway transmission process can be simply summarized as the Hg Homo sapiens *patched 1-Smoothened-Glioma associated oncogene homolog* (*Ptch1–Smo–Gli*) process. As the most important nuclear transcription factor in the Hg pathway, *Gli-l* is responsible for regulating many downstream effector factors of the pathway and binds to the promoter of downstream genes in the Hg signaling pathway to directly regulate the transcription and expression of target genes (Figure 2). Recent studies have shown that the Hg pathway is abnormally activated in various liver diseases (95, 96). In addition, the Hg signaling pathway can promote the proliferation of tumor cells, inhibit apoptosis, and promote the occurrence of HCC. Therefore, the Hg signaling pathway is closely related to hepatic fibrosis and HCC (97). The Hg signaling pathway not only participates in cell growth and differentiation but also plays an important role in tissue and organ damage repair and immune regulation. However, abnormal activation of the Hg signaling pathway can also lead to abnormal development and even tumors.

2.2.1 Hg signaling and hepatic fibrosis

Many studies have shown that the immune cell-mediated microenvironment of hepatic fibrosis is closely related to the activation of the Hg signaling pathway (98). Natural killer T (NKT) cells also produce Sonic Hedgehog (SHH), promote collagen secretion, and transform stationary HSCs into MYFs, resulting in hepatic fibrosis (99, 100). The human Hg protein is highly expressed in stationary HSCs, and the key gene of the Hg signaling pathway (*Gli-1 Gli-2*) cannot be detected. However, after 24 h of culture, the expression of human Hg interacting protein in HSCs decreased by 90% and the Hg signaling pathway ligands SHH and Gli-1 increased significantly, leading to activation of the Hg signaling pathway (101). The pathological characteristics of hepatic fibrosis include excessive synthesis and insufficient degradation of ECM, leading to its deposition in the liver. Persistent liver fibrosis may develop into cirrhosis and increase the risk of HCC. Inhibition of the Hg pathway (using Smo antagonists or by knocking out the *Smo*) can reduce the activation of quiescent HSCs, reduce the production of MYF HSCs, and reduce the degree of hepatic fibrosis (Table 1). Although the Hg signaling pathway is associated with quiescent HSC activation, the activation mechanism is unclear. Although the Nobel Prize winners Wieschaus and Nussland-Volhart reported the Hg pathway in 1980, its importance in dictating hepatic fibrosis and HCC outcomes has emerged much more recently (102). Fan et al. found that suppressing the activation of HSCs could alleviate hepatic fibrosis in mice induced by CCl_4 and a 3,5-diethoxycarbonyl-1,4-dihydrocollidine diet for 8 weeks via the Hg

pathway (103). In mice or patients with hepatic fibrosis, inhibition of glutaminase blocked the accumulation of MYFs and fibrosis progression. Du et al. reported that knockout of the Hg signaling intermediate heptahelical transmembrane G protein-coupled receptor SMO or knockdown of Yes-associated protein (YAP) inhibited the expression of glutaminase, the rate-limiting enzyme in glutaminolysis, in mice and patients with hepatic fibrosis (99). Hg signaling regulates glutaminolysis to inhibit HSC activation. *In vivo* and *in vitro* studies confirmed that procyanidin B2, a flavonoid extract that is abundant in grape seeds and has pharmacological effects, alleviated CCl_4-induced hepatic fibrosis in mice by inhibiting the activation of HSCs and angiogenesis via the Hg pathway during hepatic fibrosis (98). In other words, the Hg pathway plays an important role during various liver injuries, such as hepatic fibrosis, inflammation-related injury, and liver carcinogenesis. Targeting the Hg pathway has become a promising treatment for hepatic fibrosis.

2.2.2 Hg signaling pathway and HCC

Abnormal activation of the Hg signaling pathway is closely related to the invasion and metastasis of malignant tumors. Aberrant activation of Hg signaling in the normal liver and HCC has been demonstrated in detail in previous studies (23). A new study found that the stage of hepatic fibrosis was associated with the degree of Hg signaling activation in patients with non-alcoholic fatty liver disease (NAFLD). Activation of Hg signaling is also associated with fibrosis in the lungs, skin, and kidneys (104). Chung et al. further investigated up-regulated hepatic expression of SHH-induced hepatic fibrosis and hepatocarcinogenesis in a transgenic mouse model (105). GANT61 (NSC136476) is a *Gli-1*- and *Gli-2*-induced transcriptional inhibitor that inhibits Hg. Wang et al. found that GANT61 significantly suppressed Hg signaling to reverse sorafenib resistance in CD44-positive HCC tissues (97). This combined administration may be effective in patients with HCC with high CD44 levels as a personalized medicine approach. Another study has shown that the Hg pathway in liver tissue of Chinese patients with HCC is activated by ligand expression, rather than by mutations, suggesting that the research prospects of Hg signaling inhibitors are very broad for a large number of patients with HCC in China (24). Currently, the role of the Hg signaling pathway in liver physiology and pathology has not been fully elucidated and requires further study.

2.3 MEK/ERK signaling pathway

HSC activation is facilitated by several mitogen-activated protein kinases (MAPKs), including MAPK/extracellular signal-regulated kinase (MEK), extracellular regulated protein kinase (ERK), connective tissue growth factor (CTGF), and insulin-like growth factor-1 (106). MEK binding to ERK results in dimerization of tyrosine (Tyr) residues, which activates the phosphatidylinositol 3-kinase (PI3K) and MAPK pathways. Blocking MEK/ERK signaling blocks MAPK and PI3K/AKT signaling pathways, thereby inhibiting HSC activation and attenuating experimental hepatic fibrosis progression (Table 1). ERK/MAPK signaling pathways are activated and involved in cell growth, differentiation, and migration during the pathogenesis of hepatic fibrosis, cirrhosis, and HCC (25, 107). The MEK/ERK signaling pathway is closely related to hepatic fibrosis and HCC (Figure 2).

2.3.1 MEK/ERK signaling and hepatic fibrosis

Studies have confirmed that ERK is a major member of the MAPK family and that its MEK/ERK signaling pathway is an important pathway for many cytokines to regulate cell proliferation and apoptosis. Foglia et al. suggested that inhibiting the MEK/ERK pathway in activated MYF-like HSCs is a key crossroad for reversing hepatic fibrosis (26). HSC activation by myofibroblastic differentiation is critical for hepatic fibrosis. Crosstalk between HSCs/myofibroblastic and tumor cells in the microenvironment alters the properties and facilitates the growth, proliferation, migration, and invasion of HCC cells. Homo sapiens *E2F transcription factor 3* (*E2F3*) acts as a transcriptional activator and increases cell proliferation through G1/S transformation. A new report has identified a novel stiffness-mediated HSC activation mechanism that is dependent on the *E2F3* (108). Liu et al. found that HCC cells cultured in an HSC-conditioned medium activated the PI3K/AKT and MEK/ERK signaling pathways following the combination of *E2F3* with the *fibroblast growth factor 2* (*FGF2*) promoter, which increased the growth and metastasis of HCC cells. In addition, gene knockout of *E2F3* mitigated DEN- and CCl_4-induced HCC in mice. The *E2F3* is also highly expressed in the HCC tissues of patients; therefore, matrix stiffness modulates HSC activation into tumor-promoting MYFs via *E2F3*-dependent MEK/ERK signaling and regulates malignant progression. The ERK pathway is critical for transducing signals from surface receptors to the nucleus and is overactivated in many tumors, including HCC, melanoma, and breast cancer.

2.3.2 MEK/ERK signaling and HCC

According to new statistics, the majority (approximately 80%) of HCC cases result from severe hepatic fibrosis and/or cirrhosis. Li et al. found that the serum cartilage oligomeric matrix protein (COMP) levels in patients with HCC were obviously higher than those in healthy people, and these patients showed more unfavorable disease parameters, including a higher incidence of vascular invasion and HCC recurrence (106). In addition, gene knockout animal experiments and different cell experiments demonstrated for the first time that COMP mainly originates from activated HSCs and promotes the growth and metastasis of HCC cells in a dose-dependent manner by activating MEK/ERK and PI3K/AKT signaling. Moreover, crosstalk was observed between hepatic fibrosis and HCC through inhibiting ERK signaling, which is a potential novel target for the prevention and treatment of HCC. Another study showed that low-density lipoprotein receptor inhibited the enhancement of intracellular cholesterol synthesis through MEK/ERK signaling and promoted the proliferation and metastasis of HCC cells (109). It has also been reported that Homo sapiens minichromosome maintenance complex component 6 promotes HCC metastasis through MEK/

ERK signaling and can be used as a novel serum biomarker for early recurrence (110). Lai et al. found that NEI-like DNA glycosylase III (NEIL3) activation of MEK/ERK signaling mediated epithelial–mesenchymal transition (EMT), that treatment resistance promoted HCC progression, and that NEIL3 induction of targeted inhibition of NEIL3 was a promising therapeutic approach in patients with HCC (111). Currently, sophoridine derived from natural products has been found to inhibit the growth of lenvatinib-resistant HCC by inhibiting rat sarcoma virus (RAS)/MEK/ERK signaling by decreasing vascular endothelial growth factor receptor 2 expression (25). Another natural product, Morusinol, inhibits HCC cell invasion and migration and targets RAS/MEK/ERK signaling by inducing autophagy, and has selective and effective antitumor activity against human HCC (112). These studies further confirm that inhibition of MEK/ERK signaling alleviates HCC.

2.4 TGF-β signaling pathway

Discovered by Tucker in 1984, transforming growth factor-β (TGF-β) is a polypeptide cell growth regulatory factor associated with the growth of various tumors. The TGF-β superfamily members include at least five isomers (TGF-β1, 2, 3, 4, 5), among which TGF-β1 is the most closely related to liver injury and disease occurrence (113). TGF-β1 is a secretory polypeptide factor, which has various biological activities, including regulating cell growth, migration, differentiation, the occurrence and development of embryos and tumors, wound healing, bone formation, and immune regulation. Normal hepatocytes either lack TGF-β1 or show low levels (114). Meanwhile, damaged liver endothelial cells cause platelets to agglutinate and release TGF-β1. Studies have shown that TGF-β1 is a crucial factor leading to hepatic fibrosis and even HCC in the process of liver injury. The drosophila mothers against decapentaplegic protein (Smad) is the substrate of the most important intracellular kinase of the TGF-β1 receptor known to date. Activated TGF-β1 receptors recruit Smads through Smad anchor proteins or directly bind to signal molecules such as MAPK and phosphorylate them, so that signals are transmitted step by step in the cell until they are transferred to the nucleus, where they regulate the expression of target genes (115) (Figure 2).

2.4.1 TGF-β signaling and hepatic fibrosis

Most literature studies have shown that TGF-β1 stimulates HSC activation and proliferation, leading to hepatic fibrosis (27, 28, 116, 117) (Table 1). TGF-β1 in the liver is mainly secreted by immune cells, HSCs, and epithelial cells, mainly through mediating the activation of HSCs to produce excessive ECM, leading to hepatic fibrosis (117). Xiang et al. reported that Physalin D alleviated CCl_4- and BDL-induced hepatic fibrosis in mice via blocking TGF-β/Smad signaling and reducing HSC activation, proliferation, and transformation (27). Compound kushen injection, an approved traditional Chinese medicine formula, reduced the inflammatory response, oxidative stress, liver compensatory proliferation, and hepatocellular death of mice with hepatic fibrosis induced by CCl_4 injection or a methionine choline-deficient diet via rebalancing TGF-β/Smad7 signaling in HSCs, which protected against hepatic fibrosis and hepatocarcinogenesis in both preclinical and clinical studies (28). Sulfatase-2 (Sulf2) also regulates hepatic fibrosis in mice induced by BDL or intraperitoneal injection of CCl_4 or TAA through inhibiting TGF-β signaling (118). *Sulf2* knockout (*Sulf2*-KO) mice showed significantly decreased collagen content and bands of bridging fibrosis compared with wild-type mice in all three models of hepatic fibrosis. Sulf2 expression has recently been shown to be upregulated in cirrhotic human liver and fibrotic mouse liver, suggesting that Sulf2 plays an important role in both fibrosis and subsequent tumorigenesis. TGF-β is highly expressed in tissues of hepatic fibrosis and HCC, so the TGF-β signaling is considered to be a marker of hepatic fibrosis and HCC. The synergistic role of TGF-β and the tissue microenvironment in modulating the cellular response of different cell types and promoting the development of hepatic fibrosis and the progression of HCC has been extensively demonstrated (29). TGF-β signaling provides a wide scope for intracellular crosstalk, such as receptor-associated Smads interacting with other signaling molecules rather than directly transmitting signals to the nucleus, and the activation of intracellular substrates other than Smad can be mediated by influencing apoptosis and other activation of other intracellular signaling pathways (119). The mechanism of treating hepatic fibrosis through targeted inhibition of TGF-β signaling has been widely discussed (119, 120).

2.4.2 TGF-β signaling and HCC

TGF-β1 is an important cytokine in the occurrence and development of HCC. As well as being an important cytokine that controls the growth and proliferation of hepatocytes, TGF-β1 is also known to be highly expressed in patients with HCC and is significantly correlated with the degree of tumor differentiation (29). Recently, cancer-associated fibroblast-mediated cell crosstalk supporting HCC progression has become a research hotspot (121). CAFs are key players in the pathogenesis of HCC; however, the complex mechanism of crosstalk between CAFs and other components of the TME is still unclear, and studies on TGF-β1 activation of CAFs are ongoing (121). Aberrant activation of TGF-β/Smad signaling facilitates tumor metastasis and is often observed in HCC. The lncRNAlnc-UTGF has been shown to mediate a positive feedback loop regulates TGF-β/Smad signaling and promotes hepatoma metastasis (122). Moreover, bone morphogenetic protein (BMP) is involved in TGF-β signaling crosstalk; indeed, Ning et al. found that TGF-β1/BMP-7 pathway imbalance induced by activation of liver polarized macrophages promotes the aggressiveness of HCC (123). Increasing evidence has shown that TGF-β signaling plays a critical role in the regulation of immune cells, including CD4+ T cells, CD8+ T cells, dendritic cells (DCs), NK cells, myeloid suppressor cells, and TAMs. TGF-β signaling mediates HCC progression through the critical regulation of various immune cells in the liver to maintain a balance between immune tolerance and activation (124). *RALYL*, a liver progenitor-specific gene, was recently found to promote tumorigenicity, self-renewal, chemotherapy resistance, and metastasis of HCC by up-regulating TGF-β signaling and subsequent PI3K/AKT and signal transducer and activator of

transcription 3 (STAT3) signaling to enhance HCC stemness (125). Increasing evidence suggests that crosstalk between ECM and TGF-β, and intracellular TGF-β signaling often exhibits crosstalk with other signals, including Jun N-terminal kinase, p38, MAPK, and NFκB, to regulate hepatic fibrosis and HCC (126). Some studies have explored the underlying molecular mechanisms of STAT3 crosstalk with Smad3/TGF-β1 signaling during EMT in patients with HCC and a rat model. Both *in vivo* (HCC patients, DEN-induced HCC rat model) and *in vitro* (HepG2, Bel7402, MHCC97H, and HCCLM3) results indicate that TGF-β1-induced EMT is dependent on Smad3-mediated Snail transcription and crosstalk of STAT3 signals in HCC cells (30). Interestingly, new studies have shown that TGF-β has a dual role in tumorigenesis, acting as a tumor suppressor in the early stages of tumorigenesis and promoting tumor progression and metastasis in more advanced cancers (31). In addition, the crosstalk between TGF-β and vascular endothelial-derived growth factor (VEGF) signals in a variety of immune cells, tumor cells, and matrix cells may further promote TGF-β-mediated immunosuppression, which may be a new mechanism for TGF-β to regulate tumor immune escape through immunosuppression in the latest tumor stage (126). However, TGF-β1 plays a role in promoting tumor growth and metastasis in the middle and late stages of the tumor. Overexpression of TGF-β1 in HCC cells does not inhibit the proliferation of HCC cells, which may be related to the defective receptor.

2.5 Wnt/β-catenin signaling

Wnt/β-catenin signaling comprises a group of evolutionarily conserved signals that play an important role in cell genesis, embryonic development, cell proliferation and differentiation, and tissue regeneration in various organisms (35). Recent studies have shown that Wnt signaling can participate in the activation of HSCs and the formation of hepatic fibrosis, which is mainly manifested in promoting collagen synthesis and collagen deposition in the liver by means of autocrine and/or paracrine mechanisms, thus reducing the apoptotic capacity of activated HSCs (36) (Table 1). Various stimulators can also play a role through the classical Wnt/β-catenin signaling pathway, ultimately promoting the occurrence and development of hepatic fibrosis. Other studies have found that abnormal activation of Wnt/β-catenin signaling is closely related to the progression and carcinogenicity of malignant tumors (127) (Figure 2). Specifically, the expression level of intracellular β-catenin is closely related to tumor metastasis and invasion of blood vessels and may lead to tumor enlargement. Wnt/β-catenin signaling is closely related to hepatic fibrosis and HCC.

2.5.1 Wnt/β-catenin signaling and hepatic fibrosis

Activation of classical Wnt/β-catenin signaling can regulate cell proliferation, survival, and behavior. New studies have found that a series of intracellular signals drive HSC activation, including Wnt/β-catenin signaling, TGF-β/Smad signaling, and Hg signaling, with complex crosstalk between them (32). Increasing evidence suggests that inhibition of Wnt signaling to β-catenin may alleviate hepatic fibrosis; however, further research is needed to determine the identity and cellular origin of the factors that activate β-catenin in HSCs (32). Liu et al. found that insulin-like growth factor binding prote-3, Dickkopf-3 (DKK-3), and DKK-1 derived from human amniotic mesenchymal stem cells (MSCs) mitigate hepatic fibrosis via suppression HSC activation through blocking Wnt/β-catenin signaling in mice induced by injecting CCl_4 via the tail vein. In addition, crosstalk between PI3K/AKT and Wnt/β-catenin signals were found during HSCs (LX-2) transfection assays in underlying mechanism studies (128). Rong et al. found that human bone marrow MSC-derived exosomes reduced CCl_4-induced hepatic fibrosis in mice through Wnt/β-catenin signaling via both cellular assays and animal experiments (129). Upstream regulatory mechanisms that inhibit hepatic Wnt/β-catenin activity may constitute targets for the development of new therapies against life-threatening diseases such as hepatic fibrosis and HCC (130). Therefore, the regulation of β-catenin is expected to become a target of anti-hepatic fibrosis therapy, as well as a direction of future research.

2.5.2 Wnt/β-catenin signaling and HCC

Numerous literature studies have shown that inhibition of Wnt/β-catenin signaling can inhibit HCC cell differentiation and proliferation and promote apoptosis during HCC progression (33, 131, 132). TAMs are an important component of the TME mediating the development of HCC. Yang et al. confirmed for the first time that the typical Wnt/β-catenin signaling crosstalk between HCC cells and macrophages promotes the polarization of M2-like macrophages, thus leading to tumor growth, migration, metastasis, and immunosuppression in HCC (133). Therefore, blocking Wnt/β-catenin signaling activation in HCC cells secreting Wnt and/or TAMs may be a potential strategy for future HCC treatment. Up to 70% of patients with HCC show up-regulation of Wnt/β-catenin signaling, and β-catenin mutations increase with HCC progression (134). Wang et al. reported that brain-expressed X-linked protein 1 (BEX1) plays a critical role in regulating cancer stem cell (CSC) properties in different types of HCC; indeed, targeting BEX1-mediated Wnt/β-catenin signaling may help to address the high recurrence rate and heterogeneity of HCC (135). Lentivirus-mediated overexpression or CRISPR/Cas9 knockout experiments have shown that glutaminase 1 (GLS1) regulates stemness and serves as a therapeutic target for the elimination of CSCs by inhibiting reactive oxygen species (ROS)/Wnt/β-catenin signaling *in vitro* and *in vivo*, while *GLS1* knockout inhibits tumorigenicity *in vivo* (136). Protein kinases play a key evolutionary conserved role in Wnt/β-catenin signaling and have been widely discussed as one of the most important drug targets in HCC therapy (34). However, inhibition of Wnt/β-catenin signaling alone is unlikely to significantly improve the prognosis of patients with HCC, and future research should focus on the combination of other therapies to improve the efficacy of Wnt/β-catenin signaling inhibitors. Currently, anti-HCC compounds targeting the inhibition of Wnt/β-catenin signaling are the most widely researched, most of which are in the clinical and preclinical research stages. As more research data become available,

achieving the best personalized treatment for HCC in the future represents the ideal goal (137–140). Inhibition of Wnt/β-catenin signaling reduces the activation, proliferation, migration, and progression of HCC cells, which has attracted extensive attention from many researchers worldwide. At present, several institutions are developing targeted drugs.

2.6 JAK2/STAT3 signaling

Many studies suggest that Janus kinase2 (JAK2)/STAT3 signaling is closely related to hepatic fibrosis, and HSC activation is a key factor in the progression of hepatic fibrosis (39). Following the occurrence of homologous or heterooligomerization of specific receptor subunits on the HSC membrane with platelet-derived growth factor, leptin, TGF-β, and other cytokines promoting hepatic fibrosis, the receptor-coupled JAKs are activated. The Tyr of the cytoplasmic segment of the receptor is then phosphorylated to the protein anchor site containing SH2, and downstream signaling protein molecules are activated to enable the target genes to play a role. Tyr residues (Tyr705) and Serine (Ser) residues (Ser727) at the end of the STAT protein can also be phosphorylated by JAKs to activate the STAT protein and form homologous or heterologous STAT protein dimers into the nucleus to bind the promoter of corresponding target genes, thus activating target gene transcription of HSCs and participating in the development of hepatic fibrosis (38). The results of animal experiments have shown that p-JAK2/JAK2 and p-STAT3/STAT3 protein levels were significantly higher in the fibrosis model group compared with those in the control group, suggesting that JAK2/STAT3 signaling was activated in the liver tissues of rats during dimethylnitrosamine-induced hepatic fibrosis and was involved in the development of hepatic fibrosis (40) (Figure 2). Moreover, many studies have shown that JAK2/STAT3 signaling activation is involved in the occurrence and development of hepatic fibrosis and HCC (Table 1).

2.6.1 JAK2/STAT3 signaling and hepatic fibrosis

JAK2/STAT3 signaling is a research hotspot in fibrotic disease, but the role of JAK2/STAT3 in the progression of hepatic fibrosis remains controversial (37, 141). Ding et al. found that HCC is closely related to chronic inflammation and fibrosis, which is called the inflammation–fibrosis–cancer axis (142). In addition, compared with the control group, JAK2/STAT3 signaling was significantly upregulated in the DEN exposure group, in that 100% of the rats in the DEN exposure group developed liver tumors at 20 weeks, with accompanying inflammatory and fibrotic stages correlated with exposure time. Most literature studies have reported that inhibiting JAK2/STAT3 signaling of HSC alleviates hepatic fibrosis both *in vivo* and *in vitro* (38, 39). Yang et al. found that magnesium (Mg) isoglycyrrhizinate improved high-fructose-induced liver fibrosis in rats by inhibiting JAK2/STAT3 and TGF-β1/Smad signaling by increasing microRNA-375-3p, but the effect of a direct interaction between JAK2/STAT3 and TGF-β1/Smads signaling on hepatic fibrosis *in vivo* needs further study (143). Studies have confirmed that quiescent HSCs, hepatocytes, and bile duct cells with an epithelial phenotype can be transformed into fibroblasts with a mesenchymal phenotype through EMT and participate in the occurrence and development of hepatic fibrosis (40). Xu et al. reported that the natural extract of brown algae, named propylene glycol alginate sodium sulfate (PSS), could significantly prevent liver injury and fibrosis induced by BDL and CCl_4 in mice. Mechanistically, PSS significantly inhibits the activation of HSCs in LX-2 cell lines incubated with 10 ng/mL TGF-β1 for 24 h by inhibiting the anti-autophagy effect of JAK2/STAT3 signaling (144). In conclusion, STAT3 may play a dual role in hepatic fibrosis because of different upstream regulatory factors. Currently, most studies suggest that STAT3 mainly plays a role in promoting hepatic fibrosis, and its expression level may be positively correlated with the degree of fibrosis.

2.6.2 JAK2/STAT3 signaling and HCC

STAT3 is closely related to the development and prognosis of HCC and can be adjusted by different target genes, affecting cell proliferation, apoptosis, invasion, migration, angiogenesis, and immune escape. Many studies have reported that directly inducing apoptosis of HepG2 cells by downregulating the JAK2/STAT3 signal transduction pathway may contribute to the development of new therapeutic strategies for HCC (145). The humanized-immune-system HCC mouse model is a newly developed animal model for the study of new targets of HCC immunotherapy, which has wide application prospects (146). Zhao et al. first demonstrated that intratumor human cluster of differentiation–positive (hCD14+) cells could produce IL-33 through DAMP/TLR4/activator protein 1, which increased IL-6 in other intratumor immune cells and activated JAK2/STAT3 signaling in HCC (146). However, the mechanism of crosstalk between human HCC and the human immune system still needs to be studied in depth (41, 147). Wei et al. recently found that TAMs mediate the EMT program of tumor cells before the invasion and speculated that EMT-programmed tumor cells can in turn recruit macrophages. In addition, crosstalk exists between TAMs and cancer cells in the TME, and IL-6 secreted by TAMs binds to the IL-6 receptor on the surface of cancer cells and phosphorylates STAT3 (pSTAT3) (148). It has been widely verified that abnormal activation (phosphorylation) of JAK/STAT3 signaling upregulates EMT, promoting HCC progression (42, 149). Liu et al. found that the homologous to the E6-AP carboxy terminus domain and RCC1-like domain 2 (HERC2) promote inflammation-induced stemness and immune evasion in HCC cells through JAK2/STAT3 signaling, the underlying mechanism of which is related to the regulatory effect of HERC2 on JAK2/STAT3 signaling participating in the crosstalk between cancer stemness and immune evasion (150). Cytokine activation of STAT3 is mediated by Tyr phosphorylation of JAK, and crosstalk between JAK/STAT3 signaling activation and EMT-mediated metastasis has been observed in HCC over the past decade (43–45). JAK2/STAT3 signaling is involved in many biological processes, including cell proliferation, angiogenesis, and migration in HCC (46).

2.7 CTGF/integrin/FAK signaling

CTGF is a multifunctional secretory polypeptide that regulates biological activities such as cell proliferation, differentiation, and adhesion and plays an important role in tissue damage repair and ECM synthesis (151). Integrins are receptor proteins on the surface of HSCs. Recent studies have confirmed that CTGF plays a positive regulatory role in the development of hepatic fibrosis (152). Focal adhesion kinase (FAK) is an important cytokine in integrin signaling, and activation of FAK further initiates a series of downstream cell signaling cascades (Figure 3). Currently, many studies have found that CTGF/integrin/FAK signaling is associated with hepatic fibrosis and HCC (47, 48, 153) (Table 1).

2.7.1 CTGF/integrin/FAK signaling and hepatic fibrosis

FAK is an important cytokine in the integrin signaling system. After the integrin binds to the extracellular ligand molecule, the cytoplasmic end binds to the N end of the FAK protein to transmit extracellular signals (Figure 3). FAK is activated by phosphorylation, which further activates a series of downstream protein kinases (152). Currently, invasive biopsy is still the gold standard for the diagnosis of hepatocellular fibrosis. Shao et al. developed a new [18F]-Alfatide imaging targeting integrin αvβ3, which provides a noninvasive method for evaluating the expression and function of integrin αvβ3 on activated HSCs in the injured liver (47). Researchers have successfully quantitatively evaluated the level of liver integrin αvβ3 and the progression of hepatic fibrosis in mouse models induced by CCl_4 and BDL; however, these studies are only at the preclinical stage, and further studies are needed (48, 153, 154). HSC activation and MYF differentiation are central to hepatic fibrosis and occur during ECM deposition (49, 155, 156). Integrin has been extensively investigated as a drug target for hepatic fibrosis, and a variety of antifibrotic drugs targeting integrin have entered the clinical research stage (50, 51, 157). Currently, clinically used integrin inhibitors, such as abciximab (targeting αIIbβ3 on platelets), natalizumab (targeting α4β1 on T-cells), vedolizumab (targeting α4β7 on T-cells), and lifitegrast (targeting αLβ2 on T cells), usually bind specifically to their target (52). Shi et al. found that the promoter methylation of the *CTGF* underwent phenotypic changes in HSCs, becoming MYF-like cells expressing α-SMA. CTGF promoted phenotypic changes of HSCs into MYFs, whereas inhibition of CTGF promoter methylation enhanced this process, suggesting that CTGF group promoter methylation may negatively regulate hepatic fibrosis (158). *In vivo* experiments showed that the severity of hepatic fibrosis in a CCl_4-induced rat liver fibrosis model was negatively correlated with the promoter methylation level of the *CTGF* in HSCs, suggesting that promoter methylation of the *CTGF* may prevent the occurrence of hepatic fibrosis. Therefore, low levels of promoter methylation of the *CTGF* may be a predisposing factor for the occurrence of hepatic fibrosis (158). After transfection of the *FAK* shRNA recombinant plasmid into HSCs, the migration and adhesion activities of the recombinant HSCs were significantly decreased compared with those of the control HSCs. In addition, *FAK* mRNA expression was significantly increased in acetaldehyde-activated HSCs, suggesting that FAK plays an important role in the activation of HSCs in hepatic fibrosis.

2.7.2 CTGF/integrin/FAK signaling and HCC

HCC usually develops from hepatic fibrosis. CTGF has been found to be overexpressed in 93 human HCC tissues compared with human non-HCC tissues—mainly in HCC cells—and increased CTGF expression was associated with the clinicopathological malignancy of HCC (159). A previous study confirmed that tumor cell-derived CTGF is a building block in the HCC microenvironment, activating nearby HSCs and delivering growth-promoting signals to HCC cells (159). This interaction is easily suppressed by anti-CTGF antibodies, suggesting that pro-tumor crosstalk between HCC cells and HSCs provides an opportunity for therapeutic intervention in HCC. Li et al. found that activation of the integrin β1/Piezo1 contributes to matrix stiffness-induced angiogenesis in HCC, and that high Piezo1 expression is predictive of poor prognosis (160). Integrins are key players in the spread of tumor cells and are expressed at different levels at different stages of tumor development (161, 162). Sarker et al. have extensively summarized the effects of integrin crosstalk with growth factor receptors on growth factor signaling and reviewed the evidence supporting the mechanistic regulation of integrin crosstalk with growth factor signaling, which has important implications for normal cell physiology and anticancer therapy (163). A new study has observed that enhanced radiation-induced G2/M cell cycle arrest is dependent on crosstalk between integrinβ1 and growth factor receptor signaling, which is a new research direction to elucidate the signaling underlying the EGFR/integrinβ1 crosstalk, which may support the development of advanced molecular targeted therapies in radiation oncology (164). Integrin crosstalk refers to the mechanism by which changes in the expression of one integrin subunit or activation of an integrin heterodimer may interfere with the expression and/or activation of other integrin subunits in the same cell. This phenomenon was first described in K562 erythroleukemia cells in 1994 (53, 165, 166). Samaržija et al. reviewed the evidence for integrin crosstalk in a range of cellular systems, with a particular emphasis on cancer, and described the molecular mechanisms of integrin crosstalk, the influence of cell fate determination, and the contribution of crosstalk to therapeutic outcomes (53). As a key player in many cancer features, integrins have been recognized as valuable tumor therapeutic targets (167, 168). Gahmberg et al. conducted a detailed summary of the regulation of integrin-integrin crosstalk on dynamic cell adhesion and found that although the mechanisms leading to integrin crosstalk are incompletely understood, they usually involve intracellular signaling and are also used by other cell surface receptors (169). The phosphorylation of integrins and key intracellular molecules play a crucial role in integrin-cytoplasmic interactions, which, in turn, influence integrin activity and crosstalk, with the integrin β-chain playing a central role in regulating crosstalk. In addition to

integrin-integrin crosstalk, crosstalk can occur between integrins and related receptors, including other adhesion and growth factor receptors.

2.8 PI3K/AKT signaling pathway

PI3K/AKT signaling plays a pivotal role in intracellular and extracellular signal transduction and is also involved in cell proliferation, apoptosis, invasion, and metastasis. PI3K is a crucial protein molecule involved in PI3K/AKT signaling (170). Activated PI3K can promote changes in the downstream substrate AKT and also activate the translocation of *AKT* to the nucleus, thus causing the expression of downstream-related genes and regulating cell proliferation, metabolism, and a series of physiological functions (Figure 3). Mammalian target of rapamycin is the downstream molecule of AKT and is normally activated to play an important role in the regulation of the cell cycle, cell growth, and proliferation (171). The mechanism of action of dexmedetomidine, apatinib, rosiglitazone, sorafenib, metformin, and baicalin may be downregulating the expression of PI3K and phosphorylation of AKT, while activating the apoptotic signaling of caspases to promote apoptosis. PI3K/AKT signaling is activated in 30%–50% of patients with HCC, and upregulation of phosphorylated AKT (p-AKT) is associated with poor survival and tumor vascular invasion in patients with HCC (172) (Table 1). PI3K/AKT signaling is also associated with the inhibition of HCC apoptosis. Therefore, PI3K/AKT signaling may be key to HCC drug development.

2.8.1 PI3K/AKT signaling and hepatic fibrosis

The PI3K/AKT signaling pathway is involved in many processes that regulate HSC activation, including collagen synthesis and cell proliferation. HSC activation is a key step in hepatic fibrosis that requires global reprogramming of gene expression, which is regulated by multiple mechanisms, including epigenetic regulation, such as DNA methylation (173, 174). Studies have confirmed that phosphoenolpyruvate carboxykinase 1 deficiency promotes platelet-derived growth factor AA expression through PI3K/AKT signaling and activates HSCs via hepatocyte-HSC crosstalk, and that this important crosstalk between hepatocytes and HSCs is mediated by paracrine signaling (54, 55). However, the effect of activating or inhibiting PI3K/AKT signaling on hepatic fibrosis remains controversial (64, 175, 176). Recent studies have shown that TGF-β crosstalk with PI3K/AKT signaling occurs in a Smad-independent manner, suggesting that specific crosstalk between macrophages and HSCs via soluble proteins could be an area for further study (177). Damaged hepatocytes and activated immune cells convert quiescent HSCs into MYFs through crosstalk. Recently, it has been reported that DC function is associated with PI3K/AKT signaling, involving functional reprogramming of immune cells, control of cellular responses, and regulation of hepatic fibrosis (56). PI3K/AKT signaling is involved in reprogramming the activity of many immune cells, particularly DCs and macrophages. The latest study by Xiang et al. showed that kinsenoside treatment improved the hepatic inflammatory microenvironment of hepatic fibrosis and reprogrammed intracellular glycolysis by inhibiting the migration and maturation of DCs via inhibition of PI3K/AKT signaling (56). PI3K/AKT signaling is an important pathway regulating HSC proliferation and transdifferentiation in the liver (57, 58). Further investigation revealed that hepatic fibrosis involved complex mutual crosstalk between PI3K/AKT signaling and TGF-β1/Smads signaling, and further study is required (59, 65).

2.8.2 PI3K/AKT signaling and HCC

PI3K can also inhibit tumor cell apoptosis, enhance cell resistance to chemotherapy-induced apoptosis, and promote postoperative tumor growth (60, 178, 179). Crosstalk between stromal and HCC cells changes the characteristics of HCC cells and promotes their growth and metastasis. FGF is also known to play an important role in the development of HCC. Indeed, Liu et al. have demonstrated that matrix stiffness contributes to the mechanical signal transduction of HSCs and promotes the growth and metastasis of HCC cells through the secretion of FGF2 (108). Li et al. also reported for the first time that activated HSC-derived COMP regulates the gene expression of mesenchymal and matrix metalloproteinase (MMP) in HCC cells through CD36, causing abnormal phosphorylation of ERK and AKT, with crosstalk between PI3K/AKT and MEK/ERK signaling (106). Intriguingly, zebrafish share the same molecular pathways as humans. Experiments using a zebrafish HCC model found that aloperine reduced the proliferation of Huh7 cells in a dose- and time-dependent manner, suggesting that the PI3K/AKT cell cycle is an important central node against HCC (61, 180, 181). PI3K/AKT signaling is responsible for metabolic reprogramming and glycolytic induction in HCC and is therefore a promising therapeutic target. Targeting PI3K/AKT signaling has a positive biological impact and a very promising therapeutic prospect in the prevention of HCC (62). Many studies have reported that PI3K/AKT is widely expressed in various types of cancer cells, representing a promising target for tumor therapy (63, 182–185). Metabolic reprogramming is a novel feature of cancer that involves multiple effects and steps and has been recognized as a hallmark of cancer (186, 187). Moreover, the reprogramming of gene expression during EMT and non-transcriptional changes are triggered and regulated by signaling in response to extracellular signals (188). Activation of PI3K/AKT signaling promotes glucose uptake and glycolysis, increases tumor cell proliferation, inhibits apoptosis and autophagy, and promotes cell survival (189–191). During HCC metastasis, PI3K/AKT stimulates EMT and increases MMP expression. Anticancer drugs regulate the proliferation, stemness, and apoptosis of HCC cells by targeting PI3K/AKT signaling (Table 1). Future studies translate these findings to increase and realize more effective treatment options for patients with HCC.

2.9 Ferroptosis

The term ferroptosis was coined in 2012 because erastin and RAS selective lethal small molecules (RSLs) selectively induce non-apoptotic programmed cell death in various cancer cells, which can

be blocked by iron chelating agents (192) (Figure 3, Table 1). Ferroptosis is an iron-dependent form of programmed cell death characterized by the accumulation of large amounts of lipid peroxidation in cells and an imbalance in the Redox state (66, 68, 69). Ferroptosis is associated with various signaling pathways, including amino acid and iron metabolism, ferritin autophagy, and cell adhesion (193–195). Many studies have shown that ferroptosis is closely related to HCC and hepatic fibrosis (70–73, 196). Although hepatic fibrosis has consistently been a global health problem, there remains a lack of effective treatment. The discovery of ferroptosis provides a new perspective to solve this problem.

2.9.1 Ferroptosis and hepatic fibrosis

Ferroptosis is a new form of regulatory necrosis involved in various hepatic diseases, including cancer, hepatic fibrosis, and ischemia–reperfusion injury (66, 192). *In vitro* assays showed that treatment with artesunate significantly triggered ferroptosis in activated HSCs (68). Yi et al. found that berberine alleviated hepatic fibrosis induced by TAA and CCl_4 in mice by inducing ferrous redox activation of ROS-mediated HSC ferroptosis, the mechanism of which involves ubiquitination-related ubiquitin–proteasome pathway-autophagy crosstalk in HSCs (69). However, the opposite view persists. The reason for these contradictory results may be related to the insufficient research on the relationship between ferroptosis and hepatic fibrosis (193–195). Ferroptosis is the result of iron homeostasis, iron deficiency, and acquired and inherited iron overload, resulting in iron metabolism disorders (70, 196). Ferroptosis has unique biological energy and morphological characteristics, which are different from other forms of programed cell death. However, the specific mechanism of ferroptosis in the process of hepatic fibrosis is still unclear, and some new experimental results are controversial (71–73). Although ferroptosis and apoptosis involve different mechanisms, a potential link between ferroptosis and apoptosis in HSCs still needs to be studied. Future research will focus on whether ferroptosis and apoptosis are closely related and whether crosstalk exists between them (73, 197, 198). In summary, the aforementioned studies suggest that inducing ferroptosis in HSCs may be a viable strategy for the treatment and/or prevention of hepatic fibrosis (67, 74, 199). However, challenges remain regarding the ability to selectively induce HSC ferroptosis with minimal impact on other healthy liver cells. Future studies are needed to determine the exact molecular mechanisms of ferroptosis and lipid metabolism involved in the pathogenesis of hepatic fibrosis (200, 201).

2.9.2 Ferroptosis and HCC

Increasing evidence supports the idea that activating ferroptosis may effectively inhibit HCC cell growth, thus providing a scientific basis for targeting ferroptosis as a new therapeutic strategy for HCC (202, 203). Thus, ferroptosis-inducing compounds are widely considered a promising approach for the development of novel anticancer drugs (204–207) (Table 1). Indeed, since its discovery in 2021, multiple studies have found that ferroptosis is the dominant pattern of radiation-induced cell death in HCC (75, 76, 208). Moreover, recent studies have reported direct crosstalk between ferroptosis and anti-tumor immunity, showing that tumor-infiltrating lymphocyte-mediated ferroptosis can effectively enhance the efficacy of immune checkpoint inhibitors (209–211). Xu and colleagues conducted an in-depth study on the prognostic characteristics of lncRNA associated with ferroptosis and established a promising prognostic model for HCC based on the differentially expressed lncRNA associated with ferroptosis, which can be used for prognostic prediction and selection of patients for immunotherapy. This is the first report on the effects of ferroptosis-related lncRNAs on the prognosis and immune response of the HCC population, providing a promising strategy to guide individualized therapy and improve prognosis prediction (210). Here, we summarized the typical involvement of ferroptosis in hepatic fibrosis and the HCC process and discussed the potential mechanism. Many studies have found that inducing ferroptosis inhibits hepatic fibrosis and HCC progression (212, 213). Preclinical studies of many natural products, chemicals, and drug carriers have revealed their ability to trigger ferroptosis; indeed, ferroptosis inducers are considered a key development direction in the future, with high efficiency and low toxicity.

2.10 YAP/HIF-1α signaling

YAP is an important transcriptional coactivator and a key nucleoplasm shuttle protein that is abnormally highly expressed in many malignant tumors, including HCC, and plays a role in transcriptional regulation mainly in the nucleus. Hypoxia-inducible factor-1α (HIF-1α) is a transcriptionally active nucleoprotein, the regulation of which through cell signaling was first discovered by Semenza and colleagues in 1995. Over the past few decades, a large body of evidence has shown that HIF-1α is closely associated with hepatic fibrosis (214). HIF-1α is stably expressed during hypoxia and forms a dimer with HIF-1β, inducing downstream gene transcription and hypoxia response (215–217). HIF-1α regulates VEGF under hypoxic conditions, controls angiogenesis, cell proliferation, and metastasis, and plays an important role in the occurrence and development of hepatic fibrosis and HCC (77, 78, 218, 219). In tumor cells, YAP and HIF-1α can bind to each other and stabilize HIF-1α proteins in the nucleus, forming the YAP-HIF-1α complex. Hypoxia regulates YAP phosphorylation and promotes *YAP* nuclear translocation, allowing it to bind to HIF-1α and promote its transcriptional activity (220–223) (Figure 3). The role of the YAP protein in the metabolic reprogramming of tumor cells has received increasing attention by researchers and has become a current research focus.

2.10.1 YAP/HIF-1α signaling and hepatic fibrosis

Hypoxia is an important feature of hepatic fibrosis, which can upregulate the expression of HIF-1α, promote the activation of HSCs, and lead to hepatic fibrosis. Improving the anoxic environment at the site of hepatic fibrosis and downregulating the expression of HIF-1α to the maximum extent can improve the therapeutic effect of hepatic fibrosis (215, 216). HIF-1α is known to stimulate collagen synthesis and chemotaxis in HSCs, as well as induce HSC migration, with activated HSCs known to play a

dominant role in sinusoidal structural changes during fibrosis through crosstalk with LSECs. HIF-1α also regulates HSC metabolic reprogramming through the deactivation of glycolytic genes (216). However, controversial conclusions still exist (217). Indeed, Fan et al. recently found that HIF-1α signaling plays an important role in the metabolic reprogramming of LPS-activated macrophages from glycolysis to oxidative phosphorylation induced by Celastrol (218). Multiple studies have confirmed that inflammation is the driving force behind hepatic fibrosis (77, 217, 218). As a transcription factor, HIF-1α reprograms the adaptive response of hypoxic metabolism and can induce fibrosis in multiple tissues (78). In addition, in tumor and stem cells, succinate induces HIF-1α to reprogram energy metabolism under hypoxic conditions. Intracellular succinate accumulation activates HSCs in a receptor-independent manner, while induction of HIF-1α acts as a transcription factor to reprogram cellular metabolism in response to stress (78, 219–221). HIF-1α represents an important transcription factor that promotes hepatic fibrosis, making it a potential therapeutic target (222–224). Under hypoxic conditions, HIF-1α subunits are stabilized by inhibition of proline hydroxylase and thus accumulate in the nucleus. *HIF-1* binds to hypoxic response elements and regulates the transcription of hundreds of genes involved in multiple processes, including angiogenesis, cell proliferation, erythropoiesis, metabolic reprogramming, and apoptosis/survival, in response to cell damage caused by hypoxia (224–226). Many studies have shown that HIF-1α mediates oxygen homeostasis, regulates the expression of multiple hypoxia stress protein genes, and significantly increases the expression in hepatic fibrosis tissues (79–81, 227, 228) (Table 1). Sun et al. found that microRNA-21 alleviates the abnormal crosstalk of hepatocytes and HSCs by inhibiting HIF-1α/VEGF signaling, ameliorating arsenite-induced hepatic fibrosis (229). Both microRNA-98 and miR-345–5p ameliorate hepatic fibrosis through inhibiting HIF-1α signaling (230, 231). However, microRNA-322/424 promotes angiogenesis to aggravate hepatic fibrosis by activating the HIF-1α signaling (232). Hypoxia significantly increases the levels of proinflammatory and profibrotic factors, and inhibition of HIF-1α is key to reducing adipose fibrosis and inflammation (82). Zhang et al. reported that Oroxylin A alleviated the angiogenesis of LSECs in hepatic fibrosis by suppressing YAP/HIF-1α signaling (83). Moreover, *in vitro* interference with YAP was found to significantly down-regulate HIF-1α protein expression, whereas the YAP plasmid showed the opposite effect in cellular assays (233–235). Recently, it has been shown that overexpression of HIF-1α-antisense RNA 1 inhibits the progression of hepatic fibrosis (236, 237).

2.10.2 YAP/HIF-1α signaling and HCC

In general, HCC occurs primarily in the context of cirrhosis resulting from chronic inflammation and advanced fibrosis. Extensive hepatic fibrosis is observed in the paracancer tissues of patients with HCC. Previous studies have shown that hypoxia can promote the release of fibrotic mediators (84). HCC cells can reprogram their energy metabolism to aerobic glycolysis, a phenomenon known as the Warburg effect. HCC is often associated with intratumor hypoxia due to the high oxygen metabolism of rapidly proliferating tumor cells. This hypoxic microenvironment promotes tumor aggressiveness and treatment resistance by activating the HIF regulatory pathway (238). Existing *in vivo* and *in vitro* evidence supports that increased matrix stiffness enhances the malignant characteristics of HCC cells and promotes invasion and metastasis in various ways, including by triggering the occurrence of EMT, promoting the formation of a pre-metastatic niche, enhancing stemness characteristics, upregulating the expression of invasion/metastasis-related genes, affecting the reprogramming of glucose and lipid metabolism, and reducing the efficacy of chemotherapy (160). Hypoxia is a key factor in inducing the transcription of HIF-1α encoding *HIF1A* and the accumulation of HIF-1α protein to promote angiogenesis (85, 239–241). HIF-1α is a key regulator of glycolytic metabolism, which mediates energy metabolic reprogramming in HCC (242). Inhibiting or interfering with the expression of HIF-1α effectively restrains energy metabolism and growth in HCC glycolytic metabolism. HCC cells undergo metabolic reprogramming, which is essential for subsequent rapid tumor growth, with lipid metabolism reprogramming identified as one of the new hallmarks of cancer (243). In the liver tissues of patients with HCC, both fatty acid binding protein 5 (FABP5) and HIF-1α are up-regulated, and their protein expression levels are associated with poor prognosis. Seo et al. recently reported that fatty acid-induced FABP5 upregulation drives HCC progression through HIF-1α-driven lipid metabolic reprogramming (243). Yang et al. recently found that hepatitis B virus X-interacting protein drives the metabolic reprogramming of HCC cells through methyltransferase-like protein 3-mediated m6A modification of HIF-1α (244). In addition, inhibition of HIF-1α and HIF-2α activity interferes with tumor growth and vascularization as well as reprogramming of the tumor immune microenvironment to promote anti-tumor immunity and improve the response to anti-programmed cell death protein 1 therapy (86, 245–248). The role of hypoxia-induced HIF-1α in HCC progression has been extensively studied, and it has been confirmed that hypoxia stress in HCC cells promotes the binding of YAP to HIF-1α in the nucleus (249–251). Bao et al. conducted a detailed review of the role of HIF-mediated metabolic reprogramming in HCC drug resistance and found that HIF-induced glucose metabolism, glucose uptake, and glycolysis were activated in HCC cells under hypoxic conditions, which promoted glucose uptake and satisfied the glucose requirement for the growth of hypoxic cancer cells (252). Moreover, long-chain non-coding RNA expressed in HCC tissues was increased by activating HIF-1α signaling to enhance HCC cell activation and proliferation, thereby promoting HCC progression (253–256). Overexpression and activation of YAP are associated with poor prognosis in patients with HCC, possibly because it promotes tumor progression and/or metastasis. Previous research has found that the existence of nuclear *YAP* is possible due to its combination with DNA transcription factors, which helps maintain its activity to help stabilize HIF-1α. Dai and colleagues showed that YAP signaling activation is not dependent on HIF-1α under the condition of low oxygen (257–259). A high density of tumor-infiltrating plasmacytoid DCs (pDCs) is associated with poor prognosis in patients with HCC. Hypoxia-induced extracellular adenosine (eADO) significantly enhances pDC recruitment to tumors via adenosine A1 receptors (ADORA1). Mechanistically, *HIF-1α* transcriptionally upregulated the expression of exonucleogenases CD39 and CD73, which are essential for

eADO production. Targeted recruitment of pDCs may become potential auxiliary HCC immunotherapy strategies, with crosstalk between inflammation and immunity reported previously (260). Reprogramming of lipid metabolism induced by HIF-1α has also been identified as a hallmark of cancer (261). Hypoxia increases the proportion of HCC cells with stem cell characteristics, whereas specific small ubiquitin-like modifier protease 1 (SENP1) promotes hypoxia-induced HCC cell stemness through HIF-1α oxygenation and a SENP1/HIF-1α positive feedback loop. Drugs specifically targeted to inhibit SENP1 may provide a novel therapeutic approach for HCC (262–264). It is known that there is a significant correlation between the anoxic microenvironment and sorafenib resistance. A new study found that β2 adrenergic receptor signaling negatively regulates autophagy, promotes HIF-1α stabilization, and reprograms glucose metabolism in HCC cells, leading to sorafenib resistance (265–267). YAP is highly expressed in the liver tissues of patients with HCC and is positively correlated with HIF-1α and pyruvate kinase isoform M2 (PKM2) expression. Gene set enrichment analysis has revealed that *YAP* overexpression in the liver tissues of patients with HCC under hypoxic conditions is closely correlated with *HIF-1α* (268). Hypoxia promotes glycolysis of HCC cells by reducing *p-YAP* expression and triggering *YAP* nuclear translocation. *YAP* activation directly interacts with *HIF-1α* in the nucleus, maintaining *HIF-1α* stability to activate *PKM2* transcription. YAP/HIF-1α signaling regulates HCC glycolysis and may represent a novel therapeutic target for HCC. However, whether YAP reprograms HCC cell metabolism requires further study.

3 Conclusion

The characteristics of fibrotic signaling that are common to cancer can be summarized as follows: 1) After reviewing the literature, we found ten fibrotic signals in HCC, all of which are related to inflammation, suggesting that inflammation plays a central role in the development of HCC. 2) When cells are stimulated by different factors, cell signals are transmitted from the extracellular to the intracellular space, and finally enter the nucleus to perform different physiological functions. In addition, fibrotic signals in HCC mediate HCC progression through critical regulation of various immune cells in the immune microenvironment in the liver to maintain a balance between immune tolerance and activation. 3) By activating or inhibiting these 10 fibrotic signals in HCC, different drugs inhibit the activation, proliferation, migration, invasion, and apoptosis of HSCs, CAFs, and HCC cells (Figures 2, 3, Table 1). 4) The inhibition of metabolic reprogramming of HSCs or HCC cells by different drugs targeting various fibrotic signaling pathways in HCC is a focus of current research. 5) Crosstalk between HSCs/MYFs and HCC cells in the microenvironment alters the properties and facilitates the growth, proliferation, migration, and invasion of HCC cells. 6) Anti-HCC drugs regulate the stemness of HCC cells by targeting various fibrotic signals in HCC, which is also a current research focus. HCC can be distinguished from other cancers in terms of fibrotic signaling as follows: 1) The precancerous fibrotic microenvironment of chronic liver disease is characterized by neovascularization, inflammation, and fibrosis. Fibrotic signals of HCC are more closely related to inflammation than those of other cancers. 2) Inflammatory fibrosis of the liver leads to immune tolerance to the microenvironment, which prevents the immune system from recognizing and clearing malignant transformed hepatocytes, MYFs, and CAFs. As the liver contains several types of immune cells, the fibrotic signal of HCC is more closely related to immunity than that of other cancers. 3) The liver is the largest metabolic organ in the body, and it is currently a hot research topic, in which studies have focused on inhibiting the metabolic reprogramming of HCC cells and the formation of HIF. 4) The fibrosis signals of HCC involve multiple cells, and the crosstalk between different cells and signaling pathways is more complex and requires in-depth research. Finally, the occurrence and development of HCC can be inhibited to varying degrees by regulating the above eight fibrosis signaling pathways, many of which interact with each other. New drugs for the prevention and treatment of HCC targeting different fibrosis signaling pathways continue to appear, and those with good targeting and minimal side effects will likely be developed in the future (Table 1).

Author contributions

Writing of the manuscript: LS, WX, and DZ. Developing the idea for the article and critically revising it: FW and JL. Supervision: XL. All authors contributed to the article and approved the submitted version.

Funding

This study was supported by the National Natural Science Foundation of China (grant: 82003849), the National Natural Science Foundation of China (grant: 81970518), the Special Doctoral Fund of Hefei Hospital Affiliated to Anhui Medical University (the 2nd People's Hospital of Hefei) (grant: 2020BSZX04), the Science and Technology Project of Bengbu Medical College (grant: 2022byzd192), and the Key Scientific Research Foundation of the Education Department of the Province Anhui (2023AH052595).

Acknowledgments

We thank LetPub (www.letpub.com) for its linguistic assistance during the preparation of this manuscript.

Conflict of interest

The authors declare that the research was conducted in the absence of any commercial or financial relationships that could be construed as a potential conflict of interest.

Publisher's note

References

1. Piñero F, Dirchwolf M, Pessôa MG. Biomarkers in hepatocellular carcinoma: diagnosis, prognosis and treatment response assessment. *Cells* (2020) 9(6):1370. doi: 10.3390/cells9061370

2. Forner A, Reig M, Bruix J. Hepatocellular carcinoma. *Lancet* (2018) 391 (10127):1301–14. doi: 10.1016/S0140-6736(18)30010-2

3. Llovet JM, Kelley RK, Villanueva A, Singal AG, Pikarsky E, Roayaie S, et al. Hepatocellular carcinoma. *Nat Rev Dis Primers* (2021) 7(1):7. doi: 10.1038/s41572-021-00245-6

4. Ganesan P, Kulik LM. Hepatocellular carcinoma: new developments. *Clin Liver Dis* (2023) 27(1):85–102. doi: 10.1016/j.cld.2022.08.004

5. Parikh ND, Pillai A. Recent advances in hepatocellular carcinoma treatment. *Clin Gastroenterol Hepatol* (2021) 19(10):2020–4. doi: 10.1016/j.cgh.2021.05.045

6. Lee YH, Tai D, Yip C, Choo SP, Chew V. Combinational immunotherapy for hepatocellular carcinoma: radiotherapy, immune checkpoint blockade and beyond. *Front Immunol* (2020) 11:568759. doi: 10.3389/fimmu.2020.568759

7. Donne R, Lujambio A. The liver cancer immune microenvironment: Therapeutic implications for hepatocellular carcinoma. *Hepatology* (2023) 77(5):1773–96. doi: 10.1002/hep.32740

8. Xue R, Zhang Q, Cao Q, Kong R, Xiang X, Liu H, et al. Liver tumour immune microenvironment subtypes and neutrophil heterogeneity. *Nature* (2022) 612 (7938):141–7. doi: 10.1038/s41586-022-05400-x

9. Zhao J, Li H, Zhao S, Wang E, Zhu J, Feng D, et al. Epigenetic silencing of miR-144/451a cluster contributes to HCC progression *via* paracrine HGF/MIF-mediated TAM remodeling. *Mol Cancer* (2021) 20(1):46. doi: 10.1186/s12943-021-01343-5

10. Bates J, Vijayakumar A, Ghoshal S, Marchand B, Yi S, Kornyeyev D, et al. Acetyl-CoA carboxylase inhibition disrupts metabolic reprogramming during hepatic stellate cell activation. *J Hepatol* (2020) 73(4):896–905. doi: 10.1016/j.jhep.2020.04.037

11. Ioannou GN. HCC surveillance after SVR in patients with F3/F4 fibrosis. *J Hepatol* (2021) 74(2):458–65. doi: 10.1016/j.jhep.2020.10.016

12. Carmona-Hidalgo B, González-Mariscal I, García-Martín A, Prados ME, Ruiz-Pino F, Appendino G, et al. Δ9-Tetrahydrocannabinolic Acid markedly alleviates liver fibrosis and inflammation in mice. *Phytomedicine* (2021) 81:153426. doi: 10.1016/j.phymed.2020.153426

13. Kisseleva T, Brenner D. Molecular and cellular mechanisms of liver fibrosis and its regression. *Nat Rev Gastroenterol Hepatol* (2021) 18(3):151–66. doi: 10.1038/s41575-020-00372-7

14. Samant H, Amiri HS, Zibari GB. Addressing the worldwide hepatocellular carcinoma: epidemiology, prevention and management. *J Gastrointest Oncol* (2021) 12(Suppl 2):S361–73. doi: 10.21037/jgo.2020.02.08

15. Zhao B, Lv X, Zhao X, Maimaitiaili S, Zhang Y, Su K, et al. Tumor-promoting actions of HNRNP A1 in HCC are associated with cell cycle, mitochondrial dynamics, and necroptosis. *Int J Mol Sci* (2022) 23(18):10209. doi: 10.3390/ijms231810209

16. Baglieri J, Brenner DA, Kisseleva T. The role of fibrosis and liver-associated fibroblasts in the pathogenesis of hepatocellular carcinoma. *Int J Mol Sci* (2019) 20 (7):1723. doi: 10.3390/ijms20071723

17. Oura K, Morishita A, Tani J, Masaki T. Tumor immune microenvironment and immunosuppressive therapy in hepatocellular carcinoma: A review. *Int J Mol Sci* (2021) 22(11):5801. doi: 10.3390/ijms22115801

18. Affo S, Nair A, Brundu F, Ravichandra A, Bhattacharjee S, Matsuda M, et al. Promotion of cholangiocarcinoma growth by diverse cancer-associated fibroblast subpopulations. *Cancer Cell* (2021) 39(6):866–82.e11. doi: 10.1016/j.ccell.2021.03.012

19. Rebouissou S, Nault JC. Advances in molecular classification and precision oncology in hepatocellular carcinoma. *J Hepatol* (2020) 72(2):215–29. doi: 10.1016/j.jhep.2019.08.017

20. Matsuda M, Seki E. Hepatic stellate cell-macrophage crosstalk in liver fibrosis and carcinogenesis. *Semin Liver Dis* (2020) 40(3):307–20. doi: 10.1055/s-0040-1708876

21. Guo S, Li W, Chen F, Yang S, Huang Y, Tian Y, et al. Polysaccharide of Atractylodes macrocephala Koidz regulates LPS-mediated mouse hepatitis through the TLR4-MyD88-NFκB signaling pathway. *Int Immunopharmacol* (2021) 98:107692. doi: 10.1016/j.intimp.2021.107692

22. Mohandas S, Vairappan B. Pregnane X receptor activation by its natural ligand Ginkgolide-A improves tight junction proteins expression and attenuates bacterial translocation in cirrhosis. *Chem Biol Interact* (2020) 315:108891. doi: 10.1016/j.cbi.2019.108891

23. Ding J, Li HY, Zhang L, Zhou Y, Wu J. Hedgehog signaling, a critical pathway governing the development and progression of hepatocellular carcinoma. *Cells* (2021) 10(1):123. doi: 10.3390/cells10010123

24. Gao L, Zhang Z, Zhang P, Yu M, Yang T. Role of canonical Hedgehog signaling pathway in liver. *Int J Biol Sci* (2018) 14(12):1636–44. doi: 10.7150/ijbs.28089

25. Zhao Z, Zhang D, Wu F, Tu J, Song J, Xu M, et al. Sophoridine suppresses lenvatinib-resistant hepatocellular carcinoma growth by inhibiting RAS/MEK/ERK axis *via* decreasing VEGFR2 expression. *J Cell Mol Med* (2021) 25(1):549–60. doi: 10.1111/jcmm.16108

26. Foglia B, Cannito S, Bocca C, Parola M, Novo E. ERK pathway in activated, myofibroblast-like, hepatic stellate cells: A critical signaling crossroad sustaining liver fibrosis. *Int J Mol Sci* (2019) 20(11):2700. doi: 10.3390/ijms20112700

27. Xiang D, Zou J, Zhu X, Chen X, Luo J, Kong L, et al. Physalin D attenuates hepatic stellate cell activation and liver fibrosis by blocking TGF-β/Smad and YAP signaling. *Phytomedicine* (2020) 78:153294. doi: 10.1016/j.phymed.2020.153294

28. Yang Y, Sun M, Li W, Liu C, Jiang Z, Gu P, et al. Rebalancing TGF-β/Smad7 signaling *via* Compound kushen injection in hepatic stellate cells protects against liver fibrosis and hepatocarcinogenesis. *Clin Transl Med* (2021) 11(7):e410. doi: 10.1002/ctm2.410

29. Caja L, Dituri F, Mancarella S, Caballero-Diaz D, Moustakas A, Giannelli G, et al. TGF-β and the tissue microenvironment: relevance in fibrosis and cancer. *Int J Mol Sci* (2018) 19(5):1294. doi: 10.3390/ijms19051294

30. Wang B, Liu T, Wu JC, Luo SZ, Chen R, Lu LG, et al. STAT3 aggravates TGF-β1-induced hepatic epithelial-to-mesenchymal transition and migration. *BioMed Pharmacother* (2018) 98:214–21. doi: 10.1016/j.biopha.2017.12.035

31. Pinter M, Jain RK, Duda DG. The current landscape of immune checkpoint blockade in hepatocellular carcinoma: A review. *JAMA Oncol* (2021) 7(1):113–23. doi: 10.1001/jamaoncol.2020.3381

32. Yan Y, Zeng J, Xing L, Li C. Extra- and intra-cellular mechanisms of hepatic stellate cell activation. *Biomedicines* (2021) 9(8):1014. doi: 10.3390/biomedicines9081014

33. Liao S, Chen H, Liu M, Gan L, Li C, Zhang W, et al. Aquaporin 9 inhibits growth and metastasis of hepatocellular carcinoma cells *via* Wnt/β-catenin pathway. *Aging (Albany NY)* (2020) 12(2):1527–44. doi: 10.18632/aging.102698

34. Li Q, Sun M, Wang M, Feng M, Yang F, Li L, et al. Dysregulation of Wnt/β-catenin signaling by protein kinases in hepatocellular carcinoma and its therapeutic application. *Cancer Sci* (2021) 112(5):1695–706. doi: 10.1111/cas.14861

35. He S, Tang S. WNT/β-catenin signaling in the development of liver cancers. *BioMed Pharmacother* (2020) 132:110851. doi: 10.1016/j.biopha.2020.110851

36. Perugorria MJ, Olaizola P, Labiano I, Esparza-Baquer A, Marzioni M, Marin JJG, et al. Wnt-β-catenin signalling in liver development, health and disease. *Nat Rev Gastroenterol Hepatol* (2019) 16(2):121–36. doi: 10.1038/s41575-018-0075-9

37. Cao G, Zhu R, Jiang T, Tang D, Kwan HY, Su T. Danshensu, a novel indoleamine 2,3-dioxygenase1 inhibitor, exerts anti-hepatic fibrosis effects *via* inhibition of JAK2-STAT3 signaling. *Phytomedicine* (2019) 63:153055. doi: 10.1016/j.phymed.2019.153055

38. Xu Y, Zhang D, Yang H, Liu Y, Zhang L, Zhang C, et al. Hepatoprotective effect of genistein against dimethylnitrosamine-induced liver fibrosis in rats by regulating macrophage functional properties and inhibiting the JAK2/STAT3/SOCS3 signaling pathway. *Front Biosci (Landmark Ed)* (2021) 26(12):1572–84. doi: 10.52586/5050

39. Ding H, Yang X, Tian J, Wang X, Ji Y, El-Ashram S, et al. JQ-1 ameliorates schistosomiasis liver fibrosis by suppressing JAK2 and STAT3 activation. *BioMed Pharmacother* (2021) 144:112281. doi: 10.1016/j.biopha.2021.112281

40. Zhang XL, Zhang XY, Ge XQ, Liu MX. Mangiferin prevents hepatocyte epithelial-mesenchymal transition in liver fibrosis *via* targeting HSP27-mediated JAK2/STAT3 and TGF-β1/Smad pathway. *Phytother Res* (2022) 36(11):4167–82. doi: 10.1002/ptr.7549

41. Zhu M, Shi X, Gong Z, Su Q, Yu R, Wang B, et al. Cantharidin treatment inhibits hepatocellular carcinoma development by regulating the JAK2/STAT3 and PI3K/Akt pathways in an EphB4-dependent manner. *Pharmacol Res* (2020) 158:104868. doi: 10.1016/j.phrs.2020.104868

42. Xu J, Zhang L, Li N, Dai J, Zhang R, Yao F, et al. Etomidate elicits anti-tumor capacity by disrupting the JAK2/STAT3 signaling pathway in hepatocellular carcinoma. *Cancer Lett* (2023) 552:215970. doi: 10.1016/j.canlet.2022.215970

43. Lin Y, Jian Z, Jin H, Wei X, Zou X, Guan R, et al. Long non-coding RNA DLGAP1-AS1 facilitates tumorigenesis and epithelial-mesenchymal transition in hepatocellular carcinoma *via* the feedback loop of miR-26a/b-5p/IL-6/JAK2/STAT3 and Wnt/β-catenin pathway. *Cell Death Dis* (2020) 11(1):34. doi: 10.1038/s41419-019-2188-7

44. Wu Q, Li L, Miao C, Hasnat M, Sun L, Jiang Z, et al. Osteopontin promotes hepatocellular carcinoma progression through inducing JAK2/STAT3/NOX1-mediated ROS production. *Cell Death Dis* (2022) 13(4):341. doi: 10.1038/s41419-022-04806-9

45. Wu S, Ye S, Lin X, Chen Y, Zhang Y, Jing Z, et al. Small hepatitis B virus surface antigen promotes Malignant progression of hepatocellular carcinoma *via* endoplasmic reticulum stress-induced FGF19/JAK2/STAT3 signaling. *Cancer Lett* (2021) 499:175–87. doi: 10.1016/j.canlet.2020.11.032

46. Yang T, Xu R, Huo J, Wang B, Du X, Dai B, et al. WWOX activation by toosendanin suppresses hepatocellular carcinoma metastasis through JAK2/Stat3 and Wnt/β-catenin signaling. *Cancer Lett* (2021) 513:50–62. doi: 10.1016/j.canlet.2021.05.010

47. Shao T, Chen Z, Belov V, Wang X, Rwema SH, Kumar V, et al. [18F]-Alfatide PET imaging of integrin αvβ3 for the non-invasive quantification of liver fibrosis. *J Hepatol* (2020) 73(1):161–9. doi: 10.1016/j.jhep.2020.02.018

48. Ulmasov B, Noritake H, Carmichael P, Oshima K, Griggs DW, Neuschwander-Tetri BA. An inhibitor of arginine-glycine-aspartate-binding integrins reverses fibrosis in a mouse model of nonalcoholic steatohepatitis. *Hepatol Commun* (2018) 3(2):246–61. doi: 10.1002/hep4.1298

49. Nishimichi N, Tsujino K, Kanno K, Sentani K, Kobayashi T, Chayama K, et al. Induced hepatic stellate cell integrin, α8β1, enhances cellular contractility and TGFβ activity in liver fibrosis. *J Pathol* (2021) 253(4):366–73. doi: 10.1002/path.5618

50. Rahman SR, Roper JA, Grove JI, Aithal GP, Pun KT, Bennett AJ. Integrins as a drug target in liver fibrosis. *Liver Int* (2022) 42(3):507–21. doi: 10.1111/liv.15157

51. Fausther M, Dranoff JA. Integrins, myofibroblasts, and organ fibrosis. *Hepatology* (2014) 60(2):756–8. doi: 10.1002/hep.27155

52. Yokosaki Y, Nishimichi N. New therapeutic targets for hepatic fibrosis in the integrin family, α8β1 and α11β1, induced specifically on activated stellate cells. *Int J Mol Sci* (2021) 22(23):12794. doi: 10.3390/ijms222312794

53. Samaržija I, Dekanić A, Humphries JD, Paradžik M, Stojanović N, Humphries MJ, et al. Integrin crosstalk contributes to the complexity of signalling and unpredictable cancer cell fates. *Cancers (Basel)* (2020) 12(7):1910. doi: 10.3390/cancers12071910

54. Kong D, Zhang Z, Chen L, Huang W, Zhang F, Wang L, et al. Curcumin blunts epithelial-mesenchymal transition of hepatocytes to alleviate hepatic fibrosis through regulating oxidative stress and autophagy. *Redox Biol* (2020) 36:101600. doi: 10.1016/j.redox.2020.101600

55. Ye Q, Liu Y, Zhang G, Deng H, Wang X, Tuo L, et al. Deficiency of gluconeogenic enzyme PCK1 promotes metabolic-associated fatty liver disease through PI3K/AKT/PDGF axis activation in male mice. *Nat Commun* (2023) 14 (1):1402. doi: 10.1038/s41467-023-37142-3

56. Xiang M, Liu T, Tian C, Ma K, Gou J, Huang R, et al. Kinsenoside attenuates liver fibro-inflammation by suppressing dendritic cells *via* the PI3K-AKT-FoxO1 pathway. *Pharmacol Res* (2022) 177:106092. doi: 10.1016/j.phrs.2022.106092

57. Mi XJ, Hou JG, Jiang S, Liu Z, Tang S, Liu XX, et al. Maltol mitigates thioacetamide-induced liver fibrosis through TGF-β1-mediated activation of PI3K/akt signaling pathway. *J Agric Food Chem* (2019) 67(5):1392–401. doi: 10.1021/acs.jafc.8b05943

58. Tang S, Li Y, Bao Y, Dai Z, Niu T, Wang K, et al. Novel cytisine derivatives exert anti-liver fibrosis effect *via* PI3K/Akt/Smad pathway. *Bioorg Chem* (2019) 90:103032. doi: 10.1016/j.bioorg.2019.103032

59. Wang R, Song F, Li S, Wu B, Gu Y, Yuan Y. Salvianolic acid A attenuates CCl_4-induced liver fibrosis by regulating the PI3K/AKT/mTOR, Bcl-2/Bax and caspase-3/cleaved caspase-3 signaling pathways. *Drug Des Devel Ther* (2019) 13:1889–900. doi: 10.2147/DDDT.S194787

60. Liu JS, Huo CY, Cao HH, Fan CL, Hu JY, Deng LJ, et al. Aloperine induces apoptosis and G2/M cell cycle arrest in hepatocellular carcinoma cells through the PI3K/Akt signaling pathway. *Phytomedicine* (2019) 61:152843. doi: 10.1016/j.phymed.2019.152843

61. Chen H, Wong CC, Liu D, Go MYY, Wu B, Peng S, et al. APLN promotes hepatocellular carcinoma through activating PI3K/Akt pathway and is a druggable target. *Theranostics* (2019) 9(18):5246–60. doi: 10.7150/thno.34713

62. Ma XL, Shen MN, Hu B, Wang BL, Yang WJ, Lv LH, et al. CD73 promotes hepatocellular carcinoma progression and metastasis *via* activating PI3K/AKT signaling by inducing Rap1-mediated membrane localization of P110β and predicts poor prognosis. *J Hematol Oncol* (2019) 12(1):37. doi: 10.1186/s13045-019-0724-7

63. Qu L, Liu Y, Deng J, Ma X, Fan D. Ginsenoside Rk3 is a novel PI3K/AKT-targeting therapeutics agent that regulates autophagy and apoptosis in hepatocellular carcinoma. *J Pharm Anal* (2023) 13(5):463–82. doi: 10.1016/j.jpha.2023.03.006

64. Xiu AY, Ding Q, Li Z, Zhang CQ. Doxazosin attenuates liver fibrosis by inhibiting autophagy in hepatic stellate cells *via* activation of the PI3K/akt/mTOR signaling pathway. *Drug Des Devel Ther* (2021) 15:3643–59. doi: 10.2147/DDDT.S317701

65. Wu L, Zhang Q, Mo W, Feng J, Li S, Li J, et al. Quercetin prevents hepatic fibrosis by inhibiting hepatic stellate cell activation and reducing autophagy *via* the TGF-β1/Smads and PI3K/Akt pathways. *Sci Rep* (2017) 7(1):9289. doi: 10.1038/s41598-017-09673-5

66. Du K, Maeso-Díaz R, Oh SH, Wang E, Chen T, Pan C, et al. Targeting YAP-mediated HSC death susceptibility and senescence for treatment of liver fibrosis. *Hepatology* (2023) 77(6):1998–2015. doi: 10.1097/HEP.0000000000000326

67. Yuan S, Wei C, Liu G, Zhang L, Li J, Li L, et al. Sorafenib attenuates liver fibrosis by triggering hepatic stellate cell ferroptosis *via* HIF-1α/SLC7A11 pathway. *Cell Prolif* (2022) 55(1):e13158. doi: 10.1111/cpr.13158

68. Kong Z, Liu R, Cheng Y. Artesunate alleviates liver fibrosis by regulating ferroptosis signaling pathway. *BioMed Pharmacother* (2019) 109:2043–53. doi: 10.1016/j.biopha.2018.11.030

69. Yi J, Wu S, Tan S, Qin Y, Wang X, Jiang J, et al. Berberine alleviates liver fibrosis through inducing ferrous redox to activate ROS-mediated hepatic stellate cells ferroptosis. *Cell Death Discovery* (2021) 7(1):374. doi: 10.1038/s41420-021-00768-7

70. Li L, Wang K, Jia R, Xie J, Ma L, Hao Z, et al. Ferroportin-dependent ferroptosis induced by ellagic acid retards liver fibrosis by impairing the SNARE complexes formation. *Redox Biol* (2022) 56:102435. doi: 10.1016/j.redox.2022.102435

71. Huang S, Wang Y, Xie S, Lai Y, Mo C, Zeng T, et al. Isoliquiritigenin alleviates liver fibrosis through caveolin-1-mediated hepatic stellate cells ferroptosis in zebrafish and mice. *Phytomedicine* (2022) 101:154117. doi: 10.1016/j.phymed.2022.154117

72. Gautheron J, Gores GJ, Rodrigues CMP. Lytic cell death in metabolic liver disease. *J Hepatol* (2020) 73(2):394–408. doi: 10.1016/j.jhep.2020.04.001

73. Shen M, Guo M, Li Y, Wang Y, Qiu Y, Shao J, et al. m6A methylation is required for dihydroartemisinin to alleviate liver fibrosis by inducing ferroptosis in hepatic stellate cells. *Free Radic Biol Med* (2022) 182:246–59. doi: 10.1016/j.freeradbiomed.2022.02.028

74. Liu G, Wei C, Yuan S, Zhang Z, Li J, Zhang L, et al. Wogonoside attenuates liver fibrosis by triggering hepatic stellate cell ferroptosis through SOCS1/P53/SLC7A11 pathway. *Phytother Res* (2022) 36(11):4230–43. doi: 10.1002/ptr.7558

75. Li B, Wei S, Yang L, Peng X, Ma Y, Wu B, et al. CISD2 promotes resistance to sorafenib-induced ferroptosis by regulating autophagy in hepatocellular carcinoma. *Front Oncol* (2021) 11:657723. doi: 10.3389/fonc.2021.657723

76. Conche C, Finkelmeier F, Pešić M, Nicolas AM, Böttger TW, Kennel KB, et al. Combining ferroptosis induction with MDSC blockade renders primary tumours and metastases in liver sensitive to immune checkpoint blockade. *Gut* (2023) 72(9):1774–82. doi: 10.1136/gutjnl-2022-327909

77. Eshaghian A, Khodarahmi A, Safari F, Binesh F, Moradi A. Curcumin attenuates hepatic fibrosis and insulin resistance induced by bile duct ligation in rats. *Br J Nutr* (2018) 120(4):393–403. doi: 10.1017/S0007114518001095

78. She L, Xu D, Wang Z, Zhang Y, Wei Q, Aa J, et al. Curcumin inhibits hepatic stellate cell activation *via* suppression of succinate-associated HIF-1α induction. *Mol Cell Endocrinol* (2018) 476:129–38. doi: 10.1016/j.mce.2018.05.002

79. Zhang F, Lu S, He J, Jin H, Wang F, Wu L, et al. Ligand activation of PPARγ by ligustrazine suppresses pericyte functions of hepatic stellate cells *via* SMRT-mediated transrepression of HIF-1α. *Theranostics* (2018) 8(3):610–26. doi: 10.7150/thno.22237

80. Yang J, Li S, Liu S, Zhang Y, Shen D, Wang P, et al. Metformin ameliorates liver fibrosis induced by congestive hepatopathy *via* the mTOR/HIF-1α signaling pathway. *Ann Hepatol* (2023) 28(6):101135. doi: 10.1016/j.aohep.2023.101135

81. Al-Hashem F, Al-Humayed S, Amin SN, Kamar SS, Mansy SS, Hassan S, et al. Metformin inhibits mTOR-HIF-1α axis and profibrogenic and inflammatory biomarkers in thioacetamide-induced hepatic tissue alterations. *J Cell Physiol* (2019) 234(6):9328–37. doi: 10.1002/jcp.27616

82. Wu K, Li B, Ma Y, Tu T, Lin Q, Zhu J, et al. Nicotinamide mononucleotide attenuates HIF-1α activation and fibrosis in hypoxic adipose tissue *via* NAD+/SIRT1 axis. *Front Endocrinol (Lausanne)* (2023) 14:1099134. doi: 10.3389/fendo.2023.1099134

83. Zhang C, Bian M, Chen X, Jin H, Zhao S, Yang X, et al. Oroxylin A prevents angiogenesis of LSECs in liver fibrosis *via* inhibition of YAP/HIF-1α signaling. *J Cell Biochem* (2018) 119(2):2258–68. doi: 10.1002/jcb.26388

84. Qu K, Yan Z, Wu Y, Chen Y, Qu P, Xu X, et al. Transarterial chemoembolization aggravated peritumoral fibrosis *via* hypoxia-inducible factor-1α dependent pathway in hepatocellular carcinoma. *J Gastroenterol Hepatol* (2015) 30(5):925–32. doi: 10.1111/jgh.12873

85. Chen H, Nio K, Tang H, Yamashita T, Okada H, Li Y, et al. BMP9-ID1 signaling activates HIF-1α and VEGFA expression to promote tumor angiogenesis in hepatocellular carcinoma. *Int J Mol Sci* (2022) 23(3):1475. doi: 10.3390/ijms23031475

86. Salman S, Meyers DJ, Wicks EE, Lee SN, Datan E, Thomas AM, et al. HIF inhibitor 32-134D eradicates murine hepatocellular carcinoma in combination with anti-PD1 therapy. *J Clin Invest* (2022) 132(9):e156774. doi: 10.1172/JCI156774

87. Yuan T, Lv S, Zhang W, Tang Y, Chang H, Hu Z, et al. PF-PLC micelles ameliorate cholestatic liver injury *via* regulating TLR4/MyD88/NF-κB and PXR/CAR/UGT1A1 signaling pathways in EE-induced rats. *Int J Pharm* (2022) 615:121480. doi: 10.1016/j.ijpharm.2022.121480

88. Khan HU, Aamir K, Jusuf PR, Sethi G, Sisinthy SP, Ghildyal R, et al. Lauric acid ameliorates lipopolysaccharide (LPS)-induced liver inflammation by mediating TLR4/MyD88 pathway in Sprague Dawley (SD) rats. *Life Sci* (2021) 265:118750. doi: 10.1016/j.lfs.2020.118750

89. Liu M, Xu Y, Han X, Yin L, Xu L, Qi Y, et al. Author Correction: Dioscin alleviates alcoholic liver fibrosis by attenuating hepatic stellate cell activation *via* the TLR4/MyD88/NF-κB signaling pathway. *Sci Rep* (2020) 10(1):18384. doi: 10.1038/s41598-020-74987-w

90. Hu N, Guo C, Dai X, Wang C, Gong L, Yu L, et al. Forsythiae Fructuse water extract attenuates liver fibrosis *via* TLR4/MyD88/NF-κB and TGF-β/smads signaling pathways. *J Ethnopharmacol* (2020) 262:113275. doi: 10.1016/j.jep.2020.113275

91. Liao X, Zhan W, Tian T, Yu L, Li R, Yang Q. MicroRNA-326 attenuates hepatic stellate cell activation and liver fibrosis by inhibiting TLR4 signaling. *J Cell Biochem* (2020) 121(8-9):3794–803. doi: 10.1002/jcb.29520

92. Zhang C, Wang N, Tan HY, Guo W, Chen F, Zhong Z, et al. Direct inhibition of the TLR4/MyD88 pathway by geniposide suppresses HIF-1α-independent VEGF expression and angiogenesis in hepatocellular carcinoma. *Br J Pharmacol* (2020) 177 (14):3240–57. doi: 10.1111/bph.15046

93. Hu N, Wang C, Dai X, Zhou M, Gong L, Yu L, et al. Phillygenin inhibits LPS-induced activation and inflammation of LX2 cells by TLR4/MyD88/NF-κB signaling pathway. *J Ethnopharmacol* (2020) 248:112361. doi: 10.1016/j.jep.2019.112361

94. Jing X, Tian Z, Gao P, Xiao H, Qi X, Yu Y, et al. HBsAg/β2GPI activates the NF−κB pathway *via* the TLR4/MyD88/IκBα axis in hepatocellular carcinoma. *Oncol Rep* (2018) 40(2):1035–45. doi: 10.3892/or.2018.6507

95. Sheng M, Lin Y, Xu D, Tian Y, Zhan Y, Li C, et al. CD47-mediated hedgehog/SMO/GLI1 signaling promotes mesenchymal stem cell immunomodulation in mouse liver inflammation. *Hepatology* (2021) 74(3):1560–77. doi: 10.1002/hep.31831

96. Gu Y, Wang Y, He L, Zhang J, Zhu X, Liu N, et al. Circular RNA circIPO11 drives self-renewal of liver cancer initiating cells *via* Hedgehog signaling. *Mol Cancer* (2021) 20(1):132. doi: 10.1186/s12943-021-01435-2

97. Wang S, Wang Y, Xun X, Zhang C, Xiang X, Cheng Q, et al. Hedgehog signaling promotes sorafenib resistance in hepatocellular carcinoma patient-derived organoids. *J Exp Clin Cancer Res* (2020) 39(1):22. doi: 10.1186/s13046-020-1523-2

98. Feng J, Wang C, Liu T, Li J, Wu L, Yu Q, et al. Procyanidin B2 inhibits the activation of hepatic stellate cells and angiogenesis *via* the Hedgehog pathway during liver fibrosis. *J Cell Mol Med* (2019) 23(9):6479–93. doi: 10.1111/jcmm.14543

99. Du K, Hyun J, Premont RT, Choi SS, Michelotti GA, Swiderska-Syn M, et al. Hedgehog-YAP signaling pathway regulates glutaminolysis to control activation of hepatic stellate cells. *Gastroenterology* (2018) 154(5):1465–79.e13. doi: 10.1053/j.gastro.2017.12.022

100. Sauzeau V, Beignet J, Vergoten G, Bailly C. Overexpressed or hyperactivated Rac1 as a target to treat hepatocellular carcinoma. *Pharmacol Res* (2022) 179:106220. doi: 10.1016/j.phrs.2022.106220

101. Chen X, Li XF, Chen Y, Zhu S, Li HD, Chen SY, et al. Hesperetin derivative attenuates CCl_4-induced hepatic fibrosis and inflammation by Gli-1-dependent mechanisms. *Int Immunopharmacol* (2019) 76:105838. doi: 10.1016/j.intimp.2019.105838

102. MaChado MV, Diehl AM. Hedgehog signalling in liver pathophysiology. *J Hepatol* (2018) 68(3):550–62. doi: 10.1016/j.jhep.2017.10.017

103. Fan J, Tong G, Chen X, Li S, Yu Y, Zhu S, et al. CK2 blockade alleviates liver fibrosis by suppressing activation of hepatic stellate cells *via* the Hedgehog pathway. *Br J Pharmacol* (2023) 180(1):44–61. doi: 10.1111/bph.15945

104. Chung SI, Moon H, Ju HL, Cho KJ, Kim DY, Han KH, et al. Hepatic expression of Sonic Hedgehog induces liver fibrosis and promotes hepatocarcinogenesis in a transgenic mouse model. *J Hepatol* (2016) 64(3):618–27. doi: 10.1016/j.jhep.2015.10.007

105. Dimri M, Satyanarayana A. Molecular signaling pathways and therapeutic targets in hepatocellular carcinoma. *Cancers (Basel)* (2020) 12(2):491. doi: 10.3390/cancers12020491

106. Li Q, Wang C, Wang Y, Sun L, Liu Z, Wang L, et al. HSCs-derived COMP drives hepatocellular carcinoma progression by activating MEK/ERK and PI3K/AKT signaling pathways. *J Exp Clin Cancer Res* (2018) 37(1):231. doi: 10.1186/s13046-018-0908-y

107. Akula SM, Abrams SL, Steelman LS, Emma MR, Augello G, Cusimano A, et al. RAS/RAF/MEK/ERK, PI3K/PTEN/AKT/mTORC1 and TP53 pathways and regulatory miRs as therapeutic targets in hepatocellular carcinoma. *Expert Opin Ther Targets* (2019) 23(11):915–29. doi: 10.1080/14728222.2019.1685501

108. Liu Z, Mo H, Liu R, Niu Y, Chen T, Xu Q, et al. Matrix stiffness modulates hepatic stellate cell activation into tumor-promoting myofibroblasts *via* E2F3-dependent signaling and regulates Malignant progression. *Cell Death Dis* (2021) 12(12):1134. doi: 10.1038/s41419-021-04418-9

109. Chen Z, Chen L, Sun B, Liu D, He Y, Qi L, et al. LDLR inhibition promotes hepatocellular carcinoma proliferation and metastasis by elevating intracellular cholesterol synthesis through the MEK/ERK signaling pathway. *Mol Metab* (2021) 51:101230. doi: 10.1016/j.molmet.2021.101230

110. Liu M, Hu Q, Tu M, Wang X, Yang Z, Yang G, et al. MCM6 promotes metastasis of hepatocellular carcinoma *via* MEK/ERK pathway and serves as a novel serum biomarker for early recurrence. *J Exp Clin Cancer Res* (2018) 37(1):10. doi: 10.1186/s13046-017-0669-z

111. Lai HH, Hung LY, Yen CJ, Hung HC, Chen RY, Ku YC, et al. NEIL3 promotes hepatoma epithelial-mesenchymal transition by activating the BRAF/MEK/ERK/TWIST signaling pathway. *J Pathol* (2022) 258(4):339–52. doi: 10.1002/path.6001

112. Zhu Z, Xiao T, Chang X, Hua Y, Gao J. Morusinol exhibits selective and potent antitumor activity against human liver carcinoma by inducing autophagy, G2/M cell cycle arrest, inhibition of cell invasion and migration, and targeting of ras/MEK/ERK pathway. *Med Sci Monit* (2019) 25:1864–70. doi: 10.12659/MSM.912992

113. Peng D, Fu M, Wang M, Wei Y, Wei X. Targeting TGF-β signal transduction for fibrosis and cancer therapy. *Mol Cancer* (2022) 21(1):104. doi: 10.1186/s12943-022-01569-x

114. Yan J, Hu B, Shi W, Wang X, Shen J, Chen Y, et al. Gli2-regulated activation of hepatic stellate cells and liver fibrosis by TGF-β signaling. *Am J Physiol Gastrointest Liver Physiol* (2021) 320(5):G720–8. doi: 10.1152/ajpgi.00310.2020

115. Cho SS, Lee JH, Kim KM, Park EY, Ku SK, Cho IJ, et al. REDD1 attenuates hepatic stellate cell activation and liver fibrosis *via* inhibiting of TGF-β/Smad signaling pathway. *Free Radic Biol Med* (2021) 176:246–56. doi: 10.1016/j.freeradbiomed.2021.10.002

116. Li J, Wang Y, Ma M, Jiang S, Zhang X, Zhang Y, et al. Autocrine CTHRC1 activates hepatic stellate cells and promotes liver fibrosis by activating TGF-β signaling. *EBioMedicine* (2019) 40:43–55. doi: 10.1016/j.ebiom.2019.01.009

117. Hu HH, Chen DQ, Wang YN, Feng YL, Cao G, Vaziri ND, et al. New insights into TGF-β/Smad signaling in tissue fibrosis. *Chem Biol Interact* (2018) 292:76–83. doi: 10.1016/j.cbi.2018.07.008

118. Nakamura I, Asumda FZ, Moser CD, Kang YNN, Lai JP, Roberts LR. Sulfatase-2 regulates liver fibrosis through the TGF-β Signaling pathway. *Cancers (Basel)* (2021) 13(21):5279. doi: 10.3390/cancers13215279

119. Dewidar B, Meyer C, Dooley S, Meindl-Beinker AN. TGF-β in hepatic stellate cell activation and liver fibrogenesis-updated 2019. *Cells* (2019) 8(11):1419. doi: 10.3390/cells8111419

120. Roehlen N, Crouchet E, Baumert TF. Liver fibrosis: mechanistic concepts and therapeutic perspectives. *Cells* (2020) 9(4):875. doi: 10.3390/cells9040875

121. Song M, He J, Pan QZ, Yang J, Zhao J, Zhang YJ, et al. Cancer-associated fibroblast-mediated cellular crosstalk supports hepatocellular carcinoma progression. *Hepatology* (2021) 73(5):1717–35. doi: 10.1002/hep.31792

122. Wu MZ, Yuan YC, Huang BY, Chen JX, Li BK, Fang JH, et al. Identification of a TGF-β/SMAD/lnc-UTGF positive feedback loop and its role in hepatoma metastasis. *Signal Transduct Target Ther* (2021) 6(1):395. doi: 10.1038/s41392-021-00781-3

123. Ning J, Ye Y, Bu D, Zhao G, Song T, Liu P, et al. Imbalance of TGF-β1/BMP-7 pathways induced by M2-polarized macrophages promotes hepatocellular carcinoma aggressiveness. *Mol Ther* (2021) 29(6):2067–87. doi: 10.1016/j.ymthe.2021.02.016

124. Chen J, Gingold JA, Su X. Immunomodulatory TGF-β Signaling in hepatocellular carcinoma. *Trends Mol Med* (2019) 25(11):1010–23. doi: 10.1016/j.molmed.2019.06.007

125. Wang X, Wang J, Tsui YM, Shi C, Wang Y, Zhang X, et al. RALYL increases hepatocellular carcinoma stemness by sustaining the mRNA stability of TGF-β2. *Nat Commun* (2021) 12(1):1518. doi: 10.1038/s41467-021-21828-7

126. Li Y, Fan W, Link F, Wang S, Dooley S. Transforming growth factor β latency: A mechanism of cytokine storage and signalling regulation in liver homeostasis and disease. *JHEP Rep* (2021) 4(2):100397. doi: 10.1016/j.jhepr.2021.100397

127. Russell JO, Monga SP. Wnt/β-catenin signaling in liver development, homeostasis, and pathobiology. *Annu Rev Pathol* (2018) 13:351–78. doi: 10.1146/annurev-pathol-020117-044010

128. Liu QW, Ying YM, Zhou JX, Zhang WJ, Liu ZX, Jia BB, et al. Human amniotic mesenchymal stem cells-derived IGFBP-3, DKK-3, and DKK-1 attenuate liver fibrosis through inhibiting hepatic stellate cell activation by blocking Wnt/β-catenin signaling pathway in mice. *Stem Cell Res Ther* (2022) 13(1):224. doi: 10.1186/s13287-022-02906-z

129. Rong X, Liu J, Yao X, Jiang T, Wang Y, Xie F. Human bone marrow mesenchymal stem cells-derived exosomes alleviate liver fibrosis through the Wnt/β-catenin pathway. *Stem Cell Res Ther* (2019) 10(1):98. doi: 10.1186/s13287-019-1204-2

130. Annunziato S, Sun T, Tchorz JS. The RSPO-LGR4/5-ZNRF3/RNF43 module in liver homeostasis, regeneration, and disease. *Hepatology* (2022) 76(3):888–99. doi: 10.1002/hep.32328

131. Fan Q, Yang L, Zhang X, Ma Y, Li Y, Dong L, et al. Autophagy promotes metastasis and glycolysis by upregulating MCT1 expression and Wnt/β-catenin signaling pathway activation in hepatocellular carcinoma cells. *J Exp Clin Cancer Res* (2018) 37(1):9. doi: 10.1186/s13046-018-0673-y

132. Huang G, Liang M, Liu H, Huang J, Li P, Wang C, et al. CircRNA hsa_circRNA_104348 promotes hepatocellular carcinoma progression through modulating miR-187-3p/RTKN2 axis and activating Wnt/β-catenin pathway. *Cell Death Dis* (2020) 11(12):1065. doi: 10.1038/s41419-020-03276-1

133. Yang Y, Ye YC, Chen Y, Zhao JL, Gao CC, Han H, et al. Crosstalk between hepatic tumor cells and macrophages *via* Wnt/β-catenin signaling promotes M2-like macrophage polarization and reinforces tumor Malignant behaviors. *Cell Death Dis* (2018) 9(8):793. doi: 10.1038/s41419-018-0818-0

134. Zhu L, Yang X, Feng J, Mao J, Zhang Q, He M, et al. CYP2E1 plays a suppressive role in hepatocellular carcinoma by regulating Wnt/Dvl2/β-catenin signaling. *J Transl Med* (2022) 20(1):194. doi: 10.1186/s12967-022-03396-6

135. Wang Q, Liang N, Yang T, Li Y, Li J, Huang Q, et al. DNMT1-mediated methylation of BEX1 regulates stemness and tumorigenicity in liver cancer. *J Hepatol* (2021) 75(5):1142–53. doi: 10.1016/j.jhep.2021.06.025

136. Li B, Cao Y, Meng G, Qian L, Xu T, Yan C, et al. Targeting glutaminase 1 attenuates stemness properties in hepatocellular carcinoma by increasing reactive oxygen species and suppressing Wnt/beta-catenin pathway. *EBioMedicine* (2019) 39:239–54. doi: 10.1016/j.ebiom.2018.11.063

137. Couri T, Pillai A. Goals and targets for personalized therapy for HCC. *Hepatol Int* (2019) 13(2):125–37. doi: 10.1007/s12072-018-9919-1

138. Wei S, Dai M, Zhang C, Teng K, Wang F, Li H, et al. KIF2C: a novel link between Wnt/β-catenin and mTORC1 signaling in the pathogenesis of hepatocellular carcinoma. *Protein Cell* (2021) 12(10):788–809. doi: 10.1007/s13238-020-00766-y

139. Deng R, Zuo C, Li Y, Xue B, Xun Z, Guo Y, et al. The innate immune effector ISG12a promotes cancer immunity by suppressing the canonical Wnt/β-catenin signaling pathway. *Cell Mol Immunol* (2020) 17(11):1163–79. doi: 10.1038/s41423-020-00549-9

140. Song J, Xie C, Jiang L, Wu G, Zhu J, Zhang S, et al. Transcription factor AP-4 promotes tumorigenic capability and activates the Wnt/β-catenin pathway in hepatocellular carcinoma. *Theranostics* (2018) 8(13):3571–83. doi: 10.7150/thno.25194

141. Lu ZN, Shan Q, Hu SJ, Zhao Y, Zhang GN, Zhu M, et al. Discovery of 1,8-naphthalidine derivatives as potent anti-hepatic fibrosis agents *via* repressing PI3K/AKT/Smad and JAK2/STAT3 pathways. *Bioorg Med Chem* (2021) 49:116438. doi: 10.1016/j.bmc.2021.116438

142. Ding YF, Wu ZH, Wei YJ, Shu L, Peng YR. Hepatic inflammation-fibrosis-cancer axis in the rat hepatocellular carcinoma induced by diethylnitrosamine. *J Cancer Res Clin Oncol* (2017) 143(5):821–34. doi: 10.1007/s00432-017-2364-z

143. Yang YZ, Zhao XJ, Xu HJ, Wang SC, Pan Y, Wang SJ, et al. Magnesium isoglycyrrhizinate ameliorates high fructose-induced liver fibrosis in rat by increasing miR-375-3p to suppress JAK2/STAT3 pathway and TGF-β1/Smad signaling. *Acta Pharmacol Sin* (2019) 40(7):879–94. doi: 10.1038/s41401-018-0194-4

144. Xu S, Mao Y, Wu J, Feng J, Li J, Wu L, et al. TGF-β/Smad and JAK/STAT pathways are involved in the anti-fibrotic effects of propylene glycol alginate sodium sulphate on hepatic fibrosis. *J Cell Mol Med* (2020) 24(9):5224–37. doi: 10.1111/jcmm.15175

145. Shen W, Chen C, Guan Y, Song X, Jin Y, Wang J, et al. A pumpkin polysaccharide induces apoptosis by inhibiting the JAK2/STAT3 pathway in human hepatoma HepG2 cells. *Int J Biol Macromol* (2017) 104(Pt A):681–6. doi: 10.1016/j.ijbiomac.2017.06.078

146. Zhao Y, Wang J, Liu WN, Fong SY, Shuen TWH, Liu M, et al. Analysis and validation of human targets and treatments using a hepatocellular carcinoma-immune humanized mouse model. *Hepatology* (2021) 74(3):1395–410. doi: 10.1002/hep.31812

147. Zhao Z, Song J, Tang B, Fang S, Zhang D, Zheng L, et al. CircSOD2 induced epigenetic alteration drives hepatocellular carcinoma progression through activating JAK2/STAT3 signaling pathway. *J Exp Clin Cancer Res* (2020) 39(1):259. doi: 10.1186/s13046-020-01769-7

148. Wei C, Yang C, Wang S, Shi D, Zhang C, Lin X, et al. Crosstalk between cancer cells and tumor associated macrophages is required for mesenchymal circulating tumor cell-mediated colorectal cancer metastasis. *Mol Cancer* (2019) 18(1):64. doi: 10.1186/s12943-019-0976-4

149. Xu Q, Liao Z, Gong Z, Liu X, Yang Y, Wang Z, et al. Down-regulation of EVA1A by miR-103a-3p promotes hepatocellular carcinoma cells proliferation and migration. *Cell Mol Biol Lett* (2022) 27(1):93. doi: 10.1186/s11658-022-00388-8

150. Liu Y, Xu Q, Deng F, Zheng Z, Luo J, Wang P, et al. HERC2 promotes inflammation-driven cancer stemness and immune evasion in hepatocellular carcinoma by activating STAT3 pathway. *J Exp Clin Cancer Res* (2023) 42(1):38. doi: 10.1186/s13046-023-02609-0

151. Riquelme-Guzmán C, Contreras O, Brandan E. Expression of CTGF/CCN2 in response to LPA is stimulated by fibrotic extracellular matrix *via* the integrin/FAK axis. *Am J Physiol Cell Physiol* (2018) 314(4):C415–27. doi: 10.1152/ajpcell.00013.2017

152. Fu M, Peng D, Lan T, Wei Y, Wei X. Multifunctional regulatory protein connective tissue growth factor (CTGF): A potential therapeutic target for diverse diseases. *Acta Pharm Sin B* (2022) 12(4):1740–60. doi: 10.1016/j.apsb.2022.01.007

153. Tang X, Li X, Li M, Zhong X, Fu W, Ao M, et al. Enhanced US/CT/MR imaging of integrin αvβ3 for liver fibrosis staging in rat. *Front Chem* (2022) 10:996116. doi: 10.3389/fchem.2022.996116

154. Schonfeld M, Villar MT, Artigues A, Weinman SA, Tikhanovich I. Arginine methylation of integrin alpha-4 prevents fibrosis development in alcohol-associated liver disease. *Cell Mol Gastroenterol Hepatol* (2023) 15(1):39–59. doi: 10.1016/j.jcmgh.2022.09.013

155. Sciurba JC, Gieseck RL, Jiwrajka N, White SD, Karmele EP, Redes J, et al. Fibroblast-specific integrin-alpha V differentially regulates type 17 and type 2 driven inflammation and fibrosis. *J Pathol* (2019) 248(1):16–29. doi: 10.1002/path.5215

156. Su X, Ma X, Xie X, Wu H, Wang L, Feng Y, et al. FN-EDA mediates angiogenesis of hepatic fibrosis *via* integrin-VEGFR2 in a CD63 synergetic manner. *Cell Death Discovery* (2020) 6(1):140. doi: 10.1038/s41420-020-00378-9

157. Xu T, Lu Z, Xiao Z, Liu F, Chen Y, Wang Z, et al. Myofibroblast induces hepatocyte-to-ductal metaplasia *via* laminin-αvβ6 integrin in liver fibrosis. *Cell Death Dis* (2020) 11(3):199. doi: 10.1038/s41419-020-2372-9

158. Shi C, Li G, Tong Y, Deng Y, Fan J. Role of CTGF gene promoter methylation in the development of hepatic fibrosis. *Am J Transl Res* (2016) 8(1):125–32.

159. Makino Y, Hikita H, Kodama T, Shigekawa M, Yamada R, Sakamori R, et al. CTGF mediates tumor-stroma interactions between hepatoma cells and hepatic stellate cells to accelerate HCC progression. *Cancer Res* (2018) 78(17):4902–14. doi: 10.1158/0008-5472.CAN-17-3844

160. Li M, Zhang X, Wang M, Wang Y, Qian J, Xing X, et al. Activation of Piezo1 contributes to matrix stiffness-induced angiogenesis in hepatocellular carcinoma. *Cancer Commun (Lond)* (2022) 42(11):1162–84. doi: 10.1002/cac2.12364

161. Peng JM, Lin SH, Yu MC, Hsieh SY. CLIC1 recruits PIP5K1A/C to induce cell-matrix adhesions for tumor metastasis. *J Clin Invest* (2021) 131(1):e133525. doi: 10.1172/JCI133525

162. Jiang K, Dong C, Yin Z, Li R, Mao J, Wang C, et al. Exosome-derived ENO1 regulates integrin α6β4 expression and promotes hepatocellular carcinoma growth and metastasis. *Cell Death Dis* (2020) 11(11):972. doi: 10.1038/s41419-020-03179-1

163. Sarker FA, Prior VG, Bax S, O'Neill GM. Forcing a growth factor response - tissue-stiffness modulation of integrin signaling and crosstalk with growth factor receptors. *J Cell Sci* (2020) 133(23):jcs242461. doi: 10.1242/jcs.242461

164. Vehlow A, Cordes N. Growth factor receptor and β1 integrin signaling differentially regulate basal clonogenicity and radiation survival of fibroblasts *via* a modulation of cell cycling. *In Vitro Cell Dev Biol Anim* (2022) 58(2):169–78. doi: 10.1007/s11626-022-00656-z

165. Uriarte I, Latasa MU, Carotti S, Fernandez-Barrena MG, Garcia-Irigoyen O, Elizalde M, et al. Ileal FGF15 contributes to fibrosis-associated hepatocellular carcinoma development. *Int J Cancer* (2015) 136(10):2469–75. doi: 10.1002/ijc.29287

166. Zheng G, Bouamar H, Cserhati M, Zeballos CR, Mehta I, Zare H, et al. Integrin alpha 6 is upregulated and drives hepatocellular carcinoma progression through integrin α6β4 complex. *Int J Cancer* (2022) 151(6):930–43. doi: 10.1002/ijc.34146

167. Hou W, Bridgeman B, Malnassy G, Ding X, Cotler SJ, Dhanarajan A, et al. Integrin subunit beta 8 contributes to lenvatinib resistance in HCC. *Hepatol Commun* (2022) 6(7):1786–802. doi: 10.1002/hep4.1928

168. Xie J, Guo T, Zhong Z, Wang N, Liang Y, Zeng W, et al. ITGB1 drives hepatocellular carcinoma progression by modulating cell cycle process through PXN/YWHAZ/AKT pathways. *Front Cell Dev Biol* (2021) 9:711149. doi: 10.3389/fcell.2021.711149

169. Gahmberg CG, Grönholm M, Madhavan S. Regulation of dynamic cell adhesion by integrin-integrin crosstalk. *Cells* (2022) 11(10):1685. doi: 10.3390/cells11101685

170. Wang Z, Cui X, Hao G, He J. Aberrant expression of PI3K/AKT signaling is involved in apoptosis resistance of hepatocellular carcinoma. *Open Life Sci* (2021) 16 (1):1037–44. doi: 10.1515/biol-2021-0101

171. Abusaliya A, Jeong SH, Bhosale PB, Kim HH, Park MY, Kim E, et al. Mechanistic Action of Cell Cycle Arrest and Intrinsic Apoptosis *via* Inhibiting Akt/mTOR and Activation of p38-MAPK Signaling Pathways in Hep3B Liver Cancer Cells by Prunetrin-A Flavonoid with Therapeutic Potential. *Nutrients* (2023) 15(15):3407. doi: 10.3390/nu15153407

172. Bang J, Jun M, Lee S, Moon H, Ro SW. Targeting EGFR/PI3K/AKT/mTOR signaling in hepatocellular carcinoma. *Pharmaceutics* (2023) 15(8):2130. doi: 10.3390/pharmaceutics15082130

173. Xu H, Zhao Q, Song N, Yan Z, Lin R, Wu S, et al. AdipoR1/AdipoR2 dual agonist recovers nonalcoholic steatohepatitis and related fibrosis *via* endoplasmic reticulum-mitochondria axis. *Nat Commun* (2020) 11(1):5807. doi: 10.1038/s41467-020-19668-y

174. Zhu X, Jia X, Cheng F, Tian H, Zhou Y. c-Jun acts downstream of PI3K/AKT signaling to mediate the effect of leptin on methionine adenosyltransferase 2B in hepatic stellate cells in *vitro* and in vivo. *J Pathol* (2020) 252(4):423–32. doi: 10.1002/path.5536

175. Zhang Z, Shang J, Yang Q, Dai Z, Liang Y, Lai C, et al. Exosomes derived from human adipose mesenchymal stem cells ameliorate hepatic fibrosis by inhibiting PI3K/Akt/mTOR pathway and remodeling choline metabolism. *J Nanobiotechnology* (2023) 21(1):29. doi: 10.1186/s12951-023-01788-4

176. Jung K, Kim M, So J, Lee SH, Ko S, Shin D. Farnesoid X receptor activation impairs liver progenitor cell-mediated liver regeneration *via* the PTEN-PI3K-AKT-mTOR axis in zebrafish. *Hepatology* (2021) 74(1):397–410. doi: 10.1002/hep.31679

177. Xie X, Lv H, Liu C, Su X, Yu Z, Song S, et al. HBeAg mediates inflammatory functions of macrophages by TLR2 contributing to hepatic fibrosis. *BMC Med* (2021) 19(1):247. doi: 10.1186/s12916-021-02085-3

178. Wang L, Feng Y, Xie X, Wu H, Su XN, Qi J, et al. Neuropilin-1 aggravates liver cirrhosis by promoting angiogenesis *via* VEGFR2-dependent PI3K/Akt pathway in hepatic sinusoidal endothelial cells. *EBioMedicine* (2019) 43:525–36. doi: 10.1016/j.ebiom.2019.04.050

179. Zhang Y, Mao X, Chen W, Guo X, Yu L, Jiang F, et al. A discovery of clinically approved formula FBRP for repositioning to treat HCC by inhibiting PI3K/AKT/NF-κB activation. *Mol Ther Nucleic Acids* (2020) 19:890–904. doi: 10.1016/j.omtn.2019.12.023

180. Zhang Y, Lv P, Ma J, Chen N, Guo H, Chen Y, et al. Antrodia cinnamomea exerts an anti-hepatoma effect by targeting PI3K/AKT-mediated cell cycle progression in *vitro* and in *vivo*. *Acta Pharm Sin B* (2022) 12(2):890–906. doi: 10.1016/j.apsb.2021.07.010

181. Liao J, Jin H, Li S, Xu L, Peng Z, Wei G, et al. Apatinib potentiates irradiation effect *via* suppressing PI3K/AKT signaling pathway in hepatocellular carcinoma. *J Exp Clin Cancer Res* (2019) 38(1):454. doi: 10.1186/s13046-019-1419-1

182. Fu H, He Y, Qi L, Chen L, Luo Y, Chen L, et al. cPLA2α activates PI3K/AKT and inhibits Smad2/3 during epithelial-mesenchymal transition of hepatocellular carcinoma cells. *Cancer Lett* (2017) 403:260–70. doi: 10.1016/j.canlet.2017.06.022

183. Yu Y, Zhao D, Li K, Cai Y, Xu P, Li R, et al. E2F1 mediated DDX11 transcriptional activation promotes hepatocellular carcinoma progression through PI3K/AKT/mTOR pathway. *Cell Death Dis* (2020) 11(4):273. doi: 10.1038/s41419-020-2478-0

184. Sun F, Wang J, Sun Q, Li F, Gao H, Xu L, et al. Interleukin-8 promotes integrin β3 upregulation and cell invasion through PI3K/Akt pathway in hepatocellular carcinoma. *J Exp Clin Cancer Res* (2019) 38(1):449. doi: 10.1186/s13046-019-1455-x

185. Wu Y, Zhang Y, Qin X, Geng H, Zuo D, Zhao Q. PI3K/AKT/mTOR pathway-related long non-coding RNAs: roles and mechanisms in hepatocellular carcinoma. *Pharmacol Res* (2020) 160:105195. doi: 10.1016/j.phrs.2020.105195

186. Zhang M, Liu S, Chua MS, Li H, Luo D, Wang S, et al. SOCS5 inhibition induces autophagy to impair metastasis in hepatocellular carcinoma cells *via* the PI3K/Akt/mTOR pathway. *Cell Death Dis* (2019) 10(8):612. doi: 10.1038/s41419-019-1856-y

187. Luo X, Zheng E, Wei L, Zeng H, Qin H, Zhang X, et al. The fatty acid receptor CD36 promotes HCC progression through activating Src/PI3K/AKT axis-dependent aerobic glycolysis. *Cell Death Dis* (2021) 12(4):328. doi: 10.1038/s41419-021-03596-w

188. Tang W, Lv B, Yang B, Chen Y, Yuan F, Ma L, et al. TREM2 acts as a tumor suppressor in hepatocellular carcinoma by targeting the PI3K/Akt/β-catenin pathway. *Oncogenesis* (2019) 8(2):9. doi: 10.1038/s41389-018-0115-x

189. Zhangyuan G, Wang F, Zhang H, Jiang R, Tao X, Yu D, et al. VersicanV1 promotes proliferation and metastasis of hepatocellular carcinoma through the activation of EGFR-PI3K-AKT pathway. *Oncogene* (2020) 39(6):1213–30. doi: 10.1038/s41388-019-1052-7

190. Xue XB, Lv TM, Hou JY, Li DQ, Huang XX, Song SJ, et al. Vibsane-type diterpenoids from Viburnum odoratissimum inhibit hepatocellular carcinoma cells *via* the PI3K/AKT pathway. *Phytomedicine* (2023) 108:154499. doi: 10.1016/j.phymed.2022.154499

191. Lu Y, Li X, Liu H, Xue J, Zeng Z, Dong X, et al. β-Trcp and CK1δ-mediated degradation of LZTS2 activates PI3K/AKT signaling to drive tumorigenesis and metastasis in hepatocellular carcinoma. *Oncogene* (2021) 40(7):1269–83. doi: 10.1038/s41388-020-01596-2

192. Pan Q, Luo Y, Xia Q, He K. Ferroptosis and liver fibrosis. *Int J Med Sci* (2021) 18(15):3361–6. doi: 10.7150/ijms.62903

193. Yu Y, Jiang L, Wang H, Shen Z, Cheng Q, Zhang P, et al. Hepatic transferrin plays a role in systemic iron homeostasis and liver ferroptosis. *Blood* (2020) 136 (6):726–39. doi: 10.1182/blood.2019002907

194. Luo P, Liu D, Zhang Q, Yang F, Wong YK, Xia F, et al. Celastrol induces ferroptosis in activated HSCs to ameliorate hepatic fibrosis *via* targeting peroxiredoxins and HO-1. *Acta Pharm Sin B* (2022) 12(5):2300–14. doi: 10.1016/j.apsb.2021.12.007

195. Zhang Q, Qu Y, Zhang Q, Li F, Li B, Li Z, et al. Exosomes derived from hepatitis B virus-infected hepatocytes promote liver fibrosis *via* miR-222/TFRC axis. *Cell Biol Toxicol* (2023) 39(2):467–81. doi: 10.1007/s10565-021-09684-z

196. Wu A, Feng B, Yu J, Yan L, Che L, Zhuo Y, et al. Fibroblast growth factor 21 attenuates iron overload-induced liver injury and fibrosis by inhibiting ferroptosis. *Redox Biol* (2021) 46:102131. doi: 10.1016/j.redox.2021.102131

197. Shen M, Li Y, Wang Y, Shao J, Zhang F, Yin G, et al. N6-methyladenosine modification regulates ferroptosis through autophagy signaling pathway in hepatic stellate cells. *Redox Biol* (2021) 47:102151. doi: 10.1016/j.redox.2021.102151

198. Yang W, Wang Y, Zhang C, Huang Y, Yu J, Shi L, et al. Maresin1 protect against ferroptosis-induced liver injury through ROS inhibition and nrf2/HO-1/GPX4 activation. *Front Pharmacol* (2022) 13:865689. doi: 10.3389/fphar.2022.865689

199. Zhang Z, Guo M, Li Y, Shen M, Kong D, Shao J, et al. RNA-binding protein ZFP36/TTP protects against ferroptosis by regulating autophagy signaling pathway in hepatic stellate cells. *Autophagy* (2020) 16(8):1482–505. doi: 10.1080/15548627.2019.1687985

200. Chen J, Li X, Ge C, Min J, Wang F. The multifaceted role of ferroptosis in liver disease. *Cell Death Differ* (2022) 29(3):467–80. doi: 10.1038/s41418-022-00941-0

201. Hao M, Han X, Yao Z, Zhang H, Zhao M, Peng M, et al. The pathogenesis of organ fibrosis: Focus on necroptosis. *Br J Pharmacol* (2022) 180(22):2862–79. doi: 10.1111/bph.15952

202. Liang JY, Wang DS, Lin HC, Chen XX, Yang H, Zheng Y, et al. A novel ferroptosis-related gene signature for overall survival prediction in patients with hepatocellular carcinoma. *Int J Biol Sci* (2020) 16(13):2430–41. doi: 10.7150/ijbs.45050

203. Wan S, Lei Y, Li M, Wu B. A prognostic model for hepatocellular carcinoma patients based on signature ferroptosis-related genes. *Hepatol Int* (2022) 16(1):112–24. doi: 10.1007/s12072-021-10248-w

204. Yao F, Deng Y, Zhao Y, Mei Y, Zhang Y, Liu X, et al. A targetable LIFR-NF-κB-LCN2 axis controls liver tumorigenesis and vulnerability to ferroptosis. *Nat Commun* (2021) 12(1):7333. doi: 10.1038/s41467-021-27452-9

205. Huang W, Chen K, Lu Y, Zhang D, Cheng Y, Li L, et al. ABCC5 facilitates the acquired resistance of sorafenib through the inhibition of SLC7A11-induced ferroptosis in hepatocellular carcinoma. *Neoplasia* (2021) 23(12):1227–39. doi: 10.1016/j.neo.2021.11.002

206. Sun X, Ou Z, Chen R, Niu X, Chen D, Kang R, et al. Activation of the p62-Keap1-NRF2 pathway protects against ferroptosis in hepatocellular carcinoma cells. *Hepatology* (2016) 63(1):173–84. doi: 10.1002/hep.28251

207. Li ZJ, Dai HQ, Huang XW, Feng J, Deng JH, Wang ZX, et al. Artesunate synergizes with sorafenib to induce ferroptosis in hepatocellular carcinoma. *Acta Pharmacol Sin* (2021) 42(2):301–10. doi: 10.1038/s41401-020-0478-3

208. He F, Zhang P, Liu J, Wang R, Kaufman RJ, Yaden BC, et al. ATF4 suppresses hepatocarcinogenesis by inducing SLC7A11 (xCT) to block stress-related ferroptosis. *J Hepatol* (2023) 79(2):362–77. doi: 10.1016/j.jhep.2023.03.016

209. Yang M, Wu X, Hu J, Wang Y, Wang Y, Zhang L, et al. COMMD10 inhibits HIF1α/CP loop to enhance ferroptosis and radiosensitivity by disrupting Cu-Fe balance in hepatocellular carcinoma. *J Hepatol* (2022) 76(5):1138–50. doi: 10.1016/j.jhep.2022.01.009

210. Xu Z, Peng B, Liang Q, Chen X, Cai Y, Zeng S, et al. Construction of a ferroptosis-related nine-lncRNA signature for predicting prognosis and immune response in hepatocellular carcinoma. *Front Immunol* (2021) 12:719175. doi: 10.3389/fimmu.2021.719175

211. Chen Y, Li L, Lan J, Cui Y, Rao X, Zhao J, et al. CRISPR screens uncover protective effect of PSTK as a regulator of chemotherapy-induced ferroptosis in hepatocellular carcinoma. *Mol Cancer* (2022) 21(1):11. doi: 10.1186/s12943-021-01466-9

212. Du J, Wan Z, Wang C, Lu F, Wei M, Wang D, et al. Designer exosomes for targeted and efficient ferroptosis induction in cancer *via* chemo-photodynamic therapy. *Theranostics* (2021) 11(17):8185–96. doi: 10.7150/thno.59121

213. Wu J, Wang Y, Jiang R, Xue R, Yin X, Wu M, et al. Ferroptosis in liver disease: new insights into disease mechanisms. *Cell Death Discovery* (2021) 7(1):276. doi: 10.1038/s41420-021-00660-4

214. Zhan L, Huang C, Meng XM, Song Y, Wu XQ, Yang Y, et al. Hypoxia-inducible factor-1alpha in hepatic fibrosis: A promising therapeutic target. *Biochimie* (2015) 108:1–7. doi: 10.1016/j.biochi.2014.10.013

215. Liu MX, Xu L, Cai YT, Wang RJ, Gu YY, Liu YC, et al. Carbon Nitride-Based siRNA Vectors with Self-Produced O_2 Effects for Targeting Combination Therapy of Liver Fibrosis *via* HIF-1α-Mediated TGF-β1/Smad Pathway. *Adv Healthc Mater* (2023):e2301485. doi: 10.1002/adhm.202301485

216. Zhang F, Hao M, Jin H, Yao Z, Lian N, Wu L, et al. Canonical hedgehog signalling regulates hepatic stellate cell-mediated angiogenesis in liver fibrosis. *Br J Pharmacol* (2017) 174(5):409–23. doi: 10.1111/bph.13701

217. Kaminsky-Kolesnikov Y, Rauchbach E, Abu-Halaka D, Hahn M, García-Ruiz C, Fernandez-Checa JC, et al. Cholesterol induces nrf-2- and HIF-1α-dependent hepatocyte proliferation and liver regeneration to ameliorate bile acid toxicity in mouse models of NASH and fibrosis. *Oxid Med Cell Longev* (2020) 2020:5393761. doi: 10.1155/2020/5393761

218. Fan N, Zhang X, Zhao W, Zhao J, Luo D, Sun Y, et al. Covalent inhibition of pyruvate kinase M2 reprograms metabolic and inflammatory pathways in hepatic macrophages against non-alcoholic fatty liver disease. *Int J Biol Sci* (2022) 18(14):5260–75. doi: 10.7150/ijbs.73890

219. Yang X, Wang Z, Kai J, Wang F, Jia Y, Wang S, et al. Curcumol attenuates liver sinusoidal endothelial cell angiogenesis *via* regulating Glis-PROX1-HIF-1α in liver fibrosis. *Cell Prolif* (2020) 53(3):e12762. doi: 10.1111/cpr.12762

220. Zheng H, Huang N, Lin JQ, Yan LY, Jiang QG, Yang WZ. Effect and mechanism of pirfenidone combined with 2-methoxy-estradiol perfusion through portal vein on hepatic artery hypoxia-induced hepatic fibrosis. *Adv Med Sci* (2023) 68(1):46–53. doi: 10.1016/j.advms.2022.12.001

221. ElBaset MA, Salem RS, Ayman F, Ayman N, Shaban N, Afifi SM, et al. Effect of empagliflozin on thioacetamide-induced liver injury in rats: role of AMPK/SIRT-1/HIF-1α Pathway in halting liver fibrosis. *Antioxidants (Basel)* (2022) 11(11):2152. doi: 10.3390/antiox11112152

222. Liu HL, Lv J, Zhao ZM, Xiong AM, Tan Y, Glenn JS, et al. Fuzhenghuayu Decoction ameliorates hepatic fibrosis by attenuating experimental sinusoidal capillarization and liver angiogenesis. *Sci Rep* (2019) 9(1):18719. doi: 10.1038/s41598-019-54663-4

223. Moczydlowska J, Miltyk W, Hermanowicz A, Lebensztejn DM, Palka JA, Debek W. HIF-1 α as a key factor in bile duct ligation-induced liver fibrosis in rats. *J Invest Surg* (2017) 30(1):41–6. doi: 10.1080/08941939.2016.1183734

224. Li HS, Zhou YN, Li L, Li SF, Long D, Chen XL, et al. HIF-1α protects against oxidative stress by directly targeting mitochondria. *Redox Biol* (2019) 25:101109. doi: 10.1016/j.redox.2019.101109

225. Wang Z, Yang X, Kai J, Wang F, Wang Z, Shao J, et al. HIF-1α-upregulated lncRNA-H19 regulates lipid droplet metabolism through the AMPKα pathway in hepatic stellate cells. *Life Sci* (2020) 255:117818. doi: 10.1016/j.lfs.2020.117818

226. Kou K, Li S, Qiu W, Fan Z, Li M, Lv G. Hypoxia-inducible factor 1α/IL-6 axis in activated hepatic stellate cells aggravates liver fibrosis. *Biochem Biophys Res Commun* (2023) 653:21–30. doi: 10.1016/j.bbrc.2023.02.032

227. Ma Y, Bao Y, Wu L, Ke Y, Tan L, Ren H, et al. IL-8 exacerbates CCl_4-induced liver fibrosis in human IL-8-expressing mice *via* the PI3K/Akt/HIF-1α pathway. *Mol Immunol* (2022) 152:111–22. doi: 10.1016/j.molimm.2022.10.011

228. Strowitzki MJ, Kirchberg J, Tuffs C, Schiedeck M, Ritter AS, Biller M, et al. Loss of Prolyl-Hydroxylase 1 Protects against Biliary Fibrosis *via* Attenuated Activation of Hepatic Stellate Cells. *Am J Pathol* (2018) 188(12):2826–38. doi: 10.1016/j.ajpath.2018.08.003

229. Sun J, Shi L, Xiao T, Xue J, Li J, Wang P, et al. microRNA-21, *via* the HIF-1α/VEGF signaling pathway, is involved in arsenite-induced hepatic fibrosis through aberrant cross-talk of hepatocytes and hepatic stellate cells. *Chemosphere* (2021) 266:129177. doi: 10.1016/j.chemosphere.2020.129177

230. Wang Q, Wei S, Zhou H, Li L, Zhou S, Shi C, et al. MicroRNA-98 inhibits hepatic stellate cell activation and attenuates liver fibrosis by regulating HLF expression. *Front Cell Dev Biol* (2020) 8:513. doi: 10.3389/fcell.2020.00513

231. Wang P, Fang Y, Qiu J, Zhou Y, Wang Z, Jiang C. miR-345-5p curbs hepatic stellate cell activation and liver fibrosis progression by suppressing hypoxia-inducible factor-1alpha expression. *Toxicol Lett* (2022) 370:42–52. doi: 10.1016/j.toxlet.2022.09.008

232. Wang Q, Zhang F, Lei Y, Liu P, Liu C, Tao Y. microRNA-322/424 promotes liver fibrosis by regulating angiogenesis through targeting CUL2/HIF-1α pathway. *Life Sci* (2021) 266:118819. doi: 10.1016/j.lfs.2020.118819

233. Fang J, Ji Q, Gao S, Xiao Z, Liu W, Hu Y, et al. PDGF-BB is involved in HIF-1α/CXCR4/CXCR7 axis promoting capillarization of hepatic sinusoidal endothelial cells. *Heliyon* (2022) 9(1):e12715. doi: 10.1016/j.heliyon.2022.e12715

234. Li X, Yao QY, Liu HC, Jin QW, Xu BL, Zhang SC, et al. Placental growth factor silencing ameliorates liver fibrosis and angiogenesis and inhibits activation of hepatic stellate cells in a murine model of chronic liver disease. *J Cell Mol Med* (2017) 21 (10):2370–85. doi: 10.1111/jcmm.13158

235. Wang J, Lu Z, Xu Z, Tian P, Miao H, Pan S, et al. Reduction of hepatic fibrosis by overexpression of von Hippel-Lindau protein in experimental models of chronic liver disease. *Sci Rep* (2017) 7:41038. doi: 10.1038/srep41038

236. Luo M, Li T, Sang H. The role of hypoxia-inducible factor 1α in hepatic lipid metabolism. *J Mol Med (Berl)* (2023) 101(5):487–500. doi: 10.1007/s00109-023-02308-5

237. He Z, Yang D, Fan X, Zhang M, Li Y, Gu X, et al. The roles and mechanisms of lncRNAs in liver fibrosis. *Int J Mol Sci* (2020) 21(4):1482. doi: 10.3390/ijms21041482

238. Vanderborght B, De Muynck K, Lefere S, Geerts A, Degroote H, Verhelst X, et al. Effect of isoform-specific HIF-1α and HIF-2α antisense oligonucleotides on tumorigenesis, inflammation and fibrosis in a hepatocellular carcinoma mouse model. *Oncotarget* (2020) 11(48):4504–20. doi: 10.18632/oncotarget.27830

239. Shi M, Dai WQ, Jia RR, Zhang QH, Wei J, Wang YG, et al. APCCDC20-mediated degradation of PHD3 stabilizes HIF-1a and promotes tumorigenesis in hepatocellular carcinoma. *Cancer Lett* (2021) 496:144–55. doi: 10.1016/j.canlet.2020.10.011

240. Wen Y, Zhou X, Lu M, He M, Tian Y, Liu L, et al. Bclaf1 promotes angiogenesis by regulating HIF-1α transcription in hepatocellular carcinoma. *Oncogene* (2019) 38 (11):1845–59. doi: 10.1038/s41388-018-0552-1

241. Huang R, Zhang L, Jin J, Zhou Y, Zhang H, Lv C, et al. Bruceine D inhibits HIF-1α-mediated glucose metabolism in hepatocellular carcinoma by blocking ICAT/β-catenin interaction. *Acta Pharm Sin B* (2021) 11(11):3481–92. doi: 10.1016/j.apsb.2021.05.009

242. Feng J, Li J, Wu L, Yu Q, Ji J, Wu J, et al. Emerging roles and the regulation of aerobic glycolysis in hepatocellular carcinoma. *J Exp Clin Cancer Res* (2020) 39(1):126. doi: 10.1186/s13046-020-01629-4

243. Seo J, Jeong DW, Park JW, Lee KW, Fukuda J, Chun YS. Fatty-acid-induced FABP5/HIF-1 reprograms lipid metabolism and enhances the proliferation of liver cancer cells. *Commun Biol* (2020) 3(1):638. doi: 10.1038/s42003-020-01367-5

244. Yang N, Wang T, Li Q, Han F, Wang Z, Zhu R, et al. HBXIP drives metabolic reprogramming in hepatocellular carcinoma cells *via* METTL3-mediated m6A modification of HIF-1α. *J Cell Physiol* (2021) 236(5):3863–80. doi: 10.1002/jcp.30128

245. Wang M, Zhao X, Zhu D, Liu T, Liang X, Liu F, et al. HIF-1α promoted vasculogenic mimicry formation in hepatocellular carcinoma through LOXL2 up-regulation in hypoxic tumor microenvironment. *J Exp Clin Cancer Res* (2017) 36(1):60. doi: 10.1186/s13046-017-0533-1

246. Chen T, Liu R, Niu Y, Mo H, Wang H, Lu Y, et al. HIF-1α-activated long non-coding RNA KDM4A-AS1 promotes hepatocellular carcinoma progression *via* the miR-411-5p/KPNA2/AKT pathway. *Cell Death Dis* (2021) 12(12):1152. doi: 10.1038/s41419-021-04449-2

247. Li Q, Ni Y, Zhang L, Jiang R, Xu J, Yang H, et al. HIF-1α-induced expression of m6A reader YTHDF1 drives hypoxia-induced autophagy and Malignancy of hepatocellular carcinoma by promoting ATG2A and ATG14 translation. *Signal Transduct Target Ther* (2021) 6(1):76. doi: 10.1038/s41392-020-00453-8

248. Liu D, Luo X, Xie M, Zhang T, Chen X, Zhang B, et al. HNRNPC downregulation inhibits IL-6/STAT3-mediated HCC metastasis by decreasing HIF1A expression. *Cancer Sci* (2022) 113(10):3347–61. doi: 10.1111/cas.15494

249. Fan Z, Yang G, Zhang W, Liu Q, Liu G, Liu P, et al. Hypoxia blocks ferroptosis of hepatocellular carcinoma *via* suppression of METTL14 triggered YTHDF2-dependent silencing of SLC7A11. *J Cell Mol Med* (2021) 25(21):10197–212. doi: 10.1111/jcmm.16957

250. Wang L, Li B, Bo X, Yi X, Xiao X, Zheng Q. Hypoxia-induced LncRNA DACT3-AS1 upregulates PKM2 to promote metastasis in hepatocellular carcinoma through the HDAC2/FOXA3 pathway. *Exp Mol Med* (2022) 54(6):848–60. doi: 10.1038/s12276-022-00767-3

251. Zhang MS, Cui JD, Lee D, Yuen VW, Chiu DK, Goh CC, et al. Hypoxia-induced macropinocytosis represents a metabolic route for liver cancer. *Nat Commun* (2022) 13(1):954. doi: 10.1038/s41467-022-28618-9

252. Bao MH, Wong CC. Hypoxia, metabolic reprogramming, and drug resistance in liver cancer. *Cells* (2021) 10(7):1715. doi: 10.3390/cells10071715

253. Liu Z, Wang Y, Dou C, Xu M, Sun L, Wang L, et al. Hypoxia-induced up-regulation of VASP promotes invasiveness and metastasis of hepatocellular carcinoma. *Theranostics* (2018) 8(17):4649–63. doi: 10.7150/thno.26789

254. Wang L, Sun L, Liu R, Mo H, Niu Y, Chen T, et al. Long non-coding RNA MAPKAPK5-AS1/PLAGL2/HIF-1α signaling loop promotes hepatocellular carcinoma progression. *J Exp Clin Cancer Res* (2021) 40(1):72. doi: 10.1186/s13046-021-01868-z

255. Lin J, Cao S, Wang Y, Hu Y, Liu H, Li J, et al. Long non-coding RNA UBE2CP3 enhances HCC cell secretion of VEGFA and promotes angiogenesis by activating ERK1/2/HIF-1α/VEGFA signalling in hepatocellular carcinoma. *J Exp Clin Cancer Res* (2018) 37(1):113. doi: 10.1186/s13046-018-0727-1

256. Wei X, Zhao L, Ren R, Ji F, Xue S, Zhang J, et al. MiR-125b loss activated HIF1α/pAKT loop, leading to transarterial chemoembolization resistance in hepatocellular carcinoma. *Hepatology* (2021) 73(4):1381–98. doi: 10.1002/hep.31448

257. Dai XY, Zhuang LH, Wang DD, Zhou TY, Chang LL, Gai RH, et al. Nuclear translocation and activation of YAP by hypoxia contributes to the chemoresistance of SN38 in hepatocellular carcinoma cells. *Oncotarget* (2016) 7(6):6933–47. doi: 10.18632/oncotarget.6903

258. Lu LG, Zhou ZL, Wang XY, Liu BY, Lu JY, Liu S, et al. PD-L1 blockade liberates intrinsic antitumourigenic properties of glycolytic macrophages in hepatocellular carcinoma. *Gut* (2022) 71(12):2551–60. doi: 10.1136/gutjnl-2021-326350

259. Hu W, Zheng S, Guo H, Dai B, Ni J, Shi Y, et al. PLAGL2-EGFR-HIF-1/2α Signaling loop promotes HCC progression and erlotinib insensitivity. *Hepatology* (2021) 73(2):674–91. doi: 10.1002/hep.31293

260. Pang L, Ng KT, Liu J, Yeung WO, Zhu J, Chiu TS, et al. Plasmacytoid dendritic cells recruited by HIF-1α/eADO/ADORA1 signaling induce immunosuppression in hepatocellular carcinoma. *Cancer Lett* (2021) 522:80–92. doi: 10.1016/j.canlet.2021.09.022

261. Chu Q, Gu X, Zheng Q, Zhu H. Regulatory mechanism of HIF-1α and its role in liver diseases: a narrative review. *Ann Transl Med* (2022) 10(2):109. doi: 10.21037/atm-21-4222

262. Cui CP, Wong CC, Kai AK, Ho DW, Lau EY, Tsui YM, et al. SENP1 promotes hypoxia-induced cancer stemness by HIF-1α deSUMOylation and SENP1/HIF-1α positive feedback loop. *Gut* (2017) 66(12):2149–59. doi: 10.1136/gutjnl-2016-313264

263. Feng J, Dai W, Mao Y, Wu L, Li J, Chen K, et al. Simvastatin re-sensitizes hepatocellular carcinoma cells to sorafenib by inhibiting HIF-1α/PPAR-γ/PKM2-mediated glycolysis. *J Exp Clin Cancer Res* (2020) 39(1):24. doi: 10.1186/s13046-020-1528-x

264. Luo D, Wang Y, Zhang M, Li H, Zhao D, Li H, et al. SOCS5 knockdown suppresses metastasis of hepatocellular carcinoma by ameliorating HIF-1α-dependent mitochondrial damage. *Cell Death Dis* (2022) 13(11):918. doi: 10.1038/s41419-022-05361-z

265. Méndez-Blanco C, Fondevila F, García-Palomo A, González-Gallego J, Mauriz JL. Sorafenib resistance in hepatocarcinoma: role of hypoxia-inducible factors. *Exp Mol Med* (2018) 50(10):1–9. doi: 10.1038/s12276-018-0159-1

266. Lv C, Wang S, Lin L, Wang C, Zeng K, Meng Y, et al. USP14 maintains HIF1-α stabilization *via* its deubiquitination activity in hepatocellular carcinoma. *Cell Death Dis* (2021) 12(9):803. doi: 10.1038/s41419-021-04089-6

267. Ling S, Shan Q, Zhan Q, Ye Q, Liu P, Xu S, et al. USP22 promotes hypoxia-induced hepatocellular carcinoma stemness by a HIF1α/USP22 positive feedback loop upon TP53 inactivation. *Gut* (2020) 69(7):1322–34. doi: 10.1136/gutjnl-2019-319616

268. Zhang X, Li Y, Ma Y, Yang L, Wang T, Meng X, et al. Yes-associated protein (YAP) binds to HIF-1α and sustains HIF-1α protein stability to promote hepatocellular carcinoma cell glycolysis under hypoxic stress. *J Exp Clin Cancer Res* (2018) 37(1):216. doi: 10.1186/s13046-018-0892-2

Frontiers in Oncology

Advances knowledge of carcinogenesis and tumor progression for better treatment and management

The third most-cited oncology journal, which highlights research in carcinogenesis and tumor progression, bridging the gap between basic research and applications to imrpove diagnosis, therapeutics and management strategies.

Discover the latest Research Topics

See more →

Frontiers

Avenue du Tribunal-Fédéral 34
1005 Lausanne, Switzerland
frontiersin.org

Contact us

+41 (0)21 510 17 00
frontiersin.org/about/contact